



PROCEEDINGS
of the

**15th International Symposium on
Water Management and
Hydraulics Engineering**

September 6th – 8th, 2017

Hotel Zora / Primošten / Croatia





UNIVERSITY OF
ZAGREB

FACULTY OF CIVIL
ENGINEERING



SLOVAK UNIVERSITY
OF TECHNOLOGY IN
BRATISLAVA

FACULTY OF CIVIL
ENGINEERING



SS. CYRIL AND
METHODIUS
UNIVERSITY IN
SKOPJE

FACULTY OF CIVIL
ENGINEERING



GDANSK UNIVERSITY OF
TECHNOLOGY

FACULTY OF CIVIL AND
ENVIRONMENTAL
ENGINEERING



BRNO UNIVERSITY OF
TECHNOLOGY

FACULTY OF CIVIL
ENGINEERING



BOKU UNIVERSITY
OF NATURAL
RESOURCES AND
APPLIED LIFE
SCIENCES

INSTITUTE OF
WATER
MANAGEMENT,
HYDROLOGY AND
HYDRAULIC
ENGINEERING

PROCEEDINGS
of the

15th International Symposium
Water Management and
Hydraulics Engineering

September 6th-8th, 2017,

Hotel Zora / Primošten / Croatia

EDITORS: Damir Bekić, Dalibor Carević, Dražen Vouk

Zagreb, September 2017

PUBLISHER:

Faculty of Civil Engineering Zagreb, Croatia, University of Zagreb
Kačićeva 26, Zagreb

EDITORS:

Damir Bekić, Dalibor Carević, Dražen Vouk

GRAFIC DESIGN

Dora Jelić
Tin Kulić

ISBN

978-953-8168-17-8

ISSN

2410-5910

Authors are completely responsible for the content and shape of their papers. Publisher, editor and organizing committee of the Symposium are not responsible for attitudes carried out in this Proceedings.

Symposium chairmen

Damir Bekić

University of Zagreb, Faculty of Civil Engineering, Zagreb, Croatia

Michał Szydłowski

Gdansk University of Technology, Faculty of Civil and Environmental Engineering, Gdansk, Poland

Andrej Šoltész

Slovak University of Technology, Faculty of Civil Engineering, Bratislava, Slovak Republic

Helmut Habersack

University of Natural Resources and Life Sciences, Vienna, Austria

Cvetanka Popovska

Ss. Cyril and Methodius University, Faculty of Civil Engineering, Skopje, Macedonia

Jaromír Říha

Brno University of Technology, Faculty of Civil Engineering, Brno, Czech Republic

Scientific advisory committee

University of Zagreb, FCE, Zagreb, Croatia

Neven Kuspilić, Živko Vuković, Goran Lončar

Gdansk University of Technology, Faculty of Civil and Environmental Engineering, Gdansk, Poland

Adam Szymkiewicz, Magdalena Gajewska, Piotr Zima

Slovak University of Technology, Faculty of Civil Engineering, Bratislava, Slovak Republic

Ján Szolgay, Peter Dušička, Štefan Stanko

University of Natural Resources and Life Sciences, Vienna, Austria

Johannes Hübl, Gerhard Kammerer, Petr Lichtneger

Ss. Cyril and Methodius University, Faculty of Civil Engineering, Skopje, Macedonia

Josif Josifovski, Petko Pelivanoski

Brno University of Technology, Faculty of Civil Engineering, Brno, Czech Republic

Jan Jandora, Miroslav Špano

Organizing committee

Damir Bekić, Dalibor Carević, Dražen Vouk - Croatia

Wojciech Artichowicz - Poland

Michaela Červeňanská - Slovak Republic

Petr Lichtneger - Austria

Goce Taseski - Macedonia

Tomáš Julínek - Czech Republic

Symposium secretariat

Hrvoje Mostečak

University of Zagreb

Faculty of Civil Engineering

Water Research Department

Kačićeva 26, 10000 Zagreb, Croatia

e-mail: wmhe2017@grad.hr

Under the auspices of



President of Croatia



Ministry of Environmental and Nature Protection



Hrvatske vode

Sponsor



Hawle Hrvatska



Hidroprojekt-ing d.o.o.



Hidroing d.o.o.

Preface

The 15th International Symposium on Water Management and Hydraulic Engineering, WMHE2017, was organised from 6 to 8 September 2017 in Hotel Zora, Primošten, Croatia. This symposium formed the follow-up of the earlier, biannual series. The original bilateral symposium between civil engineering faculties of Gdansk University of Technology (Poland) and University of Zagreb (Croatia) was held back in 1984 in Gdansk under the original name „Research on Hydraulic Engineering“. The symposium has since been spread to partner universities: Slovak University of Technology in Bratislava, Ss. Cyril and Methodius University in Skopje (Macedonia), University of Natural Resources and Applied Life Sciences in Vienna (Austria) as well as Brno University of Technology (Czech Republic). This successful series nowadays is regularly organized between partners.

The aim of this conference series is to encourage and facilitate the interdisciplinary communication in the field of water management and hydraulic engineering. Interdisciplinary aspect of symposium is an opportunity for researchers, practitioners, policymakers and industry representatives to meet at one place and encounter industry-academia interaction and collaborative innovation. During this three days event, discussion on different water management issues was encouraged including aspects of ecosystems and sustainable development. Participating countries could rely on similar political and cultural heritage same as similar position in processes of integration into the EU.

Selection of the symposium topics supports interdisciplinarity in new researches among different sectors of water engineering. The papers were presented in seven topics:

1. Climate Change Impacts and Policies
2. Catchment and River Systems
3. Water Supply and Wastewater Systems
4. Hydraulic Structures
5. Coastal Engineering
6. Geotechnical Engineering
7. EU Projects, Societies and Industry

Topic 1 - Climate Change Impacts and Policies deals with climate change impact on aquatic systems, climate change & hydrological modelling and data management, environmental policy and legislation and hydro-meteorological applications, products and services.

Topic 2 - Catchment and River Systems focuses on new trends in flood risk management, flood forecasting and flood management in small catchments, sediment transport and sustainable sediment management, integrated river-basin management and ecosystem restoration, land-atmosphere interactions, quality control of hydrologic simulations, plausibility data and models, groundwater resources - spatial distribution, monitoring, quality and remediation and groundwater-surface water interaction.

Topic 3 - Water Supply and Wastewater Systems deals with urban water systems - modelling, design and management, advanced technologies for water and wastewater treatment, water pollution & water-related environmental and health issues and challenges in final disposal of treated wastewater and sludge.

Topic 4 - Hydraulic Structures gives papers on design and management of dams and reservoirs, development and implementation of hydro power plants, river engineering structures - past and future, bridge scour risk - assessment, monitoring and management and inland navigation - design, implementation and utilisation.

Topic 5 - Coastal Engineering shows coastal & marine physics, ecology and management and coastal engineering - climate change and ocean energy.

Topic 6 - Geotechnical Engineering focuses on investigation works for remediation of hydraulic structures, implementation of Eurocode 7 in the design of hydraulic structures and application of geosynthetics in hydraulic engineering.

Topic 7 - EU Projects, Societies and Industry deals with connecting industry, academia and societies, experiences from EU funded water management projects and experiences from EU funded projects on water supply and wastewater systems.

Two sessions were scheduled for presentations according to specific topics for more than 150 participants. Within the framework of the meeting 63 full papers and 10 abstracts were presented through

55 oral presentations and 14 posters. During the conference there were three keynote lectures. The most interesting papers qualified by the scientific committee board were proposed for publishing in special issues of journals *Gradevinar* (ISSN **1333-9095**) and *Acta Hydrologica Slovaca*. Social events included gala dinner, technical tour at Peruča dam and excursions to Split and Trogir.

We thank symposium chairmen, scientific advisory committee and organising committee for their valuable contribution on the ideas and the definition of symposium topics and themes. We also thank all the authors for their excellent contributions to these proceedings and all the participants for their contribution to this successful symposium, either in the form of an oral presentation or poster or in the form of their attention in the presentation and contributions to the discussions.

The symposium was held under the auspices of President of Croatia, Ministry of Environmental and Nature Protection of Croatia and Croatian Waters.

See you all at the 16th WMHE in 2019!

Damir Bekić
Dalibor Carević
Dražen Vouk
Editors

Content

1. CATCHMENT AND RIVER SYSTEMS	1
CONSIDERING THE EFFECTS OF HUMAN ACTIVITIES IN FLOOD HAZARD ASSESSMENT	2
HYDROLOGICAL AND HYDRAULIC ANALYSIS OF RIVER CROSSINGS.....	9
FLOODS: NEW CONCEPTS EMERGE - OLD PROBLEMS REMAIN	19
ANALYSIS OF THE SEDIMENT FROM SMALL WINTER PORT ON THE DRAVA RIVER ...	27
COMPARISON OF DIFFERENT COMPUTATIONAL METHODS FOR FLOOD MITIGATION	33
UNSATURATED ANALYSES OF EXTREME RAINFALL INFLUENCE ON THE LANDSLIDE STABILITY	42
COMPARISON OF EROSION MODELLING AND BATHYMETRY MEASUREMENTS OF SEDIMENT TRANSPORT IN THE SVACENICKY CREEK BASIN IN SLOVAKIA	52
FLOOD MODEL AT RACINOVCI AND RAJEVO SELO USING THE 2D MODEL IN HEC-RAS	60
FLOOD MODELING OF WETLAND RESTORATION IN EZERANI NATURE PARK, PRESPA LAKE WATERSHED.....	69
ANALYSIS OF ICE REGIMES ON THE DANUBE IN DALJ IN 2012. AND 2017.....	76
FLOOD MANAGEMENT IN URBAN BASINS OF THE CITY OF GDAŃSK	84
2. WATER SUPPLY AND WASTEWATER SYSTEMS.....	93
ANALYSIS OF WATER QUALITY OF THE KARAŠICA-VUČICA RIVER.....	94
HYDRAULIC MODELLING OF DEMAND GROWTH IN TOURIST ISLANDS, CASE STUDY: GALÁPAGOS, ECUADOR.....	113
URBAN SEDIMENT MANAGEMENT – FROM THE RIVER TO THE SEWER	128
STORMWATER MANAGEMENT IN THE URBAN ENVIRONMENT	137
COMPUTER ANALYSIS OF HYDRAULIC CONDITIONS IN A SANITARY CHAMBER	147
3. HYDRAULIC STRUCTURES	156
MORPHODYNAMIC IMPACT OF SCOUR COUNTERMEASURES ON RIVERBED DEVELOPMENT	157
POOL FISHWAY HYDRAULIC ANALYSIS.....	165
HYBRID MODELLING OF OVERFLOWING BROAD-CRATED WEIR-PHYSICAL AND NUMERICAL COMPARISON	174
BED ROUGHNESS EFFECT ALONG SUBMERGED HYDRAULIC JUMP	181
EXPERIMENTAL RESEARCH ON FLOW CONDITIONS AT SELF-CLEANING RACKS.....	190
EFFECT OF VERTICAL SHAPES OF SHAFT INTAKE STRUCTURES ON FLOW VELOCITY DISTRIBUTION	196
4. COASTAL ENGINEERING.....	202
MEASUREMENTS OF WATER CIRCULATION IN MARINA OPATIJA-CROATIA.....	203
5. GEOTECHNICAL ENGINEERING	213
IMPLEMENTATION OF EUROCODE 7 IN THE DESIGN OF FLOOD PROTECTION EMBANKMENTS IN CROATIA.....	214
REMOTE SURVEYING OF FLOOD PROTECTION EMBANKMENTS	224
INVESTIGATION WORKS FOR REMEDIATION OF HYDRAULIC STRUCTURES	244
AUTHOR INDEX.....	254

1. CATCHMENT AND RIVER SYSTEMS

CONSIDERING THE EFFECTS OF HUMAN ACTIVITIES IN FLOOD HAZARD ASSESSMENT

GAŠPER RAK¹, FRANCI STEINMAN²

¹ University of Ljubljana, Faculty of Civil and Geodetic Engineering, Slovenia, Gasper.Rak@fgg.uni-lj.si

² University of Ljubljana, Faculty of Civil and Geodetic Engineering, Slovenia, Franci.Steinman@fgg.uni-lj.si

1 Abstract

Increasing trend of a frequency and intensity of flood phenomenon and also even more frequent human encroachment in a water-corridors and floodplains are main reasons for flood being one of most serious disaster. For more effective flood hazard and risk management the European Union adopted Flood Directive in 2007, on base of which all EU nations prepared legislation on the methodology for determination of flood hazard and risk areas. Classification of flood areas is taking into account several criterions and flood hazard assessment for high water scenarios with different return periods. Despite important anthropogenic influences and their impact on flood hazards, legislation on the process of flood hazards mapping usually does not obligate to consider anthropogenically induced scenarios that occur during extreme and extraordinary events like embankment breaching or failure of other flood protection measures, irregular or limited operation of the hydro mechanical equipment at hydraulic structures etc. As important human influence should also be considered the stochastic land-use changes in line with economic, environmental and social interests. To reduce the risk in flood prone areas, infrastructure facilities, such as embankments, etc., are being planned as mitigation measures. Such measures can change the runoff regime and divert the hazard of flooding to other areas. Moreover, construction of levees changes the retention capacity of floodplains areas, which can have a significant impact on the peak attenuation and propagation time extension of flood waves and consequently on the flood safety of the downstream areas. The article presents introducing of exceptional events analysis in flood hazard and risk assessment, with different examples of direct and indirect human-induced extreme flood events, analysed with detailed hydraulic modelling.

Keywords: flood hazard, anthropogenic effects, flood risk mapping, legislation, runoff regime

2 Introduction

For reduction or more effective flood risk management and other risk associated with water with an appropriate spatial planning, which is primarily aimed at reducing the vulnerability with preventive measures, the European Parliament and the Council of the European Union adopted the Flood Directive in 2007. The Flood Directive required from EU member states to ensure that the flood hazard maps (KRPN) and flood risk maps were completed to the end of 2013, and that the flood risk management plans were completed to the end of 2015. To meet the objective Slovenia adopted *Rules on the methodology for determining the areas threatened by floods and associated erosion of inland and marine waters, and the method of classifying land in hazard classes (Government of the Republic of Slovenia (RS), 2007)* and *Decree on conditions and limits for the implementation of activities and interventions in place in areas threatened by flooding and the associated erosion of inland and marine waters (RS, 2008)*. With this legislation Slovenia has prepared detailed regulation on management with water-related hazards as well as to aim more effective zoning of riparian areas, which are subject of land use restriction.

Today there is much talk about climate change, but it should be stressed, that the risk is mainly increased due to anthropogenic interventions in areas, where considering of vulnerability is not sufficient. There are many reasons: the intensive land use and thereby increasing of economic value of buildings and infrastructure within flood endangered areas, reducing of retention areas, which are flooded during flood events, providing only of minimal flood protection measures and improper maintenance of them etc.

(Loat, 2003). With an event, which carries the risk, it should be considered acceptable risk, manageable risk, which was for an example taken in account in project design, and residual risk. Catastrophic event in the past have shown that adverse effects can only be partially mitigated by the structural measures and that flood protection measures in Slovenia as well as in elsewhere have limited range of functionality, while vulnerability and consequently the risk of inhabitants, buildings and activities increase.

Flood protection measures and other interventions in the water and riparian areas are dimensioned with ie. »design discharge«, to which protected areas are safe (e.g. Q100+freeboard) or reduction of flood hazard is achieved. With reduction of hazard, protected areas became very attractive for more intensive land use and thus a damage potential in the flood events is increased. In flood risk analysis there is usually not taken into account what happens in the case of extraordinary events, e.g. braking flood protection measures, in incorrect or limited operation or even failure of hydro-mechanical equipment at hydro-engineering facilities. As adverse anthropogenic effects on flood hazard management can also be considered the inadequate maintenance of flood protection infrastructure as well as uncontrolled changes of land use in retention areas. The changes of land use are leading to changes in run-off regime, according to the conditions which were taken into account in design of interventions and spatial planning. An illustrative example of adverse effects of water, as consequence of uncontrolled land use in riparian area, are damages at a channel-type power plant Formin during flood event in 2012, where discharge exceeded the discharge capacity of overgrown channel of Drava River and water found other, destructive path.

This paper presents two examples of anthropogenic impact on changing of flood hazard. In the first case, the impact of uncontrolled changing of land use during infrastructure lifespan on the run-off regime and consequent changing of the flood risk in the affected area is presented. In the second case, it presents sudden or progressive failure of flood protection embankment during extreme and extraordinary events.

3 Uncontrolled land use changing in riparian areas

Riparian areas and floodplains, particularly in flatland areas, present great potential for development, but at the same time these areas, with their retention capacity influence the runoff regime, flood wave attenuation, lengthening of the propagation time and consequently the flood risk reduction of downstream areas. Due to conflict of interests in spatial planning, in siting of building and infrastructure as well as in long term planning of land use and preserving of environment, prudent strategy of spatial development and planning of interventions in riparian areas is necessary. The essential task is, how to preserve run-off regime in influenced area with appropriate land use and at same time not cause adverse effects on downstream areas. »Freezing« the state in the affected area is difficult, because spatial developments are always dynamic, but it necessary to analyse the potential negative impacts of spatial changes. With legislation, prepared in accordance with the Flood Directive, interventions in flood endangered area are restricted, although there may be different changes in the area.

In the extensive floodplains of plain Krško-Brežiško polje, which have significant retention capacity and an impact on run-off regime, the construction of HPP Brežice is in finishing phase. HPP and other related interventions present water infrastructure, which covers a long stretch of watercourse and changes the run-off regime significantly as well as flood risk in the area of influence. With selected indicators such as a flood wave peak attenuation, propagation time over studied area, the extent of the flooded area and distribution of water depths and velocities etc., it is possible to clearly analyse as well as to show the response of run-off regime to the processes of spatial changes in the area. Hereafter, the impact of land use changes in riparian areas as consequence of "unintentional" anthropogenic influences – e.g. a gradual afforestation of retention areas due to the abandonment of agriculture activities and vice versa, an extension of agricultural areas into forest areas, is presented.

The figure 1 presents four scenarios of afforestation and disforestation, where the proportion of areas with forest and agriculture land use is changing within the extent of flooding with 100 years return period. Because distribution of land use in analysis was mainly linked to the parcel boundaries, in

gradual changing of land use the connections between the neighboring parcels were also taken into account.

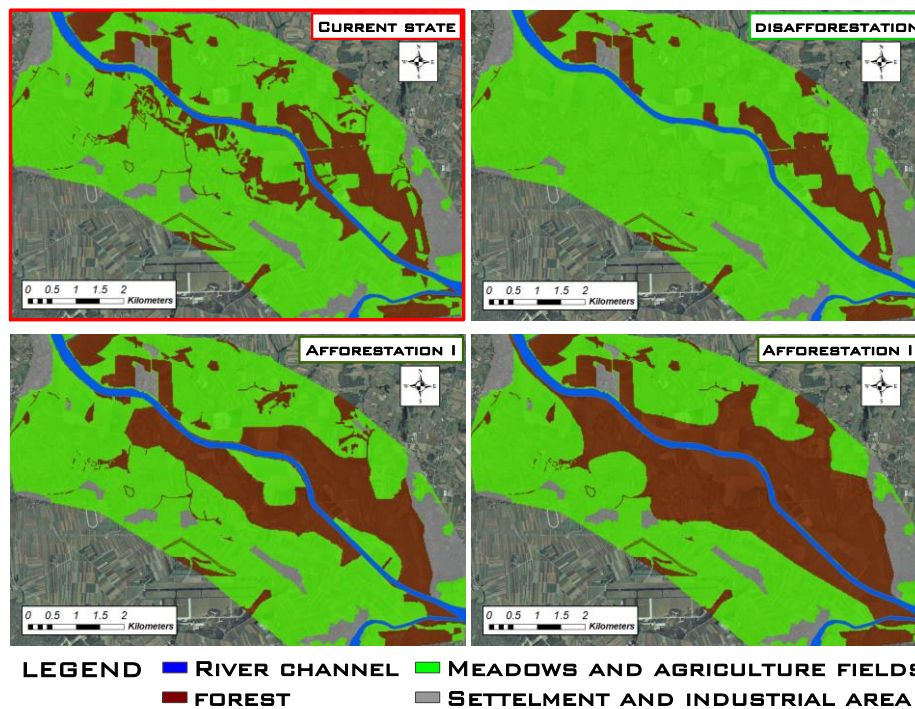


Figure 1: Examples of different proportions of specific land use areas considered in calculations.

In the preparation of flood hazard maps and flood risk maps for the events with 100-year return period are, beside extent of flooded area, also taken into account the distribution of water depth (1. criterion) and its velocity (momentum of water flow; 2. criterion) (RS, 2007). Data on the depth and velocity of water is essential for determining the intensity of the event, as momentum of water directly threatens non-resistant (vulnerable) inhabitants and buildings. For an example, an individual object is resistant to a certain water depth and velocity, while at greater depth or velocity either human lives or the stability of the object could be at risk. By changing the proportion of extent of the particular land use the hydraulic response of flooded areas is shown as changing of the extent of flooding and the spatial distribution of flooded areas, and thus flood hazard classes on the KRPN (Šantl and Rak, 2010), which are determined in accordance with legislation (RS, 2007). The land use in flood endangered areas is only partly restricted, because legislation (RS, 2008) regulates the interventions in accordance with Classification of Types of Constructions (CC-SI) and 5 types of activities that are possibly carried out therein. However, changes of flood hazard in relation to all land use (e.g. afforestation) in entire influenced inundation is important information for all users of the area.

From the analysis can be concluded that the positive impact of increasing the extent of forest area can be seen in determining of flood hazard according to 2. criterion. The afforestation increases the extent of the entire flooded area as well as the extent of the area with maximum depths (water depths above 1.5 m), while the velocity of water flow decreases rapidly. As mentioned before the areas with water flow velocities over 1 m/s are subject of tighter restrictions. But it is necessary to take into account that the 1. criterion is typically predominant in determining of flood hazard in inundation of flatland. With increasing the extent of agriculture area or areas at lower roughness velocities of water flow increase, while the extent of flood areas decrease. Peak discharge of flood wave at downstream boundary is also increased, while the propagation time is reduced. Generally, we can say that all selected indicators reflect

opposite trend in the afforestation and in disforestation. Absolute as well as relative changes of indicator values decrease with increasing a length and peak discharge of the flood wave (Rak et al., 2016). Figure

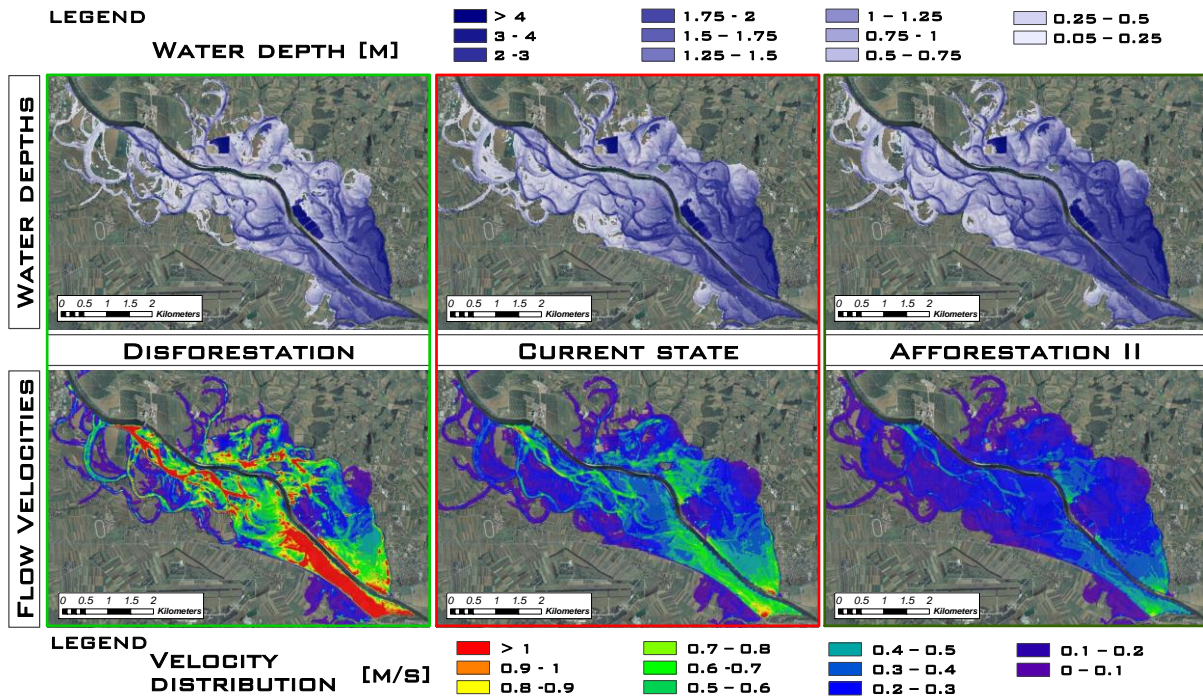


Figure 2: A comparison of the extent of the flooded area and water depths for flood wave with the peak discharge of 3750 m³/s (above) and a comparison of the spatial distribution of local (cell) velocities (below) for different ratios between the agricultural and forest areas.

With changing of land use are, in addition to run-off regime, affected also the peak-discharge of outflow hydrograph and propagation time of flood wave, and consequently flood hazard of downstream areas. With disforestation and the increasing of agriculture areas the volume of water spilled onto the retention increase, but at the same time, at low roughness of retention the velocities of parallel water flow in floodplains are high, ie. the order of magnitude of velocities in the river channel, thus water mass is not significantly retained and coincidence of wave peaks in the channel and over floodplains has a negative effect on peak attenuation. Increasing the roughness slows the water flow over the retention, which causes the return of the water mass from the retention into the channel at a later stage of the hydrograph and contributes less to the peak of the outflow hydrograph. At a certain increase in hydraulic roughness, which is different for different flood waves, water flow over the retention is too slow and water levels are consequently too high for the water mass of the flood wave peak to spill onto the retention area. Water flow over the retention is slow and only marginally contributes to the peak of the hydrograph in the output profile, but the volume of water spilled onto the retention is too small that the run-off regime over the retention would have a significant impact on flood wave transformation (Rak et al., 2016). Extension of propagation time of flood wave is very important for downstream areas as it increase available responsible time for preparation of flood protection measures and to mitigate the adverse effects of flood events, while the greater peak attenuation has impact on reducing of the intensity of the event. Increasing vegetation density on floodplains decrease velocities and thus the associated erosion hazard. Table 1 presents the variation of the analysed parameters in the process of increasing or decreasing the extent of agricultural areas relative to the current state of land use.

Table 1: The impact of disforestation and afforestation on the analysed parameters (narrow HW wave Q_{100} with the peak discharge $3750 \text{ m}^3/\text{s}$).

	narrow flood wave $Q_{100}=3750 \text{ m}^3/\text{s}$					
	100 % Agriculture areas	Disforestation I	Current state	Afforestation case A	Afforestation case B	100 % Forest areas
Peak attenuation	- 13.7 %	- 2.9 %	128 m^3/s	+ 11.3 %	+ 36.1 %	+ 63.0 %
Propagation time	- 7.1 %	- 3.6 %	280 min	+ 3.6 %	+ 10.7 %	+ 10.7 %
Extent of flooded area	- 6.8 %	- 5.7 %	19.1 km^2	+ 1.6 %	+ 2.2 %	+ 4.5 %
Area with water depth < 0.5 m	+ 11.2 %	+ 2.5 %	4.5 km^2	- 5.0 %	- 18.1 %	- 18.9 %
Area with water depth 0.5 - 1.5 m	- 7.7 %	- 7.5 %	7.8 km^2	+ 1.9 %	- 3.3 %	- 3.9 %
Area with water depth > 1.5 m	- 17.9 %	- 9.1 %	6.8 km^2	+ 5.7 %	+ 22.1 %	+ 29.7 %
Area with water velocity > 1 m/s	+ 127.0 %	+ 118.9 %	0.6 km^2	- 11.3 %	- 70.3 %	- 99.3 %
Avg. water depth on floodplains	- 12.8 %	- 6.7 %	1.5 m	+ 4.0 %	+ 14.0 %	+ 19.6 %
Avg. water velocity on floodplains	+ 16.9 %	+ 9.6 %	0.4 m/s	- 8.8 %	- 27.3 %	- 38.5 %

Presented impacts already occur with stochastic changes of land use, while dedicated intervention are separately analysed. The decision to give priority to downstream areas or to take into account the needs and requirements of users of retention areas as much as possible or to find compromises, it is difficult task of »guardian of spatial planning«. There are procedures to clarify the tasks and responsibilities for spatial planning, but the question, who will take care for long-term preservation of retention capacity of floodplains, remains.

4 Flooding caused by failure of flood protection measures

With implementation of flood protection measures (FPM), it is expected that their maintenance and operation ensure functioning in accordance with project conditions throughout the entire lifespan of infrastructure. As is shown in figure 3, the efficiency decreases with time due to ageing of FPM and other processes (the soil consolidation etc.). Without maintenance the FPM quickly lose effect of freeboard (see DIN 31 054, 2003) and thus FPM passes into the area, where the probability of failure or even collapse is higher.

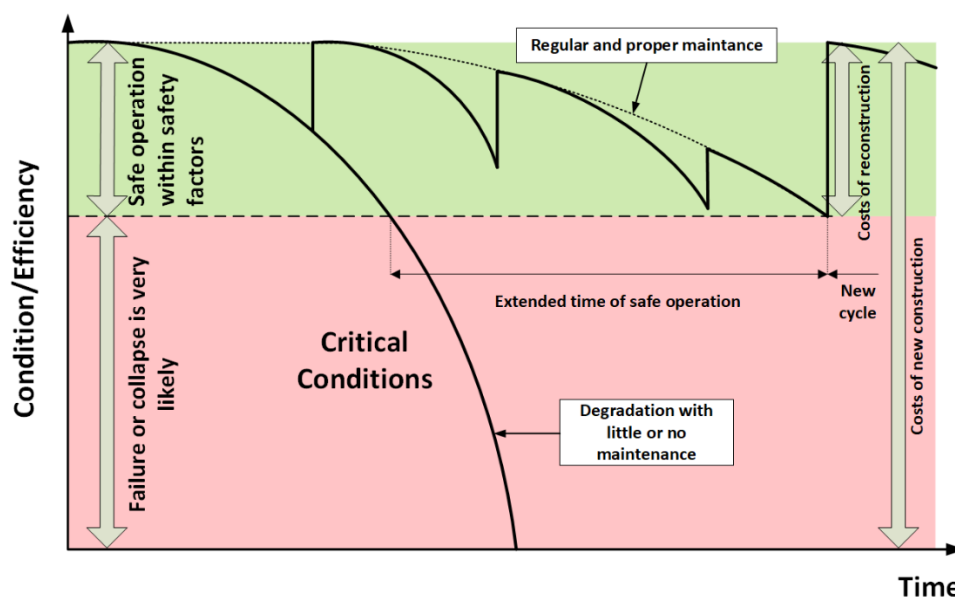


Figure 3: Changing of FPM efficiency regarding their conditions and scope of maintenance. (Rak and Steinman, 2014).

The figure also shows that regular maintenance ensures functionality of FPM over a longer period of time, however, the ageing process cannot be stopped and the reconstruction or later even the new construction, according to the rules of the respective state-of-the-art, is necessary. Good management also requires good decision-making, ie. to reconstruct the damaged/collapsed FPM in shorter periods of time or to maintain their function with regular maintenance as long as possible.

Once the structural FPMs are completed, the process of consolidation is taking place, which depends on the built-in soil, heterogeneous load-bearing capacity of terrain etc. Therefore, to preserve the flood protection function of measures, it is necessary to periodically maintain the level of embankment as well as to check/improve their stability. In the period between the two interventions in the FPM, the critical sections may occur in the locations, where settlements are greater and possibility of embankment overflow increase. In design of FPM only the normal conditions (covered with design discharge) are usually taken into account, although extraordinary events (clogging of the bridge openings, mudslides in river channel etc.) should also be considered. Among the extraordinary events can also be considered failure and breaching of FPM, which should be, properly constructed and maintained, capable of withstanding loads without any structural damages. At the critical point of FPM the instantaneous-collapse can occurs, e.g. part of flood protection wall, or gradual breaching, where overflow of embankment causes the depth and lateral erosion and consequently the increasing of breach dimension. The amount of water spilled onto floodplain is increasing, while water flow gradually propagates in areas, which are, according to the maps of flood hazard map, regarding as areas with acceptable flood risk, while there the flooding of settlement areas, infrastructure, etc. occur. Overflow of FPM can also occur in the case of extreme events, ie. flood events in which peak discharge significantly exceeds the design discharge. FPMs for protection of important areas are designed with discharge with 100-year return period and additional freeboard. In the cases, when water levels exceed level of implemented measures, we are talking about the occurrence of »force majeure«. Analysis of such scenarios can be intended to prepare guidelines, restrictions, requirements and prohibitions in spatial planning, as well as in planning the coordinated operations of the services for protection and rescue during the extraordinary events. In preparing the scenarios of flooding, it is also necessary to analyse the critical location of failure, to predict timing of erosion processes and breaching, and to consider increasing of the opening through which water is spilled onto floodplain, as well as the final width of the destructed section of the FPM and the beginning of overflow of the embankment (in relation to the course of the flood wave). Propagation of flooding due to overflow and collapse of FPM is, for selected temporal dynamic, presented with maps of flood hazard in figure 4. They show the states of flooding after the first hour and after 10 hours from the beginning of the occurrence of concrete wall collapse.

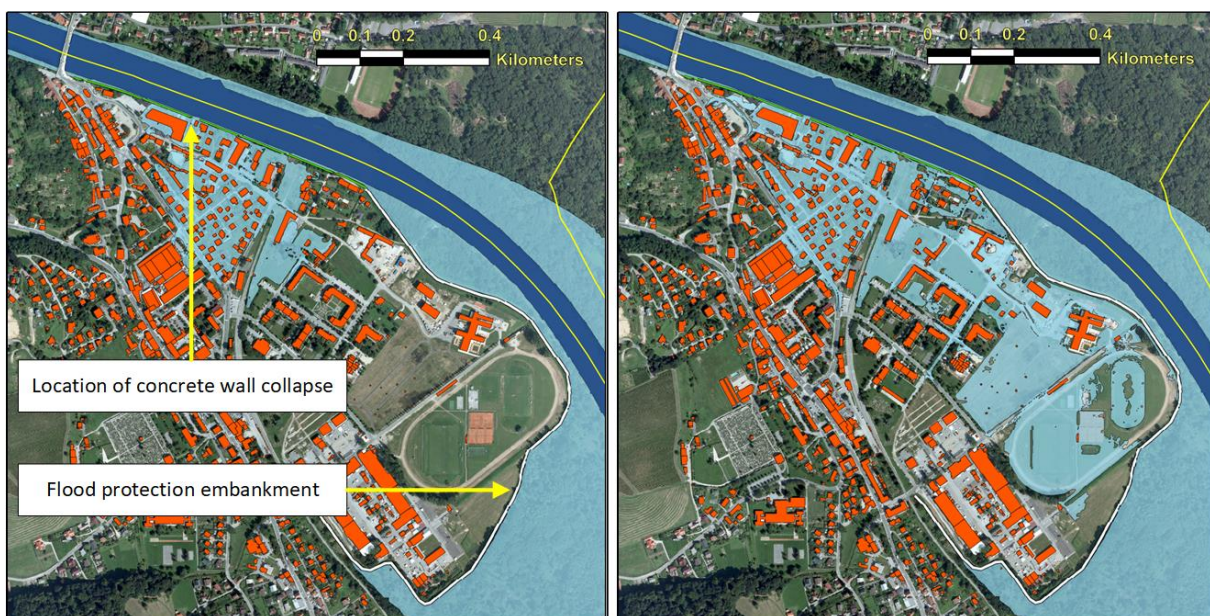


Figure 4: Propagation of flooding 2 hours (left) and 4 hours (right) after the collapse a part of flood protection wall.

5 Conclusions

The paper presents just a few examples of the possible impacts of anthropogenic activities with significant influence on flood risk, but adverse effects can be predicted and analysed with hydraulic researches of run-off regime in river channels and riparian areas. With analysis it is possible to improve the emergency plans of services for protection and rescue, as well as the preparation of practical solutions and guidelines, which should be considered in planning of the spatial development and in finding the appropriate solutions to achieve the objective of spatial development strategy. The preparation of such expert basis enable the inclusion of concerns in spatial planning, which would hinder or even paralyse measures of protection and rescue, as well as to prevent taking of excessive risk. The planning of land use should take into account expertise and experiences, which has shown, that the land use can be significantly changed after implementation of intervention in riparian areas, which affects the achievement of the objectives of FPM. Reduced flood risk is attracting more intensive use of riparian areas, and thus increasing the damage potential in occurrence of flood events. From completion of FPMs to their change or degradation the land use has to be monitored or, if necessary, an inappropriate land use has to be restricted in the influenced area through the entire lifespan of FPMs to avoid harmful effects of flooding. Effective and comprehensive plan for sustainable development of the area should certainly include the systematic management of flood endangered areas, taking into account both temporal and spatial dynamic.

References

- [1] Loat, R. 2003. Risk management in Switzerland. Biel.
- [2] Rak, G. 2013. Hydraulic Analysis of Floodplain Land Use Effects on Flood Wave Propagation. Master's thesis, Ljubljana, University of Ljubljana, Faculty of Civil and Geodetic Engineering.
- [3] Rak, G., Steinman, F. 2014. Kaj se zgodi ko PPU odpovedo – Poplavni scenariji v Gornji Radgoni. 25. Mišičev vodarski dan: 83-90.
- [4] Rak, G., Slokar, M., Steinman, F. 2014. Slovensko – avstrijsko sodelovanje pri poplavah zaradi porušitve protipoplavnih ukrepov na območju Gornje Radgone in Bad Radkersburga. Ujma: 245-254.
- [5] Rak, G., Müller, M., Kompare, K., Steinman, F. 2014. Vpliv zaraščenosti poplavnih površin na potovanje poplavnih valov. Gradbeni vestnik, 2-12.
- [6] Rak, G., Kozelj, D., Steinman, F. 2016. The impact of floodplain land use on flood wave propagation. Natural hazards 83; 1: 425-443.
- [7] Republic of Slovenia, Ministry of the Environment and Spatial Planning, 2007. Rules on the methodology for determining the areas threatened by floods and associated erosion of inland and marine waters, and the method of classifying land in hazard classes, Official Gazette of RS, Nos. 60/07.
- [8] Republic of Slovenia, Ministry of the Environment and Spatial Planning, 2008. Decree on conditions and limits for the implementation of activities and interventions in place in areas threatened by flooding and the associated erosion of inland and marine water, Official Gazette of RS, Nos. 89/08.
- [9] Steinman F., Mueller M., Kozelj D., Rak G., Analiza poplavljanja mejne Mure/Abflussuntersuchung der Grenzmur. UL FGG, VGI. May 2012, EU project DRA-MUR-CI SI-AT 2007-2013.
- [10] Šantl S., Rak, G. 2010. Flood hazard and run-off regime analysis - approach with use of different types of hydraulic models, Gradbeni vestnik, Ljubljana, 147–156.

HYDROLOGICAL AND HYDRAULIC ANALYSIS OF RIVER CROSSINGS

BORJANA BOGATINOSKA¹

¹ *University of Ss Cyril and Methodius, Faculty of Civil Engineering, Macedonia, borjana95@gmail.com*

1 Abstract

River crossings are unique component of bridge and pipeline construction projects. River crossings construction techniques typically require devoted crews and specialized equipment, specific engineering design and specific planning and regulatory approval considerations. Crossings pose risks to the success of the projects and to environmental disturbances. Success of the projects depends on the hydrological and hydraulic analysis of the river.

This paper deals with some results out of hydrological and hydraulic analyses of Podmolska River in south-western part of the Republic of Macedonia. The river is a tributary of Crna River and according to the watershed area it is considered as a small watershed. The applied methods in hydrological analysis were defined by the existing and available hydro meteorological data. Physical geographical watershed characteristics were defined by Digital Elevation Model (DEM), land use and land cover by CORINE 2006, while in hydraulic modelling HEC-RAS was used.

Additionally, environment impacts are briefly discussed considering that the cumulative effects of construction activities within watercourse and riparian areas can magnify the outcome of a storm or flood event and can stress the aquatic populations.

Keywords: hydrological, hydraulic, drainage basin, discharge hydrograph, fuel pipeline, erosion.

2 Introduction

The project, National gasification system in the Republic of Macedonia, LOT 2, from the city Kavadarci to Bitola, is part of the complex gasification system that will enable the development of the existing gas infrastructure and in the period from 2010-2040 should be established in the territory of the country. Its projected route crosses different types of natural obstacles, however we concentrated our attention on the crossing with the river Podmolska that is 18 km from the city of Prilep.

The main purpose of this research is to study, calculate and analyse the hydrological and hydraulic characteristics of the watershed up until the crossing with the pipeline.

In the research, an analysis is made using the software ArcMap and together with the gathered information from the meteorological station near the city Prilep, the flood waters are calculated for few return periods using the SCS method.

For the obtained return period, hydraulic analysis are made using the HEC-RAS software and based on the results couple of different building techniques are commented considering the impacts on the environment.

3 Methods

3.1 Hydrological analysis

3.1.1 Drainage basin characteristics

Drainage basins are local open systems. A drainage basin is an area of land drained by a river and its tributaries (river system). It includes water found in the water table and surface run-off. There is an imaginary line separating drainage basins called a watershed. Usually, this is a ridge of high land. The geometry of a drainage basin and its stream system is usually described by measurements of linear, areal and relief aspects. The first two categories are planimetric, while the third one is related to the vertical variability of the drainage basin forms (Popovska et al. 2011). These geometrical characteristics of the drainage basin are analysed by using the Digital Terrain Model (DTM):

1. The basin area until the crossing with the gas pipeline is $A=29.37 \text{ km}^2$;
2. The length of river Podmolska is $L_R=6.5 \text{ km}$;
3. The basin length (the longest path) is $L_S= 12.97 \text{ km}$;
4. The watershed length is $L_V= 31.16 \text{ km}$;
5. Coefficient of rotundity:

$$m = \frac{L_V}{2 \cdot \sqrt{\pi \cdot A}} = 1.62 \quad (1)$$

6. The average width of the basin:

$$B_{SR} = \frac{A}{L_S} = 2.26 \quad (2)$$

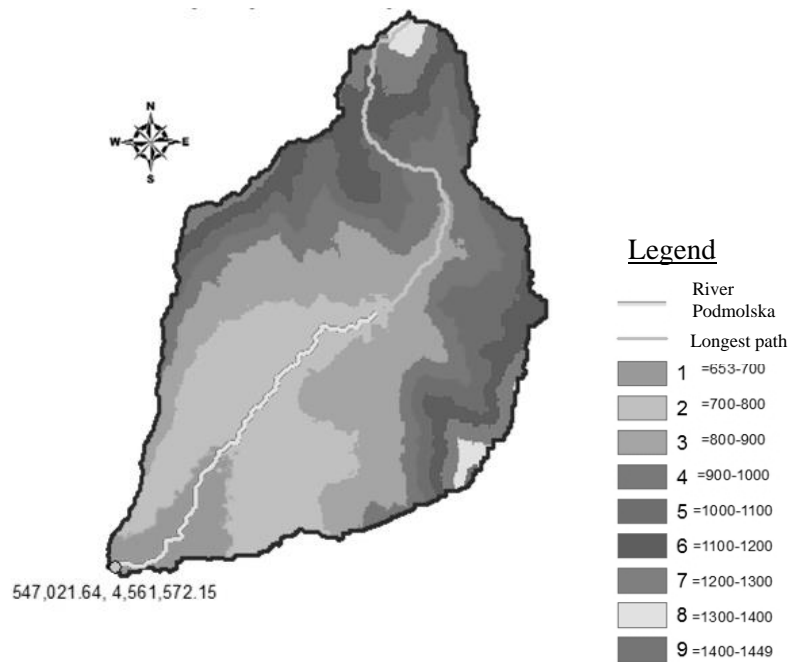


Figure 1. Height distribution of the watershed of river Podmolska

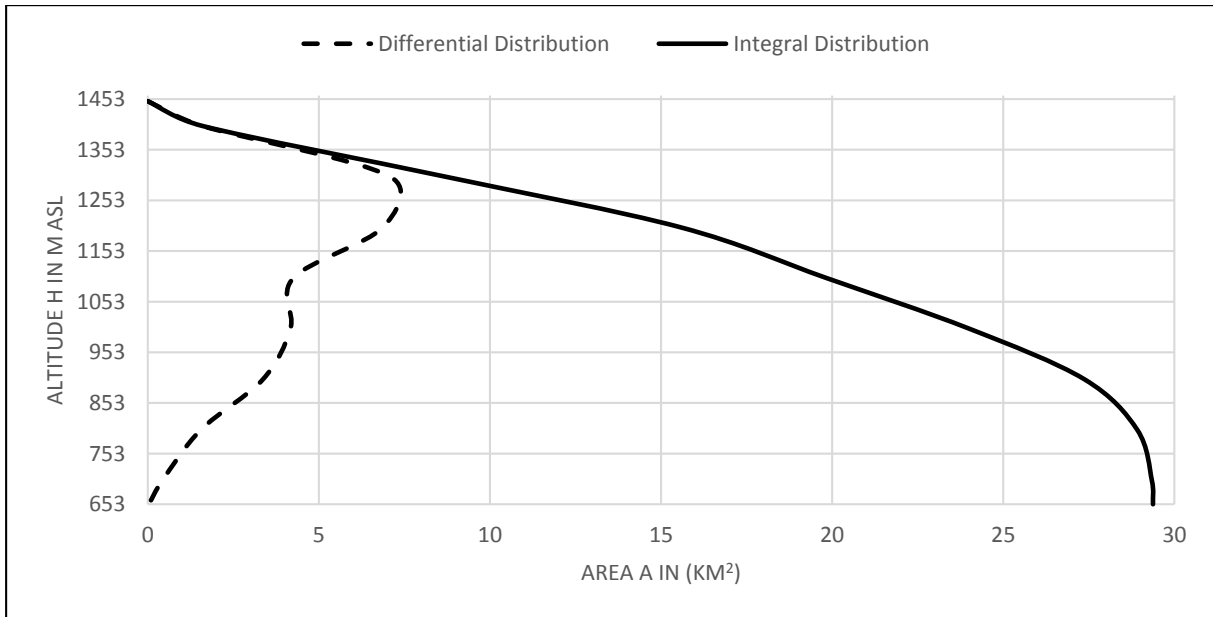


Figure 2. Hypsometric curve (River Podmolska)

Besides the above mentioned drainage characteristics, very important in hydrological analysis are the physical-geographical characteristics, such as: geographical location, climate, vegetative cover and land use, geological structure, geomorphological conditions and other. The land cover and land use characteristics may be analysed by the use of GIS based on Corine Land Use Classification Model.

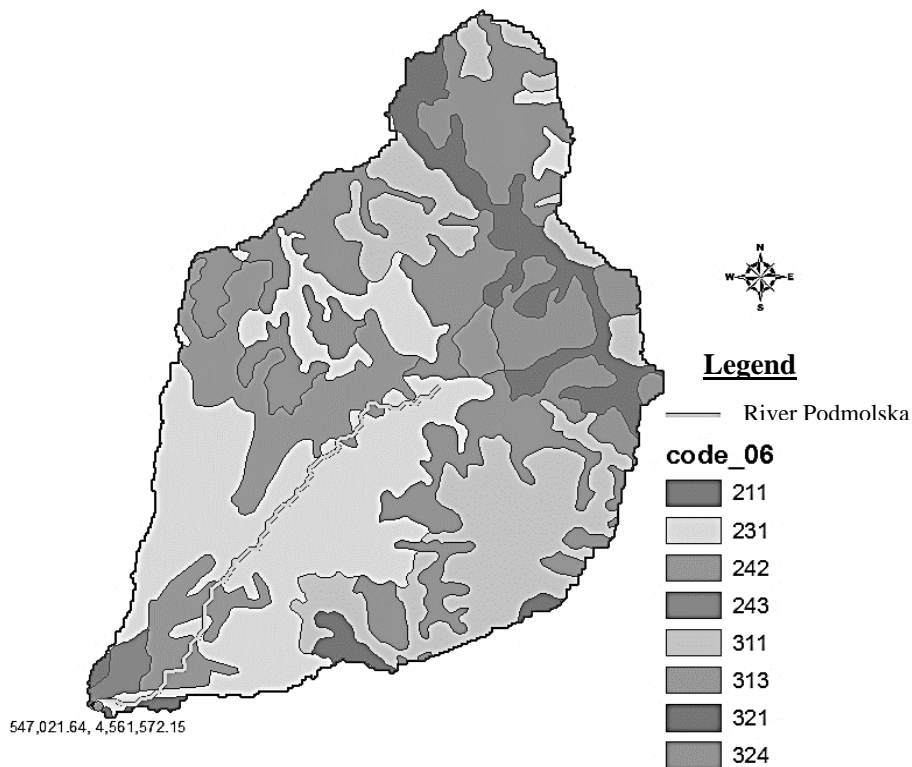


Figure 3. Land use characteristics of the drainage basin of river Podmolska

Table 1. Land use and land cover by CORINE 2006

No.	Code	Land use type	Area in km ²
1	211	Agricultural areas (Non-irrigated arable land)	0.121
2	231	Agricultural areas (Pastures)	8.476
3	242	Agricultural areas (Complex cultivation patterns)	3.275
4	243	Land principally occupied by agriculture, with significant areas of natural vegetation	0.287
5	311	Forest and semi natural areas (Broad-leaved forest)	5.809
6	313	Forest and semi natural areas (Mixed forest)	0.289
7	321	Forest and semi natural areas (Natural grasslands)	2.415
8	324	Forest and semi natural areas (Transitional woodland-shrub)	8.701
			Σ= 29.37km ²

The hydro meteorological characteristics are one of the most important factors that have direct influence on the discharge from one catchment area as a result of the storm waters and their processes. One of the most important climate elements that effect the design and exploitation of the structures (gas pipeline) are the following: air temperature, humidity, precipitation, wind, sun radiation.

As a result of the not existing available monitoring data in the drainage basin, the data from the nearest meteorological station (in the city Prilep) is used in the analysis. The geographical location of the meteorological station in Prilep is defined with the following coordinates: Hs=673 m, φ=41°20', λ=21°34'.

Table 2. Probability of occurrence of the maximum annual rainfall

PROBABILITY OF OCCURRENCE p (%)	DURATION t (min)										
	5	10	20	40	60	90	150	300	720	1440	24 h
	h(mm)	h (mm)	h (mm)	h (mm)	h (mm)	h (mm)	h (mm)	h (mm)	h (mm)	h (mm)	h (mm)
50	5.26	8.31	11.39	13.92	15.20	17.73	19.43	23.94	27.54	31.17	32.35
20	6.88	10.95	15.59	19.32	21.26	27.01	29.82	34.46	38.25	42.97	44.26
10	7.96	12.71	18.37	22.91	25.27	33.16	36.70	41.44	45.33	50.78	52.15
4	9.31	14.92	21.88	27.43	30.34	40.93	45.38	50.24	54.29	60.65	62.12
2	10.32	16.56	24.48	30.79	34.10	46.69	51.83	56.78	60.93	67.97	69.52
1	11.32	18.19	27.06	34.12	37.83	52.41	58.23	63.26	67.52	75.24	76.86

(Shkoklevski, Todorovski, 1993)

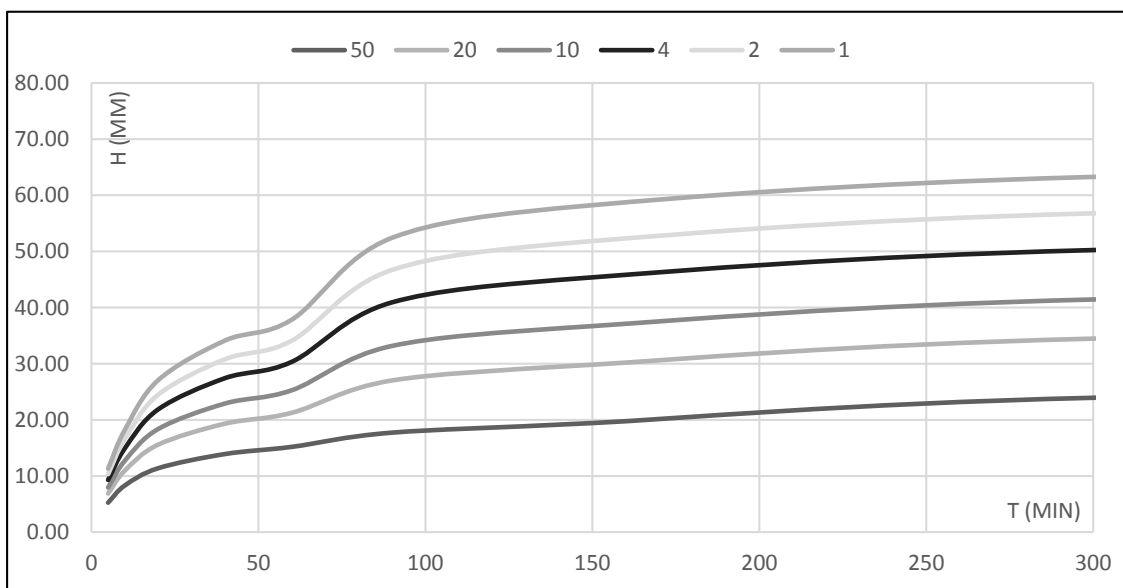


Figure 4. Curves representing the rainfall height, durrance and the occurrence probability

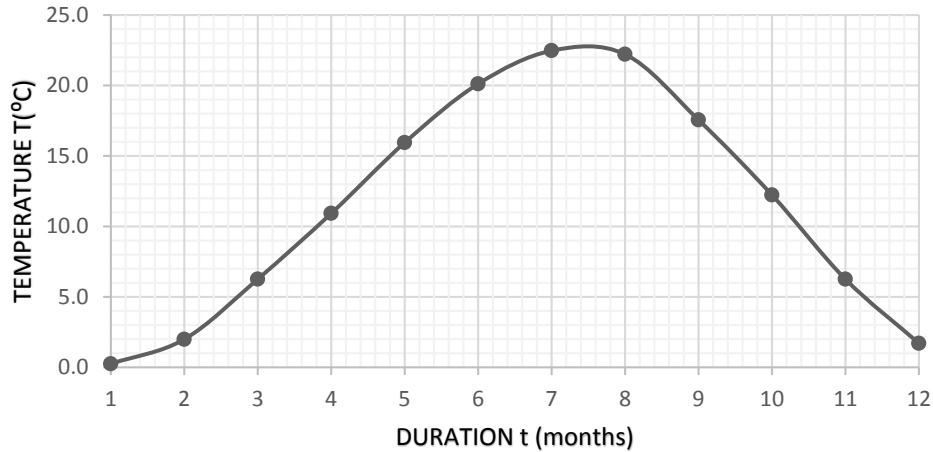


Figure 5. Average monthly air temperature data from the period 1981-2010

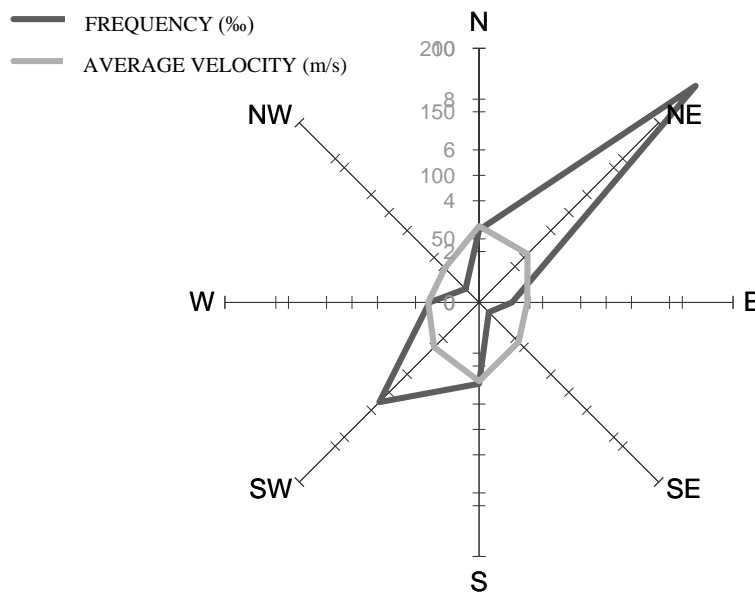


Figure 6. Wind rose with 8 directions (Meteorological monitoring station Prilep-Macedonia)

3.1.2 SCS Method

In practise, most commonly, there is a need of defining the unit hydrograph for drainage basins in the absence of data from systematic measurements of the water stage and the flow. In such cases, methods synthesizing the data from observed and well-studied similar basins can be applied in defining hydrographs of the unmeasured and less studied basins. Extensive literature exists on various ways of calculating the synthetic hydrograph, however, one of the most commonly used is the proposed Soil Conservation System Method from 1969.

In Table 3. are presented the topographical-hydrological parameters, necessary for calculating the synthetic hydrograph.

Table 3.

Coefficient dependent on the drainage basin characteristics			
	$k = \frac{Tr}{Tp} = F(A)$	$k =$	1.12 (-)
Rising time	$Tp = f(A)$	$Tp =$	1.56 (h)
The time of concentration (according to the SCS method) where Lt is the length of the river in km and St is the average slope of the drainage basin in ‰			
	$Tc = (0.868 \cdot \frac{Lt^2}{St})^{0.385}$	$Tc =$	0.47 (h)
The time of concentration			
	$Tc = To = 1,864 \cdot A^{0.39} \cdot Ss^{-0.31}$	$To =$	2.02 (h)
Time of effective rainfall duration			
	$Tk = Tc \cdot (1 + Tc)^{-0.2}$	$Tk =$	1.62 (h)
Time from Q=Qmax to the center of gravity of the rainfall hyetograph			
	$C = Tp \cdot (k - 1)/3$	$C =$	0.062 (h)
The rising time			
	$Tp = \frac{Tk}{2} + To - C$	$Tp =$	2.77 (h)
Recession time			
	$Tr = k \cdot Tp$	$Tr =$	3.10 (h)
Time of direct runoff			
	$Tb = Tp + Tr$	$Tb =$	5.87 (h)

The volume of the direct runoff hydrograph may be computed with the drainage basin parameters ($W = PeA$) or with the geometry of direct runoff hydrograph ($W = Q_{max}T_B/2$), from where the maximum discharge of direct runoff (peak of the hydrograph) may be computed:

$$Q_{max} = \frac{2 \cdot Pe \cdot A}{T_B} \quad (3)$$

where Pe is effective rainfall in (mm), A is the drainage basin area in (km^2), and T_B is time of direct runoff in (hr). Effective rainfall considers all rainfall losses occurring before the beginning of the runoff, including interception, infiltration and depression storage. Based on curve number method the effective rainfall is computed by the following equation:

$$Pe = \frac{(P - 0.2D)^2}{P + 0.8D} \quad (4)$$

where P is total rainfall depth in (mm) and D is maximum possible retention in (mm). This equation indicated $P > 0.2D$ ($Pe = 0$ when $P \leq 0.2D$). The use of this equation for estimating the depth of effective rainfall during storm requires an estimation of the maximum possible retention D . The Natural Research Conservation Service conducted research to approximate D for various soils and cover conditions. The following simple equation was proposed:

$$D = \left(\frac{1000}{CN} - 10 \right) \cdot 25.4 = 64.216mm \quad (5)$$

where CN is a runoff curve number varying between 0 and 100. Rearranging the (4) equation, D is related to the curve number CN as follows:

$$CN = \frac{1000}{10 + 0.0394 \cdot D} = 79.82 \quad (6)$$

Overview of the maximum discharges for the analysed profile, for the calculated time of concentration $Tk = 97.2$ min is presented in table 4.

Table 4. Overview of the maximum discharge

RETURN PERIOD	TOTAL RAINFALL	EFFECTIVE RAINFALL	DISCHARGES
T (YEARS)	P (mm)	Pe (mm)	Q _{MAX} (m ³ /s)
10	33.16	4.883	13.682
25	40.93	8.547	23.947
50	46.69	11.682	32.733
100	52.41	15.085	42.266

3.2 Hydraulic analysis

In the HEC-RAS software, firstly the geometrical characteristics are defined: 5 cross sections from the situation of the gas pipeline (figure 7) i.e. 2 before the crossing with the river, 2 after the crossing and 1 in the exact crossing spot and the distance between them is 20m. Secondly is determined the left and right bank of every profile and finally is defined Manning’s coefficient value that is different in the banks ($n=0.045$) and in the channel ($n=0.035$). For the final calculations, the chosen regime is mixed.

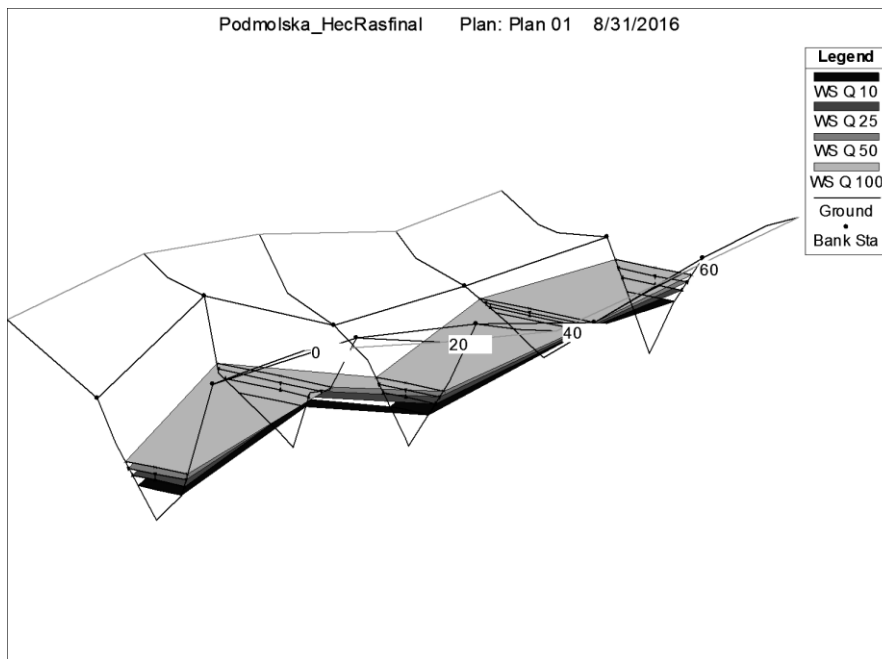


Figure 7. 3D model for different return periods (T=10, 25, 50 and 100 years)

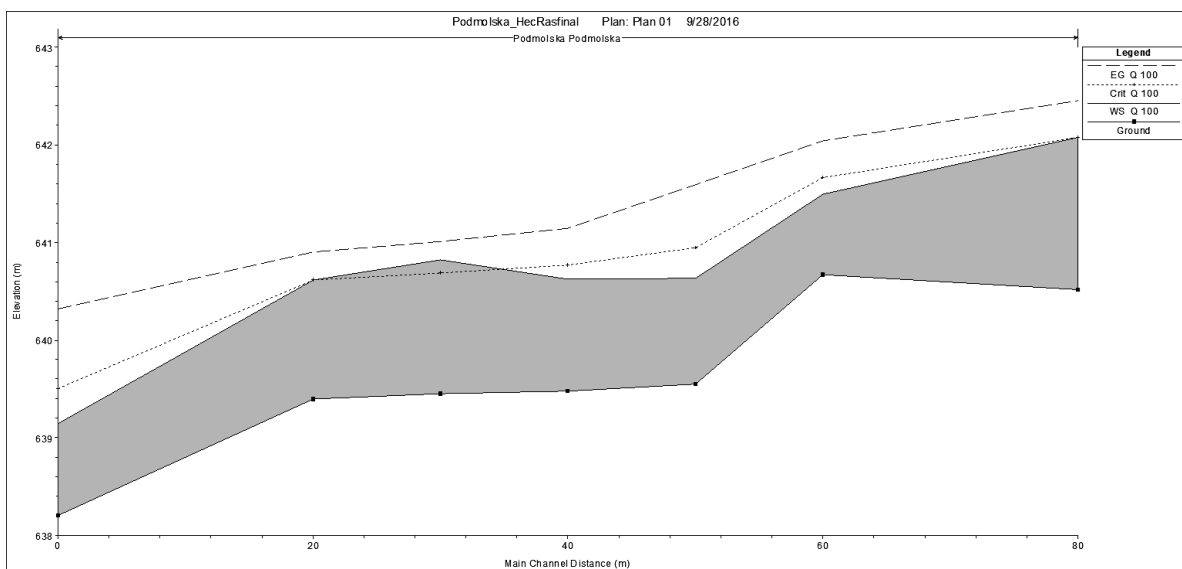


Figure 8. Profile plot with the calculated discharge $Q=42.26\text{m}^3/\text{s}$ for a return period $T=100$ years

Table 6. Hydraulic parameters for the profiles for different return periods (T=10, 25, 50, 100)

River station	Profile	Q Total (m ³ /s)	Min. Ch. El (m asl.)	W.S. Elev (m)	Crit W.S (m)	E.G Elev (m)	E.G Slope (m/m)	Velocity (m/s)	Flow Area (m ²)	Top Width (m)	Froude No.	Shear Ch (N/m ²)
80	Q 10	13.68	640.52	1.02	0.99	1.24	0.012252	2.11	6.48	12.83	0.95	59.96
	Q 25	23.95	640.52	1.24	1.24	1.55	0.012903	2.45	9.79	16.13	1	75.85
	Q 50	32.73	640.52	1.41	1.41	1.75	0.012393	2.59	12.62	18.5	1	81.94
	Q 100	42.27	640.52	1.56	1.56	1.93	0.01198	2.72	15.53	20.65	1	87.34
60	Q 10	13.68	640.67	0.63	0.63	0.8	0.016024	1.8	7.61	23.7	1.01	50.39
	Q 25	23.95	640.67	0.7	0.79	1.03	0.027546	2.54	9.44	26.32	1.35	96.76
	Q 50	32.73	640.67	0.76	0.9	1.21	0.033574	2.96	11.07	28.45	1.51	127.94
	Q 100	42.27	640.67	0.82	1.	1.38	0.037561	3.29	12.85	30.6	1.62	154.43
40	Q 10	13.68	639.22	0.63	0.89	1.54	0.090859	4.21	3.25	10.29	2.39	279.07
	Q 25	23.95	639.22	0.86	1.12	1.68	0.054934	4.01	5.97	13.95	1.96	228.73
	Q 50	32.73	639.22	0.99	1.26	1.84	0.046203	4.07	8.05	16.21	1.84	223.43
	Q 100	42.27	639.22	1.12	1.4	2	0.041649	4.17	10.14	18.19	1.78	226.02
20	Q 10	13.68	639.4	0.77	0.77	0.97	0.015191	1.97	6.95	18.04	1.01	57.04
	Q 25	23.95	639.4	0.97	0.97	1.21	0.013979	2.2	10.91	22.6	1.01	65.77
	Q 50	32.73	639.4	1.11	1.11	1.37	0.013441	2.26	14.48	27.91	1	68.03
	Q 100	42.27	639.4	1.22	1.22	1.51	0.01306	2.38	17.72	30.85	1	73.18
0	Q 10	13.68	638.21	0.55	0.8	1.45	0.107518	4.19	3.26	11.86	2.55	288.87
	Q 25	23.95	638.21	0.71	1.01	1.76	0.082411	4.54	5.28	13.91	2.35	304.66
	Q 50	32.73	638.21	0.82	1.16	1.95	0.070611	4.71	6.95	15.41	2.24	310.06
	Q 100	42.27	638.21	0.93	1.3	2.12	0.061509	4.83	8.75	16.88	2.14	310.55

From Table 6, it is obvious that as a result of the steep slopes in the area of the crossing with the pipeline, the regime is supercritical, and the shear stress in the bottom of the river is high (230–280 N/m²) and that could possibly cause damage, even cutting the pipeline. As a result, measures for protecting the zone around the pipeline are necessary.

4 Results and discussion

For the pipelines to transport the necessary energy across the country, sometimes they need to cross bigger or smaller rivers. The impact on the environment has a big influence on the design of the pipelines, and major companies have taken this in account.

Pipelines that cross perennial, intermittent, and ephemeral stream channels should be constructed to withstand floods of extreme magnitude to prevent rupture and accidental contamination of runoff during high flow events. Pipelines crossing at the surface must be constructed high enough to remain above the highest possible flood flows at each crossing, and pipelines crossing below the surface must be buried deep enough to remain undisturbed by scour and fill processes typically associated with passage of peak flows. A hydraulic analysis should be completed during the pipeline design phase to avoid repeated maintenance of such crossings and eliminate costly repairs and potential environmental degradation associated with pipeline breaks at stream crossings. (Fogg, 2010)

While the construction is taking place, the assembling of the pipeline in the location could cause short term pollution of the water with solid particles, oil or fuel leaks from the vehicles or the equipment. In preparation for new access roads and establishing the construction zones around the pipeline fundamentals, when choosing a technique for the design and execution of the crossings with the pipeline, we should take in account the following guidelines:

- Erosion of sediments due to removal of the soil cover,
- Leakage of fuel and oil from the equipment and the vehicles,
- Changes in the riverbed and banks,
- Disruption of aquatic habitats.

The excavation of the pipeline usually should not exceed depth bigger than 2.0 meters and therefore less chances of occurrence of groundwater, however if they arise and we apply any type of drainage systems, there is a possibility of this effecting the hydrology in the location in terms of prolonged drainage. Drainage in sandy soils with surface pumps can cause rinsing on the top layer of the soil, which can create gaps and pockets in the soil around the site of the excavation.

5 Conclusion

The choice of design, execution and the technique of crossing the water flow through the pipeline depends on the following factors:

- The stability of the location where the pipeline intersects with the river,
- The width and depth of the water at the location of intersection,
- The discharge at the time of installation,
- Topography and accessibility to the location (e.g. the geometry of the banks),
- The material in the bottom of the riverbed and banks.

In this case, for the river Podmolska, the proposed solution is to place the pipeline under the river at a depth of about 1.2 m (from the requirement to prevent freezing of the soil) so that in the downstream direction after the pipeline would be set up a protective threshold of gabions filled with stones with $d=100-200\text{mm}$ ($d_{\text{max}}=300\text{mm}$) so that the wires that hold the stones would act as a kind of reinforcement. After the gabions should be formed a coating of crushed stone with length of about 2-3m, and in upstream direction from the gabions should be placed coating from arranged stone. (Figure 10)



Figure 9. The location where the pipeline will intersect with the river

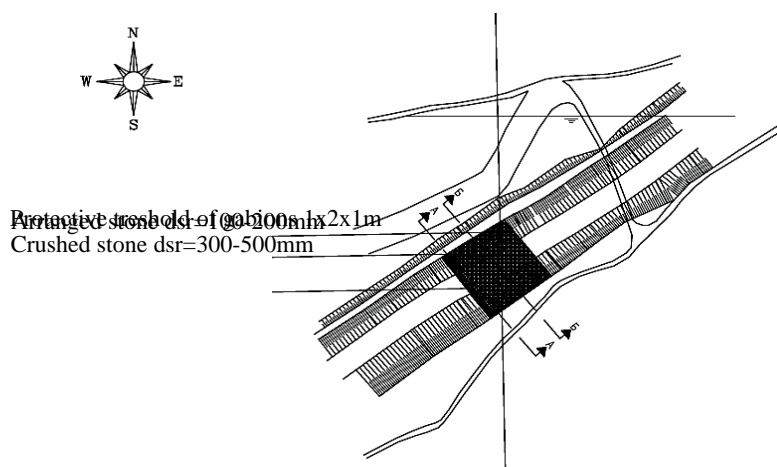


Figure 10. Situation of the river crossing with 2 cross sections

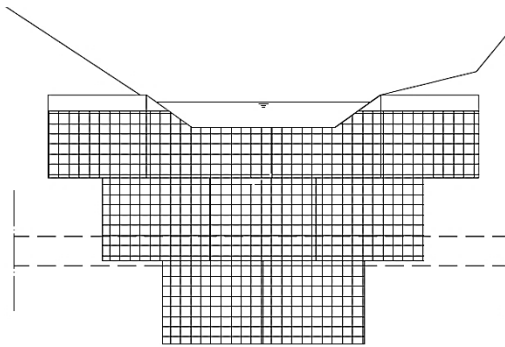


Figure 11. Cross section A-A

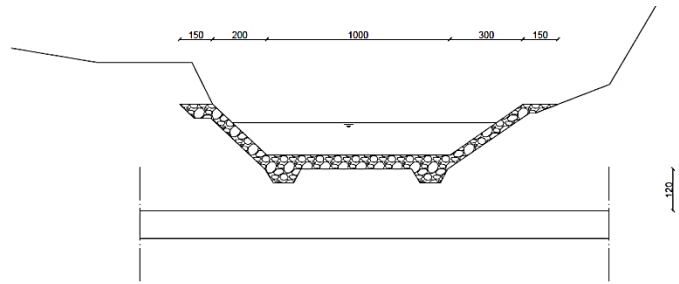


Figure 12. Cross section B-B

References:

- [1] Popovska, P., Stavric, V., Sekovski, D.: Hydrology and hydraulic structures in environmental engineering, Skopje, 2011.
- [2] Shkoklevski, Z., Todorovski, B.: Intenzivni vrnezi na Republika Makedonija, Faculty of Civil Engineering, Skopje, 1993.
- [3] Fogg, J., Hadley, H.: Hydraulic considerations for pipeline crossing stream channels, U.S Bureau of Land Menagment Papers, Paper 14, Nebraska, 2010.

FLOODS: NEW CONCEPTS EMERGE - OLD PROBLEMS REMAIN

OGNJEN BONACCI¹

¹ Faculty of Civil Engineering, Architecture and Geodesy, University of Split, 21000 Split, Matice hrvatske 15, Croatia, obonacci@gradst.hr

1 Abstract

Floods have had a significant impact on mankind and environment throughout the history by causing severe humanitarian, environmental, and financial disasters. Modern societies endeavour to defend against flood hazards by infrastructure protection plans, efficient resource management and insurance plans. Such protection mechanisms can be effective only if they are designed on the basis of scientific methods founded on a close cooperation between different branches and institutions. Protective measures are often counterproductive. They may result in higher damages than those which would otherwise occur. The definite conclusion is that a flood protection system which guarantees complete safety is an illusion. At the same time, flooding brings many benefits particularly for ecological variability and soil fertility. The paper treats flood control measures and some different concepts and approaches, as well as international initiatives organised in order to reduce damages caused by flood, especially to protect human lives.

Keywords: flood, floodplain, levee, ecology, flood control

2 Introduction

Flood is a consequence of migration of a boundary between land and water bodies, reflecting the normal interaction of the atmosphere, hydrosphere and lithosphere [1]. The following two major factors are responsible for flood generation and its specific characteristics: (1) interactive geophysical processes between the atmosphere, hydrosphere and lithosphere; (2) the geographic characteristic of flooded area.

Floods equally affect countries large and small, rich and poor, regardless of their political system, thus presenting formidable barriers to national, regional and even global development. Two thirds of people on the Earth live in flood-prone areas, nearby rivers and in coastal zones. Worldwide, floods have caused greater economic damage and loss of human life than any other type of natural disaster. It seems that nowadays extreme floods occur with higher frequency. The reasons for this conclusion can be objective, as well as subjective. Possibly the most important objective reason is the global change, which includes climatic change or variability, population increase and their massive settling in flood-prone areas, massive land-use changes, as well as inadequate flood protection measures. The subjective reason can be explained by the fact that information and memory about historical floods are forgotten. Memories are short-lasting. The significance of flood as disaster appears only in the context of human perception. At the same time, recent public information system has enabled instantaneous knowledge of any catastrophic event on the planet. Each flood event instantaneously attracts much publicity.

Understanding the geophysical processes which govern flood development is of crucial importance in order to choose successful strategies and undertake efficient protective measures. Predicting current and future flood risk represents a major challenge for climatology, hydrology, hydraulics, geomorphology, ecology and landscape management. The complex nature of flood risk challenges established risk assessment methodologies and their modelling components, such as hydrologic and hydraulic simulation. In practice, flood risk predictions are characterised by great uncertainty. The flood management decision-makers need to evaluate and clearly communicate with different scientific disciplines and social groups, including scientists, politicians and people threatened by flood. Scientists and practitioners should take into account that there are many commonalities in the origin of floods and

landslides, soil erosion, water pollution transport etc. Unfortunately, little joint research is conducted.

3 Different kinds of floods - different protection measures

In literature, there are many different flood systematisations and/or categorisations. This is not a formal issue, because each different category of floods requires different theoretical and practical approach, which would explain them and provide efficient protection against their dangerous consequences. Herchy [2] gives the following six flood categories: (1) riverine overbank flooding; (2) riverine gorge and canyon flooding; (3) landslide or glacier-blocked rivers; (4) estuarine and deltaic flooding; (5) coastal flooding; (6) volcanic flooding. Mandych [1] defined three different kinds of floods: (1) river floods; (2) inundation of seacoast; (3) floods on inland seas and lakes. The river floods are divided into eleven categories: (1) long duration floods of melt water; (2) short duration floods of melt water; (3) ice gorge floods; (4) ice jam floods; (5) long duration floods of rainwater; (6) floods of monsoon rains; (7) flash floods; (8) dam break floods; (9) backwater floods; (10) mudflows; (11) floods caused by icing. Inundation of sea coast can be caused by three different forms: (1) tides; (2) storm surges; (3) tsunamis. Floods on inland seas and lakes can be caused by: (1) tides; (2) wind surges; (3) seasonal flooding; (4) seiches. Earthquakes shifting massive sheets of rock have an effect on hydrological and hydrogeological processes, affecting groundwater and surface water rising in rivers, lakes, and reservoirs [3]. Human-induced earthquakes can cause flood. Witman [3] gives example of the earthquake which struck Pawnee, Oklahoma (USA) in early September 2016, and supposed that it represents a wastewater-induced quake.

Some of the main flood-intensifying conditions depend on basin, drainage network and stream channel characteristics. The more or less stable characteristics are: (1) basin area; (2) basin topography. Variable characteristics are: (1) storage capacity; (2) infiltration; (3) channel length; (4) roughness etc. Variable characteristics can change very fast by man-induced actions, which generally intensify the flood response of the basin on precipitation.

Recently, special attention has been dedicated to urban floods as the most destructive and the most dangerous kind of flood. Rapid urbanisation drastically decreases the capacity of water retention. It increases the flood peak and volume, as well as velocity of overland flow. Flash floods in urban areas have been very frequent and extremely dangerous in the last decade [4]. The main cause of urban flash flooding is severe thunderstorm attended by intensive rainfall. Urban floods can be intensified because of: (1) urbanisation, i. e. inadequate land use; (2) canalisation of natural open stream flows; (3) failures of city protection dikes; (4) inflow from main recipient during high stages into urban drainage system; (5) discharge due to blockage of drains and street inlets; (6) soil erosion and/or transport of material that clogs drainage system etc.

For urban floods in urban areas, special attention should be given to a concept called ***Flooding from Other Sources-FFOS***. The objective of ***FFOS*** is to take into account the possibility and significance of many different flood causes, especially in urban areas, but not only in them. There are the following eight flood sources [5]: (1) pluvial flooding caused by high-intensity or prolonged heavy rainfall leading to overland flow and ponding; (2) flooding due to blockage of sewerage and other part of drainage system, or flooding caused by high water levels in recipient (open watercourses, lakes, marshes, underground space etc.); (3) flooding from small, very often neglected and dry water courses; (4) groundwater flooding as a consequence of prolonged infiltration and/or fast water level rising in karst areas; (5) groundwater flooding from flow through alluvial aquifers connected with water in the adjacent river; (6) failures of infrastructures such as levees and reservoir dams etc.; (7) flooding from tsunami.

Statistical analysis of floods is a very popular approach to flood research. In a fast changing river basin landscape, mainly because of massive human intervention and constructions, the methods of statistical and mathematical analysis of flood have become questionable. The global changes or variability, as well as other local, regional and global natural changes, add more dubiousness. The ***probable maximum flood (PMF)*** is the largest flood that could conceivably occur at a particular location, usually estimated from probable maximum precipitation, and where applicable, snow melt, coupled with the worst flood producing catchment conditions [6]. This concept was developed with the aim to solve many problems

concerning flood occurrence. It seems that success in practical application of this method is weak.

Flood flow frequency analysis based on observations is uncertain because of: (1) limited data set; (2) difficulties of measurements during the high water, which result in low accuracy of measured data; (3) strong, uncontrolled and unknown natural and human-induced changes in hydrological regime; (4) presence of outliers etc. One of the fundamental assumptions in traditional flood analysis is the stability of climate and geophysical factors influencing flood development, which guarantee stationarity of hydrological and climatological data series. This assumption is being increasingly questioned due to man-induced activities and climate variability [7]. It is crucial to develop suitable parameter estimation techniques to cope with the non-stationarity of hydrometeorological and geophysical input processes of flood management.

One of the main problems in the flood management is that most of the existing flood protection systems have been designed on the assumption that the past is the key to the future. Present engineering measures are often counterproductive and result in higher damages than those which would otherwise occur. This approach needs to be re-examined and replaced with a new and efficient one [8]. Man-made structural interventions in catchments and river channels generally change them in a wrong way and cause flood intensification [9]. Long systems of levees can cause many negative ecological consequences and decrease groundwater recharge by changing natural relationship between surface water and groundwater.

Today, we comprehend that a long system of levees alone cannot represent a definitely safe solution of flood protection. Reinforcements and rising of levees made flood hazard less frequent in protected area and increased it downstream. Figure 1 represents the best example of the previous statement. It illustrates the evolution of the Mississippi River levees from the very beginning until today [10]. Extreme enlargement and rising of levees did not prevent floods. It is evident that floods in the Mississippi river basin area have been rather frequent and more destructive in the last decade. As the levees got higher and higher, so did the floods.

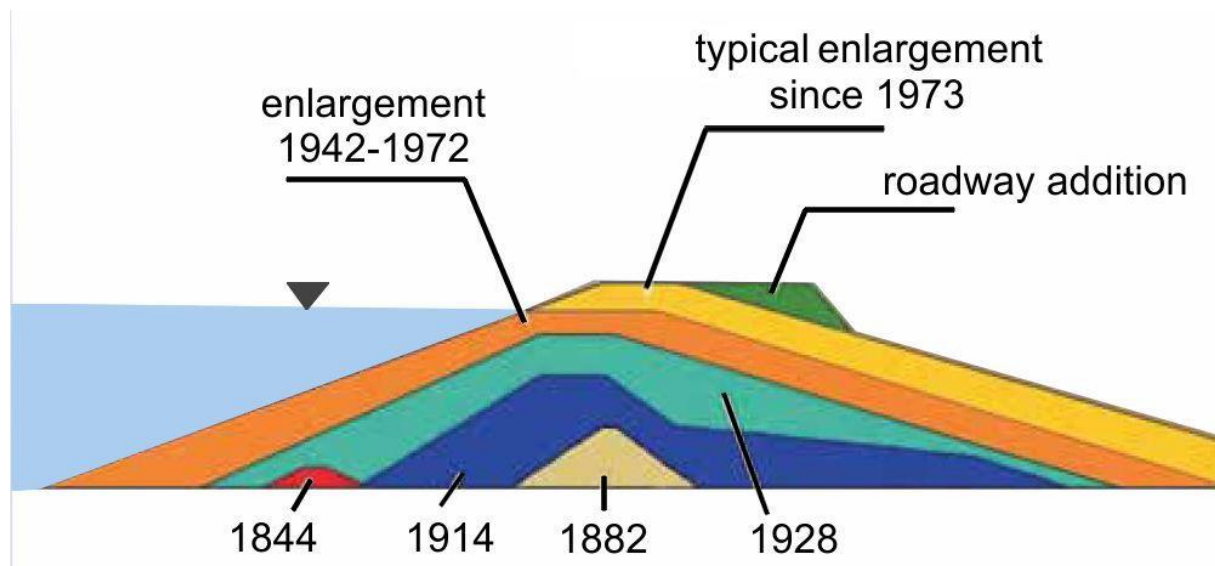


Figure 1 Illustration of evolution of the Mississippi River levees from the beginning until today [10]

Non-structural measures are an attractive alternative and effective addition to structural measures. Their most important advantage is in fact that they help reduce the loss of lives and property. Non-structural measures include: (1) real-time forecasting; (2) early warning system; (3) insurance; (4) land use

planning.

4 Floodplain

Open stream flows with naturally associated floodplains are systems for the transmission of water and sediment. They have been developed and adopted naturally over a long period. During the last 5000 years, floodplains have been the preferred place for socio-economic development. It is well-known that floodplains and wetlands play a crucial role in decreasing the flood peak and volume, thus alleviating the worst flood-induced damages. In order to protect their properties and life, people tried to reduce negative flood consequences by undertaking different measures. Man-made structures, especially levees and dams, drastically, instantaneously and mostly dangerously change natural flow and ecological regime.

Floodplain is the area that is irregularly, but more or less frequently, covered with water during high waters in its adjacent open stream. The extent of a floodplain depends on individual geomorphologic and vegetation characteristics. The interaction between the river and its floodplain has a crucial ecological role. In floodplain there are many highly diverse habitats, which quickly change in time and space [11].

In most part of the world, floodplains and low-laying coast have attracted economic development. In arid and mountain landscape they represent the only space easy for communication and agricultural production. It is estimated that half of more than 7 billion people living on the Earth are located in the floodplains and low-laying coasts. The floodplains are of major socio-economic and ecological importance [12]. Floodplains protect downstream parts of rivers from flooding.

Floods bring many benefits, particularly for ecological variability and soil fertility. It promotes exchange of materials and organisms between habitats, and plays a key role in determining the level of biological productivity and diversity. The beneficial aspects of flooding are less obvious to many people, and particularly to those whose dwellings are at risk of flood inundation [13].

Floodplain restoration is one of the crucial goals of the *Integrated Flood Management (IFM)* approach. For achieving success in this complex procedure, the most important prerequisites imply floodplain ecology. A concept of floodplains restoration could be a successful solution, but in many cases it is unfeasible in practice, because it very often presents insuperable legal and social difficulties.

Dutch river water management policy and scientists established a new programme called *Making space for the river* as the response to extreme floods in 1993 and 1995 [14]. The idea is to restore the flood storage capacity and to enhance the river's natural values. The programme comprises 39 measures for enlargement of the discharge capacity of the main Dutch rivers. Many independent scientists believe that this programme is controversial and extremely expensive (two billion Euros). More space for the rivers means less space for housing, business areas, intensive and safe agriculture etc.

Removal of dams can be treated as one kind of floodplain restoration. In USA this is a new and relatively broadly recommended procedure, while in Europe experts are not sure about the positive effects of this approach. There is great scientific uncertainty over potential environmental benefits arising from it. A scientific framework is lacking in considering how tremendous variation in dam and river attributes determines the ecological impacts of dams and the restoration potential following dam removal [15].

5 New methods, concepts, approaches, initiatives, institutions

The modern concept of flood risk assessment and management combined with uncertainty analysis includes new ideas and approaches to hydraulic and hydrologic modelling, model calibration and validation, as well as measures for flood mitigation and cost-effectiveness of these measures. The observation data for the extreme flood events are scarce, which represents a substantial obstacle in flood

risk management. During the last decades, a lot of new and more or less different methods, concepts, initiatives, approaches, organisations have appeared at national and international levels. It seems that these valuable initiatives did not achieve the necessary goals. This can be supported by Balmforth's [16] opinion: "It can be argued that the developed world is more resilient to flooding."

International Flood Initiative (IFI) is UNESCO-International Hydrological Programme (IHP) and World Meteorological Organisation (WMO) joint action dedicated to the UN International Decade for action called **Water for life** (2005-2015). **IFI** is organised in order to improve co-operation between UNESCO, WMO and many other organisations dealing with flood management. It integrates land and water resources development, includes the institutional components of flood management, and recognises the critical importance of stakeholder participation and cultural diversity.

As nowadays problems in flood water management cannot be solved by technical and legal measures alone, UNESCO and WMO had started initiative called **IFM**. It belongs to the framework of **Integrated Water Resources Management** [17]. Figure 2 schematically shows IWRM concept. **IFM** addresses issues of human security and sustainable development from the perspective of flood management [17].

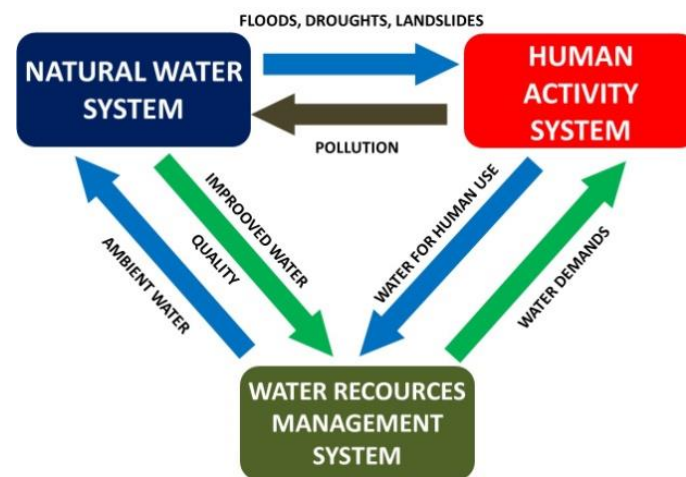


Figure 2. Schematic representation of Integrated Water Resources Management concept

In October 2005, the Japanese government established the **International Centre for Water Hazard and Risk Management (ICCHARM)** under the auspices of UNESCO. Its mission is to serve as the **Global Centre of Excellence for Water Hazard and Risk Management** by, inter alia, observing and analysing natural and social phenomena, developing methodologies and tools, building capacities, creating knowledge networks, and disseminating lessons and information in order to help governments and all stakeholders manage risks of water-related hazards (especially floods and associated hazards) at global, national, and community levels [18].

United Nations General Assembly established the **United Nation University (UNU)** in 1973. On June 2004 **UNU** officially opened a new institute in Bonn dedicated to study of the environment and security (**UNU-EHS**). The main goal is to strengthen the capacity of governments to respond to natural disasters (especially flood), and establish sustainable land management practices.

Risk-based management of the European rivers [19] involves the integrated application of three key-principles: (1) be well informed; (2) manage adaptively; (3) take a participatory approach. Their recommendation is that river and flood should be managed at the basin scale.

Foundation **Milwaukee's urban rivers land trust** focused its efforts on conservation and protection of riparian corridors creating open space along Milwaukee's Rivers for public access, walkways and

recreation which helps revitalise surrounding neighbourhoods and improve water quality.

Room for the River plan designed by a Dutch government intended to address flood protection, master landscaping and the improvement of environmental conditions in the areas surrounding the Netherlands' rivers. The project was active from 2006 to 2015.

Making Space for the River concept presents not only opportunities and synergies, but also risks as it crosses established institutional boundaries and touches on multiple stakeholder interests, which can easily clash [14]. It requires spanning the mind-space which people think about river basin and system. Johnson et al. [20] stress: "Not only ... making space for the water is a must, but also how we can make space for water".

The **RiverCare** research programme of the **Netherlands Centre for River Studies (NCR)**, investigate the mid-term effects of some of the river interventions which were constructed as part of the **Room for the River** project [21]. **RiverCare** is a research programme in which the partners of **NCR** with several other public and private parties collaborate to monitor the consequences of measures. The monitoring data will be used to improve the fundamental understanding of the behaviour of rivers, map the consequences of the measures for hydraulics, morphology and ecology and to improve the current models. The data, knowledge and models will be used to improve the design and maintenance of measures and cut costs of river management. **RiverCare** aims at fundamentally improving the understanding of adaptations in river systems in the next 10 to 50 years.

The goals of **Natural Water Retention Measures** are to safeguard and enhance the water storage potential of landscape, soil, and aquifers, by restoring ecosystems, natural features and characteristics of water courses and using natural processes. They support **Green Infrastructure** by contributing to integrated goals dealing with nature and biodiversity conservation and restoration, landscaping, etc. They are adaptation measures that use nature to regulate the flow and transport of water so as to smooth peaks and moderate extreme events (floods, droughts, desertification, salinization) [22].

The **Delta Programme** is tasked with ensuring that flood risk management and the freshwater supply will be sustainable and robust by 2050, and that Dutch will be designed in a manner that enables it to continue to cope resiliently with the greater extremes of climate [23].

To promote the systematic use of paleoflood evidence, the **Floods Working Group of the Past Global Changes (PAGES)** project organised the first interdisciplinary workshop on past flood variability [24]. The meeting brought together geologists, geographers, historians, meteorologists, climatologists, statisticians, and hydrologists who investigate past flood events globally. Despite the wealth of flood archive data, it is still challenging to compare different data sets or integrate these data into risk assessments.

The success of practical application of the flood risk assessment measures depends of the knowledge of geophysical processes occurring during flood and uncertainties in measurement data and modelling, as well as organisation of the flood protection system. The flood risk mapping is a relatively new concept based on **GIS** tools, which plays an important role in the definition of flood-prone area. At the same time, it has some major constrains. The rapid growth in the experience of flood risk mapping has yet to be translated into a formal set of practically applicable standards [25].

Definite conclusion about most of new methods, concepts, approaches, initiatives and organisations dealing with flood attenuation and river restoration or revitalisation is that their good intention did not considerably improve flood management. Their costs are very high and the success is questionable. Characteristic example is the Jubilee River [14], [26]. The Jubilee River is an 11.6 km long and approximately 45 metres wide hydraulic channel in southern England. It was constructed in the late 1990s and early 2000s to take the overflow from the River Thames and thus alleviate flooding to areas in and around the towns of Maidenhead, Windsor, and Eton (suburb of London). Although successful in

its stated aims, residents of villages downstream claim it has increased flooding [27].

6 Conclusions

Flood management control should respect precautionary principles and must be deeply integrated in the system of general water management and planning. Precautionary approach copes with uncertainties in the assessment and management of flood risk. Prevention is definitely better than curing the consequences.

One of the main reasons for the unsatisfactory state of flood management issue is the complexity of time and space scale processes involved in this extremely dynamic process. For improving flood hydrology, it is of the utmost importance to better understand and more efficiently introduce the temporal and spatial variations of effective precipitation. This is especially important for a more accurate real-time forecasting of flash floods. Shortly before the flood and during the flood, a critical difficulty lies in the efficient integration of different governmental and local initiatives and agencies.

In order to successfully adapt to future devastating floods, the scientists and the world leaders need to make decisions that reduce damages and especially losses of human life. The great obstacle is that the decision-makers do not have the information they need to undertake efficient measures. Open access to all available data and information is particularly essential.

Recently, different types of flash floods have caused substantial damage. Because of a short time (from few minutes to few hours) between falling of intensive precipitation and the formation of extreme peak of flood hydrographs, it is not possible to organise any efficient protective measures. In these cases, the key factors for flood damages alleviation, especially in urban areas, lies in the previous organisation of urban landscape. Urban storm water management includes natural retention measures, training of people, organisation of flood protection measures before, during and after flood occurrence.

One of the crucial questions in flood analysis, which is not objectively solved thus far, is: “What is the crucial flood characteristic: maximum discharge or maximum water level?” For flood modelling, maximum discharge is accepted as a more important factor than maximum water level. In practice, the characteristic of maximum water level is a real and better understood measure for laymen. Measuring flood with a high accuracy by any of the standard methods of stream flow measurements is onerous [2]. In many cases, especially during flash floods in karst areas, it is not possible to measure discharge at all. The same situation is in some other types of floods, as for example: (1) groundwater flooding as a consequence of infiltration and fast water level rising in karst areas; (2) groundwater flooding from flow through alluvial aquifers connected with water in the adjacent river etc.

Absolute protection against floods does not exist. It seems that the concept called *Living with floods* should be accepted. It is necessary to live with the awareness of the possibility of floods [28]. The best solution is to better understand and to adapt to this invincible natural force more adequately. It is of crucial importance to indicate potential flood problems at an early stage, to take measures to prevent people from drowning and reduce damage as much as possible [29]. All flood management measures should take care of the environment and insure sustainable development. *IFM* [13] conclusion dealing with environmental aspects of flood management is that: “There are no universal criteria to determine environmental friendly flood management practices. It is crucial to adopt practices that suit the particular circumstances in a given hydro-climatic, topographical and socio-economic setting and follow a rational and balanced approach in addressing environmental issues in flood management.” Although the study of flood management is in steady progress, a lot remains to be done.

References:

- [1] Mandych, A.F. Classification of Floods (Chapter), Encyclopedia of Life Support. Natural Disasters Vol. II, ed. W.M. Kotlyakov, UNESCO, Eolss Pbl. Co., pp. 63-88, 2010.
- [2] Herchy, R.: The World's Maximum Observed Floods. IAHS Publication No. 271: pp. 355-360, 2002.

- [3] Witman, S.: River's Rise Linked to Oklahoma's Largest Earthquake, *Eos*, 98, pp. 7-8, 2017.
- [4] Hoffius, K.: River Flood Disasters, Deutsches IHP/OHP Nationalkomitee, Koblenz, 1997.
- [5] Hankin, B., Waller, S., Astle, G., Kellagher, R.: Mapping Space for Water: Screening for Urban Flash Flooding. *Journal of Flood Risk Management*, 1(1), pp. 13-22, 2008.
- [6] www.hurstville.floodstudy.com.au, 19.03.2017.
- [7] Strupczewski, W.G., Singh, V.P., Feluch, W.: Non-Stationary Approach to At-Site Flood Frequency Modelling, I. Maximum Likelihood Estimation. *Journal of Hydrology*, 248, pp. 123-142, 2001.
- [8] Kussisto, E., Lemmelä, R., Libsher, H., Nobilis, F.: Climate and Water in Europe, Some Recent Issues. World Meteorological Organization. Technical Report of Rapporteurs - Working Group on Hydrology. Helsinki, 1994.
- [9] Bonacci, O.: River-the Bloodstream of Landscape and Catchment. *Acta Hydrotechnica*, 29(50), pp. 1-12, 2016.
- [10] CIRIA C731: The International Levee Handbook. CIRIA, London, 2013.
- [11] Gordon, N.D., McMahon, T.A., Finlayson, B.L., Gippe, C.J., Nathan, R.J.: *Stream Hydrology - an Introduction for Ecologists*, Second edition, Wiley, Chichester, 2004.
- [12] Marriott, S.B., Alexander, J.: *Floodplains: Interdisciplinary Approaches*. The Geological Society, London, 1999.
- [13] WMO: Environmental Aspects of Integrated Flood Management. Associated Programme on Flood Management, WMO No.1009, 2006.
- [14] Warner, J.F.: A Tale of Two Channels for the Thames (Chapter), *Making Space for the River – Governance Experiences with Multifunctional River Flood Management in US and Europe*, eds. J.F. Warner, A. van Buuren & J. Edelenbos, IWA Publishing, London, pp. 103-120, 2013.
- [15] LeRoy Poff, N., Hart, D.D.: How Dams Vary and Why It Matters For the Emerging Science of Dam Removal. *BioScience*, 52(8), pp. 659-668, 2002.
- [16] Balmforth, D.: Editorial, *Journal of Flood Risk Management* 1, pp. 1-2, 2008.
- [17] UNESCO/WMO: *Water Resources Assessment*. UNESCO, Paris, 1991.
- [18] <http://www.icharm.pwri.go.jp>, 19.03.2017.
- [19] Brils, J., Harris, B.: *Towards Risk-Based Management of European River Basins: Key Findings and Recommendations of the RISKBASE Project*, EC FP6 reference GOCE 036938, Utrecht, The Netherlands, 2009.
- [20] Johnson, C., Penning-Rowsell, E., Tapsell, S.: *Aspiration and Reality: Flood Policy, Economic Damages and the Appraisal Process*. *Area*, 39(2), pp. 214-223, 2007.
- [21] <http://www.ncr-web.org/rivercare/about>, 20.03.2017.
- [22] <http://ec.europa.eu/environment/water/adaptation/ecosystemstorage.htm>, 20.03.2017.
- [23] <https://deltaprogramma2017.deltacommissaris.nl/viewer/publication/1/1-delta-programme>, 19.03.2017.
- [24] Swierczynski, T., Ionita, M., Pino, D.: Using Archives of Past Floods to Estimate Future Flood Hazards, *Eos*, 98, pp. 8-9, 2017.
- [25] Hankin, B., Waller, S., Astle, G., Kellagher, R.: Mapping Space for Water: Screening for Urban Flash Flooding. *Journal of Flood Risk Management*, 1(1), pp. 13-22, 2008.
- [26] Bonacci, O.: Space for the River - Prostor za Rijeku. *Hrvatske Vode*, 23(93), pp. 222-231, 2015.
- [27] https://en.wikipedia.org/wiki/Jubilee_River, 19.03.2017.
- [28] Kundzewicz, Z.W.: Floods in the 1990s: Business as Usual? *WMO Bulletin*, 47(2), pp. 155-160, 1998.
- [29] Sprokkereef, E.: Flood Forecasting for the River Rhine in the Netherlands. *IAHS Publication No. 271*, pp. 347-352, 2002.

ANALYSIS OF THE SEDIMENT FROM SMALL WINTER PORT ON THE DRAVA RIVER

TAMARA DADIĆ¹, LIDIJA TADIĆ², IVANA BARIŠIĆ³

¹ Faculty of Civil Engineering Osijek, Croatia, tamaradadic@gfos.hr

² Faculty of Civil Engineering Osijek, Croatia, ltadic@gfos.hr

³ Faculty of Civil Engineering Osijek, Croatia, ivana@gfos.hr

1 Abstract

Riverbed sediment is affecting form of the river and changing its cross sections on locations where sedimentation is a dominant process. Deposited sediments should be monitored and excessive amounts dredged out. This is especially the case in river ports where water velocities are very low. This paper will provide insight into sediment characteristics, pollution and its potential use in civil engineering. Sediment samples were taken from Osijek Winter port which is a port for small fishing boats on the Drava River in the center of the town.

Keywords: sediment, Winter port Osijek, Drava River, pollution, heavy metals

2 Introduction

Sediment particles of mineral and organic matter accumulate as the result of physical, chemical, and biological processes, both natural and anthropogenic. Human activities can affect river sediments by accelerating the rate of accumulation and introducing contamination [1]. Riverbed sediment is affecting form of the river and changing its cross sections on locations where sedimentation is a dominant process. Deposited sediments should be monitored and excessive amounts dredged out in order to maintain normal river activities, mobility and satisfied minimum depths. This is especially the case in river ports where water velocities are very low.

Generally, dredged sediments are very soft soils with low mechanical strength, extremely high moisture content and usually contaminated. Sediments accumulate contaminants, such as pathogens, nutrients, metals, and organic chemicals and serve as sources of pollution to the ecosystems they are connected with. Intensive contamination occurs wherever there are population, industrial, or agricultural centers [1, 2]. As contaminants do not degrade (or degrade very slowly), they can be a source of environmental issues for long periods of time [1, 3].

Management of contaminated sediments is a complex problem at several levels. At the technical level, controlling input is difficult because of the many sources of contaminants. At the legal level, ports are obligated to monitor, dredge and deposit sediments regardless of its contaminations and pay for it. Proper management of contaminated sediments is becoming more complicated because of increasing environmental concerns [4]. Conventional disposal solutions for dredged sediments, such as depositing into landfills, are gradually becoming restricted in many countries in order to protect environment. The beneficial uses of dredged sediments are becoming increasingly interesting in terms of environmental protection and sustainable development.

For an alternative usage of these sediments in civil engineering or agriculture, detailed research and laboratory analysis are needed. So far, there is no systematical monitoring of sediment quality in any river port in Croatia. This paper will provide insight into sediment characteristics, pollution and its potential use in civil engineering. Sediment samples were taken from Osijek Winter port.

3 Methods

3.1 Location and sediment sampling

Osijek Winter port is a port for small fishing boats on the Drava River in the center of the town (Figure 1). The Drava River is the fourth largest and fourth longest Danube tributary, and it connects the Alps with the Danube and the Black Sea. Total length of the Drava river is 749 km and it is the second longest river in Croatia, with the length of 330 km. Water levels of Drava River near Osijek is significantly affected by the Danube River. The vicinity of the Drava and Danube confluence proved to be of utmost importance due to the backwater impact. Hydrological analyses of the maximum water level records for the period from 1926 to 2014 showed that maximum Drava water levels at Osijek are under a stronger influence of the Danube river. The joint influence of high water levels of both rivers exerts the strongest influence but possibility of its occurrence is very small [5].



Figure 1. Osijek Winter port on the Drava River

Osijek Winter port is used by local fishermen and it can accommodate four large ships, thirteen small ships, seventeen vessels and four water mills. Winter port has total area of more than 55 000 m² with mooring length of 200 m [6].

Sediment samples were taken from this location during winter period in year 2016. Winter port sediment samples extraction was performed using small sampling equipment for extraction of undisturbed samples called sediment core sampler, type Beeker (Eijkelkamp) (Figure 2a). This sampler works on the principles of pressure and vacuum. Two main parts of the equipment are cutting head and piston. At the bottom of the cutting head there is a membrane which is used for opening and closing of the cutting head in order to keep the sample into the tube. This kind of equipment is intended for a maximum sampling depth of 5 metres, but the depth can be increased using extension rods. Samples are shown in Figure 2b.



Figure 2. a) Sediment core sampler, type Beeker b) sediment samples

3.2 Laboratory analyses

All analysis and results shown in this paper were part of the project CLEAR BASIN: Research of River-Port Sediment and its Potential use in Civil Engineering financed by the Danube Region Project Fund.

Sediment samples from 8 locations in Winter port were divided, according to depths, into lower and upper layer, each approximately 30 cm in length. Recovered material samples were processed, prepared and delivered for laboratory testing. Basic engineering physical-mechanical properties, as well as chemical properties, usually determined for standard soil types, were determined in the Laboratory for Soil mechanics (Faculty of Civil Engineering, Belgrade, Serbia). Chemical analyses were conducted in laboratory at Department for Chemistry, University of Osijek. In order to take into account potential environmental hazard of sediment usage in civil engineering, heavy metals concentrations were also determined using external services (Institute of Public Health Osijek, Baranja County and Faculty of Agriculture in Osijek, University of Osijek). All physical-mechanical properties were determined for both layers together, and chemical analysis and heavy metal concentrations were determined for each layer separately [7].

For determination of trace elements Cd, Pb, As, Ni in sediment, EN ISO 15586:2008 [8] standard using atomic absorption spectrometry with electrothermal atomization was used. For Hg level measurement, AAS 019 REV [9] standard was used, while for determination of Fe, Mn, Zn, Cu, Co and Cr destruction by aqua regia was used, as a method providing the fastest, safest and the most precise analytical results with an accuracy of more than 5%. These tests were conducted in laboratories at Institute of Public Health Osijek, Baranja County and Faculty of Agriculture in Osijek, University of Osijek.

4 Results and discussion

4.1 Physical-mechanical properties

According to the obtained results, sediments from Drava River are classified as low plasticity clay. According to AASHTO (American Association of State Highway and Transportation Officials) classification of soils for highway construction purposes [10], Drava River sediments are classified as A7-6 (silt-clay materials which have high plasticity indexes in relation to liquid limit and which are subject to extremely high volume change).

According to Croatian and Serbian regulations [11, 12], based on Atterberg limits (liquid limit (LL) \leq 65% and plasticity index (PI) \leq 30%), tested sediments satisfy the requirements for embankment construction. Proctor test showed that, according to optimal moisture content, additional treatment needs to be conducted (in terms of material treatment – stabilization), in order for the material to be used in embankment or road subgrade construction [7].

4.2 Chemical properties

In order to gain full insight into characteristics and potential environmental hazard of river port sediment, samples for chemical analyses and determination of heavy metal concentration were taken and grouped according to depths on upper (surface) and lower layer.

Obtained pH and texture results as well as macro-element concentration are shown in Table 1.

Table 1. pH and Macro-element total concentration (mg/kg) results

	TEXTURE	pH	Na	K	Ca	Mg
Upper layer	loam	7.15	5.556	67.330	459.305	191.735
Lower layer	silty loam	7.15	6.003	73.609	488.757	211.707

The pH value of soil is an important environmental factor and each type of soil has a certain level of acidity and pH, depending upon its composition, native vegetation and rainfall amounts. According to the results presented in Table 1, tested sediments can be classified as neutral (pH = 6.6 - 7.3). This is favourable result regarding potential release of metals since in soils with low pH, many metals are more mobile and available for uptake compared with neutral or alkaline soils which can affect toxicity and bioavailability of the metal contaminants to terrestrial organisms.

4.3 Heavy metal concentrations

For the presence of heavy metals in the environment, natural and anthropogenic activities are responsible. However, the occurrence of elevated levels of trace metals in the sediment can be a good indication of man-induced pollution and high levels of heavy metals can often be attributed to the anthropogenic influences, rather than natural enrichment of the sediment by geological origin. That is why the investigation of heavy metals in sediments, as the essential and dynamic part of the river basin, could be used to assess the anthropogenic and industrial impacts on the riverine ecosystems.

The results of heavy metal concentrations analysis are presented in Picture 3.

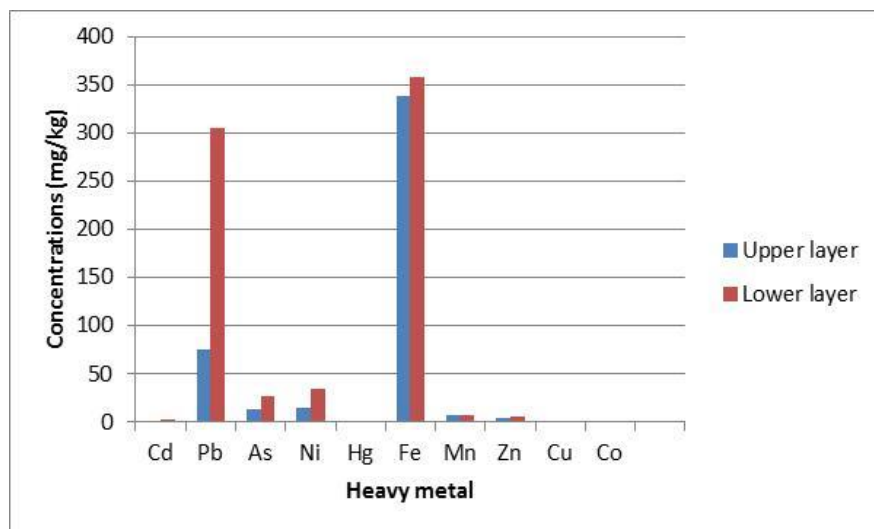


Figure 3. Heavy metal concentrations analysis

Highest concentrations were observed in the lower sediment layer. Generally, Fe and Pb are present in highest concentrations for both tested sediment layers, while the lowest values are obtained for Co and Cu. At the national level, in Croatia, the only guideline for heavy metal concentrations is the one for agricultural soils [13].

There are several approaches listed in [2] for sediment quality classification. These approaches generally set two threshold levels, one below which effects rarely occur [e.g., the lowest effect level, (LEL), threshold effect level (TEL), effects range low (ERL), minimal effect threshold (MET), and threshold effect concentration (TEC)] and one above which effects are likely to occur [e.g., the severe effect level (SEL), probable effects level (PEL), effect range median (ERM), toxic effect threshold (TET), and probable effect concentration (PEC)]. In Table 2 are listed first and second threshold levels (TEL and PEL) for several heavy metal concentrations.

Table 2. Lowest and probable effect sediment quality guidelines for metals (mg/kg) [2]

	Cd	Pb	Ni	Hg	Zn	Cu	Cr
TEL	0.6	35	18	0.17	123	35.7	37.3
PEL	3.53	91.3	36	0.486	315	197	90

According to criteria listed in Table 6, upper layer is or below TEL (Ni, Zn, Cu and Cr) or between threshold effect level and probable effects level (Cd, Pb, Hg). Heavy metal concentrations from lower layer are much higher and for some elements even exceed PEL (Pb and Hg).

There are also Serbian regulations for sediment quality [14], which are based on whether this sediment will be extracted or not (Table 3). These regulations are the least restrictive and for some elements, allowable concentrations are higher for not extracted and for other for extracted sediment.

Table 3. Limit values for assessing the status and sediment quality [14]

	Cd	Pb	Ni	Hg	Zn	Cu	Cr
Not extracted	6,4	310	44	1,6	430	110	240
Extracted	2	530	35	0,5	480	36	380

4.4 Sedimentation process in Winter port

In order to analyse sedimentation process in Winter port, cross sections from 1968 and from 2017 are compared (Figure 4). Although it was expected that sedimentation would be dominant, most of the cross section from 2016 is lower than the cross section from 1968. This means that Winter port in Osijek is well maintained and excessive amounts of sediment are dredged out.

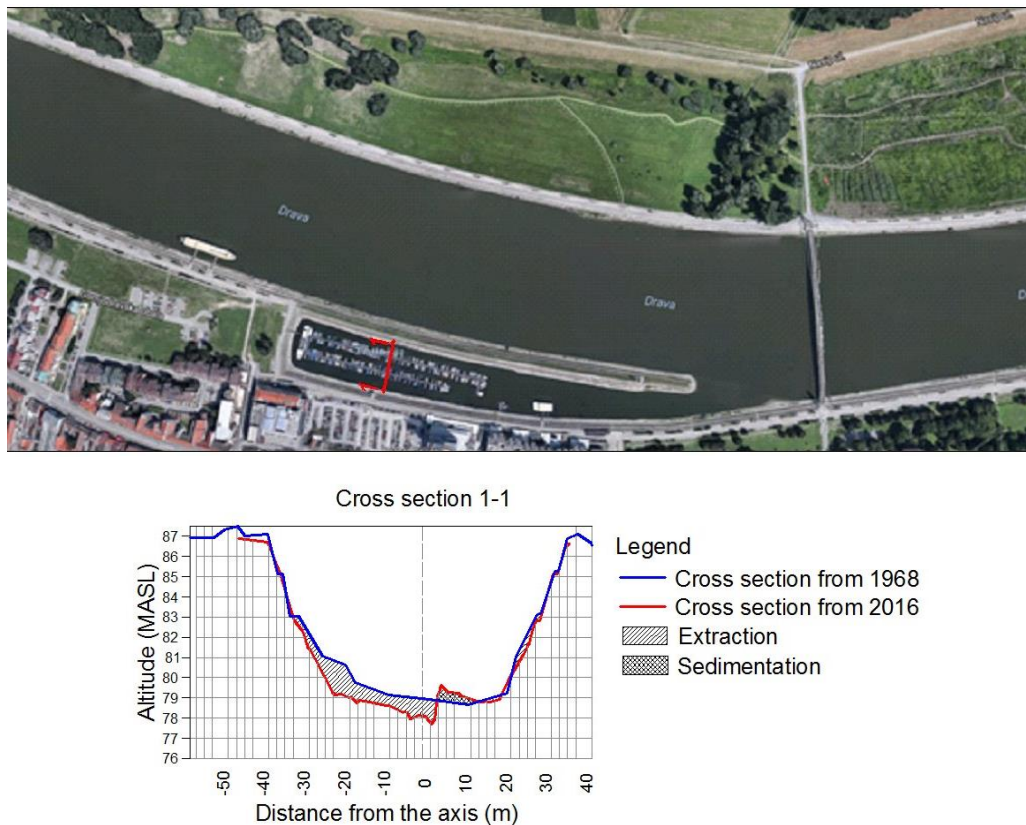


Figure 4. Cross section from Osijek Winter port on the Drava River

5 Conclusion

Sediment particles of mineral and organic matter accumulate in rivers as the result of physical, chemical, and biological processes, both natural and anthropogenic. Human activities can affect sediments by accelerating the rate of accumulation and introducing contamination. Accumulation is especially dominant where water velocities are very low. This is the case in river ports where, beside accumulation, contamination is emphasized also. In order to keep normal port functions, sediment should be regularly extracted. Problem is its deposition in many countries so new ways of its usage, such as material in civil engineering, are investigating.

There is no monitoring of river ports sediments in Croatia so, in order to investigate quality and properties of riverbed sediments, from Osijek Winter port on Drava river sediment samples were extracted and divided into two layers. Basic physical-mechanical properties, as well as chemical properties and heavy metal concentrations are determined. According to the obtained results, sediments from Drava River are classified as low plasticity clay. Regarding Croatian and Serbian regulations tested

sediments satisfy the requirements for embankment construction but Proctor test showed that additional treatment needs to be conducted in terms of stabilization. Obtained heavy metal concentrations showed that lower sediment layer is more contaminated than upper one, especially regarding lead.

In order to observe sedimentation process, cross sections of Winter port from 1968 and from 2017 were compared. According to bottom elevations, in this port excessive sedimentation isn't a problem and normal port activities are not compromised with same dredging practice and intensity.

Further analysis of sediment, and from several different locations, are needed in order to investigate magnitude of its contamination and properties for its possible use in civil engineering.

Acknowledgements

Activities and results shown in this paper are part of the project Research of River-Port Sediment and its Potential use in Civil Engineering funded by EU Strategy for Danube Region (lead partner: Faculty of Civil Engineering Osijek, partners: Faculty of Civil Engineering Belgrade, Department of Chemistry Osijek and Port authority Osijek).

References:

- [1] Fondriest Environmental, Inc., Sediment Transport and Deposition-Fundamentals of Environmental Measurements, 2014, http://www.fondriest.com/environmental-measurements/parameters/hydrology/sediment-transport-deposition_16.5.2017.
- [2] Burton, G.A.: Sediment quality criteria in use around the world, *Limnology*, 3, pp. 65–77, 2002.
- [3] EPA, NOAA, USACE, & USFWS: Contaminated Sediment Remediation Guidance for Hazardous Waste Sites, 2005, United States Environmental Protection Agency: Office of Solid Waste and Emergency Response, EPA-540-R-05-012.
- [4] Committee on Contaminated Marine Sediments, Marine Board, Commission on Engineering and Technical Systems, National Research Council: Contaminated Sediments in Ports and Waterways, Cleanup Strategies and Technologies, NATIONAL ACADEMY PRESS, Washington, D.C., 1997 - <https://www.nap.edu/read/5292/chapter/3#18>
- [5] Dadić, T., Tadić, L., and Bonacci O.: The Drava and Danube impacts on the floods in Osijek throughout history, *Hrvatske vode*, 23(94), pp. 287-294, 2016.
- [6] Survey report on sample extraction - Location selection and field research –, 01_PA1a-C2, Research of River-Port Sediment and its Potential use in Civil Engineering, 2016
- [7] Survey report on initial laboratory tests – Basic engineering and chemical properties analyses –, 01_PA1a-C2, Research of River-Port Sediment and its Potential use in Civil Engineering, 2016.
- [8] EN ISO 15586:2008: Determination of trace elements using atomic absorption spectrometry with graphite furnace
- [9] AAS 019 REV-standard for HG level measurement
- [10] United States Department of Agriculture, SCS: AASHTO-(American Association of State Highway and Transport Officials), Study guide, 1987.
- [11] IGH :GTR -General technical requirements for road works, Zagreb, Croatia, 2001.
- [12] Earthworks on road construction, Official Gazette 48/84, Belgrade, Serbia
- [13] Ministry of Agriculture, Croatian Government: Pravilnik o zaštiti poljoprivrednog zemljišta od onečišćenja, Zagreb, Croatia: Official Gazette 9/14, 2014.
- [14] Uredba o graničnim vrednostima zagađujućih materija u površinskim i podzemnim vodama i sedimentu i rokovima za njihovo dostizanje, "Sl. glasnik RS", br. 50/2012

COMPARISON OF DIFFERENT COMPUTATIONAL METHODS FOR FLOOD MITIGATION

ADAM JANÍK¹, ANDREJ ŠOLTÉSZ²

¹ *Department of Hydraulic Engineering, Faculty of Civil Engineering, Slovak University of Technology in Bratislava, Radlinského 11, 810 05 Bratislava, Slovak Republic, adam.janik@stuba.sk*

² *Department of Hydraulic Engineering, Faculty of Civil Engineering, Slovak University of Technology in Bratislava, Radlinského 11, 810 05 Bratislava, Slovak Republic, andrej.soltesz@stuba.sk*

1 Abstract

There are several methods of flood mitigation calculation used in our country as well as modern programming tools offering another possibility of modelling the flood process. This paper aims to compare results from different methods of flood mitigation calculation using the same prospective reservoir. The methods presented and compared in the article are: classical graphic-computational method, numerical modelling method as well as the third one using standard hydraulic equations. Results of these three methods are summarized, compared and described in the contribution.

Keywords: flood mitigation, detention reservoir, hydraulic modelling, flood wave, hydrograph

2 Introduction

Flood mitigation or transformation of a flood wave is an effect on the flood wave caused by a reservoir or a lake. This phenomenon, which is very positive from a flood protection point of view, consists of reducing peak discharge of the flood and also its delay in time. For the flood situations there is a special volume secured in reservoir that is called retention volume. It is a reserve in water level elevation that is always ready to be filled during a flood. In a special type of reservoir – the detention reservoir – major part of its volume is intended to retain flood water. The whole process of flood mitigation has to be calculated in the phase of study and also project of a reservoir. In fact, the retention volume is mostly proposed according to this calculation. Other situation might be examining effect of already existing structure where the dimensions of all functional structures are intended. This case may occur also when hydrological institutes re-evaluate the design flood waves according to recent data [1].

During the proposal of a retention volume of either reservoir or detention reservoir, the aim is to reduce the peak discharge under the value of harmless outflow according to chosen N-year design flood wave. The value of a harmless outflow is usually determined by the capacity of water course downstream, that is mostly limited by cross-stream structures like bridges or larger covers and in many cases also culverts. The fact is that the value of harmless outflow determines the solution significantly.

There are two types of retention volume; controlled and uncontrolled. The shape of the outflow hydrograph depends on type of a retention volume. If a controlled retention volume is used, the outflow from the reservoir can be managed by an operator. In case of an uncontrolled retention volume, the value of an outflow only depends on the filling of a retention volume, respectively on elevation of water level that determines the pressure head on bottom outlets or overflow head on spillway.

Most of the detention reservoirs are built with uncontrolled retention volume to ensure their automatic function during a flood. If a controlled retention volume is used it must be proven by a calculation that in the event of incorrect operation or failure of the structure (outlet remains closed) the safety of the entire structure will not be endangered.

The solution of flood mitigation is done graphically or more frequently numerically from the initial water elevation in reservoir or in case of dry detention reservoir from the elevation of the bottom. The calculation gradually simulates the transition of a flood wave in the reservoir for given elevation of the spillway and configuration of bottom outlets. Finding the needed value of retention volume leads to optimization task, where according to the configuration of functional structures and given harmless outflow the retention volume has to be minimized.

There are several methods of flood mitigation calculation used in our country. All of them are based on the basic balance equation of a reservoir:

$$Q_{in} dt - Q_{out} dt = dV \quad (1)$$

In this article, several methods of flood mitigation computation are performed and compared on the same detention reservoir and using the same design flood wave.

3 Methods

The first and very important characteristic needed to perform the simulations is intercepted volumes line for the chosen profile of detention reservoir. This requires some basic geodetic data about the locality, gathered either by 3D scanning, digital terrain model or in form of standard cross-sections. Another relevant data that come from configuration of the functional structures is a function of outflow according to water level elevation in reservoir. There are several ways how to obtain this function and they depend on the type of a detention reservoir. Hydraulic equations for culverts, orifices and overflow can be used as well as mathematical modelling in chosen software. In this case, simulation in HEC-RAS software was used. Finally, from the intercepted volumes line (function of intercepted volume in reservoir according to water level elevation) and function of outflow according to water level elevation in reservoir a function of outflow according to the intercepted volume can be constructed, which is important function used in every of the chosen methods for flood mitigation calculation. For purposes of this comparison, the same function of outflow has been used.

3.1 Chosen detention reservoir, design flood wave

The detention reservoir chosen for purpose of comparison of different flood mitigation computational methods comes from a study of flood protection of a village in under-mountain locality in western Slovakia [2]. This proposed reservoir is situated in a valley above the village and its realization (with other proposed reservoirs) would ensure flood protection for the village without any channel regulations in the village itself. The reservoir is proposed to be 7,6 m high with dam crest elevation of 289,8 m a. s. l. and emergency spillway elevation 289,0 m a. s. l. The reservoir has one square bottom outlet which width and height are 0,7 m and the elevation of its centre is on 282,85 m a. s. l. As the bottom outlet is not situated in the elevation of former natural riverbed but slightly above, it has some permanently intercepted volume of about 3000 m³ depending on the actual inflow. The length of the dam in crest is approx. 70 m. The intercepted volumes line of this reservoir is shown in Fig. 1.

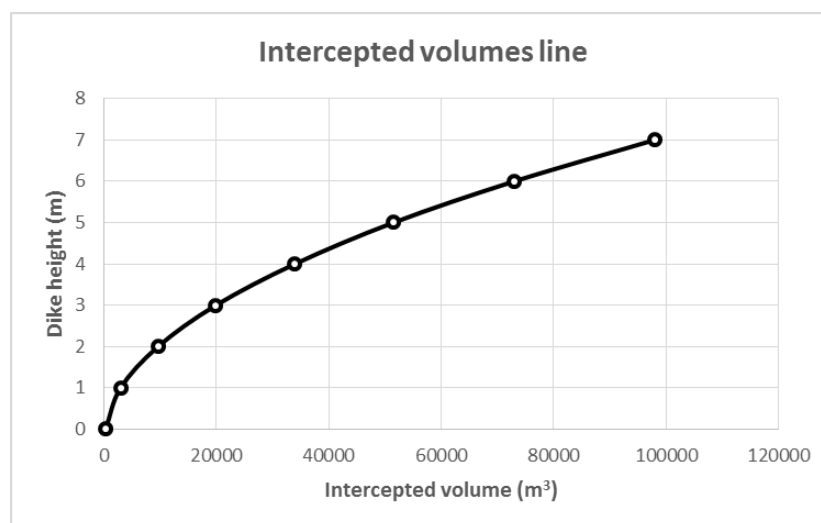


Figure 1. Intercepted volumes line of proposed reservoir.

A flood wave that came from reconstruction of a real flood event in village was used as a design flood wave for this reservoir. The record of the flood wave comes from a stage hydrograph under the

confluence of two streams. This flood wave had to be divided in two separate streams above village Pila using mathematical modelling in HEC-RAS. The proposed reservoir is located on one of these streams. The design flood wave was very rapid - the time of rise of the flood wave was only 3 hours. The peak discharge had a value of $11,4 \text{ m}^3 \cdot \text{s}^{-1}$ (average discharge is $0,3 \text{ m}^3 \cdot \text{s}^{-1}$). The flood wave is shown in Fig. 2.

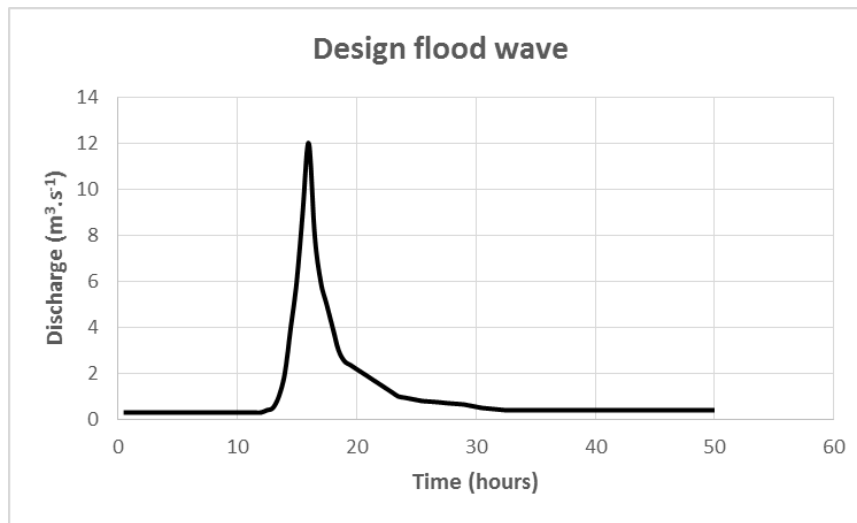


Figure 2. The design flood wave used in simulations.

3.2 The Klemeš method

The Klemeš method is a graphic-computational method that comes out from solving four connected graphs characterized function parameters of reservoir - intercepted volumes line, inflow and outflow hydrograph, a function of water level in time and a functionality of outflow according to retention volume. It was originally formed for uncontrolled retention volumes of multi-purpose reservoirs, which retention volume is situated above the spillway and the flood water overflows through the spillway without any possibilities of control. To adopt this method for purposes of detention reservoirs, the outflow characteristics of the outlets have to be incorporated into the function of outflow from the reservoir according to water level elevation.

The basis of this method is formed by flood hydrograph, which is then divided into the intervals by chosen time step Δt . It is appropriate to choose constant value of time interval especially when using fine divisions. Every interval has its average value of inflow Q_{in} . Then a transformation line in the same scale has to be constructed next to the inflow graph. The transformation line is in this case the function of outflow from the reservoir according to water level elevation $Q_{out} = f(V)$. Next step is to calculate transformation angle for each time interval that comes out from the same scale of discharge as the inflow hydrograph. Assuming that two sides of a rectangled triangle are drawn, its hypotenuse represents transformation angle [3].

The simulation is then constructed from inflow to the transformation line where transformation angle is constructed. Intersection of the transformation line with the line in transformation angle shows the value of outflow for the first interval. By repeating this process, a complete outflow hydrograph can be obtained. By adding the intercepted volumes line (in scale) under the transformation line, the user is also able to obtain function of water level elevation in time in the reservoir (Fig. 3). The results show that the peak discharge has been reduced from the original $11,4 \text{ m}^3 \cdot \text{s}^{-1}$ to a value of $3,66 \text{ m}^3 \cdot \text{s}^{-1}$ and has been delayed by 2 hours.

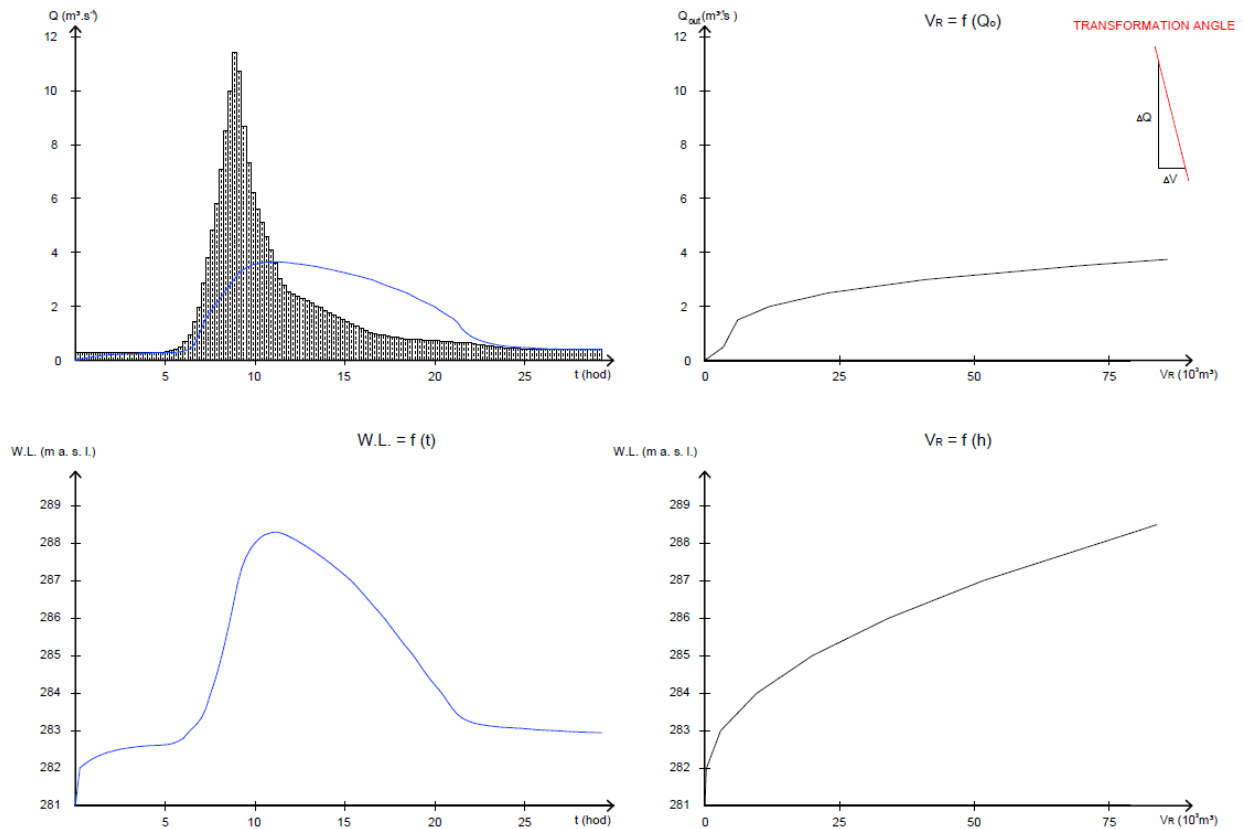


Figure 3. Simulation of flood wave mitigation – Klemeš method.

3.3 HEC-RAS modelling

Another possibility of performing the flood mitigation simulation is offered by mathematical modelling in various software. Because of availability, good experience and due to the range of gathered data, HEC-RAS program has been chosen for this modelling. Another reason was that the system is designed for application in the flood plain management and the flood insurance studies to evaluate floodway encroachments.

In general, to simulate a flood wave using the HEC-RAS program, an unsteady flow analysis has to be performed. There are two ways of modelling detention reservoirs in the HEC-RAS program. The user can choose the creation of storage areas connected with weirs or (as in this case) culverts or weirs, with many cross-section profiles upstream from the construction, to ensure detailed and correct calculations of the water levels behind the structure [4].

The computation in software is done automatically and relatively quickly according to geodetic, hydrological and initial data. The worst part in this case is gathering and processing the input data. User has also to choose profiles, in which the hydrographs will be illustrated and for comparison with a simulation without any measures has to be done.

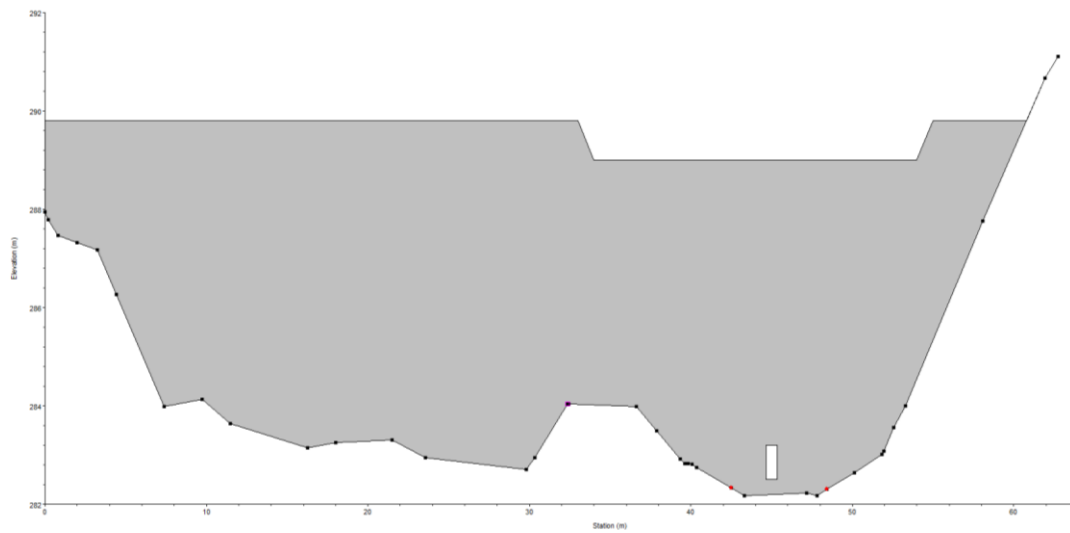


Figure 4. Detention reservoir in form of an inline structure in HEC-RAS software.

The result of the hydraulic modelling of the detention reservoir is shown in Fig. 5. The comparison was done at a specific profile below the detention reservoir. The peak discharge has been reduced from the original $11.4 \text{ m}^3\text{s}^{-1}$ to a value of $3.54 \text{ m}^3\text{s}^{-1}$ and has been delayed by 2 hours.

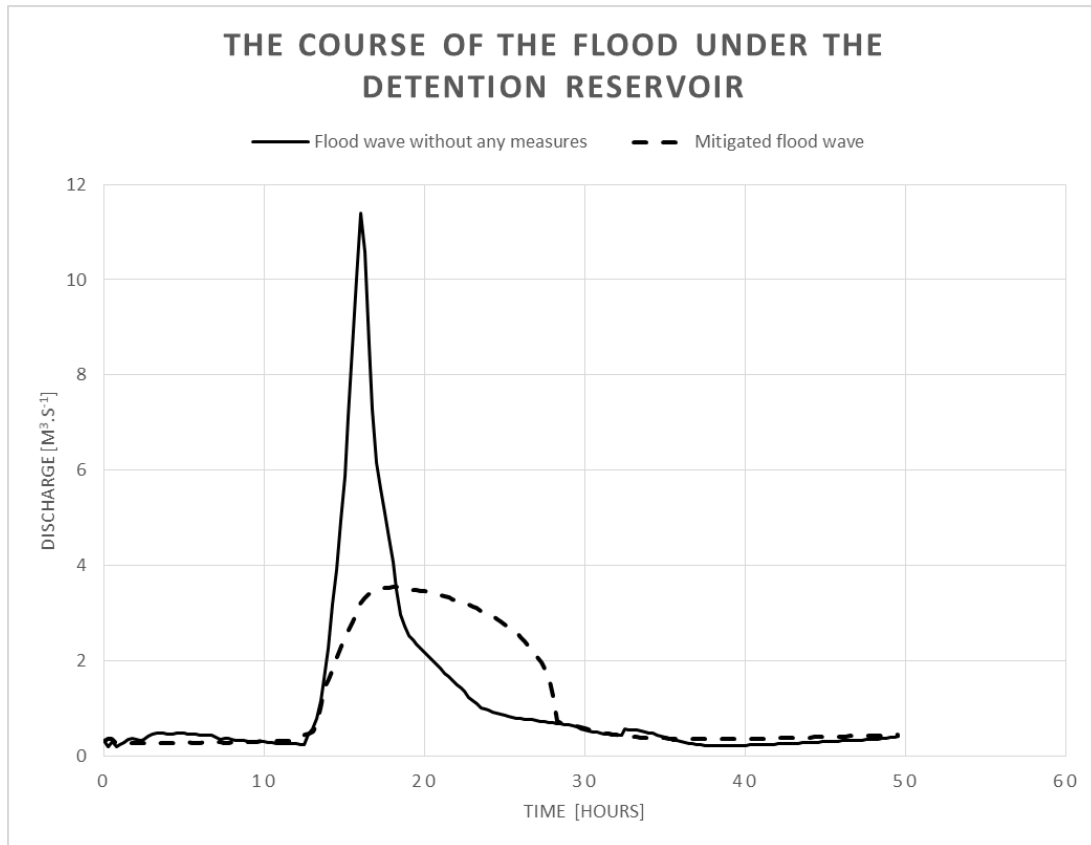


Figure 5. Mitigation of the flood wave in HEC-RAS software.

3.4 Numerical solution

Nowadays the most common solution of flood mitigation comes from numerical solution, which is related to development of computer programs, especially table editors. These programs significantly reduce time needed to provide the whole calculation in comparison with the past manual computations. The solution comes from solving equation (1) in chosen time interval. For each time step a change in volume of water is determined, what leads then to new value of outflow dependent on the elevation of water level. By repeating this process for the time where the flood wave is passing the reservoir we are given complete values of outflow that can be compared then with inflow values and illustrated in hydrograph. The very basic solution is based on calculation of the outflow capacity according to the water level elevation using outlet equations.

In this case, the function of outflow according to the intercepted volume has already been given. The first solution came from solving the basic equation of reservoir (1) simply as:

$$(Q_{in} - Q_{out}) \cdot \Delta t = \Delta V \quad (2)$$

The error of this simplification should be minimized by using a very small time step, i.e. 15 minutes. Whole computation has been done in table for the time of filling and emptying of detention reservoir. The results are displayed in Fig. 6. Using this method the peak discharge has been reduced to a value of $3,41 \text{ m}^3\text{s}^{-1}$ and has been delayed by 2,25 hours, as well.

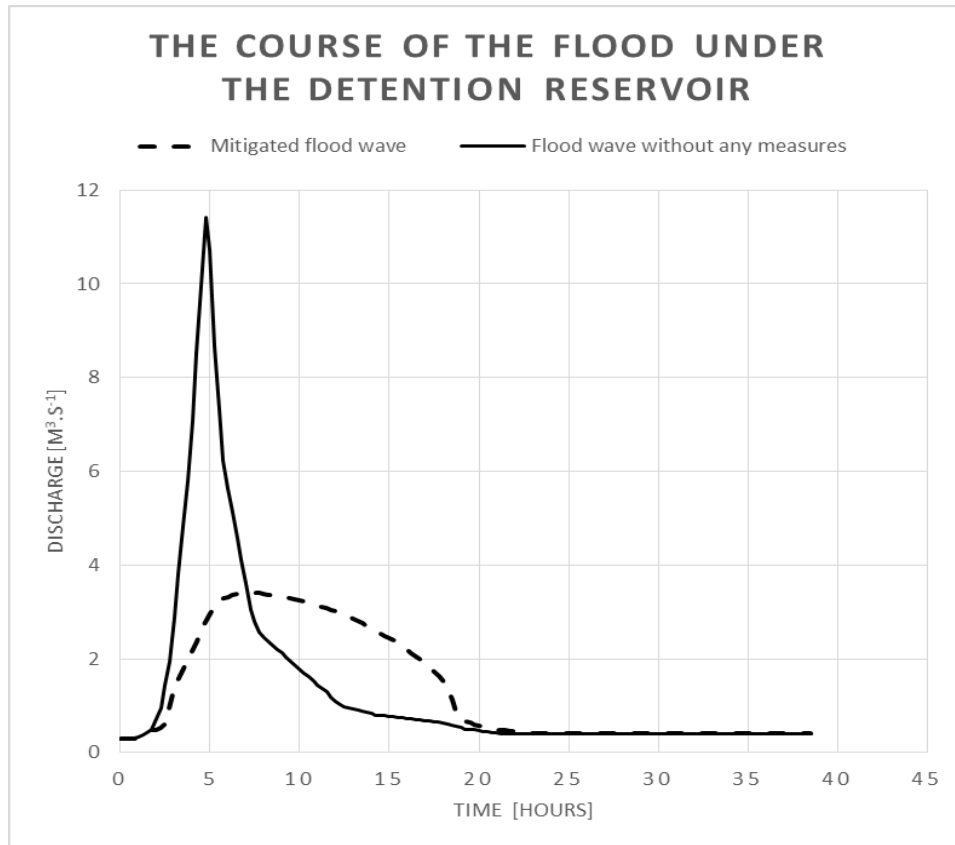


Figure 6. Mitigation of the flood wave by simplification of differential equation.

The equation (1) can be solved after adjustment by 4-stage Runge-Kutta method [5]:

$$V_1 = V_0 + \frac{K_1 + 2K_2 + 2K_3 + K_4}{6} \quad (3)$$

Where

$$V(t) = V_0 \text{ and } V(t + \Delta t) = V_1, \quad (4)$$

$$\begin{aligned} K_1 &= \Delta t \cdot [Q_{in}(t) - Q_{out}(V_0)], \\ K_2 &= \Delta t \cdot \left[Q_{in}\left(t + \frac{\Delta t}{2}\right) - Q_{out}\left(V_0 + \frac{K_1}{2}\right) \right], \\ K_3 &= \Delta t \cdot \left[Q_{in}\left(t + \frac{\Delta t}{2}\right) - Q_{out}\left(V_0 + \frac{K_2}{2}\right) \right], \\ K_4 &= \Delta t \cdot [Q_{in}(t + \Delta t) - Q_{out}(V_0 + K_3)]. \end{aligned} \quad (5)$$

The accuracy of the solution is strongly dependent on the chosen time interval Δt . With small values of Δt the approximate error is small, but it may lead to an unnecessarily more demanding calculation with larger amount of individual calculations and may also lead to rounding errors that occur, for example, when summing up very small numbers with large numbers. From another point of view, the incremental step size can accumulate approximation errors that may appear to be average considering one approximation step, but can lead to significant accumulated errors in a large number of steps. The length of the time step is therefore chosen by applying the relationship [6]:

$$|K_2 - K_3| \approx 0,05 K_2 \quad (6)$$

Using 4-stage Runge-Kutta method the peak discharge has been reduced to a value of $3,40 \text{ m}^3\text{s}^{-1}$ and has been delayed also by 2,25 hours (Fig.7). The result is in fact very similar to the previous one.

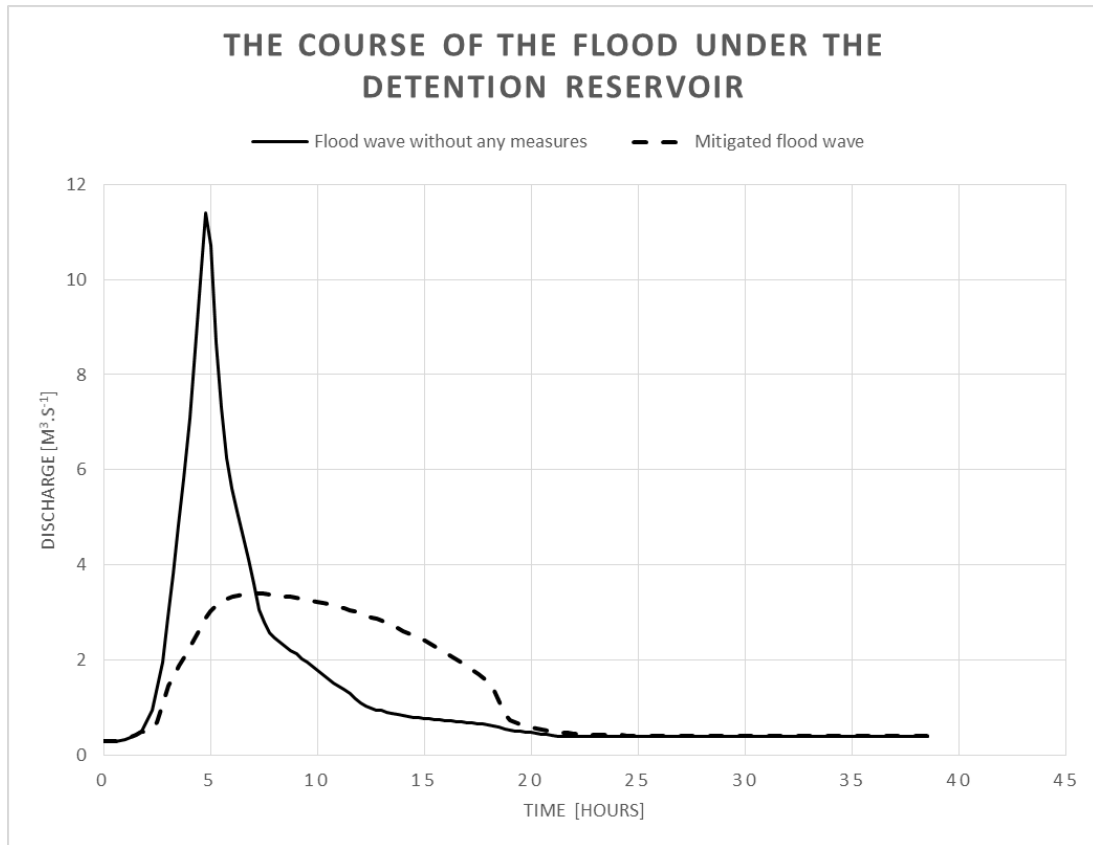


Figure 7. Mitigation of the flood wave by using 4-stage Runge-Kutaa method.

4 Results and discussion

The results of all methods are gathered and compared in Table 1. As it can be seen, every used method brought almost the same result, only a very small differences occur. It would be very interesting to compare these results with a real situation or a physical model but both of these possibilities are financially very demanding.

Table 1. Comparison of flood wave mitigation results by different methods

METHOD USED		PEAK INFLOW (m³.s ⁻¹)	PEAK OUTFLOW (m³.s ⁻¹)	REDUCTION (%)	TIME DELAY (HOURS)
KLEMEŠ METHOD		11,4	3,66	68	2
HEC-RAS			3,54	69	2
NUMERICAL SOLUTION	Simplification of differential equation		3,41	70	2,25
	4-stage Runge-Kutta method		3,40	70	2,25

5 Conclusion

Three different flood mitigation methods have been examined for the same flood protection measure - proposed detention reservoir situation. Design flood wave with peak discharge of 11,4 m³.s⁻¹

passed the reservoir and the effect of it was analysed. The results show that in this particular case methods gave very similar results with slight differences. That leads to a conclusion that any of these methods used in a study or a project of a detention reservoir would give appropriate results that could be used for correct design of detention reservoir as a proper flood protection measure.

Acknowledgements

The paper was supported by the VEGA Grant agency under contract No. 1/0800/17 Optimization of the flood protection of municipalities in river basin of mountain streams.

References:

- [1] Kelčík S., Pindjaková T., Šoltész A.: Assessment and design of the flood protection measures in the district of Levice (Slovakia), *Pollack Periodica*, Vol. 11. No. 1, 2016, pp. 25–34.
- [2] Pindjaková T., Kelčík S., Šoltész A.: Simulation of flood progress on the Gidra River, *Pollack Periodica*, Vol. 11. No. 1, 2016, pp. 25–34.
- [3] Lukáč, M., Bednárová, E.: *Nádrže a Priehrady*, Bratislava: STU in Bratislava, 2001.
- [4] HEC-RAS Programme, Hydrologic Engineering Centre, River analysis system, US Army Corps of Engineers, 2008.
- [5] Szymkiewicz, R.: *Numerical Modeling in Open Channel Hydraulics*, First edition, Springer, 2010.
- [6] Říha, J., Sedláček, M., Smrž, P., Veselý, R., Žatecký, S.: *Návrh a realizace suchých nádrží z pohledu technickobezpečnostního dohledu*, First edition, Prague: Ministry of the Environment of the Czech Republic, 2014.

UNSATURATED ANALYSES OF EXTREME RAINFALL INFLUENCE ON THE LANDSLIDE STABILITY

JOSIF JOSIFOVSKI ¹, STANISLAV LENART ², BOJAN SUSINOV ³

¹ Faculty of Civil Engineering, "Ss. Cyril and Methodius" University, Skopje, R. Macedonia, jjosifovski@gf.ukim.edu.mk

² Slovenian National Building and Civil Engineering Institute, Ljubljana, Slovenia, stanislav.lenart@zag.si

³ Faculty of Civil Engineering, "Ss. Cyril and Methodius" University, Skopje, R. Macedonia, susinov@gf.ukim.edu.mk

1 Abstract

In the past couple of years, the region of South-East Europe as consequence of a climate change there are more gust rainfall events. Often they are main trigger for activation of many new landslides but also reactivation of old ones. They were quite an expected and in many cases, there were significant material losses in some even a human loss. This situation strengthens the position with the national regulatory bodies that there is a need to reevaluate the existing risk maps and set new practice. As a part of this initiative, the paper presents only one case history out of many re-evaluated with the effects of saturation or partial saturation on the slope stability. Hence, the behaviour of the slopes will be controlled by their hydro-mechanical conditions and soil-atmosphere interaction that earlier was not anticipated. The pore water pressure changes within a slope in some cases significantly reducing the soil strength. Climatic factors such as precipitation, evapotranspiration and runoff may also have a substantial impact on slope stability.

The paper presents a numerical investigation of the „Ramina” landslide, a natural landslide located in urban area near the city of Veles in Central Macedonia subjected to excess climatic perturbations. A specific short term of gust rainfall is considered as trigger landsliding event. In the beginning, the study case is briefly described later to be analysed using the finite element method with coupled thermo-mechanical calculation. Model wise, the van Genuchten’s hydraulic model is used in combination with Mohr–Coulomb elastoplastic material models. Finally, the results summarize the critical comments regarding the mathematical formulation used to describe atmospheric-soil interaction and the influence of different aspects on the accuracy is briefly discussed.

The rainfall infiltration effects in the literature are usually critical for shallow landslides, but here it proven that also the deep sited landslides with high GWL could be destabilized. It was also proven that relatively short (12 h) but gust rainfall (10 mm/h) could have a significant influence on the overall (global) stability. Conclusive discussion for the simulated hydro–mechanical numerical effects with suggestions for possible model improvements.

Keywords: unsaturated soil, landslide, climate change, rainfall, coupled hydro-mechanical analysis.

2 Introduction

In the past couple years, in South-East Europe, number of landslide occurrences have increased. They are usually followed by flooding’s associated with significant and concentrated rainfall in certain locations. Such storm events had caused significant devastation to infrastructure and even human life. To keep up with the nature we have to re-evaluate the existing risk maps thoroughly, based on advanced calculations that include the effects of saturation or partial saturation of the soil on slope stability [5].

It is well known fact that the behaviour of the slopes is controlled by their hydro-mechanical conditions and by soil-atmosphere interaction. Climatic factors such as precipitation, evapotranspiration and runoff water may also have a substantial impact on slope stability through a change in the pore water pressure significantly reducing the soil strength.

In terms of numerical modelling, the stability analysis of partially saturated slopes is a complex and time dependent problem with many variables. The more advanced approaches require implementation of hydraulic models with input data obtained from the Soil Water Retention Curve (SWRC). Moreover, the time dependent hydro-mechanical behaviour of the soil is best described in a coupled format, taking both deformation and groundwater flow into account, in which mixed equations of displacement and pore pressure, called, have to be solved simultaneously in a coupled hydro-mechanical approach [2].

The study implements some advanced modelling aspects defining a complex climate-soil system with the main objective was to determine the rainfall influence on the slope failure.

3 Site descriptions

The „Ramina” is natural landslide located in highly urbanized hilly area of city Veles, Macedonia, on the left bank of the river Vardar. In the past it has been reactivated several times, last time in 2002 with major deformations leading to severe damage of the infrastructure and buildings.

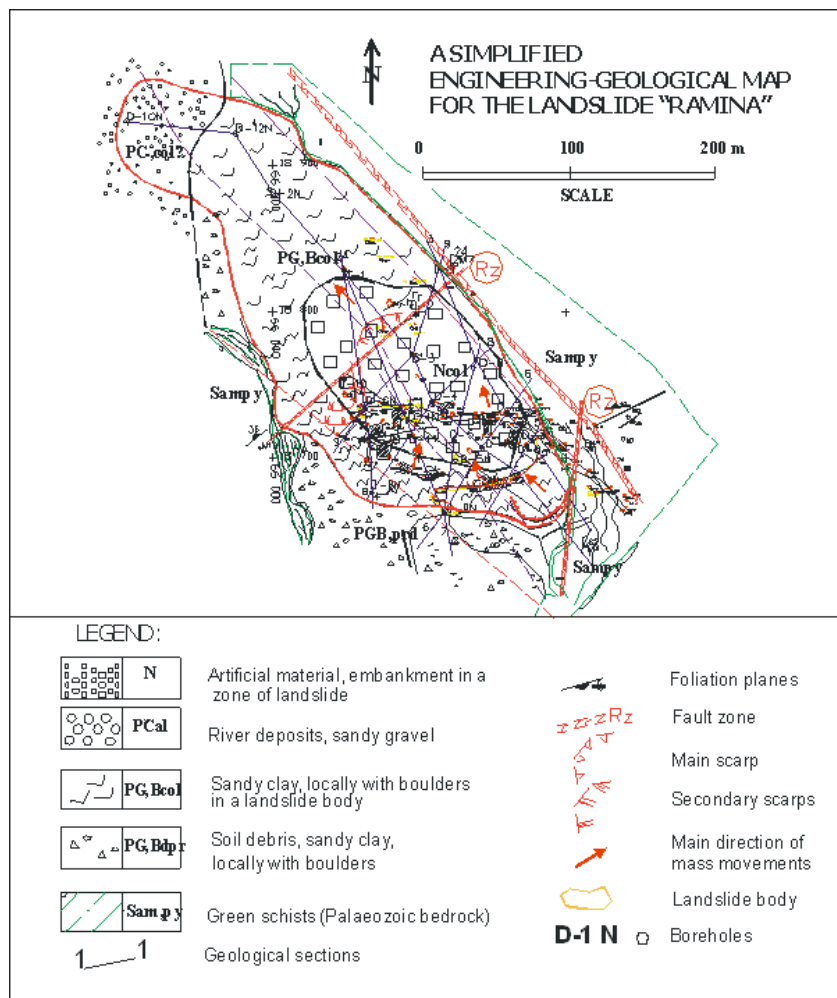


Figure 1. Simplified Engineering Geological profile

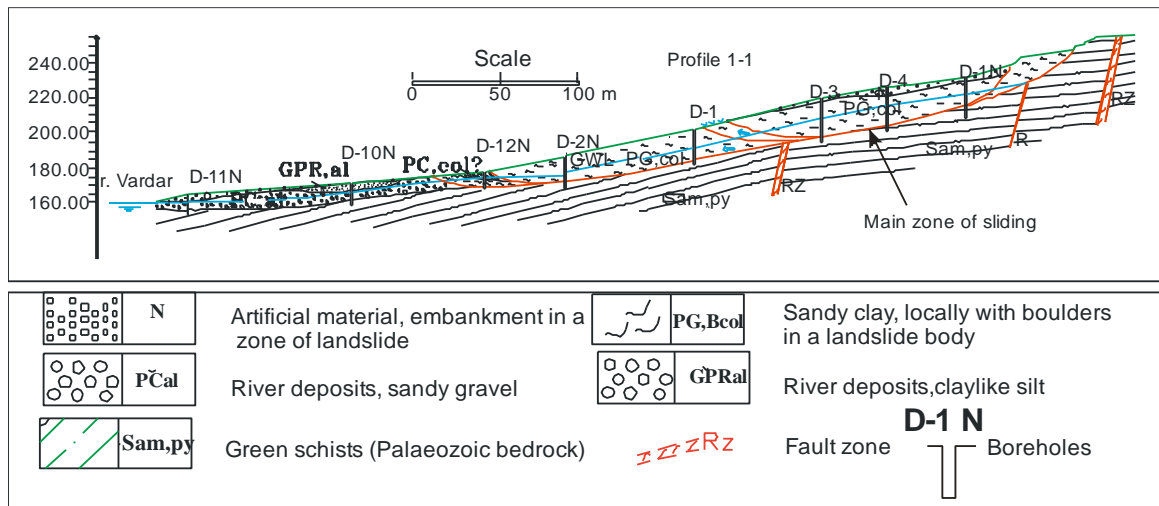


Figure 2. Typical geological profile of „Ramina” landslide

The influence of Continental and Mediterranean climate in Macedonia unequally spreads the precipitations through throughout the year with intensity between 400-900 mm/y, thus long-time arid periods from (summer-autumn) and short wet seasons exist. A season of gust rainfall in period from December to March averages with monthly precipitation of around 140 mm/month or as maximal daily precipitation of 70 mm. The elevation of the slope is around 1000 m above sea level sited on the transition of relatively steep mountain slopes to a river valley. Actually, it is attacked by a surface and ground water from wider catchment area, moreover there is no vegetation to reduce the effects of heavy rainfall events. The average slope angle is around 15° and maximal 22°. The landslide is about 500 m long with average width of about 100 m and height of 95 m (fig. 1). The estimated maximum depth of the shear zone is 24 m. The sliding system is comprised of two parts (fig.2), the “upper” with a length of 350 m, width 110 m, height 60 m and “lower” with length of 200 m, width 90 m, height 35 m and depth up to 18 m. The total area of the landslide is estimated to be 37,600 m² with around 475,200 m³ of sliding mass, ranking as one of the largest in the Balkans, and possibly in South East Europe [3].

The geotechnical investigations indicate a sliding zone on the contact between weathered bedrock (Palaeozoic amphibolitic schists, highly foliated and faulted) and low plasticity claylike mass. The hydrogeological conditions indicate that the zones with increased water contents relate to the sliding zone. A sub-artesian effect is also present in almost all boreholes [4]. The GWL is detected at 8 m of depth while in the lower part it was around 2 m below the terrain.

4 Numerical modelling

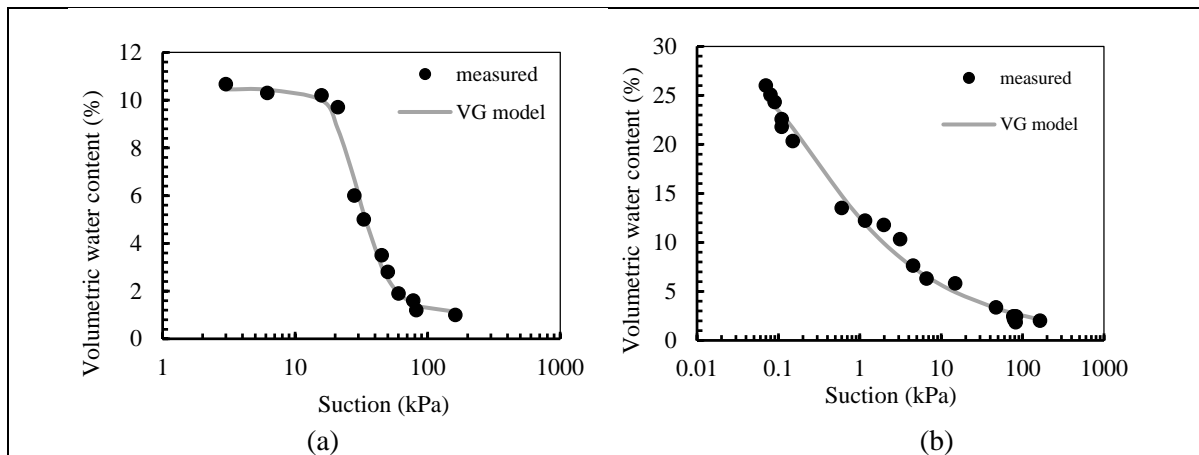
To analyse mechanical behaviour of saturated or partially saturated soils by means of numerical method e.g. finite element method, in proper manner, it is necessary to take into account both deformation and groundwater flow. For time dependent behaviour, this leads to mixed equations of displacement and pore pressure, called coupled hydro-mechanical approach, which have to be solved simultaneously [2].

The task was to perform a coupled hydro-mechanical analysis of slope stability on the presented case histories. The calculation using the finite element software Plaxis [1] is performed, which enables fully coupled hydro-mechanical analysis. This type of analysis is able properly to evaluate the effects of rainfall and water infiltration on the slope stability. The shear strength of the unsaturated soil is examined based on effective stress concept considering suction. The finite element method with shear strength reduction technique was employed to evaluate the stability using the factor of safety (FoS). For the soil material an elastic-perfectly plastic small strain Mohr-Coulomb (MC) model was employed with special attention put on definition of mechanical and hydraulic parameters critical for realistic simulation. For simplicity, a homogeneous profile with soil parameters given in Table 1 is assumed.

Table 1. Soil material parameters for MC model

Parameter / Soil material	Sandy-Clay	Clay
Unit weight γ (kN/m ³)	20.14	20.2
Eff. friction angle ϕ' (°)	23	22
Eff. Cohesion c' (kPa)	12	15
Eff. Poisson's ratio ν' (/)	0.32	0.30
Elastic modulus E' (kPa)	10000	7000

For definition of the hydraulic models at the Slovenian National Building and Civil Engineering Institute tensiometer laboratory test is performed to determine the suction in the material samples for different water content. Through the measured data a nonlinear SWRC fitting (fig. 3) after UNSODA [10] database was made.

**Figure 3.** SWRC of (a) Sandy-Clay and (b) Clay from „Ramina” landslide profile

The hydraulic model is defined by of Van Genuchten model parameters [7] given in Table 2.

Table 2. Hydraulic data of Van Genuchten model

Soil	k_{sat} (m/s)	θ_s (%)	θ_r (%)	(1/kPa)	n (-)
Sandy-Clay	1E-6	38.70	10.45	0.35	4.17
Clay	1E-8	27.80	0.10	9.50	1.35

In the „Ramina” case a constant rainfall infiltration is assumed with 10 mm/h on the free surface plus additional 1 m³/h on left inflow boundary. The right model boundary is open outflow because the slope ends with open recipient, namely the river Vardar. A runoff not greater than 0.5 mm/h is assumed due to the surface characteristics at the site (s for moderate urbanized area). In the model no vegetation and temperature is not considered, therefore the evapotranspiration effects are not analysed. As for the mechanical part of the modelling only Dirichlet boundary conditions are defined. In the restrain vertical direction of the right and left boundary and totally fixed in the bottom. On the schist contact an interface elements are employed to check for developing shear tresses. The mesh updating is necessary as often the case when due to deformation the finite elements are moving from saturated to unsaturated zone and vice versa due to the occurrence of large straining.

5 Results

The analysis produced wide range of results clearly depicting the influence of the heavy rainfall on the hydro-mechanical material parameters. Generally, the position of phreatic level and the distribution of pore water pressure are governed climate conditions (groundwater flow boundary conditions) with suction above phreatic level where with time in the case of downward flux (i.e. precipitation) suction decreases (and degree of saturation increases) and the water level rises.

In the following text some of the results from the coupled flow-deformation analysis will be presented, the specific are chosen which without any doubt show how the rainfall influences on the slope stability. Usually the displacement are the most significant in this type of analysis, thus below in figure 4(a) and 4(b) are presented the model predictions.

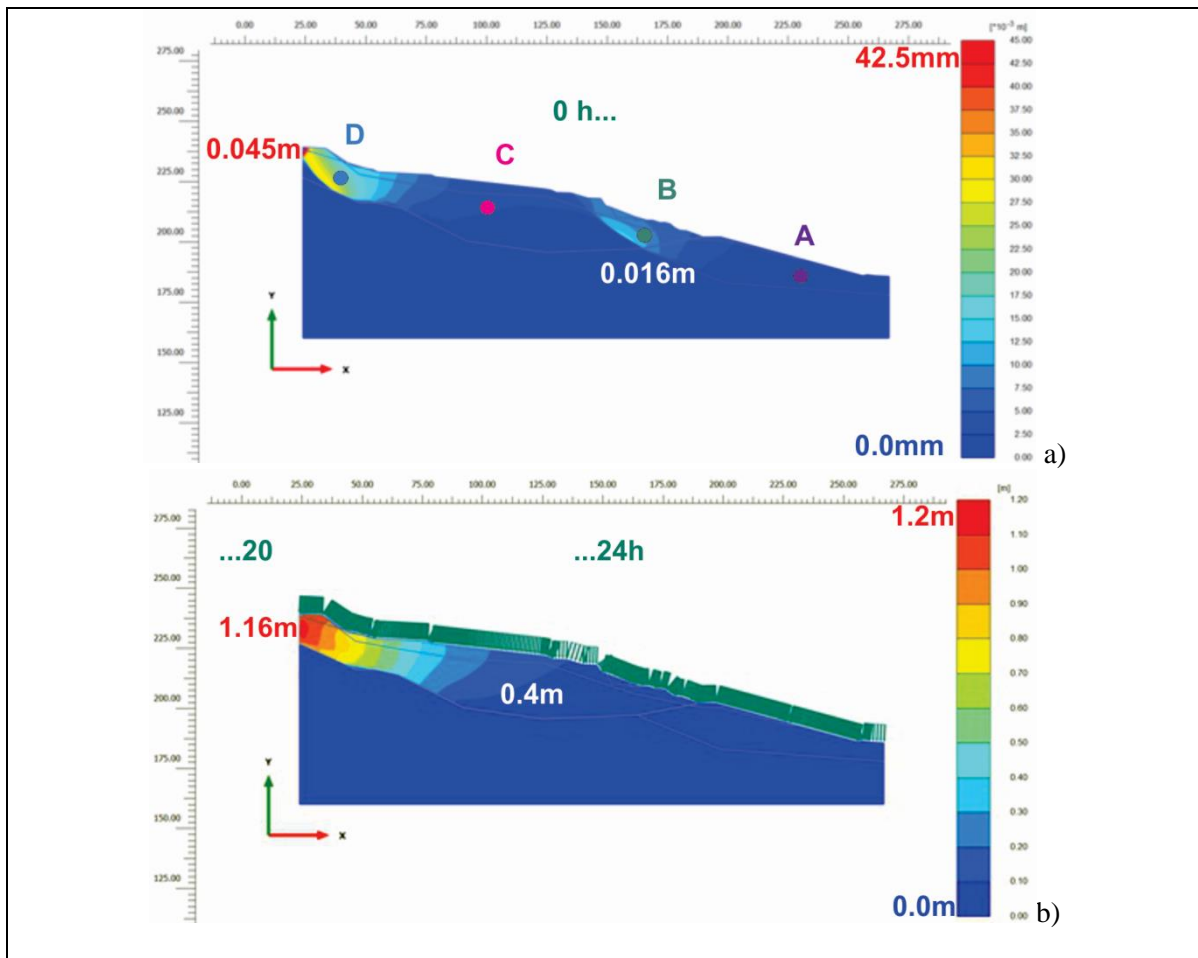


Figure 4. Total landslide displacement at (a) $t_0=0h$ and (b) $t=24h$

In figure 4(a) the graph of total landslide displacements for static conditions are depicted. At initial time $t_0=0$ s the sliding did not occur, only a displacement of 4.5 cm are registered at the top and 1,6 in the middle of the landslide clearly forming a two potential sliding zones. The sliding surface is obviously on the contact sliding zone is along the contact between low plasticity clay-like materials and the bedrock, represented by Palaeozoic amphibolitic schists, highly foliated, faulted and locally weathered. Comparably, in figure 4(b) the slope displacements after 24 h of constant precipitation and infiltration are presented. The displacements at the top are still maximal they have increased by 30 times creating a landslide scarp with 1.2m deformation. Clearly there is a deep sliding mechanism where it could be argued that the single sliding mass is breaking into two (figure 10a) due to the presence of the buttress in the middle. The displacements in the middle of the landslide are 3 times smaller than those on the top but still significant. The obtained results are confirmed with the inclinometer measurements. They are captured in photography; see in figure 10(b). To understand better the deformation mechanism, development of the sliding surface, it is necessary to analyse the result as time dependent displacements in certain points of the landslide, see figure 5.

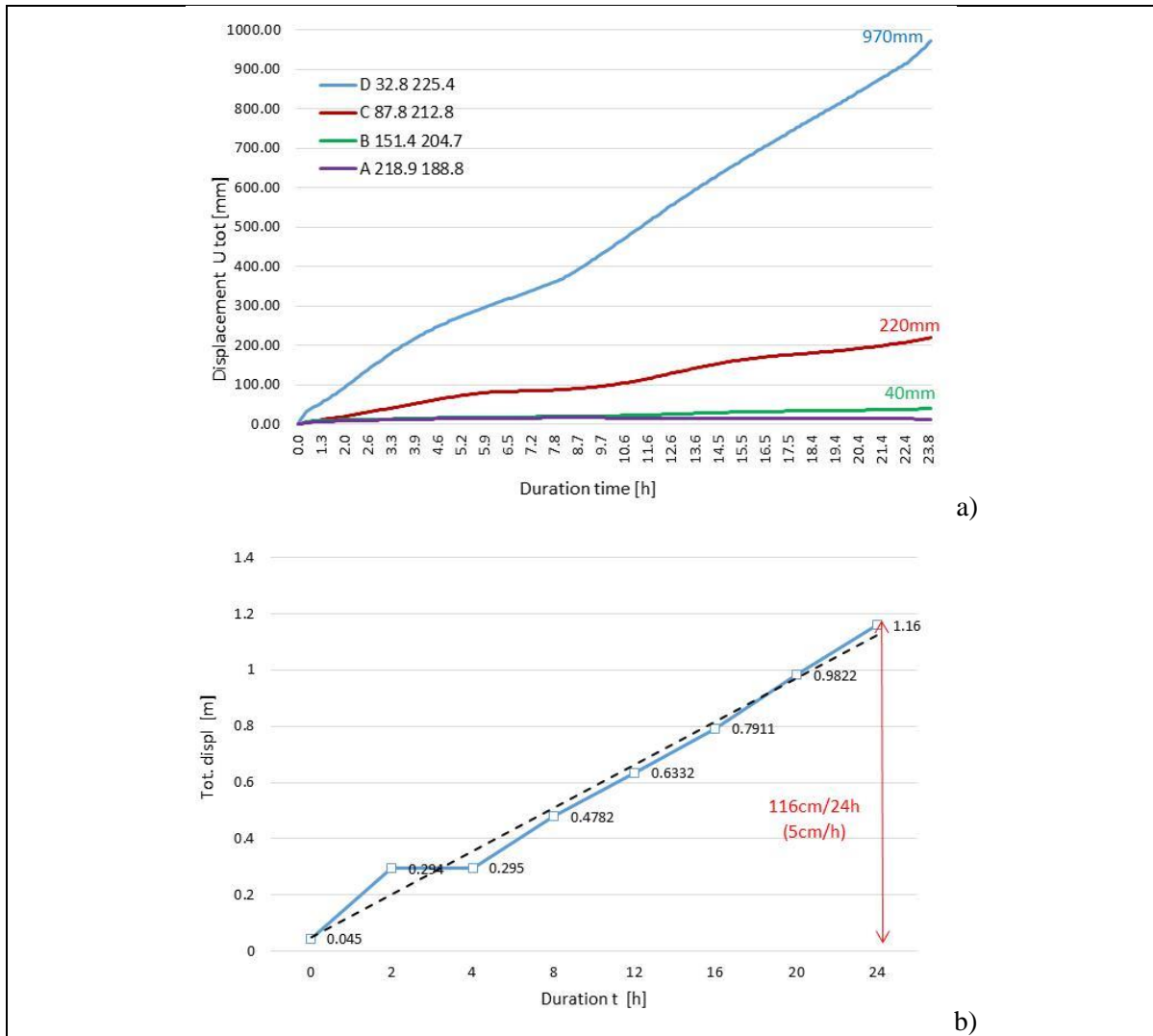


Figure 5. Time dependent total displacement at (a) selected points and (b) max. value

From the beginning all the points show a gradual increase in the displacements, figure 5(a), hence the point D positioned at the top is with the highest increase rate and point A positioned at the toe with lowest. Analysing the maximal displacement, which are located at the top of the landslide, in figure 5(b), show again a gradual increase from the very beginning with a rate of 5 cm/h thus describing a failure mechanism with no stabilization effect and continuous deformations or mass movement during the whole time of the rainfall.

The key factor influencing the displacements is the development of pore water pressure (PWP) which is negative by nature destabilizing the soil, but above the saturation level a positive contra part develops in form of suction acting with a stabilizing effect. This force is surely reduced by the infiltration rate and raise in the GWL, which in this analysis is time dependent. Gradually with time the pore water pressure equals the shear resistance of the material at certain points and the sliding occurs. Therefore, in figure 6 the pore water pressure is presented at initial time and after 24h.

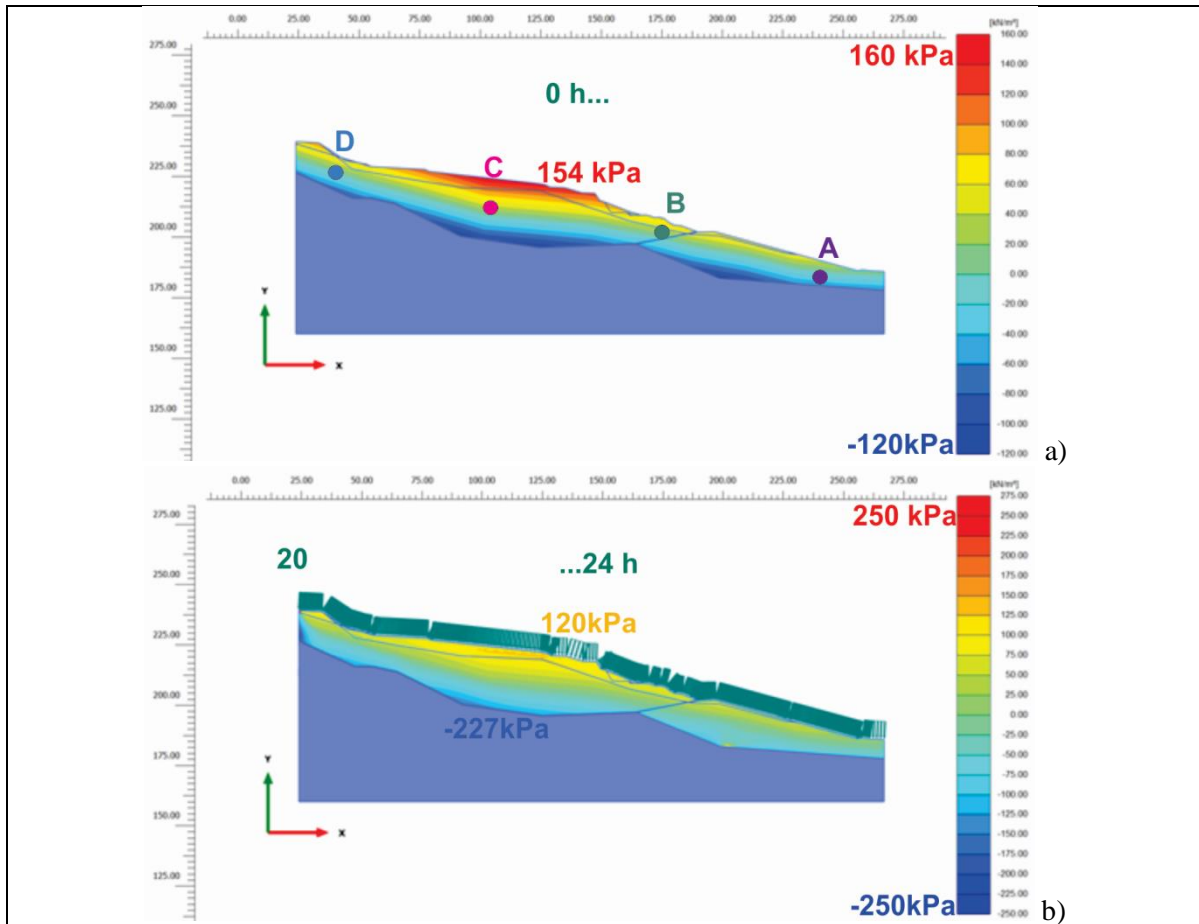
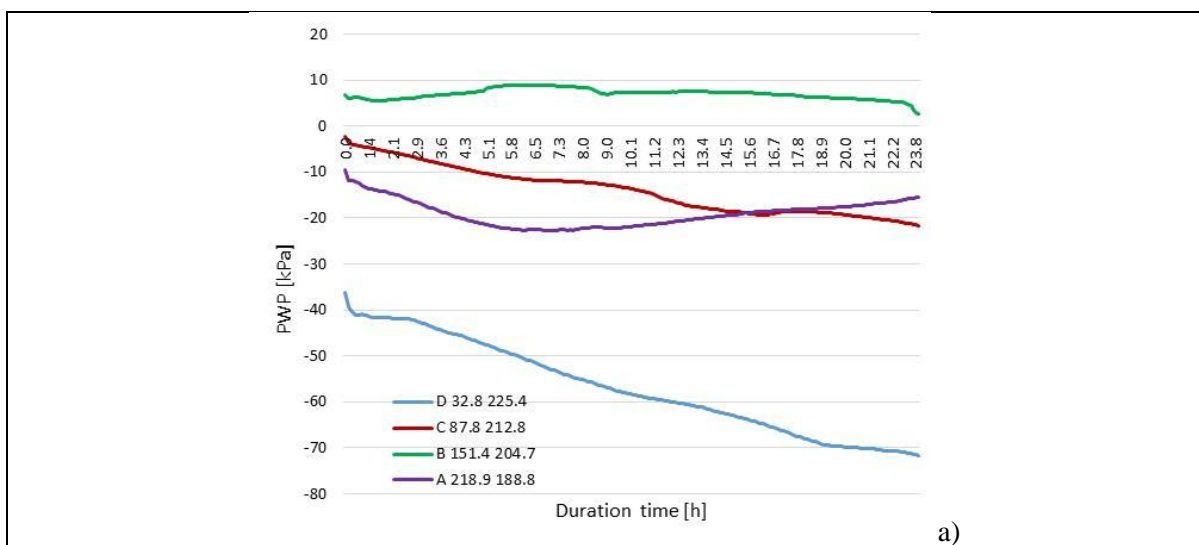


Figure 6. PWP graph at (a) 0h and (b) 24h

As expected in the beginning the suction forces at the top soil layer are higher (from 154 kPa) and decreases with time (to 120 kPa) which is still enough to insure from local instabilities. In contrast, the pore water pressure increases almost twice after 24h from -116 kPa to -227 kPa. The time dependent development of the negative pore pressure (point A, C and D) and suction at point B is shown in figure 7(a).



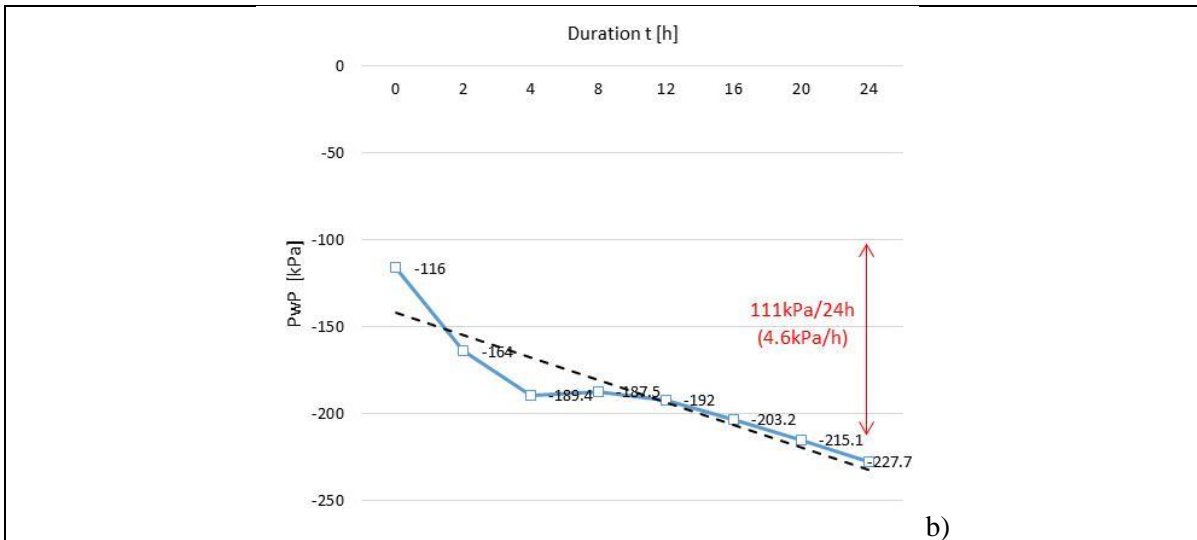


Figure 7. Time dependent development of PWP at (a) points A, B, C, D and (b) max. value

In general, when looking at the maximal PWP values there is almost a gradual increase with the time, see figure 7(b), from 111 kPa in 24h of constant rainfall or rate of 4.6 kPa/h. There is a slight stabilization between 4 and 8h, which is probably an effect of strain accumulation. The strain shear increments are largest in the plastic zones where the sliding occurs (figure 8a).

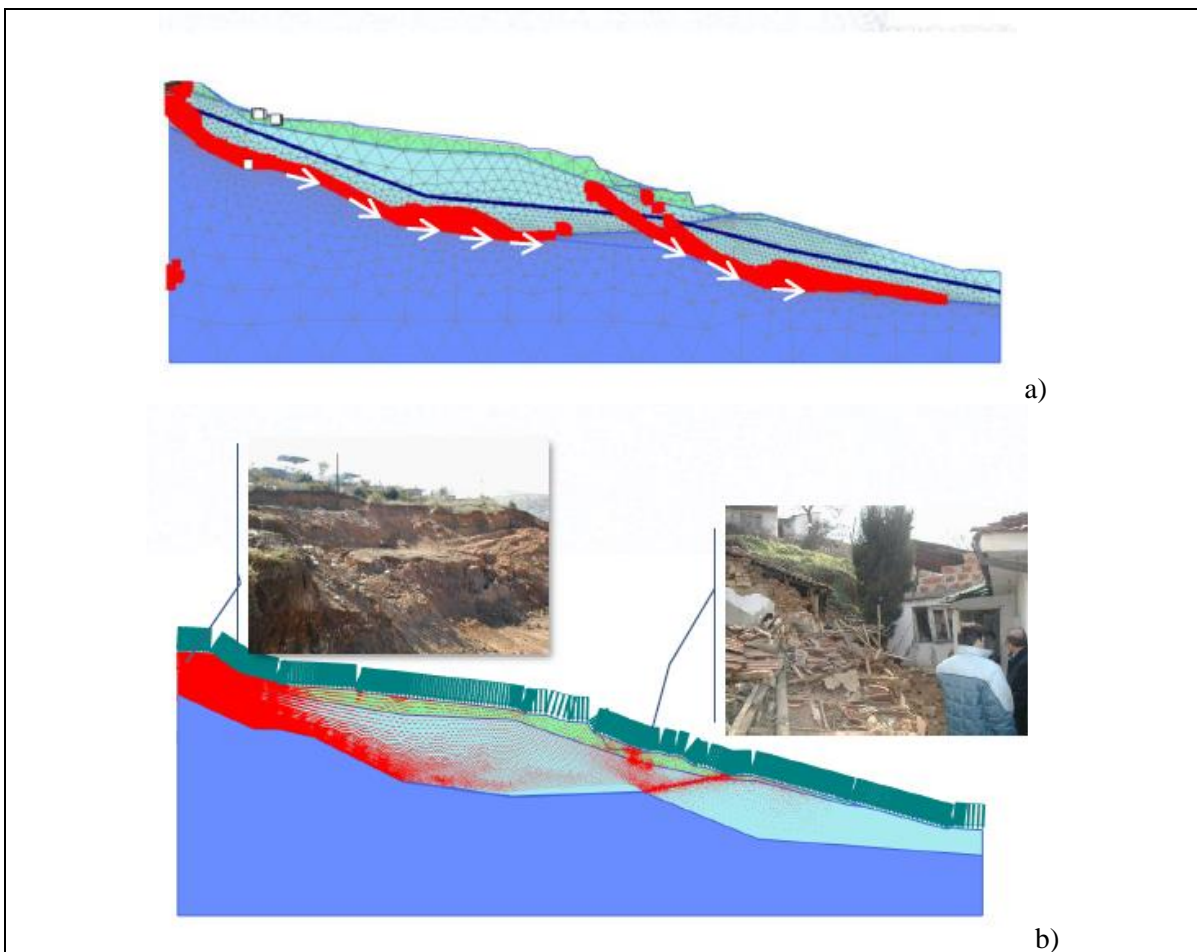


Figure 8. Sliding mechanism described through (a) plastic zones and (b) total displacements

The results show a sliding mechanism where the upper part of the slope starts to move due to the rainfall event that cause a significant rising of the water table and the pore water pressures. Thus, different

ground water levels develop in the upper and lower part of the slope, representing a trigger for the sliding of the upper mass and the loading at the top of the lower mass. The slope deformations, recorded by means of inclinometers located along sections of the slope different from the analysed one (about 0.5 m displacement in the middle of the landslide), have been qualitatively compared with the ones simulated through the hydro-mechanical analysis (depicted in figure 4b). The comparison appears to qualify the hydro-mechanical simulation of the failure mechanism so far presented as reasonable.

After the simulation of 24 h plastic analysis an overall stability check has been performed using phi-c reduction method. In figure 9 the deformation diagram is presented which is ensured with FoS=1.03.

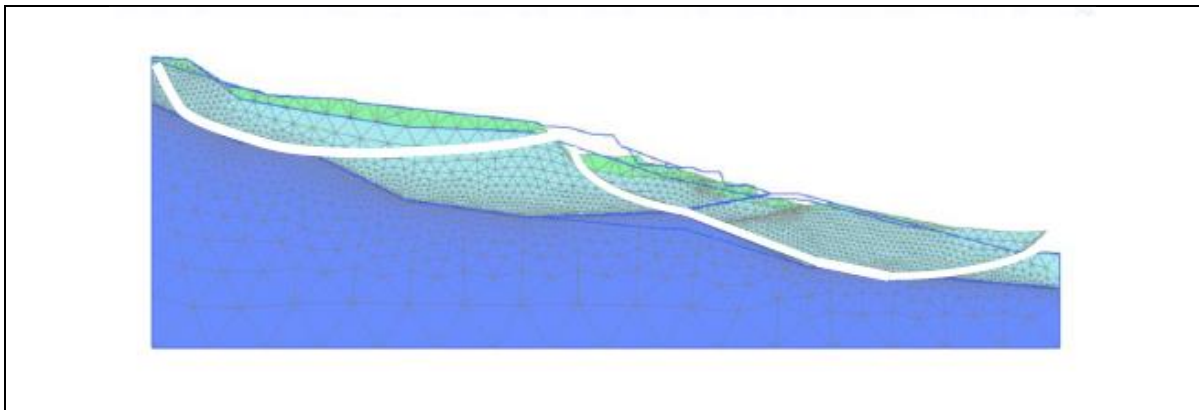


Figure 9. Diagram from global stability after 24h

After the plastic deformation and mass displacement, the stability is still problematic because the calculated factor is practically non-existent. The landslide is in labile equilibrium with potential to be re-activated after any other similar event.

6 Conclusion

The consequences of climate change on landslide rate, size and frequency are difficult to predict because they depend on a range of variables. The precipitation (mostly in rainfall) is among the most important factors especially severe storm would cause flash floods with intense erosion and landsliding. In addition to the above direct influences, the indirect impact of climate change on landslide is exerted through changes of vegetation cover, quality and density, runoff, overland flow and oversaturation would increase raising the rate of erosion and frequency of landslides. Rainfall is often the main factor for landsliding. The modelling has shown that suction responses to rainfall vary on a number of different timescales [8]. On shorter timescales (ranging from minutes to hours and days) heavy rainfall which was of primary interest in this study produced very interesting results. The rainfall infiltration effects in the literature [9] are usually critical for shallow landslides, but here it proven that also the deep sited landslides with high GWL could be destabilized.

The combination of rainfall infiltration and GW inflow to the slope is the main reason for destabilization in Macedonia around 60% of all the total number. Therefore, the need to asses that impact of climate change and reevaluate current landslide risk maps especially near infrastructure and urban areas is necessary [6].

The presented coupled hydro-mechanical analysis underlines the importance to check on heavy rainfall scenarios (10 -20 mm/h) with relatively short duration (3 - 6 h) because as shown they could have a significant influence on stability, thus should be considered in future with given probability of occurrence. In the analysis it has been evaluated the influence in the sense of infiltration and duration of rainfall on the slopes. It was proven that relatively short but gust rainfall could have a significant influence on the overall (global) stability. According to the statistics this type of events are to be expected frequently.

Other modelling aspects of climate-vegetation-soil system such as: influence of cracks and fissures, root water uptake were not considered, thus there are still but a few improvements in this model [11].

Acknowledgements

This paper is result of collaboration between Faculty of Civil Engineering in Skopje and Slovenian National Building and Civil Engineering Institute from Ljubljana in the framework of COST action TU1202 – a European network that addresses the impacts of climate change on engineered slopes for infrastructure activities, where the research transfer through short-term scientific missions was adequately supported.

References:

- [1] Hughes, D., Karim, M.R., Briggs, K., Glendinning, S., Toll, D., Dijkstra, T., Powrie, W., Dixon, N.: A Comparison of numerical modelling techniques to predict the effect of climate on infrastructure slopes, XVI European Conference on Soil Mechanics and Geotechnical Engineering, Edinburgh, 2015.
- [2] Galavi, V., Internal report: Groundwater flow, fully coupled flow deformation and undrained analysis in Plaxis 2d and 3D, 2010.
- [3] Josifovski, J., Gjorgjevski, S., Susinov, B.: Ramina Landslide from a Natural Hazard to Remediation, 1st Regional Symposium on Landslides in the Adriatic-Balkan Region with 3rd Workshop of the Japanese-Croatian Project on ‘Risk Identification and Land-Use Planning for Disaster Mitigation of Landslides and Floods in Croatia, Zagreb, 2013.
- [4] Josifovski, J., Lenart, S.: Some Experience in Numerical Modelling of Unsaturated Slope Instabilities, 3rd European Conference on Unsaturated Soils – “E-UNSAT 2016”, Volume 9, E3S Web of Conferences 9, 08005, 2016.
- [5] Plaxis bv. Plaxis 2D AE. Scientific Manuel, 2016.
- [6] Seki, K.: Hydrol. Earth Syst. Sci. Discuss., 4 : SWRC fit - a nonlinear fitting program with a water retention curve for soils having unimodal and bimodal pore structure, 2007, p407-437.
- [7] van Genuchten, T.M.: A closed-form equation for predicting the hydraulic conductivity of unsaturated soils, Soil Science Society of American Journal, 44, 1980, p.892–898.
- [8] SAFELAND – Living with landslide risk in Europe: Assessment, effects of global change, and risk management strategies.
- [9] Casini, F., Serri, V., Springman, S.M.: Hydromechanical behaviour of a silty sand from a steep slope triggered by artificial rainfall: from unsaturated to saturated conditions, Canadian Geotechnical Journal, 50(1), 2015, p.28-40.
- [10] Jovanovski, M., Peshevski, I., Markoski, B., Petrusheva, S., Susinov, B.: Landslide Inventory Map of the Republic of Macedonia, statistic sand description of main historical and slide events, 1st Regional Symposium on Landslides in the Adriatic-Balkan Region with 3rd Workshop of the Japanese-Croatian Project on ‘Risk Identification and Land-Use Planning for Disaster Mitigation of Landslides and Floods in Croatia, Zagreb, 2013.
- [11] Springman, S.M., C. Jommi, C., Teyssere, P.: Instabilities on moraine slopes induced by loss suction: a case history, Géotechnique, 53(1), 2003, p.03–10.

COMPARISON OF EROSION MODELLING AND BATHYMETRY MEASUREMENTS OF SEDIMENT TRANSPORT IN THE SVACENICKY CREEK BASIN IN SLOVAKIA

SILVIA KOHNOVÁ ¹, KAMILA HLAVČOVÁ ¹, YVETTA VELÍSKOVÁ ², VALENTIN SOČUVKA ²,
ZUZANA STUDVOVÁ ¹

¹ Slovak University of Technology, Faculty of Civil Engineering, Department of Land and Water Resources Management, Radlinského 11, SK 810 05 Bratislava, Slovakia, silvia.kohnova@stuba.sk, kamila.hlavcova@stuba.sk

² Institute of Hydrology, SAS, Dúbravská cesta 9, 841 04 Bratislava, Slovakia, veliskova@uh.sav.sk

1 Abstract

The erosion, transport and deposition of sediments in small valley reservoirs represent a significant impact on their operations, mainly with regard to reducing the volume of their accumulation. The aim of this study was to quantify erosion processes and sediment transport in the Svacenicky Creek basin, where a flood protection reservoir was built in 2012. The small water reservoir of Svacenicky Creek is a part of the flood protection measures in Turá Lúka and is located in the western part of Slovakia, close to the town of Myjava. The town of Myjava in recent years has been threatened by frequent floods, which caused heavy material losses and significantly limited the quality of life of the local residents. To estimate the amount of sediments transported from the basin, we applied the USLE 2D erosion model and compared the results with the results of the actual bathymetry of the polder. The measurements were provided by a modern Autonomous Underwater Vehicle (AUV) hydrographic instrument. From the sediment data measured and the original geodetic survey of the terrain at the time of the construction of the polder, we calculated changes in the storage volume of the polder during its four years of operation. The results show that in the given area, there has been a gradual clogging of the bottom of the polder caused by erosion. We estimate that within the four years of the acceptance run, 10,515 m³ of bottom sediments on the Svacenicky Creek polder have accumulated. It therefore follows that a repetitive surveying of the sedimentation is very important for management of the water reservoir.

Keywords: soil erosion, reservoir storage volume, sediment, bathymetry, Svacenicky Creek

2 Introduction

Reservoir sedimentation can be considered as a process by which sediments are transported to reservoirs and accumulated until the reservoir become completely filled. The transport and accumulation of sediments depend on many factors, but mostly on the size of the sediments. The mechanisms contributing to reservoir sedimentation are well known but not yet fully physically described. Field observations on reservoir sedimentation processes started about 1936, but the majority of publications on this topic have only appeared since the 1980s [1]. Field surveys have been reported since the 1960s. We can only find exceptional papers published before 1950. Most methods for the sustainable use of reservoirs were proposed in the 1980s and 1990s.

Dam construction creates an extremely efficient trap for sediments in a valley. Due to the dynamics and morphology of a river catchment over the years, a reservoir loses the storage capacity for which it was initially designed as the sediments accumulate. The routing of sediments that contribute to the sedimentation of a reservoir must be assessed on a river basin scale with adequate conceptual models. These models have to consider the relevant key environments and their interrelationships: the sources, pathways and storage [2], [3], [4], [5], [6],[7],[9], [10].

The erosion rate of a catchment can generally be determined by the estimation of sediment yields, which can be quantified in various ways: from reconnaissance methods through catch pits used for measurements of the flow and sediment loads or from the quantities of sediment trapped in water reservoirs. Many of the problems associated with sampling of river sediments can be avoided when data derived from reservoir surveys are used to estimate sediment yields [11].

The aim of this study was to quantify the erosion processes and sediment transport in the Svacenicky Creek basin, where a flood protection reservoir was built in 2012. The small water reservoir of the Svacenicky Creek is a part of the flood protection measures in Turá Lúka and is located in the western part of Slovakia close to the town of Myjava. To estimate the amount of sediments transported from the basin, we applied the USLE 2D erosion model and compared the results with the results of the actual bathymetry measurements of the polder.

3 Methods

3.1 Bathymetry measurement of the polder

For the hydrographic research and data mapping of the Svacenicky Creek polder, the AUV EcoMapper device was used. AUVs represent devices which are currently used in a wide range of hydrographic research, marine geoscience, and the military, commercial, and policy sectors. In general, they have the shape of a torpedo and were originally developed for military purposes. The first AUV was developed at the Applied Physics Laboratory at the University of Washington as early as 1957 by Stan Murphy and Bob Francois. The vehicle was used to study diffusion, acoustic transmissions, and submarine wakes [12]. During the 1980s AUVs were also applied for water exploration and hydrographic surveys. The IFREMER L'Epaulard is considered one of the most significant instruments, and was built by ECA in association with the French Oceanology Research Institute in the 1980s. The IFREMER L'Epaulard was used for oceanographic surveys with a depth range of up to 6000 m. In subsequent years the research and development of new AUV devices has permitted their use in inland conditions and has also increased the area of the measurements of biological and geochemical parameters.

YSI EcoMapper

EcoMapper is a device which is capable of moving on surface and subsurface water levels independently and performing logging of data. This device is ideal for coastal and shallow water applications such as hydrographic surveys and spatial environmental monitoring. Its survey mission can be performed in water with depths of more than one meter and it is fully capable of subsurface operations down to 100 m. EcoMapper was developed by the YSI Company (USA) and is designed for the quick and easy collection of bathymetry, sonar and water quality data.



Figure 1. YSI EcoMapper side view (YSI, 2009)

The EcoMapper device consists of hardware (Fig.1) and the Vector Maps software program, which was designed for mission planning and for the partial analysis of measured data. Physically, the vehicle can be divided into 3 distinct parts. The bow section contains water quality sensors that interact with an aquatic environment and a Doppler Velocity Log (DVL) for underwater navigation. The middle section includes an on-board computer, the electronic components, batteries, and weights to balance the vehicle. The tail section contains a propulsion system and GPS antennas for navigating on water surfaces. The physical design permits its easy deployment from the shore by one person. All the external components on the vehicle can be easily replaced. The external replaceable components include the water quality sensor, handle and balance assembly, vehicle antennae, control planes, propeller, and cowling [13].

3.1.1 Estimation of soil losses

The estimation of soil erosion processes was provided on a yearly basis, therefore the Universal Soil Loss Equation (USLE) and the Sediment Delivery Ratio (SDR) models were applied.

The USLE method is the basic empirical method which is suitable for calculating the average annual soil loss from field studies or assessing the erosion vulnerability areas in terms of permitted water erosion or proposed critical slope lengths. The USLE 2D modification equation is used to calculate the LS space – variable factor (combined slope length L and slope steepness S) in a two-dimensional space; it is based on a raster grid and digital elevation model. The raster structure of the digital elevation model allows for taking into account the slope's variability in the separate cells of a square grid area, together with increasing the slope's length in the direction of the surface runoff. Increasing the slope length in the model is expressed by a unit contributing area, which is defined by several algorithms.

The basic expression of the relationship by [8], defined the interaction between the length and steepness of the slope. The formula of the topographic factor of an irregular slope has the shape:

$$LS = \sum_{j=1}^N \frac{S_j * \lambda_j^{m+1} - S_j * \lambda_{j-1}^{m+1}}{(\lambda_j - \lambda_{j-1}) * (22,13)^m} \quad (1)$$

where

S_j - factor of the slope steepness for the j - th element (m / m),

λ_j - the length between the lower boundary of the j - th element and the upslope field boundary (m).

The equation can be expanded to three-dimensional topography:

$$LS = \sum_{i,j} \frac{S(i,j) * \lambda(i,j)_{outlet}^{m+1} - S(i,j) * \lambda(i,j)_{inlet}^{m+1}}{(\lambda(i,j)_{outlet}^{m+1} - \lambda(i,j)_{inlet}^{m+1}) * (22,13)^m} \quad (2)$$

where

LS - the topographical factor for one parcel or a whole river basin,

$\lambda(i,j)$ - the slope length at the input for the i, j - th grid cell (m),

$\lambda(i,j)$ - the slope length at the output for the i, j - th grid cell (m),

$S(i,j)$ - the slope factor for the i, j - th grid cell,

m - the slope length exponent.

The authors [8], expressed the factor of the slope steepness for individual cells by several algorithms.

For estimating the sediment transport from a watershed, we applied the SDR model, which represents the ratio between the total annual soil loss and the annual amount of the sediment transport:

$$SDR = 1.366 \cdot 10^{-11} \cdot F^{-0,0998} \cdot RP^{0,3629} \cdot CN^{5,444} \quad [-] \quad (2)$$

where

F – catchment area (km²),

CN – CN curve number,

RP – relief ratio (m/km).

Finally, for conversion of results from volume to weight unit the values of volume density of sediments which was estimated from the real field measurements of bed sediments in the Svacenicny Creek polder were used.

4 Case study

The Svacenicny Creek polder is a part of the flood protection measures in Turá Lúka and is located in the western part of Slovakia close to the town of Myjava, Fig.2. The Svacenicny Creek flows into the Myjava River at 69.0 river km, close to Turá Lúka. The Svacenicny Creek polder, which was built in 2012, can reduce a 100-year maximum design flood of 16.00 m³.s⁻¹ to 0.21 m³.s⁻¹. The projected volume of the polder's storage capacity is 215,808 m³, and it is able to capture a flood wave of 207,330 m³.

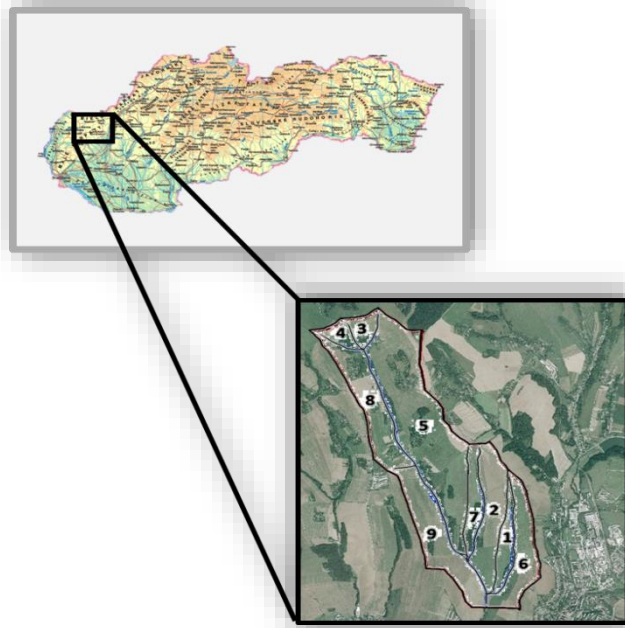


Figure 2. Location of the Svacenicky Creek catchment and the Svacenicky Creek polder within the territory of Slovakia.

Before the field bathymetry measurements take place, the mission planning must be predefined, Fig. 3. The EcoMapper then follows the predefined mission plan created by the user in the graphical user environment of Vector Map Software. Finally, the predefined mission represents 84 navigation points. During the measurements a certain distance had to be kept from the shore polder, due to the dense vegetation and shallow depth, especially in the northern part of the polder. After entering the navigation points, cross sections of a distance of 10-12 meters were created. The total length of the measurement was 2878.97 m. The EcoMapper’s velocity was set at 3.7 km h⁻¹; one measurement took about 60 minutes. The collecting interval of the qualitative and depth data was set at 1 second. The total amount of data collected during the measurement of the water level was 3004 for each parameter.

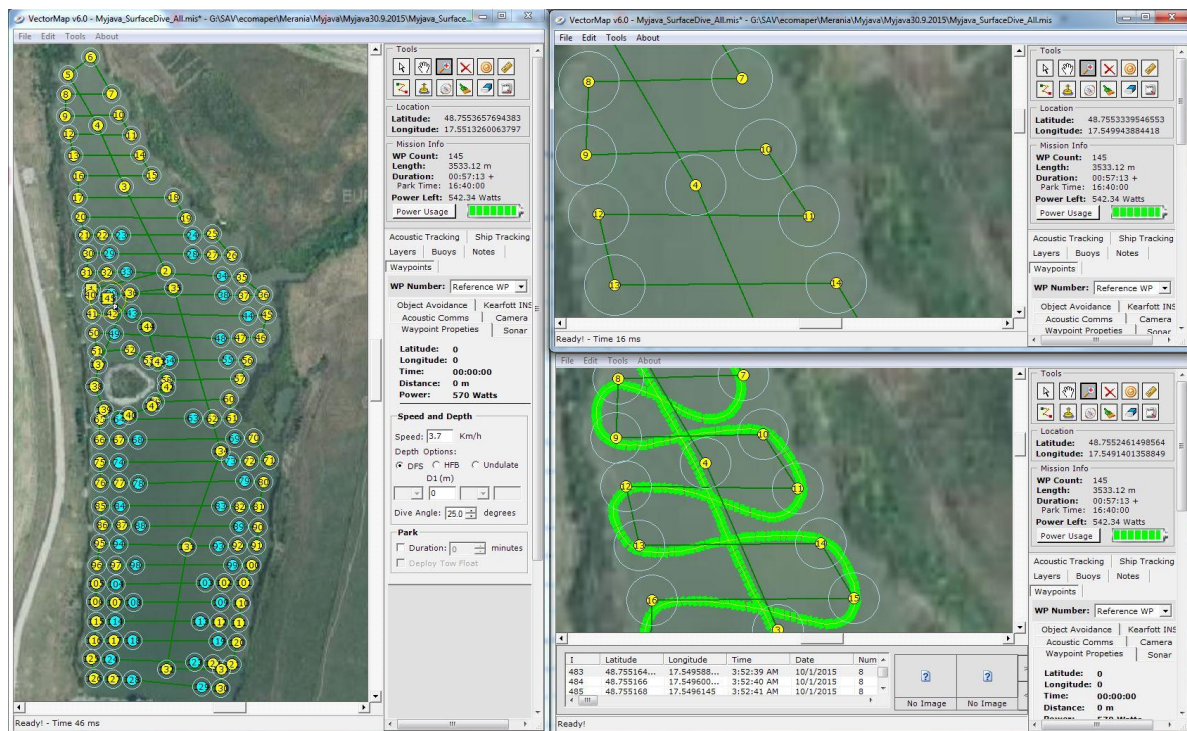


Figure 3. Mission planning in the VectorMap software program.

5 Results and discussion

First, the geodetic points measured during the polder's construction were used for the creation of a digital terrain model to characterize the original morphology of the polder bed, Fig. 4. and was only modelled in the flooded area. A resolution of 1 square meter per cell of the digital terrain model was chosen. During the bathymetry measurement on September 22, 2015, a water level height of 316.45 m. a. s. l. was estimated. Subsequently, a network of sediment points was used for creating the actual morphology of the polder bed after the process of sedimentation, Fig. 5. However, during the creation of the digital terrain model of the sediments, it was very difficult to define the morphology in the areas without the actual measured points. These areas had a water depth lower than 20 cm; due to the low water level, the EcoMapper could not provide any measurements. In this case, the same resolution of the raster was chosen.

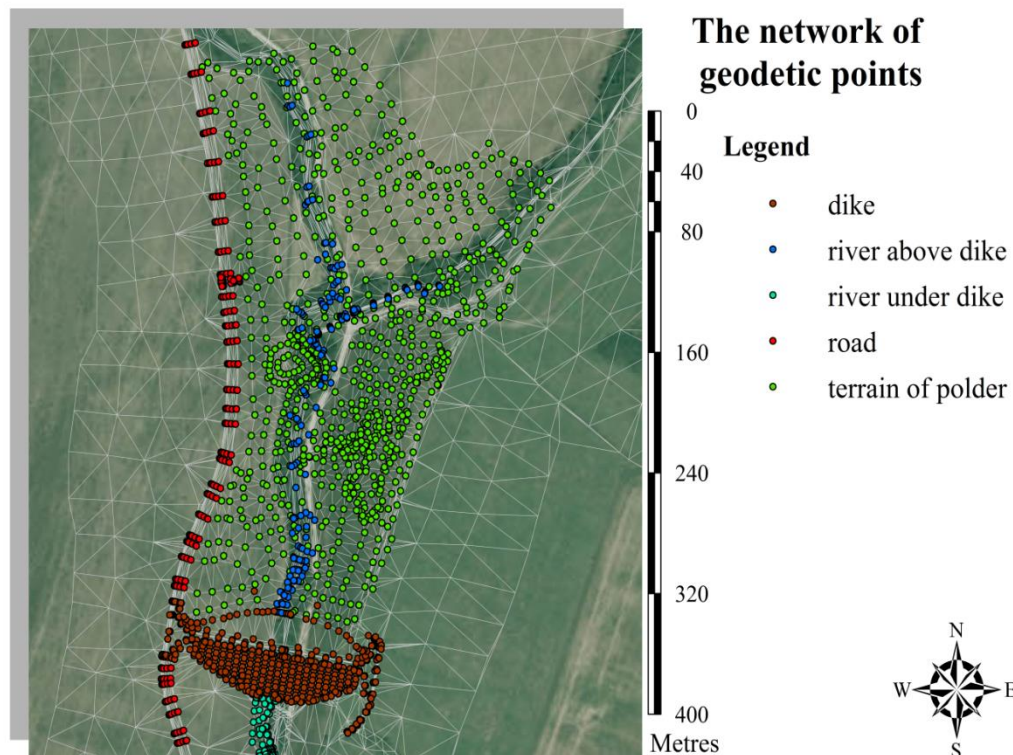


Figure 4. The network of geodetic points of the Svaceny Creek polder area using ArcMap 10.1 software.

The analysis was based on calculating the differences in height between the digital terrain model of the polder bed and the digital terrain model of the sediments. The results of this analysis are shown in Fig. 6. In the flooded area, a maximum height of 1.74 m of the sediments was identified. This maximal height of the sediments was localized near the dike. Other areas, where the erosion processes have washed away the sediments, are marked in yellow, orange and red. The maximal depth of the terrain decreased by the erosion processes was identified as around 0.54 m.

Table 1 presents an estimation of the increase in the bottom sediments after the 2015 measurements. Since 2012-2015, the sediments have increased by 10,474 m³ and have therefore reduced the retention volume to 42,864 m³.

Table 1. Comparison of the sediment yield amounts

Year of Measurement	Volume of sediments (original state) (m ³)	Retention volume of the polder in m ³ (water level 316.45 m. a. s.l)	Increase in bottom sediments (m ³)
2012	0	53,338	0
2015	10,694	42,864	10,474

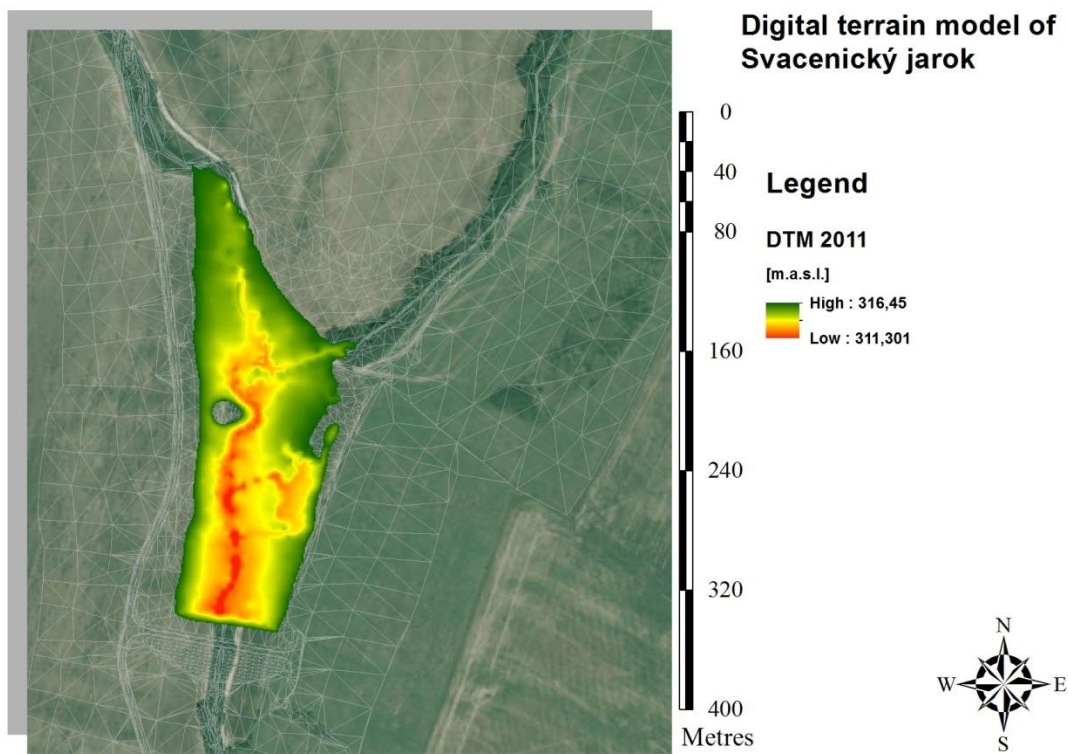


Figure 5. Digital terrain model of the polder bed (just after construction) (ArcMap 10.1).

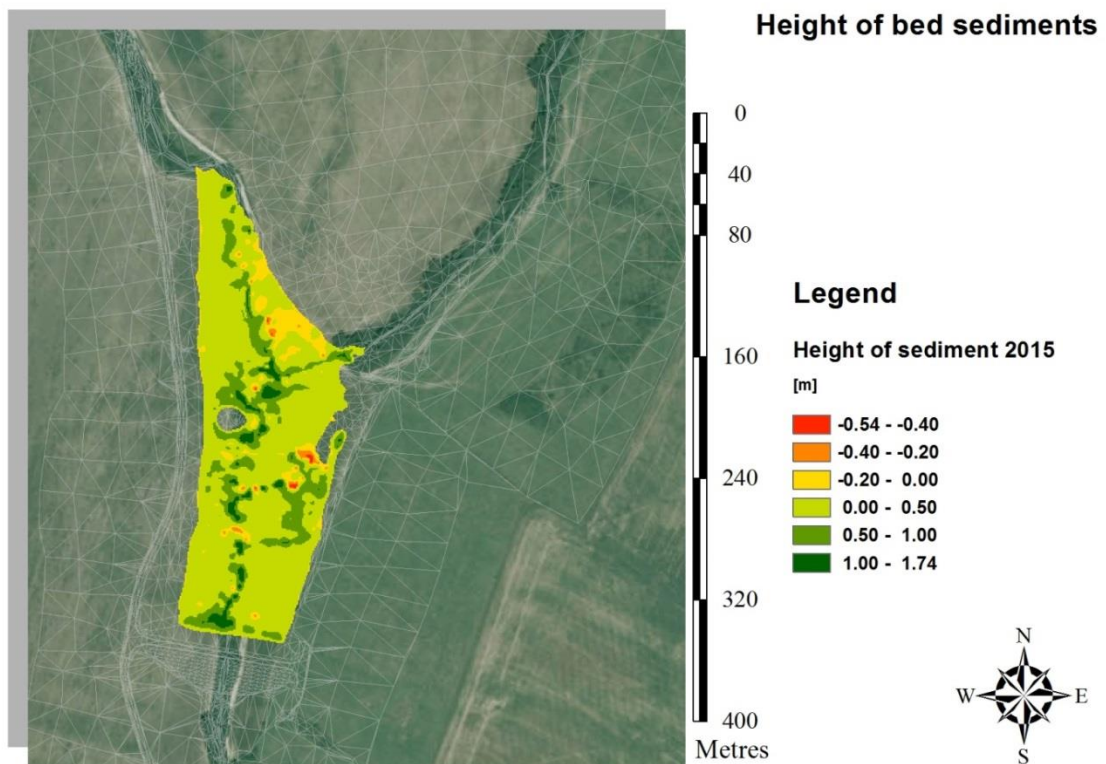


Figure 6. Digital terrain model of the bottom sediments (2015) (ArcMap 10.1).

Subsequently, we applied the USLE 2D erosion modelling to estimate the soil loss at the Svacenicky Creek catchment. The USLE is an empirical model with many limitation but it is still the most widely used prediction equation in the world. Empirical models are often criticised for simplification of the catchment processes and ignoring the heterogeneity of catchment characteristics. On the other side empirical models are frequently used in preference to more complex models in situations with limited data and parameter inputs, and are useful as a first step in identifying potential sources of sediment generation. The comparison of the mean annual soil erosion and sediment transport from the Svacenicky Creek basin with measurements of the sediment yields in the polder using the AUV EcoMapper for the period of four years after the polder’s construction is presented in Tables 2 and 3.

Table 2. Modelling of the mean annual soil erosion and sediment transport from the Svacenicky Creek basin

Erosion modelling	Method	Soil loss
Soil loss	USLE+USLE 2D	8680.16 t.year ⁻¹
Ratio of sediment transport	SDR	0.473
Sediment transport		4112.96 t.year ⁻¹

Table 3. Measurement of the sediment yields in the polder of Svacenicky Creek

Measurement	Method	
Sediment yield in 2015	AUV EcoMapper	10474 m ³
Annual average of sediment yield (2012-2015)		10474/4 years=2618.5 m ³
Annual average of sediment yield		4994.41 t

The results presented confirmed our theories about the on-going sedimentation processes in the Svacenicky Creek polder. According to the analysis presented, we determined that during the last four

years, over 10,474 m³ of sediment on the area of the Svacenicky Creek basin have accumulated. The sediment transport was estimated to be 4112.96 t year⁻¹ using the modelling. Finally, it can be stated that during the last four years, about 10,500 m³ of sediments accumulated in the Svacenicky Creek polder.

6 Conclusion

The main objective of this study was to quantify the soil loss from the agriculturally arable lands and sediment transport to the dry water reservoir (polder) of the Svacenicky Creek. The AUV EcoMapper was used to gather the data on the Svacenicky Creek polder in September 2015. Based on the field measurements of the bottom bathymetry, the current status of the clogging of the reservoir was evaluated. The results confirmed our theories about the on-going sedimentation processes in the Svacenicky Creek polder. According to the analysis presented, we determined that during the last four years, over 10,474 m³ of sediment on the area of the Svacenicky Creek basin have accumulated. The sediment transport was estimated to be 4112.96 t.year⁻¹ using the modelling. Finally, it can be stated that public awareness of the problem of reservoir sedimentation and its relation to the sustainability of reservoirs should be increased by a more appropriate transfer of knowledge from researchers to entities that intervene on the topic and the general public.

Acknowledgements

This work was supported by the EU-FP7 RECARE project under the 603498 project ID, by the Slovak Research and Development Agency under Contract No. APVV-15-0497 and VEGA Grant Agency No 1/0710/15.

References:

- [1] De Cesare, G., Lafitte, R.: Outline of the historical development regarding reservoir sedimentation. 32nd IAHR Congress, Venice, 2007.
- [2] Owens, P.: Conceptual models and budgets for sediment management at the river basin scale. *Journal of Soils and Sediments*, 5, pp. 201–212, 2005.
- [3] Williams, J.R.: Sediment routing for agricultural watersheds. *AWRA, Water Resources Bulletin*, v. 11, 5, pp. 965-974, 1975.
- [4] Walling, D.E.: The sediment delivery problem. *J. Hydrology*, No. 65, pp. 209-237, 1983.
- [5] Lane, L.J., Hernandez M., Nichols M.: Processes controlling sediment yield from watersheds as functions of spatial scales. *Environmental Modelling and Software*, 12, 4, pp. 355-369, 1997.
- [6] Van Rompaey, A.J.J., Verstraeten, G., Van Oost, K., Govers, G., Poesen, J.: Modelling means annual sediment yield using a distributed approach. *Earth Surfaces Proc. Landforms*, No. 26, pp. 1221-1236, 2001.
- [7] Fasching, R.A., Bauder, J.W.: Evaluation of agricultural sediment load reductions using vegetative filter strips of cool season grasses. *Water Environ. Res.*, 73, 5, pp. 590-596, 2001.
- [8] Foster G.R., Wischmeier W.H.: Evaluating irregular slopes for soil loss prediction. *Transactions of the ASAE*, 17, pp. 305-309, 1974.
- [9] Nelson, E.J., Booth, D.B. Sediment sources in an urbanizing, mixed land-use watershed. *J. Hydrology*, 264, pp. 51-68, 2002.
- [10] Abril, B., Knight, D.W.: Stabilising the Paute River in Ecuador. *Proceedings of the ICE. Civil Engineering*, 156, 1, pp. 32-38, 2004.
- [11] Lawrence, P.: Guidelines on field measurement procedures for quantifying catchment sediment yields, TDR project R5836, Report OD/TN77, HR Wallingford, 1996. (<http://eprints.hrwallingford.co.uk/177/1/ODTN77.pdf>, the last view on 20 March 2017)
- [12] Vijay, .S.: AUTONOMOUS UNDERWATER VEHICLES, Seminar on Autonomous Underwater Vehicles, PESCE Mandya, <http://www.scribd.com/doc/55826714/Autonomous-Underwater-Vehicles-2011>
- [13] YSI Ecomapper operation manual, 2009, YSI (Yellow Springs Instruments)

FLOOD MODEL AT RACINOVCI AND RAJEVO SELO USING THE 2D MODEL IN HEC-RAS

Slobodan Kolaković¹, Goran Jeftenić^{1*}, Matija Stipičić¹, Srđan Kolaković¹, Ljubomir Budinski¹

¹ Faculty of Technical Sciences, Trg Dositeja Obradovića 6, Novi Sad 21000, Serbia

1 Abstract

In this study conditions in the middle reaches of the river Sava will be analysed, during April, May and June 2014, when the historical maximum of flow and water level of this river was registered, and when catastrophic floods occurred. Flooding of the territory of Slavonia and Srem will be simulated with the water that reached the defended field by coming through levee breaches at Racinovci and Rajevo Selo, then merged with flood water from the west and formed a parallel stream with the river Sava. As a result of these events villages, fertile agricultural land and forests were flooded causing damage of immeasurable proportions. Based on all measurements directly from the field and the available data from competent institutions 1D model for unsteady flow in the river bed will be created as well as 2D model for flooding of abovementioned territories, whose results will show the real situation that occurred in the bed of the river Sava in May 2014. For the purposes of this analysis, it is necessary to form a DTM riverbed, floodplain and potential retentions (flooded areas), from data obtained by the traditional methods and data based on geographic information system (GIS). Hydraulic model will be created by means of software package HEC-RAS 5.0. which has RAS Mapper option with the possibility of importing digital terrain models made in GIS. HEC has added the ability for mapping of the inundated area, as well as animations of the flooding inside of the RAS Mapper features. This study shows the visual representation of streamline for flood wave in spring of 2014.

Keywords: Hydraulic analysis, 1D unsteady flow, flooding, river Sava

2 Introduction

Numerical modelling of plane flows is of great importance for hydro technical practice. In fact, many flows cannot be described with linear models due to specific morphological conditions imposed by planar characteristic of the flow. In addition, some problems require such level of details which cannot be achieved without use of plane and spatial models [1]. Numerical models may use either one-dimensional (1D) or two-dimensional (2D) models. Although the 1D modelling approach could be useful in some contexts, mainly for artificial channels, it presents several limitations for overflow analysis [2]. When water begins to overflow it becomes a 2D phenomenon and the use of a 2D model is more suitable. Thus, 2D numerical models were successfully applied for flood modelling. The discharge is used as upstream boundary condition of the main river channel and then a 2D simulation is performed [3]. One of the most popular hydraulic models is the American model HEC-RAS developed by the U.S. Army Corps of Engineers (USACE). In the year 2016 HEC-RAS announced and released its new HEC-RAS version 5.0 with 2D capabilities [4].

In this study are analysed the 2014 flood event on Sava river using the 2D capabilities of the new HEC-RAS-v5.

Location which is analysed in this paper includes the river Sava River from 206 + 000 km to 264 + 892 km as well as protected area in Croatia, Serbia and Bosnia and Herzegovina, which includes populated cities from Rajevo Selo to Račinovci. Due to the large amount of rainfall during May 2014, these settlements were flooded. The main cause of heavy rainfall, which exceeded one third of the total annual rainfall at some locations, was unusually slow-moving large deep cyclones from the Mediterranean across the Balkan Peninsula. In addition, the territory of the Republic of Serbia has already been exposed to an extremely wet period in April with a great amount of rainfall. This rainfall had already caused flooding throughout the country, which caused great material damages. Rainfall that followed was

falling continuously on 14 and 15 May and the amount of rainfall was the highest one ever registered. Due to these effects of heavy rains there was a levee breaches near Rajevo Selo (KM 233 + 880) and Račinovci (KM 212 + 878) and overflow of the river Sava basin causing damage of catastrophic proportions estimated at over 1.8 billion US dollars [5]. Water poured from the river across plains of Slavonia and Srem, leaving behind the tragic consequences. Result of this flood of epic proportions was 24,250 hectares of flooded territory, with eight settlements, infrastructure, fertile agricultural land, and great forest area.

3 Methods

3.1 Modelling of DTM

Gathering all the necessary data for any kind of numerical modeling represents one of the most challenging tasks for engineers. For the purposes of this analysis, it is necessary to form a DTM riverbed, floodplain and potential retentions (flooded areas), from data obtained by the traditional methods and data based on geographic information system (GIS) since combination of global and conventional technologies can provide best results. The conventional way of making geodetic and topographic maps related mainly to the cadastral and topographic-cadastral plans and with its update does not correspond to the specific needs of the user. For this purposes digitization was realized with manual method based on vectorization of existing topographic maps of 1: 5000. All points that represent the performance of the terrain height are vectorised and grouped in databases (Figure. 1). Embankment lines, river axis and point in inundation areas are also vectorised, and as such stored in the databases providing basis for later creation of digital terrain model in the GIS software package.

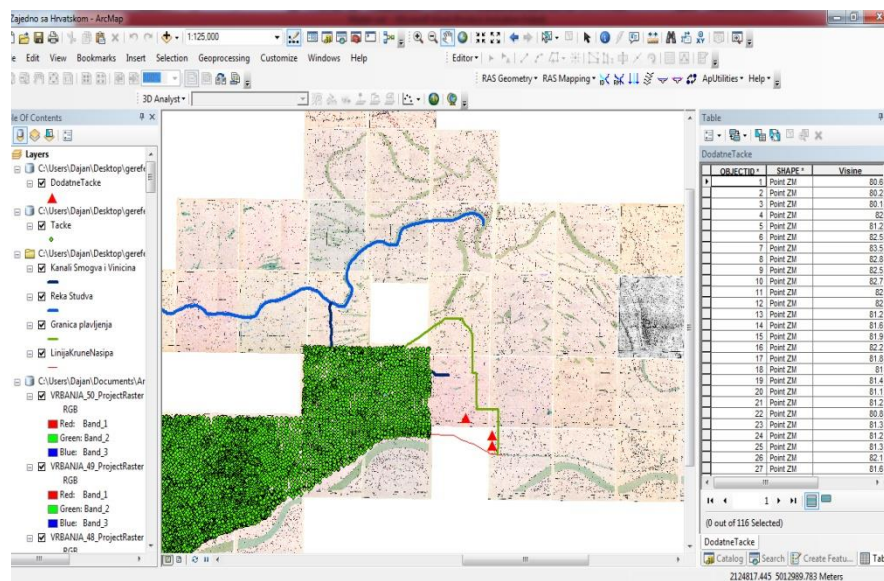


Figure 1. Vectorization of points and attribute setting

Software package HEC - RAS 5.0.0 has RAS Mapper option which offers the possibility of importing terrain models made in GIS. After imported DTM environment, it is necessary to form a DMT riverbed based on data of cross sections obtained by bathymetric measurements, and then merge them into a single DTM whereupon the ultimate model for hydraulic calculations is formed.

3.2 Numerical simulation

HEC-RAS 2D is based on finite element method as a numerical scheme, and therefore has the ability to develop structural or non-structural budget network. This additional option is very convenient to use just in case of water penetration into the defended territory to show how water is allocated according to the retention basin.

The present study used combination of 1D and 2D model when the main rivers are modelled as 1D and the floodplains are modelled as 2D (Figure 2). Model with the combination is faster than fully 2D but requires the user to define the connections between the 1D and the 2D models.

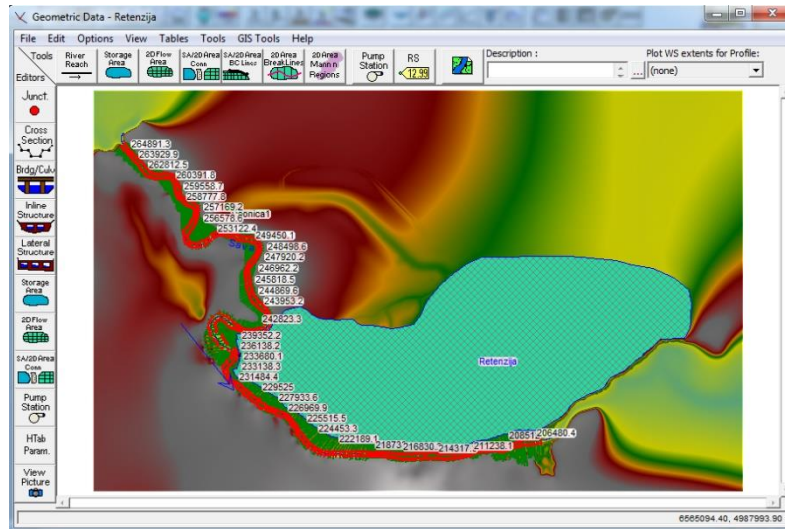


Figure 2. Vectorization of points and attribute setting

The new HEC-RAS-v5 solves either the 2D Saint Venant equations or the 2D diffusive wave equations:

$$\frac{\partial \zeta}{\partial t} + \frac{\partial p}{\partial x} + \frac{\partial q}{\partial y} = 0 \quad (1)$$

$$\frac{\partial p}{\partial t} + \frac{\partial}{\partial x} \left(\frac{p^2}{h} \right) + \frac{\partial}{\partial y} \left(\frac{pq}{h} \right) = - \frac{n^2 pg \sqrt{p^2 + q^2}}{h^2} - gh \frac{\partial \zeta}{\partial x} + pf + \frac{\partial}{\rho \partial x} (h\tau_{xx}) + \frac{\partial}{\rho \partial y} (h\tau_{xy}) \quad (2)$$

$$\frac{\partial q}{\partial t} + \frac{\partial}{\partial y} \left(\frac{q^2}{h} \right) + \frac{\partial}{\partial x} \left(\frac{pq}{h} \right) = - \frac{n^2 qg \sqrt{p^2 + q^2}}{h^2} - gh \frac{\partial \zeta}{\partial y} + qf + \frac{\partial}{\rho \partial y} (h\tau_{yy}) + \frac{\partial}{\rho \partial x} (h\tau_{xy}) \quad (3)$$

where h is the water depth (m), p and q are the specific flow in the x and y directions (m^2s^{-1}), ζ is the surface elevation (m), g is the acceleration due to gravity (m s^{-2}), n is the Manning resistance, ρ is the water density (kg m^{-3}), τ_{xx} , τ_{yy} and τ_{xy} are the components of the effective shear stress and f is the Coriolis coefficient (s^{-1}). When the diffusive wave is selected the inertial terms of the momentum equations (Eqs. (2) and (3)) are neglected [3,6].

Initially, this study considered both options the 2D Saint Venant equations and the 2D diffusive wave. The results of both methods are similar, but simulation solving the 2D diffusive wave equations is more stable and much faster. For these analysis the method with 2D diffusive wave equations are accurate enough.

For 2D simulation of flooded area was needed to define a closed polygon and the computation cells inside the polygon. The selected equations are solved with an implicit finite volume algorithm. The finite volume solution approximates the average integral on a reference volume and allows a more general approach to unstructured meshes. The solution of the equations is similar to the HEC-RAS 1D unsteady flow solution. Hydraulic property tables are computed before starting calculations. Elevation volume relationships are computed for each cell and elevation hydraulic properties (wetted perimeter, area) relationships are computed for every computational cell face, similar to the cross section preprocessing in 1D. Then, the equations are solved with an iterative scheme with a maximum of 40 iterations [3].

The computation cells may be arranged in a staggered or a non-staggered grid composed by polygons between 3 sides and 8 sides [3].

In this study was used a non-staggered grid:

-total number of cells: 120 701;

- Max. cell size 38245.24 m²;
- Min. cell size 100.83 m²;
- The average cell size 2,510.47 m².

Allocation of numerical cells in close proximity to spillways is of great importance. They should be placed in a way that the grid elements tend to form square shapes which are easier to implement. The problematic points are always the initial moments of flooding and the transition from 1D to 2D flow. Direct observation of the terrain provided data on rupture dimensions and quantity of the presented flooded area. The first levee breach occurred during enormously high water level of the river, on its curve on the 233 + 800th kilometer. Its width in the crown was about 109 m, and the level at which the demolition stopped is about 84.5 meters above sea level. Breach happened on 17.05.2014. at 14:55, and was preceded by a breakdown in the soil, which caused flushing of fine particles of sand leading to sag in the zone of the levee crown. Breach at Racinovci occurred shortly afterwards. At around 4:25 pm on the same day on a flat section of the Sava river at 212 + 878 kilometer, near the Croatian and Serbian border levee collapsed, which was caused by leakage and increased pressure in the body of the levee because the spring was very rainy and the soil waterlogged. The bottom of the spillway is 82.12 meters above sea level, and the final width of the crown is around 70 m.

Before calibration of the combined 1D riverbed model and 2D flooded area model, only calibration for river bed of Sava for the flood wave in 2013 was done. For the verification of the model was used flood wave from 2010.

After input of all the required parameters and completion of mosaic which included digital terrain model, hydrological data, Manning's coefficients, etc., it has been proceeded to the final numerical model of flooding. Simulation is carried out with time step $t=2$ minutes for the calculation, and the number of iterations for 1D flow is limited to 20, whereas for the 2D stream number of iterations is bigger, 50. Although the calibration of the models showed that the Manning's coefficients in the main bed were much smaller than usual, because in the mathematical model the Manning's coefficient does not have any physical meaning, it's mainly correction parameter. In the modeling of the flood, when the water expands across the floodplain and makes flow extremely unsteady adopted Manning's coefficient for the main river bed is 0.025 which is close to the real, while its value for the floodplain is 0.05. This choice of Manning's coefficient, taken for the purpose of corresponding to levels measured in the peak time of the flood, will later result in mistakes which will be defined further. Flooded territory is a place where after rupture of embankment water began to pour, and it was a kind of inundation with Manning's coefficient of 0.06. Namely, when the water poured through the cracks in the levee, it began to fill the space with the lowest terrain level creating itself privileged flows, basically creating a river next to the river filling up territories closest to the levee first and then those most distant, in proportion to its energy. Visual representation of streamlines is shown in Figure 3.

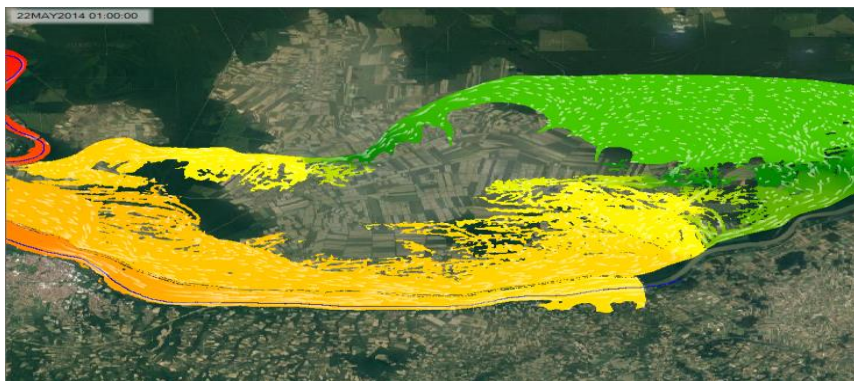


Figure 3. Visual representation of streamlines

4 Results and discussion

One of the primary goals is to interpret stacking of observed water levels and the levels in the model for the period April - June 2014. For this comparison hydrograph at Zupanja was used at river 264 + 891.3 kilometer.

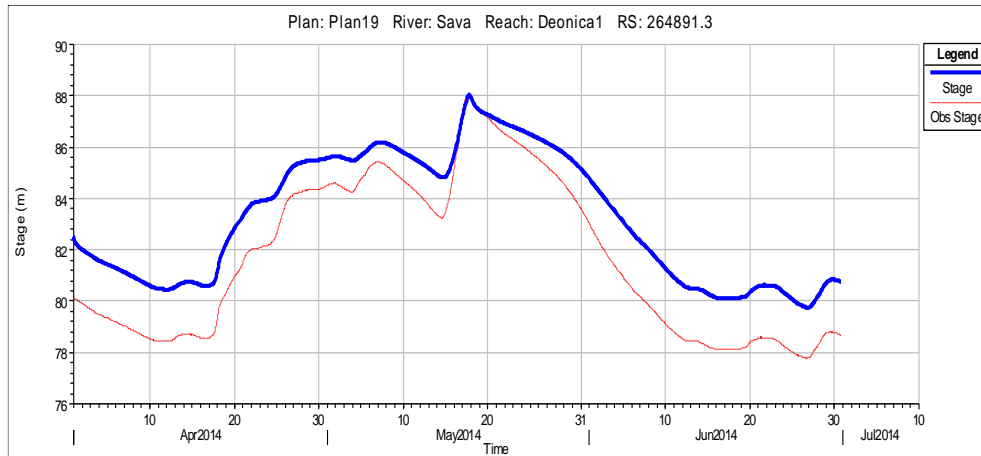


Figure 4. Observed and calculated stage at station Zupanja

Figure 4 shows that the water levels coincide in the period from 16 to 22 May, when the flow rates were in rank with centennial flows, exceeding 4200 m³/s. It has already been stated that adopted value of Manning’s coefficient for the entire section of the main riverbed was 0.025, and for the inundation 0.05, which is a problem for numerical calculations for smaller flows. However, this wasn’t the subject of the research, the emphasis is on the fact that adopted coefficients provided matching parameters of flow and levels at measuring stations in the flood period.

In this paper emphasis is on the subject of a two-dimensional flow across defended territory after rupture of levee. Levee breaches in the hydraulic sense will work as side spillway, and overflow will be calculated for sharp-edged spillway. At Figure 5 and 6 dependence between flow at spillway at Rajevo village and time is graphically showed. The levee, as graphic shows, opened around 3:00 pm 17. May and progressively expanded under flood woes, up to a maximum flow of 670 m³ /s, when it started declining until May 28, when the flow stopped through this breakthrough. During this time, through this breakthrough has passed 220 million m³ of water, which flooded surrounding villages, spreading eastward towards border between Croatia and Serbia and together with water leakage from another breakthrough created a parallel flow to the river Sava.

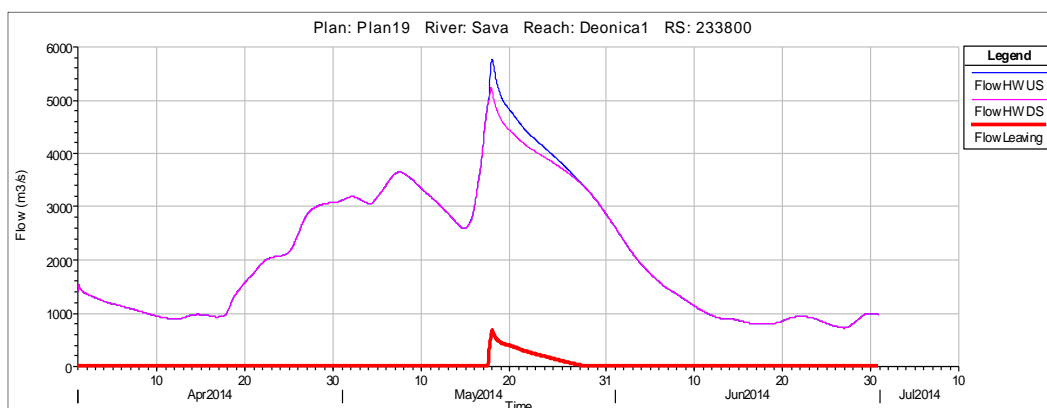


Figure 5. Discharge through levee breach near Rajevo Selo

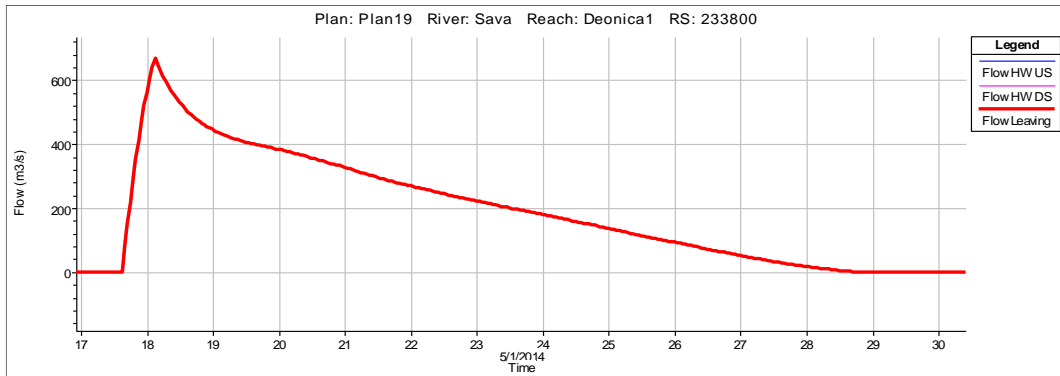


Figure 6. Discharge through levee breach near Rajevo Selo

Figure 7 also clarifies how breakthrough at settlement Račinovci manifested. Soon after 4:00 pm water penetration through cracks started filling up surrounding terrain of lower levels, and then more remote parts in proportion to its energy. However, this graph shows irregularities during the period when the flow in the river bed drops below 4200 m³/s when above mentioned phenomenon of dependence between Manning’s coefficient and flow quantity lead to non-matching data obtained by calculation and measured data. On that occasion, junction of 1D and 2D flow reaches the point where flow every half hour changes the direction and runs from river, and then back to the river, which is manifested with sharp change of flow at the graph. After some time, when water level of the river decline to the point where it’s equalized with the level in littoral area and achieve a tendency of constant decline, the water from the flooded area will return to the riverbed, which graph shows as a negative flow in the period from 24 May to June 1. Maximum flow through this opening is obtained by calculation and its value is 827 m³/s, and it will contribute to flooding with an additional 80 million m³ of water.

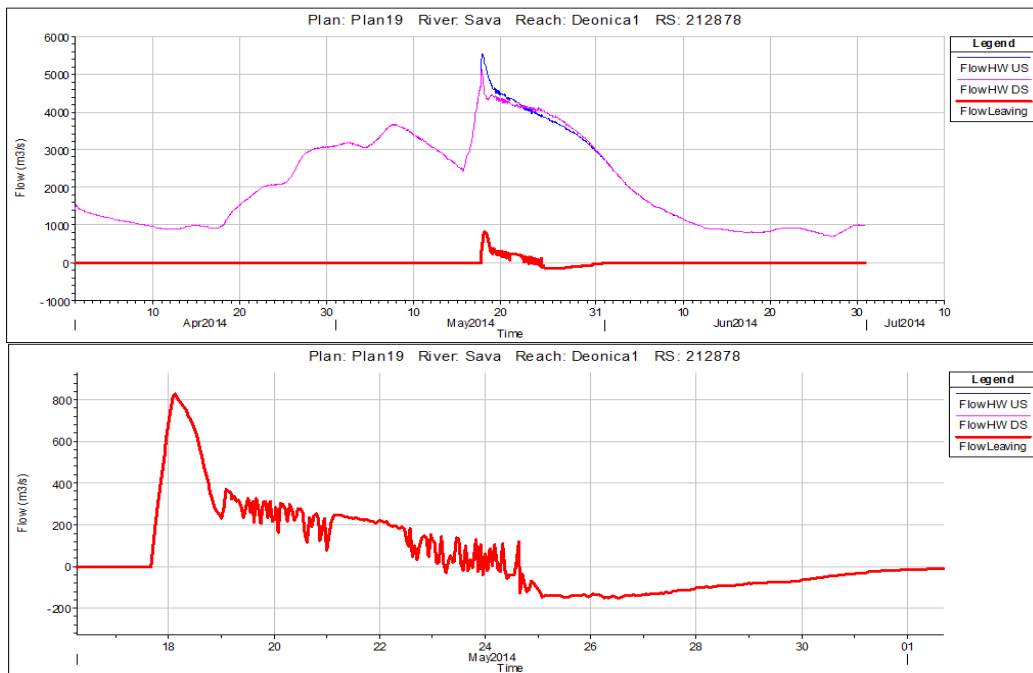


Figure 7. Discharge through levee breach near Racinovac

In Figure 8 - 11 shows the situation in which are shown the locations of penetration of levees and expansion of flooded area over time.

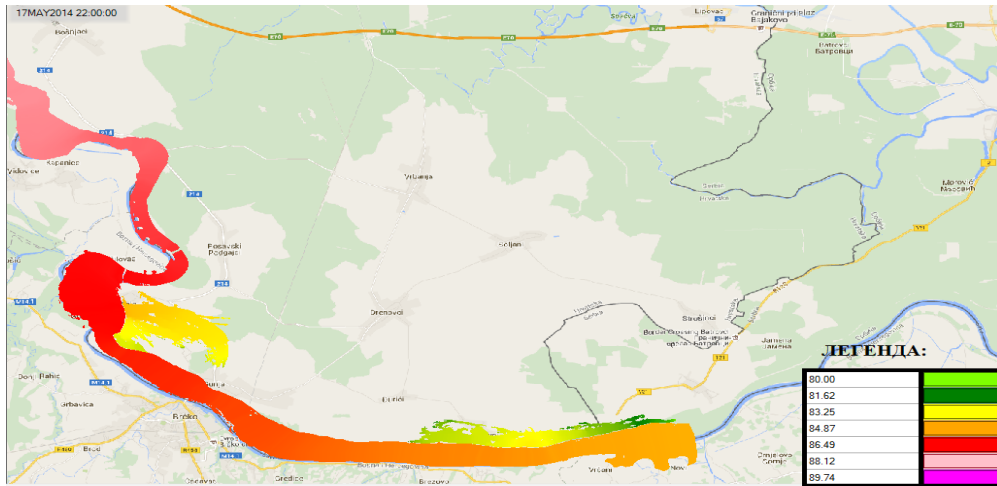


Figure 8. Situation map at the beginning of floods

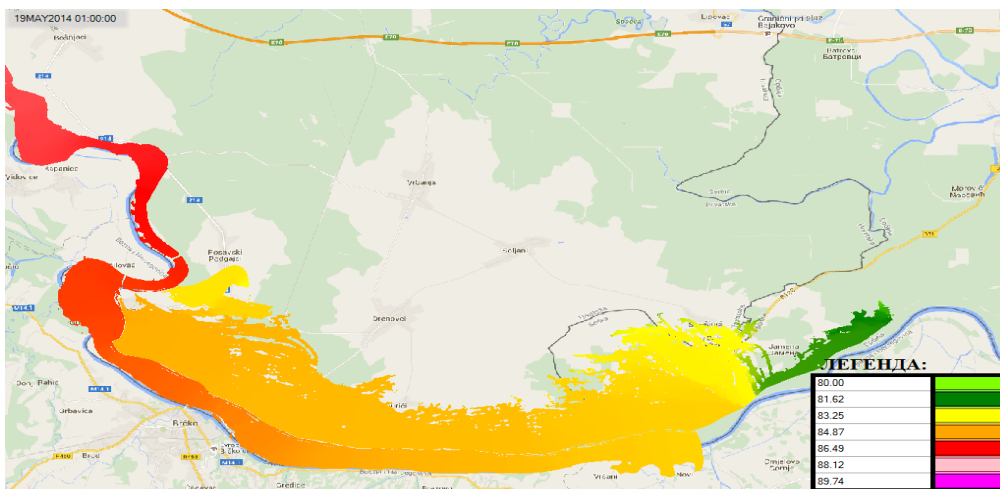


Figure 9. Situation map of flooded area and water level on the 2th day of floods

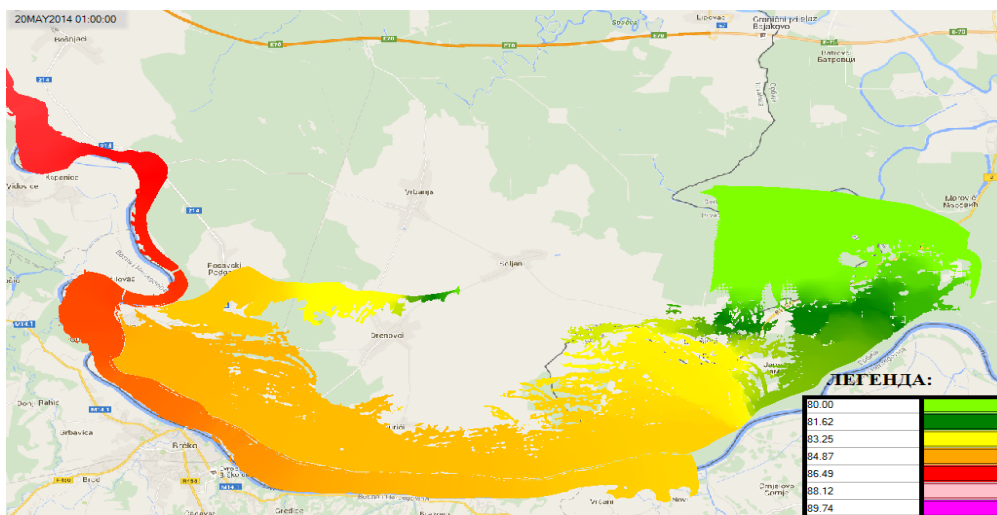


Figure 10. Situation map of flooded area and water level on the 4th day of floods

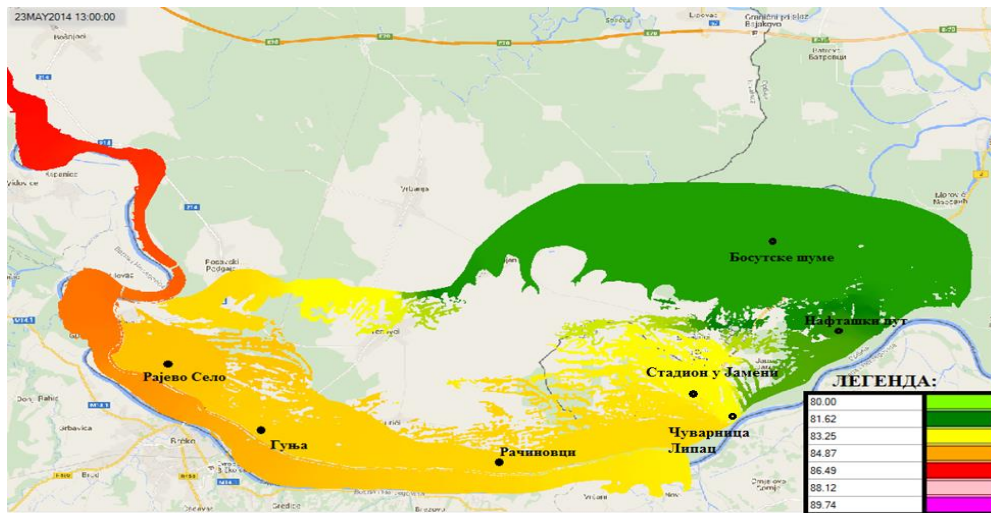


Figure 11. Situation map of flooded area with gauging points of water level

5 Conclusion

This study shows that the new HEC-RAS version 5 is an important tool for studying and understanding flood events.

The simulation shows very good performance when comparing the simulation results with flood extent registered on the field. Besides, the simulation provides additional information like flood depth, flow velocity and flood duration.

Model has been shown that in some areas the water maintained for a relatively short time (5-7 days), while in some a considerable amount of water accumulated and maintained for a longer period of time. From the aspect of this study the improvement of measures for flood protection in the middle course of the Sava is the most emphasized. This area is very rich in forests, especially on the left bank of the river Sava, where the level of terrain is low, showing a great potential to develop as retention in the future. In the upper section of the river Sava for relief from high water upstream there are Lonja and Odrovsko retention basins, while in the lower reaches reduction of the flood peak can be dampened with Obedska Bara. But in the middle course of the Sava, where floods took place there are no retentions in which can be released large amount of water to minimize the hydrograph flood peaks in large cities along the Sava. In accordance with the tendencies of the European organizations, with special reference to the Framework Directive on the assessment and management of flood risks this paper has shown that in the future we have something to think about. It is high time to start thinking about establishing retention area in the rich forests that is bordered by the Sava River levee in the south, and the Bosut and Studva on other sides. This area has a large accumulation potential and it could be used for permanent effective flood protection in the long period.

Acknowledgements

This work is supported by Ministry of Education and Science, Republic of Serbia (Grant No. TR37003, TR37018).

References:

- [1] Jovanovic M., Osnove numeričkog modeliranja ravanskih otvorenih tokova, Univerzitet u Beogradu, Građevinski fakultet Beograd. 1998.
- [2] Srinivas K, Werner M, Wright N. Comparing forecast skill of inundation models of differing complexity – the case of Upton upon Severn. In: Allsop W, Samuels P, Harrop J, Huntington S, editors. Flood risk management: research and practice. London: Taylor and Francis Group; ISBN 978-0-415-48507-4, 2009.
- [3] Moya Quiroga V., Kurea S., Udoa K., Manoa A., Application of 2D numerical simulation for the analysis of the February 2014 Bolivian Amazonia flood: Application of the new HEC-RAS version

- 5, *Revista Iberoamericana del Agua* 3, pp. 25–33, 2016.
- [4] Brunner G., Combined 1D and 2D modelling with HEC-RAS, US Army Corps of Engineers pp. 130, 2014.
- [5] Siebert S., Teizer J., Mobile 3D mapping for surveying earthwork projects using an Unmanned Aerial Vehicle (UAV) system, *Automation in Construction* vol. 41, pp. 1-14, 2014.
- [6] Brunner G. HEC-RAS River Analysis System – 2D Modeling User’s Manual, US Army Corps of Engineers - Institute for Water Resources - Hydrologic Engineering Center (HEC), Davis, 2015.

FLOOD MODELING OF WETLAND RESTORATION IN EZERANI NATURE PARK, PRESPA LAKE WATERSHED

CVETANKA POPOVSKA ¹, ANGELCO PANOV ², DIMITRIJA SEKOVSKI ³

¹*Faculty of Civil Engineering, Republic of Macedonia, popovska@gf.ukim.edu.mk*

²*PointPro Consulting, Republic of Macedonia, angel.panov@pointpro.com.mk*

³*United Nations Development Programme, Republic of Macedonia, dimitar.sekovski@undp.org*

1 Abstract

The canalization of the river delta of Golema Reka extending along the northern shores of Lake Prespa disconnected the riverbed from its natural floodplain, reducing the filtering capacity of the former wetland against the upstream pressures. The ongoing UNDP-backed *Lake Prespa Restoration Programme* formulated an engineered wetland design to restore area's natural filtering functions and create additional ecosystem benefits. This paper summarizes the findings of the hydraulic modelling of the engineered wetland using HEC-RAS for a number of flooding scenarios, and land-use limitations.

Keywords: Wetland Restoration, Ezerani Nature Park, Flood Modeling, HEC-RAS

2 Introduction

The development pressures in the Prespa Lake watershed have caused considerable loss of valuable landscape elements that provided critical ecological services and contributed to the watershed's ecological integrity. The combined influence of the natural and human factors has particularly harsh impact on the Ezerani wetland area – a natural high value ecosystem located along the northern shoreline of the Lake Prespa. Located at river delta of Golema Reka – the largest and currently most degraded tributary of the Lake – the Ezerani wetland has played an important filtering function, helping to mitigate upstream human pressures.

The canalization of the river delta in the 1990s is considered to be among the most significant human intervention. Disconnecting the river channel from its natural floodplain dramatically reduced the wetland area and its filtering capacity. As a result, considerable quantities of pollutants and nutrients are being continuously discharged into the Lake (Figure 1). The occasional flood events are the reason for individual or locally organized interventions in the river channel – its strengthening and deepening being the most common flood control practice. This disturbance allows the river forces to further incise the alluvial river channel, which also affects the stability of existing structures.

The ongoing UNDP-backed Lake Prespa Restoration Programme formulated and adopted a management plan for the area (part of a recently re-designated protected area – Ezerani Nature Park) that foresees significant wetland restoration/engineering activities, in order to provide: a) water retention of Golema Reka, allowing the wetlands to slow and filter inflows from the watershed, b) tertiary treatment of the wastewater from the existing nearby municipal Wastewater Treatment Plant (WWTP), c) flood control function, d) retention of untreated wastewaters in event of high hydraulic load or WWTP malfunction, and e) additional wetland related benefits (wildlife habitat, recreational and aesthetic values, biomass generation).

To be able to assess comparatively various wetland restoration alternatives, a few alternatives have been evaluated against a number of assessment factors (financial, economic, environmental and social). The alternatives differ in the ambition of the restoration objectives and include full or partial restoration of the former riverbed, use of existing abandoned fishponds or a compensation of the lost wetland area, regulation/stabilization of the existing riverbed as a flood control measure, etc. Based on a multi-

criteria, and cost-benefit analysis, as well as community-based prioritization, the process proposed a single restoration alternative.

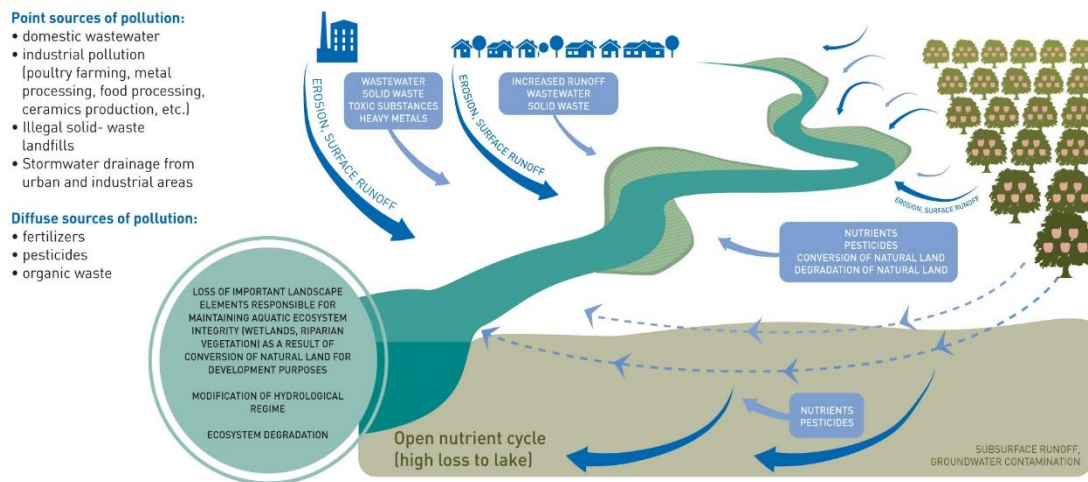


Figure 1. Summary of effects of the degraded Ezerani wetland – opening of nutrient cycle and modifying the hydrological regime

The proposed alternative takes into account the multitude of limitations (e.g., legal, land-use structure, financial, organizational, cultural), avoiding – to the extent possible – the use of private land. Such an approach greatly improves the possibilities for implementing the wetland restoration plan, as well as sustainability prospects of the intervention. It includes creation of a sufficient wetland area that would ensure filtering of Golema Reka in combination with the effluent from the WWTP.

2.1 Proposed technical solution

From a technical perspective, the selected wetland restoration option presents a complex hydraulic system comprising: a) a continuation of the existing upstream regulation of Golema Reka in length of 1,280 m (to provide better protection of the frequently flooded developed/agricultural land); b) lifting the level of the regulated riverbed by constructing a barrier / water distribution structure; c) two open canals to divert low flows in the retention area; d) a downstream weir to enable retention of the adopted design discharge; e) left and right embankments connected to the downstream weir (the right embankment closes the retention area by connecting to the embankments of the existing fishponds; and f) a pipeline for delivering the effluent from the existing WWTP to the retention/wetland area. The conceptual design for this restoration plan is presented in Figure 2.

This approach is adapted to consider the existing conditions of the riverbed and limitations imposed by the current land-use. The design is composed of the following functional hydraulic elements: a) inlet section with protective carpet upstream of the barrier dam; b) barrier dam with weepholes, a small spillway for evacuation of average discharge and a large spillway for evacuation of high discharges with volume greater than the retention area; c) stilling pool for energy dissipation of the overflow discharges; d) transitional section for connecting the stilling pool with the natural riverbed of Golema Reka and e) earth embankments for creation/closing of the retention area. Besides the filtering functions, the wetland restoration needs to avoid – to the extent possible – temporary or permanent flooding of private land.

The hydraulic dimensioning of structures was carried out for normal flow conditions in Golema Reka with long-term average monthly discharges with probability of 80% as well as for maximum discharges with return period of 20 and 50 years. The maximum Q20 flow corresponds to the discharge capacity of the existing bridges upstream of the wetland. Q50 is selected as a design discharge for sizing the large spillway as the height of the embankments for creation of the retention area is determined by the local infrastructure. The embankments and the barrier dam create together a retention area of approximately 100 hectares and sufficient volume to accommodate the design flood wave. The left embankment (735.7 m long) which extends eastwards joins the embankment of the existing fishpond. The right embankment

is 1,215 m long and it extends westwards. It has more significant height variations and connects to the left bank of the old riverbed of Golema Reka.

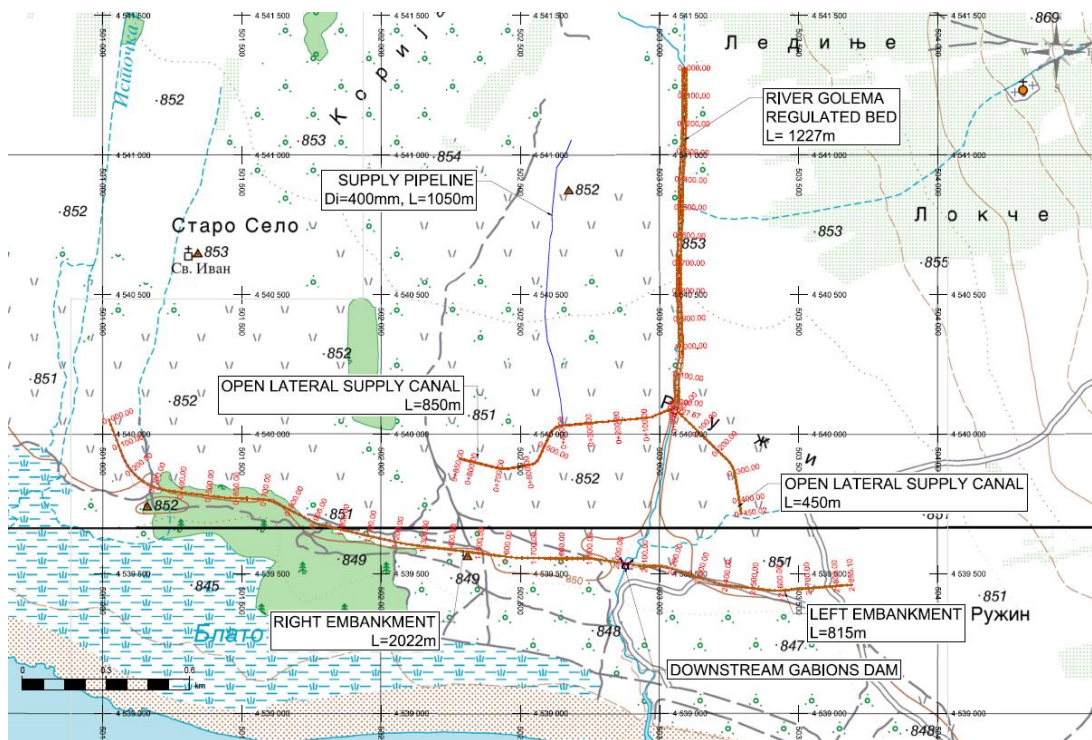


Figure 2. Layout of the conceptual technical solution for Ezerani wetland restoration

3 Methods

The hydraulic modelling of this engineered wetland was carried out by using HEC-RAS – designed to simulate one and two-dimensional calculations for a network of natural and constructed channels. This software contains several river analysis components: 1) steady flow water surface profile computations; 2) one and two-dimensional unsteady flow simulation; 3) movable boundary sediment transport computations; and 4) water quality analysis. All four components use a common geometric data representation and common geometric and hydraulic computation routine.

The unsteady flow simulation component is capable to combine one and two-dimensional flow through a full network of open channels and floodplains. The hydraulic calculations for cross-sections, bridges, culverts, weirs and other hydraulic structures developed for the steady flow component were incorporated into the unsteady flow module. Special features of the unsteady flow component include: levee breaching and overtopping, dam break analysis, pressurized pipe systems and pumping stations.

The unsteady flow component is based on 2D Saint Venant equations or on 2D Diffusion Wave equations and the user can easily switch between equation sets. In general, the 2D Diffusion Wave equations allow the software to run faster and have greater stability properties. The equations are solved by implicit finite volume method which algorithm allows larger computational time steps than explicit methods. 2D flow areas can start completely dry and handle a sudden rush of water into the area. Additionally, the algorithm can handle subcritical, supercritical, and transitional flow regime such as hydraulic jump.

For 2D flow analysis a digital elevation model (DEM) of the area was prepared based on detailed geodetic survey of the corridor of Golema Reka and the Ezerani wetland (Figure 3). This model was improved around the bridges to avoid the flow discontinuities. The corrections were done by RAS Mapper using orthophoto map with resolution 0.5 m and topographic map in scale of 1:25,000.



Figure 3. Flooded area on DEM placed over orto map as a base.

The investigated area was defined as computational mesh with cells of different shapes and sizes (1x1 m in the riverbed to 5x5 m in the wetland/floodplain). The underlying terrain and the computational mesh are pre-processed in order to develop detailed elevation-volume relationships for each cell, and also detailed hydraulic property curves for each cell face (elevation vs. wetted perimeter, area, and roughness). The roughness coefficient (n) for the cells is estimated to be $0.03 \text{ m}^{-1/3}$ s for the riverbed and $0.05 \text{ m}^{-1/3}$ s for the wetland/floodplain areas.

The boundary conditions that can be applied are external and internal/structures. The external boundary condition at upstream end is simulated with flow hydrographs, and at downstream end with normal depth at steady flow. The internal boundary condition was flow calculated by weir equation. The hydrographs at upstream river section in flood simulation were obtained by SCS Curve Number Method by the use of precipitation data from nearest meteorological station in Resen (Restoration of Golema Reka, UNDP Project, 2006). The obtained hydrographs with different return periods are shown in Figure 4. The computational time step applied was 5 seconds and the simulation was performed until the flood wave reaches the downstream boundary section. The simulation scenarios carried out for a period of 48 to 72 hours.

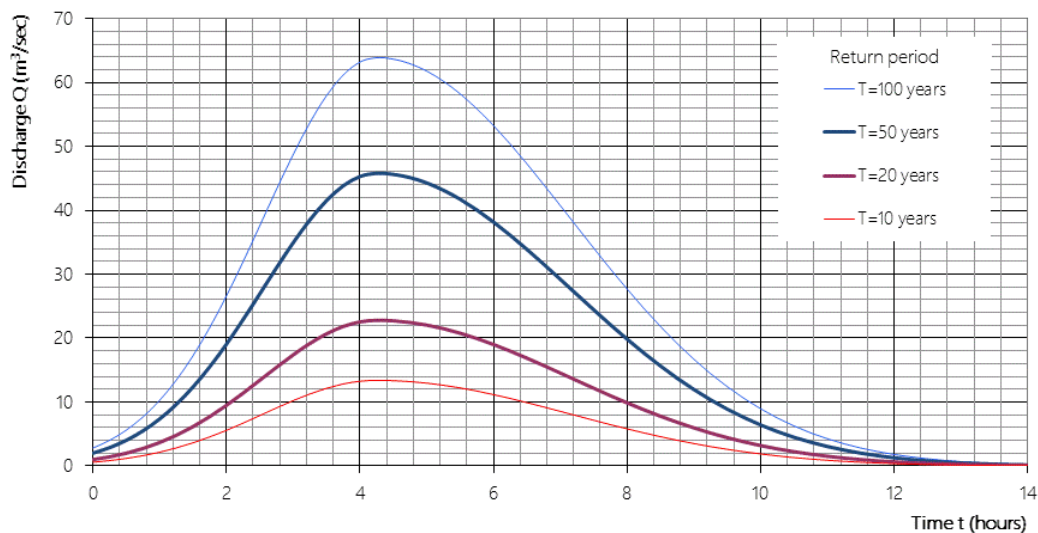


Figure 4. Flow hydrographs with different return periods at upstream river section.

4 Results

As part of the hydraulic modelling exercise the following five scenarios were analysed to assess the functionality of the proposed restoration design (to achieve the retention of nutrient/pollutant enriched water and avoid flooding of private property):

Scenario 1: normal conditions. All structures are fully operational. The initial river flow is at its average monthly value ($Q=1.5 \text{ m}^3/\text{s}$) and the flood wave has a return period of 20 years ($Q=22.8 \text{ m}^3/\text{s}$). The results show that the flood wave is completely retained, reaching water level elevation of 850.44 m asl which is below the elevation of the spillways. The retention time of the flood wave is over 40 hours and the water is released through the weepholes placed on the barrier dam.

Scenario 2: half of the weepholes are out of operation. The flow conditions upstream the dam remain the same as in the first scenario. The simulation shows good retention of the flood wave, reaching water level elevation of 850.59 m asl that initiates minor flow over the large spillway.

Scenario 3: all weepholes are out of operation. The flow conditions remain the same. The obtained results show decrease in retention capacity and achieving water level elevation of 850.86 m asl. There is an overflow of approximately $6 \text{ m}^3/\text{s}$.

Scenario 4: all weepholes and the secondary/small weir are out of operation. All other flow conditions remain the same. The obtained results show decrease in retention capacity, and water level elevation of 851.06 m asl. There is an overflow of approximately $6.5 \text{ m}^3/\text{s}$.

Scenario 5: all weepholes and the secondary/small weir are out of operation. The initial river flow is at its average monthly value ($Q=1.5 \text{ m}^3/\text{s}$) and flood wave is with return period of 50 years ($Q=45.8 \text{ m}^3/\text{s}$). The results show water level elevation of 851.4 m asl that is below the top of embankments. The maximum overflow on the large spillway is $19.0 \text{ m}^3/\text{s}$ that is below its designed capacity. Hence, the stability of all structures is confirmed.

The simulations of the flooded area and the retention capacity over time (from 27 September 2015 at 01:30 to 29 September 2015 at 00:00) for the conditions described in Scenario 5 are presented in Figures 5 and 6. The resulting hydrographs from the hydraulic simulations are shown in Figure 7.

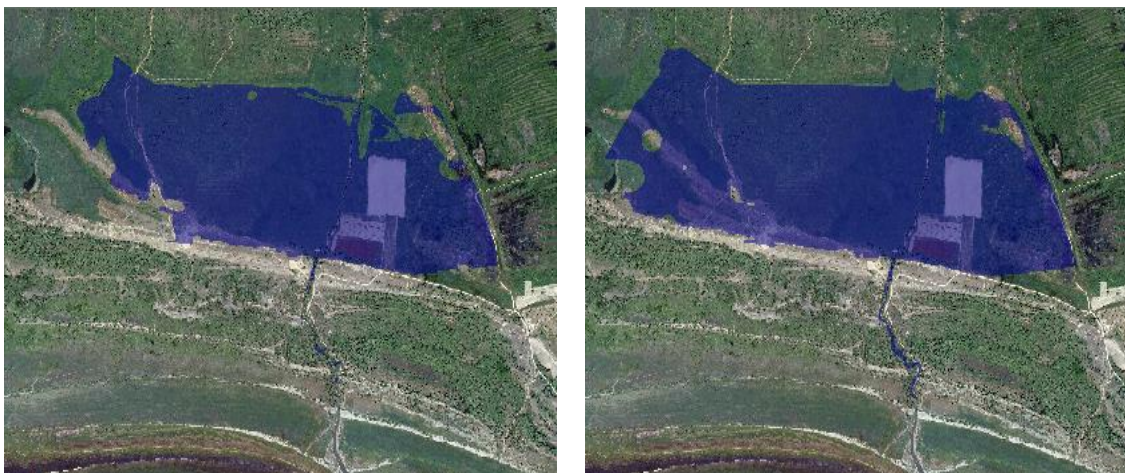


Figure 5. Simulation of flooding at $Q_{50}=45.8 \text{ m}^3/\text{s}$. Left: 27 Sept 2015 at 01:30 ($Q_{\text{inflow}}=1.5 \text{ m}^3/\text{s}$, $Q_{\text{spillway}}=1.5 \text{ m}^3/\text{s}$, $WS=850.60 \text{ m asl}$). Right: 27 Sept 2015 at 06:15h ($Q_{\text{inflow}}=45.8 \text{ m}^3/\text{s}$, $Q_{\text{spillway}}=9.39 \text{ m}^3/\text{s}$, $WS=851.1 \text{ m asl}$).

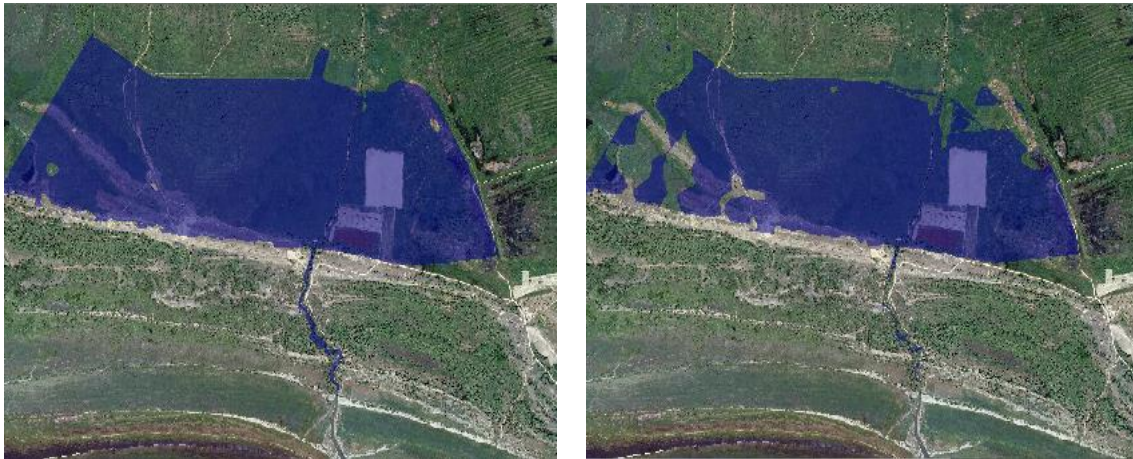


Figure 6. Simulation of flooding at $Q_{50}=45.8\text{m}^3/\text{s}$. Left: 27 Sept 2015 at 10:00h ($Q_{\text{inflow}}=19.85\text{m}^3/\text{s}$, $Q_{\text{spillway}}=18.99\text{m}^3/\text{s}$, $WS=851.39\text{m asl}$). Right: 29 Sept 2015 at 00:00h ($Q_{\text{inflow}}=1.5\text{m}^3/\text{s}$, $Q_{\text{spillway}}=2.17\text{m}^3/\text{s}$, $WS=850.82\text{m asl}$).

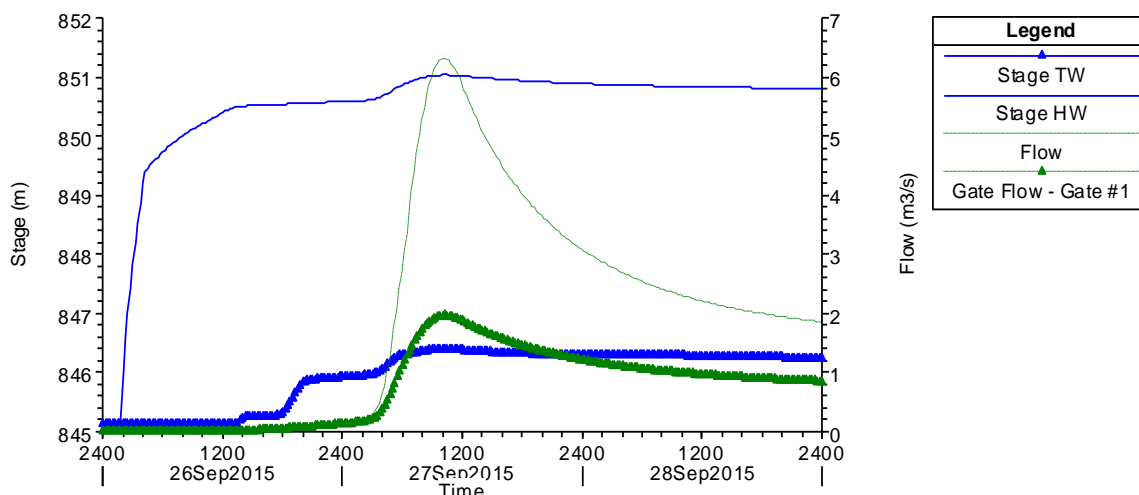


Figure 7. Stage (HW-head water, TW-tail water) and flow hydrographs at the downstream dam profile.

5 Conclusion

This brief analysis of the main environmental problems in Golema Reka watershed in Prespa region shows that most of them are related to the human activities and current socio-economic and political conditions, and thus special attention should be given to them when the restoration and protection measures are being designed. The main problems are: serious decline of water quantity and quality, significant reduction of biological diversity, significant erosion and sediment load into the lake, frequent flooding of agricultural lands, insufficient monitoring, insufficient water management, low public awareness.

This paper deals with case study on wetland restoration/engineering designs that are often limited by a number of constraints, including: a) regulatory (e.g., imposed by planning documents, flood control standards); b) technical (need to incorporate existing structures, ensuring stability); c) financial (e.g., land expropriation, capital investment and maintenance costs); d) societal/cultural (competing interests between different land-uses). Land ownership and development plans need to be given due consideration in the design process. Flood modelling can help in identifying solutions that will avoid flooding of private land, and can be very useful in communicating the findings with the affected communities and building consensus on the restoration goals. The selected restoration design for the Ezerani wetland area

helps fulfil the primary objectives of the initiative (sufficient retention area and improved filtering capacity), by minimizing the conflict with the competing land-uses.

References:

- [1] Popovska, C., Bonacci, O. (2007). *Basic Data on the Hydrology of Lakes Ohrid and Prespa*. Hydrological Processes, Wiley InterScience
- [2] Popovska, C., Sekovski, D. (2011). *Hydrological Sub-watershed Analysis of the Prespa Region*, International Conference 'Earth on the Edge: Science for a Sustainable Planet', International Union of Geodesy and Geophysics (IUGG), Melbourne, Australia
- [3] Sekovski, D., Popovska, C. (2013). *Ecohydrological Solutions to River Corridor and Wetland Restoration – The Concept for the Golema Reka River in the Prespa Lake Basin*, Twelfth International Symposium on Water Management and Hydraulic Engineering (WMHE 2013), Bratislava
- [4] Sekovski, D., Popovska, C., Zdraveski, N. (2012). *Applying the Ecohydrological Approach at Watershed Scale to Restore Freshwater Ecosystems*, Conference on Water Observation and Information System for Decision Support (BALWOIS), Ohrid
- [5] UNDP (2006). *Restoration of Golema Reka*, Basic Design, Geing, Skopje
- [6] UNDP (2011). *Prespa Lake Watershed Management Plan*, Geotehnicki inženiring, Skopje
- [7] UNDP (2012). *Feasibility Study for Wetland Restoration*, Ambisat, Madrid
- [8] UNDP (2013). *Basic Design for Wetland Restoration*, Hidroenergo Inženiring, Skopje

ANALYSIS OF ICE REGIMES ON THE DANUBE IN DALJ IN 2012. AND 2017.

MARIJA ŠPERAC ¹, TOMISLAV SLUNJSKI ²,

¹ *J.J.Strossmayer University of Osijek Faculty of Civil Engineering, Vladimira Preloga 3, 31000 Osijek, Croatia, msperac@gfos.hr*

² *Hrvatske vode, VGO Dunav i donja Drava, Služba zaštite od štetnog djelovanja voda, Splavarska 2a, 31000 Osijek, Croatia, tomislav.slunjski@voda.hr*

1 Abstract

The regime of ice in rivers represent the spatial and temporal regularity of occurrence in watercourses. In hydrological terms distinguish ice drift and a static ice. Ice regime of natural rivers is influenced by climate, water regime and channel morphology. Since channel morphology and water regime are influenced by river dams, changes in ice conditions can be expected. Regular ice phenomena observation mostly dates back to the 19th century. During this long-term observation period, the human impacts on the river hydrology and morfology have become more and more intensive. River ice regime could characterise by the date of drift-ice appearance, freeze-up, break-up and river ice disappearance, furthermore the duration of ice-affected and ice-covered season. Ice-on is the date of ice appearance, when ice drifting starts. Freeze-up is the date of continuous and immobile ice-cover occurrence. Break-up is the date, when the ice cover begins to move downstream and open water areas appear. Ice-off is the date of ice disappearance, when the river becomes ice-free. The Danube is the second length of the rivers in Europe, long 2857 km (188 km in Croatia). Flows through the nine European countries or is their border river. For the water regime of the Danube is characterized by big water level fluctuations. Danube freezes only for the strong winter, the lower course of the thickness of the ice is up to 60 cm. Therefore, navigation occasionally suspended from mid-December to early March. In this paper, we analysed the two ice regime on the Danube in Dalj in Croatia, recorded in 2012 and 2017. The consequence of ice on watercourses is to create backflow and reduce the flow profile, which can result in the appearance of ice floods. To prevent the appearance of ice floods on the Danube, the ice was broken by icebreakers, and in some places are mined with explosives.


Keywords: ice regimes, Danube, Croatia, ice flood, icebreaker







2 Introduction


Ice regime of natural rivers is influenced by climate, water regime and channel morphology. Regular ice phenomena observation mostly dates back to the 19th century. In hydrological terms distinguish ice drift and a static ice.

The ice formation process on the rivers can be divided into several phases shown in Table 1.

Table 1. [1]

FRAZIL	The first stage in river ice formation is when crystals start to form and grow. But the water movement interrupts crystal growth and the crystals don't join together to form a sheet. Instead you get a mixture of ice crystals and water that looks like a wet slushie. The crystals are called frazil and the mixture of crystals and water is called frazil slush.	
--------	--	---

<p>PANCAKE</p>	<p>As the temperature drops frazil ice clusters start to freeze together and form plates of ice called pancake ice or frazil pans. These are usually rounded and often have raised edges formed by the repeated collisions with other pancakes. Areas of frazil slush usually separate the pancakes.</p>	
<p>BORDER ICE</p>	<p>Solid ice usually begins to form along the shore of the river. There is less movement of water here so ice forms more easily and the temperature in the shallow water along the shore drops faster on a cold night. Both factors lead to a margin of ice along each shore, a condition referred to as border ice or shore ice. Border ice may continue to grow gradually toward the center until the river freezes over.</p>	
<p>FREEZUP</p>	<p>If the temperature drops quickly enough the frazil slush and frazil pans in the center of the river may freeze up quickly and cover the center of the river all at once. Sometimes this mass of ice, which is semi-solid at first, may restrict the flow of water and form an ice jam.</p>	
<p>SHEET ICE</p>	<p>Whether by the border ice meeting in the center or by a more rapid freeze up of the pancake/frazil ice, when the river is completely covered it is referred to as sheet ice. As the cold weather continues the ice becomes thicker and thicker. But unlike lake ice, where the thickness is uniform and safe to walk on, river ice may have thin spots.</p>	
<p>CANDLE ICE</p>	<p>These freeze-thaw cycles produce a honeycomb of water and long hexagonal crystals of ice called candles. This ice is referred to as "rotten ice" and even though it may still be many inches thick is not solid enough to walk on safely.</p>	
<p>BREAKUP</p>	<p>As the water begins to rise during the spring melt the rotten candle ice gives way, cracking into blocks that float downriver. If there are constrictions in the river, such as where bridge abutments have been placed out into the river, the breakup ice may jam the river and cause flooding. Unfortunately it is often our human manipulation of the river that causes these constrictions and since we usually do this in our towns and villages, it is usually the towns and villages that are damaged by ice jams.</p>	

<p>ANCHOR ICE</p>	<p>Ice attached to the streambed is called anchor ice. It forms under a variety of circumstances in areas where the water is shallow enough to freeze all the way from the surface down to the bottom. It is more likely to form in the headwaters, in the shallows along the edges of the river, or in riffle areas. It is more likely to form in colder winters and when there is less snow insulating the surface</p>	
--------------------------	--	---

Study area

The Danube is the second longest river in Europe, long 2857 km (188 km in Croatia). Flows through the nine European countries or is their border river.

Throughout its flow through the Republic of Croatia, Danube is an interstate that runs along the area of high-density population and environmentally sensitive area of Kopački Rit Nature Park.

In this paper, we analysed the two ice regime on the Danube in Dalj in Croatia, recorded in 2012 and 2017. Dalj is the village located on the right bank of the Danube in Croatia. It represents a critical point for the defense of the ice and flood. (Figure 1.)

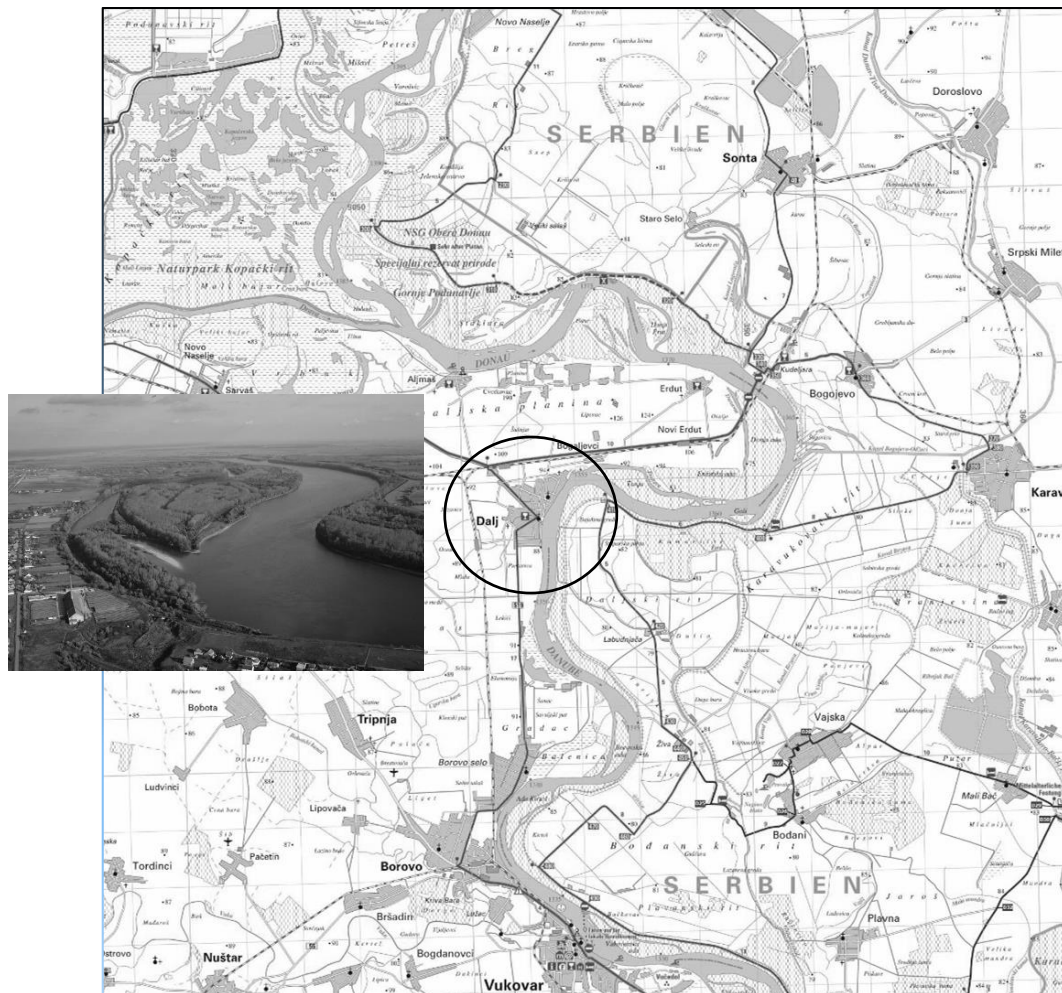


Figure 1. Position of Dalj on Danube River in Croatia

3 Ice regimes on the Danube in Dalj

3.1 Ice regime in February 2012

Due to the long-term, very cold air temperature at the end of January and early February 2012 on the territory of the Republic of Croatia, but also in Central Europe, ice formation occurred on the Danube. In this period, the extremely cold air temperature and intense ice formation on the Danube caused a slowdown and the water level was rising steeply registered downstream on the territory of the Republic of Serbia, while this growth was less pronounced in the Republic of Croatia.

On 07 February 2012, the percentage of floating ice exceeded 25% of the Danube water surface. Due to the forecasts of extremely cold air temperatures and the observed significant increase of floating ice, with a large possibility of creating a ice jam on critical profiles icebreakers have started breaking down the ice on Danube, with the most time spent on preventing flooding in Dalj until 22 February 2012. [2] (Figure 3.)

Ice jam has formed near Dalj with thicknes 20 – 30 centimeters.

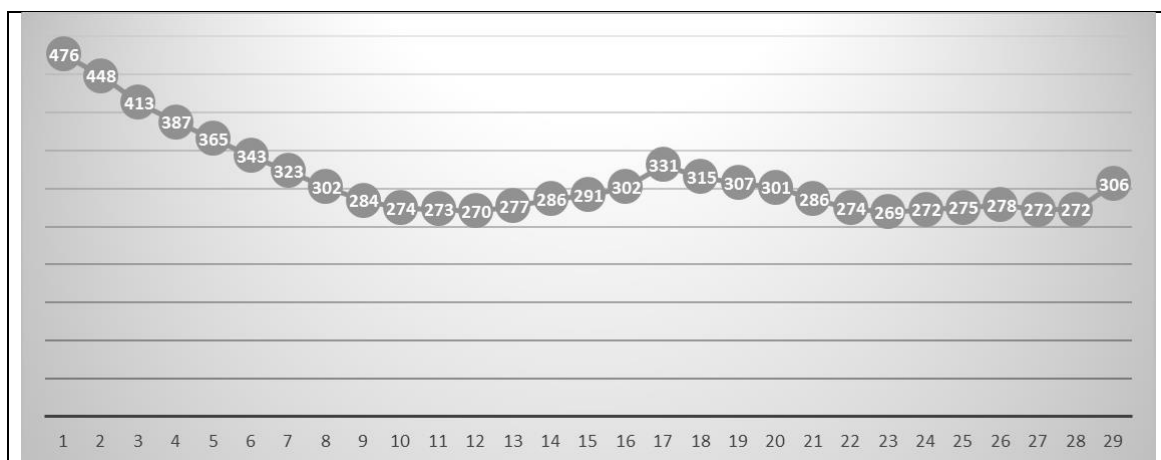


Figure 2. Water level in February 2012 [3]



Figure 3. Floating ice in February 2012 [4]

3.1.1 Description of hydro meteorological conditions

During the winter 2011/2012 the average winter air temperatures (December, January and February) were predominantly higher than the perennial average (1961-1990) in the continental part of Croatia. According to the distribution of percentiles, thermal conditions in Croatia for winter 2011/2012 are described in the dominant category normally.

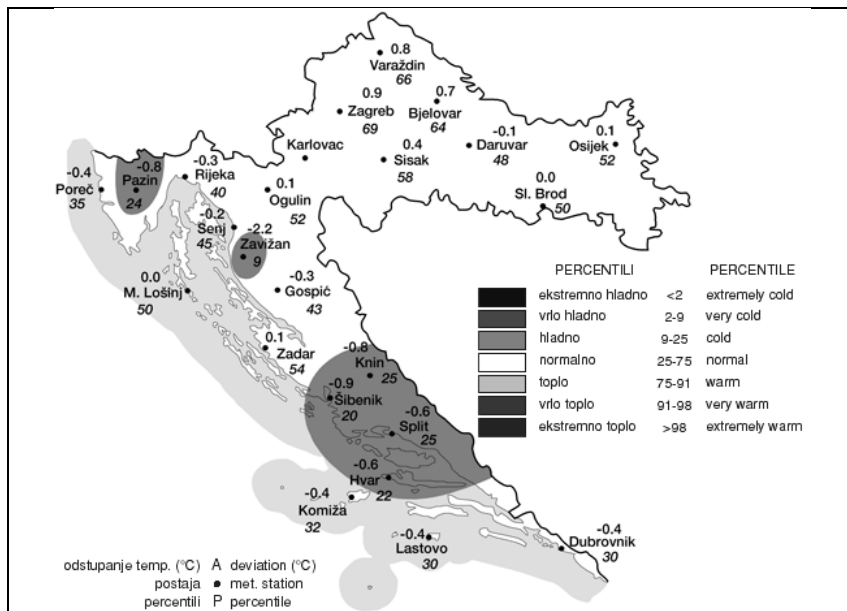


Figure 4. Air temperatures anomalies in winter 2011/2012 [5]

The average monthly air temperature in February 2012 was below the perennial average (1961-1990), indicating a negative sign of temperature anomalies. According to the distribution of percentiles, thermal conditions in Croatia in February 2012 are described in the dominant category very cold.

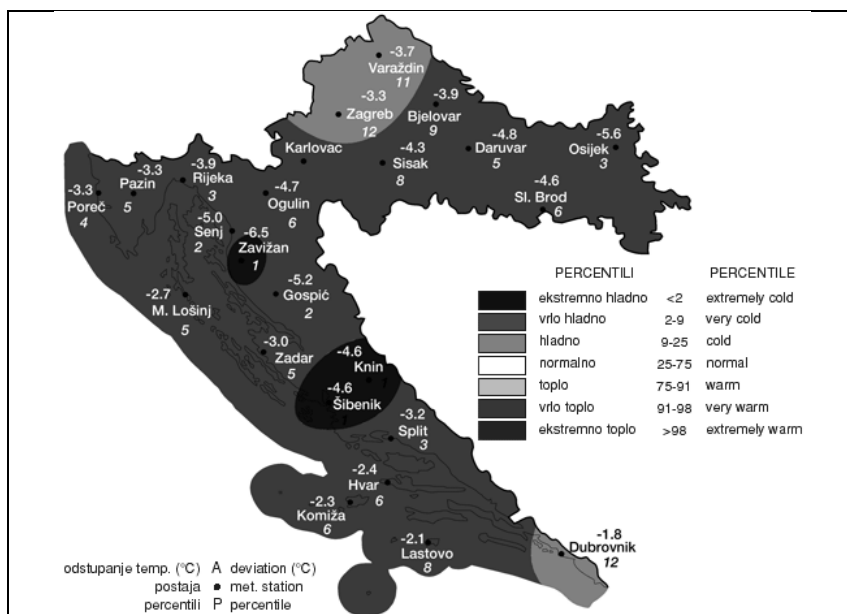


Figure 5. Air temperatures anomalies in February 2012 [5]

3.2 Ice regime in January 2017

Due to the long-term, very cold air temperature in January 2017 on the territory of the Republic of Croatia, but also in Central Europe, ice formation occurred on the Danube. In this period, the extremely

cold air temperature and intense ice formation on the Danube caused a slowdown and the water level was rising steeply registered in the Republic of Croatia in Dalj.

On 09 January 2017, the percentage of floating ice exceeded 25% of the Danube water surface and the ice jam is formed near Dalj. Due to the forecasts of extremely cold air temperatures and the observed significant increase of floating ice upstream, with a large possibility of creating another ice jam on critical profiles icebreakers have started breaking down the ice on Danube on 16 January 2017. with the most time spent on preventing flooding in Dalj until 31 January 2017. [6] (Figure 7.)

Ice jam has lenght of 11 km from Dalj to Savulja with alluvium thicknes 2 – 3 meters.

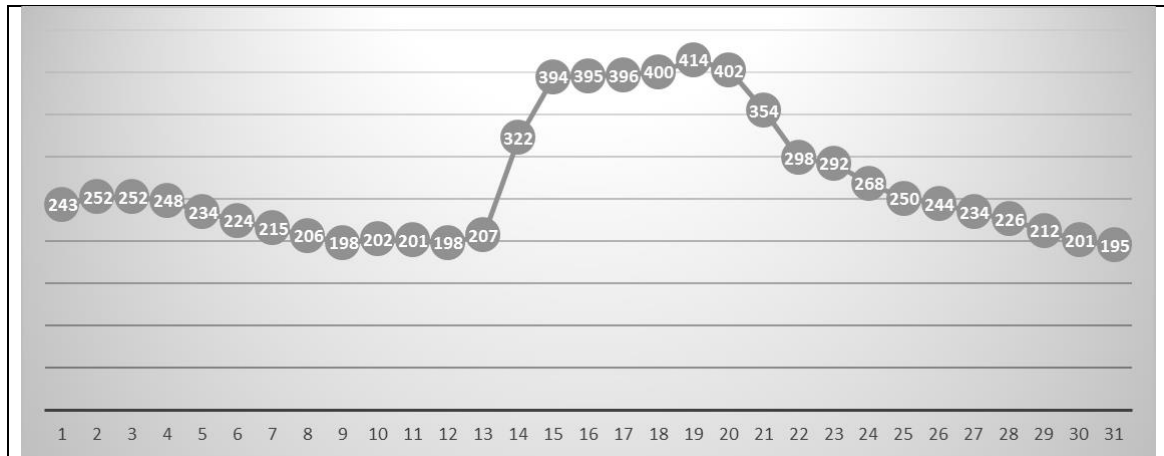


Figure 6. Water level in January 2017 [7]



Figure 7. Icebreaker breaks ice jam in January 2017 [8]

3.2.1 Description of hydro meteorological conditions

During the winter 2016/2017 the average winter air temperatures (December, January and February) were predominantly lower than the perennial average (1961-1990) in the continental part of Croatia. According to the distribution of percentiles, thermal conditions in Croatia for winter 2011/2012 are described in the dominant category normally.

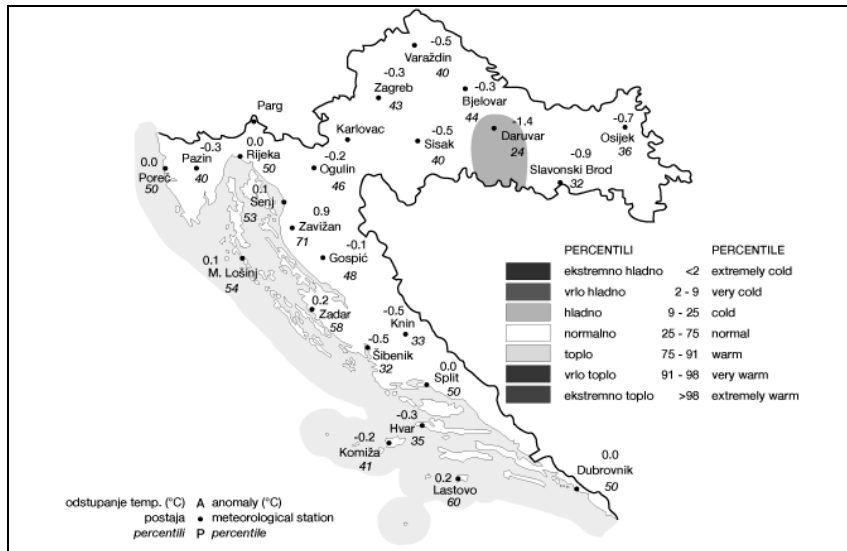


Figure 8. Air temperatures anomalies in winter 2016/2017 [5]

The average monthly air temperature in January 2017 was below the perennial average (1961-1990), indicating a negative sign of temperature anomalies. According to the distribution of percentiles, thermal conditions in Croatia in January 2017 are described in the dominant category very cold.

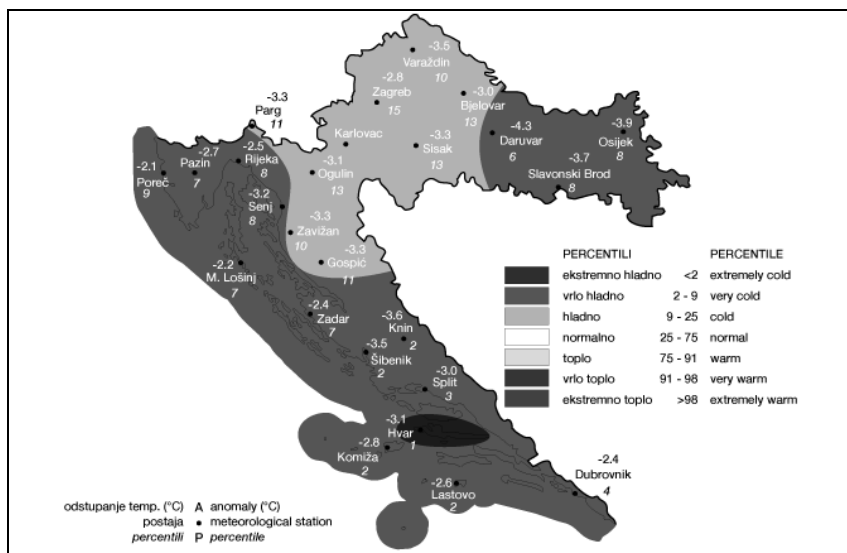


Figure 9. Air temperatures anomalies in January 2017 [5]

4 Conclusion

The regime of ice in rivers represent the spatial and temporal regularity of occurrence in watercourses. River ice regime could characterise by the date of drift-ice appearance, freeze-up, break-up and river ice disappearance, furthermore the duration of ice-affected and ice-covered season. Ice-on is the date of ice appearance, when ice drifting starts. Freeze-up is the date of continuous and immobile ice-cover occurrence. Break-up is the date, when the ice cover begins to move downstream and open water areas appear.

Research has many times detected significant changes in the river ice regime in the Northern Hemisphere over the past decades/centuries. The historical records of freeze-up dates and break-up dates show significant trends. As a result of changes in the dates of ice phenomena the ice-affected season has also decreased, on average by 2–38 days per century according to observations in the Northern Hemisphere. [9]

On the River Danube, the occurrence and the duration of river ice phenomena has changed since the start of river ice observations. Later first ice appearance and freeze-up, earlier breakup and final ice disappearance were observed. River ice formation is directly controlled by winter air temperatures. Climate change could be the reason of the changes in river ice regime. Non-climatic factors also affect the river ice regime of the Danube. Many anthropogenic intervention were made along the river, all of these works have the same effect: they lessen the occurrence and the duration of river ice phenomena. Therefore, these interventions alone are not be able to cause these changes in river ice regime, but accelerate the effects of climate change. Correlation analysis confirmed that the total number of ice-affected days is in strong relationship with mean winter temperature. Since the start of river ice observations, along the Danube the mean winter temperature has increased by 1.2–1.5 °C on 100 years average. This warming up of the winter climate could be hold responsible for changes in river ice regime of the River Danube. [10]

At the time of the ice regime on the Danube in Croatia, it was threatened by ice floods. Cooperation between Croatia, Serbia and Hungary eliminated the danger of ice flooding on the Danube. To prevent the appearance of ice floods on the Danube, the ice was broken by icebreakers, and in some places are mined with explosives.

References:

- [1] <http://www.denniskalma.com/river/ice.html>, 01.06.2017.
- [2] Croatian Water Management, January/May 2012, number 198, year XX., ISSN 1330-321X, UDK 628.1 Croatian waters, water level archive, 2012
- [3] Croatian waters, photography archive, ice defense, 2012
- [4] Croatian Meteorological and Hydrological Service, http://klima.hr/ocjene_arhiva.php, 20.04.2017.
- [5] Croatian Water Management, January/March 2017, number 218, year XXV., ISSN 1330-321X, UDK 628.1
- [6] Croatian waters, water level archive, 2017
- [7] Croatian waters, photography archive, ice defense, 2017
- [8] M. Klavins, A. Briede, V. Rodinov: Long term changes in ice and discharge regime of rivers in the Baltic region in relation to climatic variability *Clim. Change*, 95 (3–4) (2009), pp. 485–498
- [9] Takács, K.: Changes in river ice regime of the river Danube, Department for Physical Geography, Eötvös Loránd University 1/c Pázmány Péter sétány, Budapest, H-1117

FLOOD MANAGEMENT IN URBAN BASINS OF THE CITY OF GDAŃSK

TOMASZ KOLERSKI ¹, DOMINIKA SZAWURSKA ²,

¹ *Gdańsk University of Technology, Faculty of Civil and Environmental Engineering, Poland, tomasz.kolerski@pg.gda.pl*

² *Gdańsk University of Technology, Faculty of Civil and Environmental Engineering, Poland, domszawu@pg.gda.pll*

1 Abstract

Over the last years, the City of Gdańsk suffers twice from flash floods. Both events were caused by intense storms which produced significant surface runoff and caused inundation private and cities properties. The first case of July 2001 flood [3], [9] was the turning point for the city authorities, who decide to look close on the flood management in small urban catchments. The aim of research projects was to establish technical solutions and procedures to be applied in case of risk of flooding due to heavy rain on all Radunia Channel tributaries. The largest basin is the catchment of the Oruński Stream. This area was recently intensely developed and according to the spatial planning the urbanisation process will proceed. The project's closure took form of decisions concerning technical solutions modifying operation mode of Gdansk Water Junction System in order to ensure an optimal distribution of flood water. After 2003, Gdansk Floodway System rebuilding propositions started to be regularly implemented. Thanks to actions initiated in the river basin of Radunia channel, no more emergency situations were observed during the flood in 2016. In the paper, the hydrologic model of the water system of Oruński Stream will be presented with particular effort paid to the new and renovated retention structures. Hydrological modelling system of HEC HMS was used to simulate the basin response on precipitation. The 16,4 km² model domain was divided into 35 sub-basins according to storm water drainage system. Both, current and proposed land use of the basin was taken into consideration. The operation of six existing and two proposed flood detention reservoirs were included in the simulations. The results showed the importance of reservoirs and water diversion structures on flood surge routing.

Keywords: Flood Management, Urban Basin, HEC HMS Modelling, Oruński Stream, Gdańsk

2 Introduction

The flood protection of the Gdańsk city, include control of three types of possible flooding come from different directions. The first is coastal flooding caused by high winds producing sea surges, next is high discharge in the Vistula River, which could be increased in the winter season by ice phenomena [1]. The last type of flooding, which is certainly the most destructive natural hazard for the city, is flash flooding caused by surface runoff on moraine hills [9]. The hills surrounding the city from the west and south were originally covered by forest and agricultural lands. Due to the city intense development, the land use of this area changed to fully developed urban areas. In effect, the natural retention of the hills reduced affecting the runoff and streamflow caused by rain water which is much intense nowadays. Number of small streams drains the moraine hills and flows down through the city, ending its course in Martwa Wisła. Oruński Stream originates in the vicinity of Otomin, western part of the city and flows eastern direction to Radunia Channel (Figure 1). On July 9th 2001, a major mesoscale convective system affected Gdańsk: 1 person was killed during the event and the economic damage is estimated at 50 million Euro. The most severe damages in city infrastructure were caused by Oruński Stream.

The study was conducted to determine the design discharge in uncontrolled urban basin. The aim of the study was to use mathematical model to analyse the precipitation effects on the river basin with the proposed reservoir and the associated flow condition. The Oruński stream basin has produced intense surface runoff in the past [2], which was caused by the high inclination of the terrain along the stream course (drop of about 100 m on 2 km distance) and decreasing natural retention. Urban development of the basin increased recently [6] and in short future its land use will change significantly. Therefore to reduce the flood potential the proposed plan is to: 1) create approximately 38 000 cubic meters dry

reservoir (Z3) and 2) regulate stream section on the distance of about 1,2 km incorporating bioengineering methods whatever possible and practical.

Sensitivity study of proposed reservoir on the Oruński stream (Z3 on Figure 1) require to include the entire reservoirs basin in calculations. The basin of the short stream section downstream to the reservoir was also included in the study in order to calculate the maximum permissible outflow from proposed reservoir. Calculations were conducted on Orunski stream basin with closing cross sections at the dam of reservoir Z4 (reservoir Augustowska). As shown on the map (Figure 1) the model domain include the upstream section of Oruński stream with its four natural tributaries as well as three main storm sewers collectors on the left side of the stream. In calculations, except of proposed reservoir (Z3), three existing reservoirs located along the stream i.e. Z1 (Świętokrzyska 1), Z2 (Świętokrzyska 2) and Z4 (Augustowska). Also, three reservoirs on storm sewers were included – W1 (Wieżycka), W2 (Jeleniogórska) and W3 (Wielkopolska). In addition planned reservoir K2 on the Kowalski stream was also included but only in cases where land use of the basin according to the city's spatial planning was included. Total flood retention possibility of all existing reservoirs exceeds 400 thousand m³, but reservoirs Z1 and Z2 alone have 340 thousand m³. The proposed reservoir is planned to be small, dry reservoir with a total storage of 41 000 m³. Reservoir storage allocation zones will be divided into three major parts as follows: dead storage zone used for recreation and sediment collection is 4 500 m³, flood control space for storage excessive flood volume which is 32 200 m³, and surcharge, related to emergency spillway operation has additional space of 4 300 m³ (see Figure 5).

The basin soil data has been collected from general soil maps available at Department of Geodesy and Cartography of the Pomorskie Provincial Office in Gdańsk. Soil types were then classified to one of four soil groups, as shown in Figure 2. The dominant soil type in the Oruński basin is classified to belong to groups B and C (average infiltration rate), and little portion of group D (low infiltration rate).

Three general scenarios were considered in a study: current condition with a land use specified according to the situation from 2016 (Case 0) and two cases with proposed basin development based on the city spatial planning (Case A and B). The Case A consider that urbanisation process will proceed without any care on basin retention. In the Case B despite the basin development the current retention is considered to be kept by incorporating modern techniques of harvesting rainwater such as permeable roads, bioswales, ditches filled with native plants or rooftop gardens. Land use of the direct basin of proposed reservoir is shown in Figure 3.

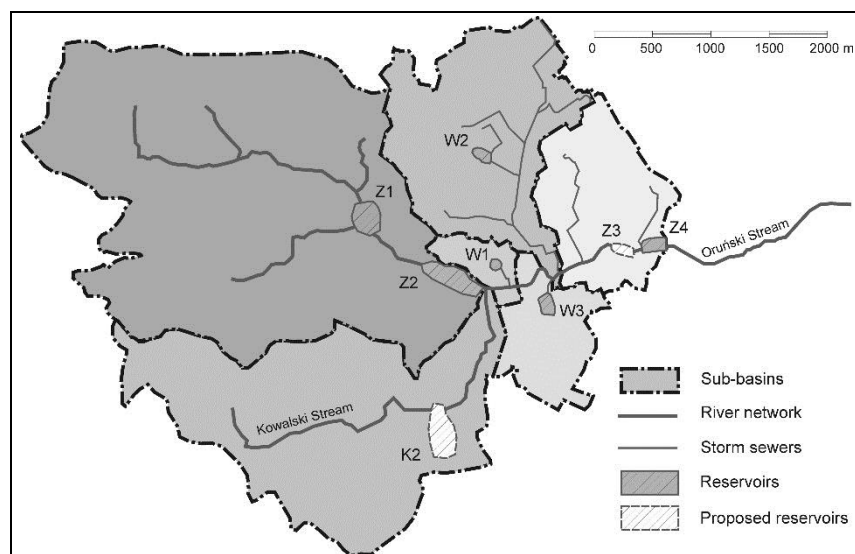


Figure 1. Model domain of Oruński Stream with selection of main sub-basins and flood retention reservoirs

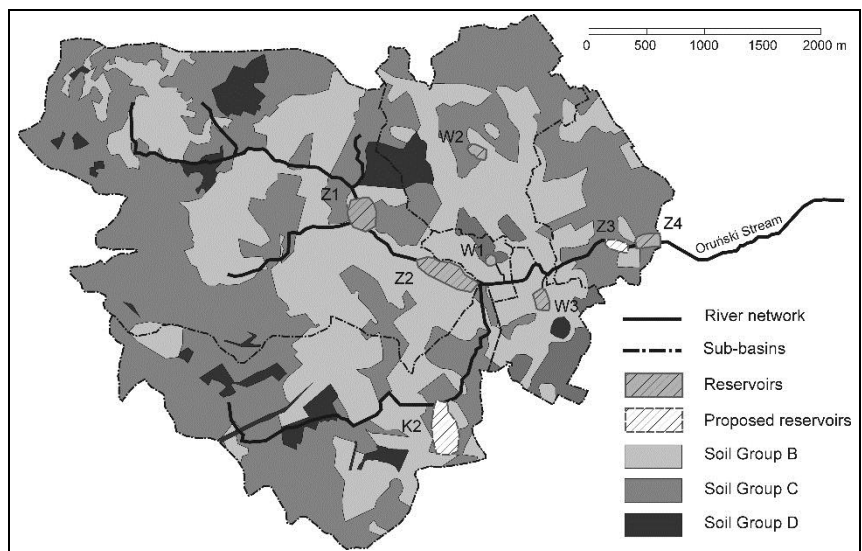


Figure 2. Soil type map of the Oruński Stream basin

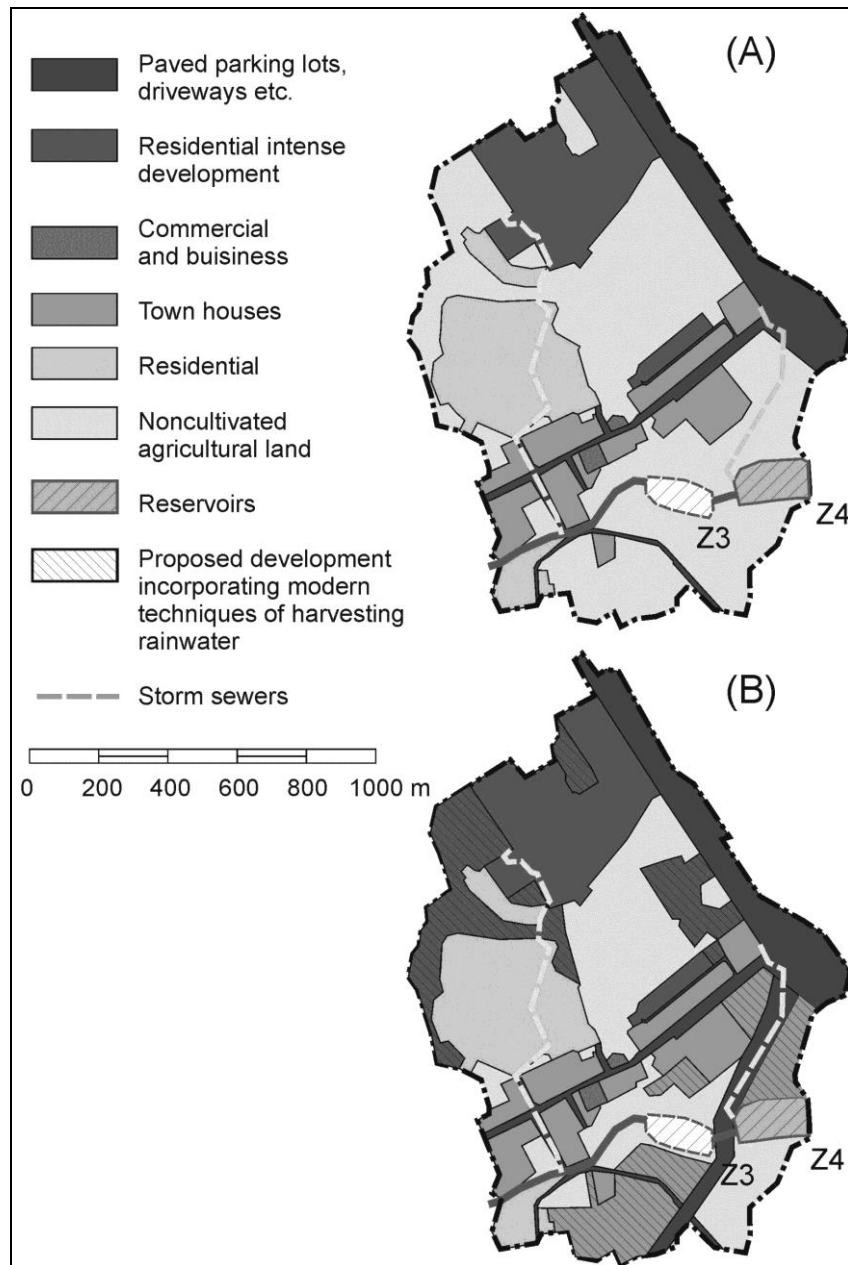


Figure 3. Land use of the direct basin of Z3 and Z4 reservoirs showing current (A) and proposed (B) conditions

3 Methods

Calculations required to design the proposed flood detention reservoir Z3 are not complicated but since the system being analysed is very complex the mathematical model was used here. All calculations were carried out by Hydrological Modeling System HEC-HMS. However each step was verified manually on single test basin. All information required to prepare input data are summarized below.

3.1 Intensity-duration-frequency method

The proposed reservoir was calculated on design flood conditions which return period is stated in the polish journal of laws where the hazard classification of dams utilizing dam height, volume of water impounded and probable effects of dam failure due to downstream. In a Polish law, it is established that the structure which is in the lowest category need to be designed on the 100 years flow and need to maintain the 200 years conditions. Even though storm water monitoring system exists in the City of Gdańsk [7], the Oruński Stream basin is not controlled. Therefore the flood surge of required return period cannot be determined based on the historical discharge data. The only possibility is to calculate

the required design flood from rainfall-runoff formulas including rainfall of specified duration and intensity which is related to the probability of the event. Determination of the design flood involves two basic steps: 1) to synthesize a hydrograph of inflow into the reservoir and 2) to model the movement of the flood through the reservoir and past the dam.

The Intensity-duration-frequency (IDF) method for extreme precipitation has been used here to determine so called 'design storm'. The IDF formulas play an important role in hydrological applications, and become particularly useful in analyses concerning urban areas [8]. Among others, it is recommended in the study area to use the IDF formula established by the Institute of Meteorology and Water Resources for the northern part of Poland as provided below [10]:

$$P = 1,42 \cdot T_d^{1/3} + \alpha \cdot [-\ln(p)]^{0,584} \quad (1)$$

In which P – total depth of precipitation [mm]; T_d – duration of rain [min]; p – return period of the storm (dimensionless; i.e. for 10 years storm $p = 0,1$); α – weighted coefficient determined on the base of duration of rain such as:

$$T_d \leq 30 \text{ min} \quad \alpha = 3,92 \cdot \ln(T_d + 1) - 1,662 \quad (2a)$$

$$30 < T_d \leq 60 \text{ min} \quad \alpha = 8,944 \cdot \ln(T_d) - 18,6 \quad (2b)$$

$$60 < T_d \leq 120 \text{ min} \quad \alpha = 4,693 \cdot \ln(T_d + 1) - 1,249 \quad (2c)$$

$$120 < T_d \leq 720 \text{ min} \quad \alpha = 2,223 \cdot \ln(T_d + 1) - 10,639 \quad (2d)$$

$$T_d > 720 \text{ min} \quad \alpha = 9,472 \cdot \ln(T_d + 1) - 37,032 \quad (2e)$$

Since the most severe conditions may be produced by rainfall of any duration all possible scenarios must be calculated to determine the design rain duration. The table below presents the results of IDF formula Eq. (1), for possible rainfall durations.

Table 1. Calculated depth of precipitation for variability of rainfall duration

T_d [min]	α	P [mm]	
		$p = 1$	$p = 0,5$
30	11,80	33,2	35,7
60	18,02	49,5	53,3
90	19,92	55,0	59,1
120	21,26	58,9	63,3
180	22,20	62,2	66,8
240	22,83	64,5	69,3
360	23,73	68,0	72,9
480	24,37	70,6	75,6
1440	31,86	93,8	100,4

For intensity of the precipitation in time the DVWK regulations were employed here. According to the recommendation single peak rainfall as shown in Figure 3 was used in a current study. The time variable precipitation will be distributed according to following rule: during the first $\frac{1}{3}$ of total time 20% of gross rainfall occurs, in the next 20% of time the 70% of total rain falls and the rest will be uniformly distributed over the remaining 50% of the time [4].

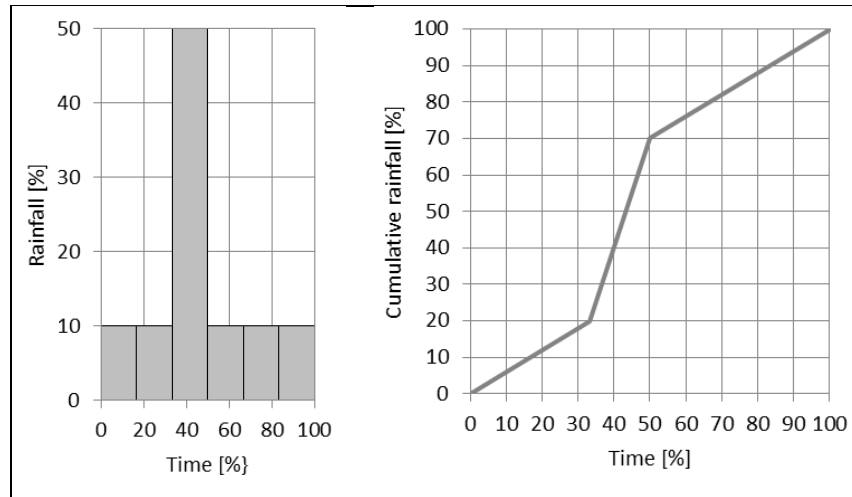


Figure 4. Rainfall intensity distribution according to DVWK [4]

3.2 Rainfall- runoff formula

To calculate excess rainfall the Soil Conservation System (SCS) procedure was applied to the Oruński Stream basin. The SCS procedure is a rainfall-runoff relation for watersheds which says that for the storm as a whole the depth of excess precipitation, P_e is always less than the depth of precipitation, P likewise, after runoff begins, the additional depth of water retained, F is less than or equal to some potential maximum retention, R . The procedure assumes that the ration of two actual and the two potential quantities are equal [5]:

$$\frac{F(t)}{R} = \frac{P_e(t)}{P(t) - I_a} \quad (3)$$

Introducing curve number parameter (CN) and substituting initial abstraction by percentage of potential abstraction ($I_a = \mu \cdot R$) will lead to final form of cumulative effective rainfall:

$$P_e(t) = \frac{\left(P(t) - \mu \cdot a \left(\frac{1000}{CN} - 10 \right) \right)^2}{P(t) + a(1 - \mu) \left(\frac{1000}{CN} - 10 \right)} \quad (4)$$

In which μ empirical constant for initial abstraction related to potential abstraction; a is a scale factor to include depth of precipitation in millimeters $a = 25,4$. The SCS dimensionless curvilinear unit hydrograph has been used in a runoff calculations. The method requires the peak discharge and time to peak to be determined. Time to peak is the time from the beginning of rain to the of the peak discharge, which could be calculated as half of the duration of excess rainfall and a lag time.

$$t_p = 0,5 \cdot T_d + t_L \quad (5)$$

In which lag time t_L was calculated base on the slope S in percent, the hydraulic length L in meters, and roughness of the terrain.

$$t_L = \frac{L^{0,8}(R + 1)^{0,7}}{4915\sqrt{S}} \quad (6)$$

The peak discharge in is calculated according to following equation:

$$Q_{max} = 2,08 \cdot F \cdot Pe \cdot t_p^{-1} \quad (7)$$

3.3 Level pool routing method

To analyse reservoirs effect on time and magnitude of the flow hydrologic routing by lumped system has been applied here. The level pool routing procedure for calculating the outflow hydrograph from reservoir assuming horizontal water surface was adopted. The input was inflow hydrograph calculated from SCS-UH procedure and storage-outflow characteristics of existing reservoirs. For proposed reservoir both storage and outlet structures are subject to design, therefore the number of possible solutions were tested. For hydrological routing inflow, outflow and storage as a function of time are related by the continuity equation:

$$\frac{dV}{dt} = I(t) - O(t) \quad (8)$$

Above equation cannot be solved therefore second equation relating storage and outflow is needed. Coupling the reservoir storage function with the continuity equation provides solvable combination of two equations with two unknowns. The specific form of storage functions depends on nature of system being analysed, and in current study it was the storage-elevation relations for all six reservoirs. It was coupled with rating curves of all existing outlet structures. Storage-outflow function of the proposed Z3 reservoir which was optimised during the numerical calculations is presented in Figure. 5

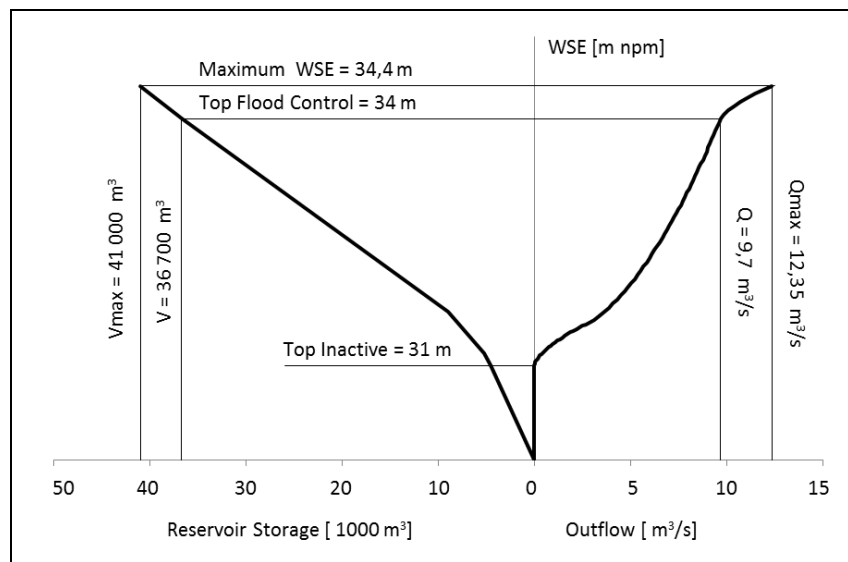


Figure 5. Storage – outflow relation for proposed Z3 reservoir

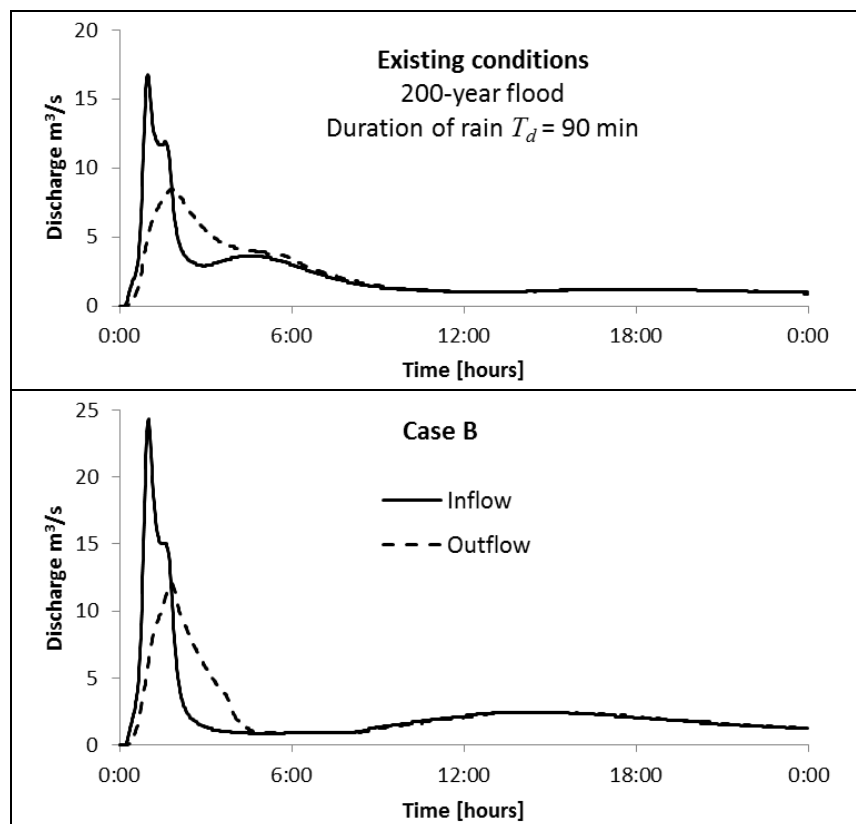
4 Results and discussion

Computations were performed for two storms return periods: 100 and 200-years storms and for whole range of possible rainfall duration times. Simulations for three different scenarios of land use were carried out which were referred to basin development as well as flood detention system operation. The system operation is planned to be updated by additional reservoir (K2) and flow diversion structure redirecting storm water from the Kowalski stream to Z2 reservoir.

Simulation results shown insufficient flood routing in case of full basin urbanisation without maintaining current retention (case A). It shows clearly that particular attention must be payed to preserve basin retention on the level of new city districts planning. The storm water drainages and sewers must be designed to not reduce current basin retention which could be reached by combining variety technical methods of harvesting rainwater. The simulation results of case B, which is a scenario with fully developed basin, but with respect of so called ‘sponge city’ solutions, shown sufficient flood detention possibility of the reservoirs system.

Table 2. Case B: Calculated maximum inflow, outflow and storage in proposed reservoir for return periods 100 and 200 years for variety of rainfall duration

Duration of rain [min]	Return period 100 years			Return period 200 years		
	Storage [1000 m ³]	Inflow [m ³ /s]	Outflow [m ³ /s]	Storage [1000 m ³]	Inflow [m ³ /s]	Outflow [m ³ /s]
30	13,8	13,9	5,8	16,4	16,0	6,4
60	29,5	21,2	9,3	34,2	24,4	11,0
90	31,5	21,3	9,8	35,9	24,3	12,0
120	31,2	20,8	9,7	35,4	23,6	11,7
180	25,8	17,9	8,5	30,4	20,2	9,5
240	24,0	16,6	8,1	28,2	18,8	9,0
360	21,3	12,4	7,5	25,0	14,0	8,3
480	19,4	10,4	7,0	22,9	11,7	7,8
1440	15,1	6,7	6,1	18,2	7,7	6,8

**Figure 6.** Simulation results of the 200 year flood routing affected by proposed reservoir for both existing and proposed basin development

It was expected, that due to significant terrain inclination, the design storms are intense but short duration. It was confirmed by simulation results of the numerical model concluding that the highest discharge is produced by 60 and 90 minutes rainfall. Even though the total precipitation depth from storms with longer duration is higher, these events produce less intense runoff and lower discharge in consequence. It is shown in Table 2, where inflow to the proposed reservoir for cases with different storm duration is presented.

5 Conclusion

Base on the simulation results conducted by using mathematical model HEC HMS following conclusions has been stated, which relates to hydrodynamics of the surface runoff of storm water in the Oruński Stream basin:

- The catchment is intensely developed and has significant inclination, which generates intense runoff with the peak occurring in relatively short time from the beginning of the rainfall. In consequence the worst case scenario is related to the basin reaction on convective storms with duration shorter than 2 hours.
- The proposed reservoir no 3, affects significant reduction of the flood surge. The reservoir is planned to be partially dry reservoir, with flood retention storage of 32 200 m³, which is sufficient to control 100 and 200 years floods in the current stage of basin development.
- In case of further basin development, it is required to keep the current retention of the catchment or even improve it by incorporating modern techniques of harvesting rainwater. In case of neglecting this practice, floods and inundations will occur more often in the basin because the existing and proposed flood protection system is not sufficient to prevent it
- In case of using good practice of ‘sponge city’ technique adapted to the development of the Oruński catchment (Case B), the proposed reservoir will guarantee the flood safety of the entire basin.

Results of the study have been discussed and accepted by Gdańskie Wody (municipal unit of the Gdańsk City). The proposed reservoir will be constructed in next years to complete flood protection system of the Oruński basin region.

References

- [1] Kolerski, T.: Modeling of ice phenomena in the mouth of the Vistula River, *Acta Geophysica*, 62(4), pp 893-914, 2014
- [2] Kolerski, T., Kowalik, M.: Wyznaczanie odpływu ze zlewni niekontrolowanych Kanału Raduni podczas powodzi w 2001 r., *Inżynieria Morska i Geotechnika* 02/2014; 35(1) pp. 3-10, 2014
- [3] Majewski, W., Jasińska, E., Kolerski, T., Olszewski T.: Zagrożenia powodziowe Gdańska oraz proponowane zabezpieczenia w świetle powodzi w lipcu 2001 r., *Gospodarka Wodna* 2006(7) p. 260-267, 2006
- [4] Maniak, U.: Hydrologie und Wasserwirtschaft (Chapter), *Niederschlag-Abfluß-Modelle für Hochwasserabläufe*, Springer Berlin Heidelberg, pp 282-380, 1988
- [5] Mays, L.W.: *Water Resources Engineering*, New York: John Wiley 2005
- [6] Olechnowicz, B. and Weinerowska-Bords, K.: Impact of Urbanization on Stormwater Runoff from a Small Urban Catchment: Gdańsk Małomiejska Basin Case Study. *Archives of Hydro-Engineering and Environmental Mechanics*, 61(3-4), pp141-162., 2014
- [7] Szydłowski, M., Zima, P., Weinerowska-Bords, K., Mikos-Studnicka, P., Hakiel, J., Szawurska D., Stormwater and snowmelt runoff storage control and flash flood hazard forecasting in the urbanized coastal basin, 14th International Symposium on Water Management and Hydraulic Engineering, Brno, pp 141-150 2015
- [8] Weinerowska-Bords, K.: Development of Local IDF-formula Using Controlled Random Search Method for Global Optimization. *Acta Geophysica*, 63(1), pp 232-274, 2015
- [9] Wołoszyn, E. The catastrophic flood in Gdansk on July 2001. In *Urban Water Management: Science Technology and Service Delivery*, pp. 115-124. Springer Netherlands, 2003.
- [10] Wołoszyn, E. Polish rainfall—runoff investigations and modification of the rational method. *Atmospheric Research* 27, no. 1-3 (1991): pp 219-229. 1991

2. WATER SUPPLY AND WASTEWATER SYSTEMS

ANALYSIS OF WATER QUALITY OF THE KARAŠICA-VUČICA RIVER

ANA AMIĆ ¹, LIDIJA TADIĆ ²

¹ *Department of Chemistry, Josip Juraj Strossmayer University in Osijek, aamic@kemija.unios.hr*

² *Faculty of Civil Engineering, Josip Juraj Strossmayer University in Osijek, Croatia, ltadic@gfos.hr*

1 Abstract

Water quality of the Karašica-Vučica River, located in an area with intensive agricultural production, was examined. Samples were taken over the period of 15 years and cover several locations along the river flow. Analysis of chemical parameters indicates a decrease in water quality, depending on location and year. Statistical analysis indicates a future increase of analysed parameters in both rivers. Obtained results indicate that it is necessary to protect the Karašica-Vučica River from further pollution, by decreasing application of mineral fertilizers and by constructing waste water treatment plants.

Keywords: water quality, nitrogen compounds, phosphorus compounds, BOD₅, COD, Karašica and Vučica rivers

2 Introduction

The Karašica-Vučica River catchment area is located in eastern Croatia (Osijek-Baranja County and Virovitica-Podravina County) in the Pannonian Plain, which is a fertile agricultural and forested land with a total area of 2,352.63 km² (1,419.87 km² of which is agricultural land). In the terms of water management, the Karašica-Vučica River catchment area consists of two hydrographical units – Vučica, which collects water from Krndija mountain, and Karašica, which collects water from Papuk mountain and lowland part of this area. Both rivers spring at the north side of Papuk mountain, flow almost parallel to Drava River, merge near Valpovo, and flow into Drava River near Petrijevci municipality. The Karašica-Vučica catchment area also contains more than 4,000 km of canals, dams, bridges, and other hydro-technical constructions [1]. According to Köppen's classification, this area has a moderate continental climate with annual precipitation between 710 mm in the lowland part to 816 mm in the highland part of the catchment. Mean annual groundwater level is approximately 3.0 m below land surface [2].

Vegetation is composed of pastures, meadows, vineyards, orchards, and deciduous forests. Dominating soil types are loam and clay, with over 70% of lowland area containing heavy clay soil what requires intensive land drainage. Figure 1 presents study area.

Water quality of the Karašica-Vučica River is highly influenced by various economic activities, main of which is food industry (agriculture, viticulture, livestock farming, fishing), as well as some other types of industry (Našicecement d.d., Belišće d.d., Viridis wood cluster, oil and gas field Beničanci) [3]. Also, Karašica and Vučica rivers or their tributaries are a wastewater recipient for some small towns and villages (domestic sewage), which are usually rich in biodegradable organic matter and surface runoff. In the last 30 years several studies have reported changes in water quality of the Karašica-Vučica River. Munjko et al. (1980) determined that the water of the Karašica River is pure before textile factory in Črnkovci, after which is loaded with plants wastewater. Measured levels of nitrates in Karašica surface waters were in 1.9 to 76 mg/L range, and in 2.5 to 45 mg/L range for the Vučica River [4]. Vidaček et al. (1999) obtained similar results – 7.6 to 74.2 mg/L of nitrates in surface water [5].

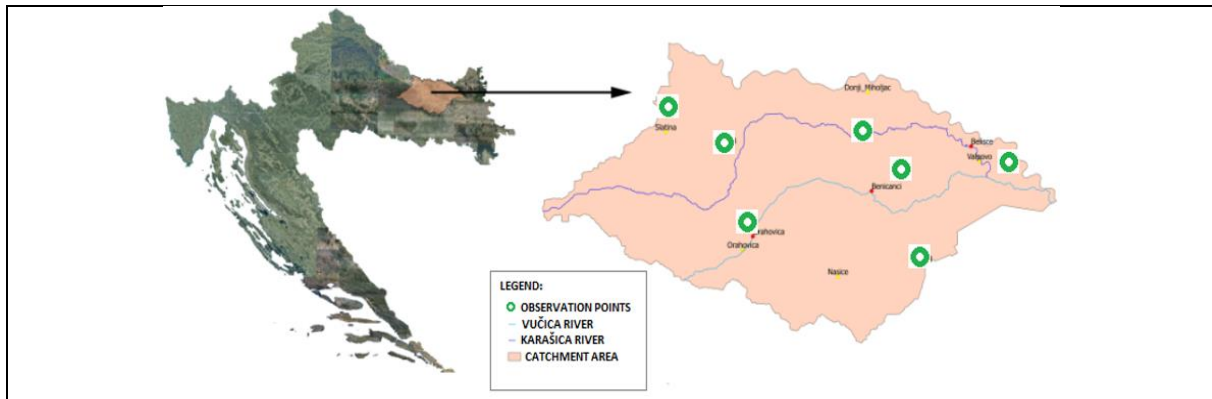


Figure 1. Study area.

Since 1991, industrial pollution dropped significantly throughout Croatia (as a result of war, destruction of agricultural and industrial facilities, as well as a result of massive emigration throughout Croatia), so the aim of our study was to analyse Karašica and Vučica rivers water quality over the period of 15 years to determine whether water quality has changed because of it. Data analysed in our study was obtained from Hrvatske vode, the national water management agency responsible for surface and ground water quality monitoring. Most of the data are from samples collected at monthly intervals. Our aim was also to determine if there were differences in water quality between measurement sites, and to predict future quality of the studied water body.

3 Methods

Monitoring that took place between 2004 and 2015 included seven sites: 1) Karašica, road Crnac-Krčenik (rural area) at 45° 44' 50" North, 17° 58' 05" East; 2) Karašica at Črnkovci (village) at 45° 42' 26" North, 18° 17' 44" East; 3) Karašica downstream of Valpovo (rural area) at 45° 66' North, 18° 42' East; 4) Vučica, Marjančaci (village) at 45° 37' 59" North, 18° 23' 39" East; 5) Vučica at Petrijevci (municipality) at 45° 36' 57" North, 18° 32' 28" East; 6) Vučica, bridge on the road Staro Petrovo Polje (rural) at 45° 44' North, 17° 58' East; 7) Vučica at Beničanci (village) at 45° 38' 18" North, 18° 10' 36" East. For two locations, Karašica Črnkovci and Vučica Petrijevci, results of water monitoring quality that took place between 1998 and 2004 were also analysed.

The major economic activity in analysed area includes intensive food production (agriculture and farming) and wood and paper industry. The wastewater coming from some villages and municipalities of surrounding areas is also being discharged into the Karašica and Vučica rivers.

Monthly sample analysis included nitrate nitrogen, nitrite nitrogen, total nitrogen (total – N), inorganic nitrogen, total phosphorus (total – P), orthophosphates, five-day biochemical oxygen demand (BOD₅) and chemical oxygen demand (COD). Samples were analysed right after collection using ion chromatography to determine the concentrations of nitrogen (HRN EN 26777:1998, HRN EN ISO 10304-1:1998, HRN ISO 7890-1:1998, HRN ISO 7890-3:1998, HRN ISO 5663:20001, HRN EN ISO 11905-1:2001, HRN EN 12260:2008) and phosphorus compounds (HRN ISO 6878:2001) and titration to measure biochemical (HRN EN 1899-1:2004, HRN EN 1899-2:2004) and chemical oxygen demand (HRN EN ISO 8467:2001) [6, 7]. All water quality parameters are expressed in milligrams per litre (mg/L).

Statistical analysis of some water quality parameters with the longest data series was performed. Analysis of linear regression and ANOVA has been performed and obtained results are presented in Figures 5, 6 and 7.

4 Results and discussion

The water quality of Karašica and Vučica rivers was determined based on comparing COD, BOD₅, nitrites, nitrates, total – N and total – P parameters. These are summarized in Tables 1 and 2, and Figures 2, 3 and 4. All parameters varied during the investigation period.

BOD₅ and COD are important parameters that describe oxygen regime in the water, and refer to biochemical reactions that occur in natural waterways. While COD measures the oxygen demand of oxidisable pollutants, BOD₅ measures the oxygen demand of biochemically degradable organic matter present in water. BOD₅ is used to determine self-purification of surface water and water load with dissolved organic matter. Contributors to this load with oxygen-depleting substances are agricultural effluents, discharge of poorly treated industrial waste (food, wood and paper, textile industry), as well as discharge of poorly treated domestic sewage from a number of local towns and villages.

Nitrite concentrations in water are usually low (0.01 mg/L), and higher values are a result of agricultural effluents. Nitrites are an important part of the nitrogen cycle, they are unstable and can transform into nitrates or ammonia. Nitrate concentrations in water are usually 0.1 mg/L, or lower. Increased concentrations of nitrates are usually a result of agricultural production (nitrogen fertilisers) and/or disposal of human and industrial waste.

Table 1. Mean annual value of analysed chemical and nutrient parameters for the Karašica River.

Karašica River							
Location	Year	Nitrites (mg/L)	Nitrates (mg/L)	Total – N (mg/L)	Total – P (mg/L)	BOD ₅ (mg/L)	COD (mg/L)
Crnac-Krčeničnik	2012	0.0478	0.2635	0.7104	0.0863	2.7	5.2
	2013	<0.01	<0.701	0.5743	0.105	1.9	3.5
	2014	0.02225	0.6423	0.8867	0.185	3.8625	9.625
	2015	0.0086	0.6858	0.0011	0.0825	3.375	4.5167
Črnkovič	1998	0.006	-	-	-	5.64	4.09
	1999	0.015	-	-	-	6.865	5.135
	2000	0.0105	0.6215	1.96	0.237	2.11	5.1575
	2001	0.009	0.678	1.25	0.1645	3.7625	4.3015
	2002	0.028	0.904	1.525	0.303	3.6775	5.27
	2003	0.01425	0.6315	1.06738	0.168	4.05	4.125
	2004	0.0243	3.2142	3.8081	0.256	3.4	5.9
	2005	0.028	1.4564	1.7171	0.1459	3.3	5.4
	2006	0.0232	0.904	1.2553	0.6402	3.2	5.6
	2007	0.013	0.7684	1.0198	0.192	2.9	5.7
	2008	0.0661	1.1978	1.4556	0.1596	3	5
	2009	0.0118	0.6127	1.1223	0.1412	1.8	4.4
	2010	0.039	1.5158	1.9958	0.2292	2.1	5.6
	2011	0.0235	0.5496	0.9708	0.1721	1.8	3.9
	2012	0.0367	0.7255	1.2982	0.2082	2.9	10
2013	0.0247	1.2444	1.73	17.138	3.2	6.3	
2014	0.02883	1.015	1.4843	0.2008	3.4	5.7	
2015	0.02258	1.0475	1.4942	0.2793	3.7	6.6	
Downstream from Valpovo	2012	0.0235	0.1235	0.6139	0.1703	2.3	4.6
	2013	0.0205	0.7884	1.1094	0.16	1.8	3.8
	2015	0.067	0.87834	2.14398	0.2373	3.437	4.875

Former national regulations in Croatia [6,7] have classified surface water in five classes (Class I being the best and Class V the worst water quality category). According to that classification, parameters shown in Table 1 would indicate that the quality of the Karašica River surface water at location Crnac-Krčeničnik varies from Class I to Class III regarding mean recorded values for most analysed parameters. The exception is year 2013, during which water quality was evaluated as Class V, with respect to values determined for total – P.

Parameters shown in Table 2 indicate that the quality of the Vučica River surface water at location Marjančaci varies between Class II and Class III (except 2007 and 2009, during which water quality was evaluated as Class V, with respect to nitrites concentration).

Current regulations in Croatia classify water quality in the categories: very good/good/moderate/bad according to hydromorphological, physical, chemical, and biological parameters. Regarding the observations of total – P, total – N, nitrites, nitrates, BOD₅ and COD concentrations water quality of Karašica and Vučica rivers may be designated as a moderate and good, respectively, with the remark that evaluations are not very reliable.

Table 2. Mean annual value of analysed chemical and nutrient parameters for the Vučica River.

Vučica River							
Location	Year	Nitrites (mg/L)	Nitrates (mg/L)	Total – N (mg/L)	Total – P (mg/L)	BOD ₅ (mg/L)	COD (mg/L)
Marjančaci	2012	0.0623	0.2824	1.2763	0.0733	2.6	3.6
	2013	0.039	<0.701	1.3021	0.14	2.6	4.7
	2014	0.03775	1.2792	1.8592	0.1825	5.4325	10.525
	2015	0.03192	1.25	1.8867	0.2456	3.575	6.642
Petrijevci	1998	0.033	-	-	-	5.57	3.015
	1999	0.077	-	-	-	3.195	6.04
	2000	0.0095	0.62145	1.8953	0.18975	2.82	5.175
	2001	0.0095	0.791	1.3593	0.234	6.3575	5.755
	2002	0.015	1.017	1.894	0.5175	4.8825	7.2125
	2003	0.01775	0.81925	1.54488	0.167875	5.55	5.175
	2005	0.0319	1.3309	1.6803	0.4029	3.7	6.1
	2006	0.024	0.9266	1.3442	0.5584	3.5	5.1
	2007	0.2747	0.5055	1.1845	0.1822	4.4	5.5
	2008	0.0741	1.4238	1.7635	0.1608	3.9	5.6
	2009	0.2747	0.5055	1.1845	0.1605	3.5	4.8
	2010	0.0819	1.3759	1.8558	0.2253	4.5	6.5
	2011	0.0816	0.4933	1.2248	0.1057	2.9	4
	2012	0.0222	0.5633	1.2008	0.1542	3.2	5.2
	2013	0.0348	1.6392	1.3008	0.2628	4.5	7
2014	0.03775	1.2792	1.8592	0.238	3.1	6.6	
2015	0.01883	0.9458	1.7209	0.1871	4.9	6.4	
Staro Petrovo Polje	2014	0.0245	1.1993	1.50725	0.2775	3.555	4.35
	2015	0.02534	1.30834	1.66834	0.1308	3.245	3.742
Beničanci	2015	0.03675	1.3475	1.920833	0.20925	3.2167	5.65

Figures 2, 3 and 4 illustrate spatial pollution of the Karašica River surface water (i.e. pollution of surface water along the river flow). Generally, considering depicted water quality parameters (total – N, BOD₅ and COD), no significant difference in the level of pollution of surface water along the river flow can be observed.

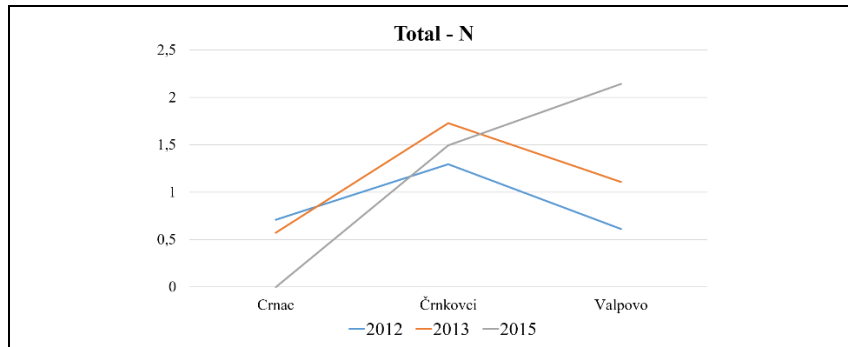


Figure 2. Mean annual value of total nitrogen for the years 2012, 2013 and 2015, along the Karašica River.

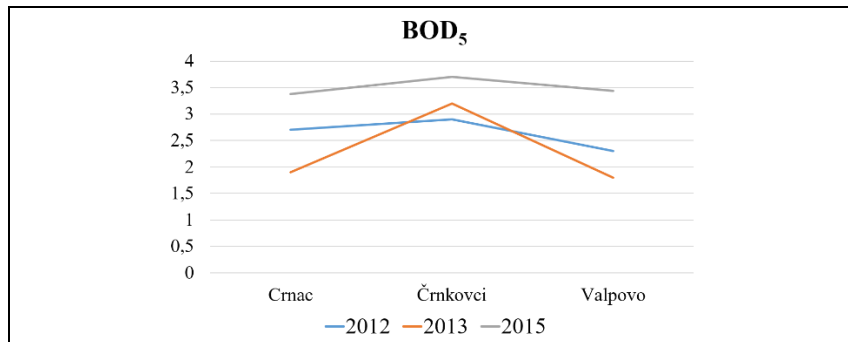


Figure 3. Mean annual value of BOD₅ for the years 2012, 2013 and 2015, along the Karašica River.

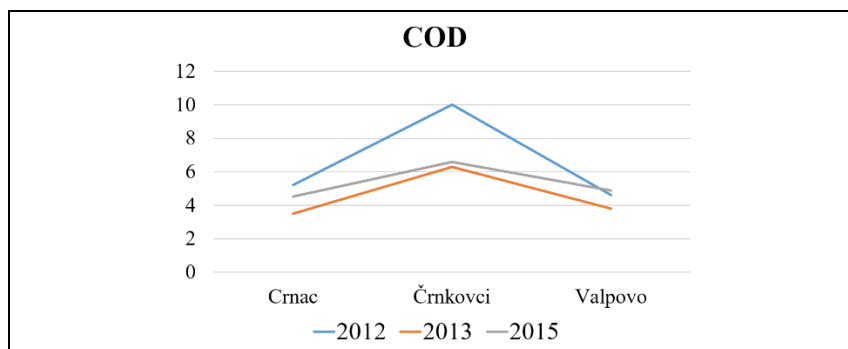


Figure 4. Mean annual value of COD for the years 2012, 2013 and 2015, along the Karašica River.

One-Way ANOVA test was applied to define the significance of the difference between two water quality parameters of Karašica and Vučica rivers. Results are presented in Figure 5. It is obvious that only time behaviour of nitrites is equal for both rivers ($p < 0,05$), while other parameters did not show significant statistical behaviour. This can be explained by different exposure to pollution and different catchment sizes of studied rivers.

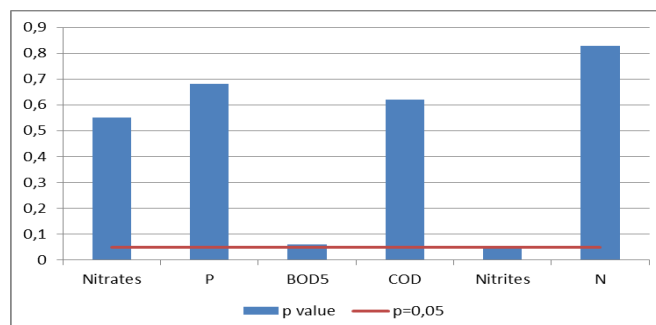


Figure 5. Statistical analysis of the difference between Karašica and Vučica rivers water quality parameters. We also performed statistical analysis to predict the change of observed parameters in the future, for the period of 2016-2020.

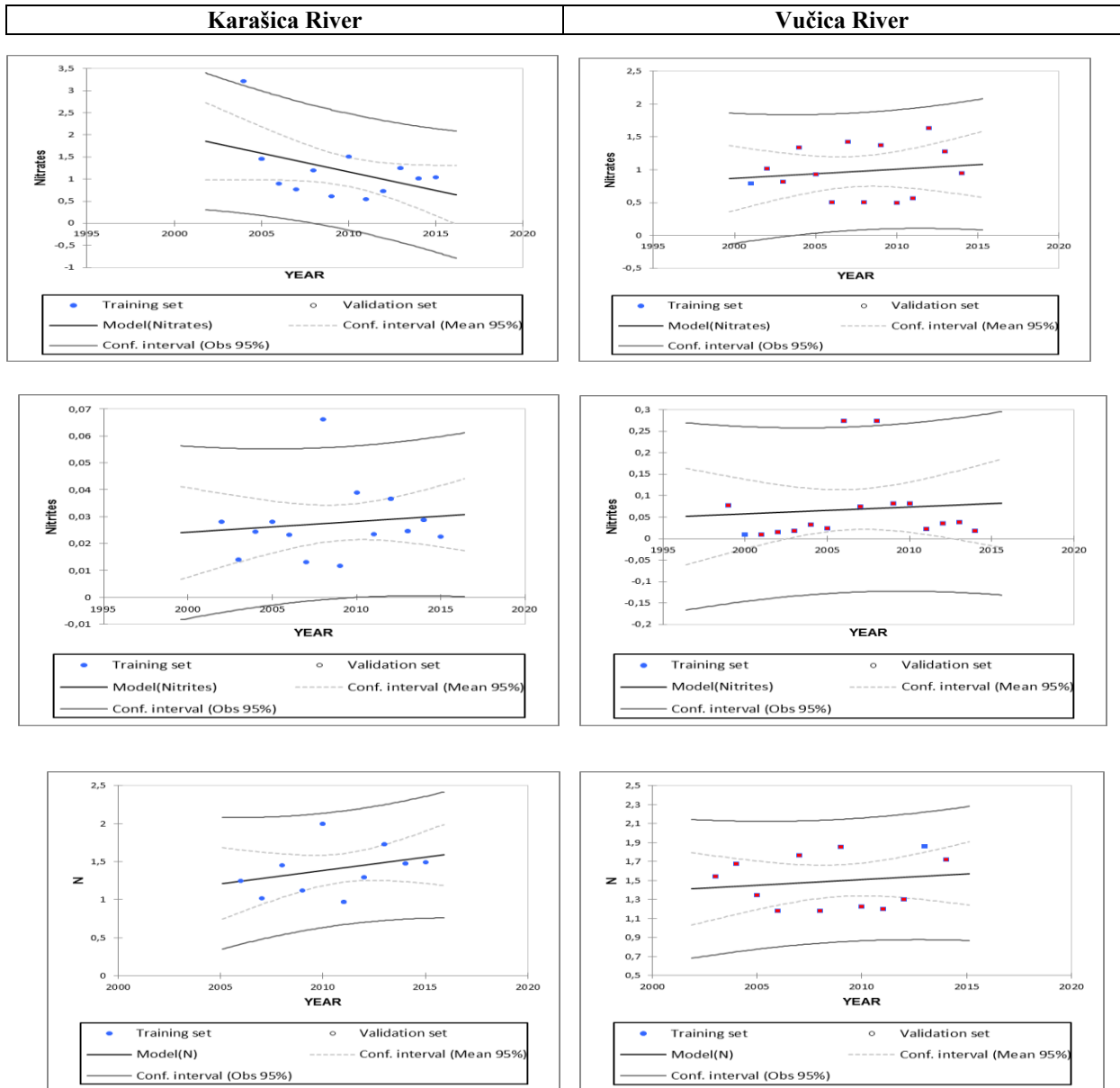


Figure 6. Linear regression of total – N, nitrites and nitrates.

According to obtained results, increasing of all parameters in both rivers can be expected, except nitrates concentration in the Karašica River.

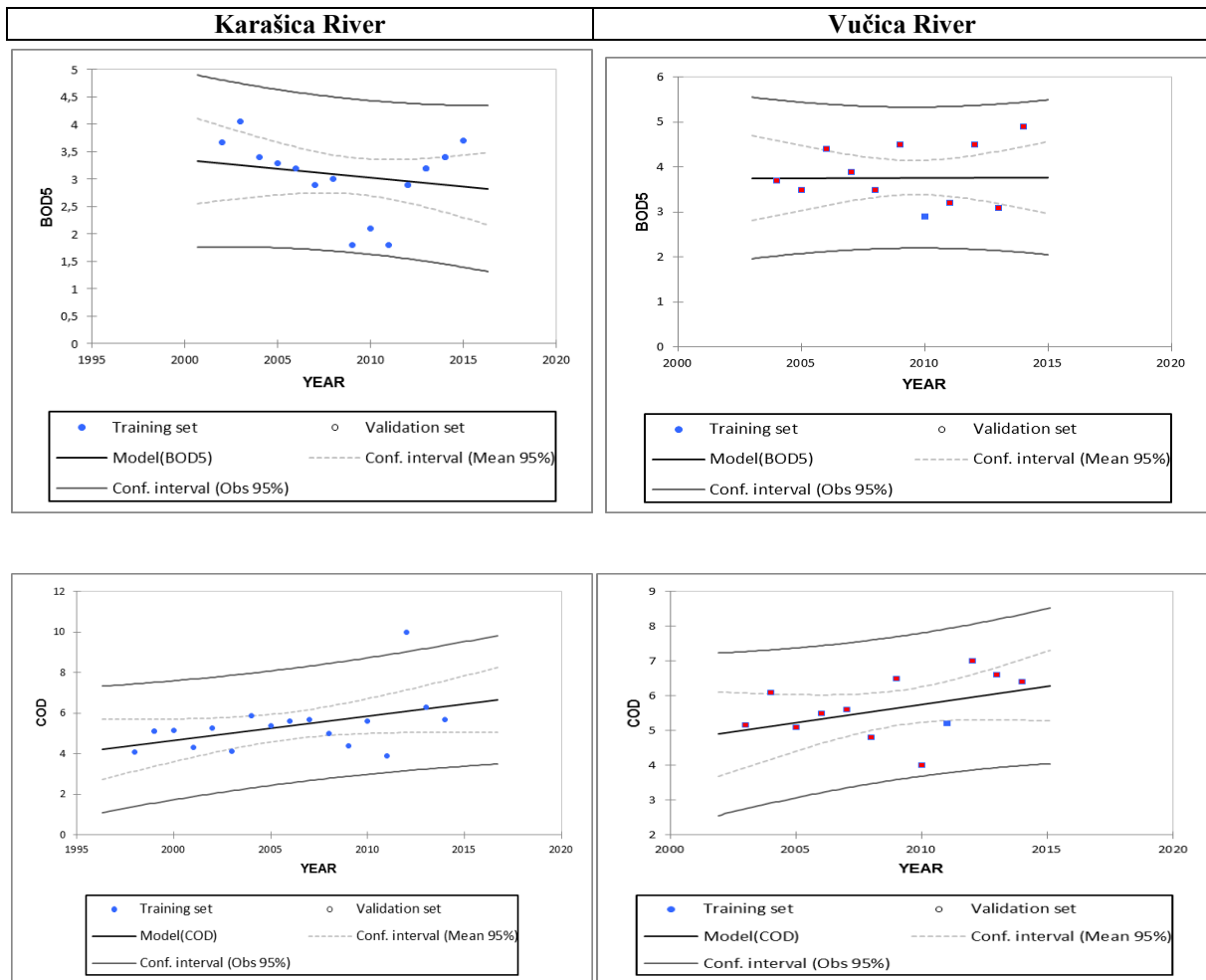


Figure 7. Linear regression of BOD₅ and COD.

Prediction of the BOD₅ and COD is similar. They are predicted to increase, except BOD₅ in the Karašica River, which means that generally the Karašica River shows slight improvement regarding self-purification abilities. The overall analysis suggests that most of the analysed parameters increased at all locations during the analysed period.

5 Conclusion

According to current regulations in Croatia [8], surface water quality of Karašica and Vučica rivers can be generally characterized as good to moderate, depending on analysed parameter and location. Quality of the Karašica River at location downstream from Valpovo is evaluated as moderate, and at two locations, road Crnac-Krčenik and Črnkovci, as good. Quality of the Vučica River at location Marjančaci is evaluated as good, at location Petrijevcı as moderate (regarding BOD₅, nitrates, total – P) to good, and at location bridge on the road Staro Petrovo Polje as poor.

In summary, quality of Karašica and Vučica rivers surface water upstream from industrial complex can be characterized as moderately polluted, with sufficient concentration of oxygen. Such conditions are ideal for excessive algal and aquatic plant growth, leading to increased eutrophication. Downstream from industrial complex, level of surface water pollution is greater, water has decreased amount of oxygen.

Obtained results (especially negative predictions of deterioration of water quality) indicate that it is necessary to take actions to protect the Karašica-Vučica River form further pollution. According to Nitrate Directive [9], potential sources of pollution (agriculture, sewage, industry) should be minimized, systems for water purification should be modernized, by agricultural production already jeopardized and vulnerable areas should be identified and protected, for instance by limiting application

of nitrogen fertilizers. Further continuous monitoring of water quality is necessary in order to insure adequate implementation of the aforesaid measures and to improve reliability of water quality categorization.

References:

- [1] Nadilo, B. Tekla voda Karašica. *Gradevinar*, 66 (2014) 2, 164-174.
- [2] Tadić, L., Dadić, T., Leko-Kos, M. Variability of Hydrological Parameters and Water Balance Components in Small Catchment in Croatia. *Advances in Meteorology*, doi:1393241-1-1393241-13, 2016.
- [3] Tadić, L. Analiza indikatora relevantnih za održivo gospodarenje vodama sliva Karašice i Vučice, Faculty of civil engineering, Zagreb, 2001.
- [4] Munjko, I., Lovrić, E., Jovinac, R. Eutrofne soli u slivu rijeka "Karašica-Vučica" sa posebnim osvrtom na problem nitrata. *Croatian Journal of Fisheries*, 35 (1980) 5, 101-105.
- [5] Vidaček, Ž., Sraka, M., Čoga, L., Mihelić, A. Nitrati, teški metali i herbicid u tlu i vodama sliva Karašica-Vučica. *Poljoprivredna znanstvena smotra*, 44 (1999) 2, 143-150.
- [6] Uredba o klasifikaciji voda [Regulation on water classification, in Croatian]. *Narodne novine* 1998/77.
- [7] Uredba o izmjenama i dopunama uredbe o klasifikaciji voda [Extension to Regulation on water classification, in Croatian]. *Narodne novine* 2008/137.
- [8] Uredba o standardu kakvoće voda [Regulation on water quality, in Croatian]. *Narodne novine* 2013/73.
- [9] Nitrate Directive 91/676 EEC, 1991.

AVERAGE PRESSURE IN A WATER SUPPLY SYSTEM

IVAN HALKIJEVIĆ¹, DRAŽEN VOUK², HANA POSAVČIĆ³

¹ Faculty of Civil Engineering University of Zagreb, Croatia, halkijevic@grad.hr

² Faculty of Civil Engineering University of Zagreb, Croatia, dvouk@grad.hr

³ Faculty of Civil Engineering University of Zagreb, Croatia, hposavcic@grad.hr

1 Abstract

The average water pressure in a water supply system is usually determined as the weighted (by some parameter) average value of all pressures. In IWA (International Water Association) methodology, average pressure is used for calculating 'Unavoidable Annual Real Losses' (UARL), which are a core component for deriving the ILI index (Infrastructure Leakage Index). This paper gives an overview and the comparison of several approaches for determining the average pressure required for the calculation of UARL. The determination of the average water pressure is based on field pressure measurements and the use of calibrated hydraulic mathematical model. Some advantages and disadvantages of each method is pointed out.

Keywords: average pressure, water losses, water systems, UARL, hydraulic mathematical model

2 Introduction

The presence of water losses is a characteristic of all water supply systems. A long-time practice in water losses accounting was based on the percentage relationship between non-revenue water and the amount of water entering the system. The IWA (International Water Association) methodology brings a piece of novelty in water losses analysis by defining water balance components. According to the methodology, water losses are divided into *apparent* and *real* losses, and they represent the difference between the amount of water entering the system and the authorized consumption within the system [1].

According to the IWA methodology, one segment of real losses are *Unavoidable Annual Real Losses* (UARL) which represent the lowest, technically possible, i.e. achievable leakage from the system [2]. The ratio of *Annual Real Losses* and *Unavoidable Annual Real Losses*, represents the *Infrastructure Leakage Index*, aka. ILI index. Since UARL are a vital component for calculating the ILI index, it is necessary to accurately determine this component of *Real Losses*.

The amount of UARL is determined according to the expression [3]:

$$UARL = (A \cdot L_m + B \cdot N_s + C \cdot L_p) \cdot P \quad (1)$$

where:

- $UARL$ - Unavoidable Annual Real Losses, [volume/time],
- L_m - network length (without service connection pipes), [km],
- N_s - number of service connections, [1],
- L_p - total length of service connection pipes between a street and a water meter, [km],
- P - average water pressure in the system, [m],
- A, B, C - coefficients that depend on the technical characteristics of the system, [1].

According to Eq (1), the average water pressure in the system is the parameter that most affects the UARL value. Therefore, it is necessary to accurately determine this value.

This paper presents two approaches for determining the average water pressure in the water supply system. The first approach is based on the water pressure field measurements, while the second one is based on the use of hydraulic mathematical model.

3 Methods to assess the average pressure

Determination of the average water pressure of the whole water supply system is based on a systematic approach in which it is necessary to determine the average pressure of every individual zone in the system. Thereby, the determination of the average water pressure can be based on:

- water pressure field measurements,
- calibrated hydraulic mathematical model.

For both approaches, it is necessary to acquire the additional data related to the geodetic survey (elevations) regarding service connection (customer meters), or specific points within the individual zone (i.e. hydrants), as well as the information regarding water supply network lengths and profiles.

3.1 Average pressure of the zone determined by field measurements

This approach requires the determination of a point in the zone called *Average Zone Point (AZP)* (usually a hydrant), for which it is assumed that the measured pressure, with sufficient accuracy, represents the pressure of the entire zone.

District Metered Area (DMA) is usually formed due to the need of determining the water balance in some part of the system. Boundaries of the zone are usually defined in terms of hydraulic criteria, the location of objects in the system and the possibility of placing measuring equipment. Thereby, pressure measurements are usually carried out at the inlet/outlet point of the zone and one (or few) points (hydrants) within the zone, mostly on the location of critical consumer or on water mains where greatest flow rates are realized [4]. Since DMA boundaries are often determined by the objects in the system (pumping stations, tanks, pressure reducing valves, etc.), it is suitable to use these locations for data acquiring since these objects usually have installed meters or it is convenient to temporarily install them due to available space.

Generally, none of these locations match the AZP, therefore, none of measurements would represent the *average zone pressure*, which is often wrongly calculated as the average pressure between the pressure at the inlet and outlet of the zone, or as the average pressure between the inlet and the critical consumer, Figure 1.

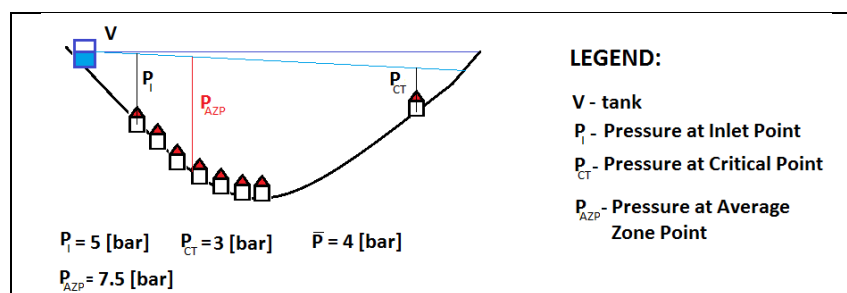


Figure 1. Error in estimating the average zone pressure as the average pressure between the inlet and the critical consumer

A systematic approach for determining the average water pressure of the entire system consists of the following steps [5]:

- determining the weighted average zone elevation,
- identifying a hydrant as the AZP of the zone,
- obtaining the pressure at the AZP for each zone,
- calculating the average pressure of the entire system.

3.1.1 Determining the weighted average zone elevation

The weighted average zone elevation, *WAGL* (\bar{H}), is calculated from geodesic (topographic) data, depending whether the density of service connections in the zone is greater or not than 20 per kilometer of network ([connections/km]).

According to studies [6], if the density of service connections in the zone is greater than 20 [connections/km], the majority of water leakage (real losses) is realized on service connections. In that case, the average elevation of the zone is calculated as the average elevation of all service connections within the zone:

$$\bar{H} = \frac{\sum_1^n h_i}{n} [m] \tag{2}$$

where:

- h_i – ground level (elevation) of the service connection [m],
- n – number of service connections [1].

Otherwise, if the density is less than 20 [connections/km], majority of real losses occur on water network, thus pipes. Then, the average zone elevation is determined as the average elevation of water supply network within the zone. If geodetic survey of the network is not available and if there is more than 100 hydrants in the zone, the average zone elevation can also be determined as the average elevation of all hydrants within the zone [4].

In this case it is necessary to create a table with elevation classes (average elevation between two elevation contours) and the corresponding mains length (or the number of hydrants) that are located between the two elevation contours. The average value of two boundary contours is joined to each class, by multiplying it with the corresponding length of the network (or with the corresponding number of hydrants), Table 1.

Table 1. An example of determining the average zone elevation for density of connections < 20 [1/km]

CONTOUR BANDS [m a.s.l.]	ELEVATION CLASS [m a.s.l.]	NUMBER OF HYDRANTS [1]	LENGTH OF NETWORK [m]	EL. CLASS x NUM. OF HYDRANTS [m a.s.l.]	EL. CLASS x LENGTH OF NETWORK [m x m a.s.l.]	AZP BY NUMBER OF HYDRANTS [m a.s.l.]	AZP BY LENGTH OF NETWORK [m a.s.l.]
(1)	(2)	(3)	(4)	(5) = (2) x (3)	(6) = (2) x (4)	(7) = $\Sigma(5) / \Sigma(3)$	(8) = $\Sigma(6) / \Sigma(4)$
10 ÷ 15	12.5	9	411	112.5	5137.5	20.5	21.0
15 ÷ 20	17.5	11	871	192.5	15242.5		
20 ÷ 25	22.5	7	394	157.5	8865		
25 ÷ 30	27.5	13	919	357.5	25272.5		
		$\Sigma =$ 40	$\Sigma =$ 2595	$\Sigma =$ 820 [m n.m.]	$\Sigma =$ 54517.5 [m x m n.m.]		

If digitized data of network features, such as elevations of hydrants and customer meters (service connections) is available, the average zone elevation can be easily determined by using GIS tools, Figure 2.

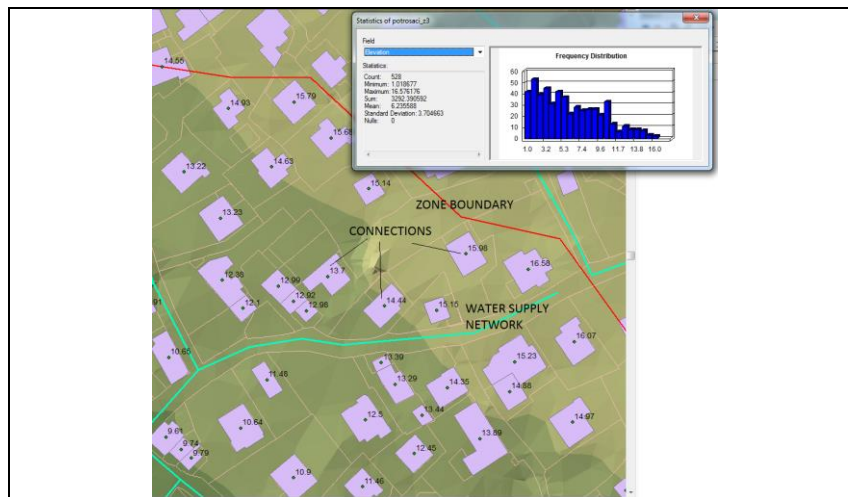


Figure 2. Using GIS tools to determine the average zone elevation

3.1.2 Identification of the hydrant as the AZP representative

After calculating the average elevation, it is necessary to select AZP for each zone, usually a hydrant. The representative hydrant is ideally located in the center of the zone. If such a hydrant does not exist, it is necessary to find a hydrant that is not far from AZP, with a minimum difference in elevation, ΔH , between the representative hydrant elevation, H_{AZP} , and the average elevation of the zone, \bar{H} .

$$\Delta H = |H_{AZP} - \bar{H}| \rightarrow 0 [m] \quad (3)$$

It is necessary to avoid the selection of hydrants that are located on smaller diameter pipes on which higher velocities may occur (>1.5 [m/s]), and it is particularly necessary, due to possible high pressure losses, to avoid measurements on service connections.

3.1.3 Measuring the pressure at the AZP

On the selected hydrant a pressure gauge is installed and pressure is continuously measured for minimum 24 [h] (better 7 days). From obtained measurements the average water pressure is calculated and corrected according to the elevation difference ΔH , (elevation difference between the hydrant used for AZP measurement and the average elevation of the zone, \bar{H}). This corrected pressure value represents the average water pressure of the whole zone, Figure 3.

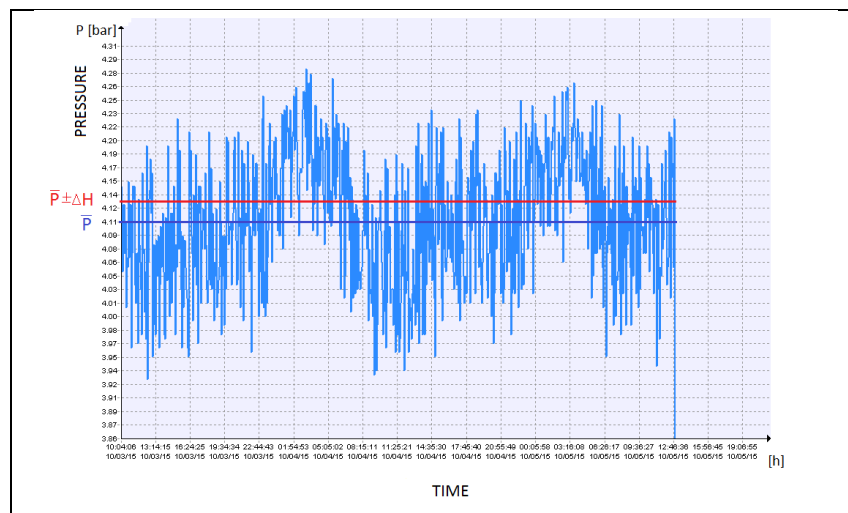


Figure 3. Measured average zone pressure

If it is possible to locate more hydrants close to the average zone elevation (\bar{H}), the measurements can be also performed on these hydrants in order to obtain more reliable value of the average pressure.

If adequate inputs (elevations) and \bar{H} could not be determined, as a final measure, the pressure on at least 3 randomly selected hydrants can be measured. The hydrants should be widely distributed within the zone (on profiles no smaller than DN 80). The average value of these 3 measurements then represent the average zone pressure.

3.1.4 Calculating the average pressure of the system

The average pressure of the entire system is calculated as the weighted average pressure from all zones. For each zone, every previously calculated average pressure is multiplied by the number of connections (for zone with more than 20 [connections/km]), or with the length of the network within the zone (for zone with less than 20 [connections/km]). These value are summed for all zones and divided by the total number of connections (or total length of the network), Table 2.

Table 2. Weighted average system pressure (example calculation of system from Section 4.)

ZONE	LENGTH OF MAINS	NUMBER OF CONNECTIONS	DENSITY OF CONNECTIONS	AVERAGE PRESSURE IN ZONE*	CORRECTION FOR AZP	NUMBER OF CONNECTIONS x AVERAGE PRESSURE	LENGTH OF MAINS x AVERAGE PRESSURE	
	Lm [km]	Ns [1]	Ns/Lm [1/km]	P [m]	ΔH [m]	Ns x P [1 x m]	Lm x P [km x m]	
1	4.92	256	52.0	52.8	1.4	13517	260	
2	12.98	691	53.2	51.7	3.8	35725	671	
3	2.93	528	180.5	35.6	0.5	18797	104	
4	12.10	274	22.6	42.3	6.0	11590	512	
TOTAL	32.93	1749	-	-	-	79629	1547	
FOR ENTIRE SYSTEM								
AVERAGE	8.23	437.3	77.1	45.6	2.9	45.5	47.0	
System density of connection is > 20/km, so best estimate of system P =							45.5	[m]

* measured values with correction of ΔH for average elevation of connections in the zone

3.2 Average zone pressure determined by the mathematical model

This approach involves the use of the calibrated hydraulic mathematical model. In order to create such a model, it is also necessary to obtain field data, thus flow and pressure measurements. Most often, field measurements are obtained in order to determine the water balance in the system, and the same data are also used for the model calibration. During the measurement campaign, usually a less attention is dedicated for the purpose of determining the average zone pressure, and subsequent measurements are, sometimes, difficult to perform (redistributed measuring equipment, not included by contract terms, deadlines of the project etc.).

It is important to evaluate the calibrated model with all available field data (preferably time-coherent), taking into account that for each zone pressure measurements are obtained at several points. The accuracy of calibrated model can be determined through a very close match between all measured and modelled values.

The advantage of using calibrated model is simpler and faster determination of the average pressure and the ability of different subsequent pressure analysis without the need for additional field data. Therefore, it is possible to obtain the average pressure in the same way, wherein field measurements are replaced by node pressure readings from the model. In addition, through the model it is possible to take into account all node pressures in the network, or at service connections, and to calculate weighted pressure value in a simple and quick way.

By using the hydraulic model, the average pressure can be obtained as:

- the average pressure in AZP,
- the average pressure in several nodes (hydrants) at the average zone elevation,
- the average pressure in all nodes (service connections) in the zone,
- the weighted average zone pressure.

3.2.1 The average pressure in AZP

This approach is equivalent to the average pressure obtained by AZP field measurements. Also, it is necessary to determine the average elevation and its associated node in the zone for which the 24-hour pressure diagram is read off, thus the average pressure is read directly from the model, Figure 4.

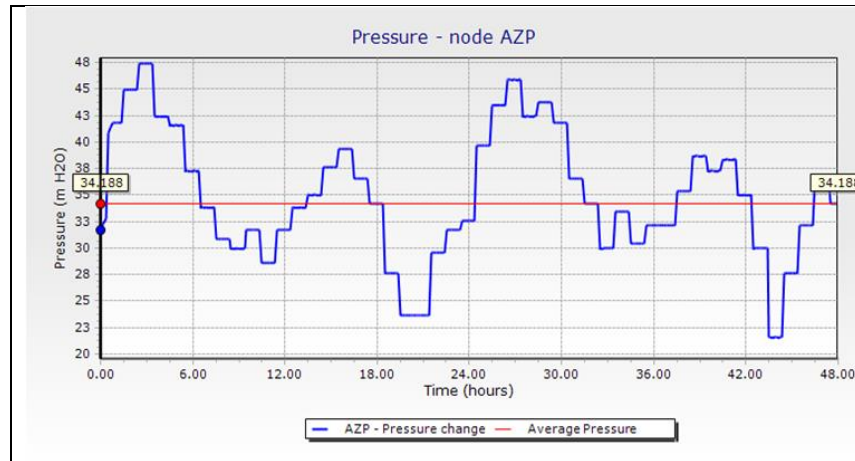


Figure 4. Average pressure in AZP read directly from the model

Since it is possible to add nodes at arbitrary locations, the advantage of using model pressure readings relative to the field measurements is the possibility of reading pressure exactly in the point that corresponds to the average elevation of the zone, \bar{H} , (without looking for conveniently located hydrants). Thus, the problem of non-existing nodes (hydrants) at the average elevation of the zone and the correction of the pressure for ΔH , is not relevant in this case, Figure 5.

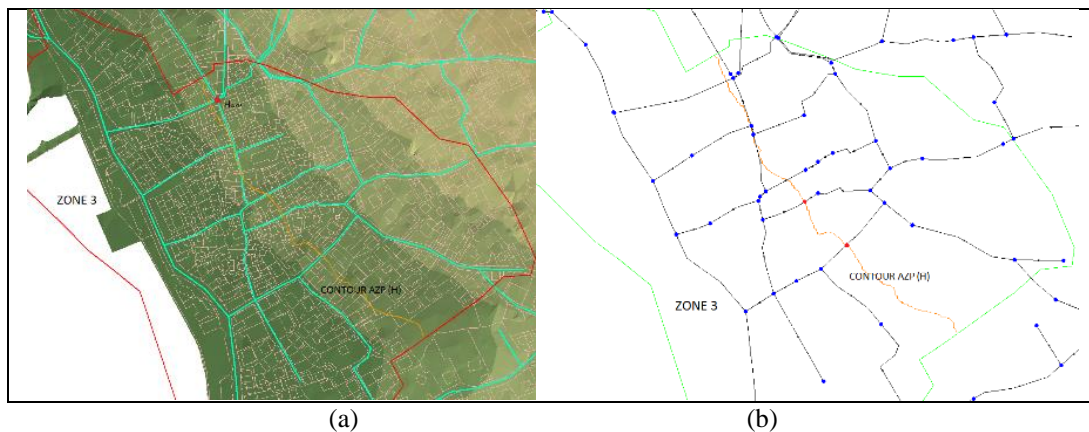


Figure 5. The possibility of determining the average pressure in the model versus the field survey
 (a) measuring the pressure in AZP in the edge of the zone with the existence of ΔH ;
 (b) reading the pressure at the \bar{H} and in the center of the zone

3.2.2 Reading average pressures in more nodes at an average elevation of the zone

The method is equivalent to pressure measurements obtained from more hydrants located at, or near the average zone elevation, \bar{H} . The procedure is carried out by drawing a contour on average zone elevation and by reading the pressure on every node that is located directly on the contour or immediately near it (take care to avoid smaller profiles). Thereby, it is possible to add suitably selected nodes for pressure value readings, Figure 5(b).

After reading the average pressures, \bar{p}_i , for 24 hours in n nodes on \bar{H} contour, it is necessary to determine their average value, \bar{P}_n .

$$\bar{P}_n = \frac{\sum_1^n \bar{p}_i}{n} [bar] \tag{4}$$

3.2.3 Determining the average pressure based on all nodes in the zone

It is performed similar to the previous method, wherein the average pressure is read in all nodes (service connections) in the zone and the average pressure is calculated according to Eq (4).

Since all the nodes in the zone are taken into account, it is very important, in the process of model building, to take into account the spatial distribution of nodes in the zone, because a larger number of nodes, for example in the area with higher pressure, will result in a higher average zone pressure than it really is, Figure 6.

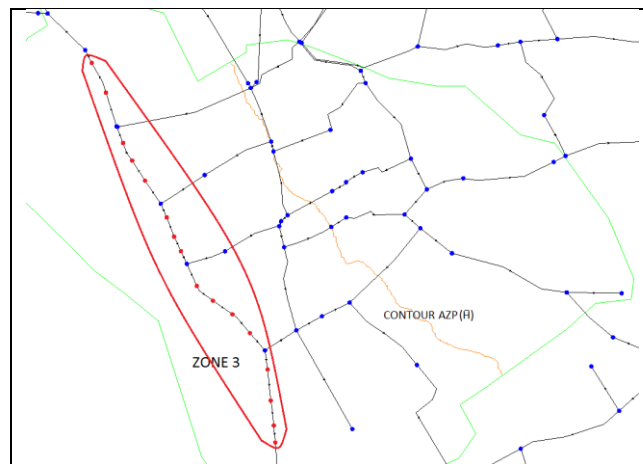


Figure 6. The higher density of nodes in the part of the zone in which higher or lower pressure values occur, affects the final average zone pressure

Therefore, it is necessary to take into account that the density of nodes in the model is uniform within a zone/system. Ideally, each node should represent one service connection with associated water consumption.

3.2.4 Determining the weighted average zone pressure

In most cases, when the node density is not uniformly distributed, or when one node does not represent one service connection, the average zone pressure can be determined as weighted node pressure. In that case, the weighted factor can be:

- The water consumption in the node,
- Node corresponding length of the water supply network.

If water consumption at node is chosen as the weighted factor it would imply that the actual number of service connections is taken into account. Therefore, it is assumed that higher consumption in node represents a greater number of service connections within a small area of the zone and the resulting pressure will be weighted with associated consumption, Figure 7.

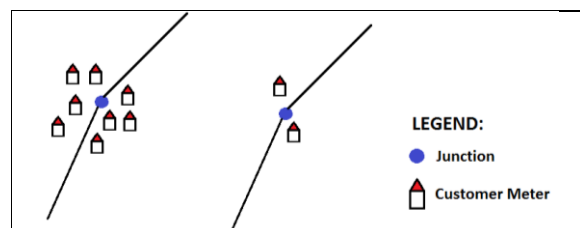


Figure 7. Calculated pressure weighted with the number of customer meters

It is necessary to consider that the water consumption of a single larger customer, whose consumption is also defined at some node, will also influence the average pressure of the whole zone.

In this case, in order to determine the average pressure of the zone, the average pressures from all nodes need to be weighted with associated consumption according to the following:

$$\bar{p} = \frac{\sum \bar{p}_i \times (1 + d_i)}{\sum (1 + d_i)} \text{ [bar]} \quad (5)$$

where:

\bar{P} – average zone pressure, [bar],

\bar{p}_i – average node pressure in 24 hours, [bar],

d_i – water consumption (water demand) in the node, [l/s].

Since the pressures in water supply network, regardless of the density of connections, occur along the entire water supply network, and not only in one point (as in the hydraulic model), it is possible to choose node belonging length of the network for weighted factor. Thus, the average pressure directly depends on the length of the network where the specific pressure value occurs. For example, if small pressures occur in the largest part of the network, the average pressure will be affected by the belonging length. This belonging length of the network is defined as the sum of the half-pipe lengths that are related to one node, Figure 8.

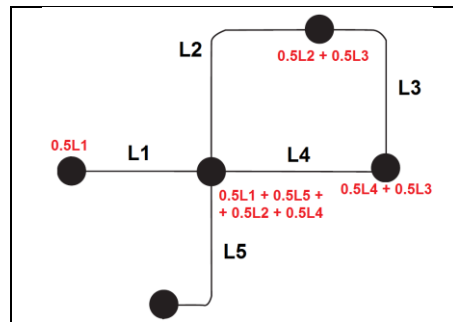


Figure 8. Node corresponding length of the network

In this case, the average zone pressure is calculated by using the formula:

$$\bar{p} = \frac{\sum \bar{p}_i \times L_i}{\sum L_i} \text{ [bar]} \quad (6)$$

where:

\bar{P} – average zone pressure, [bar],

\bar{p}_i – average node pressure in 24 hours, [bar],

L_i – the length of water supply network that belongs to each node in the zone, [m].

3.2.5 The average pressure of the whole system

In case where the average zone pressure is determined as the average pressure of all nodes in the zone, or as the weighted (with length of the network or consumption in the node) average pressure, the average pressure of the entire system is determined as the mean average pressure of all zones, according to Eq (4).

If the average zone pressure is determined by pressure readings in one or more nodes at the average zone elevation, then the pressure from each zone, depending on the density of connection, needs be weighted with number of service connection or with the belonging length of the network, as in Table 2.

4 Calculation example

In the following an example of the average water pressure is given for a water supply system divided in 4 pressure zones, Figure 9.

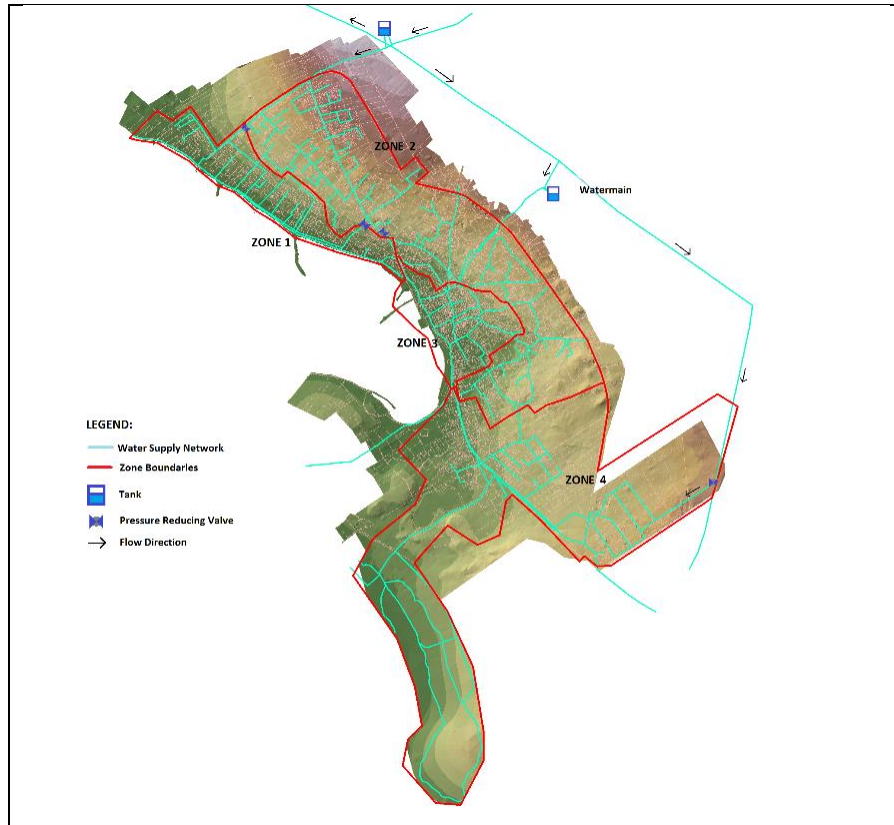


Figure 9. Analysed average pressure in gravity water supply network

The system is supplied from two tanks and through pressure reducing valve located at the entrance to the zone 4. Tanks and mentioned pressure reducing valve are connected to a water main located at high elevations above the system. In the process of system zoning, field flow and pressure measurements were gathered, upon which the hydraulic mathematical model was built and calibrated. The results of calibration are shown in Figure 10.

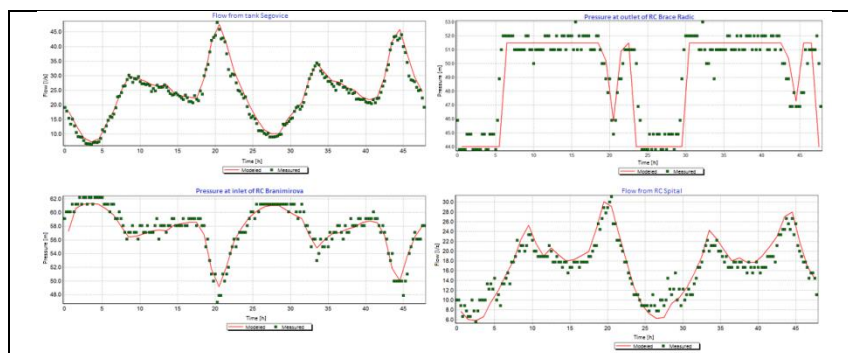


Figure 10. The results of calibration of the mathematical model of water supply system from Figure 9

The basic characteristics of the system relevant for average pressure determination are given in Table 3.

Table 3. Some characteristics of the analysed water supply system

WATER SUPPLY NETWORK	ZONE 1	ZONE 2	ZONE 3	ZONE 4	Σ
Number of connections [1]	256	691	528	274	1749
Length of network [km]	4.92	12.98	2.93	12.10	32.93
Density of connections [1/km]*	52.0	53.2	180.5	22.6	
Average elevation of connections [m a.s.l.]	7.3	23.0	6.2	10.6	

* the average density of connections of the whole system is 77.1 [1/km]

With calibrated model the average pressure is determined for each zone and ultimately for the entire system according to methods explained in Section 3.2. Obtained results are shown in Table 4.

Table 4. Average zone pressures

AVERAGE ZONE PRESSURES for 24 [h] [m]				
Method for determining the average pressure	ZONE1	ZONE 2	ZONE 3	ZONE 4
Average pressure in a node at the average zone elevation (center of the zone)	52.6	52.3	34.2	42.8
Average pressure for 5 nodes at the average zone elevation (throughout the zone)	51.6	47.9	33.9	42.4
Average pressure of all nodes in the zone	54.2	43.4	36.8	37.5
Average pressure of all nodes with additional nodes in high pressure subzones	54.6	44.6	37.0	41.2
Average pressure weighted with node consumption	54.2	43.6	36.7	38.6
Average node pressure weighted with the corresponding length of the water network	54.9	44.0	35.0	38.3

Results show that the difference in the average pressure within the same zone, depending on the used method, vary considerably. In this case, the difference between average pressures ranges from 0.3 [bar] for Zone 1, to 0.9 [bar] for Zone 2. This difference in average pressure for a certain zone, significantly affects the reliability of UARL calculation.

The results for average pressures of the entire system are given in Table 5. It may be noted that, due to the averaging pressure values from all zones, ultimately, the difference between methods is considerably lower.

Table 5. Average pressures for the entire system

AVERAGE PRESSURE FOR THE ENTIRE SYSTEM	
Method for determining the average pressure	P_{system} [m]
Average pressure in a node at the average zone elevation (center of the zone)	45.4
Average pressure for 5 nodes at the average zone elevation (throughout the zone)	43.4
Average pressure of all nodes in the zone	43.0
Average pressure of all nodes with additional nodes in high pressure subzones	44.3
Average pressure weighted with node consumption	43.3
Average node pressure weighted with corresponding length of the water network	43.1

5 Conclusion

The average system pressure obtained by field data is 45.5 [m] (Table 2), suggesting that the first approach, which relates to the average pressure obtained in one point, at the average zone elevation (AZP), is the most accurate. According to this method, the average pressure is 45.4 [m]. However, since it is necessary to determine the average pressure of the entire system, and the pressure occurs across the water supply network, the method in which the node pressure is weighted with corresponding length of the network should be preferred.

Each of above methods for determining the average pressure result with a different average pressure value and the difference between methods can be very significant.

Both approaches have certain advantages and disadvantages. With filed measurement, the real pressure values in each zone can be obtained directly. The disadvantage of this approach is in the necessity of obtaining a large number of time-coherent measurements at a number of locations in each zone (eg. at each service connection). This requires a lot of measuring equipment which is usually not available. Also, the proper functioning of pressure measuring devices is questionable, wherein the failure of the device, or measuring with degree of error, is usually present.

On the other hand, the calibrated model also requires many field flow and pressure measurements.

The average water pressure for systems pressurized with pumping stations, can be determined in the same manner as described above.

References

- [1] American Water Works Association: Water Audits and Loss Control Programs (M36): AWWA Manual of Practice 3rd Edition, April 2, 2009.
- [2] THORNTON, J.; Water Loss Control, 2nd edition, McGraw-Hill Education, 2008.
- [3] LAMBERT, A. O.; MCKENZIE, R. D.; Practical Experience in using the Infrastructure Leakage Index, International Water Association Conference 'Leakage Management: A Practical Approach', Cyprus, November, 2002.
- [4] ILMSS Ltd; Guidelines relating to the Assessment and Calculation of Average Pressure in Water Distribution Systems and Zones, 28th July, 2013.
- [5] RENAUD, E.; SISSOKO, M.T.; CLAUZIER, M.; GILBERT, D.; KHEDHAOUIRIA, D.; Comparative study of different methods to assess average pressures in water distribution zones, Waterloss 2012, Feb 2012, Manille, France. 9 p., 2012. <hal-00779645>
- [6] LAMBERT, A.; TAYLOR, R.; Water Loss Guidelines – Water New Zealand, February, 2010.

HYDRAULIC MODELLING OF DEMAND GROWTH IN TOURIST ISLANDS, CASE STUDY: GALÁPAGOS, ECUADOR

MARIA FERNANDA REYES PEREZ ¹, NEMANJA TRIFUNOVIĆ ¹, SAROJ SHARMA ¹, MARIA KENNEDY ¹,

¹ IHE Delft Institute for Water Education, The Netherlands, m.reyesperez@un-ihe.org, n.trifunovic@un-ihe.org, s.sharma@un-ihe.org, m.kennedy@un-ihe.org

1 Abstract

Tourist islands worldwide have five characteristics in common: (1) natural beauty, (2) sunny and dry climate, (3) travellers who like to enjoy both at maximum affordable luxury, (4) local population who wish to capitalise with income from tourism, and (5) vulnerable environment with scarce potable water and energy resources that need protection. Renowned for its unique wildlife, Galápagos Archipelago in Ecuador is one of the most challenging examples where all these issues have to be brought in optimal balance. This manuscript presents the network hydraulic modelling in Puerto Ayora, the main tourist hub of Santa Cruz Island, which is threatened by exponential tourism rates over the last two decades. Currently, the water supply there is characterised by insufficient quality and quantity of brackish, untreated and practically non-potable water. The distribution is intermittent with households massively relying on individual roof tanks and bottled drinking water, however with surprisingly wide range of specific demands, between 50 and well above 400 lpcpd. That raises concerns about illegal tourist water use and unnecessary wastages while filling the household roof tanks. The hydraulic model built in EPANET software was used with two objectives: (1) to assess the levels of water losses from the spilling of the roof tanks and justify the applied intermittency regime, and (2) to check conveying capacity of the network by proposing rehabilitation measures for the most environmentally responsible future demand growth scenario. The hydraulic simulations to address the first objective were run in pressure-driven demand mode (PDD) using emitter coefficients for different scenarios of supply, while the future demand scenario was analysed in standard demand-driven mode of calculation (DD) to assess the need for intermittent supply and accumulation of water in the roof tanks. The results show significant water losses from the tanks contributing to the intermittency purely as a negligence of local population. Furthermore, a moderate network renovation will be needed for future demand scenario in case of continued (limited) use of the roof tanks. Although done on a relatively small case, the research points that the hydraulic modelling of distribution networks in tourist islands poses quite a complex problem due to transient flow conditions caused by intermittency, numerical instability caused by numerous tanks existing in the model, and difficult calibration from unknown and inaccurate data needed to build a reliable model. Yet, these analyses offer preliminary conclusions of high environmental relevance.

Keywords: water distribution, network modelling, tourist demand, intermittent supply, PDD analysis, water leakage

2 Introduction

Water demand tends to exceed the available supply capacity, especially in many developing countries, as a result of rapid population growth [1]. As a consequence, Intermittent Water Supply (IWS) regimes are introduced with the aim of limiting that demand. Furthermore, in arid regions the problem is amplified by low conveying capacity in the distribution network, often too deteriorated to deliver the required demands [2]. Even though the water distribution should be equitable and efficient [3], IWS have become a norm rather than an exemption [4], mainly due to necessity rather than the initial design [3].

IWS varies depending on the region and situation, ranging from a few hours per day to a few hours per week. Therefore, the consumers need to store as much water as possible during service hours, to compensate the periods of interruption. Therefore, individual storage facilities play important role in intermittent supply networks, since they are the only supply when the service is unavailable. Often, this

type of systems is characterized by inadequate pressures, high peak factors in the distribution system [5], and failure of pumps and pipes to carry the required water in the times of supply [2].

Network modelling software commonly uses the so called Demand Driven Analysis (DDA) as the default hydraulic solver. This assumes that the nodal demands are known functions of time and are independent of the pressure available in the system [6]. The hydraulic simulation then produces the nodal pressures and pipe/pump flows which satisfy those fixed nodal demands, presenting reasonable and close-to reality solutions (but under regular supply conditions). This approach assumes that the nodal demands are always delivered, regardless of the pressures throughout the distribution system, since the algorithm formulates the needed equations to solve the unknown nodal heads [7]. At the same time, this algorithm is unable to capture accurately the behaviour of intermittent systems, operating under irregular conditions.

A number of studies, such as those by [8], [9] and [10], based mainly on field investigations, discuss the restrictions of DDA. These studies suggest the use of the Pressure Driven Analysis (PDA), which assumes a fixed demand above given pressure threshold, zero demand below the given minimum pressure, and proportional relationship between the pressure and the demand for the pressure range between the threshold and the minimum values [7]. The PDA approach uses the concept of orifices at system nodes, with the aim of replicating a pressure-demand relation in the modelling process, suggesting that PDA can be more effective than DDA when simulating intermittent conditions. The EPANET software uses the PDA concept through Emitter Coefficients (EC), which model pressure-dependant flows from sprinkler heads, as developed by [11], describing the concept of EC by using similar relationships as in Eq. (1).

$$H_i = H_i^{\min} + K_i Q_i^n \quad (1)$$

In this case, an emitter is modelled as a setup of a dummy pipe which is connected to the actual node, with a dummy reservoir whose nodal elevation (z) equals the initial head. Hence, $H_i^{\min} = z_i$ and:

$$Q_i = \frac{1}{K_i^{1/n}} (H_i - z_i)^{1/n} \quad (2)$$

The K-value in Eq. (2) refers to the resistance of the dummy pipe. Finally,

$$Q_i = k_i \left(\frac{P_i}{\rho g} \right)^\alpha \quad ; \quad \frac{P_i}{\rho g} = H_i - z_i \quad ; \quad \alpha = 1/n \quad ; \quad k_i = \frac{1}{K_i^\alpha} \quad (3)$$

where k_i is the EC in node i and α is an emitter exponent with theoretical value of 0.5. EC was first introduced to simulate operation of fire hydrants. Several other PDA approaches have been based on further improvement of the EC concept, such as the one by [12]. However, extensive field data collection is required for determination of the relationship between nodal heads and flows [7].

3 Case study description

Tourist islands face pressure to tackle the scarcity aiming to optimise the revenues from tourism while providing sufficient environmental protection. With more than 60% of the total population, Puerto Ayora is the main urban settlement and touristic centre of the Galápagos Archipelago, located on Santa Cruz Island. It has a distribution network built approximately 30 years ago, which consists of approximately 2,500 service connections and supplies brackish water to approximately 12,000 inhabitants, intermittently [13]. Because of insufficient maintenance, the network has high leakage levels whose actual figure has not been established accurately, yet. Most households have their own storage facilities, mainly in the form of roof-tanks and/or cisterns, perceiving the supply as unreliable and insufficient.

Also, the fixed water-tariff structure (paid per month regardless the level of domestic consumption) seems to be the main cause of excessive water wastage within the premises, also emerging from leakages and spillage from the roof tanks and cisterns. Puerto Ayora has been confronted by exponential increase of local population and tourism over the last decades [13], while the local authorities have not been able to cope with this growth, causing a significant impact on the water supply.

The water supply system has an intermittent regime, with the aim of preserving scarce water resources. However, this intermittency is also believed to be caused by the lack of proper management and by sensitive political issues [14]. Because of this regime adopted by the municipality authorities, the local population perceive the system as unreliable. The water is supplied three hours per day on average, depending on the location of the neighbourhood. There are no individual water meters installed, leading to significant water wastage. In addition, the fact that the system has been built in an improvised way, adapting it to the fast population increase, makes the service levels low. For this reason, the municipality has divided the town into five distribution zones with different schedules of supply. Due to the lack of monitoring/data and various forms of illegal extractions [14], the overall water demand in Puerto Ayora has been very difficult to estimate.

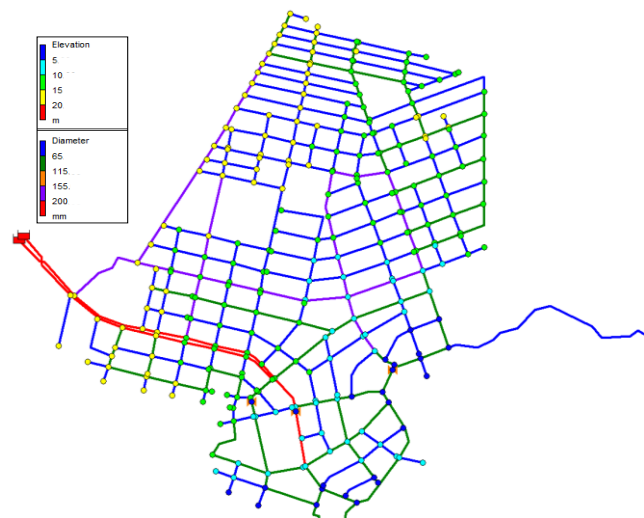


Figure 1. Layout of Puerto Ayora water supply network

The research presented in this manuscript analysed the hydraulic performance of the network in Puerto Ayora, with specific attention to the water losses from spilling of the roof tanks. During the fieldwork data collection, a peculiar situation was observed regarding the local complaints on the lack of water combined with overwhelming amount of wastage from the overflow of the household roof tanks. The reason is the likely absence of float valves and the fact that the owners do not shut-off the faucets manually when the tank is already full (they may not be even at home at that moment). Therefore, an attempt was made to develop a modelling methodology for quantification of the overflows of household roof tanks and further reassess the currently applied IWS regime with the PDA approach. On the latter, the research aimed to assess the network conveyance capacity in the future and the need for IWS and roof tanks, and propose suitable rehabilitation measures, for what has been indicated as the maximum demand growth scenario indicated in the research, described in previous publications. These demand scenarios were simulated by applying DDA.

4 Methodology

The hydraulic network model was built in the EPANET software, as shown in Figure 1, which consists of 2 reservoirs, 284 nodes and 367 pipes. An estimation of nodal demands was done based on the total population and the demography per m².

To check the robustness and numerical stability of the EPANET hydraulic solver, a variant was also developed by modelling each node connected to a tank of the size anticipated from the number of occupants supplied from it, and its elevation corresponding to that of the node. An average of five inhabitants per household was assumed and an average tank height of 1.5 m above the ground level. All tanks were assigned the initial depth of 1 m, the minimum depth = 0 m, and the maximum depth = 3 m. Also, a check-valve was modelled on a short dummy pipe, to prevent backflow from the tank (i.e simulate the inlet arrangement from the top).

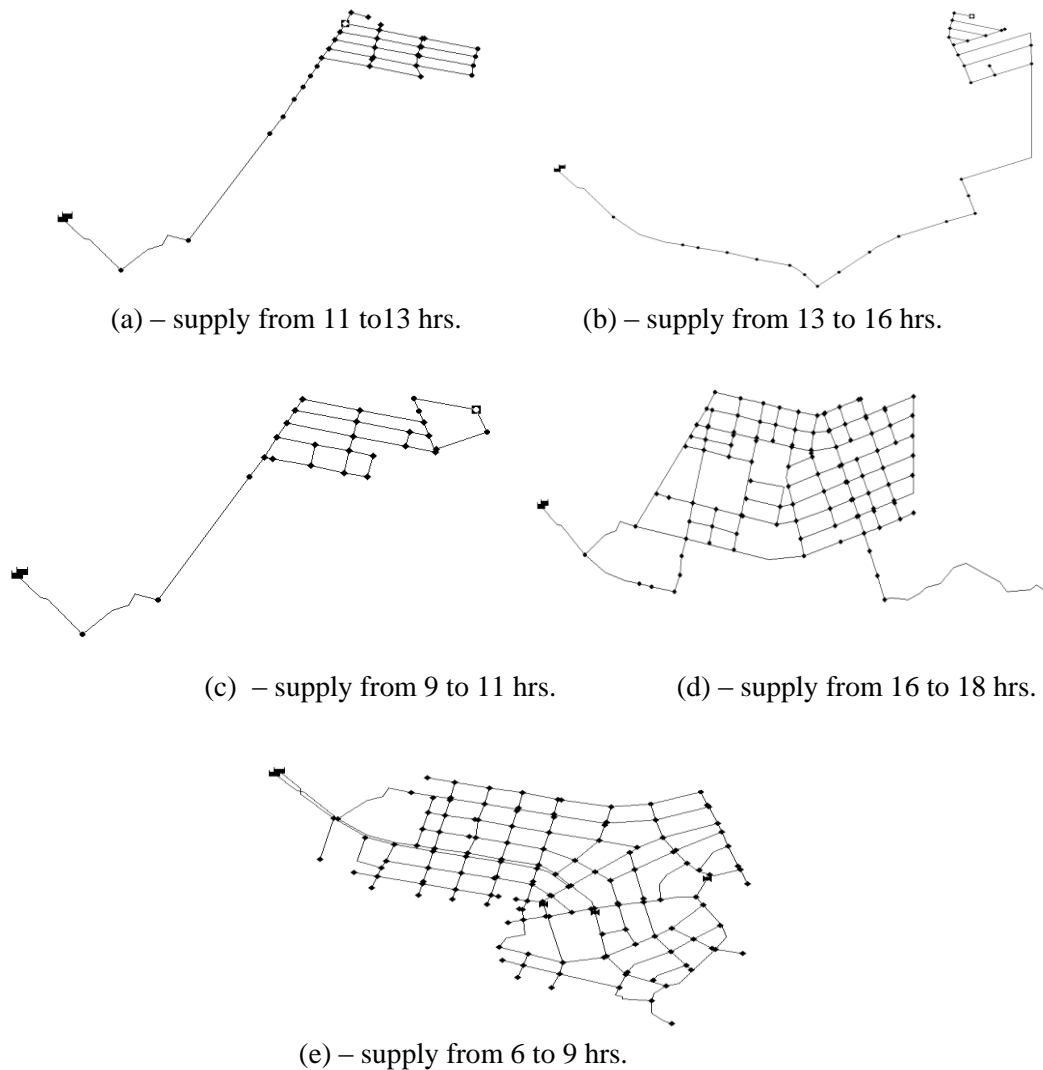


Figure 2. Layouts of five supply zones of distribution according to the Municipality of Santa Cruz.

Alternatively, the PDA was simplified in order to enable the rationing as applied in reality. To make it possible, the network with emitter coefficients was divided into five small sub-systems (Figure 2), capturing the five distribution zones created by the Municipality. Different EC values were tried for each zone and supply hours, in an attempt to match the previously reported total amount of supply per day (which is approx. 5,000 m³ for the horizon 2015, including the leakage), ending with the adopted EC value of 0.5, as an average. Moreover, the assessment of the overflow of nodal tanks was done per zone, for several scenarios created by varying the leakage levels, the average volume of individual storage, and the percentage of the level of the tank filled at the moment the water supply starts in a particular distribution zone. The volumes considered in making the balance per each node of the five sub-models are further shown in Eqs.4 to 10.

$$V_i^{avl} = n_{h,i} X_1 \quad (4)$$

V_i^{avl} is the total available individual storage volume in node i (in m^3), $n_{h,i}$ is the number of households served from the node, and X_1 indicates the average storage volume available per household (m^3).

$$V_i^{c24} = n_{c,i} X_2 \quad (5)$$

V_i^{c24} is the total volume consumed in node i over 24 hours (in m^3), $n_{c,i}$ is the number of consumers served from the node, and X_2 indicates the average specific demand per capita (lpcpd).

$$V_i^{s24} = Q_i^{EC} h_i^s \left(1 - \frac{X_3}{100}\right) \quad (6)$$

V_i^{s24} is the total volume supplied to node i over 24 hours (in m^3); this is an IWS that occurs during h_i^s hours at the flow Q_i^{EC} (in m^3/h) based on the available pressure calculated in EPANET using the EC. X_3 indicates the average leakage percentage in node i .

$$V_i^{cIWS} = \sum_{j=1}^{h_i^s} \frac{V_i^{c24}}{24} pf_{j,i} \quad (7)$$

V_i^{cIWS} is the total volume consumed in node i (in m^3) during the IWS period of h_i^s hours, at hourly peak factors $pf_{j,i}$ applied depending on the period of the day when the IWS takes place. Hence, the actual volume accumulated in the tank(s) of node i during the IWS period is $V_i^{s24} - V_i^{cIWS}$. Assuming X_4 to be the variable that indicates the percentage of the total available volume V_i^{avl} already occupied at the moment when the IWS starts, the buffer of volume in the tank(s) of node i , V_i^{buf} , when the IWS stops, will be:

$$V_i^{buf} = V_i^{avl} \left(1 - \frac{X_4}{100}\right) - (V_i^{s24} - V_i^{cIWS}) \quad (8)$$

Possible negative result in Eq. 8 will indicate the overflow i.e. the spilling from the tank(s) of node i . Furthermore, when the IWS stops, the tank(s) will be discharged for the volume $V_i^{c24} - V_i^{cIWS}$ suggesting the initial volume before the IWS starts again to be:

- 1) $V_i^{avl} - (V_i^{c24} - V_i^{cIWS})$, if the overflow was taking place during the IWS ($V_i^{buf} < 0$);
- 2) $V_i^{avl} - V_i^{buf} - (V_i^{c24} - V_i^{cIWS})$, if the overflow was not taking place during the IWS ($V_i^{buf} \geq 0$).

In both of these cases, the result can in theory be negative, suggesting the water shortage and/or insufficient volume of the tanks. Assuming that this is not the case, some indication exists while assessing the values for X_4 . Sample calculation done for IWS Zone 1 shown in Figure 2 is given in Table 1, taking $X_1 = 1.5 m^3$, $X_2 = 163$ lpcpd, $h_i^s = 2$ hours, $X_3 = 17.5\%$, $pf_1 = 1.29$, $pf_2 = 1.66$, and $X_4 = 0$. With these, the total overflow amounts at approximately $114 m^3$, which is about 42% of the total volume supplied (of $269 m^3$). The full analysis was done for the entire network, judging the influence of each variable. Finally, the water supply network was assessed for the future demand under four tourist and local population growth scenarios.

Table 1. Assessment of tanks' overflow in IWS Zone 1

ID _i	n _{c,i}	n _{h,i}	V ^{avl} (m ³)	X ₂ (lpcpd)	h _i ^s (hrs)	V _i ^{e24} (m ³)	V _i ^{eIWS} (litres)	V ₂ ^{eIWS} (litres)	Q ^{EC} (l/s)	V _i ^{s24} (m ³)	V _i ^{s24} - V _i ^{eIWS} (m ³)	V _i ^{buf} (m ³)
J-1	31	6	6.2	163	2	5.1	272.9	351.2	2.1	12.4	11.7	-5.5
J-2	29	6	5.8			4.7	252.1	324.4	2.0	12.1	11.5	-5.8
J-3	18	4	3.6			2.9	157.0	202.1	2.1	12.5	12.2	-8.6
J-42	15	3	3.0			2.5	133.1	171.3	2.1	12.4	12.1	-9.1
J-43	27	5	5.4			4.4	238.1	306.4	2.0	11.8	11.3	-5.8
J-44	15	3	3.0			2.5	132.2	170.1	2.0	11.8	11.5	-8.5
J-45	27	5	5.3			4.3	233.3	300.2	2.1	12.5	11.9	-6.6
J-46	39	8	7.8			6.4	342.1	440.3	2.0	11.9	11.2	-3.4
J-47	23	5	4.5			3.7	198.8	255.8	2.1	12.6	12.1	-7.6
J-48	47	9	9.3			7.6	408.9	526.2	2.0	11.6	10.7	-1.3
J-50	27	5	5.4			4.4	238.3	306.7	1.8	10.5	10.0	-4.5
J-64	28	6	5.7			4.6	249.4	321.0	2.0	11.7	11.1	-5.4
J-65	54	11	10.9			8.8	475.7	612.1	2.1	12.5	11.4	-0.5
J-66	27	5	5.4			4.4	237.6	305.8	2.1	12.5	11.9	-6.5
J-67	44	9	8.9			7.2	389.5	501.3	2.0	12.1	11.2	-2.3
J-68	28	6	5.6			4.5	244.3	314.3	2.2	12.8	12.3	-6.7
J-69	35	7	7.1	5.8	311.0	400.2	2.2	13.2	12.5	-5.4		
J-70	29	6	5.8	4.7	254.1	326.9	2.0	12.1	11.5	-5.7		
J-78	54	11	10.8	8.8	473.6	609.4	2.1	12.7	11.6	-0.8		
J-79	47	9	9.3	7.6	407.9	524.9	2.0	11.8	10.9	-1.6		
J-80	26	5	5.2	4.2	227.6	292.9	2.0	11.7	11.2	-6.0		
J-81	34	7	6.8	5.5	298.0	383.5	2.3	13.5	12.9	-6.1		

5 Simulations, results and discussion

5.1 Current situation simulated with nodal tanks

The first simulation runs were conducted with the network model with individual nodal tanks. The statistics of this model indicates 578 nodes, 286 tanks and 940 pipes. The larger number of pipes originates from the setup of the discharge from the tanks that consists of a dummy pipe and the node with the attached consumption pattern, and another dummy pipe on the upstream side of each tank, which is a check valve. In this way the model becomes rather bulky, reflecting the actual reality but with high chance of being numerically instable.

As expected, the simulation runs could have not yield tangible results. The model appeared to be very sensitive to the definition of the tank properties and the initial water levels. As soon as the tank was emptied or filled from the imbalance between the demand and supply, based on the EPANET settings, the tank would be disconnected from the network. The multiple occurrences of this nature inflict numerical instability, which was also experienced by significantly longer simulation and resulting in negative pressures in the network. Hence, the calibration of such a model appears to be very complex and it seems that with this amount of tanks, the model could work only if these are not entirely emptied or completely full, but will have sufficient amount of water throughout the entire day. In that case, analyses of any irregular scenario become practically impossible, which was the main reason to abandon this way of modelling.

5.2 Results of Pressure Driven Approach with Emitter Coefficients

The alternative way of modelling was therefore adopted using the approach illustrated by the above Eqs. 4 to 8 and in Table 1. The 16 selected scenarios based on assumed values X_1 to X_4 , as well as the buffer volume are shown in Table 2. Two specific demand scenarios (X_2) correspond to the figures obtained by the field survey described in [14], and earlier pilot measurements done by the municipality. Similarly, the leakage scenarios (X_3) were set by assuming the physical leakage to be 50% of the total NRW levels (assessed at 35% and 50%, respectively). The negative buffer from 2nd figure shows the value reduced

for 30%, which is believed to be the percentage of the households having the float valves installed on their roof tanks, according to [14].

In terms of the percentage from daily supply, the results show relatively wide range: between approximately 4 and 32 %, which points the sensitivity of input data. Based on the field observations, it is believed that Scenario 6 may be the closest to the reality, with remark that the tank levels at the beginning of the IWS next day may well have different filling percentages, based on the consumption pattern of the previous day; hence, the values of X_4 need specific validation compared to the other three variables.

Table 2. Scenarios for the estimate of tank overflows in Puerto Ayora

X_2 (lpcpd)	X_3 (%)	X_1 (m ³)	X_4 (%)	V_t^{buf} (m ³)	$V_t^{buf} (2)$ (m ³)	% total daily supply
163	Scenario 1					
	17.5	1	0	-1327	-929	18.6
	Scenario 2					
	17.5	1	50	-2301	-1611	32.2
	Scenario 3					
	17.5	2	0	-423	-296	5.9
	Scenario 4					
	17.5	2	50	-709	-496	9.9
	Scenario 5					
	25	1	0	-1053	-737	14.7
	Scenario 6					
	25	1	50	-1957	-1370	27.4
Scenario 7						
25	2	0	-287	-201	4.0	
Scenario 8						
25	2	50	-1053	-737	14.7	
195	Scenario 9					
	17.5	1	0	-1285	-900	18.0
	Scenario 10					
	17.5	1	50	-2239	-1567	31.3
	Scenario 11					
	17.5	2	0	-411	-287	5.7
	Scenario 12					
	17.5	2	50	-1285	-900	18.0
	Scenario 13					
	25	1	0	-1016	-712	14.2
	Scenario 14					
	25	1	50	-1900	-1330	26.6
Scenario 15						
25	2	0	-298	-208	4.2	
Scenario 16						
25	2	50	-1016	-712	14.2	

The sensitivity of the four X-variables was further analysed against the tank overflow in somewhat wider range than the one applied in the 16 scenarios. This analysis showed that the highest sensitivity belong to the variables X_1 and X_4 , which underpins the need of further fieldwork in order to validate the available volume of household storages and the initial level, every day, of the tanks before the IWS kicks-off. However, X_3 and X_4 influence the overflow volume to a lesser extent.

5.3 Demand Driven Analysis for future growth modelling

The analyses of the future demand growth were done by applying DDA. The results obtained from the demand scenarios show the percentage of the nodes in three different pressure ranges (less than 0, 0 to 10, and greater than 10 meters of water column - mwc) for the daily demand scenario at maximum consumption hour at 6:00 am (Table 3). Not surprisingly, the supply in year 2045 for the very fast- and

fast growth is practically impossible, regarding the size and capacity of the current network; the simulations show that already at year 2020, the network will start to perform poorly. Therefore, a major renovation would need to be considered, resulting in extremely high financial burden for the Municipality. Also, those would consider a long period of construction with permanent disturbances to the tourists and local population. Only in the slow growth scenario the network would perform optimally for the next 30 years, showing that the nodal pressures would hardly drop below 20 mwc at the peak hour. The research results reported in previous studies, put the moderate growth scenario (3% annual growth for local population and 4% annual growth for tourist visitors) as the preferred one by the majority of stakeholders, and the maximum recommended one in order to cover water demand with supply. Two options were considered under this scenario in order to solve the water deficit and lack of pressures in the moderate growth scenario at year 2045.

Table 3. Percentage of nodes with different ranges of pressure at peak hour (6:00 hrs)

% of nodal pressures						
VERY FAST GROWTH				FAST GROWTH		
Year	< 0 mwc	0 - 10 mwc	> 10 mwc	< 0 mwc	0 - 10 mwc	> 10 mwc
2015	0%	0%	100%	0%	0%	100%
2020	5%	7%	87%	0%	0%	100%
2025	85%	1%	14%	0%	10%	90%
2030	86%	1%	13%	48%	24%	28%
2035	86%	1%	13%	75%	8%	17%
2040	90%	2%	8%	84%	2%	14%
2045	93%	3%	4%	86%	0%	14%
MODERATE GROWTH				SLOW GROWTH		
2015	0%	0%	100%	0%	0%	100%
2020	0%	0%	100%	0%	0%	100%
2025	0%	3%	97%	0%	0%	100%
2030	0%	7%	93%	0%	0%	100%
2035	3%	56%	41%	0%	0%	100%
2040	53%	20%	27%	0%	0%	100%
2045	72%	9%	19%	0%	0%	100%

The first one included a partial renovation of the network, increasing some of the pipes' capacity, assuming there would be enough water for distribution. For this analysis, the average consumption of 163 lpcpd was used, assuming a management strategy proposed to reduce the water demand in the future. The average is assumed to be constant throughout the year, with no major seasonal variations. An intervention to guarantee the minimum pressure of 25 mwc was analysed, knowing that the authorities want to target elite tourism. In order to satisfy the demand at the end of the planning horizon, the approximate investment adds up to nearly 200,000 EUR, which seems a bit low in view of the population growth rate. However, this cost does not include the high excavation costs of volcanic rock, which will increase the total cost considerably.

The previous analysis also shows that the roof tanks could become redundant in the future, to larger extent for the sake of water quality risks. Alternatively, in the second option these tanks were still considered, because they traditionally have a high public acceptance. Tanks have also a positive hydraulic impact into the renovation of the distribution network, which could be then based on the average flow rather than the peak hourly flows. In the second option, using an average flow in the network of 121 l/s in the year 2045 were assumed (*pf* value closer to 1). For this value, Table 4 shows the balancing volume on the maximum consumption day.

Table 4. Analysis of balancing volume on the maximum consumption day in 2045, for moderate population growth scenario.

Hour	Tank In (m ³ /h)	Tank Out (m ³ /h)	Peak Factor	In-Out (m ³ /h)	Cumulative Volume (m ³ /h)
1	322.6	167.5	0.5	155.1	155.1
2	322.6	167.5	0.5	155.1	310.2
3	322.6	167.5	0.5	155.1	465.3
4	322.6	167.5	0.5	155.1	620.4
5	322.6	167.5	0.5	155.1	775.5
6	322.6	701.5	2.2	-378.9	396.6
7	322.6	360.3	1.1	-37.7	358.9
8	322.6	379.2	1.2	-56.6	302.3
9	322.6	391.9	1.2	-69.3	233.0
10	322.6	404.5	1.3	-81.9	151.1
11	322.6	407.7	1.3	-85.1	66.0
12	322.6	524.6	1.6	-202.0	-136.0
13	322.6	372.9	1.2	-50.3	-186.3
14	322.6	372.9	1.2	-25.0	-236.7
15	322.6	347.6	1.1	-6.1	-261.7
16	322.6	328.7	1.0	-104.0	-267.8
17	322.6	426.6	1.3	-192.5	-371.8
18	322.6	515.1	1.6	-211.5	-564.3
19	322.6	534.1	1.7	155.1	-775.8
20	322.6	167.5	0.5	155.1	-620.7
21	322.6	167.5	0.5	155.1	-465.6
22	322.6	167.5	0.5	155.1	-31.5
23	322.6	167.5	0.5	155.1	-155.4
24	322.6	167.5	0.5	155.1	-0.3
Balancing volume (Max. Cum. Vol + ABS. Min. Cum. Vol.)					775.5 +775.8= 1551.4

As observed in Table 4, this steady state calculation results in balancing volume of 1,551.4 m³. If it is assumed that the population in year 2045 will be 37,236 inhabitants (INEC, 2010) and an average occupation of 5 inhabitants, there would be a total of 7,447 households, resulting in average individual storage tanks of 0.21 m³. This option means that the investment costs of the tanks should be taken into consideration. These costs could be assumed either by the owners of each property or by the municipality. Alternatively, a central service tank(s) could also be constructed due to a favourable topography of the area, but placing it in densely populated (tourist) area may pose a problem.

6 Conclusions

Three modelling approaches elaborated in this manuscript included nodal tanks, the PDA and the DDA, for the current and future demand in Puerto Ayora. In the first one, it was very complicated to replicate the actual individual storage in the model. The EPANET software becomes unstable due to different water level patterns in each tank that sometimes becomes full and sometimes empty. More detailed information would be needed for proper calibration of such a model, which would still not solve the deficiency of numerical algorithm.

The PDA of present demand reflects partially the situation with the household storages. It can be concluded that there may be a significant amount of water lost due to the overflow of the roof tanks. Consequently, the local authorities in Puerto Ayora, as well as local residents, have erroneous idea of the “need” for individual storage to compensate the lack of water in the hours of no supply, which to the large extent may result from the negligence. Furthermore, the sensitivity analysis suggests which input data should be verified with priority. The result show the size of individual household tanks and the initial level when the supply begins have more impact on the overflow, than the leakage percentage or per capita demand. Despite the fact that many assumptions were made, this analysis provides a practical approach to measure the volume that might be spilled from household tanks, which seems to be the main source of water wastage.

Regarding the future assessment, in the case of very fast- and fast growth scenario, a major renovation of the network will be needed. Therefore, the moderate growth scenario would be more adequate one. For this scenario, a gradual network renovation was proposed, considering the replacement of main pipes. With this option, the roof tanks could be removed. On the other hand, by calculating the gross balancing volume on the maximum consumption day, the roof tanks will be needed to cover the peak hour supply, but the IWS regime could be avoided, meaning no major investment into the network renovation but into the storage provision, be it in the form of individual household tanks or a centralised storage in the town. The size of the future tanks seems relatively smaller in comparison with the current average tank size; which hints that present household tanks have bigger dimensions than it is necessary and as a result, the demand is also higher.

Finally, the research points that the hydraulic modelling of distribution networks in tourist islands poses quite a complex problem due to: (1) numerical instability caused by multiple tanks existing in the model, and (2) difficult calibration from lots of unknown and inaccurate data needed to build a reliable model.

References:

- [1] Ingeduld, P., Svitak, Z., Pradhan, A. and Tarai, A.: Modelling intermittent water supply systems with EPANET, 8th annual water distribution systems analysis symposium, Cincinnati, 2006.
- [2] Ameyaw, E. E., Memon, F. A. and Bicik, J.: Improving equity in intermittent water supply systems, *Journal of Water Supply: Research and Technology-Aqua* 62(8), pp. 552-562, 2013.
- [3] Vairavamoorthy, K., Gorantiwar, S. D. and Mohan, S.: Intermittent water supply under water scarcity situations, *Water international* 32(1), pp.121-132, 2007.
- [4] Seetharam, K. and Bridges, G.: Helping India Achieve 24x7 Water Supply Service by 2010, Roundtable Discussion on Private Sector Participation in Water Supply in India, June 15-16, 2005.
- [5] Cheung, P., Van Zyl, J. and Reis, L.: Extension of EPANET for pressure driven demand modeling in water distribution system, *Computing and Control for the Water Industry*, pp. 311-316, 2005.
- [6] Ozger, S. S. and Mays, L.: A semi-pressure-driven approach to reliability assessment of water distribution networks. *Proceedings of the Thirtieth Congress of the University of Arizona*, 2003.
- [7] Martinez, F., Signes, M., Savall, R., Andrés, M., Ponz, R. and Conejos, P.: Construction and use of dynamic simulation model for the valencia metropolitan water supply and distribution network. *Water Industry Systems: Modeling and Optimization Applications*, In: Savic, DA and Walters, GA, pp. 155-174, 1999.
- [8] Germanopoulos, G.: A technical note on the inclusion of pressure dependent demand and leakage terms in water supply network models, *Civil Engineering Systems* 2(3), pp 171-179, 1985.
- [9] Soares, A., Reis, L. and Carrijo, I: Head-driven simulation model (HDSM) for water distribution system calibration. *Advances in Water Supply Management*, 1, pp. 197-207, 2003.
- [10] Hayuti, M. and Burrows, R.: Sequential solution seeking dda based hda (sss-dda/hda) approach. *Proc. of Decision Support in the Water Industry under Conditions of Uncertainty-ACTUI*, 2004.
- [11] Rossman, L. A.: EPANET 2: users manual, 2000.
- [12] Pathirana, A.: EPANET2 desktop application for pressure driven demand modeling. *Water Distribution Systems Analysis*, pp. 65-74, 2010.
- [13] Censo de Población y vivienda del Ecuador, Instituto Nacional de Estadísticas y Censos (INEC), 2010.
- [14] Reyes, M., Trifunovic, N., d'Ozouville, N., Sharma, S. and Kennedy, M.: Quantification of urban water demand in the Island of Santa Cruz (Galápagos Archipelago), *Desalination and Water Treatment* 64, pp. 1-11, 2017.

LIQUID RESIDENCE TIME IN VORTEX CHAMBERS

MARLENA A. GRONOWSKA-SZNELER¹, JERZY M. SAWICKI¹

¹*Gdańsk University of Technology, Faculty of Civil and Environmental Engineering, Department of Hydraulic Engineering, ul. Narutowicza 11/12, 80-233 Gdańsk, Poland, e-mail: jsaw@pg.gda.pl*

1 Abstract

Liquid circulation in vortex chambers generates centrifugal force which has considerable effects on the flow. Centrifugal force enhances gravitational separation of suspension (vortex separators), as well as allows regulation of liquid discharge or division of liquid stream (vortex flow control devices). Furthermore, many researchers claim that fluid circulation elongates the effective residence time of liquid inside a vortex chamber in comparison to non-circulative flow. The paper presents authors' research on this issue. Measurements performed on a laboratory test stand indicate that liquid average residence time for circulative flow exceeds 50% of plug-flow time, whereas, for non-circulative flow residence time reaches only 10% of plug-flow time.

Keywords: centrifugal force, circulative motion, residence time, storm waste water, vortex chamber

2 Introduction

The principal characteristic of flow-through vortex chambers is liquid horizontal circulation around vertical axis of the device. Such circulation is most commonly induced by inlet pipe placed at a tangent to chamber wall. Circular velocity field generates centrifugal force which is a significant factor in theoretical description and operation of hydraulic objects.

In general, there are two relevant effects achieved by introduction of centrifugal force:

- influence on particles suspended in fluid;
- rise in pressure towards chamber wall.

The first effect is widely used as a factor responsible for (in case of centrifuges) or at least enhancing mechanical removal of suspension. It is employed in cyclones (e.g. [1]) and hydrodynamic vortex separators HDVS (e.g. [2], [3]). On the contrary, the second effect is the basis for vortex flow control devices that can be divided into two groups:

- vortex valves;
- vortex dividers (e.g. storm overflows).

Frequently, both effects are combined together in one device, e.g. in known technical constructions such as SWIRL or STORM KING.

Nevertheless, regardless of the way in which circulation is utilized, it is the source of another important effect - elongation of liquid residence time inside the chamber. This fact has been noted by numerous researchers. For instance, Andoh and Saul [4] made a general statement that vortex chambers work better than analogical objects without fluid circulation. This results from the fact that interior of vortex chamber is used more efficiently than in case of non-circulative devices. Analogical conclusion may be found in paper by Eubaia and Algarmadi [5] that were conducting research on influence of circulative motion on efficiency of wastewater disinfection.

Theoretical methods of residence time (RTD) determination have been widely discussed in literature (e.g. [6], [7]). As this is a complicated matter, very often researchers make use of simplified 1D models with limited accuracy of results.

That is why, in case of existing objects (or their physical models) empirical methods are preferred such as experimental determination of average liquid residence time RTD as the first moment on the residence time distribution curve $E(t)$. This method had already been proposed eighty years ago [8], however, it became popular in the middle of the 20th century [9]. Authors of this paper made use of this method to

identify and evaluate influence of circulation on residence time RTD in a flow-through chamber, as well as compare experimental RTD with its technical measure (plug-flow time) for various configurations of outlet pipe.

3 Methods

In order to determine time characteristics of vortex chambers, authors of the paper performed a series of measurements on a functional model of vortex chamber in the form of a flow-through chamber. For each configuration of inlet and outlet pipes residence time distribution curve $E(t)$ was created.

Firstly, concentration $c(t)$ of Rhodamine WT tracer at the outlet cross-section was measured using Cyclops-7 colorimeter from Turner Designs, USA. Function $E(t)$ was calculated for known value of discharge Q and mass of the tracer dose M :

$$E(t) = \frac{c(t)Q}{M} \quad (1)$$

Secondly, values of chosen synthetic indicators were determined:

- average residence time t_A equal to the first moment on the residence time distribution curve $E(t)$:

$$t_A = \int_0^{\infty} tE(t) dt \quad (2)$$

- modal time t_M calculated as the time of maximum concentration of the tracer at the outlet displayed on the residence time distribution curve $E(t)$, averaged over 5 consecutive measurements for each configuration;
- plug-flow time t_{PF} according to the formula:

$$t_{PF} = \frac{V}{Q} \quad (3)$$

calculated for known value of discharge Q and height of water surface H in each configuration and for fixed diameter of the chamber $D = 2R = 0.80$ m.

Schematics and dimensions of the test flow-through chamber, as well as configurations of inlet and outlet pipes are shown in Fig. 1. Altogether, three groups of inlet and outlet configurations were investigated:

1. Inlet pipe at a tangent to chamber wall and axial outflow through a vertical pipe:
 - upper orifice overflow (configuration PG),
 - perforated side surface of outlet pipe – 9 rows of openings with diameter $d = 5$ mm in 1 cm intervals (configuration PP),
 - three rectangular openings 29 mm x 15 mm in outlet pipe side surface located 2 cm above chamber bottom (configuration PD).
2. Inlet pipe symmetrical to chamber wall with vertical liquid inflow and outlet pipe near the opposite wall:
 - inlet submerged 3 cm below water surface (configuration WP),
 - inlet located 5 cm above chamber bottom (configuration WD).
3. Inlet pipe tangent to chamber wall (as in configurations P) and outlet pipe located at various points along the perimeter inside the chamber (configurations TA, TB, TC, TD, TE and TF as seen in Fig. 1).

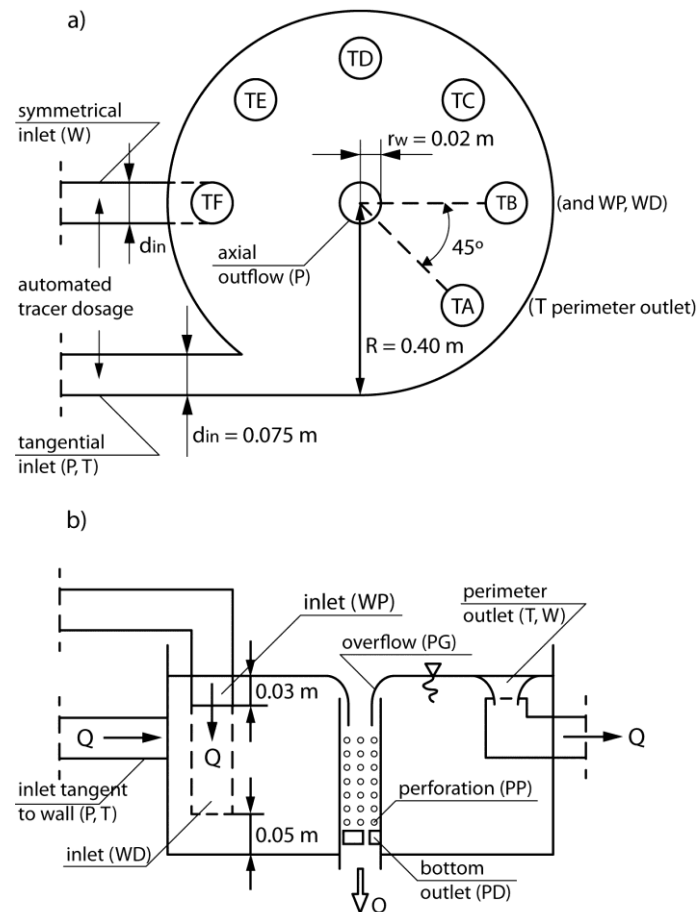


Figure 1. Schematics of test flow-through chamber: a) top view; b) cross-section (R – chamber radius, d_{in} – inlet diameter, r_w – outlet radius, Q – discharge)

The third group of combinations cannot be accepted as rational from hydraulic point of view. Nevertheless, such solutions can be found in catalogues offered by producers of devices for removal of suspension. That is why, authors of this paper decided to investigate three additional combinations of flow, clearly for cognitive reasons:

1. Liquid circulation (tangent inlet) and forced flow in the central part of the chamber (effect of outlet pipe location, “P” series).
2. Liquid circulation (tangent inlet) and no flow in the central part of the chamber (outlet pipe along the chamber perimeter, “T” series).
3. Non-circulative flow and forced flow in the central part of the chamber (location of inlet and outlet pipes, “W” series).

4 Results and discussion

Sample residence time distribution curves $E(t)$ for each group of configurations obtained in the course of measurements are presented in Fig. 2 (for configurations PG, WD and TB).

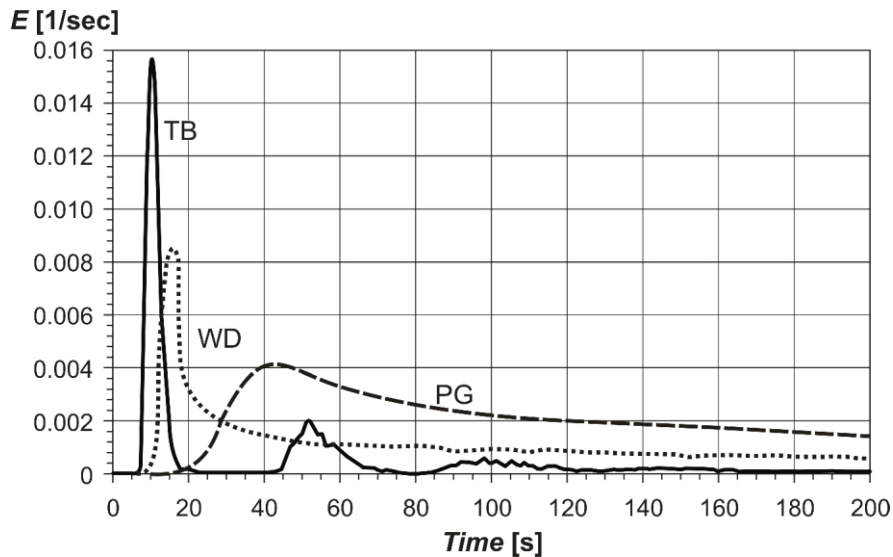


Figure 2 Sample residence time distribution curve $E(t)$ for different configurations

Analysis of obtained residence time distribution curves $E(t)$ confirm the statement made by Veerapen *et al.* [2], that vortex chamber ensures high level of mixing – first portions of tracer appear at the outlet after a short period of time, then tracer concentration increases to a maximum value, and finally exponentially decreases. Characteristic times (t_A , t_M and t_{PF}) determined for the investigated device are presented in Table 1. Additionally, Table 1 includes relative values of average time t_A and modal time t_M related to plug-flow model time t_{PF} calculated according to relation (3).

Table 1. Time characteristics of liquid flow in the test vortex chamber (for investigated configurations and combinations of inlets and outlets)

CONF./COMB.	Q [l/s]	H [m]	t_{PF} (sec)	t_A (sec)	t_A/t_{PF} (-)	t_M (sec)	t_M/t_{PF} (-)
PG (1)	0.340	0.240	355	217	61	42	12
PP (1)	0.335	0.133	199	116	55	32	16
PD (1)	0.315	0.132	210	118	56	29	14
WP (2)	0.60	0.266	223	57	26	16	7
WD (2)	0.60	0.270	226	66	29	15	7
TA (3)	0.60	0.263	220	21	10	8	4
TB (3)	0.60	0.255	213	23	11	10	5
TC (3)	0.60	0.260	218	24	11	15	7
TD (3)	0.60	0.269	225	30	13	19	8
TE (3)	0.60	0.261	219	36	16	24	11
TF (3)	0.60	0.253	212	40	19	27	13

5 Conclusions

Results of measurements confirm the qualitative statement that circulation generated in vortex chambers can increase the usage of device volume to a significant degree. In order to achieve such an effect, liquid must be forced to flow in the central part of the chamber. If liquid circulation is accompanied by radial flow, average residence time t_A reaches almost 60% of plug-flow time t_{PF} . This means that dead and stagnant zones occupy less volume than the active layer of liquid flow. Even though centrifugal force generated by circulation is not a key factor in the process of separation of suspension (as in centrifuges), threefold longer average residence time t_A than in case of flow without circulation (configurations W) is very advantageous.

Moreover, modal residence time t_M is also elongated (becomes circa two times longer). After this time period, main portion of the tracer mass M introduced into the system leaves the chamber. This means that, according to the reaction rate curve, effective level of reduction of substance concentration is higher

for systems with fluid circulation. This conclusion is similar to the one given by Eubaia and Algarmadi [5] that vortex disinfection tank has the same efficiency as a non-circulative tank of threefold volume. Finally, research conducted by the authors indicate that configurations "T", where location of inlet pipe generates circulation and outlet pipe is situated near the chamber wall, are definitely less beneficial.

Acknowledgments

Scientific research has been carried out as a part of the Project "Innovative resources and effective methods of safety improvement and durability of buildings and transport infrastructure in the sustainable development" financed by the European Union from the European Fund of Regional Development based on the Operational Program of the Innovative Economy.

References:

- [1] White L.C. (1932) Results of research on cyclone dust collectors, *Power*, 75, 344-346.
- [2] Verapeen J.P., Lowry B.J., Couturier M.F., (2005) Design methodology for the swirl separator, *Aqua. Eng.*, 33, 21-45.
- [3] Gronowska-Szneler M.A., Sawicki J.M. (2014) Simple design criteria and efficiency of hydrodynamic vortex separators, *Water Sci. and Techn.*, 70(3), 457-463.
- [4] Andoh R.Y.G., Saul A.J. (2003) The use of hydrodynamic vortex separators and screening systems to improve water quality, *Water Sci. and Techn.*, 47(4), 175-183.
- [5] Eubaia A.E., Algarmadi S.M. (2013) Tracer study investigation into hydrodynamic vortex separator characterization, *J. of Eng. Sc. Assint Univ.*, 41(3), 1352-1363.
- [6] Haas C.N. (1996) Moment analysis of tracer experiments, *J. Environ. Eng.*, 122(12), 1121-1123.
- [7] O'Doherty T., Egarr D.A., Faram M.G., Guymer I., Syred N. (2009) Assessment of residence time in a hydrodynamic vortex separators by applying distribution models, *J. of Process Mech. Eng.*, 223(E3), 179-188.
- [8] MacMullin R.B., Weber M. (1935) The theory of shortcircuiting in continuous-flow mixing vessels in series and kinetics of chemical reactions in such systems, *Transactions AIChE*, 31(2), 409-458.
- [9] Danckwerts P.V. (1953) Continuous flow systems. Distribution of residence times, *Chem. Eng. Sci.*, 2, 1-13.

Notation:

$c(t)$ – concentration of the tracer, D – vortex chamber diameter,
 d_{in} – inlet diameter, H – height of water surface, M – mass of the tracer dose,
 Q – discharge, R – chamber radius, r_w – outlet radius,
 t_A – average residence time, t_M – modal time, t_{PF} – plug-flow time

URBAN SEDIMENT MANAGEMENT – FROM THE RIVER TO THE SEWER

JOHANNES SCHOBESBERGER ¹, JOHANNES FISCHER ², CHRISTINE SINDELAR ³,
HELMUT HABERSACK ⁴

¹ *University of Natural Resources and Life Sciences, Austria, johannes.schobesberger@boku.ac.at*

² *University of Natural Resources and Life Sciences, Austria, johannes.fischer@boku.ac.at*

³ *University of Natural Resources and Life Sciences, Austria, christine.sindelar@boku.ac.at*

⁴ *University of Natural Resources and Life Sciences, Austria, helmut.habersack@boku.ac.at*

1 Abstract

This study deals with sedimentation problems and the investigation of a sediment trap. Sediment samples of the natural and urban catchment area were taken to compare the grain sizes and the geological composition with samples from the sediment trap. A physical model test of the sediment trap was set up to investigate its operation capability based on LDA measurements. The results indicate sediment input from the urban catchment area. The physical model tests showed that sediments begin to flush out of the sediment trap well below the one year flood. In future, the focus is to optimize the function of the sediment trap.

Keywords: urban sediment management, hydraulic assessment of sediment trap, physical model, Laser Doppler Anemometry, sediment transport, sediment source

2 Introduction

Sedimentation in sewerage systems is a very common topic. Often there is a high number of sediment sources, which are responsible for the sediment input. In some sections of the sewerage system in Vienna, Austria, there are problems caused by sedimentation. Sediments from a creek called “Erbsenbach” rising in the “Wienerwald” and material from the urban catchment area are potential sources of these sediments. Starting from its source the Erbsenbach has a free flowing section of about 3.2km with a natural catchment area of 3.1km² and a mean annual flow of 0.04m³/s. Afterwards the creek discharges into the sewerage system of Vienna (19th district). The vaulted section is about 2.0km long and at the end of the mixed water sewer, a sediment trap is located which should reduce the sediment input into the following sewer section called “right main sewer”. The sediment trap is 12.0m long and consists of two 2.0m wide pools, which are separated by a middle wall. The depth of the sediment trap is 1.2m and each pool has a slope of 0.025. Especially at large discharges, the accumulated sediment in the sediment trap flushes out. Accordingly, this leads to sedimentation in the right main sewer further downstream. In this area, an automatic excavation of the sediments is not possible which means that the excavation must be done manually. The primary goals of this study are to find the source of the accumulated sediments and to prove the hydraulic operational capability of the sediment trap. To detect the sediment sources, samples of the sediments in the natural and the urban catchment area were collected to compare the grain sizes and the geological composition with sediment samples of the sediment trap and the right main sewer. To determine the sediment transport rates at the free flowing sections of the Erbsenbach bed load measurements were carried out. The final step was to build a physical model of the sediment trap, which should provide information on the hydraulic conditions, for example the hydraulic capability, by varying discharges.

3 Methods

This section describes the approach of the sampled sediments, the measured bed load of the Erbsenbach and the methods applied for the physical sediment trap model.

3.1 Sampling the natural and urban catchment area

To detect the sediment sources it was necessary to divide the project catchment area (CA) into a natural and urban catchment area. First four sediment samples along the course of the Erbsenbach were taken. Therefore, a wooden frame (50x50cm) was used to define the sample spots. To sample the urban catchment area, sediments from four sludge traps were gathered. The purpose of the sludge trap samples is the collection of sediments and materials, which are spilled from the streets into the sewerage system during a precipitation event. Figure 1 shows the catchment areas and the location of the sample spots.

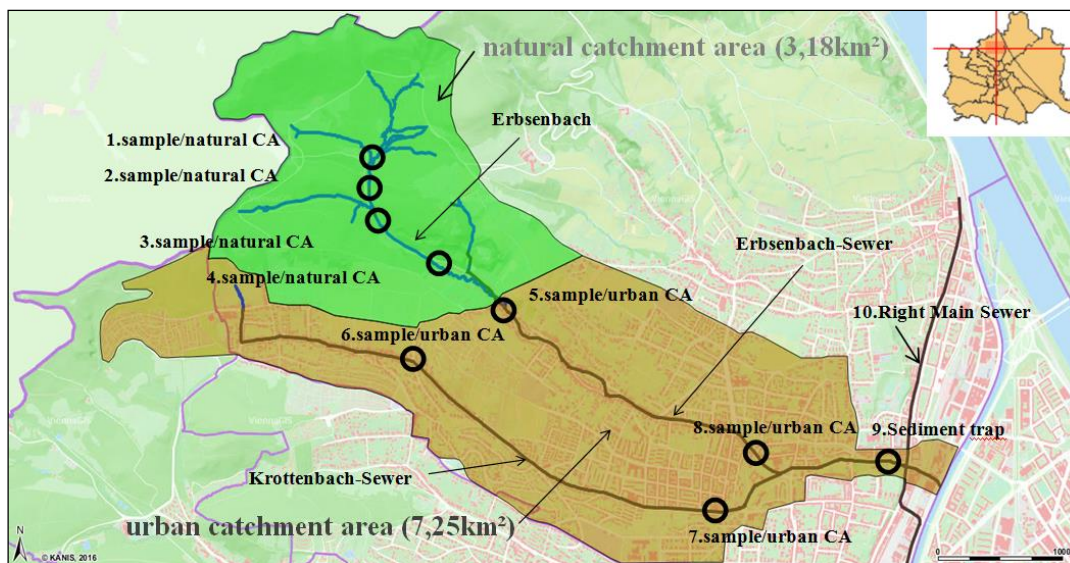


Figure 1. Natural and urban catchment area with sample spots

To analyse the sediment samples a sieve machine with a mechanical shaker was used for creating the sieve analyses and the characterised grain size diameter (d_{10} to d_{90}) for each sample. The characterised grain size diameter served as basis for the geological analyses. To determine the geological composition a so called “scree analyse” has been implemented. The natural area is located in the Flysch area, regarding to the geological situation. In this area rocks like marl, sandstone and shale are dominating. Some pre-tests of the geological composition of the samples from the catchment areas revealed that three different rock types are dominating. To find the source of the sediments the “scree analyse” has been done for flysch stones, lime and a defined rest, which includes concrete, brick and organic material like wood and faeces. This means, if there is a high amount of flysch stones in the sediment trap samples, it is likely that the sediments are arising from the natural catchment area. On the other hand, if there is a high amount of lime or other material in the sediment trap samples it is indicating sediment input from the urban catchment area.

3.2 Measurement of the bed load transport

The Erbsenbach has a free flowing section before it discharges into the sewerage system. In this reach bed load transport may occur. Therefore, it was necessary to measure the amount of the transported sediments. The mean annual flow of the Erbsenbach is about 0.04 m³/s. Pre-measurements revealed that there is no bed load transport at this discharge. Because of that, the measurements were performed during precipitation events. For measuring the bed load three different devices were used.

- Hand sampler (length and width of the sampler opening is 25:25cm)
- Large Helley-Smith sampler (length and width of the sampler opening is 15:15cm)

- Fixed mounted sediment sampler (length and width of the sampler opening is 50:50cm)

Depending on the discharge, one of the three mentioned measurement devices was used. The fixed mounted sediment sampler delivered long-term bed load results. The hand sampler and the Helley-Smith sampler were used for short term and heavy rainfall events. Overall, eight bed load measurements at different discharges were conducted. The water level at the profile (cross section) of the bed load measurement spot was determined by a flood marker. The discharge was calculated assuming a Strickler value of $45\text{-}55\text{m}^{1/3}\text{s}^{-1}$. Therefore, it was possible to relate the bed load to the corresponding discharge.

3.3 Physical sediment trap model and experimental procedure

The primary goal of the physical model test was to observe the hydraulic capability of the sediment trap. Therefore, the sediment trap model at a scale of 1:10 was built at the Hydraulic Laboratory of the University of Natural Resources and Life Sciences Vienna (Fig 2.). The total length of the physical model is 5.5m and it consists of a 2.5m long inlet reach and a 1.3m long outlet reach. The profile of the inlet and outlet reach is a stretched circular cross section with dimensions 26/20 centimetre. At the end of the inlet, there is a short widening section with an opening angle of 20° . After the widening section, two sediment trap pools are located. The depth of each pool is 0.2m with a length of 1.2m. The physical model represents the free surface channel of the projected sewerage system part and so it was built without a top. This was also necessary for measuring the water level. Because of the free flowing regime, the Froude model law was used requiring that the Froude numbers are the same in the scaled model and under nature conditions [1]. Giesecke and Mosony [2] defined a critical velocity Eq.(1), which should not be exceeded in the sediment trap. The sediment trap is a concrete building and so the Strickler value k_{st} was set to $70\text{m}^{1/3}\text{s}^{-1}$ for further calculations [3].

$$u_{Gr} = k_{st} * R_{hy}^{1/6} \sqrt{0,03 * \left(\frac{\rho_s}{\rho} - 1\right) * d} \quad (1)$$

For Eq.(1) R_{hy} stands for the hydraulic radius, the factor 0.03 for the shields parameter, d represents the grain diameter and ρ_s and ρ are sediments ($2.65\text{kg}/\text{dm}^3$) and water ($1.0\text{kg}/\text{dm}^3$) densities, respectively. The method for determining the hydraulic capability of the sediment trap was to compare the measured velocity at different discharges with the calculated critical velocity u_{Gr} .

$$\frac{v_{measured}}{u_{gr}} < 1 = \text{sedimentation}$$

$$\frac{v_{measured}}{u_{gr}} > 1 = \text{sediment transport and flushing}$$

If the ratio of $v_{measure}$ to u_{gr} is smaller than one the hydraulic capability of the sediment trap is given and sedimentation will be the primary process. On the other hand, if the ratio $v_{measured}/u_{gr}$ is higher than one, transported sediments do not settle and sediments already accumulated in the sediment trap will be flushed out. To measure the flow velocities in the sediment trap a 2D-LDA-System (Laser Doppler Anomometry) consisting of two diode pumped solid state (DPSS) lasers was used. LDA is a non-intrusive optical measurement system based on the Doppler Effect, which does not influence the flow and provides two-dimensional (horizontal and vertical) velocities. For measuring two-dimensional velocities, two pairs of laser beams at different wavelengths (532nm and 564nm) are necessary. The beams intersect in one point, which represents the measurement point/volume. The size of the measurement volume is smaller than one millimetre. Small particles (with a size of a few μm), which follow the flow pass the measurement volume and scatter the laser light back to the receiving optic. The scattered light is shifted by the Doppler frequency, which is proportional to the velocity [4]. For the measurements, the laser power was set to 100mA. A recording time of 90 seconds turned out as a representative duration. The LDA Systems was mounted on a traverse displaceable in X/Y/Z directions. The velocities were measured on a defined grid with a spacing in X/Y/Z of 8/4/2 centimetres,

respectively. Figure 2 shows the layout of the 1:10 scaled sediment trap and the LDA measurement areas.

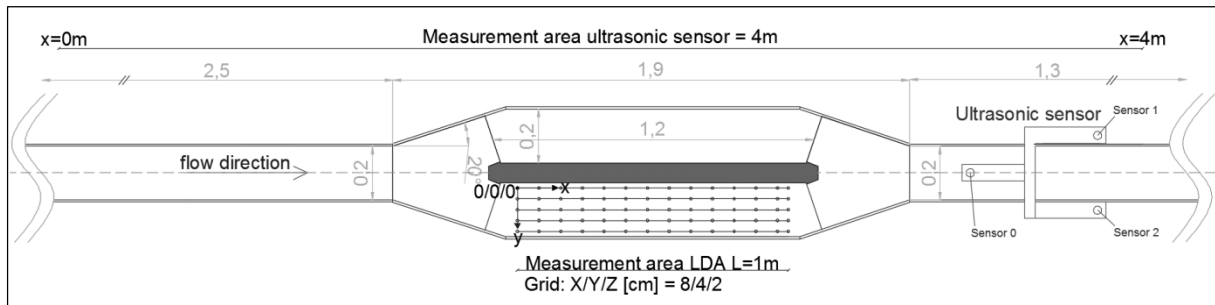


Figure 2. Layout of the model and its measurement areas

For defining representative test scenarios, pre measurements with a partly filled sediment trap were conducted. The aim of these measurements was to find out at which discharge sediments begin to flush out of the sediment trap. Table 1 shows the defined scenarios based on the results of the pre measurements.

Table 1. Defined scenarios for the physical model tests

Scenarios	Model discharge [m ³ /s]	Natural discharge [m ³ /s]	Expected Process Sedimentation/Begin flushing /flushing
1. Scenario	0.002	0.63	Sedimentation
2. Scenario	0.008	2.5	Begin flushing
3. Scenario	0.016	5.1	Complete flushing
3.1. Scenario	0.016	5.1	Sedimentation

For the scenarios defined in Table 1, LDA measurements were performed and for calculating the hydraulic parameters, the water level was detected using three ultrasonic sensors.

4 Results and discussion

In this chapter, the results from the field measurements as well from the physical model test are presented and explained.

4.1 Results and discussion - Sampling the natural and urban catchment area

For all samples a sieve analyses and the geological composition was carried out. Figure 3 illustrates the results from the sieve analyses as a box plot. There the range of the characterized grain size diameter (d_{10} to d_{90}) for each sample is displayed as 25 and 75 quartile. In between, the median represents the d_{50} of the characterized grain size diameter. As Figure 3 shows the range of the grain size diameter from the natural catchment area is larger than from the urban catchment area and does not fit with grain size diameters from the sediment trap or the right main sewer. The d_{50} of the sediment trap and of the right main sewer are 3.58mm and 4.5mm, respectively. The average of the d_{50} values from the natural catchment area is 9.1mm and from the urban catchment 3.9mm. Comparing the d_{50} 's of the sediment trap and the right main sewer, it is more likely that most of the sediments in the sediment trap arise in the urban catchment area. To prove this hypothesis the geological composition of the samples was investigated.

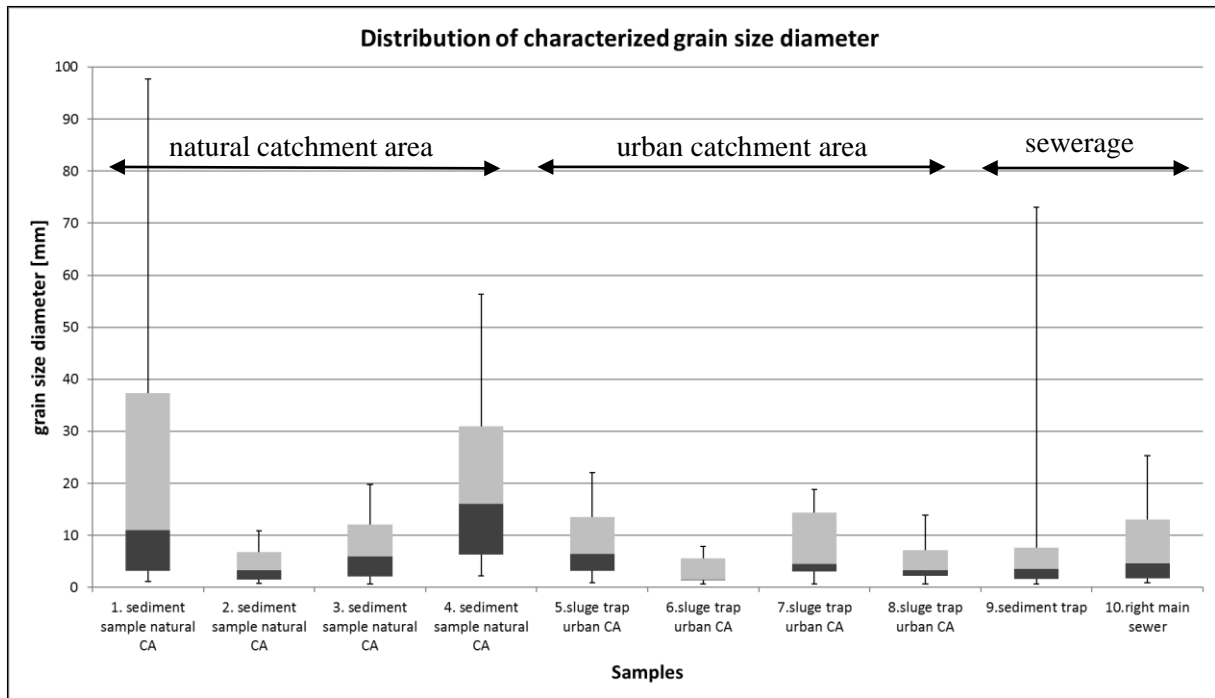


Figure 3. Grain size diameters of all samples displayed as a box plot displayed as 25-75% quartile

It turned out, that the primary part of the geological composition in the natural catchment area consists of flysch stone which fits to the geological situation in this area. As shown in Table 2, for samples one to four, the percentage ratio of flysch stone is not smaller than 85 percent. In addition, some small ratios of rest could be found in the samples of the natural catchment area. It is likely that they originate from bordering areas like yards or streets located in the natural catchment area. The change of the geological composition of the sludge trap samples in the urban catchment area is striking. In this case, the defined rest is the dominating rock (up to 79%) and in contrast to the samples from the natural catchment area, parts of limestone have been detected. Considering the geological composition of the samples from the sediment trap and the right main sewer also lime and rest are the main rock types. With two and four percent, the ratios of flysch stone in the sediment trap and the main sewer are vanishingly low. Based on this observation and regarding the results of the sieve analyses, one can conclude that the accumulated sediments in the sediment trap and the main sewer come mainly from the urban catchment area.

Table 2. Geological composition of the sediment samples in percent

Sample	FLYSCH	LIME	REST
1.SAMPLE/NATURAL CA	100	-	-
2.SAMPLE/NATURAL CA	93	-	7
3.SAMPLE/NATURAL CA	85	-	15
4.SAMPLE/NATURAL CA	89	-	11
5.SAMPLE/URBAN CA	9	16	75
6.SAMPLE/URBAN CA	4	12	84
7.SAMPLE/URBAN CA	7	14	79
8.SAMPLE/URBAN CA	10	16	74
9.SEDIMENT TRAP	2	27	71
10.RIGHT MAIN SEWER	4	62	34

4.2 Results and discussion - Measurement of the bed load transport

For determining the sediment transport at the free flowing section of the Erbsenbach bed load measurements were carried out. Figure 4 shows the hydrograph of the Erbsenbach (grey graph) and the amount of the trapped sediments in dependence of the discharge during the measurement events.

The red brackets indicate the measurement period of the permanent sediment sampler and its highest discharge events.

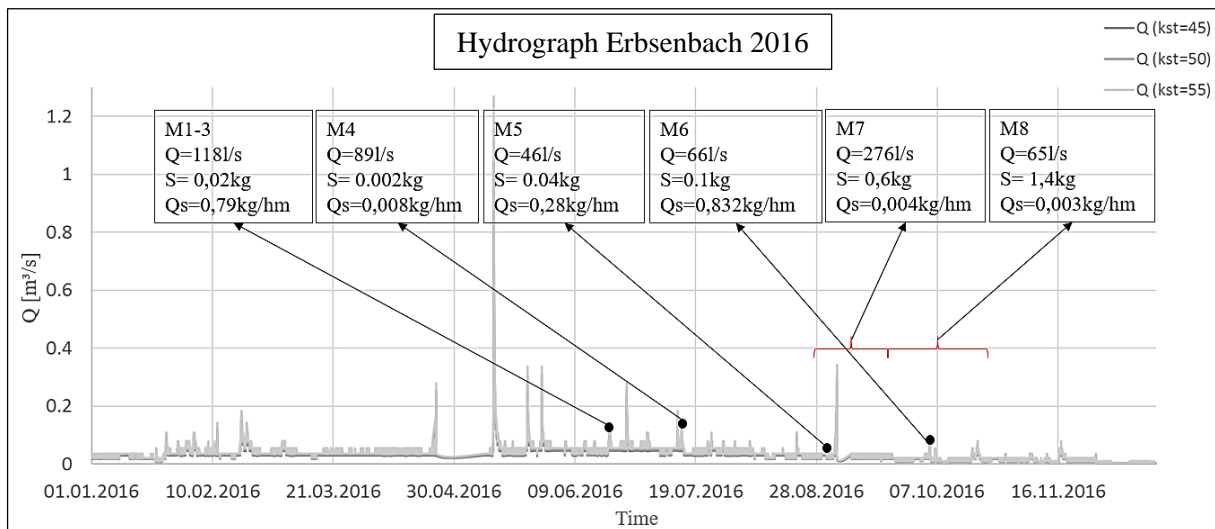


Figure 4. Hydrograph of the Erbsenabch and the amount of trapped sediments. (“M” – measurement; “Q”=discharge of the Erbsenabch; “S”=caught sediment in kg; “Qs”=amount of sediment per one meter width and one hour time)

As illustrated in Figure 4 the amount of captured sediments during the measurements is very low even for the long term measurements with the fixed sediment sampler. The measurement time for M1-M6 was set to 30 minutes. The highest bed load amount for these measurements was 0.1kg (M6). For M7 and M8 (fixed sediment sampler) the maximum captured sediment amounts to 1.4kg during 60 days. Furthermore, no relationship between the amount of the bed load and the discharge was detected. In summary, it can be stated that during the project period the sediment input from the free flowing section of the Erbsenabch can be neglected. In addition, the results from the bed load measurements suggest that the sediments do not arise in the natural catchment area of the Erbsenabch. Under conditions with increased discharge (up to 0.3m³/s), the amount of the caught bed load material achieved less than one kilogram per meter width. Furthermore, this is another indication for urban sediment input into the sewerage system.

4.3 Results and discussion – Physical sediment trap model

For investigating the hydraulic capability of the sediment trap a physical model was built at a scale of 1:10. Figure 7 shows the measured velocities at different longitudinal sections of the right sediment trap pool for scenario 1 to 3.1. The distance from the longitudinal section at Y=180 to the outer boundary of the sediment trap is 20mm and Y=20 is 20mm apart from the middle separation wall, which is located between the two sediment trap pools. The highest velocities in scenario 1 have been detected at Y=180 with a maximum of 0.35m/s. At this section, the vectors are directed horizontally and are getting smaller in downstream direction of the sediment trap. Regarding the other planes the direction of the vectors are changing/turning, which indicates a vortex in Y- and Z-direction. The contour plot in the background of the vector plot illustrates the ratio of measured velocities to critical velocity u_{gr} . The critical velocity is calculated for the characteristic grain size $d_{50}=3.57\text{mm}$ (equal to 0.357mm under model conditions) of the sediments which have been sampled in the sediment trap. If the ratio $v_{measured}/u_{gr}$ is smaller than one (yellow colour) then no sediment movement in the sediment trap is expected. On the other hand, if the ratio between the mentioned velocities is larger than one (blue colour) sediment transport will occur. For scenario1, the calculated critical velocity is 0.27m/s. The contour plot for scenario 1 indicates that there are only small areas near the water level with velocities higher than 0.27m/s. In this case, the sediments will stay in the sediment trap. Regarding Scenario 2 the critical velocity is 0.28m/s at the discharge of 8l/s. The highest velocities occur near the outer boundary with a maximum value of 0.76m/s. Similar to scenario 1 the direction of the vectors are changing at the Y=100 section. The blue

area indicating sediment spill is more distinct than in scenario 1, in particular at $Y=180$, and reaches down to $Z=20\text{mm}$ above the sediment trap bottom. If the sediment trap would be partly filled with sediments, sediment transport and further sediment flushing will occur. In scenario 3 the discharge was set to 16l/s . At this discharge one sediment trap pool is supplied with a higher flow rate than the other pool. Figure 5 shows the different water supply in relation to the discharge. Ink was used to visualize the flow. As shown in Figure 5 for scenario 1 and scenario 2 the flow was divided equally in both pools. For scenario 3 only one sediment trap pool was supplied.

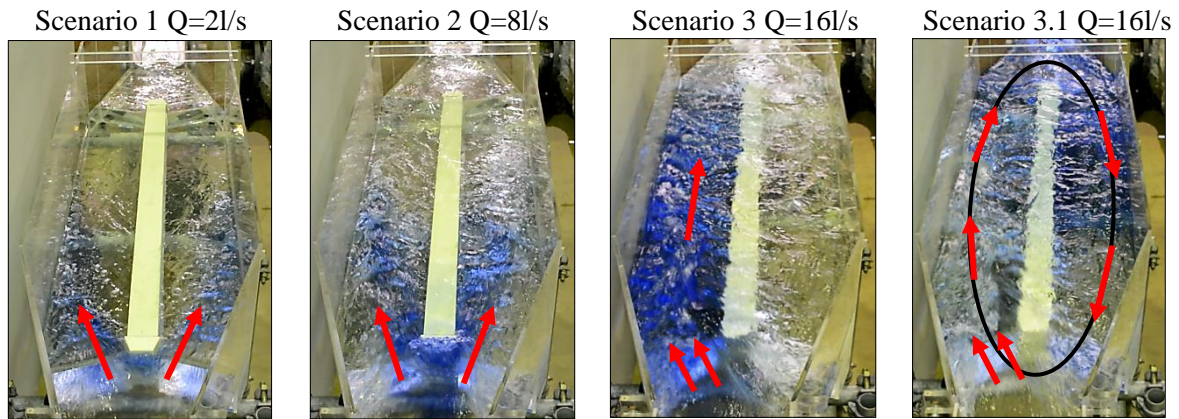


Figure 5. Model tests with ink for describing the flow conditions

This effect is caused by the widening section and a too large widening angle (40°) at the beginning of the sediment trap. The discharge can switch to the other pool by manually disturbing the flow at the inlet. When the flow switches to the other pool it stays there steady. A similar phenomenon can be found for diffusers with large opening angles. There the mentioned state is described as steady two dimensional stall, where the separated flow near the throat just follows one diverging wall. At the other diverging wall a fix stall with low velocities compared to the through flow blocks a significant fraction of the available flow area and the blockage accounts for the low performance in this region [5]. Further Renau describes the state as “stable to small internal disturbances, but the stall can be switched from one diverging wall to the other by a large disturbance at the inlet or exit of the diffuser”. The widening angle 2θ of the sediment trap inlet equals 40° . The ratio of the length of the widening section N and width at the beginning of the widening W_1 is about 2.3. As it is shown in Figure 6, the result (black point) for the widening of the sediment trap is situated directly on line b-b, which represents the “fully developed two-dimensional stall”.

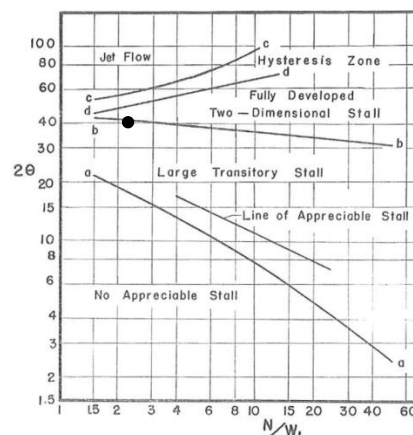


Figure 6. Flow regimes in straight wall diffusers [5]. The black point shows the state fully developed two-dimensional stall for the sediment trap inlet.

Because of that state the velocities of the supplied pool increase as well as the areas with a ratio $v_{measured}/u_{gr}$ larger than one. The maximum velocities for scenario 3 are larger than $1,1\text{m/s}$. In contrast to scenario 1 and 2 the direction of the vectors does not change. As the contour plot for scenario 3 in Figure 7 shows, the sediment spill area (blue area) reaches down to the bottom of the sediment trap. This

indicates sediment transport and sediment flushing in the supplied sediment trap pool. Because of the one-sided flow at a discharge of 16l/s the pool which was not supplied was investigated in scenario 3.1. As the vectors in Figure 7 show there is no consistent flow direction. The maximum velocity is about 0.25m/s, which is more than four times less than the maximum velocity in the other pool (scenario 3). The ratio of $v_{measured}/u_{gr}$ didn't exceed the value one in the whole measurement area and so no sediment transport will occur. Because the pool in scenario 3.1 will not be supplied with discharge, transported sediments upstream will not be spilled into it, which decreases the sedimentation process in the sediment trap.

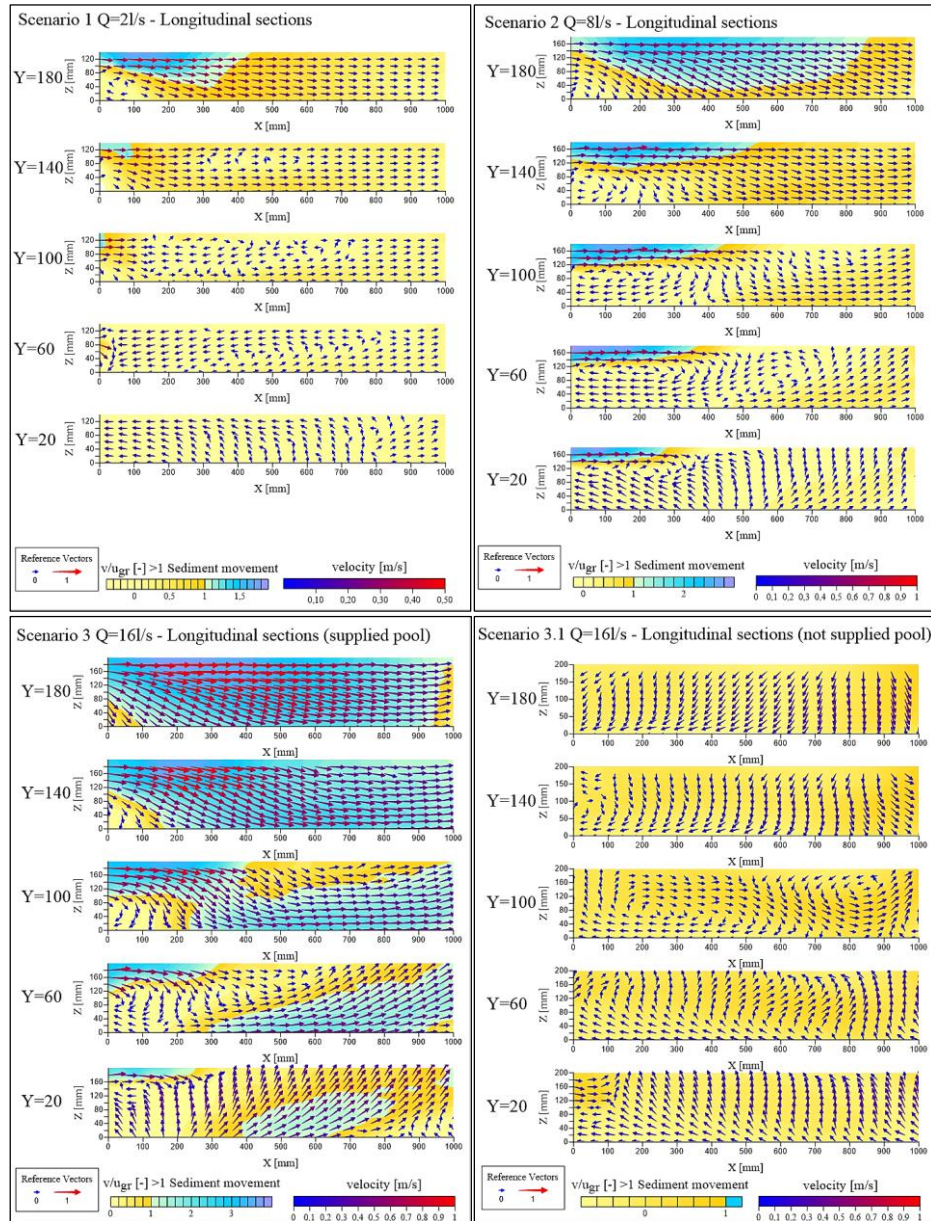


Figure 7. Longitudinal vector and contour plots for all four scenarios. The colour of the vectors correspond to their value (red – high velocity; blue – small velocity). The contour plot shows areas of sedimentation (yellow area – $v/u_{gr} < 1$) and sediment movement (blue area – $v/u_{gr} > 1$)

5 Conclusion

The aims of this project were (i) to find the sources of the accumulated sediments in the sediment trap as well as in the right main sewer and (ii) to test the hydraulic capacity of the sediment trap with physical model tests. Therefore, sediment samples of the relevant natural and urban catchment areas were taken

to determine the grain sizes and the geological composition of the sediments. After comparing the grain sizes and the geological composition with the sampled material of sediment trap, one can conclude that the sediments of the sediment trap originate in the urban catchment area. There, the amount of limestone (15%) and other material (78%) agrees very well with the corresponding rates of limestone (21%) and other material (71%) of the sediment trap. In the natural catchment area no lime stone and high amount (up to 100 percent) flysch stone was found. In addition, the characterized grain size diameters d_{50} of 3.9mm and 3.6mm for the urban catchment area and for the sediment trap, respectively, agree very well. In contrast, the average d_{50} of all samples from the natural catchment area is 9.1mm. Because of the high velocities during periods with high discharges, full sedimentation in the sediment trap is no longer possible and the already accumulated sediments flush out. The physical model tests resulted in full flushing at a discharge of 16l/s, which corresponds 5.1m³/s under nature conditions. During the field measurement campaign (four months), this event occurred 13 times. At this discharge the flow is not evenly distributed and only one sediment trap pool is supplied. This discharge is well below the one year flood event. For the future, the focus will be set on the optimization of the hydraulic capability of the sediment trap and the reduction of flushing sediments by means of the physical model.

Acknowledgments:

This research was funded by Wien Kanal. We thank the employees from Wien Kanal and Franz Ottner from the Institute of Applied Geology (IAG) for their support during the project period.

References:

- [1] Kobus, H.: Wasserbauliches Versuchswesen, 2. Auflage, Hamburg-Schriftenreihe des Deutschen Verbandes für Wasserwirtschaft und Kulturbau, 1984.
- [2] Gieseke, J., Monsoyi, E.: Wasserkraftanlagen – Planung, Bau und Betrieb, 5. Auflage, Berlin-Springer-Verlag Berlin Heidelberg, 2009.
- [3] Bollrich, G.: Technische Hydromechanik 1 – Grundlagen, 7. Auflage, Berlin-Beuth Verlag GmbH, 2013.
- [4] Ruck, B.: Laser-Doppler-Anemometrie, AT-Fachverlag GmbH Stuttgart, 1987.
- [5] Renau, L. R., Johnston, J. P., Kline, S. J.: Performance and Design of Straight,
- [6] Two-Dimensional Diffusers, Journal of Basic Engineering 3 (1967), Nr. 1, pp. 141-150, 1967.

STORMWATER MANAGEMENT IN THE URBAN ENVIRONMENT

MARIJA ŠPERAC¹, DINO OBRADOVIĆ²,

¹ Josip Juraj Strossmayer University of Osijek, Faculty of Civil Engineering, Vladimira Preloga 3, 31000 Osijek, Croatia
msperac@gfos.hr

² Josip Juraj Strossmayer University of Osijek, Faculty of Civil Engineering, Vladimira Preloga 3, 31000 Osijek, Croatia
dobradovic@gfos.hr

1 Abstract

Issues related to integral stormwater management in the urban environment. The paper shows the importance of integral stormwater planning and management in urban areas and gives a summary of the methods and procedures for controlling stormwater runoff. Drainage of stormwater is solved integrated with multidisciplinary teamwork and applying a series of administrative and technical measures aimed at reducing the negative impact of a switched hydrological regime of runoff and pollution of rainwater entered into the water recipient. It explains the basic, commonly used concepts, such as integral approach and stormwater. Terms like infiltration, retention, and detention are explained. Also, alternative concepts are shown, i.e. detention, infiltration, (sub) surface retention, and water in the landscape. Sustainable urban drainage systems (SUDS) are systems designed to efficiently manage the drainage of surface water in the urban environment. These systems reduce pollution levels and rainwater runoff from urbanized areas. Some examples of typical SUDS elements have been provided at the end of the paper. Paper will present the various possibilities of using rainwater as a resource as opposed to considering it as something that simply needs to be hidden in sewers.

Keywords: device, drainage, management, stormwater, SUDS, treatment, urban environment

2 Introduction

2.1 Integral stormwater management

Stormwater management is a major and growing challenge nationwide, with stormwater pollution, flooding and other impacts imposing serious impacts on water quality, public health and local economies [1]. Integral water management is essentially the management of the supply and demand for water. Integral management is linked to sustainability and to the criteria of water sustainability. Globally, about one fifth of the available water quantities are being utilised. However, there are water resource problems because those resources are not equally distributed. Most of the water involved is not consumed but returns to the circular flow of water and thus becomes available for further use, after treatment or a natural self-cleaning process [2]. In general, the term sustainability includes the policies and strategies that meet the society's present needs, without compromising the ability of future generations to meet their own needs [3]. A balance in the demand is required for the sustainability of the water system, regarding water consumption and its availability. Measures for increasing water availability include the reuse of treated wastewater, building accumulations, and the use of alternative sources. Finally, reducing losses in the distribution system can also increase the amount of water in the system without increasing water catchment from nature [2].

The most significant advantage of the integrated approach for planning and management of stormwater over the traditional approach is its highly positive impact on the distinct biophysical features of the urban environment (it prevents the creation of thermal islands and reduces the negative effects of stormwater on the urban space and on the recipient) with optimal economic effects. In addition, this approach improves the quality of housing and the quality of life, improves ecological, economic, and social characteristics, and generally improves the protection of the space, while improving the microclimate and mitigating the effects of droughts, and it also mitigates or even eliminates the consequences of

climate change [4]. A new generation of management practices has emerged to effectively manage stormwater while simultaneously building vibrant, attractive communities [1].

Green infrastructure is a cost-effective, resilient approach to managing wet weather impacts that provides many community benefits. While single-purpose gray stormwater infrastructure- conventional piped drainage and water treatment systems- is designed to move urban stormwater away from the built environment, green infrastructure reduces and treats stormwater at its source while delivering environmental, social, and economic benefits [5].

2.2 Stormwater quality in urban area

Water in any composition must be clean in order to be visually and socially attractive. In general, urbanization converts permeable natural soils into paved surfaces and roofs while vegetation is moved. This process decreases evaporation, decreases infiltration whereas runoff is increased. Urban runoff is also polluted due to building materials, traffic pollutants and other sources. Reported effects on receiving waters include: flooding, erosion, sedimentation, temperature rise, dissolved oxygen depletion, eutrophication, toxicity, and reduced biodiversity.

In Europe, around 75 % of the population live in urban areas and this is projected to increase to about 80 % by 2020. Stormwaters, flowing into storm sewers, are known to significantly increase the annual pollutant loads entering urban receiving waters and this results in significant degradation of the receiving water quality. Knowledge of the characteristics of stormwater pollution enables urban planners to incorporate the most appropriate stormwater management strategies to mitigate the effects of stormwater pollution on downstream receiving waters [6]. Stormwater runoff from urban and suburban areas generates numerous pollutants. The areas include residential areas, parks, commercial areas, industrial areas and road/highways. Table 1 summarizes the pollutants commonly found in stormwater and their possible sources.

Table 1. Possible sources of pollutants in stormwater [7]

	Soil erosions	Vehicles	Human/animal waste	Fertilizers	Household chemicals	Industrial processes	Paints and preservatives
Solids							
Metals							
Oil, greese and organics							
Nutrients							

Non-point pollution is a major source of pollutants in urban environments. A wide range of pollutants deposited on urban catchment surfaces are transported with stormwater during the wet weather periods and ultimately enter aquatic receiving waters [7].

3 Procedures with stormwater in urban environments

3.1 Infiltration

The process of penetrating of water from the ground surface under gravity is called infiltration. Many factors influence the infiltration rate. It mainly depends on condition of soil surface, existing land cover, properties of soil beneath [8]. During the rain infiltration loss occurs quickly almost exclusively from the water that has reached the ground surface. The water infiltrating into the soil moves downward through larger soil pores under the force of gravity. The smaller surface pores take in water by capillarity [9]. Infiltration components are used to capture surface water runoff and allow it to infiltrate (soak) and filter through to the subsoil layer, before returning it to the water table below. Infiltration components can be incorporated into a range of SUDS components [10].

Due to its ability to purify water, the natural layer of soil functions as a long term and effective groundwater protection during the infiltration of rainfall through the vegetated layer of soil. Soil retains harmful substances from stormwater and removes them from the water through various chemical and biological processes. A revitalized layer of soil is an excellent stormwater filter. Buildings should have specific spacing on the boundary with adjacent lots. In addition, the rules regulating construction should

require that a small section of land be set aside for a green area and some additional space, both in populated and in unpopulated areas. These green areas are used not only to beautify the space around the building; they can also be used as an ideal space for the infiltration of stormwater from the roofs [11].

The most rational way is to drain the water over solid soil, through surface channels, or through shallow wells, to a vegetated surface where infiltration is possible. In this way, vegetated surfaces can be useful in two ways - as elements of urban zone design, and for the infiltration of stormwater [11].

Figure 1 shows a rain garden. A rain garden is primarily used to manage runoff from roofs (and relatively unpolluted areas). Plants in a rain garden should be able to withstand periods of ponding and dry periods and, ideally, maintain or enhance the pore space in the underlying soils via deep rooting systems [10].

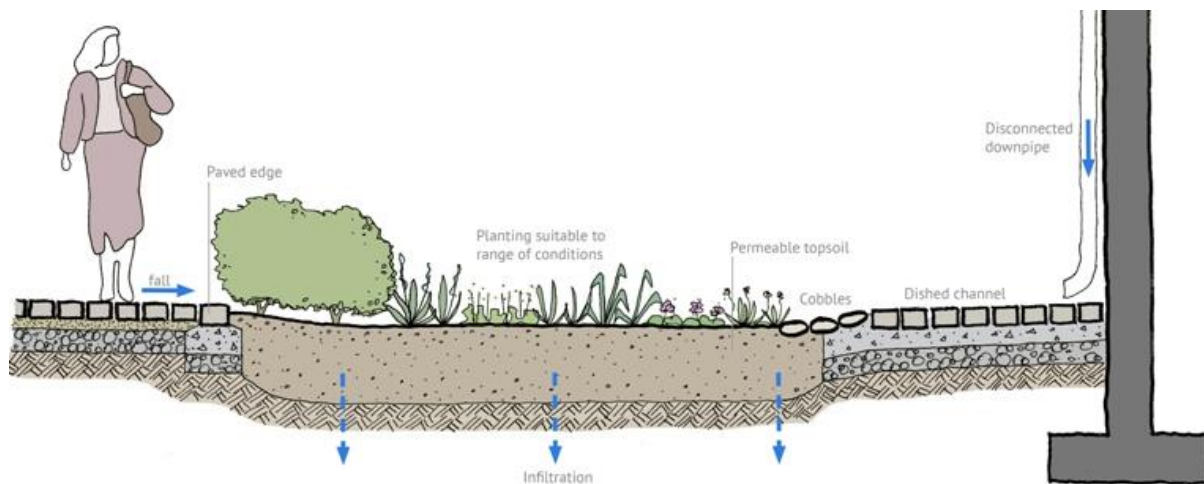


Figure 1. Rain garden [12]

In industrial areas, all usable areas are usually paved or banked with some other material, thus preventing the possibility of infiltration of rainwater through the soil. The aggravating circumstance in this case is that it is also necessary to build a set of stormwater drains or stormwater treatment facilities. The simplest, most cost effective and most efficient way to drain stormwater is through green areas [11].

Some of infiltration type devices are: infiltration trenches, grass filter strips, grass swales and pervious pavements. Infiltration trenches are provided to enhance the infiltration of storm water into the ground. Grass filter strips are stripes of grassed soil surfaces introduced between the urban impervious surfaces and the storm drains to slow down and partially infiltrate runoff. Grass swales are depressions in the grassed terrain designed to function as small unlined channels in which stormwater runoff is slowed down and partially infiltrated along their course. Pervious pavements are permeable surfaces where the runoff can pass and infiltrate into the ground. Pervious pavements facilitate peak flow reduction, ground recharge and pollution filtering. There are three types of pervious pavements: porous asphalt pavements, porous concrete pavements and garden blocks [8].

3.2 Retention

Retention is the reservation of water in case of heavy rainfall and its gradual release to the ground / sewerage. In this way, large water waves and floods can be prevented and there is no need to dimension the drainage system with large cross section pipes.

A retention pond, sometimes called a "wet pond," has a permanent pool of water with capacity above the permanent pool designed to capture and slowly release the water quality capture volume over 12 hours [13]. The design of capacity is based on the runoff generated from the basin due to a design storm [8]. The permanent pool is replaced, in part, with stormwater during each runoff event so stormwater runoff mixes with the permanent pool water [13]. A retention basin can also provide water quality benefits by reducing sediments and attached pollutants [14]. Retention ponds can be very effective in removing suspended solids, organic matter and metals through sedimentation, as well as removing soluble pollutants like dissolved metals and nutrients through biological processes [13]. A retention

basin can also provide water quality benefits by reducing sediments and attached pollutants [14]. Additionally, sunlight and oxygen break down greases and oils [15].



Figure 2. Example of stormwater retention pond (basin) [16]

Retention ponds are one of the most effective storm water management installations for removing storm water pollutants. Sedimentation of solids occurs in the open water and wetland bench. Nutrients are removed in the open water by photosynthesis and by bacteria attached to wetland plants. Since retention ponds have the capability of removing soluble pollutants, they are suitable for sites where nutrient loadings are expected to be high [17]. Maintenance activities include repairing erosion, removing sediment, and managing the vegetation. Repairing erosion early can save significant costs, both in the erosion and the resulting sedimentation that can end up needing to be removed from the basin [14]. Retention ponds provide two primary services. First, they retain the runoff before releasing it into streams. They release the water at flow rates and frequencies similar to those that existed under natural conditions. The flood volume held in a retaining pond reduces the impact on downstream stormwater systems. The second benefit of the retaining ponds is that they provide pollutant removal through settling and biological uptake. Ponds remove 30-80% of certain pollutants from water before it enters nearby streams. Common pollutants reduced are sediments, bacteria, greases, oils, metals, total suspended solids, phosphorous, nitrogen, and trash. Ponds are one of the most effective tools at providing channel protection and pollutant removal in urban streams. Essentially, retention ponds provide water quality and quantity control [18].

Aquatic vegetation is often associated with wet ponds. Vegetation such as grasses and plants are able to establish themselves in the permanent pool of wet ponds thus providing extra pollutant removal. The aquatic plants and grasses serve as an extra filter in the pond. They assimilate dissolved pollutants and, by biological uptake, transform pollutants into less toxic materials. Microorganisms often establish themselves in wet ponds and aid in the breakdown of pollutants [18]. Some benefits are water quality control, water quantity control, amenity value, habitat creation value and biological treatment [17].

3.3 Detention

Detention ponds, also called dry detention ponds, are basins that receive and hold runoff for release at a predetermined rate, thereby reducing the peak runoff delivered to storm sewers and streams. The ponds generally are earthen structures constructed either by impoundment of a natural depression or excavation of existing soil. Captured runoff is released through multi-level outlet structures consisting of weirs, risers, orifices or pipes, which provide for increased discharge as water levels in the basin increase. They help to prevent localized flooding and, if designed to do so, provide some water quality benefits and reduce streambank erosion downstream [19].

Detention ponds serve as important flood control features. They are usually dry except during or after rain or snow melt. Their purpose is to slow down water flow and hold it for a short period of time such as 24 hours. Urban areas rely on these structures to reduce peak runoff rates associated with storms,

decreasing flood damage [20]. Detention ponds have been one of the most widely used stormwater management practices. However, they should not be used as a one size fits all solution. If pollutant removal efficiency is an important consideration, detention ponds may not be the most appropriate choice. Detention ponds require a large amount of space to build [21].



Figure 3. Example of stormwater detention pond (basin) [10]

Detention ponds can be designed for a variety of storm events and purposes. The land area available for construction, slope of the site and contributing area are all factors to be considered. Also, an emergency spillway is usually required to allow for safety during flood events. Although detention ponds can vary in size and shape, they all function to settle stormwater particles and reduce peak flows. All of the ponds are designed to be separate from local groundwater supplies to prevent movement of dissolved pollutants from surface water to groundwater sources [20]. Dry ponds, detention ponds, do not have dead storage and dry out between storms [18].

Properly maintained detention ponds can be very effective at removing certain pollutants and providing necessary storage volumes during larger storm events. Improperly maintained ponds can increase the discharge of pollutants downstream, increase the risk of flooding downstream, increase the instability of downstream channels, and lead to aesthetic and nuisance problems [22]. Some benefits of detention ponds are: reduces peak rate of runoff, alleviates flooding, cost effective, can be designed to address water quality, space surrounding pond can be landscaped to enhance and provide habitat for wildlife [19].

Detention ponds are best used in areas where there is four or more hectares of land. On smaller sites, it is difficult to control water quality and other options may be more appropriate. Detention ponds generally use a very small slope to divert water. The system works by allowing a large collection area, or basin, for the water. The water then slowly drains out through the outlet at the bottom of the structure. Sometimes concrete blocks and other structures act as a deterrent to slow the water flow and collect extra debris [23].

4 Sustainable urban drainage systems (SUDS)

There are four main categories of benefits that can be achieved by SUDS: water quantity, water quality, amenity and biodiversity. These are referred to as the four pillars of SUDS design. SUDS can take many forms, both above and below ground. Some types of SUDS include planting, others include proprietary/manufactured products. In general terms, SUDS that are designed to manage and use rainwater close to where it falls, on the surface and incorporating vegetation, tend to provide the greatest benefits. Most SUDS schemes use a combination of SUDS components to achieve the overall design objectives for the site [24].

Conventional stormwater drainage, whose main purpose is the rapid removal of all stormwater from the urban landscape, has been found to have some undesirable effects on the urban environment such as lowering the water quality of receiving water bodies due to increased sediment yields and related contaminant fluxes, a decrease in hydrological amenity and an increase in flood risk. Also, conventional

stormwater drainage is said to be expensive in terms of the costs of developing and maintaining the infrastructure, while its overall effectiveness as a flood risk management option has also been questioned. In the last two decades, solving the problem of stormwater drainage in developed countries is given great attention by applying planning and design techniques known as Low Impact Development (LID) to USA and Canada, Sustainable Urban Drainage Systems (SUDS) in the UK or Water- Sensitive Urban Design (WSUD) in Australia. Drainage of stormwater is handled integrated, multidisciplinary teamwork and applying a series of administrative and technical measures aimed at reducing the negative impact of the changed hydrological regime of runoff and pollution of storm water carried in the receiving waters. This is an innovative approach that relies on ecological principles to plan and design drainage according to natural mode of runoff, i.e. to manage groundwater resources at source by using evenly distributed decentralized micro drainage and purification systems and/ or best practices for integrated stormwater management.

Sustainable drainage systems provide the ideal opportunity to bring urban wetlands and other wildlife friendly green spaces into our towns and cities and link these with existing habitats creating blue and green corridors. Well-designed SUDS should also be an amenity and education resource for the community, providing high-quality public green space in which to relax, play and enjoy wildlife. However, whilst there are many good examples of this already, there is still a long way to go before SUDS fulfil their potential to integrate surface water management and water quality improvements with people and wildlife benefits. SUDS provide the ideal opportunity for local authorities to deliver multiple benefits and for little or no extra cost. Also, these solutions are very often cheaper to build and maintain than conventional drainage solutions [25].

Increasing use of SUDS will help us overcome a variety of challenges we face, namely:

- a rapidly changing climate (including an increasing urban heat island effect),
- increasing loss of permeable surfaces through development and urban creep,
- inadequate capacity of existing sewerage systems,
- poor water quality in streams and rivers, and
- a lack of wildlife habitats in urban areas and a lack of connectivity with suburban/rural areas.

SUDS will:

- manage volume and flow rates of run-off to reduce the downstream flow and destructive power of surface water, and reduce the risk of flooding,
- improve water quality by reducing pollution locally and downstream in streams, rivers and estuaries,
- encourage natural groundwater recharge to help maintain river and stream flows in periods of dry weather, and support wetlands in the wider landscape,
- protect and enhance water quality and provide significant opportunities for wetland habitat creation,
- support the well-being of people and communities and increase the amenity value of developed land, and
- increase evapotranspiration and climate regulation in urban areas.

Table 2. Examples of typical SUDS elements [26]

	<p style="text-align: center;">Infiltration from surface</p> <p>Infiltration from surface occurs when disconnecting the downspouts and discharging the rainwater on the permeable surface.</p>
	<p style="text-align: center;">Soakaway or infiltration trench</p> <p>A soakaway (dry well, infiltration well) is a pit in the ground, stabilised with a porous material wrapped in geotextile and covered with topsoil and vegetation. An infiltration trench is a soakaway shaped geometrically like a trench, for example, 60 cm wide, 1 m deep and several metres long.</p>
	<p style="text-align: center;">Rain garden</p> <p>A rain garden is a depression in the terrain designed to receive, store and filter runoff from roofs or surfaces and is also designed as a specially planted area with selected plants that can cope with dry and with wet conditions.</p>
	<p style="text-align: center;">Swales</p> <p>A swale is a rain garden placed in the side of a road, with a soakaway underneath. Typically, the swale also serves as a traffic harassment.</p>
	<p style="text-align: center;">Green roof</p> <p>Green roofs are roofs covered with a multi-layer system consisting of: growth medium, drainage layer and water-proof membrane. Green roofs delay runoff from roofs, and the total runoff volume is less than that from conventional tiled roofs. The degree of delay and volume reduction increases with the thickness of the growth medium. Green roofs insulate buildings against warming and can provide a habitat for certain insect and birds. Retained water evaporates.</p>
	<p style="text-align: center;">Permeable pavement</p> <p>Permeable pavement provides a horizontal surface suitable for walking or driving but also allows rainwater to infiltrate. The infiltration capacity of the permeable pavement depends on the design and on the hydraulic capacity of the base course and the soil underneath and alongside.</p>
	<p style="text-align: center;">Trenches</p> <p>Trenches are used for transporting water above ground in places where open trenches do not inconvenience road users. Trenches can be a recreational element in an urban landscape.</p>
	<p style="text-align: center;">Ditches</p> <p>A ditch is a narrow channel dug in the ground, typically used for drainage alongside a road or the edge of a field.</p>

The delivery of SUDS fits elegantly within the remit of GI, in terms of water management and flood prevention. Green infrastructure (GI) is a concept that describes a network of inter-connected, multifunctional green and blue spaces designed to meet the environmental, social and economic needs of a community. SUDS creates a drainage network, however unlike a conventional drainage system, SUDS relies on mainly natural approaches to provide drainage. The above ground drainage networks, if correctly designed and delivered, provide effective green corridors where biodiversity can thrive, due to

controlled flows of clean water. Thus the synergies between delivering SUDS and providing a GI network can be readily appreciated. The main benefits of GI regarding hydrology are rainfall interception, increased soil infiltration, water uptake, water storage and delaying and decreasing peak flows all of which decrease the volume of water that requires management. In more detail, depending on size and species, big trees have the potential to intercept 80% of precipitation where smaller trees may only have 16% rainfall interception.

Green infrastructure has great potential to decrease the volume of stormwater needing management at all levels. Rainfall interception, mainly by trees, reduces the amount of water reaching the ground. Increased infiltration of soils through root growth and root turnover increases the rate at which water is relocated from the surface to the subsoil/groundwater. Vegetation removes water from the ground through transpiration and therefore increases the capacity of the soil to store water. Finally, the remaining stormwater can be stored in ponds, wetlands and other open spaces within the floodplain and prevent damages to homes and other properties [27].

SUDS have many more advantages than disadvantages on the environment and population. There are numerous advantages in using SUDS, and some of advantages are: low-cost way to reduce rate and volume of runoff; easy to integrate into green space; easy maintenance; effective water filtration and pollutants removal; regulates groundwater level; stimulates biodiversity; provide a variety of pollutant treatment mechanisms, such as filtration, adsorption into soil particles, biological uptake (by plants); sound/ noise absorption; habitat for urban wildlife [28]; reduced flooding risks; minimises public and environmental impacts as a result of decreased pollutants; reducing potable water demand through rainwater harvesting; reducing stormwater inflow into sewer systems; etc.

Some disadvantages of SUDS are: use of large areas; with no regular inflow or water aeration, anaerobic conditions and algal blooms may happen (retention ponds); not appropriate for steep roofs, maintenance of roof vegetation (green roofs); constructed wetlands need large area and sensitive to overloading, especially in cold climate areas [28]; may be initially expensive to construct SUDS.

5 Stormwater management in Croatia

Stormwater management in Croatia is far from sustainable. In Croatia, stormwater is drained in a classic way, which includes drainage pipes connected to a wastewater treatment plant or discharge into the recipient. Due to such solutions, urban floods are common occurrences in Croatia, they happen as a result of high rainfall intensity and the inability of the sewage system to accept large amounts of stormwater. These occurrences are more evident in urban environments, especially in towns along the Adriatic coast. One of the solutions for this problem is the integral drainage approach. The integral approach uses almost no pipes or stormwater precipitation canals. Stormwater is treated naturally: by infiltration underground and by evapotranspiration.

There are initiatives in the Republic of Croatia aimed at the popularization of green infrastructure (GI) and at the education related to the possibilities of its implementation through the Croatian Green Building Council, but these are only pioneering activities. A wider involvement is needed, based on the inclusion of the overall professional and scientific public [29]. Croatia has been a member of the European Union since 2013, and the recommendation of the European Commission (2013) to implement green infrastructure has aroused interest in urban and spatial planning institutions [30].

At present there is no legislation addressing the problem of stormwater management in more detail. Stormwater is only recognized as a wastewater but any other related aspects are not covered. The existing legislation is primarily engaged in wastewater treatment at wastewater treatment plants and effluent quality requirements from WWTP. Current practice of urban planning favours conventional sewage and drainage solutions while SUDS are not recognized as a possible alternative. Also the possibilities for energy savings by collecting and using stormwater are not covered by any document at the national level. The possibility of the energy efficiency through effective stormwater management is not included in the municipal Sustainable Energy Efficiency Action Plan. Main water regulations (Acts) have been adjusted with the regulations at European level, but as well as European regulations, still do not provide direct guidelines, actions or at least principle solutions for stormwater management [31]. SUDS provide the ideal opportunity for local authorities to deliver multiple benefits and for little or no extra cost. In fact, these sustainable solutions- SUDS are very often cheaper to build and maintain than conventional

drainage solutions [25]. All examples of SUDS listed in Table 2 are to a lesser extent applied to the Republic of Croatia, with the exception of the soakaway that is not applied.

Finally, it is worth mentioning that the term green infrastructure is defined in Article 9, paragraph 1, subparagraph 52 of the Nature Protection Act (NN 80/13), in the definition section, and it also appears in Article 7, paragraph 3 of this Act [32].

6 Conclusion

Stormwater management in urban area means to manage *surface runoff* in urban areas where *run-off* cannot infiltrate because the surfaces are impermeable. Any urban development will affect or make an impact (mainly negative impact) on its environment. Stormwater management is the science of limiting these negative impacts on the environment and enhancing the positive impacts, or catering for the hydraulic needs of a development while minimising the associated negative environmental impacts. Climate changes and the fast growing urbanization, which is causing increasing problems, should be initiators for a new way of thinking. The integral approach is an innovative approach that relies on the ecological principles of planning and designing drainage according to the natural runoff.

Today, interest is growing for using green structures (typical SUDS elements) for retrofits and for controlling combined sewer overflows.

In many countries (and even in Republic of Croatia) the application of these alternative drainage solutions is very small or none. The future of urban sewage is just related to these methods of drainage. Therefore it is necessary to introduce the wider community with the benefits and opportunities of sustainable drainage systems, and the design of new systems and reconstruction of existing in the maximum extent possible, apply green infrastructure.

References:

- [1] EPA, United States Environmental Protection Agency: Community Solutions for Stormwater Management, A Guide for Voluntary Long- Term Planning, draft, pp. 1, 2016.
- [2] Gereš, D.: Održivi razvoj vodnog gospodarstva, Hrvatski savez građevinskih inženjera, Sabor hrvatskih graditelja 2004, Cavtat, pp. 925-935, 2004.
- [3] Draper, J.: Urban Design and Stormwater Management: An Integrated Approach to Public Hardscape Design, Clemenson University TigerPrints, Theses, Paper 1084, pp. ii, 2011.
- [4] Milićević, B. D., Anđelković, N. Lj., Mitić, M. P.: Nužnost integralnog pristupa planiranju i upravljanju atmosferskim vodama na primeru grada Pirota, Tehnika-kvalitet ims, standardizacija i metrologija, 15, 6, pp. 1065-1072, 2015.
- [5] EPA, United States Environmental Protection Agency: What is Green Infrastructure, <https://www.epa.gov/green-infrastructure/what-green-infrastructure>, 28.05.2017.
- [6] Floris C. Boogaard, C. F., van de Ven, F., Langeveld, J. G., van de Giesen, N.: Stormwater Quality Characteristics in (Dutch) Urban Areas and Performance of Settlement Basins, Challenges 2014, 5, pp. 112-122., 2014.
- [7] Rupak Aryal, R., Vigneswaran, S., Kandasamy, J., Naidu, R.: Urban stormwater quality and treatment, Korean J. Chem. Eng., 27, 5, pp. 1343-1359, 2010.
- [8] Hydrology for Urban Stormwater Drainage, https://ocw.un-ihe.org/pluginfile.php/445/mod_resource/content/1/Urban_Drainage_and_Sewerage/3_Urban_Hydrology/Urban_Hydrology/Urban_hydrology_note.pdf, 27.05.2017.
- [9] Sen, S.: Infiltration: Concept and Factors Affecting Infiltration, <http://www.yourarticlelibrary.com/water/infiltration/infiltration-concept-and-factors-affecting-infiltration/60457/>, 20.05.2017.
- [10] Susdrain: Infiltration overview, <http://www.susdrain.org/delivering-suds/using-suds/suds-components/infiltration/infiltration.html>, 20.05.2017.
- [11] Kovačević, A., Agić, Dž.: Održivo upravljanje kišnicom, Uputstvo za infiltraciju i korištenje, Centar za ekologiju i energiju, Tuzla, pp. 4, 12, 14, 2012.
- [12] <http://picasaweb.google.com/111313736746690275084/SusdrainWebsiteSketches#5782907023732993138>, 27.05.2017.
- [13] Retention pond, Urban Drainage and Flood District, Urban Storm Drainage Criteria Manual

Volume 3, T-7, 2015.

- [14] Sustainable Stormwater Management, <https://sustainablestormwater.org/2009/05/28/stormwater-101-detention-and-retention-basins/>, 27.05.2017.
- [15] Southwest Florida Water Management District: How To Operate & Maintain Your Stormwater Management System, pp. 10.
- [16] <https://www.pinterest.com/pin/317996423671553908/>, 26.05.2017.
- [17] Dublin City Council: Greater Dublin Strategic Drainage Study- Environmental management policy, Retention ponds, site control, <http://www.dublincity.ie/sites/default/files/content/WaterWasteEnvironment/WasteWater/Drainage/GreaterDublinStrategicDrainageStudy/Documents/Vol%203%20-%20%20Retention%20Ponds.pdf>, 02.06.2017.
- [18] Jordan, A. K.: The use of retention ponds in residential settings, Department of Earth Sciences, University of South Alabama, Mobile, AL, <http://www.southalabama.edu/geography/fearn/480page/02Jordan/Jordan.htm>, 25.05.2017.
- [19] Dauphin County Conservation District: Best Management Practices Fact Sheet, Detention Ponds
- [20] Laramie County Conservation District: Best Management Practices for Stormwater Runoff: Ponds, 2011.
- [21] Mississippi Department of Environmental Quality: Erosion Control, Sediment Control and Stormwater Management on Construction Sites and Urban Areas, Volume 2, Stormwater Runoff Management Manual, Chapter 4: Best Management Practices Design, Dry Detention Pond, pp. 144, 2011.
- [22] SEMSWA, Southeast Metro Stormwater Authority: Maintaining Detention Ponds, pp. 1
- [23] Wessler Engineering, <https://info.wesslerengineering.com/blog/stormwater-basins-detention-retention-ponds>, 30.05.2017.
- [24] Woods Ballard, B., Wilson, S., Udale-Clarke, H., Illman, S., Scott, T., Ashley, S., Kellagher, R.: The SuDS Manual, CIRIA, Department for Environment Food & Rural Affairs, London, 2015.
- [25] Graham, A., Day, J., Bray, B., Mackenzie, S.: Sustainable drainage systems, A guide for local authorities and developers, 2012.
- [26] Hoffmann, B., Laustsen, A., Jensen, I. H., Jeppesen, J., Briggs, L., Bonnerup, A. et al.:
- [27] Sustainable Urban Drainage Systems: Using rainwater as a resource to create resilient and liveable cities, State of Green, 2015.
- [28] Bartens, J. and The Mersey Forest Team: Green Infrastructure and Hydrology, 2009, http://www.greeninfrastructurenw.co.uk/resources/GI_&_Hydrology_Report_May_2009.pdf, 04.06.2017.
- [29] Estonia Latvia Programme, (D)rain for life: Handbook on sustainable urban drainage systems, <http://drainforlife.eu/attachments/article/64/DFL%20SUDS%20Handbook%20final.pdf>, 18.07.2017.
- [30] Ćosić-Flajsig, Gorana: Zelena infrastruktura u Europskoj uniji i izazovi/mogućnosti primjene u Hrvatskoj, <http://seminar.tvz.hr/materijali/materijali19/19G07.pdf>, 03.06.2017.
- [31] Hrdalo, I., Tomić, D., Pereković, P.: Implementation of Green Infrastructure Principles in Dubrovnik, Croatia to Minimize Climate Change Problems, Urbani izziv, 26, (special issue), pp. S38-S49, 2015.
- [32] Vukovic, Z., Halkijevic, I., Kuspilic, M., Ercegovac, K.: E²STORMED Strategic Action Plan for Zagreb, Zagreb, pp. 8, 9., 2015.
- [33] Zakon o zaštiti prirode, Narodne novine, Službeni list Republike Hrvatske, NN 80/13, Zagreb, 2013.

COMPUTER ANALYSIS OF HYDRAULIC CONDITIONS IN A SANITARY CHAMBER

PIOTR ZIMA ¹

¹ *Gdańsk University of Technology, Faculty of Civil and Environmental Engineering, Poland, pzim@pg.gda.pl*

1 Abstract

This paper presents analysis of hydraulic conditions of sewage flow down the slipway (ramp) in the collecting sanitary chamber connecting 3 collectors on the inlet: $\varnothing 600$, $\varnothing 800$ and $\varnothing 1400$ and one on the outlet $\varnothing 1600$ mm, with a maximum difference of elevation 5 m. The mathematical model has been made and hydraulic calculations were carried out in steady flow conditions. Then wastewater surface elevation, energy grade line elevation, critical depth and the value of average velocity were computed in adopted cross-sections of the model. Adhesion of flux to the surface of the slipway and conditions of energy dissipation in the basin below the ramp were also checked.

Keywords: sanitary chamber, sewage system, hydraulic calculations, sewage flow, collectors connection

2 Introduction

When designing a sanitary sewage system very common problem is connection of sewage collectors located on different heights. In such cases, the collecting sanitary chambers are used. Streams are combined in the chamber by proper shaping of the slipways. The dimensions of these chambers are limited, and the ordinates of the collectors outlets are very different. In this case important is proper shaping of the ramp surface at the juncture of the wastewater streams. In an improperly designed chamber it will be occurred the collision of wastewater streams and the formation of strong turbulence and eddies. This increases the velocity of wastewater, which grabs a significant amount of air and injects into drains. Then air is blown out through the sewer manholes, causing an unpleasant odour, often at a considerable distance from the chamber. Therefore, an important part of a well-made design of such a chamber are appropriately contoured surfaces of slipways and stilling basin to dissipating the flow energy of wastewater, which will minimize the adverse effects of rapid mixing of the streams. One method is to verify proposed design solutions by mathematical modelling. These simulations can be done within the existing programs performing calculations in the field of CFD, but it is a very time-consuming process. In practical applications, you can use the available software to perform the calculation of flow in sewers.

This paper presents analysis of hydraulic conditions of sewage flow down the slipway in the collecting sanitary chamber connecting 3 collectors on the inlet: $\varnothing 600$, $\varnothing 800$ and $\varnothing 1400$ and one on the outlet $\varnothing 1600$ mm, with a maximum difference of elevation 5 m. The details of the construction and basic dimensions of the sanitary chamber are shown in Figure 1 (horizontal view) and in Figure 2 (basic section – A-A) – extract from the documentation of the Gdansk Water and Wastewater Infrastructure (GWWI). Adhesion of flux to the surface of the slipway and conditions of energy dissipation in the basin below the ramp (the junction of collectors: inlet $\varnothing 800$ and outlet $\varnothing 1600$) were also checked. There are two methods: the ramp shape was compared to the shape of a wastewater stream freely flowing from a pipe and to the Creager profile.

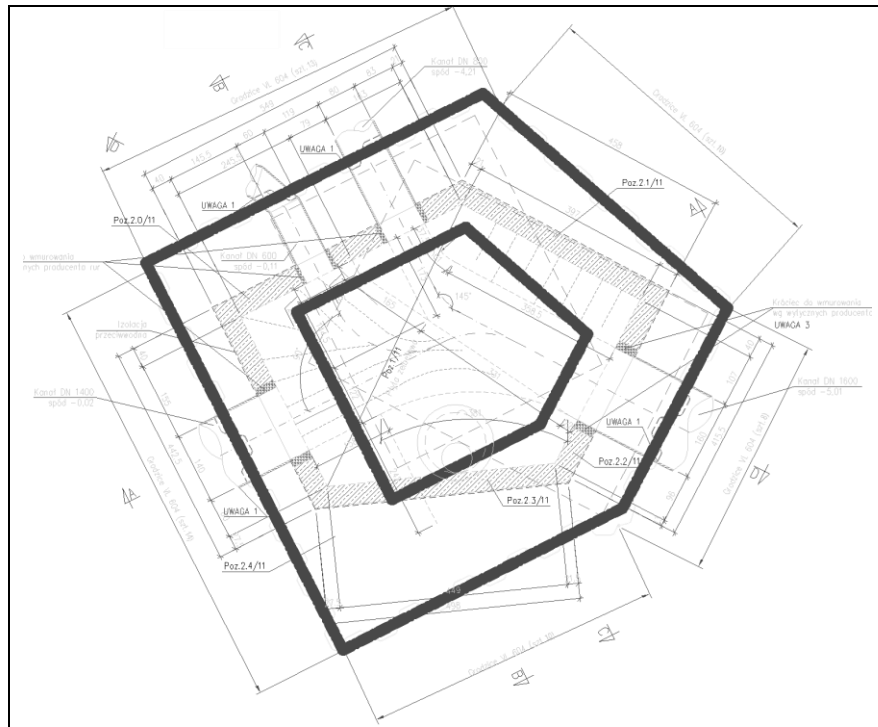


Figure 1. Horizontal projection of the sanitary chamber (source: GWWI)

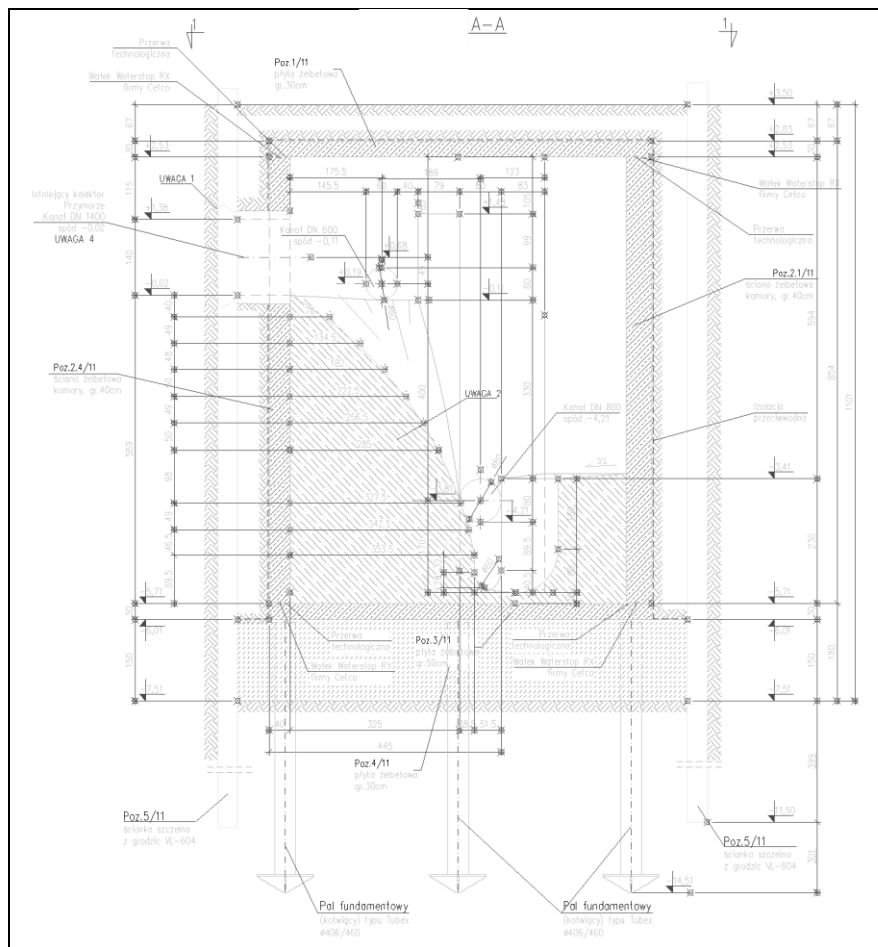


Figure 2. Main vertical section (A-A) of the sanitary chamber (source: GWWI)

3 Methods

The mathematical model has been made in HEC-RAS program on the basis of the available project documentation (Figure 3). This model take into account the data on the position of the collectors adjacent to the chamber, the geometry of the chamber together with shape of the slipway and dissipation basin inside. The three-dimensional model of the chamber is presented in Figure 4.

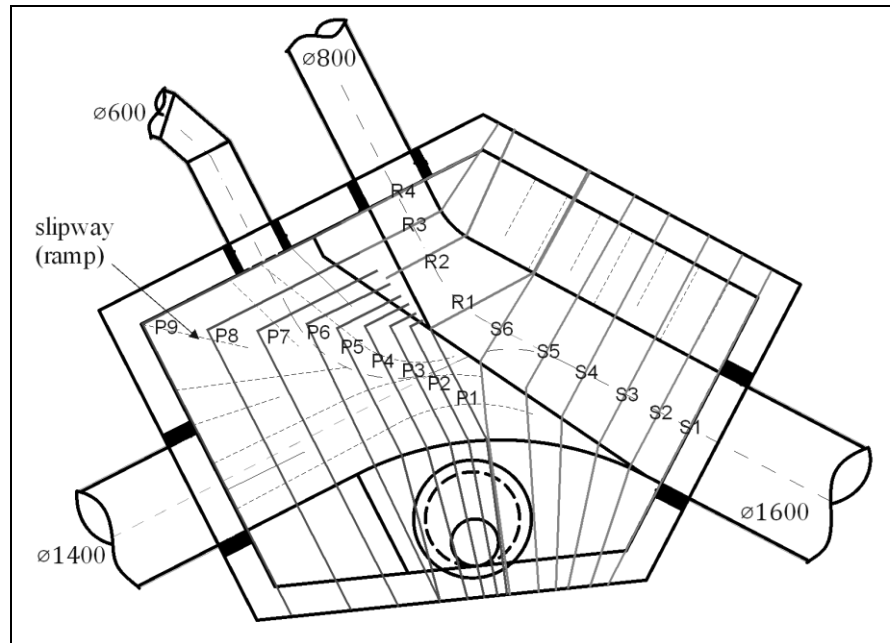


Figure 3. Adopted computational cross-sections in mathematical model of the sanitary chamber

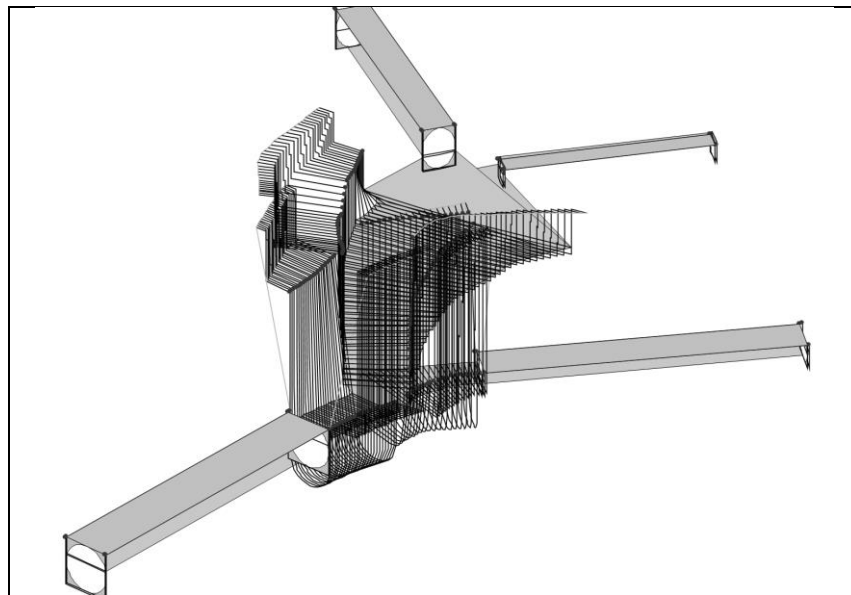


Figure 4. Model of the sanitary chamber in HEC-RAS program

HEC-RAS [1] has been developed by the U.S. Army Corps of Engineers in Hydrologic Engineering Center. It allows to perform flow calculations with free surface and under pressure, steady and unsteady flow conditions, including both sub- and supercritical flow. In calculations, the equation of the mechanical energy balance of the stream at cross-section i and $i+1$ is used [2]:

$$z_i + h_i + \frac{\alpha u_i^2}{2g} = z_{i+1} + h_{i+1} + \frac{\alpha u_{i+1}^2}{2g} + h_e \quad (1)$$

where:

z – elevation of the main channel sections [m],
 h – depth of water at cross sections [m],
 α – velocity weighting coefficients [-],
 u – average velocities at cross sections [m/s],
 g – gravitational acceleration [m/s²],
 h_e – total energy head loss [m].

Energy losses in the model are covered by friction (Manning's formula) and contraction between the computing cross-sections. In addition, in case of change of flow direction (defined by angle), additional local losses are taken into account. Where we are dealing with a supercritical flow, for calculations the equation of momentum conservation is used. This is the implementation of the second Newtonian dynamics principle for the mass of liquid between two cross sections (i and $i+1$) [2]:

$$\frac{\beta Q_{i+1}^2}{gA_{i+1}} + A_{i+1}h_{i+1} + \frac{A_i + A_{i+1}}{2}LS_0 - \frac{A_i + A_{i+1}}{2}LS_f = \frac{\beta Q_i^2}{gA_i} + A_i h_i \quad (2)$$

where:

Q – flow rate [m³/s],
 β – momentum coefficient [-],
 A – area of the cross section [m²],
 S_f – slope of the energy gradient [m],
 S_0 – slope of the channel [m],
 L – distance between sections i and $i+1$ [m].

In case of high flow velocity, the location of the wastewater surface depends on the aeration. This phenomenon should be taken into account in the analysis of strongly supercritical flows (Froude number $Fr > 1.6$). HEC-RAS uses two formulas. When $Fr \leq 8,2$ the wastewater surface is calculated according to the formula [1]:

$$\frac{h_n}{h} = 0,906 \cdot e^{0,0615 \cdot Fr} \quad (3)$$

where:

h_n – water depth with air entrainment [m],
 Fr – Froude number.

Whereas when $Fr > 8,2$ following formula is used [1]:

$$\frac{h_n}{h} = 0,620 \cdot e^{0,1051 \cdot Fr} \quad (4)$$

To check the conditions of adhesion of the wastewater stream to the ramp surface, we obtain appropriate relationships by solving the equation of conservation of momentum Eq. (2), in which we reject the viscosity and accept the constant pressure. Using the relationship between the displacement and the velocity of the sewage, we obtain an equation of the stream shape [3]:

$$z = H + x \cdot tg\alpha - \frac{1}{2}g \left(\frac{x}{v_0 \cdot \cos\alpha} \right)^2 \quad (5)$$

where:

H – elevation of the collector outlet above the datum [m],
 x – distance from the collector outlet [m],

α – angle of inclination of the collector outlet to horizon [m],
 v_0 – velocity of sewage stream at the collector outlet [m/s].

Condition Eq. (5) was used in simulations made using the HEC-RAS program, each time checking the adhesion of the stream to the ramp and taking into account the fact that it was detachment from surface. The second approach used in analysing of the position of the stream relative to the ramp was to compare the ramp shape with the Creager profile [4]. This is a profile described by dimensionless coordinates defining the profile of the shape of the bottom surface of a freely falling stream. In literature [4] two curves are published: for the upstream face inclined with respect to the outlet 90° and 45° (Table 1). In order to obtain the coordinates describing the curve for a given flow rate, multiply the z coordinate by forming the elevation of the energy grade line H_0 .

Table 1. Coordinates of the Creager profile

x/H_0	z/H_0	
	90°	45°
0.0	-0.126	-0.043
0.1	0.036	-0.010
0.2	-0.007	0.000
0.3	0.000	-0.005
0.4	-0.006	-0.023
0.6	-0.060	-0.090
0.8	-0.147	-0.189
1.0	-0.256	-0.321
1.2	-0.393	-0.480
1.4	-0.565	-0.665
1.7	-0.873	-0.992
2.0	-1.253	-1.380
2.5	-1.960	-2.140
3.0	-2.820	-3.060
3.5	-3.820	-4.080
4.0	-4.930	-5.240
4.5	-6.220	-6.580

4 Results and discussion

After performing the numerical model of the analysed chamber together with the adjacent sections of the sewage collectors, hydraulic calculations were carried out in steady flow conditions. First, flow rates and appropriate boundary conditions in all collectors were adopted. For the downstream cross-sections were adopted appropriate slope of energy line, for outflow from collectors - critical depth, and in junctions - momentum mode with friction and proper tributary angle. The maximum values of wastewater flow into the chamber by individual collectors and their slopes (information obtained from **GWWI**) were taken into account. On the inflow: $\varnothing 600 - Q_{max} = 0,53 \text{ m}^3/\text{s}$ and $I = 0,56\%$, $\varnothing 800 - Q_{max} = 0,26 \text{ m}^3/\text{s}$ and $I = 0,14\%$, $\varnothing 1400 - Q_{max} = 1,59 \text{ m}^3/\text{s}$ and $I = 1,40\%$, and on the outflow: $\varnothing 1600 - Q_{max} = 2,38 \text{ m}^3/\text{s}$ and $I = 0,12\%$. Next wastewater surface elevation (WS), energy grade line elevation (EG), critical depth (Crit) and the value of average velocity were computed in adopted cross-sections of the model.

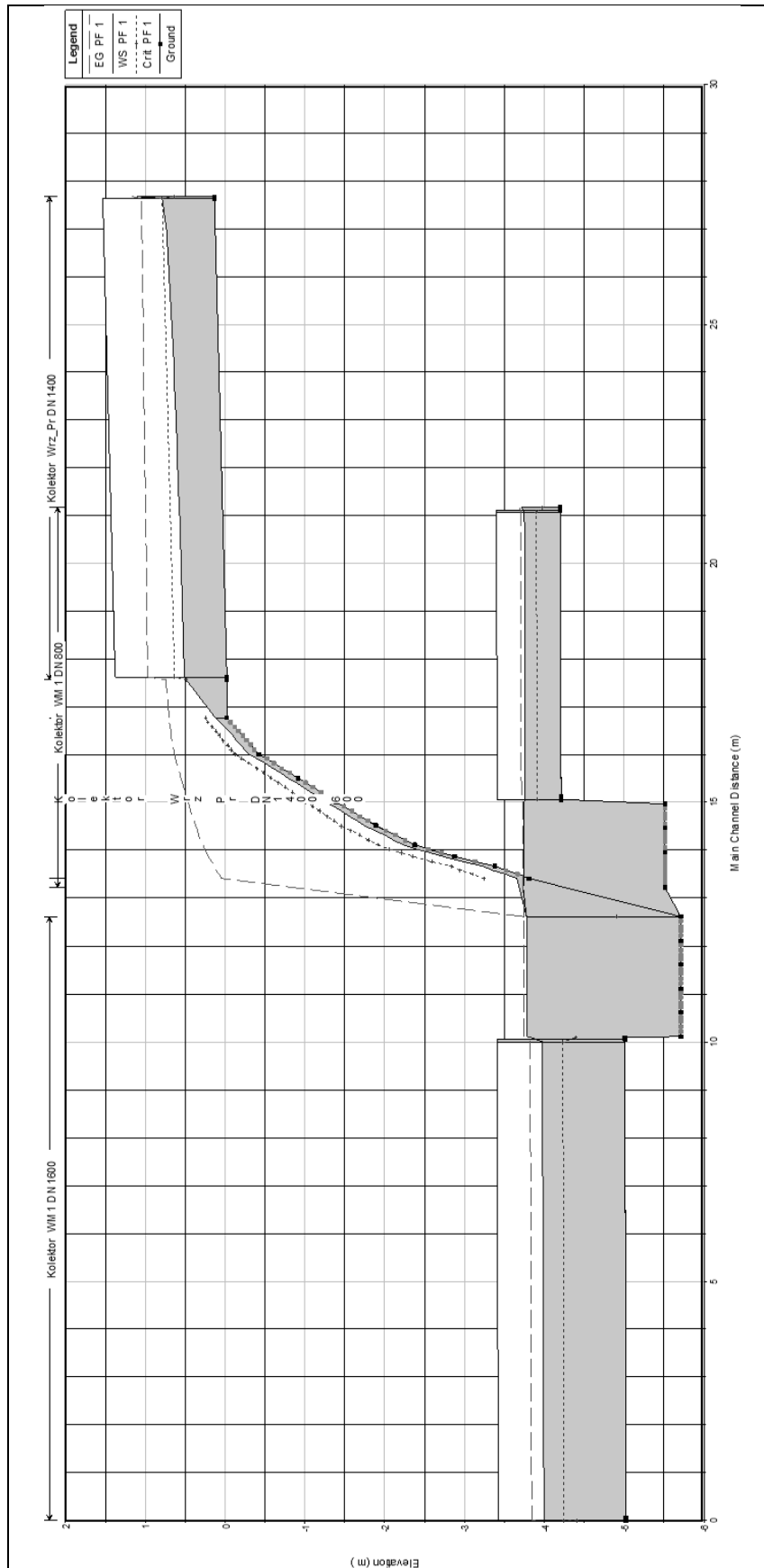


Figure 5. The longitudinal profile of wastewater along the main collectors axes and along the ramp (HEC-RAS) Depending on the value of the Froude number, the formulas Eq. (3) and Eq. (4) have been used to correct the position of the wastewater surface due to aerating. Calculation results for the assumed maximum

flow distribution are graphically represented as the wastewater surface profile along the main collectors axis ($\varnothing 800$, $\varnothing 1600$ and $\varnothing 1400$) and along the chamber (within the main collector - $\varnothing 800 \div \varnothing 1600$) and along the slipway (ramp) in the chamber (Figure 5). The fulfillments of the collectors $\varnothing 1400$ and $\varnothing 600$ were below the critical depth, and flow was supercritical (Froude number $Fr > 1$) with velocity respectively: $v = 2.24$ m/s and $v = 2.06$ m/s. Then the two wastewater streams merge together and run down reaching velocity at the base of ramp $v = 8.53$ m/s and fall into the dissipation basin. There is energy dissipation, connection to the stream from collector $\varnothing 800$ and flow out by collector $\varnothing 1600$ in subcritical conditions ($Fr < 1$, depth greater than the critical depth, velocity in the basin $v = 0.85$ m/s, velocity in the collector $v = 1.26$ m/s). Detailed results in the form of ordinates: the body of the ramp (slipway), location of the wastewater surface, the energy grade line, the critical depth and the mean velocity along the ramp are summarized in Table 1. By analysing its content, it is clear that the sewage flows from the $\varnothing 1400$ collector are in the supercritical regime (the depth at the outlet of the collector is below the critical depth), and the velocity along the ramp increases from more than 2 m/s at the outlet of the collector, to over 8.5 m/s at its base, before entering to the dissipation basin in the main collector line.

Table 2. Results of numerical simulation of sewage flow in the sanitary chamber

CROSS-SECTION	Q [M ³ /s]	ELEVATION [MASL]				v [M/s]	COMMENTS
		bottom	wastewater surface	critical depth	energy grade line		
KS1400	1.59	-0.02	0.49	0.49	0.74	2.24	$\varnothing 1400$
P9	2.12	-0.02	0.12	0.25	0.7	2.62	Spilway (ramp) in sanitary chamber
P8	2.12	-0.42	-0.3	-0.12	0.64	4.3	
P7	2.12	-0.91	-0.79	-0.58	0.55	5.17	
P6	2.12	-1.39	-1.26	-1.01	0.47	5.89	
P5	2.12	-1.89	-1.75	-1.46	0.37	6.57	
P4	2.12	-2.38	-2.24	-1.91	0.28	7.19	
P3	2.12	-2.88	-2.73	-2.36	0.21	7.77	
P2	2.12	-3.38	-3.22	-2.83	0.13	8.29	
P1	2.12	-3.81	-3.65	-3.25	0.05	8.53	
S6	2.38	-5.71	-3.78	-4.91	-3.74	0.83	Dissipation basin in sanitary chamber
S5	2.38	-5.71	-3.78	-4.91	-3.74	0.83	
S4	2.38	-5.71	-3.78	-4.91	-3.74	0.84	
S3	2.38	-5.71	-3.78	-4.91	-3.74	0.85	
S2	2.38	-5.71	-3.78	-4.91	-3.74	0.85	
S1	2.38	-5.71	-3.78	-4.91	-3.74	0.86	
KS1600	2.38	-5.01	-3.83	-4.4	-3.75	1.26	$\varnothing 1600$

In the last stage of the work has been done verification of conditions of stream adhesion to the slipway. Different curvatures of surface of ramps for collector $\varnothing 1400$ (main part of slipway) and $\varnothing 600$ were adopted in the chamber project. For this reason they have been checked independently. Two approaches were used here. In the first it has been calculated position of the stream which would has been formed as the free outlet from the collector (assuming given flow rate and slope of collector). In the analysed case $\alpha = 0$, and the formula Eq. (5) simplifies to the following [3]:

$$z = H - \frac{x^2 \cdot g}{2v_0^2} \quad (6)$$

In the second approach the shape of the slipway surface was compared to Creager profile (for the 45° and 90° upstream cross-section location). This article analyses both curves (slipways below collectors $\varnothing 1400$ and $\varnothing 600$). The results are presented in Table 3 and Figure 6. These figures show the surface of the ramp (solid line), the line calculated from Eq. (6) (big dashed line), and the surfaces of Creager profiles (dashed and dashed-dotted lines, respectively for the 45° and 90°). The results of calculations showed that the designed curvature of the slipway should ensure adherence of stream of sewage for the part the ramp below outlet of collector $\varnothing 1400$ (even for maximum flow). However, in the case of part of the slipway surface below collector $\varnothing 600$, the condition of stream adhesion is satisfied only in the case

of the first of the adopted methods of verification. But despite this, it was decided to accept the designed shape of the slipway surface.

The calculations have been confirmed by the observation of flow through the chamber after its construction and putting into operation.

Table 3. Results of calculation of sewage surface over the slipways (ramps)

SLIPWAY BELOW COLLECTOR DN1400							SLIPWAY BELOW COLLECTOR DN600						
CHAMBER		FORMULA (6)		CREAGER PROFILE			CHAMBER		FORMULA (6)		CREAGER PROFILE		
x	z	x	z	x	Z(90°)	z(45°)	x	z	x	z	x	Z(90°)	z(45°)
0.000	-0.110	0.000	-0.110	0.000	-0.110	-0.113	0.000	-0.020	0.000	-0.020	0.000	-0.020	-0.024
0.100	-0.110	0.185	-0.150	0.192	-0.148	-0.168	0.761	-0.420	0.220	0.067	0.076	-0.025	-0.037
0.300	-0.210	0.370	-0.268	0.448	-0.274	-0.315	1.347	-0.910	0.440	0.209	0.380	-0.132	-0.164
0.575	-0.510	0.555	-0.466	0.576	-0.362	-0.417	1.818	-1.390	0.660	0.446	0.532	-0.215	-0.264
0.850	-1.000	0.740	-0.743	0.896	-0.669	-0.745	2.227	-1.890	0.880	0.777	0.836	-0.449	-0.525
1.100	-1.480	0.925	-1.099	1.088	-0.912	-0.993	2.563	-2.380	1.100	1.203	1.292	-0.972	-1.069
1.300	-1.980	1.110	-1.534	1.408	-1.364	-1.480	2.850	-2.880	1.320	1.723	1.672	-1.510	-1.646
1.475	-2.470	1.295	-2.048	1.728	-1.915	-2.068	3.100	-3.380	1.540	2.338	2.052	-2.163	-2.346
1.600	-2.970	1.480	-2.642	2.048	-2.555	-2.721	3.274	-3.860	1.760	3.048	2.432	-2.923	-3.121
1.700	-3.470	1.665	-3.314	2.368	-3.265	-3.464	3.425	-4.350	1.980	3.852	2.812	-3.767	-4.002
1.721	-3.950	1.850	-4.066	2.688	-4.091	-4.321	3.535	-4.816	2.200	4.751	3.192	-4.747	-5.021

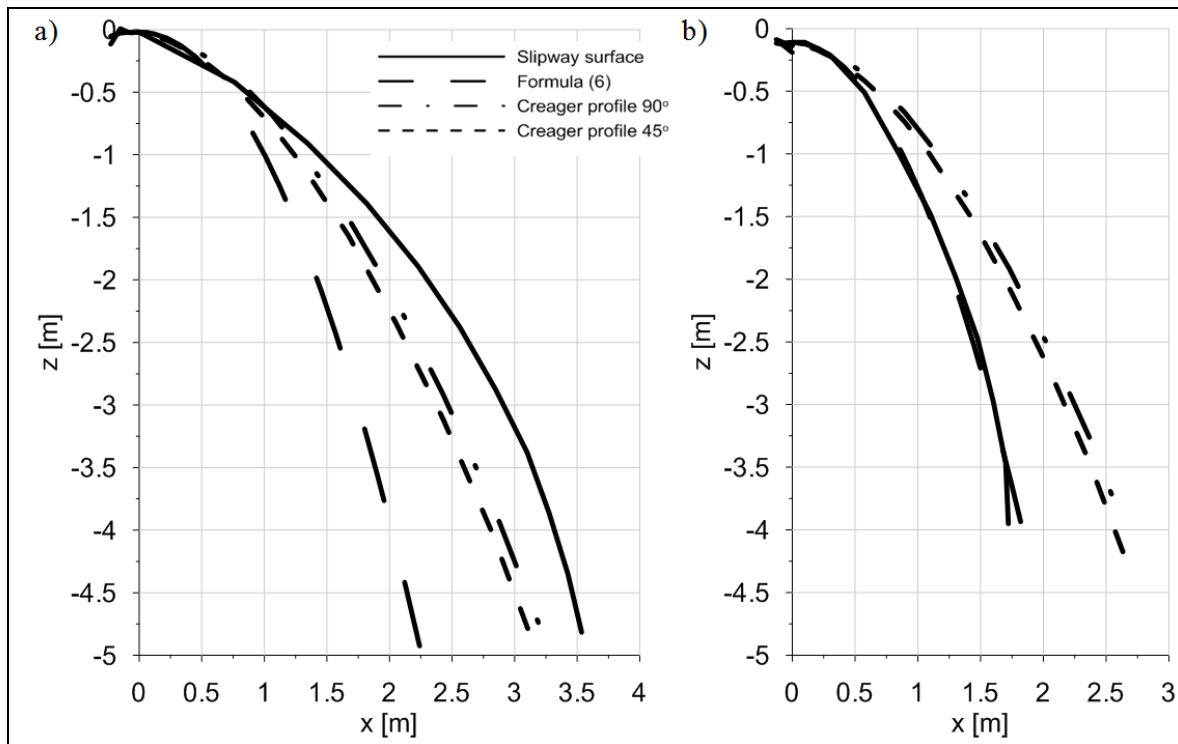


Figure 6. Results of calculation of sewage surface over the slipways (ramps):
 a) below collector \varnothing 1400, b) below collector \varnothing 600

5 Conclusion

Hydraulic calculations have shown that sewage flows down the ramp in the investigated sanitary chamber are in a supercritical regime and achieve a maximum velocity of over 8.5 m/s at its base. Next they fall into the dissipation basin where the energy is dissipated and the flow regime changes from super- to subcritical. It means that the outflow of the wastewater from the chamber to the main collector ($\varnothing 1600$) will be carried out under subcritical conditions without transferring the hydraulic jump beyond the dissipation basin in the chamber. Connection of sewage streams flowing into the chamber by the main collector ($\varnothing 800 \div \varnothing 1600$) with the stream flowing down the ramp takes place at the dissipation basin, without piling up sewage above its invert channel.

Checking the condition of adherence of the wastewater stream to the ramp has shown that in the case of the part of the ramp below collector $\varnothing 1600$ as well as the parts below the collector $\varnothing 600$, the wastewater stream should not be torn off the ramp surface.

High velocity of wastewater on the slipway (from over 2 m/s to over 8.5 m/s) can significantly affect the ramp surface damage caused by increased sand friction and mineral slurry in wastewater. In order to prevent this, the strengthening of the slipway surface should be taken into account in order to increase its abrasion resistance (reinforced concrete should be used).

References:

- [1] HEC-RAS River Analysis System, Hydraulic Reference Manual, US Army Corps of Engineers, Davis, 2010.
- [2] Szymkiewicz, R.: Numerical Modeling in Open Channel Hydraulics, Book Series: Water Science and Technology Library, vol. 83, Springer Dordrecht, Heidelberg, London, New York, 2010.
- [3] Sawicki, J.,M: Mechanics of Flows, Gdansk University of Technology Publisher, Gdańsk, 2009 (in Polish).
- [4] Senturk, F.: Hydraulics of Dams and Reservoirs, Water Resources Publication, 1994.

3. HYDRAULIC STRUCTURES

MORPHODYNAMIC IMPACT OF SCOUR COUNTERMEASURES ON RIVERBED DEVELOPMENT

GORDON GILJA ¹, NEVEN KUSPILIĆ ², DORJA TEČIĆ ³

¹ *University of Zagreb Faculty of Civil Engineering, Croatia, ggilja@grad.hr*

² *University of Zagreb Faculty of Civil Engineering, Croatia, kuspa@grad.hr*

³ *University of Zagreb Faculty of Civil Engineering, Croatia, dtecic@student.grad.hr*

1 Abstract

Local scour at bridges is natural phenomenon that occurs when structure is placed in riverbed in a way that effects flow pattern. Riverbed can be protected from scour by implementation of scour countermeasures on riverbed section that is expected to be eroded. Scour countermeasures most commonly placed in the vicinity of bridge piers or abutments. Placement of scour countermeasures must be evaluated using numerical models in order to investigate their influence on flow pattern. Inadequately placed scour countermeasures can have adverse effect on morphodynamic development of riverbed, initiating scour hole development further away from the bridge, thus causing bank undermining and flow displacement. In cases where riprap is used as scour countermeasure it can be of large proportions and have significant influence on the flow, sediment transport and consequently riverbed erosion. This paper investigates morphological development of Sava River reach at the bridge that has 3 groups of piers located in the riverbed around which riprap scour countermeasures were placed. Flow is accelerated through constricted bridge openings, inducing erosional and depositional patterns that are evident in bridge profile and on downstream reach. In addition to scour countermeasures, weir has been constructed immediately upstream of the bridge profile. Flow overtopping the weir creates hydraulic jump in the bridge profile behind the weir, in which energy is dissipated and riverbed is further deepened. For analysed river reach coupled hydrodynamic/sediment transport model is established in order to describe flow patterns and estimate morphodynamic development of the riverbed. Three different scenarios are evaluated under three characteristic flow events and variables that indicate further riverbed development are compared. It is shown that riverbed hasn't reach equilibrium state at this point and further erosion and riverbed evolution can be expected on this river reach. This insight highlights the need for plan of action on scour-susceptible bridges.

Keywords: Bridge scour, local scour, sediment transport, morphodynamic development, Sava River

2 Introduction

Bridge construction imposes new hydraulic conditions locally on downstream river reach adjacent to the bridge. Elements of bridges placed in main river channel are primarily exposed to hydraulic loads imposed by water flowing around them. In addition to this direct load riverbed in vicinity of their foundations, if susceptible to erosion, can be degraded to that extent where foundations no longer can fulfil their purpose and withstand design load [1]. Among historically recorded bridge collapses and failures, water related hazards partake as most common cause. Several studies have described bridge failures around the world and concluded that primary cause of bridge failure in 50 % or more was hydraulic loading [2-7].

Hydraulic loading is classified under temporary load category for bridge design purposes. For its unsteady nature, both temporally and spatially, it must be considered for some characteristic flow events such as high-recurrence interval floods (*i.e.* 100-year flood). Stability of structures placed in water can be affected by riverbed erosion. During design, hydraulic loading on bridge is considered for flow field in historical conditions and scour countermeasures are designed accordingly. However, during bridge construction and installation of scour countermeasures additional loads can be imposed on riverbed,

under which river morphology changes and in turn alters flow field at bridge approach that induces scour. Next to structures flow is concentrated, resulting in higher velocity, local shear stress and turbulence intensity. These forces combined erode the riverbed in bridge vicinity and alter flow pattern around piers and abutments. If significant changes in the flow pattern occur at bridge location, they can possibly render scour countermeasures ineffective and cause bridge failure. Quantification of these changes is extremely difficult yet crucial because they control long-term morphological development of riverbed and consequently flow pattern around bridge piers. Hydraulic design and realistic representation of bridge hydraulics is crucial when impact on sediment regime needs to be analysed. For this purpose, numerical modelling must be applied on wider river reach to fully describe combined impact of designed bridge elements, scour countermeasures and temporary structures used during construction.

In Croatian practice, numerous bridges on Sava river have been identified as scour susceptible due to anthropogenic influence and flow alterations. Most significant was failure of railway Jakuševac Bridge in 2009 when freight train was passing over it during high flow conditions [8]. This failure is closely related to construction of transversal weir in Sava riverbed immediately upstream [9], as well to river training works conducted throughout history that resulted in longitudinal slope increase and disruption of sediment regime balance [10]. Another example on Sava River is Slavonski Šamac Bridge where weir has been left in riverbed after bridge reconstruction in 2004 [11]. Weir is partially blocking the flow through bridge profile, spanning 2/3 of the river width from the right bank. As a result, flow has been deflected towards the left bank where riverbed is deepened and bank undermined. Beside these two given examples there are several other bridges on Sava River endangered by hydraulic related hazards. In proximity of several bridges transversal weirs have been built, and their influence on morphodynamical changes was never investigated. They pose imminent threat to bridge stability and morphodynamical evolution of riverbed. One of such bridges is motorway bridge Ivanja Reka in Zagreb. Bridge piers are founded on a group of 6 piles 1,2 m in diameter, 14 m long. Concrete pile cap dimensions 5,20 m x 8,80 m, 1,5 m thick, on top of piles provides foundation for bridge piers which are built in pairs on top of a single pile cap. Around the piles is installed riprap scour countermeasure. Top of riprap is levelled with pile cap and extends from all of its edges by incline (1:2 slope) until it reaches riverbed. Extent of such scour countermeasures significantly constrict flow through the bridge profile, causing scour (Figure 1).

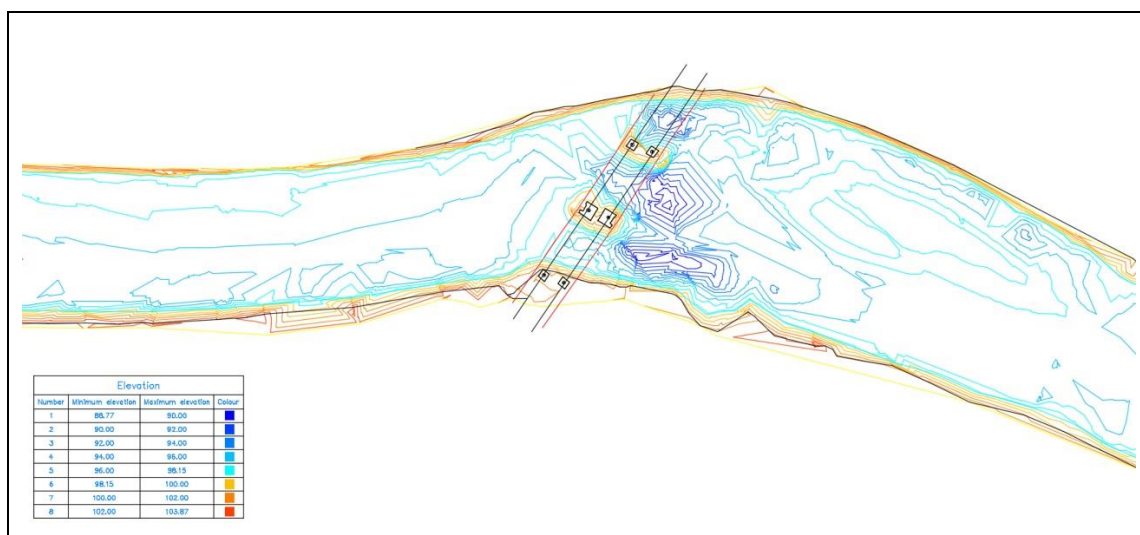


Figure 1. Bathymetry of the Sava riverbed around the bridge

In addition to scour countermeasures, low crest access weir has been constructed from right bank next to the upstream pier faces, towards the pier located furthest away, next to the left bank. Flow over this weir causes hydraulic jump to form downstream of it, increasing scour potential in the bridge profile. Material eroded from the bridge profile is deposited immediately downstream where flow velocity and

turbulence intensity are reduced upon flow expansion. Deposited material has formed a gravel bar which divides flow into two branches around it, causing undermining of the both banks.

In this paper consequences of current scour countermeasures state are estimated, and compared to long-term influence of riverbed restoration. For possible restoration two solutions were considered: 1) simple removal of riprap protection; and 2) armouring of the riverbed with riprap outlining historical bathymetry. Scour potential is evaluated using empirical relations that have been calibrated in previous research on Sava River.

3 Methods

In the initial phase of research, general scour on analysed river reach was estimated in order to define long-term sediment regime trend. This was especially important because analysed river reach is located in transitional area between upper and middle Sava River regime, as well as taking into consideration training works conducted on this reach. General scour was evaluated using Laursen's criteria given in Eq. (1).

$$v_{cr} = K_U \cdot h^{1/6} \cdot d_{50}^{1/3} \quad (1)$$

where: v_{cr} = velocity threshold for sediment incipient motion [m/s], h = mean flow depth [m], d_{50} = diameter of representative grain size [m], $K_U = 6.19$ [1].

In addition to numerical investigation, general scour was evaluated by comparison of geometry of cross-sections upstream and downstream of bridge site where influence of the bridge hydraulics is insignificant. Through analysis of river cross-section change in order to evaluate general scour it can be concluded that general scour is not present in the previous 15 years. Same trend is confirmed when Laursen's criteria is applied to results of numerical model on the analysed reach (shown in the results). Since riverbed is globally stable, scour at the bridge location was investigated using equations for prediction of equilibrium scour developed for clear-water conditions.

Equation used is the one developed by Jain (1982) because it can be applied to complex pier geometry and wide piers due to installation of riprap that acts as a bridge element and pile cap. This particular equation was selected based on its validity proven in previous research [12, 13]. Equilibrium scour depth calculated using Jain's equation is:

$$\frac{h_S}{b} = 1.84 \cdot \left(\frac{h}{b}\right)^{0.3} \cdot Fr_{cr}^{0.25} \quad (2)$$

where: h_S = equilibrium scour depth [m], b = effective column width [m], h = approach flow depth [m], Fr_{cr} = Froude number for beginning of motion [1].

Advantage of this particular equation is that it uses grain size as input parameter through Froude's number for beginning of motion as a reflection of local flow field that is most important force in scour development. Evident impact of bridge piers on the flow pattern and morphological development of the riverbed can be seen from flow field survey given on the following figure (Figure 2):

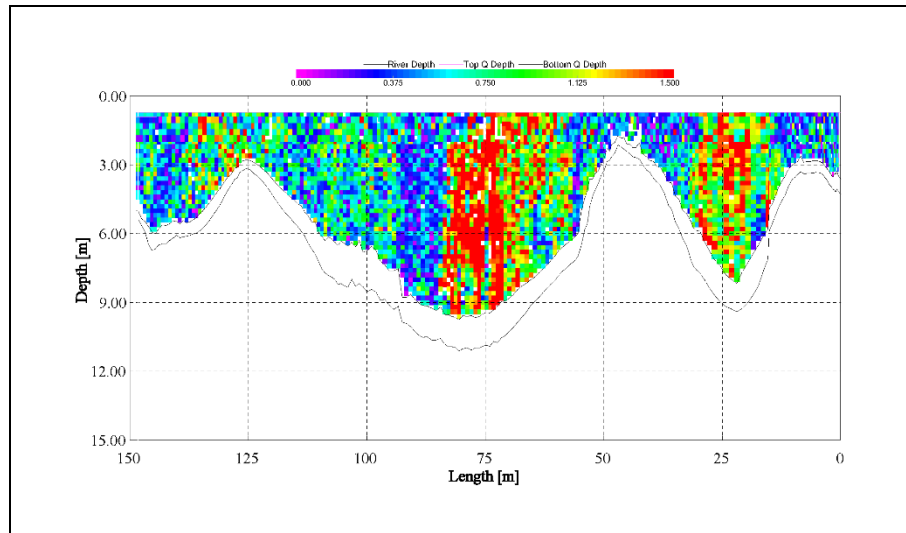


Figure 2. Instantaneous velocity profile in the bridge profile from ADCP survey

Investigation of current state of the flow field used in scour estimation was calculated using 2D numerical model established in the zone of bridge influence. Numerical model is calibrated using flow velocity measurements from field survey and results of 1D model defined for longer reach that covers river reach length between 2 gauging stations. ADCP survey conducted on two field campaigns. Flow field was measured using ADCP RioGrande 1200 kHz on 20 cross-sections, 10 upstream and downstream from the bridge. Flow field was recorded for two discharges: 200 m³/s and 610 m³/s. For each profile flow velocity field was collected as paired ADCP and GPS data which enables geolocation of each recorded ensemble.

Influence of pier removal on flow pattern and equilibrium scour depth is investigated using 2D numerical model and empirical equations. In this conditions riprap surrounding piles is removed, allowing flow to pass through them. Bridge profile geometry is still highly irregular, as well as flow velocity distribution. Equation developed by Jain cannot be applied for design conditions because it cannot account for complex pier geometry when pile cap and piles are exposed to flow. Appropriate local pier scour equation recommended by the Federal Highway Administration [4] for such conditions is HEC-18 pier scour equation that evaluates scour for a complex pier through its components: pier stem, pile cap and pile group. HEC-18 pier scour equation is based on the CSU equation and is suitable for application in clear-water pier scour conditions. Equilibrium scour depth calculated using HEC-18 equation is:

$$\frac{h_S}{h} = 2,0 \cdot K_1 \cdot K_2 \cdot K_3 \cdot K_4 \cdot \left(\frac{b}{h}\right)^{0,65} \cdot Fr^{0,43} \quad (3)$$

where: K_1 = pier shape coefficient [1], K_2 = flow attack angle coefficient [1], K_3 = bedform coefficient [1], K_4 = bed armoring coefficient [1], Fr = Froude number [1].

Scour for complex piers is calculated using modifications of Eq. (3) for each of the elements of complex pier: pier stem, pile cap and pile group. For each element coefficients related to geometry and specific positioning are used to determine attributed scour. For calculation, geometry of each element is replaced by equivalent sized pier and flow conditions are adjusted accordingly. Finally, to calculate overall scour depth all three scour components are added together. Following figure outlines decomposition of complex bridge pier elements and superposition of their respective scour depths (Figure 3).

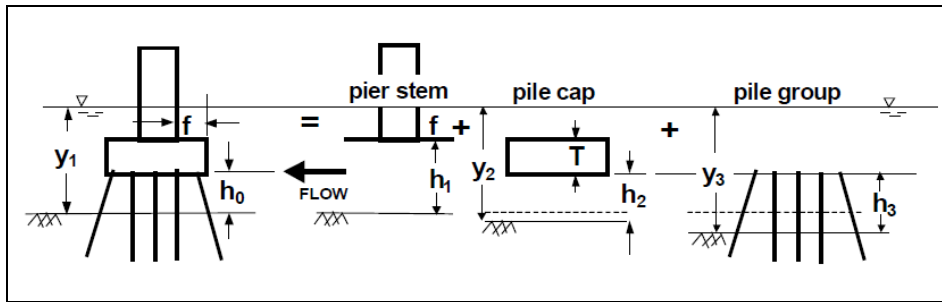


Figure 3. Scour components for a complex pier defined by Jones and Sheppard [4]

After evaluation of local scour, long term sediment regime is evaluated to account for morphological development following restoration works. Long term sediment regime trend is evaluated using results of coupled flow and sediment transport 2D numerical model. Influence of proposed channel alterations is evaluated by investigation of flow velocity change longitudinally along the river reach and locally at bridge piers.

4 Results and discussion

General erosion doesn't occur on the analysed reach for mean flow conditions. Flow velocity is under 1 m/s and doesn't pose a threat to riverbed stability. Results of longitudinal velocity distribution for historical state and two design states for 100-years return period flood are given in the figure below (Figure 4). Because this river reach is characterized with gravel-bed, critical velocity for incipient motion is high (over 2.4 m/s). For 100-year flood highest profile velocities are upstream of the bridge, on the approach section. Despite increase of the velocity compared to mean flow, flow velocity is still lower than incipient motion threshold. Locally, highest velocities are in the bridge profile, next to the riprap installed around bridge piers.

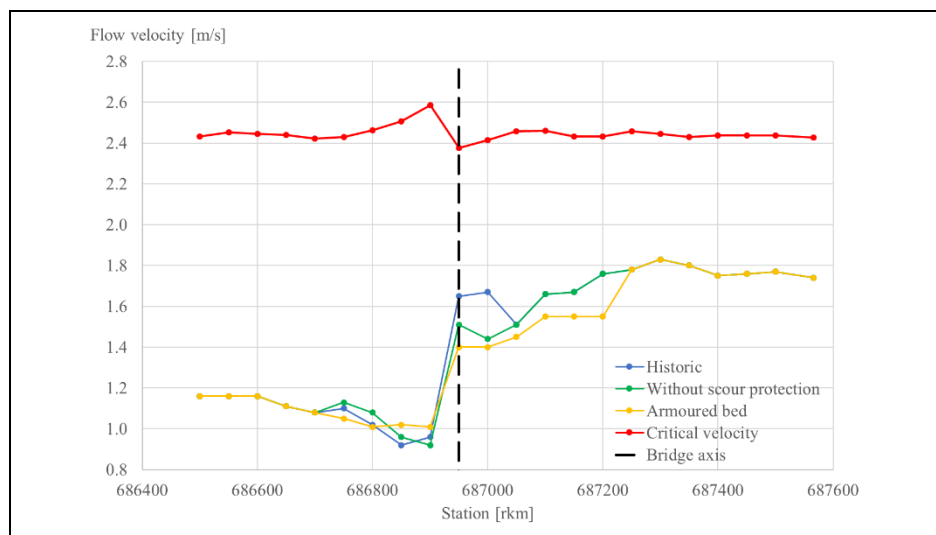


Figure 4. Longitudinal velocity distribution on the analysed reach

Immediately downstream of the bridge profile where riverbed is eroded, flow velocity drops by 50 % on average due to flow expansion and riverbed deepening. Downstream of the scour hole flow is accelerated, but due to riverbed widening velocity is still on average 40 % lower than upstream of the bridge.

Velocity distribution calculated using numerical model confirms initial assumption outlined after conducting field survey campaign that positioning of bridge piers and significant amount of riprap used for riverbed stabilization has consequences on downstream riverbed stability, morphological development and flow pattern. After calculation of detailed flow pattern and evaluation of general

riverbed stability, local scour was investigated. Using Jain's equation for equilibrium scour under clear-water conditions results were compared to measured scour hole depth. It has been shown that Jain's equation can be used to reliably estimate scour depth around piers with installed riprap protection. Following figure (Figure 4) shows calculated scour depth as a function of flow depth at bridge approach section. Scour depth is given separately for each pier, as flow characteristics are applied individually for piers from numerical model results. According to Jain's equation, scour around bridge piers has reached equilibrium conditions and further deepening of scour holes is not anticipated for current flow regime.

In order to evaluate possible river restoration on this location, scour depth is calculated for flow conditions resulting from riprap removal. Hypotheses is that in that case, since scour has reached its equilibrium depth, morphological development of the riverbed wouldn't continue. According to bridge design, piles are 18 m deep and can withstand flow forces acting on them upon riprap removal. Equilibrium scour depth calculated with Jain's equation correlates well with field measurements for both piers (Figure 4). Scour hole next to the left pier is smaller than the other two (8 m compared to 10 m, Figure 1). This is consequence of positioning of left pier next to the bank, where bank protection is falling in the scour hole and armouring its bottom. Also, according to the numerical model results, majority of the flow is flowing next to the right bank during high flow conditions. This flow pattern explains why simple empirical equation is overestimating equilibrium scour depth at this pier.

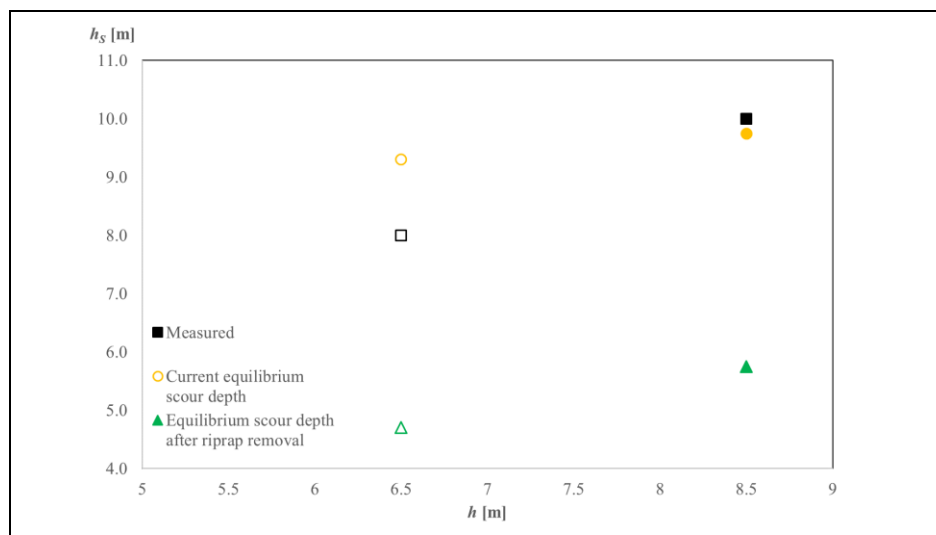


Figure 4. Equilibrium scour depth as a function of flow depth for 100-year flood

Results of equilibrium scour for 100-year flood show that removal of the riprap protection would significantly decrease scour potential at the bridge piers. With removal of riprap there is no more flow profile contraction at the bridge location because foundation piles are relatively narrow, with pile cap positioned high above the riverbed and therefore has low impact on scour depth. Following figure (Figure 5) shows comparison of flow field at current state and design state with removed riprap protection. Removal of riprap results in more evenly distributed flow velocity across river width, both upstream and downstream of bridge profile. For mean flow conditions flow is no longer deflected towards the left bank, although highest flow velocities are still occurring next to the left bank because of natural river morphology. Overall, flow velocity is reduced, and therefore lower potential for scour development is achieved. Existing scour holes are left present in the riverbed, and they act as stilling basin for flow accelerated through bridge profile. Their presence constrains effect of riprap removal to bridge profile, while flow pattern remains unaffected 150 m downstream of the bridge. Riprap removal has no influence of scour potential distribution, i.e. right pier is more exposed to flow as in the current flow conditions.

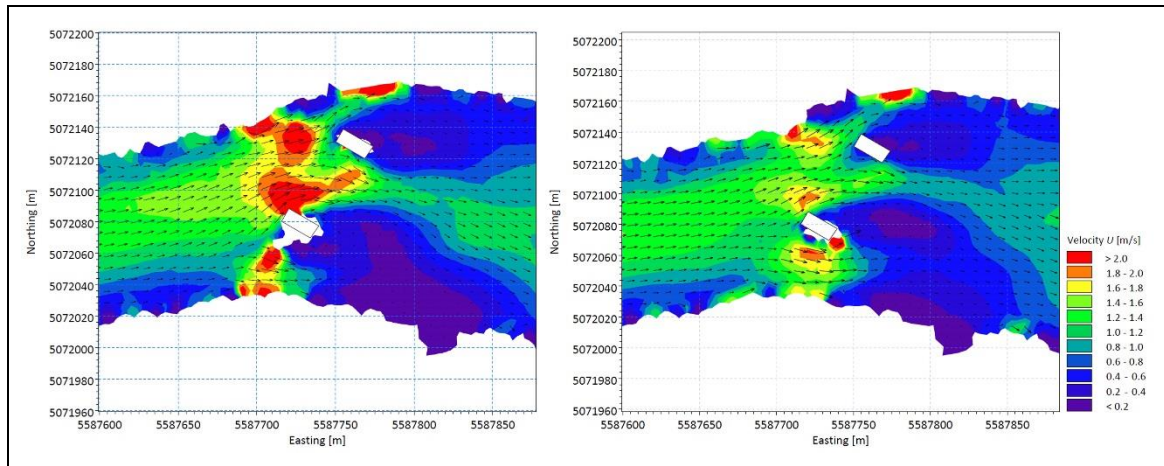


Figure 5. Flow field for: a) current state; b) state after riprap removal

It has been showed previously that general scour is not present on this reach and that riverbed is stable in long-term sediment regime conditions. Gravel bar formed downstream of the bridge from scoured material has significant influence on flow pattern. Its existence divides the flow into two branches, further annulling any flow pattern change induced in the bridge profile. After flow pattern change has been investigated under proposed restoration works, it was necessary to investigate how will it affect gravel bar existence. Morphological development of riverbed investigated with coupled flow / sediment transport model showed no significant change in river bathymetry for current state and riprap removal. Flow around gravel bar for 100-year flood conditions is too low to initiate gravel motion.

Riverbed restoration, including filling of scour holes and armouring riverbed on its historical elevation, initiates morphological development of unprotected riverbed (Figure 6). Flow accelerated on reconstructed reach initiated sediment movement which is deposited immediately on armoured bed where velocity decreases. Downstream of armoured reach accelerated flow undermines gravel bar, initiating morphological changes primarily in flow bifurcation around it. Accelerated flow shows potential for sediment movement further downstream of the gravel bar.

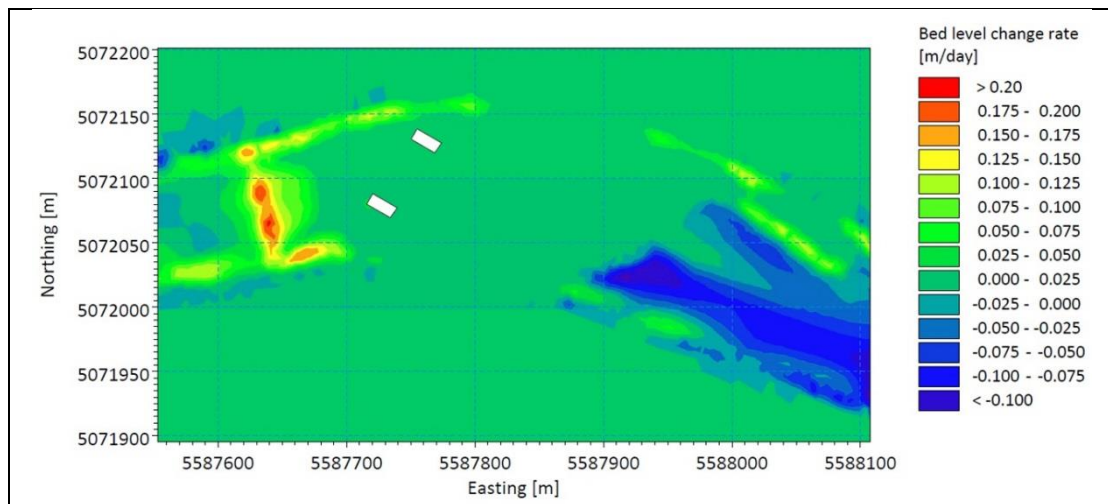


Figure 6. Morphological development for armoured bed

5 Conclusion

In this paper local scour around complex bridge piers with installed riprap scour protection was evaluated. Investigation of long-term sediment regime showed that otherwise stable riverbed is extensively eroded at the bridge location because of installed scour countermeasures. It has been

confirmed that Jain's equation can be applied for equilibrium scour depth estimation for piers protected with riprap. Proposed riverbed restoration technique that includes complete removal of riprap showed significant decrease in local scour potential compared to current state. This investigation revealed undesired effect of installed riprap protection that resulted in effect opposite to its purpose, i.e. riprap induced more scour than it would be present without it. Gravel bar formed from material eroded from scour holes governs flow pattern downstream, and only extensive bed armouring would affect its morphological development. Insights gained from this investigation can be used for plan of action on other bridges on Sava River that are scour-susceptible because scour protection installed around them are not designed in accordance to flow pattern.

References:

- [1] Kuspilić N., Gilja G., Bekić D., Zubčić K.: Podvodni pregled stupova mostova i korita vodotoka, Mjerenja, ispitivanja i monitoring na prometnicama, eds. S. Lakušić, Građevinski fakultet Sveučilišta u Zagrebu, Zagreb, pp. 262-286, 2013.
- [2] Wardhana K., Hadipriono F.: Analysis of Recent Bridge Failures in the United States, *Journal of Performance of Constructed Facilities*, 17(3), pp. 144-150, 2003.
- [3] Smith D. W.: Bridge failures, *Proceedings of the Institution of Civil Engineers*, 60(3), pp. 367-382, 1976.
- [4] Arneson L. A., Zevenbergen L. W., Lagasse P. F., Clopper P. E. Evaluating Scour at Bridges, *Hydraulic Engineering Circular No. 18*. U.S. Department of Transportation, Federal Highway Administration; 2012.
- [5] Maddison B.: Scour failure of bridges, *Proceedings of the Institution Civil Engineers - Forensic Engineering*, 165(FE1), pp. 39-52, 2012.
- [6] Yao C., Briaud J.-L., Gardoni P.: Risk Analysis on Bridge Scour Failure, *International Foundations Congress and Equipment Expo*, San Antonio, Texas March 17-21, pp. 1936-1945, 2015.
- [7] Briaud J.-L., Gardoni P., Yao C.: Bridge Scour Risk 6th International Conference on Scour and Erosion, Paris, France August 27-31, pp. 1193-1210, 2012.
- [8] Kuspilić N., Bekić D., McKeogh E., Gilja G.: Monitoring of river channel morphodynamical changes in the zone of bridge piers, *Proceedings of the First International Conference on Road and Rail Infrastructure (CETRA 2010)*, Opatija, Croatia May 17-18, 2010., 2010.
- [9] Gilja G., Oskoruš D., Kuspilić N.: Erosion of the Sava riverbed in Croatia and its foreseeable consequences, *BALWOIS Conference on Water Observation and Information System for Decision Support*, Ohrid, Republic of Macedonia May 25-29, 2010, pp. 123-124, 2010.
- [10] Gilja G., Kuspilić N., Bekić D.: Impact of morphodynamical changes on the bridge stability: Case study of Jakuševac bridge in Zagreb, *Current events in hydraulic engineering*, eds. J. M. Sawicki & P. Zima, Gdansk University of Technology, Gdansk, pp. 112-122, 2011.
- [11] Gilja G., Kuspilić N., Bekić D.: Influence of riverbed degradation on bridge safety, *CONGRESS OF CROATIAN BUILDERS 2012*, Cavtat, Croatia, Croatian Society of Civil Engineers, 15. - 17. 11. 2012., pp. 795-806 2012.
- [12] Kuspilić N., Bekić D., Gilja G.: Praćenje morfodinamičkih promjena korita vodotoka u zoni stupova mostova, *Prometnice - nove tehnologije i materijali*, eds. S. Lakušić, Građevinski fakultet Sveučilišta u Zagrebu, Zavod za prometnice, Zagreb, pp. 69-112, 2010.
- [13] Sheppard D. M., Demir H., Melville B. W.: Scour at Wide Piers and Long Skewed Piers, *Transportation Research Board*, Washington, DC, 2011.

POOL FISHWAY HYDRAULIC ANALYSIS

EVA OCVIRK ¹, GORDON GILJA ², DAMJAN BUJAK ³

¹ Faculty of Civil Engineering, University of Zagreb, Croatia, ocvirk@grad.hr

² Faculty of Civil Engineering, University of Zagreb, Croatia, ggilja@grad.hr

³ Faculty of Civil Engineering, University of Zagreb, Croatia, dbujak@grad.hr

1 Abstract

Artificial barriers such as dams, weirs, drops, gates, etc. interrupt fish migration on natural watercourses. Pool fishways are one of the most commonly used structures for enabling fish to pass an obstacle. The main principle of pool fishway consists in dividing up a channel from the headwater to the tailwater by building cross-walls to form a succession of stepped pools and riffles. The flow passes through small openings in the cross-walls. The desired geometry of the pools was evaluated using an 3D numerical model and the numerical model was verified using field conditions as a physical model in scale 1:1 at SHPP Ilovac on Kupa River.

Keywords: pool fishway, numerical model, physical model

2 Introduction

In the contemporary approach to river regulation, it is thought that the river is a line ecosystem in which the principle of river continuum applies. The concept of river continuum tries to explain long-term changes and the development of biological communities in watercourses ecosystems, in order to preserve biodiversity across the watercourse [1, 2]. Over the past few years, the public awareness of the importance of environmental conservation and the need to use renewable energy sources has been growing. One of the renewable energy sources is water power, therefore the construction of small hydropower plants has increased in popularity. Small hydropower plants do not change significantly the flow regime and obstacles do not cause significant backwater impact. Furthermore, they do not have a significant impact on nature, except that by interrupting continuity, they influence the migration of organisms into the watercourse.

In order to address the problem of migration of fish species, fishways are being built [3]. The fishway is usually a canal equipped with elements that enable the desired hydraulic characteristics required to allow the fish to swim in the fishway. Technical fishways are pool fishways (cross-walls with opening, cross-walls with weirs, cross-walls with weirs and openings), vertical slot fishways, Denil fishways, canal with increased roughness, weir and culvert fishways, and special types – fish lifts, fish locks, screw jack fishways, eel ramps, Natural types of fishways try to imitate a natural riverbed, the most common types are rock ramp fishways and bypass fishways. The uniqueness of this type is the presence of a rocky substrate at the bottom which increases the roughness of the riverbed. Since the stone substrate is usually not sufficient to allow favourable hydraulic conditions on shorter sections, further damping of the natural course can be accomplished by placing larger stone blocks. This also creates places suitable for fish to rest. Each of these paths has a domain within which it is suitable for use. Special types are either intended for certain types of fish or are applied in conditions where there is no choice of a simpler solution. Different problems arise in the upstream and downstream transition and in this paper the emphasis is on upstream migration. It is important for the fish to pass through the fishway with as little energy and as little effort as possible, without injury and predator activity [4].

3 Flow characteristics in fishways

Passing through a fishway in the upstream direction is not always an easy task for fish. Flow velocity, water depth, turbulence characteristics and flow rate must correspond to the physical capabilities of fish. Fish swim at three different speeds:

- 1) burst speed – maximum speed, it lasts for only a few seconds and demands a long time of recovery.
- 2) prolonged speed – about 5 body lengths per second and fish can use it up to 200 minutes.
- 3) sustained speed – about 2 body lengths per second, sustainable for more than 200 minutes.

When designing fishways the goal is to determine the flow rate, water level, a certain canal width and flow velocity in the canal, depending on the needs of fish species to determine the required number of pools, their length and the total length of fish pass. Fishways shouldn't be designed to require the usage of bursting speed (except in the flow contraction areas), but rather to require the prolonged speed which fish can use long enough to pass through the fishway. There is no need for fishways to require the usage of cruising speed as it is desirable that longer fishways have places for fish to rest [5]. In sections with barriers permitted flow velocity is achieved, while in the pools calmer zone is created, which enables fish to rest if needed [2]. In this paper, pool fishways – cross-walls with opening are analysed using a 3D numerical model calibrated on field survey at pool fishway of SHPP Ilovac (Figure 1 and Figure 2).

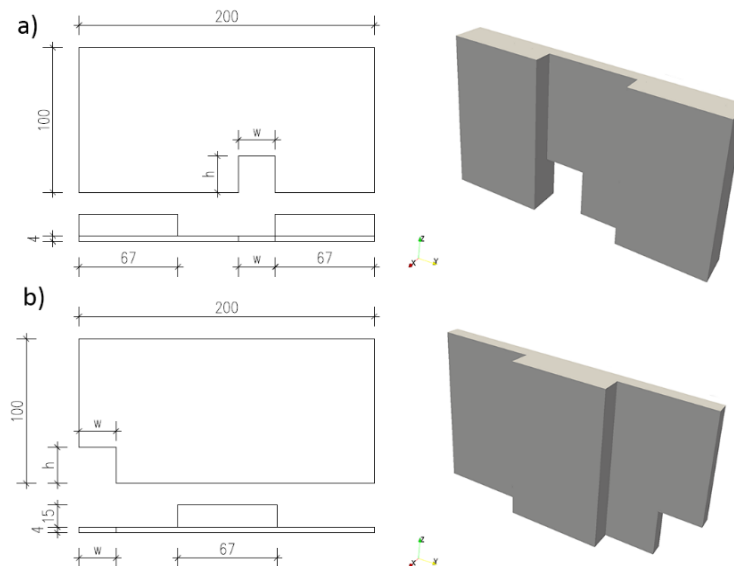


Figure 1 Cross-walls with openings dimensions inside pool fishways; a) plan, top and isometric view of the cross-wall that has the opening roughly in the middle b) plan, top and isometric view of the cross-wall that has the opening on the left side, next to the wall of the fishway



Figure 2 Pool fishway at SHPP Ilovac under construction

Turbulence and vortices are unavoidable in natural flows, and their impact on fish swimming is not entirely explained. Due to the possibility that small fish are caught and confused by vortices and turbulence, it is assumed that the impact is negative. Some studies suggest that fish know how to use the turbulence, propulsion caused by swimming fish and other vortices, in order to swim successfully. It is suspected that the size of the vortex influences the behaviour of fish in swimming the most [6, 7]. Because of other aquatic organisms (weaker swimmers), turbulence should be as small as possible. At pool fishways, the maximum volumetric dissipation power is a general indicator of the agitation level (i.e. rough turbulence intensity indicator) and it is recommended that it should be about $150\text{-}200\text{ W/m}^3$ depending on the type of fish. It is defined as the function of water density, water flow, water level difference in front and behind the pool opening, light length and pool width and average water depth measured in the centre of the pool.

Furthermore, the relevant local indicators are the velocities at a point whose maximum value must not exceed 2 m/s (at the points of flow contraction), and a depth not less than 0.2 m [2, 8]. Fish prefer when they know the "flow pattern", so it is desirable to repeat the geometrical pattern, which is usually present in most fishways. At pool fishways recirculation zones are created - areas bordered by vortices. Because of the weaker vertical component, they can be treated as two-dimensional. There is a close link between this indicator and volumetric dissipation power [9]. Vortices can catch smaller fish so crossing the fishway becomes questionable. The situation when the vortex is smaller than the fish is not problematic, but if it is bigger, the fish move chaotically [8].

For the past 15 years, more and more energy is invested in a detailed study of the flow structure in the fishways [8, 9, 10, 11]. Aim of this paper was to determine how geometry of openings and their consecutive layout impacts flow characteristics in the fishway basins.

4 Methods

Research has been conducted using 2D and 3D models to gain insight in the flow fields of variety of fishway types. Though 3D models take considerably more time to compute than 2D, flow field inside fishways is frequently highly three dimensional in character and thus 3D models are often a requirement. Cross-walls with openings at the bottom of the wall produce a fast jet of water entering the downstream pool and creating a 3D flow pattern in the pool that depends on the geometrical design of the downstream cross-wall. Jet velocity through the cross-wall opening is critical for fish migration. Fully 3D models can adequately resolve flows with a considerable vertical flow component.

A 3D numerical model *interFoam* that is a part of the open source *OpenFOAM* [12] package has already been used in various free surface two-phase flow cases such as wave impacts on breakwaters and dam breaks [13, 14]. Multiphase VOF (volume of fluid) solver *interFoam* relies on the definition of an indicator function. Its application is based on a Eulerian description of each fluid on an immovable mesh and the description of the interface between the two fluids by means of a transport equation for the indicator function. This function indicates the fraction of the cell volume being occupied by one phase (denoted by α). The advection equation for the volume fraction are solved using the multidimensional universal limiter (MULES). The solver *interFoam* resolves the continuity equation Eq (1) and the unsteady Reynolds-averaged Navier-Stokes equation that governs the flow Eq(2).

$$\nabla \cdot \vec{v} = 0, \quad (1)$$

$$\frac{\partial \rho \vec{v}}{\partial t} + \nabla \cdot (\rho \vec{v} \vec{v}) = -\nabla p + \nabla \cdot (\bar{\tau} - \rho v' v') + \sigma k \nabla \alpha + \rho \vec{g} \quad (2)$$

$$\frac{\partial \alpha}{\partial t} + \nabla \cdot (\alpha \vec{v}) = 0 \quad (3)$$

In the Navier-Stokes equation ρ denotes the fluid density, \mathbf{v} indicates the velocity field, t specifies time, p indicates pressure, σ denotes surface tension and mean local curvature is specified by k . Cells fully occupied by water have a value of 1 ($\alpha = 1$), whereas cells fully occupied by air assigned a value of 0 ($\alpha = 0$). Cells at the interface between two phases have a value of α between 0 and 1, depending on the presence of each phase inside the mesh cell. The volume fraction in each cell is calculated using a volume fraction transport equation Eq(3). With this description of the governing equation, each cell of the mesh is defined by a velocity vector, pressure, and volume fraction. At the interface density Eq(4) and viscosity Eq(5) are being linearly interpolated between the two phases in accordance with the α fraction assigned to each cell. Thus, using the VOF method, the whole domain can be described using a single momentum conservation equation.

$$\rho = \rho_1 \alpha + \rho_2 (1 - \alpha) \quad (4)$$

$$\mu = \mu_1 \alpha + \mu_2 (1 - \alpha) \quad (5)$$

However, in the VOF approach the end position of the interface is not known and it is described by a number of cells with finite volume. Thus, the surface tension effect (that is surface in nature) needs to be converted into a volume effect (3D) that can be incorporated into the main momentum equation valid for the entire domain.

Numerical models have been made for SHPP Ilovac on Kupa river. A pool fishway built on the SHPP Ilovac is a concrete channel with constant slope from headwater to tailwater, divided in 14 pools. Each pool 2 m width and 2.5 m length. The goal of the analysis is to show the dependence of required water depth and cross-wall opening velocities on cross-wall opening size. Analysis of fishways was conducted for various geometries of openings in cross-walls (25x25 cm, 30x30 cm and 40x40 cm) and various flows (75 l/s to 175 l/s with a step of 25 l/s).

Conditions in the fishway have been determined by field measurements using ADV instrument to measure flow velocities. Furthermore, in order to establish a tool that enables accurate determination of the hydraulic characteristics of the flow in pool fishways, a 3D numerical model has been established and calibrated using field data.

The mesh was created using open source tools blockMesh (creates a coarse base mesh across the domain) and snappyHexMesh (iteratively refines and conforms the mesh to the provided surface). The various cross-walls were previously created in Blender as surface .stl files and imported into the mesh process through snappyHexMesh. Hexagons were used to mesh the domain and low non-orthogonality (maximum non-orthogonality in the mesh was below 8°) and skewness (maximum skewness was below 0.5) were achieved.

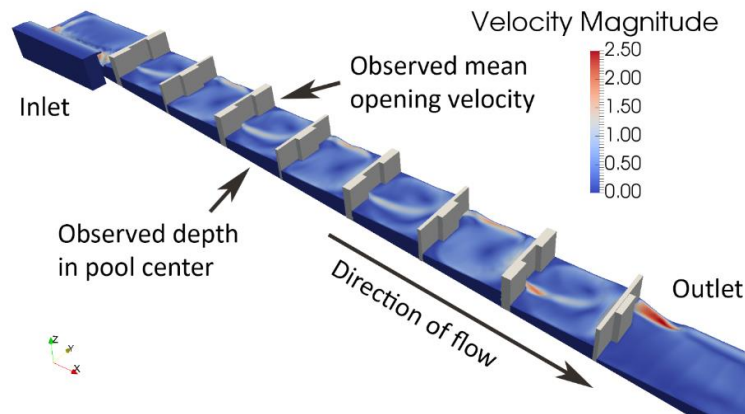


Figure 3 Isometric view of the fishway with specified locations of the observed opening for mean velocities and pool for depths (case with 30x30 cm openings and 125 l/s flow rate)

Steady state convergence of the flow was ensured by continuously monitoring the water depth in the fishway pools, the velocity field and total volume of water inside the domain. Most models took 400 s to reach steady state. Courant number was maintained below 1 across all the cells of the grid to assure temporal stability of the numerical model. The turbulence model that was evaluated to best describe the flow field was the two-equation k - ω SST model. The SST formulation combines the k - ω formulation in the boundary layer, that makes the model useable all the way to the wall, with the k - ϵ formulation in the free stream and thereby avoids the common k - ω problem that the model is too sensitive to the inlet free stream turbulence conditions.

At the inlet, a fixed velocity and α ($\alpha = 1$) value were assigned to provide a constant desired flow rate that enters into the domain. To account for the downstream water level a Dirichlet uniform velocity boundary condition was also assigned that results in the wanted water level at the outlet. The outlet velocity vector was calculated using the provided flow rate at the inlet divided by the desired area of the submerged cross section at the outlet. The outlet water level was set to 0.5 m for all cases.

After the water enters the domain, it overflows over a weir at the right side of the fishway the same as it was constructed at SHPP Ilovac (Figure 2). The cross-wall in the middle of the model that seemed to be the least influenced by the boundary conditions was chosen as the relevant locations for observing mean velocity and depth (Figure 3). The fishway has a constant slope of 6° .

5 Results and discussion

There are two types of cross-walls used in SHPP Ilovac and consequently are implemented in the mesh (Figure 1). They are alternately constructed, starting with the cross-wall with the opening roughly in the middle right after the weir where water enters the domain. As the cross-walls alternate there are two distinct flow patterns that can occur in the fishway pools, depending which cross-wall is upstream and which downstream.

In the case when the upstream opening is in the middle of the cross-wall, there is a strong jet of water entering the pool due to water level difference between the observed pool and the upstream pool (Figure 4). In the centre of the jet, velocities can go as high as 2.5 m/s depending upon the flow rate and the opening dimensions (other factors also influence the velocities in the jet like the fishway slope, but these were constant throughout all the cases) (Figure 4– a)). This strong jet hits the downstream cross-wall and which develops small vertical vortices in front of the wall which give the flow a distinct three-dimensional character (Figure 4– c)). When viewing the flow pattern from the top (Figure 8– b)), the jet itself splits the flow pattern into two large vortices, with the end of the jet gravitating towards the downstream opening.

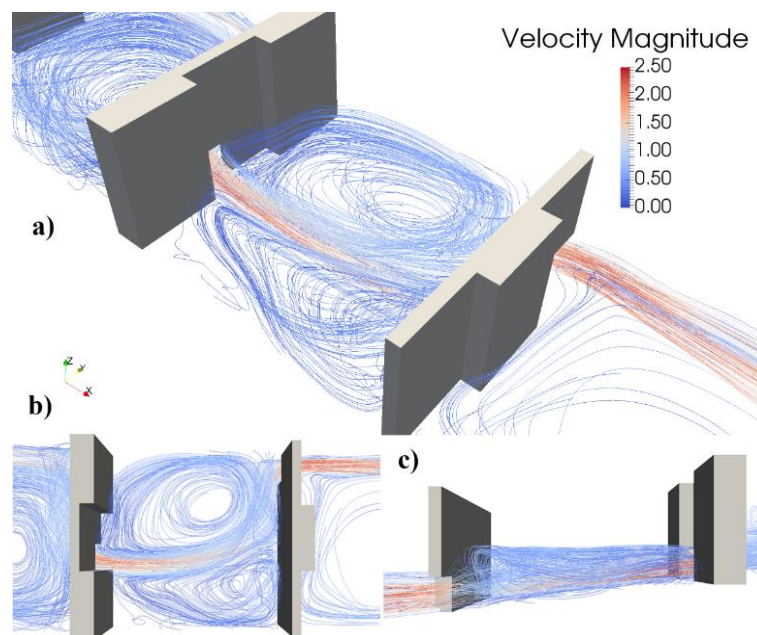


Figure 4 Streamlines depicting the velocity field at steady state in the pool downstream of the observed cross-wall opening (Figure 3); a) isometric view of flow field b) top view c) profile view (case with 30x30 cm openings and 125 l/s flow rate)

It was discussed in previous research that vortices that are larger than fish can get confused during their passage through the fishway, but there were no specific constraints regarding the velocities that can occur in these vortices [6, 7]. As the velocities in the observed vortices are rather low (below 0.5 m/s), it is the authors hypothesis that the vortices will not confuse the fish but rather provide places where the fish can rest between the challenging jets inside openings which they need to pass through.

If the upstream opening is on the left side of the cross-wall, differences in the flow pattern can be observed (Figure 5). The velocities in the centre of the jet are about the same (up to 2.5 m/s) as the water level difference between the upstream and observed pool is the same (Figure 5– a)). As the jet passes next to the left wall of the fishway it hits the downstream cross-wall and then flows parallel to the cross-wall to the downstream opening. In the rest of the pool a circular motion occurs which can be easily observed in the plan view (Figure 5– b)). The formed vortex is bigger than the two separate vortices in the previous case (Figure 4), but the velocities inside the vortex are roughly the same (below 0.5 m/s) which, as previously said, is hypothesised not to confuse fish. In conclusion, the flow pattern repeats between the two mentioned which is preferable for fish to be familiar with the pattern in order to pass through the fishway [9, 11]

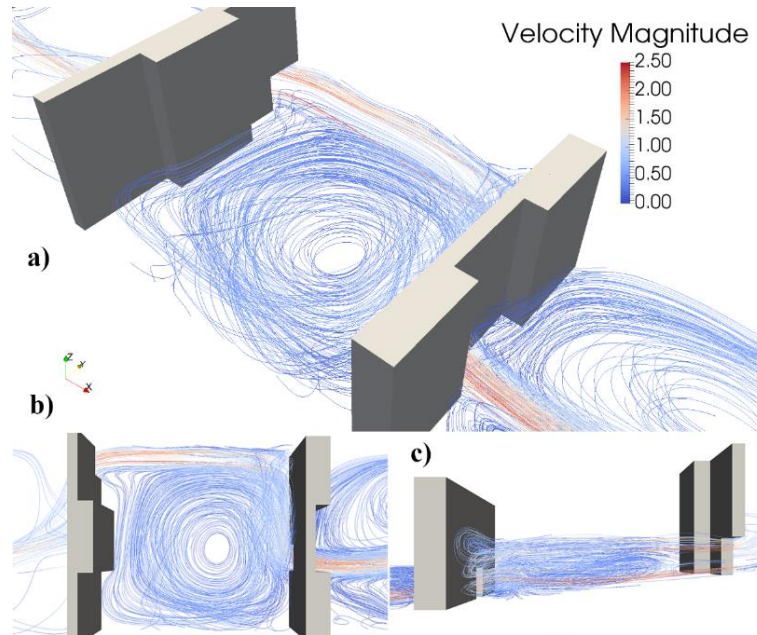


Figure 5 Streamlines depicting the velocity field at steady state in the pool upstream of the observed cross-wall opening (Pogreška! Izvor reference nije pronađen.); a) isometric view of flow field b) top view c) profile view (case with 30x30 cm openings and 125 l/s flow rate)

Analysing water depth data observed at the specified pool in the middle of the fishway (Figure 3), a contour plot was constructed (Figure 6). Depth in the centre of the pool was chosen because it represents the average depth in the pool. It comes as no surprise that higher flow rate and smaller openings result in a higher water depth in the pool. Water depth below 0.2 m does not satisfy the constraint put forward by previous research about the minimum water depth in pools to fulfil the needs of the fish passing through [2, 8]. If the openings should be bigger due to fish size, higher flow rate in the fishway is needed to provide the minimum water depth which is expected. It should be noted that in some cases the openings were not fully submerged when observing the upstream side of the cross-wall due to low flow rate, big area of the opening or both (these cases are marked by a red box around the dot). The water depth can be approximated with a plane that depends on opening dimensions and flow rate with satisfying goodness of fit ($R^2 = 0.93$).

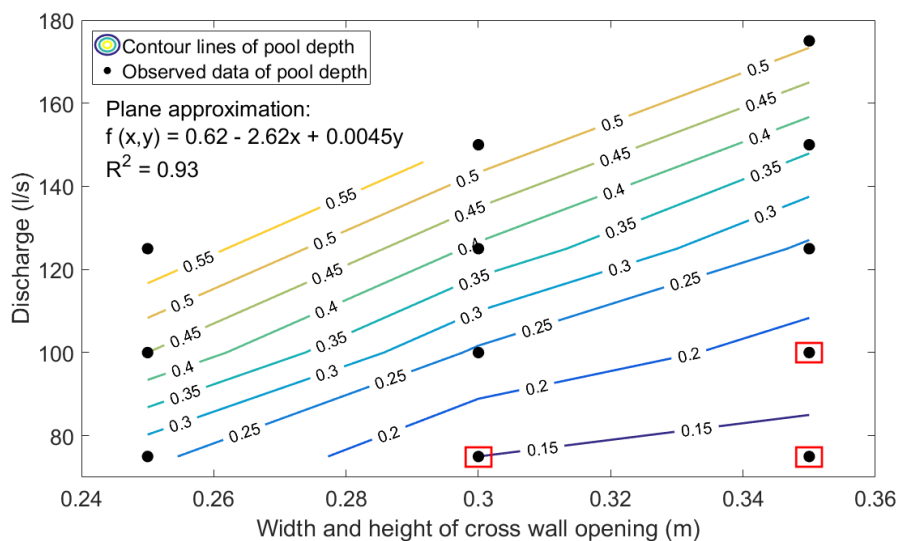


Figure 6 Contour lines that interpolate water depth data inside the pool observed on the numerical models, that depend on the cross-wall opening width and height (width and height were always the same) and flow rate specified at the inlet; red boxed indicate cases when the opening was not fully submerged

Mean water velocities are also represented as a function of opening dimensions and water flow rate (Figure 7). Most of the observations point to an expected increase in mean water velocities in openings with increasing flow rate, but then again there are exceptions. If the opening is not fully submerged, due to smaller water depths at the opening, the velocity needs to increase to maintain the same flow rate. All observed mean velocities are below the maximum permitted velocity threshold of 2 m/s, defined by previous research [2]. The mean velocities can also be approximated with a plane that depends on opening dimensions and flow rate with sufficient goodness of fit ($R^2 = 0.77$) with the least accurate approximation begin for the partly submerged openings.

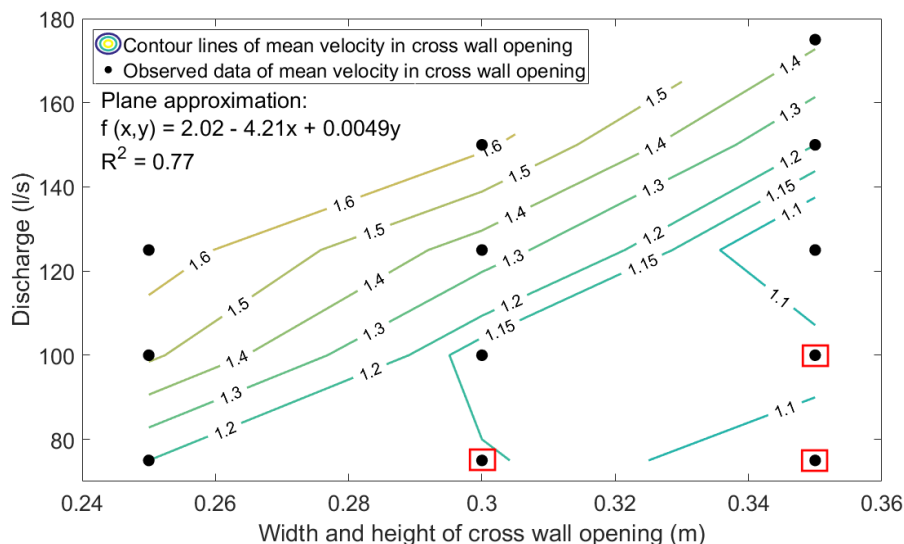


Figure 7 Contour lines that interpolate water depth data inside the pool observed on the numerical models, that depend on the cross-wall opening width and height (width and height were always the same) and flow rate specified at the inlet; red boxed indicate cases when the opening was not fully submerged

6 Conclusion

This paper showed that numerical models can simulate flow conditions on pool type fishways that correspond those in the nature. Analysis of results in the paper show that the cross-wall opening size and discharge entering the fishway determine the pool water level and flow velocities in cross-wall openings. Adequate pool water levels and velocities are necessary for the assurance of fish migration through the fishway. The spatial distribution of the velocity field inside the pools can only be influenced by the spatial arrangement of consecutive pool openings. Hence, it is always important to carefully arrange the upstream entrance/exit from the fishway as an initial generator of flow in pools.

References:

- [1] Jovanović, M.: Riblje staze u skolpu 'naturalnog' uređenja malih vodotoka, *Vodoprivreda*, vol. 43, pp. 217-226, 2011.
- [2] FAO (Food and Agriculture Organization of the US), DVWK (German Association for Water Resources and Land Improvement): *Fish passes – Design, dimensions and monitoring*, FAO, DVWK, Rome, Italy, 2002.
- [3] Prša, M., Rebrina, M., Srednoselec, I.: *Analiza geometrijskih karakteristika ribljih staza u ovisnosti o hidrauličkim uvjetima tečenja*, University of Zagreb, Zagreb, 2013.
- [4] PIANC, The World Association for Waterborne Transport Infrastructure: *Fish passage, report n° 127*, Bruxelles, Belgium, 2013.
- [5] Dumont, U.: *The New DWA Design Manual on Fish Passes (ID 16454)*, 9. International conference on hydraulics, Vienna, Austria, 2012.
- [6] Liao, J.C.: *The review of fish swimming mechanics and behaviour in altered flows*, *Philosophical Transactions of The Royal Society B: Biological Sciences*, vol. 362 (1487), pp.1973-1993, 2007.

- <http://www.ncbi.nlm.nih.gov/pmc/articles/PMC2442850/> (10.02.2015.)
- [7] Sokoray-Varga, B., Weichert, R., Lehmann, B., Nestmann, F., (): *Time-Resolved PIV Measurements to Investigate the Characteristics of the Turbulent Structures in a Vertical-Slot Fish Pass* (ID 16332), 9. International conference on hydraulics, Vienna, Austria, 2012.
- [8] Calluau, D., Pineau, G., Texier, A., David, L.: *Modification of vertical slot fishway flow with a supplementary cylinder*, Journal of Hydraulic Research, vol. 52, No. 5, pp. 614-629, 2014.
- [9] Tarrade, L., Texier, A., David, L., Larinier, M.: *Topologies and measurements of turbulent flow in vertical slot fishways*, Hydrobiologia, vol. 609, pp. 177-188, 2008.
- [10] Calluau, D., Cornu, V., Bourtal, B., Dupuis, L., Refin, C., Courret, D., David, L.: *Scale Effects of Turbulence Flows in Vertical Slot fishways: Field and Laboratory Measurement Investigation* (ID 16332), 9. International conference on hydraulics, Vienna, Austria, 2012.
- [11] Wu, S., Rajaratnam, N., Katopodis, C.: *Structure of Flow in Vertical Slot Fishway*, Journal of Hydraulic Engineering, vol. 125, no. 4, pp. 351-360, 1999.
- [12] Weller, H. G., Tabor, G., Jasak, H., Fureby, C.: A tensorial approach to computational continuum mechanics using object-oriented techniques, Computers in physics, vol. 12, no. 6, Nov/Dec 1998.
- [13] Jacobsen, N. G., Fuhrman, D. R. and Fredsoe, J.: A Wave Generation Toolbox for the Open-Source CFD Library: OpenFoam®, Int. J. of Numerl. Meth. Fluids., pp. 1073-1088, 2012., DOI: 10.1002/flid.2726
- [14] Zhainakov, A. Z. and Kurbanaliev, A. Y.: Verification of the open package OpenFOAM on dam break problems, Thermophysics and Aeromechanics, 20(4)., 2013., doi: 10.1134/S0869864313040082.

HYBRID MODELLING OF OVERFLOWING BROAD-CRESTED WEIR-PHYSICAL AND NUMERICAL COMPARISON

MARTIN ORFÁNUS¹, JÁN RUMANN², MICHAL DUŠIČKA³, TOMÁŠ KINCZER⁴

¹ Faculty of Civil Engineering STU in Bratislava, Slovakia, martin.orfanus@stuba.sk

² Faculty of Civil Engineering STU in Bratislava, Slovakia, jan.rumann@stuba.sk

³ Faculty of Civil Engineering STU in Bratislava, Slovakia, michal.dusicka@stuba.sk

⁴ Faculty of Civil Engineering STU in Bratislava, Slovakia, toms.kinczer@stuba.sk

1 Abstract

The project developed at the department of hydraulic engineering, Faculty of Civil Engineering STU in Bratislava consist of two main branches involved to cooperate and control the results of each other. The first branch was the physical model of broad-crested weir installed in collapsible canal in hydraulic laboratory and the second was numerical CFD model of broad -crested weir created in same scale. Broad-crested weirs with its multiple purpose possibilities are widely used across the hydraulic engineering.

Keywords: broad-crested weir, physical model, CFD, hybrid modelling, hydraulic research

2 Introduction

The broad crested weirs are repeatedly used to determine the discharge. The broad crested weir crest is horizontal; the upstream and downstream walls are vertical and the discharge coefficient is constant in relatively high rectangular sharp-edged weirs with a broad crest and without lateral contraction $0.1 \leq h/t \leq 0.3$ and $h/s < 0.15$, where s [m] is the height of the weir [1]. Standard criteria in terms if the weir is sharp or broad-crested is $t > 2\div 3 h$ and one of most common empirical calculation of discharge above the sharp-crested weir is

$$Q = \frac{2}{3} \mu_p b \sqrt{2gh_0^{2/3}} \quad (1)$$

Where Q is discharge, b is width, μ_p is discharge coefficient and h_0 is upstream total head according the figure 1.

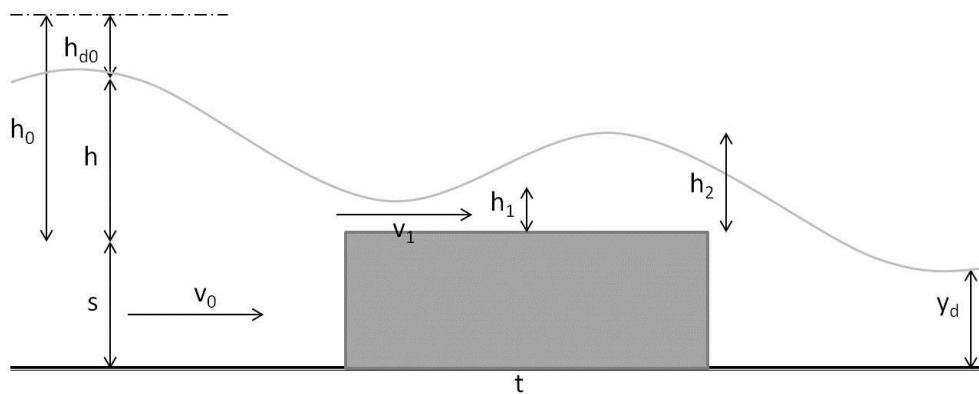


Figure 1. Broad-crested weir scheme [2]

3 Methods

The solution took the place in two stages:

- Measurement on physical model
- Simulation using a CFD model

3.1 Physical modelling

The advantage of the physical model is that, while adhering all the principles of hydraulic research, it is an accurate way to obtain flow information for a given task. However, physical research is relatively expensive, complex, time consuming and problems are difficult to construct (Figure 2).

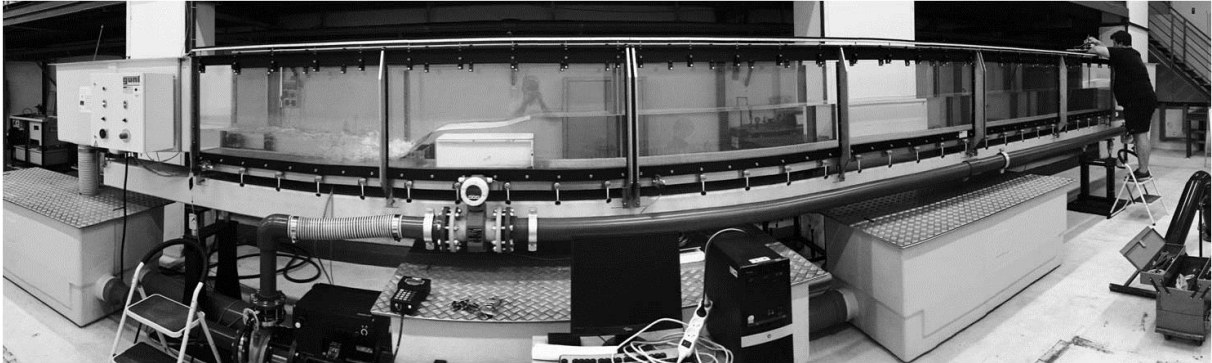


Figure 2. Broad-crested weir - physical model

The primary task of the physical modelling part of research was the measurement of the water levels in different locations along the canal and velocity fields using a point gauge and an Acoustic Doppler 2D Anemometer (FlowTracker). The velocity measurements were performed in 5 vertices with a division at a depth of 0.03 m (Figure 3) near the object of broad crested weir with dimensions of $t = 0.497$ m and $s = 0.151$ m.



Figure 3. Broad-crested weir (velocity measurement)

FlowTracker allows to measure the selected number of points in the vertical direction from a water depth of 2 cm with a speed range of 1 cm.s⁻¹ up to 4.5 cm.s⁻¹ in the vertical line. The device allows to measure and diagnose the discharge automatically and at the same time set the boundary conditions of the profile.

3.2 Numerical modelling

The RANS conservation equations are derived from the N-S equations, by applying the Reynold's decomposition that decompose the liquid flow properties into their time-mean value and fluctuating component. The mean velocity is defined as a time average for a period t that is larger than the time scale of the fluctuations. The time average of the fluctuations over t tends to zero, meaning the turbulence components do not contribute to the bulk mass transport. The time-dependent RANS equations for continuity and momentum conservation are reported below

$$\frac{\partial}{\partial x_i} (\rho \bar{u}_i) = 0 \quad (2)$$

$$\rho \frac{\partial \bar{u}_i}{\partial t} + \rho \frac{\partial}{\partial x_j} (\bar{u}_i \bar{u}_j) + \rho \frac{\partial}{\partial x_j} (\overline{u'_j u'_i}) = -\frac{\partial \bar{p}}{\partial x_i} + \mu \frac{\partial^2 \bar{u}_i}{\partial x_j^2} + \rho g_i \quad (3)$$

where ρ is fluid density, x_i is the it direction vector, u_j is the Reynolds averaged velocity in the it direction; p_j is the Reynolds averaged pressure; and g_i is the sum of body forces. The decomposition of the momentum equation with Reynolds decomposition generates the Reynolds stresses term, $-\rho \overline{u'_i u'_j}$, from the nonlinear convection component. Because the Reynolds stresses are unknown variables, the realizable k - ε model proposed by Shih et al. (1995) is used to resolve the closure problem. The realizable k - ε model suitable for boundary free shear flow applications consists of a turbulent kinetic energy equation and a turbulence energy dissipation rate equation, respectively reported below

$$\frac{\partial k}{\partial t} + \bar{u}_j \frac{\partial k}{\partial x_j} = \frac{\partial}{\partial x_j} \left(\frac{\nu_t}{\sigma_k} \frac{\partial k}{\partial x_j} \right) - \overline{u'_i u'_j} \frac{\partial \bar{u}_i}{\partial x_j} - \varepsilon \quad (4)$$

$$\frac{\partial \varepsilon}{\partial t} + \bar{u}_j \frac{\partial \varepsilon}{\partial x_j} = \frac{\partial}{\partial x_j} \left(\frac{\nu_t}{\sigma_\varepsilon} \frac{\partial \varepsilon}{\partial x_j} \right) + C_1 S \cdot \varepsilon - C_2 \frac{\varepsilon^2}{k + \sqrt{\nu \varepsilon}} \quad (5)$$

where

$$C_1 = \max \left[0.43, \frac{\eta}{\eta + 5} \right], \quad \eta = S \cdot \frac{k}{\varepsilon}, \quad S = \sqrt{2 \cdot S_{ij} \cdot S_{ij}} \quad (6)$$

and the constants: $\sigma_k^{1/4}$ 1.0, $\sigma_\varepsilon^{1/4}$ 1.2, and $C_2^{1/4}$ 1.9. In these equations, k is the turbulent kinetic energy; ε is the turbulent energy dissipation rate; S is the mean strain rate; $\nu \varepsilon$ is the eddy viscosity; ν is the fluid viscosity; and $u'_j i$ and $u'_j o i$ are defined in Eqs. (2) – (3). Hence, the turbulent flow field is determined by solving a system of four equations including the governing equations [see Eqs. (2)–(3)] and the k - ε turbulence model [see Eqs. (4) – (6)]. The numerical solver used in the current study is the pressure-based solver, which is well-suited for incompressible flows governed by motion based on pressure gradients [3].

The simulations took place after measurements in the laboratory. The main objective was to compare mathematical simulations with the measurements on physical model and calibrate the CFD model for the different settings so that the deviations of velocities and water levels are as small as possible. Model geometry and boundary conditions were identical with the physical model at the same scale. The monitored points had the same position and density as the measured points as shows the figure 4.

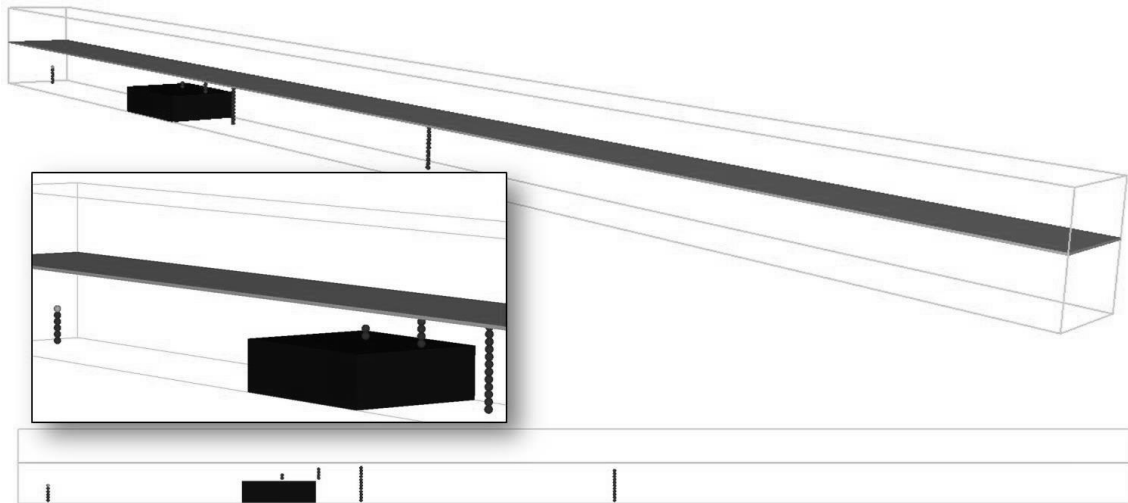


Figure 4. Sharp-crested weir (CFD model setup, with dimensions of $t = 0.497$ m and $s = 0.151$ m.)

The simulations were divided into 3 series in which the influence of the changes on mathematical model parameters on the precision of the simulation result was gradually evaluated:

- Impact of the computational mesh resolution

It was considered homogeneous with a density ranging from 0.1m up to 0.00625m

- Influence of turbulent model change

Series include 6 simulations with turbulence models: $k-\varepsilon$, one-equation turbulent energy model, Prandtl mixing length, $k-\omega$, RNG, LES.

- Influence of the aeration model

There are 5 simulations in the series, which represents different approach to aeration modelling, as follows: without aeration, empirical aeration model, aeration model with mixing and transport of the first order for water and air at 20 ° C and considering surface tension, a full two-phase model (Water air), a full-fledged two-phase model (water air) with an active model of tracking and adiabatic bubbles, and a change in the state.

4 Results and discussion

The primary objective of the project was to verify the accuracy and possibilities of using the CFD model Flow3D, Flowscience Inc. of water flow with free surface and to obtain a knowledge database from the field of parametric input of the simulation of flow and the influence of the individual parameters on simulation accuracy.



Figure 5. Accuracy of CFD for different mesh resolution varying from 0.1m up to 0.00625m

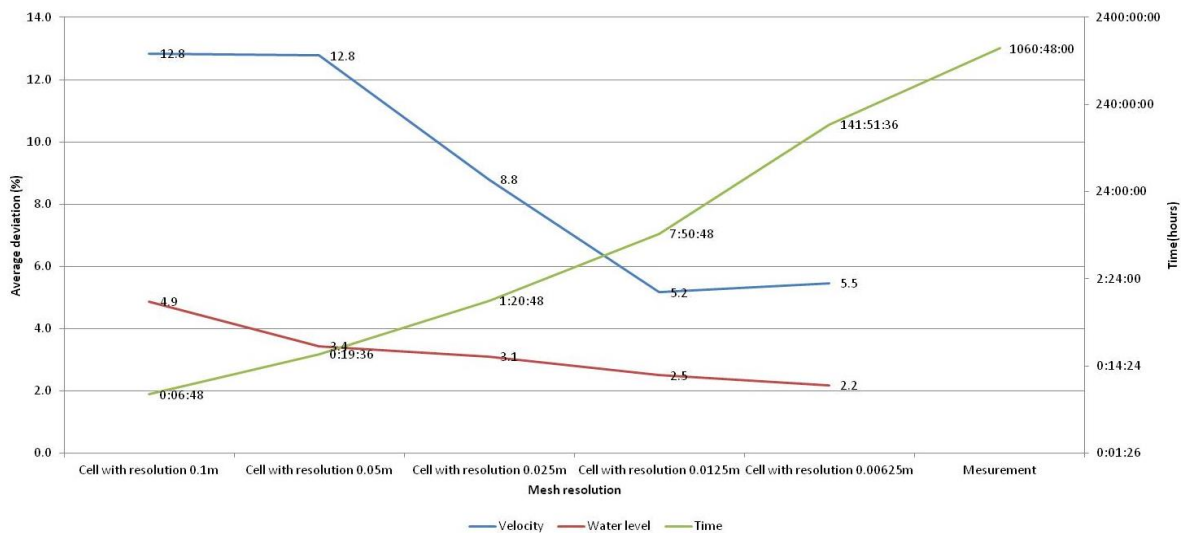


Figure 6. CFD and experiment overall comparison (mesh resolution)

Series 1 was tasked with verifying the dependency of resolution (Figure 6), respectively. The density of the computational and the accuracy of the modelled phenomenon. A very important part of simulations is their time-consuming performance. Frequent user error is ignoring the so-called "Mesh independency". The boundary where the resolution of the computational mesh is such that its further thickening does not affect the result. Frequently, this limit is exceeded and thus the calculation time is unnecessarily extended.

Table 1. Flow velocity deviations with different mesh resolution compared to measurement

Depth (m)	Cell with resolution 0.1m	Cell with resolution 0.05m	Cell with resolution 0.025m	Cell with resolution 0.0125m	Cell with resolution 0.00625m	Measurement
0.02	0.131	0.168	0.187	0.226	0.202	0.217
0.04	0.247	0.220	0.208	0.237	0.208	0.232
0.06	0.248	0.230	0.217	0.243	0.215	0.241
0.08	0.250	0.239	0.223	0.249	0.222	0.244
0.1	0.251	0.243	0.228	0.252	0.229	0.248
0.12	0.250	0.248	0.234	0.254	0.235	0.248
0.14	0.246	0.249	0.240	0.253	0.241	0.251
0.16	0.240	0.249	0.246	0.249	0.247	0.253
0.18	0.235	0.248	0.253	0.243	0.251	0.249
0.2	0.229	0.242	0.258	0.234	0.253	0.255
0.22	0.210	0.235	0.261	0.221	0.253	0.252
0.24	0.191	0.225	0.262	0.196	0.250	0.245

Numerous turbulent models were tested to find most suitable alternative in terms of accuracy and time consumption (Figure 7).

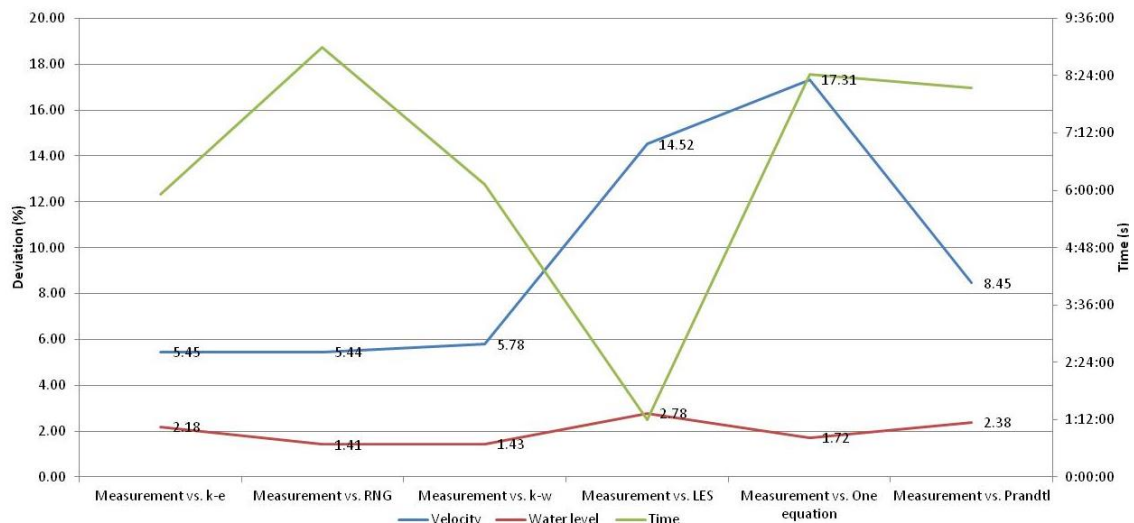


Figure 7. CFD and experiment overall comparison (turbulent model)

5 Conclusion

Broad crested weirs are normally used in medium and large rivers and canals for water regime control, flow behaviour for sustained smoothed water surface by ensuring the subcritical regime and as measuring tool.

The main task was to compare the results of different parametric set-up of the numerical simulation of water flow above the structure of broad-crested weir. As the benchmark of comparison was set-up the physical model (Figure 6) with total discharge of 25 l/s. Comparisons were carried out in several aspects. Measurements of water level and six profiles of velocity field measurements with up to 11 locations for each profile.

According the compared results, parameters of CFD model were tested and modified to get the best possible conformity. Modified parameters such as mesh resolution, turbulent model, air entrainment

effect was systematically modified and compared with physical model through the water level and velocity field measurements.

It should be stated that such a hydraulic problem is suitable for mathematical modelling with the mesh resolution with at least of 0.0125 m cell size (Figure 7) for uniform mesh. In relation to turbulent model, the best alternative is two equation model such a $k-\varepsilon$ (Figure 8). Such a parameterisation gives the most accurate results but slow down the calculation in some cases for almost 8 times.

Acknowledgements

This work was supported by the Slovak Research and Development Agency under Contract No. APVV-15-0489.

This paper was supported by the Grant agency VEGA under contract No. 1/0361/17.

The authors would like to thank for financial contribution from the STU Grant scheme for Support of Young Researchers.

References:

- [1] Říha J., Zachoval Z.: Flow characteristics at trapezoidal broad-crested side weir. J. Hydrol. Hydromech., 63, 164–171, 2015.
- [2] Mäsiar, E., Kamenský, J.: Hydraulika II. Bratislava. STU in Bratislava. 1989.
- [3] Carbone M., Garofalo G., Piro P.: Comparison between CFD and Surface Overflow Rate Models to Predict Particulate Matter Separation in Unit Operations for Combined Sewer Overflows, J. Environ. Eng., ASCE, 2014.
- [4] Orfánus M., Rumann J., Kinzer T., Dušička M.: Hybrid modelling of overflowing broad-crested weir. Technical paper. STU in Bratislava. 2015.

BED ROUGHNESS EFFECT ALONG SUBMERGED HYDRAULIC JUMP

UMUT TÜRKER¹, DANIEL FOROUGHI²

¹ Eastern Mediterranean University, N. Cyprus, umut.turker@emu.edu.tr

² Eastern Mediterranean University, N. Cyprus, daniel.foroughi@cc.emu.edu.tr

1 Abstract

The behaviour of the hydraulic jump on rough beds are analysed from the point of view of conjugate depths, dimensionless friction effect, bed roughness, and the roller length. Specifically, a new relationship for the roller length and dimensionless friction effect is obtained by solving the one-dimensional momentum and continuity equations, based on the assumption that the friction force due to surface roughness follows power relationship with the flow velocity. The validity of the proposed equations is tested through previously published experimental results and verify that the developed equations perform reasonably well. It is clearly revealed that as the strength of hydraulic jump increases the dimensionless friction effect enlarges while the dimensionless roller length reduces.

Keywords: bed roughness, conjugate depth, friction effect, hydraulic jump, roller length

2 Introduction

In fluid flow, when a change in flow conditions from supercritical to subcritical occurs accompanied by a stationary, abrupt turbulent rise in water level considerable amount of energy dissipates. This phenomenon occurs naturally and easily observed when hydraulic jump occurs in open channel. Different researchers ([1], [2]) have defined hydraulic jump several times and in general, simply define the hydraulic jump as a rapid transition of flow from a high velocity condition into slower motion. Controlled hydraulic jump can be used for energy dissipation purposes at hydraulic structures in order to minimize the scour damages. The increase in water level downstream of the hydraulic jump helps obtaining higher heads for water distribution purposes like in irrigation channels and the chaotic behaviour of water during the jump helps to mix different chemicals without extra energy requirements especially at water purification works. Among these applications, it is necessary to control the position of hydraulic jump and to force more energy to dissipate during the jump. For such purposes, roughened beds like corrugated bed, stilling basins, gravel bed, or combination of these are generally preferred during design considerations. Two dominant hydraulic jump characteristics are the length of the jump and the conjugate depths before and after the jump. These characteristics are illustrating the amount of energy dissipation during the jump [1].

Bed roughness along the jump decreases the length of the jump and the tailwater depth in open channels. The decrease in the length of the jump on the other hand helps to decrease the length of the stilling basins at the downstream of the hydraulic structure and thus minimize the cost of the structure.

So far, several times it is proved that rough beds lead to reduction of the length of the jump and depth of the tailwater ([3], [4], [5] and [6]). It is obvious that, whenever the interaction of the rough bed with flow occurs, shear stress increases and more energy dissipate consequently.

Recently, roughness effects on hydraulic jump studies are improved to the analyses on corrugated beds. The early results show that the length of the jump on corrugated beds is half of the jump length on smooth beds while Froude number range from 4 to 10 and three different relative roughness values from 0.25 to 0.5 [3]. The results show that the downstream water depths in hydraulic jumps over corrugated basins are significantly smaller than jumps on smooth beds.

Early studies on hydraulic jump regarding the rough beds were initiated when relative roughness was considered as basin parameter and upstream Froude number was chosen as flow parameter [4]. The results initiated new discussions on hydraulic jump while searching for the effect of roughness and Froude number on conjugate depths.

Later, the laboratory experiments assessed the effects of impervious rough bed on hydraulic jump properties [5]. Experiments held in horizontal rectangular flume with two different roughness geometries, one with prismatic bars and another with gravel cemented on the basin. The laboratory observation showed that both sequent depth and the length of the hydraulic jump reduced due to the surface roughness.

The studies and analysis on the depth ratio change due to wall friction [7] show that the Blanger equation is not valid for hydraulic jumps along rough beds. The experimental studies on hydraulic jump over rectangular, roughened stilling basin tested the effects of slope of the stilling basin on the flow characteristic, such as the relationship in between the conjugate depths [8].

Experimental works for the hydraulic jump on horizontal rough beds analytically solved through the momentum equation to formulate the relationship between effective variables like sequent depths, upstream Froude number, and the roughness height. Results showed that, bed roughness diminishes the conjugate depth ratio [9]. Another achievement was the definition of an effective upstream Froude number that yields universal predictions for sequent depth ratio, jump length, roller length, jump profile, and the other hydraulic jump characteristics that are definitely independent of bed roughness [10].

In this current study, the momentum equation is used together with the resistive force to obtain a reasonable friction coefficient in different rough bed characteristics. For applying this, dimensionless friction effect, β is introduced to the momentum equation, which is modified by the resistive forces as a retarding force. The β values help to generate the reasonable friction coefficients, which are related to the geometry of the roughness.

3 Theoretical consideration

3.1 Dimensionless friction effect

Considering a system defined by a control volume as given in Fig. 1, Newton's second law states that the sum of all external forces acting on the system is equal to the time rate of change of linear momentum of the system;

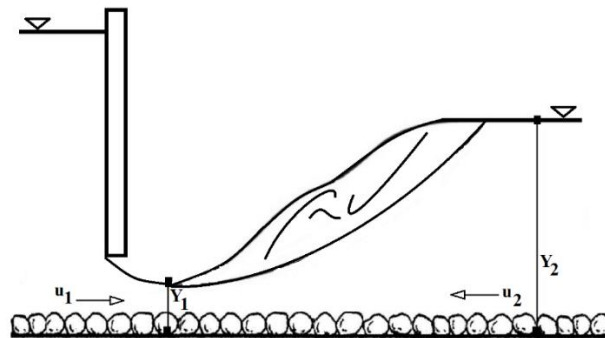


Figure 1. Schematic definition of hydraulic jump over a rough bed.

$$\bar{F} = \frac{d\bar{P}}{dt} \quad (1)$$

The resultant force \bar{F} includes all surface and body forces acting on the system and rate of change of momentum, $d\bar{P}/dt$ can be solved through Reynolds Transport Theorem. Under the assumption of small channel slope (weight component of the control volume can be ignored), steady and incompressible flow conditions, the resultant momentum equation in the direction of flow can be depicted as

$$F_{p1} - F_{p2} - F_d = \rho Q(u_2 - u_1) \quad (2)$$

F_{p1} and F_{p2} are the hydrostatic pressure forces. F_d is the flow resisting force, u_2 and u_1 are the sub-critical and super-critical flow velocities, respectively and Q is the discharge of the flow. The hydrostatic forces can be written in terms of the distance from the water surface to the centroid of the upstream h_c , area of rectangular cross section, A , and specific weight of the fluid, ($\gamma = \rho g$), as $F_p = \rho g h_c A$. This will change Eq. (2) into,

$$\rho g h_{c1} A_1 - \rho g h_{c2} A_2 = \frac{\rho g}{g} Q(u_2 - u_1) + F_d \quad (3)$$

Dividing all the terms by ρg ; and inserting $Q/A = u$ in terms of u_1 and u_2 results in;

$$\frac{Q^2}{A_1 g} + h_{c1} A_1 = \frac{Q^2}{A_2 g} + h_{c2} A_2 + F_d \quad (4)$$

In the case of rectangular channel the discharge can be defined in terms of unit discharge, q in which unit discharge is the ratio between the discharge and the width of the rectangular channel, B . Therefore, Eq. (4) can be re-arranged as

$$B \left[\frac{q^2}{y_1 g} + h_{c1} y_1 - \frac{q^2}{y_2 g} + h_{c2} y_2 \right] = \frac{F_d}{\rho g} \quad (5)$$

The flow resisting force is dependent on the speed of the flow and in general terms can be written as

$$F_d = C_f \bar{u}^2 \quad (6)$$

Here C_f depend on the shape and size of the surface, and the kind of medium. The flow resisting force caused by the interaction of fluid and the rough bed surface depends on and is proportional with the density of the fluid, ρ , mean velocity, u , gravitational acceleration, g , and the surface area, A_b , in which the friction force is acting in parallel. Inserting all these variables into Eq. (5) will result in;

$$\rho g B \left[y_1^2 F_f^2 \left(\frac{y_2 - y_1}{y_2} \right) + \frac{1}{2} (y_1 - y_2)(y_1 + y_2) \right] = \frac{1}{2} C_f \rho u_{avg}^2 A_b \quad (7)$$

After dividing all terms by ρg and y_1^2 one can obtain Eq. (8). The right hand side of the Eq. (8) consists of the variables that signifies the dimensionless friction effect, β .

$$\beta = \alpha C_f \quad (8)$$

in which,

$$\alpha = \frac{u_1^2}{y_1^2 g} \frac{A_b}{B} \quad (9)$$

Re-arranging Eq. (7) accordingly will result in;

$$2F_f^2 \left(\frac{y_2 - y_1}{y_2} \right) + \left(\frac{y_1^2 - y_2^2}{y_1^2} \right) = \beta \quad (10)$$

In the case of $\beta = 0$ where C_f is 0, Eq. (9) reduces to famous Belanger Equation. However, If $\beta \neq 0$ where $C_f \neq 0$ the resultant relationship can be given as,

$$\left(\frac{y_2}{y_1} \right)^3 - (2F_f^2 + 1 - \beta) \left(\frac{y_2}{y_1} \right) + 2F_f^2 = 0 \quad (11)$$

According to Alhamid and Negm (1996), the average velocity at upstream section can be used as a representative velocity, u_1 as an assumption for simplicity of driving the model. Rechecking the derived model with the experimental results proved that this assumption works well. Therefore, the average velocity is taken as $u_{av} = u_1$.

3.2 Roller length along the hydraulic jump

The experimental studies performed lately suggest that one can assume roller length, L_r proportional to the difference between the sequent depths as

$$\frac{L_r}{y_1} = a \left[\frac{y_2}{y_1} - 1 \right] \quad (12)$$

in which coefficient a is generally ranging between 5 and 6. Instead of empirical approach well known energy loss equation can be worked out to generate modified energy dissipation equation along the hydraulic jumps over rough surfaces. The energy dissipation along hydraulic jump is defined as

$$E_1 - E_2 = \Delta E = \frac{(h_2 - h_1)^3}{4h_1 h_2} \quad (13)$$

which is valid for the assumption of negligible friction effects. On the other hand, the energy loss due to friction should be considered in relation to the bed surface roughness. Roller length is a function of

difference of conjugate depths, bed roughness height, Froude number, and the energy dissipation along the hydraulic jump as

$$L_r = f(Fr_1, \Delta E, k_s, \Delta y) \quad (14)$$

Thus the following relationship can be established;

$$\frac{L_r}{Fr_1} = f \frac{\Delta E}{\Delta y} k_s \quad (15)$$

4 Results and discussion

4.1 Variation of dimensionless friction effect with upstream Froude number

The performance of hydraulic jump depends on the magnitude of upstream Froude number. Therefore, the dimensionless friction effect defines the resistive effects of surface roughness along the hydraulic jump depending on the thickness of the roughness. Figure 2 and Figure 3 plots the relationship between β and Fr_1 for different bed roughness heights, k_s . The plots are based on the experimental results of [5] and [9]. The dimensionless friction effect used in Figure 2 and Figure 3 is calculated through Eq. (9). Results show that for small Froude numbers β increases as k_s increases. However, as the occurrence of strong hydraulic jump increases, steep increase on β is observed independent of k_s . Clearly, as the strength of hydraulic jump increases, the turbulence effect on jump takes over the resisting forces on the hydraulic jump. From undular ($1.0 < Fr < 1.7$) to oscillating ($2.5 < Fr < 4.5$) hydraulic jumps the bed roughness dominates the resisting forces. On the other hand, it is observed that turbulence effects are more effective when Froude number gets greater than 4.5 indicating steady and strong jumps.

It can be also observed that for $Fr > 9$ the dimensionless friction effect and Froude number behaves independent of bed roughness height, k_s and thus the relationship between the parameters becomes unpredictable. This is due to the strong turbulence at high Froude numbers. As a result, the trends of Figure 2 and Figure 3 depicts that β is not only a function of Fr but also stimulated from the magnitude of bed roughness height. The best fit line equation of experimental results and the coefficient of correlation, R^2 is represented by power relationship in Table 1.

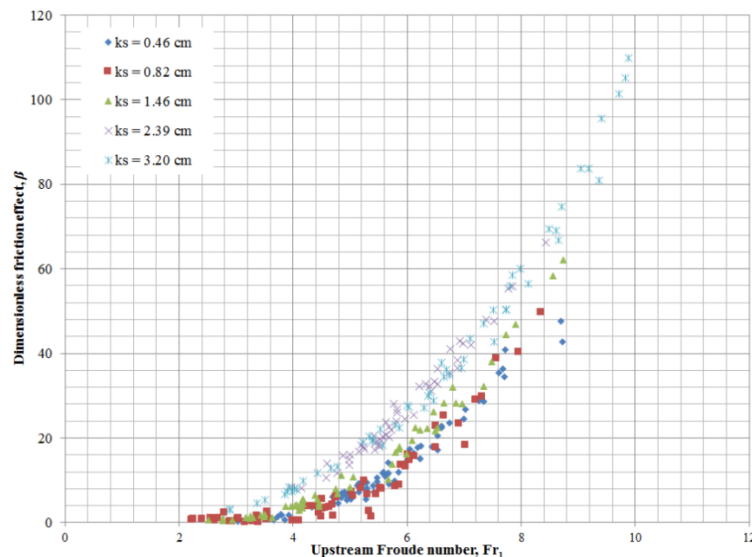


Figure 2. The relationship between the upstream Froude number and the dimensionless friction effect for the data set gathered from the work of [9]

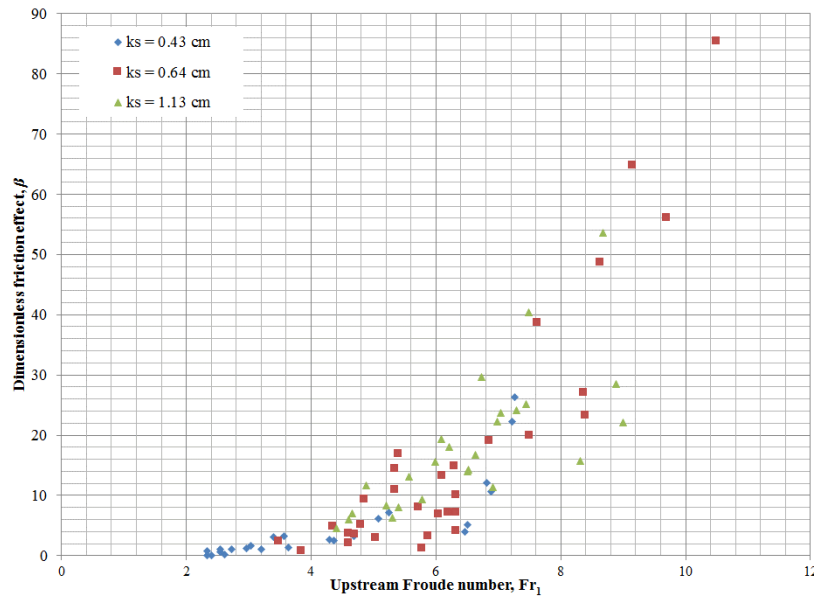


Figure 3. The relationship between the upstream Froude number and the dimensionless friction effect for the data set gathered from the work of [5]

Table 1. The equation of power relationship of Froude number and dimensionless friction effect

Figure No	Bed roughness height, (cm)	Equation type	Coefficients a_1 , n , and Correlation coefficient, R^2	Data set reference
2	0.46	$\beta = a_1 (Fr_1)^n$	$a_1 = 0.0025$; $n = 4.79$ $R^2 = 0.94$	Carollo, et al. (2007)
2	0.82		$a_1 = 0.0065$; $n = 4.10$ $R^2 = 0.70$	
2	1.46		$a_1 = 0.012$; $n = 4.05$ $R^2 = 0.97$	
2	2.39		$a_1 = 0.1372$; $n = 2.93$ $R^2 = 0.97$	
2	3.20		$a_1 = 0.1561$; $n = 2.84$ $R^2 = 0.99$	
3	0.43	$\beta = a_1 (Fr_1)^n$	$a_1 = 0.0232$; $n = 3.28$ $R^2 = 0.78$	Hughes and Flack, (1984)
3	0.64		$a_1 = 0.0129$; $n = 3.66$ $R^2 = 0.72$	
3	1.13		$a_1 = 0.1445$; $n = 2.51$ $R^2 = 0.71$	

4.2 Variation of friction factor with dimensionless friction effect

According to Eq. (8) and Eq. (9), the magnitude of friction coefficient due to bed roughness can be estimated through the ratio between β and α . Figure 4 and Figure 5 show the relationship between β and α for two different studies. Both studies show that there exists a linear relationship between the two variables and it is obvious that as β increases α also increases. The linear relationship between variables is clear in Figure 4. However, the results given in Figure 5 are not clearly depicted similar results but still can be accepted as linear trend. Any slope of any solid line representing the best fit line of given curves at different bed roughness heights can help to calculate the magnitude of friction coefficient. The equations of best fit lines obtained through the regression analysis of experimental data are summarized in Table 2. The result shows reliable solutions for friction coefficient, since the slope of the best fit lines increased as the bed roughness coefficient increases.

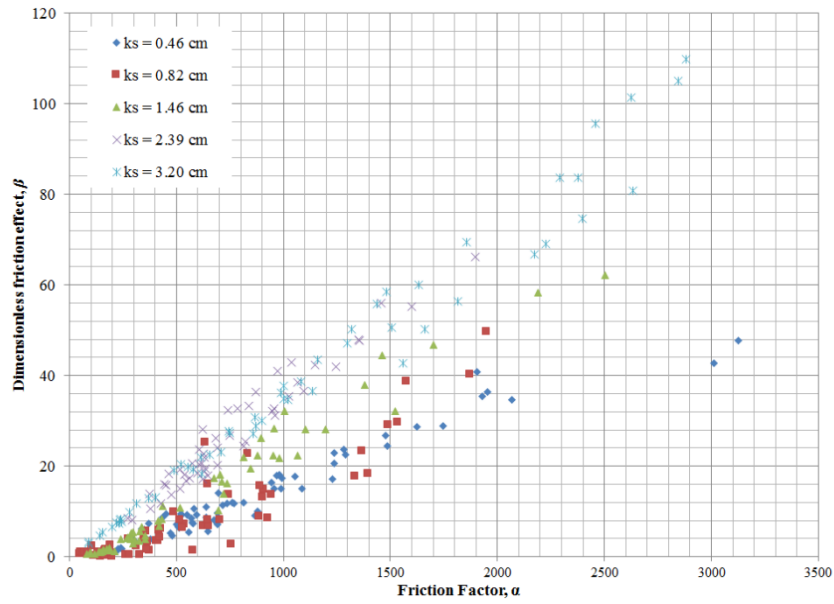


Figure 4. The relationship between the dimensionless friction effect and the friction factor. The slopes of the trends are increasing as the bed roughness height increases. The data set is gathered from [9]

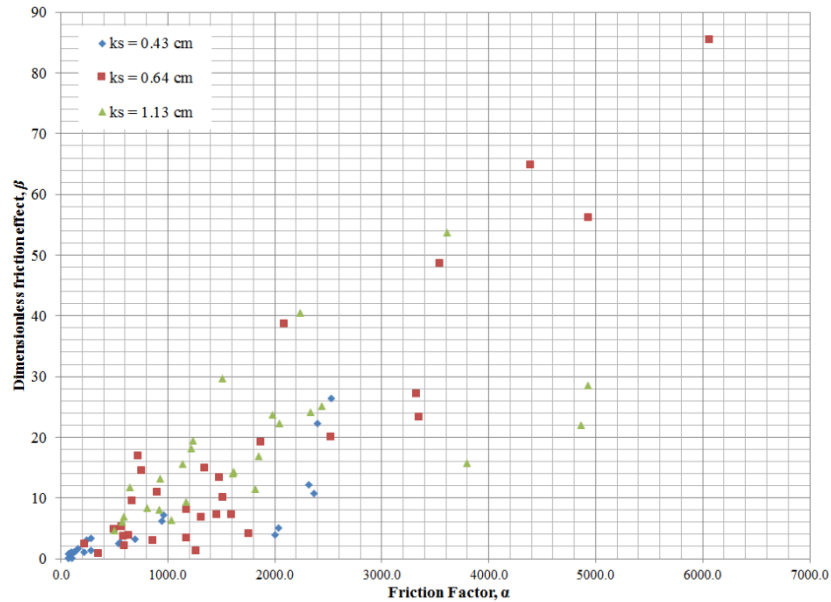


Figure 5. The relationship between the dimensionless friction effect and the friction factor. The slopes of the trends are increasing as the bed roughness height increases. The data set is gathered from [5]

Table 2. The equation of linear relationship of dimensionless friction effect and friction factor

Figure No	Bed roughness height, (cm)	Equation type	Coefficients m_1 , c , and Correlation coefficient, R^2	Data set reference
4	0.46	$\beta = m_1\alpha + c$	$m_1 = 0.0173$; $c = -1.44$ $R^2 = 0.95$	Carollo, et al. (2007)
4	0.82		$m_1 = 0.0213$; $c = -3.37$ $R^2 = 0.85$	
4	1.46		$m_1 = 0.0279$; $c = -3.28$ $R^2 = 0.97$	
4	2.39		$m_1 = 0.037$; $c = -1.60$ $R^2 = 0.95$	
4	3.20		$m_1 = 0.035$; $c = -0.32$ $R^2 = 0.97$	
5	0.43	$\beta = m_1\alpha + c$	$m_1 = 0.0062$; $c = -0.071$ $R^2 = 0.69$	Hughes and Flack, (1984)
5	0.64		$m_1 = 0.0132$; $c = -5.63$ $R^2 = 0.85$	
5	1.13		$m_1 = 0.0056$; $c = 7.85$ $R^2 = 0.37$	

Considering the results of regression analysis through evaluating the coefficient of determination, R^2 , it can be observed that friction coefficient increases as the bed roughness height increases. There is a meaningful relationship between dimensionless friction effect and the friction factor since coefficient of determination is close to one.

4.3 Roller length definition based on dimensionless roughness effect

The roller length studies are nowadays motivated to find an equation for roller length as a function of hydraulic jump properties. Based on Eq. (11), roller length was defined as dimensionless, with upstream water depth. In general, the relationship between dimensionless roller length, L_r/y_1 and roller length ratio is searched out independent on the variations in the bed roughness height (k_s). On the other hand, it is expected to have changes in the roller length related with the energy losses that occurs due to the bed friction effects. This forces the scientists to focus on the energy dissipation of hydraulic jump that should be more than the energy dissipation for smooth surfaces. The strength of hydraulic jump that is measured through the magnitude of Froude number is also an important parameter that reflects the changes in the length of the roller. Therefore, a relationship that will reflect the weights of all those variables and parameters on the length of the jump should be considered while deriving an empirical relationship. This can be achieved through the relationship given in Eq. (15).

The variation of roller length, L_r/Fr_1 with respect to bed roughness, difference between conjugate depths and energy dissipation along the jump are given in Figure 6 and Figure 7. The figures are depicted with all experimental results, which have been pointed out before. Along the horizontal axes of Figure 6 and Figure 7 as the Froude number increases (increase in the gap between conjugate depths) the representative relationship approaches to origin while generating an increase in the roller length ratio. This is the evidence of long roller length distances for strong hydraulic jumps. As the difference between conjugate depths decreases the resisting effects of bed roughness dominates the length of the hydraulic jump and the roller length increases.

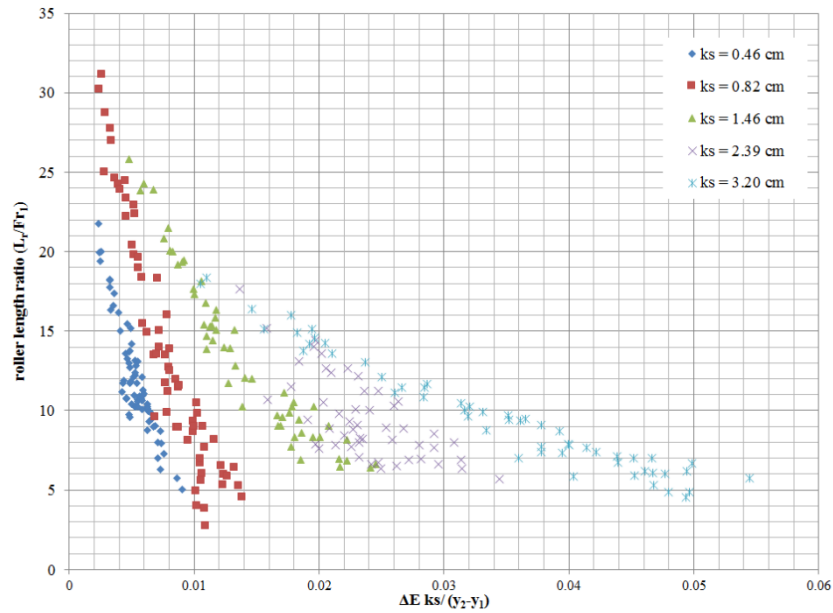


Figure 6. Change in roller length with respect to the energy dissipation during hydraulic jump for [9]

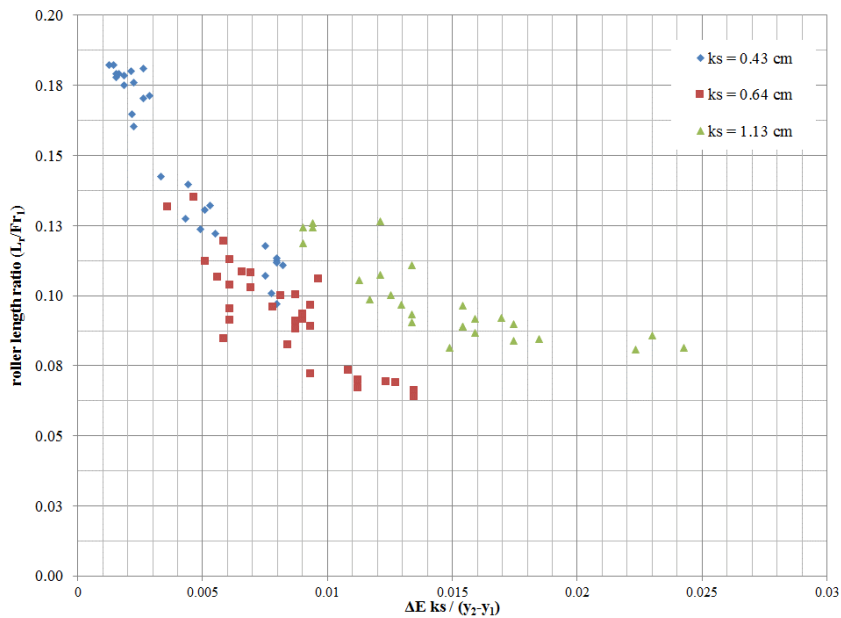


Figure 7. Change in roller length with respect to the energy dissipation during hydraulic jump for [5]

5 Conclusion

This study introduced a solution for the hydraulic jump on rough bed by integrating the flow resisting force into the momentum equation. It is assumed that the well-known Belanger’s equation is not satisfactorily representing the relationship between conjugate depth and Froude number in the case of jumps on rough surfaces. Under this assumption, momentum equation is rewritten to integrate the effect of flow resisting forces on physical behaviour of the hydraulic jump. Using the experimental results of previous studies like [5] and [9], the parameters like dimensionless friction effect, and friction factor are evaluated. The parameters help to decide on the upper limits of bed roughness that is effective in calculating flow resisting forces. As the Froude number of flow increase the effect of bed roughness in resisting the hydraulic jump conditions attenuates, while the turbulent behaviour of jump dominates the flow resisting effects. The results show that the friction coefficient increases as the thickness of the bed roughness increases. The empirical roller length (L_r) equation is also improved when it is collaboratively

used together with the upstream Froude number, energy dissipation, and difference between the conjugate depths and by the height of bed roughness.

Even though in most of the analyses good trends are obtained between the parameters, yet it is not possible to obtain only one equation representing the effect of bed roughness on the magnitudes of dimensionless friction effect, or roller length. It is expected that in the future studies, the outcomes of this study can be further developed with new generation models of optimization theories like artificial neural network or genetic algorithm to simulate all the variables in one relation.

References:

- [1] Chow, V. T. (1959). *Open Channel Hydraulics*. (McGraw-Hill International: New York, USA).
- [2] Munson, B. R., Young, D. F., Okiishi, T. H., Huebsch, W. W., (1990). *Fundamentals of Fluid Mechanics*, (John Wiley & Sons, Inc.).
- [3] Ead, S. A., and Rajaratnam, N. (2002). Hydraulic Jumps on Corrugated Beds. *Journal of Hydraulic Engineering*, 138(7), 656-663.
- [4] Rajaratnam, N. (1968). Hydraulic Jumps on Rough Beds. *Transaction, Engineering Inst. of Canada*, (11), A-2, 1-8.
- [5] Hughes, W. C., and Flack, J. E. (1984). Hydraulic Jump Properties over a Rough Bed. *Journal of Hydraulic Engineering*, 110(12), 1755-1771.
- [6] Negm, A. A. M. (1996). Hydraulic jumps at positive and negative steps on sloping floors. *Journal of Hydraulic Research*, 34(3), 409-420.
- [7] Hager, W. H., Bremen, R., and Kawagoshi, N. (1990). Classical hydraulic jump: length of roller, *Journal of Hydraulic Research*, 28(5), 591-608.
- [8] Alhamid, A. A., Negm, A. M., (1996). Depth ratio of hydraulic jump in rectangular stilling basins. *Journal of Hydraulic Research*, 34(5), 597-604.
- [9] Carollo, F. G., Ferro, V., and Pampalone, V. (2007). Hydraulic Jumps on Rough Beds. *Journal of Hydraulic Engineering*, 133 (9), 989-999.
- [10] Afzal, N., Bushra, A., Seena, A. (2011). Analysis of turbulent hydraulic jump over a transitional rough bed of a rectangular channel: universal relations. *Journal of Engineering Mechanics*, 137(12), 835-845.

EXPERIMENTAL RESEARCH ON FLOW CONDITIONS AT SELF-CLEANING RACKS

MIROSLAV TVRDOŇ¹, JÁN RUMANN², PETER DUŠIČKA³, TOMÁŠ KINCZER⁴,

¹ *Slovak University of Technology in Bratislava, Faculty of Civil Engineering, Department of hydraulic Engineering, Slovakia, miroslav.tvrdon@stuba.sk*

² *Slovak University of Technology in Bratislava, Faculty of Civil Engineering, Department of hydraulic Engineering, Slovakia, jan.rumann@stuba.sk*

³ *Slovak University of Technology in Bratislava, Faculty of Civil Engineering, Department of hydraulic Engineering, Slovakia, peter.dusicka@stuba.sk*

⁴ *Slovak University of Technology in Bratislava, Faculty of Civil Engineering, Department of hydraulic Engineering, Slovakia, tomas.kinczer@stuba.sk*

1 Abstract

An important part of any small hydropower plant is the intake structure. Its main function is to provide sufficient discharge of water for the hydropower plant and to prevent the large floating objects carried by the stream to get to the hydropower plant. In many cases, this structure requires a weir construction across the riverbed which is often environmentally unacceptable. In cases where such a construction is not possible, another kind of the intake structure has to be used, for example a bank water intake. An important part of these low-head intakes are the coarse racks which prevent floating objects to get in the hydraulic system of the turbine and endanger the operation of the entire hydropower plant. These floating objects are captured on screenings and afterwards they should be cleaned (removed from the screening). The cleaning for low-head small hydropower plants is usually manual. A new type of self-cleaning racks has been tested in the hydraulic laboratory of the Department of Hydraulic Engineering at the Faculty of Civil Engineering in Bratislava. Compared to the conventional design of the racks with minimal flow resistance, the new design of racks has far larger hydraulic resistance in order to effect the flow to float the object along the racks. The experiments were aimed to determine the optimal inclination of the racks to minimize the hydraulic resistance on the flow in the intake structure and achieve a self-cleaning effect keeping the racks clean of the floating debris. The experiments were realized on a model in experimental flume for different variations of inclination of the racks.

Keywords: low-head small hydropower plants, intake structures, coarse racks, hydraulic research, physical modelling, velocity fields

2 Introduction

Screenings (racks) are an essential part of every intake structure build as a part of hydraulic or hydropower structures. Their purpose is to prevent dragging of the floating debris along with water into the hydraulic system of the structure. A number of additional requirements are put on the screenings and their supporting construction, e.g. the ability to resist the design loads, to allow the operational maintenance and cleaning, not to induce too large hydraulic resistance to the flow, etc. Criteria for the selection of the suitable design depend mostly on the quantity and attributes of the floating objects carried by the water, weather conditions, demands for self-service, design requirements and economic costs.

Cleaning of the screenings is necessary to keep them in required operational conditions. Usually the cleaning requires cleaning mechanisms or heavy manual labour. Mechanical cleaning of the screenings by cleaning machines requires higher investment costs for the structure but provides automated cleaning. Manual cleaning requires personnel and cannot be automated. There are several screening types which do not require additional cleaning, because they have a self-cleaning ability [1].



Figure 1. Prototypes of inclined bar racks in Slovakia (Roveň, Pezinok)

One type of the self-cleaning screenings are the flat rack inclined in the flow direction. In Slovakia prototypes of these type of screening design are used at the intake structure of the Roveň small hydropower plant (SHPP) and another application of these screening is in one test relief chamber in the sewer system of the city of Pezinok (Figure1).

The racks are created by flat metal bars inclined in the main flow direction at a specific angle. This design provides higher resistance to the flow through the racks resulting in higher hydraulic losses but it affects the flow at the racks in a way that the floating debris is mostly being carried by the main flow in its direction along the racks and it does not stay on the racks (Figure 2). The design of such self-cleaning racks is being used in operation with very good results. Our research is focused on hydraulic conditions on inclined racks with self-cleaning ability with respect to varying inclination angle. A basic study on flow parameters at variously inclined flat bar racks that has been carried out is described in this paper.

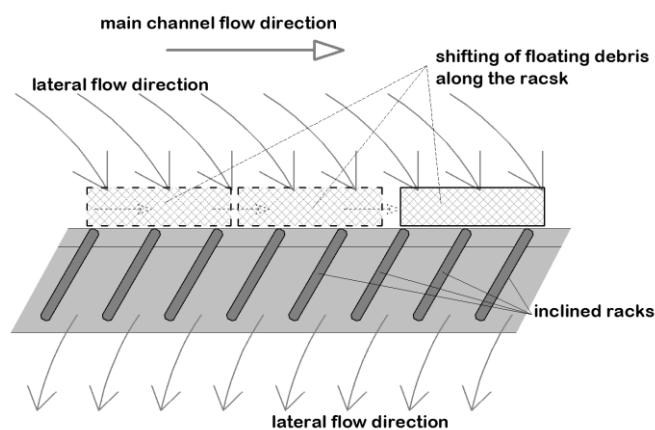


Figure 2. Scheme of the inclined flat bar racks principle

3 Methods

For research on the flow conditions at the self-cleaning inclined racks a physical model has been established in the Hydraulic laboratory of the Department of Hydraulic Engineering of the Faculty of Civil Engineering, Slovak University of technology in Bratislava. Flow condition on variously inclined bar racks were measured and evaluated.

3.1 Experimental setup

The physical model of the inclined racks was built within an experimental channel (Figure 3, 7). The channel with a rectangular cross-section is 0.60 m wide and 10 m long with a horizontal bed made of plastic. A side weir in the right wall has been built approximately 6 m from the upstream end of the

channel. The width of the side weir is 0.30 m and the height of the weir crest above the channel bed is 0.05 m. The water level in the channel as well as the discharge distribution was regulated by a sluice gate at the end of the channel. Racks with different inclination have been placed in the weir to simulate similar flow conditions as in a relief chamber of a sewer system.

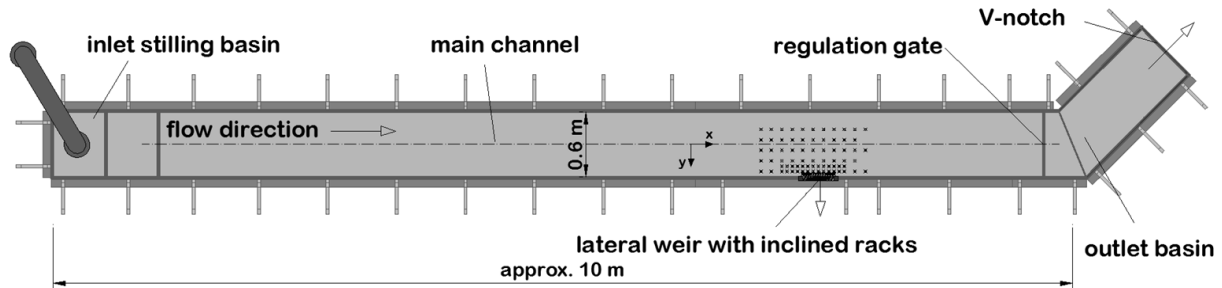


Figure 3. Schematic layout of the experimental channel

The model of the flat bar racks is made of plastic flat bars 4 mm thick and 40 mm wide. The racks are attached to the lateral weir at an angle α with a distance of the centre points of 24 mm. The shape and basic parameters of the racks is in Figure 4. Racks with different inclination angle were tested. The inclination angle was varying between negative angle values (inclination in opposite direction to the main flow direction) to positive values (inclination in the main channel direction).

In the channel inlet the discharge of 30 l.s^{-1} was established and the depth in the channel was established by the regulation gate at the end of the main channel so that the discharge in the outlet was 20 l.s^{-1} .

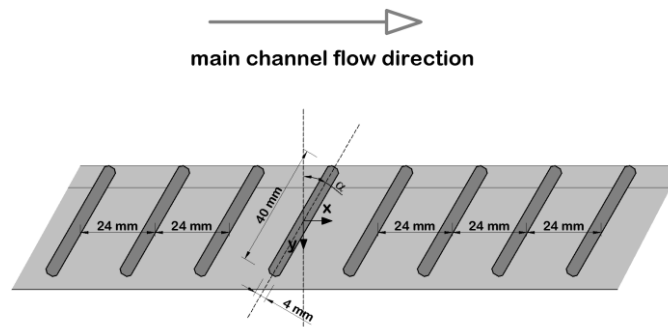


Figure 4. Scheme of the racks model

3.2 Measuring equipment

According to the changes of the inclination angle of the racks, water levels and flow velocities in a defined grid of points in the channel were measured. The distance between the points of the measurement grid varied between 2.5 cm, 5 cm and 10 cm in both directions (Figure 5). Overall 85 points of the main grid were used for the measurements.

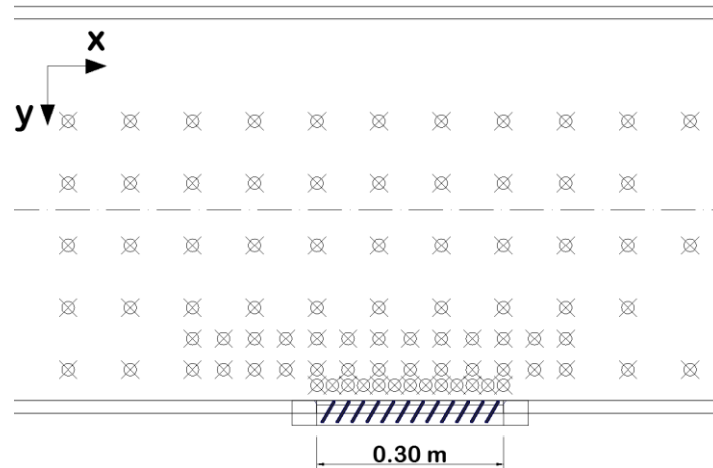


Figure 5. Layout of measurement points

For water level measurements a level gauge was used with the precision of measurement of 1mm. Additional water levels were measured in the channel axis in three profiles – starting profile of the channel, profile above the measurement grid and profile upstream the regulation gate at the end of the channel. The water levels in these profiles were measured and recorded by ultrasonic water level gauges with precision of 1 mm.

FlowTracker, a 2D handheld Acoustic Doppler Velocimeter (ADV) unit has been used for measuring velocity components in the measurement grid. This ADV device is a single point Doppler current meter designed for field velocity measurements. It measures velocities with a range as low as 0.001 m/s and up to 4.5 m/s with the accuracy of 1% of the measured velocity in a one-second sample. The velocities are measured in two directions v_x and v_y relative to probe orientation in a fixed distance of 10 cm from the tip of the probe in a cylindrical sampling volume with 6 mm in diameter and 9 mm in length (Figure 6) [2]. The velocities were measured each second with a sampling frequency of 10 Hz over averaging time of 30 s for each point of the measurement grid. Therefore, the recorded velocity values were average of 300 individual velocity measurements. The velocities were measured in the depth of 2.5 cm relative to the actual water level (the closest to the water level surface as possible) assuming that the most of the debris flowing in the water flows near the surface.

Discharge in the channel was measured by magnetic flow meter in the intake and by a V-notch in the outlet of the main channel.

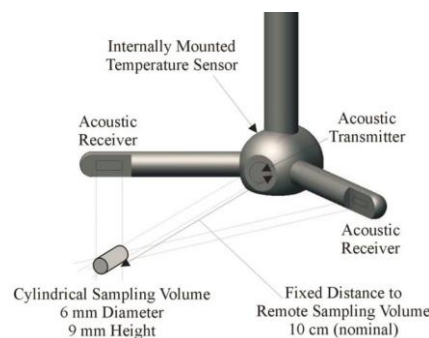


Figure 6. Illustration of the 2D ADV probe used for measurements [2]



Figure 7. Measurements on the model

4 Results and discussion

For each inclined racks model five series of velocity measurements in measurement grid points were carried out. Then the measured values were averaged and analysed. The main objective was to determine the effect of the inclination angle of the flat bar racks on the velocity vectors. The velocities were analysed for total velocities, v_x and v_y components in the direction according to Figure 5. Example of the measurement results can be seen in Figure 8. The result are show for the racks with the inclination angle $+45^\circ$ (where $+$ means inclination in the direction of the main channel flow).

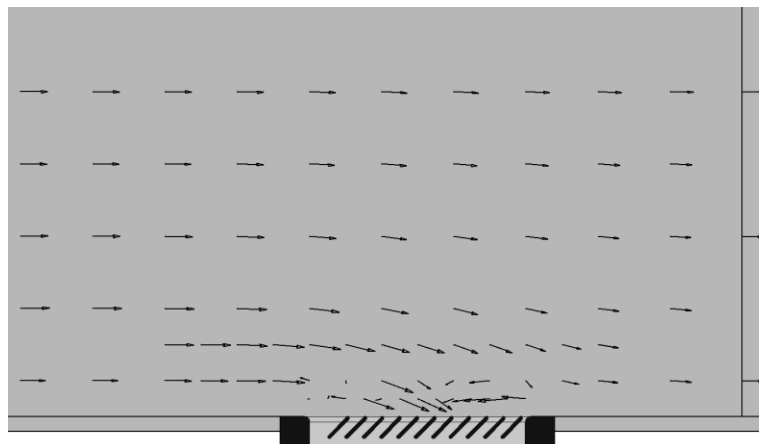


Figure 8. Example of measured velocity vectors for inclination angle of the racks $\alpha = +45^\circ$

Due to the basic hydraulic set-up (a lateral weir perpendicular to the main channel axis) and the size of the lateral weir, the character of the measured velocity fields is strongly affected by phenomena of the side overflow [3] – Figure 8. Therefore, just the mid-section of the weir can be used for evaluation of the effect of the flat bar racks inclination angle on the velocity vectors, where the velocity vector changes are significantly affected by the changes of the inclination angle of the racks. In this viewpoint the lateral weir model with the racks is relatively short. According the dimensions of the channel and the flow conditions the model should be longer than the original 30 cm to decrease the effect side overflow.

The main effect of the flat bar inclination angle on the velocity can be seen for v_y velocity component. With the increase of the angle in positive direction the average v_y componetns at the racks are decreasing, reducing the force of water flow in the y -direction (Figure 9). Additional advantage of the positive inclination angle of the flat bar racks is that the inclination creates a flat like surface on the rack wall reducing the possibility of mechanical “catching” of floating debris on the racks.

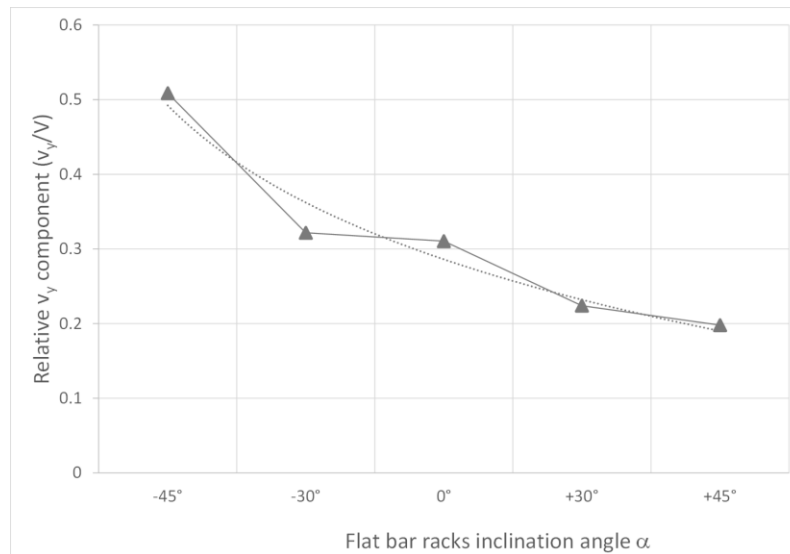


Figure 9. Relation between relative v_y component and angle of inclination of the flat bar racks

5 Conclusion

Physical model of inclined flat bar racks has been established for research on basic relations between the design (inclination) of the flat bar racks and flow velocity parameters near water surface at the racks with respect to the self-cleaning ability of such racks. Results of the research are represented as follows:

- increasing the inclination of the flat bar racks in the flow direction affects the flow velocities at the racks,
- the v_y velocity components decrease with the increase of positive inclination angle α ,
- self-cleaning ability (shifting floating debris along the racks) was observed starting with the racks with inclination angle $+30^\circ$
- the side weir overflow phenomena affects the flow velocities, therefore the area of the side weir used for evaluation of the measurement results had to be reduced,
- the ADV device used for the measurements was a suitable tool for the basic measurements of flow velocity components, for detailed flow analysis, the resolution and required measurement precision could not be obtained due to the installation of the device.

Acknowledgements

This paper was supported by the Grant agency VEGA under contract No. 1/0361/17 and by the Slovak Research and Development Agency under Contract No. APVV-0680- 10.

References:

- [1] Tvrdoň, M., Rumann, J.: Coarse Screenings with Self-Cleaning Ability on Intake Structures of Small Hydropower Plants. 13th International Symposium on Water Management and Hydraulic Engineering, Bratislava, pp.255-258, 2013.
- [2] FlowTracker® Handheld ADV®, Technical Manual, August 2006, <http://www.sontek.com>
- [3] Hager, W.H.: Lateral Outflow Over Side Weirs, Journal of Hydraulic Engineering, Volume 113, Issue 4, 1987

EFFECT OF VERTICAL SHAPES OF SHAFT INTAKE STRUCTURES ON FLOW VELOCITY DISTRIBUTION

MICHAL DUŠIČKA¹, JÁN RUMANN², PETER DUŠIČKA³, TOMÁŠ KINCZER⁴

¹ Slovak University of Technology in Bratislava, Faculty of Civil Engineering, Department of hydraulic Engineering, Slovakia, michal.dusicka@stuba.sk

² Slovak University of Technology in Bratislava, Faculty of Civil Engineering, Department of hydraulic Engineering, Slovakia, jan.rumann@stuba.sk

³ Slovak University of Technology in Bratislava, Faculty of Civil Engineering, Department of hydraulic Engineering, Slovakia, peter.dusicka@stuba.sk

⁴ Slovak University of Technology in Bratislava, Faculty of Civil Engineering, Department of hydraulic Engineering, Slovakia, tomas.kinczer@stuba.sk

1 Abstract

In Slovakia, several small hydropower plants utilizing the hydropower potential at existing water structures have been built. The design of these structures has been effected by the need of low investment costs and short construction times minimizing the impacts to the existing water structure and their operations. Therefore, a shaft intake - a specific design of intake structures has been used overcoming the vertical difference in water levels over a short distance. The shape of these structures is characterized by a vertical shaft, which leads the water from headwater to turbines. The flow conditions in these shaft intake structures are often complicated and the flow conditions at the turbine intakes are inhomogeneous, which is caused by sudden changes in flow direction. The inhomogeneity of water flow causes asymmetrical load on the mechanical parts of the turbine units, which leads to their problematic behavior and defects in performance. An experimental research in the hydraulic laboratory of the Department of Hydraulic Engineering of the Faculty of Civil Engineering in Bratislava has been realized. It was focused on determination of the effects of vertical shape of a “shaft” intake on flow conditions at the turbine intake with respect to vertical homogeneity of velocity distribution. For these purposes a model of a shaft intake in experimental flume has been built. The experimental results have been compared with results of mathematical modelling of flow in the shaft intake. The results prove effecting the vertical flow velocity distribution in the turbine intake profile by the vertical shaping of the “shaft” intake structure.

Keywords: intake structures, low-head small hydropower plants, shaft intake, flow velocity distribution, flow homogeneity, hydraulic research

2 Introduction

There are several large water works built in the past in Slovakia. All this existing water structures have several purposes and their hydropower potential is not fully utilized. Unfortunately, suitable building sites for large water structures are have been exhausted and the current situation leads to construction of smaller water structures. Except for new sites, they began to be used idle flows of large water works, for example biological discharges. Several small hydropower plants utilizing the hydropower potential of idle flows at existing water structures have been already built. It is an additional energy use of this locations. Large water structures usually use earth- fill dams. So intake structures of new small hydropower plants have to overcome this dams, which can mean some extra requirements versus open space construction sites. They are usually time and space restrictions resulting from the operation of a large water work. It is because the construction site must be dry during opening of earth-fill dam. So the construction must be done during technical shutdown of water structure or construction site must be protected by temporary blocking to create dry construction site. In both cases, the function of larger water structure has higher priority. The most affected part of such small hydropower plant is the intake structure which is usually built through the earth-fill dam. Other parts of small hydropower plant are

usually built on air part of the dam. Intake structure and temporary blocking in it are used as substitute for opened part of earth-fill dam during construction. And then during operation intake structure ensure water flow for turbines of hydropower plant directly from a water source (in this case it is usually reservoir or diversion cut). So intake structure is one of the most important part of whole small hydropower plant.

However, intake structures in projection and realization does not receive sufficient attention. As a result of this is the several operational problems at small hydropower plants, where water intake design was neglected. Most deficiencies in the design of the intake structure arises by copying designs from the already constructed objects with similar parameters. Despite the similarity in such sites, copying of the design does not mean the same results. Operational problems mainly affect negatively small hydropower plant with low installed power and even they become a limiting factor for their further development. Identical conditions for the construction of water intake at two different locations are practically non-existent and therefore it is necessary always to create design individually. Respectively already used design has to be reviewed for new conditions and if it is necessary it has to be modified.

3 Shaft Intake Structures

Small hydropower plants mentioned in introduction chapter usually use shaft intake structure to overcome earth-fill dams. They are named according to their shape. The design of these structures has been effected by the need of low investment costs and short construction times minimizing the impacts to the existing water structure and their operations. Therefore, a shaft intake - a specific design of intake structures has been used overcoming the vertical difference in water levels over a short distance. The first part is leaded horizontal as a conduit or channel and it is used to overcome dam and other possible obstacles. Next part is vertical shaft which leads inflow directly to intake piece of turbine. Engine room of small hydropower plant is usually located on dam heel. There are two sharp changes of flow direction close to each other (figure 1).

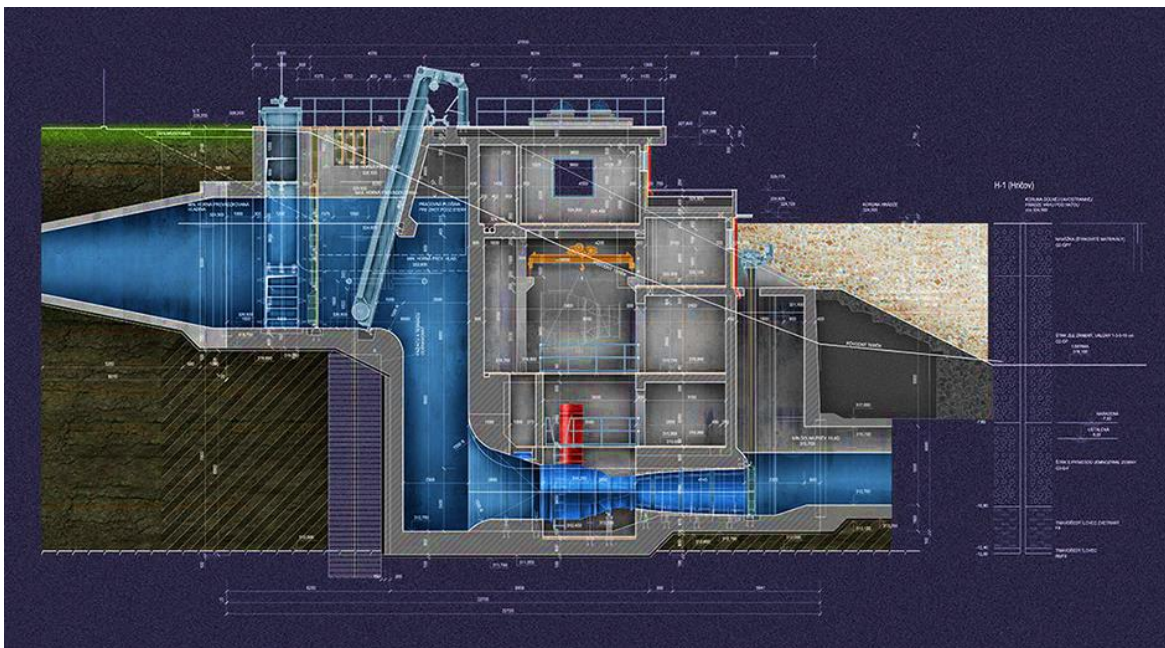


Figure 1: original design of small hydropower plant in Hričov with shaft intake structure (www.vodotika.sk).

4 Negatives of Shaft Intake Structures

The negatives of shaft intake structures are most often caused by efforts to save money, place and time during planning and realization. Perpendicular changes of direction cause higher hydraulic losses than streamline shaped intake objects [1]. Higher hydraulic losses mean lower electricity production and

hence lower profits. At the same time construction is simpler and therefore it is probably cheaper. The issue of hydraulic losses is well known to engineers skilled in the art.

The second negative is the inhomogeneously distributed velocity field at the turbine inflow. This problem is often neglected. The shape of the shaft intake structure has such a significant effect on the water flow which results in to rough operation of turbine. This has negative impact on the efficiency of the electricity production. And also service life of some mechanical parts of the turbine is shortened.

5 Inhomogeneous Distribution of Velocity Field

Lower efficiency of electricity production during rough turbine operation has been proven by physical research of Fisher and Franke [2]. The objective criteria for assessing the homogeneity of the field on the profile of turbine inlet were published in this research. The second part of their work is dedicated to completing the turbine manufacturer criteria with the criterion of the homogeneity of the longitudinal components of the turbine inlet profile. This criterion is a realistic compromise between the risk of loss of turbine efficiency and the cost of the building component of the intake structure. They used a series of tests and measurements on physical models of hydropower intakes to determine this criterion. The water flow character in the inlet facility was the subject of interest in this research. The water flow disorders were observed, for example, by the coloring of the streamlines. The impact of these disturbances on the flow stability was monitored. It was subsequently compared with the results of measurements on scaled prototypes of turbines. Based on this, intake structures can be divided into two categories: intake structures with flow disturbances and intake structures without significant flow disturbances. Their criterion is graphically represented at Figure 2. The curve of the real measured velocity field must be compared with the curve of this criterion. The curve of this criterion is a wrapping curve. If the measured values are below this curve distribution of velocity field the operation of turbine should be smooth. If the measured values are above this curve it indicates that the rough operation of turbine.

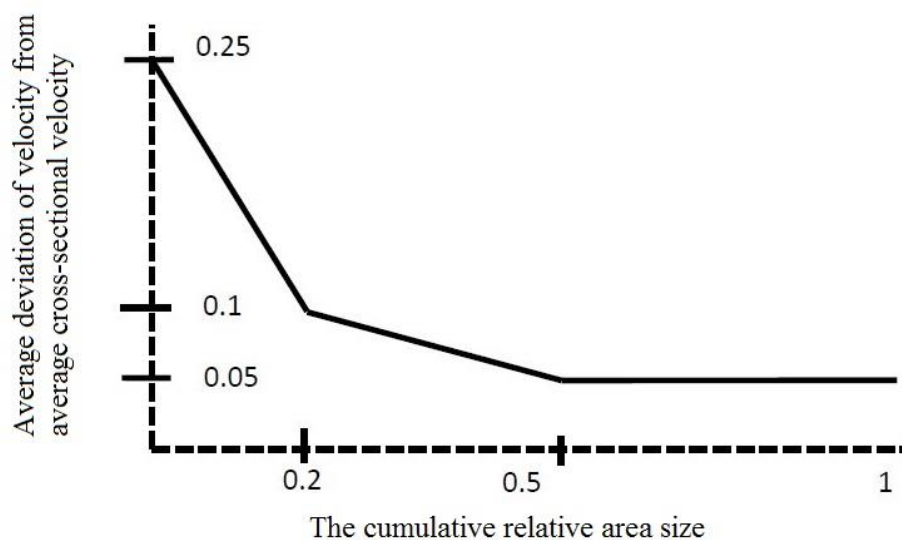


Figure 2: Evaluation criterion by Fisher and Franke.

Research based on this finding out has been carried out in the Czech Republic [2]. Measured data from real intake structures have been applied on the Fisher and Franke criterion. Losses of turbine efficiency have been confirmed by measuring of generator output. Result is that efficiency can be reduced even up to 3%. The example of this measurement is shown at figure 3.

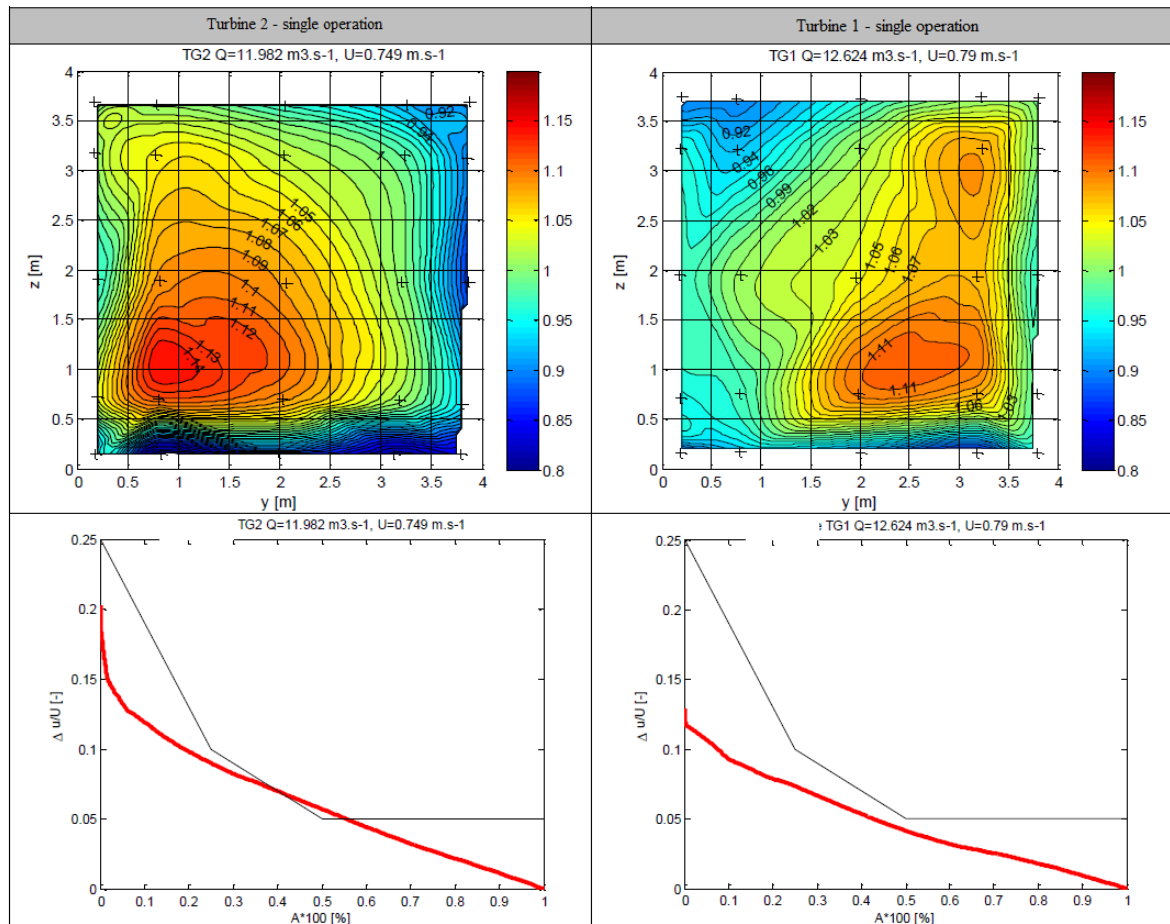


Figure 3: Comparison of measurements of two identical turbines with a different position in the intake structure.

An increased load on the mechanical parts also leads to a shorter service life of the turbine. Turbine manufacturers themselves therefore specify the conditions applied to the guaranteed turbine parameters (performance of turbine, efficiency etc.). Breach of these conditions may lead to that the guaranteed parameters of the turbine will not be achieved. Warranty conditions may also be breached. No research of the shaft intake structure has been done yet.

6 Research of Shaft intake structures

We expect operation conditions with flow disturbances according to our experiences. So we have started with research of shaft intake structures in laboratories of Department of Hydraulic Engineering at Slovak University of Technology. This research is based on comparison between different shapes of intake structures. We assume that the shaft causes inhomogeneous distribution of velocities on turbine intake especially by the vertical line. We have decided to eliminate other influence by using 2D physical model. Axial section of the intake structure is expanded all over the width of canal. Flowrate is set by the specific velocities in upper part of intake structure.

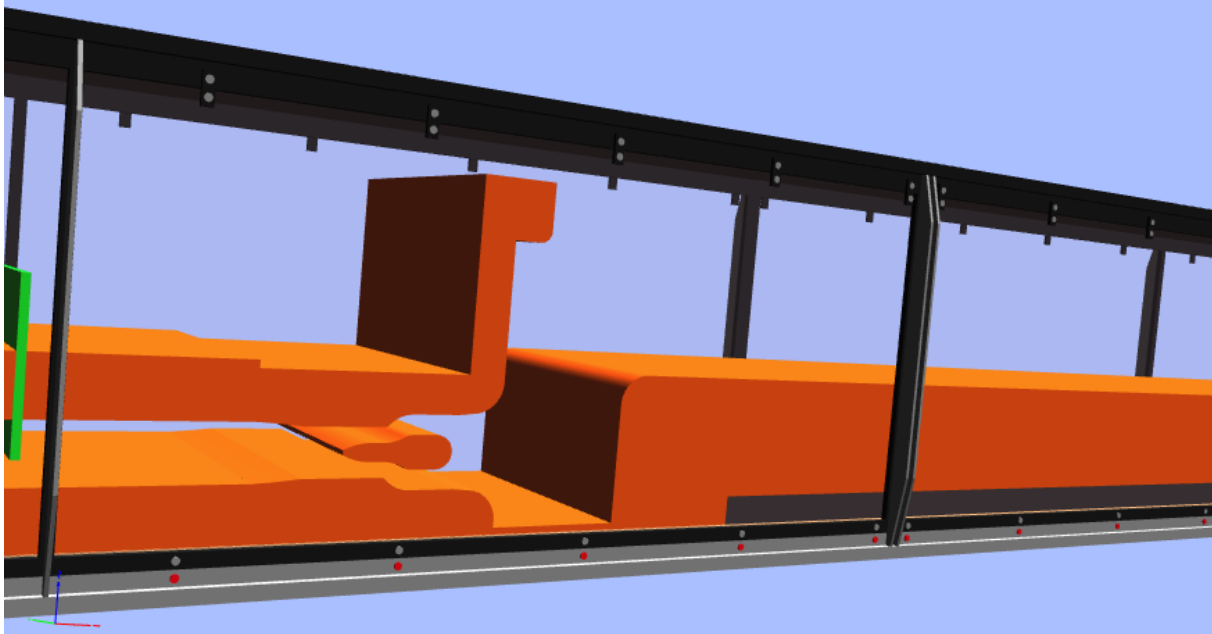


Figure 4: Visualization of physical model

We use particle image velocimetry (PIV) to measure vector maps of water flow in different intake structures. Whole model is divided into stable part and into modifiable one. Measurement of individual gating objects is performed on these days. The figure 5 shows the statistics vector map in the space in front of the turbine. It is a variant without construction to overcome the vertical difference. We plan to publish the results of other measurements together after their processing and evaluation.

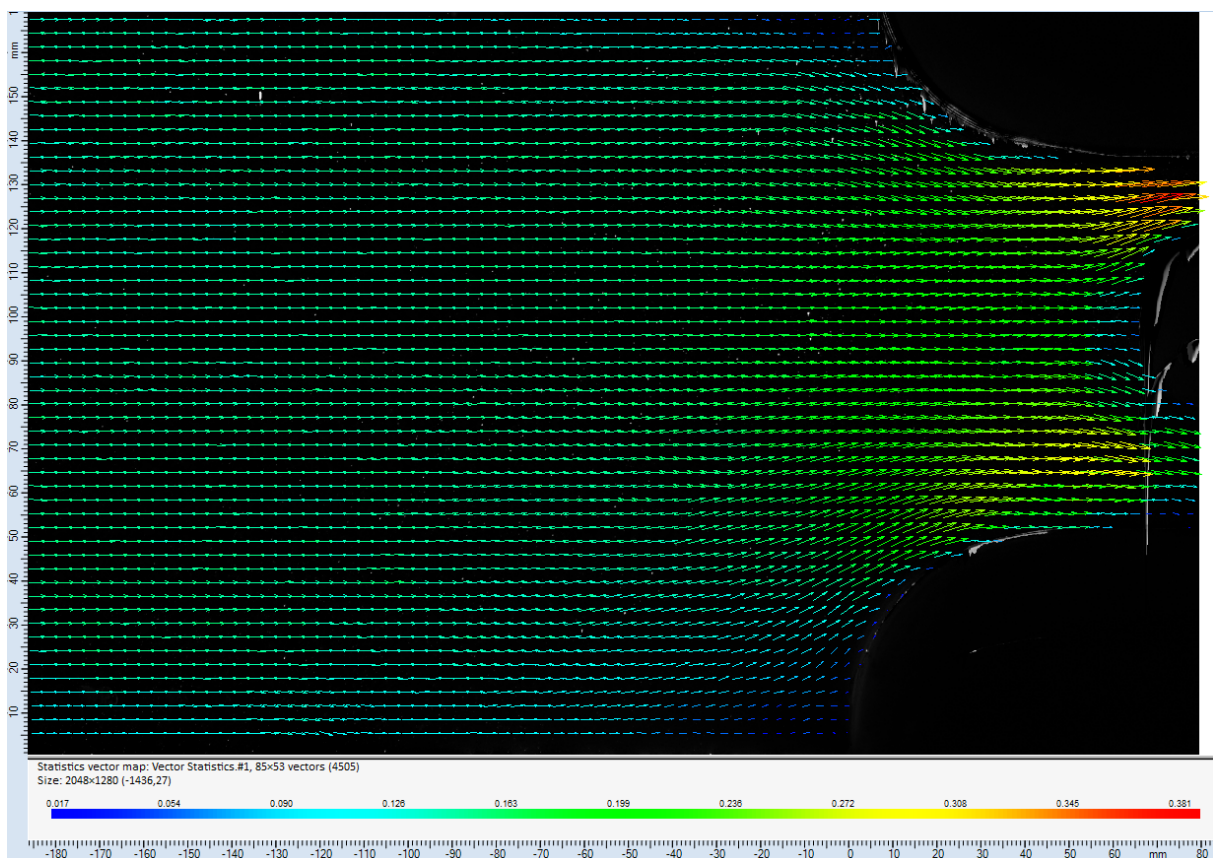


Figure 5: Example of statistic vector map – intake structure without construction to overcome the vertical difference

7 Conclusion

Our Department of Hydraulic Engineering has experiences with the measurement of different hydraulic values on the intake structures of this type. This experiences confirms problems of inhomogenously distributed velocity fields on intake structures caused by inappropriate hydraulic design. That is the reason why we have ambition to explore more about hydraulic properties of shaft intake structures. Which was not subject of any research before.

We want to achieve the relevant results with a combination of physical modeling and 3D mathematical modeling. And this knowledge should also be supplemented by experiences and measurement on the real shaft intake structures in operating. We expect that it will be possible to prove the existing hydraulic conditions of the affected small hydropower plants. We also expect that proposals to improve their hydraulic conditions will be possible to design based on results of research.

Next there will be necessary of this proposals to adapt them in to specific conditions of locations for the small hydropower plants if we want to achieve successful implementation in to operation.

In this research, we would like to contribute to solving the problems of shaft intake structures on small hydropower plants.

Acknowledgment

This paper was supported by the Grant agency VEGA under contract No. 1/0361/17 and by the Slovak Research and Development Agency under Contract No. APVV-0680- 10.

References

- [1] Mäsiar, E., Kamenský, J. *Hydraulika pre stavebných inžinierov I*. 1st ed. Bratislava: Alfa, 1985, 344p.
- [2] Fisher, R. K., Franke, G. *The Impact of Inlet Flow Characteristics on Low Head Hydro Projects; WaterPower*. 1987
- [3] Kantor, M. *Metody komplexního hydrotechnického posouzení návrhu nízkotlakých vodních elektráren: disertačná práca*. Praha: ČVUT, 2014. 148 p.
- [4] Dušička, P., Šulek, P. *Energetické využívanie vodných zdrojov*. 1st ed. Bratislava: STU, 2012. 90s. ISBN 978-80-227-3.
- [5] Dörfler, P., Sick, M., Coutu, A.: *Flow-Induced Pulsation and Vibration in Hydroelectric Machinery*, London, 2012, ISBN 978-1-4471-4252-2
- [6] Sassaman, T., Gemperline, E., Halstead, K., Lamkin, K., Kocahan, S. *Modeling: Physical Models: Why Hydro Developers Use Them in the Computer Age*. [online]. 2009 [cit. 2015-15-06]
- [7] Lichtneger, P. *Intake flow problems at low-head hydropower: Dresdner Wasserbauliche Mitteilungen*, Heft 39 (2009), P. 259-266.
- [8] Lampa, J., Lemon, D.: *Turbine flow measurement in intakes with the acoustic scintillation flow meter*, HydroTurbo 2012.

4. COASTAL ENGINEERING

MEASUREMENTS OF WATER CIRCULATION IN MARINA OPATIJA-CROATIA

DALIBOR CAREVIĆ¹, DAMJAN BUJAK², RATKO RAMUŠČAK³, TIN KULIĆ⁴, ANTE GAŠPAR⁵

¹ Faculty of Civil Engineering, University of Zagreb, Croatia, car@grad.hr

² Faculty of Civil Engineering, University of Zagreb, Croatia, dbujak@grad.hr

³ Faculty of Civil Engineering, University of Zagreb, Croatia, rramuscak@grad.hr

⁴ Faculty of Civil Engineering, University of Zagreb, Croatia, tkulic@grad.hr

⁵ Faculty of Civil Engineering, University of Zagreb, Croatia, agaspar@grad.hr

1 Abstract

The circulation of water between a harbor and the connecting sea is generally the result of natural parameters such as local tidal range, wind conditions, wave climate and water density differences (Fischer, 1979, Shwartz, 1988, Nece, 1984, Falconer, 1991). Depending on the geographical location, one or more of these variables can dominate the exchange properties of a harbor. This paper presents site measurements conducted in marina Opatija (Croatia) during 40 days of winter period. These measurements make able to get an insight in real processes, i.e. wind influence, which is hard to produce in a laboratory; the influence of wave actions and some other phenomena that could be observed only in nature.

Keywords: water renewal, flushing culvert, field measurements, breakwater, wind waves

2 Introduction

A critical feature that must be considered in harbor design and construction is the water quality within the basin, which depends on water renewal between the harbor and the surrounding water body [1]. To reduce water pollution, marinas should be located, designed, built and maintained to coexist with fish and wildlife habitats that exist in the vicinity [2]. Potential negative impacts related to marinas (e.g. habitat destruction, especially in ecologically sensitive areas) can be avoided, mitigated or significantly reduced by environmentally conscious development and planning, observance of recommended environmental best management practices and adherence to environmental regulations. Water quality in a harbor depends largely on the rate of flushing in the basin, which depends in turn on how well water circulates inside the marina. Recent studies have shown that adequate flushing improves water quality, reduces or eliminates water stagnation and helps maintain biological productivity and aesthetic appeal [3].

The circulation of water between a harbor and the surrounding sea is generally the result of natural generators of flow such as local tidal range, wind conditions, wave climate and water density differences [4–7]. Depending on the geographical location, one or more of these factors can dominate the exchange properties of a harbor. If pollutant concentrations are allowed to increase above critical levels, then the result is sub-standard water quality as characterized by a reduction in dissolved oxygen and the presence of algal blooms. Detrimental water quality within a harbor can be avoided by reducing the potential sources of pollutants, and by maintaining an optimal flushing rate. The water renewal rate is a function of structural factors such as the plan form geometry of the harbor, entrance dimensions of the harbor; water depth, bed slope, etc. [6,7], which are well investigated. Flushing rate, in low tide oscillation areas, are often improved using flushing culverts (pipes or rectangular openings in a breakwater body, diameter/dimension $D \sim 1\text{m}$), which are the most cost-effective method used in port engineering. The purpose of culverts is to enable the exchange of open sea water and the sea water contained within a protected maritime zone. Conducted research on flushing culverts, partially elaborate the basic physical processes of the flushing culverts functioning. They mainly focus only on two circulation generators: wind actions (shear stress) and waves forcing. Tidal forcing has often been omitted as insufficient for flushing processes in areas of observation.

Surface wind waves hitting the seaward side of the breakwater under a certain incident angle are generated through the action of winds blowing from particular directions. In the process, flushing culverts, under the influence of waves, allow the flow of sea water through the body of breakwaters hence enriching the harbor's 'dead zones' with fresh sea water [8,9]. Most research was conducted under the assumption that wave energy transmission translates into volume flow through the culvert. Lately some research was done, that measured the velocities inside the culvert directly [10]. The researchers observed that wave transmission does not necessarily lead to net volume inflow through the culvert. Wind forcing on the flushing culverts functioning is modestly investigated through the use of numerical models [11,12]. Authors combined two positions of the openings in the breakwater body with different directions of the wind and unique wind velocity. Both investigated positioning of openings in breakwater body in presence of only wind forcing. Researchers made general conclusion that water exchange is influenced by positions of openings in breakwater and wind direction. The importance of the openings position on the overall harbor flushing rate and the possibility of the flushing time reduction up to 50% was emphasized.

The application of the culverts is justified in low tidal range areas (such as Adriatic Sea, Aegean Sea) where tidal range is insufficient for adequate water exchange [13]. Due to these reasons, all significant researches connected to flushing culverts come from countries with similar oceanographic conditions, from Greece and Turkey in Aegean Sea [8–11,13–18].

In an initiative to further improve flushing culvert design, extensive field measurements have been conducted in ACI marina Opatija to examine the influence of various natural generators on culvert flow.

3 Methods

It has been established, that there have not been any field measurements conducted in marinas with constructed culverts. Measuring in nature can give insight into processes that are difficult to produce in a laboratory (e.g. wind influence). The Opatija marina is chosen as suitable location, since it has 8 built-in 1 m diameter culverts placed in the breakwater. The top of the culvert is positioned at the mean sea level and the offset distance between each culvert is 0.5 m. The Opatija site also has favorable orientation in terms of wind, with frequent north-northeast and south-southwest winds.

On February 15, 2017, five ADCP devices, four CTD probes, one PCM device, anemometer and camera were positioned in ACI marina Opatija (Figure 5). ADCP (Acoustic Doppler current profiler) is a hydraulic flow meter similar to a sonar. The device measures sea depth using a pressure sensor at the top of the ADCP and can also measure temperature. It slices the depth into bins by the user defined bin size and then measures velocities at each bin utilizing the Doppler effect of sound waves. ADCP transmits sound waves and measures the frequency shift in waves reflected from particles flowing in the water at each bin. By using multiple beams in four cardinal directions, it is possible to determine the velocity magnitude and direction of flow in numerous bins in the sea, depending on the frequency of the signal being transmitted. It should be considered, that ADCP devices have a blind spot just above the head of the device, before the first bin starts (this value for each ADCP can be observed in Table 2).

Divers positioned the ADCP2 roughly 2 m away from the culvert and the sensor head was 0.4 m below the bottom of the culvert (Figure 6). Vessels can be in a very close proximity to the flushing culvert and consequently, their movement in the marina can affect the hydrodynamics at the measuring location of ADCP2 (vessel position at equipment deployment can be observed on Figure 6 and Figure 7). The height of the water column above the ADCP at deployment was 1.3 m which is close to the mean sea level. A concrete slab spanning 12 m is above the culvert leeward exit and ADCP2 where goods are transported and transferred to vessels in the marina.



Figure 5. Layout of measuring devices in small marina Opatija; ADCP- sea current profiler, CTD- salinity and temperature; PCM- velocity and discharge in the flushing culvert; Anemometer – wind magnitude and direction

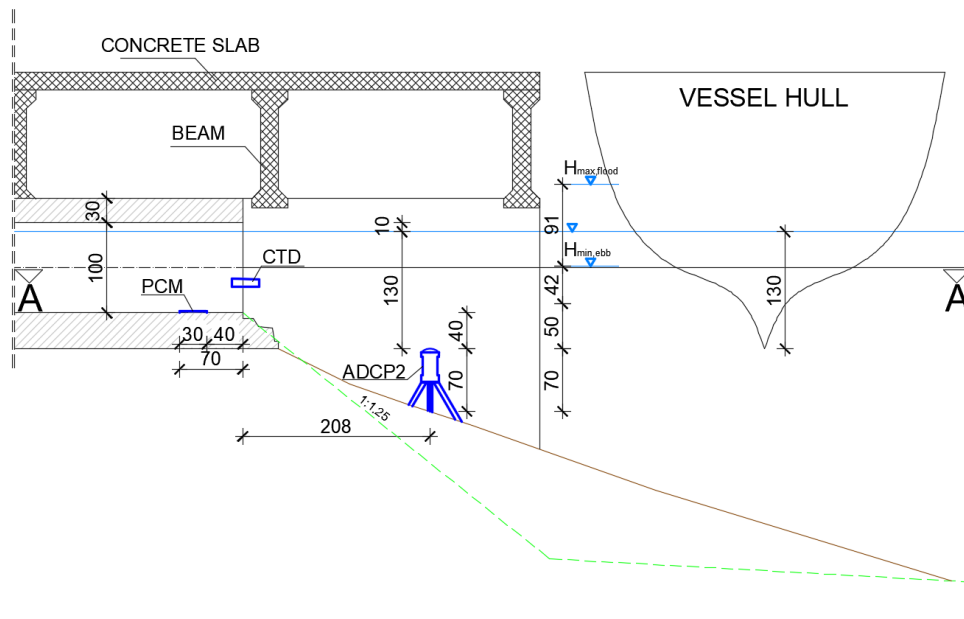


Figure 6. Cross section (B-B from Figure 7) of the breakwater at the position of the flushing culvert

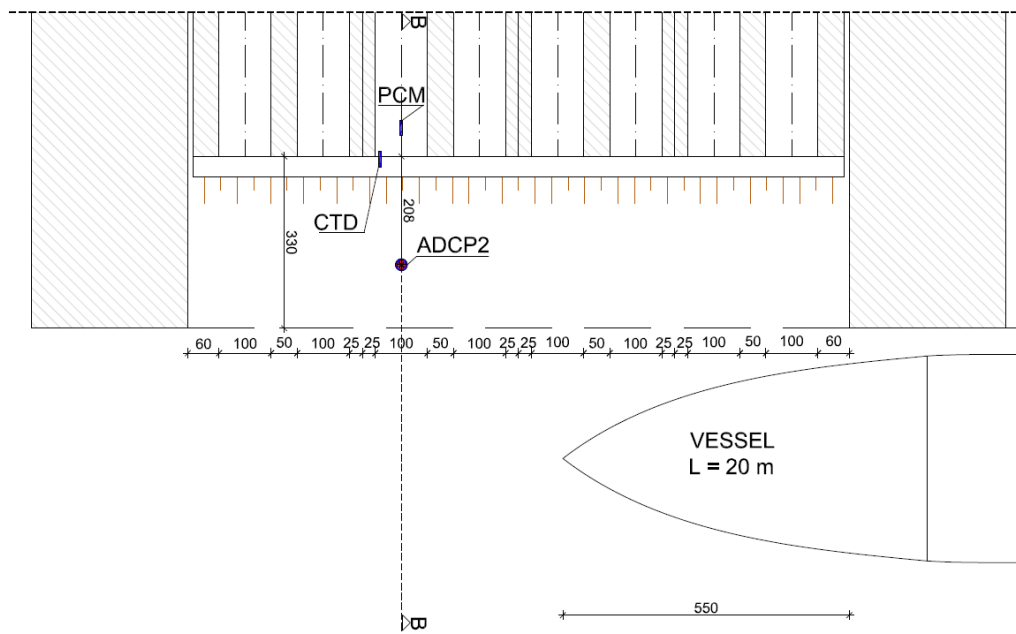


Figure 7. Plan of device deployment (A-A from Figure 6)

Table 2. ADCP settings, location depth and temperature and measuring period

	depth [m]	temp [°C]	first bin height [m]	cell size [m]	instrument frequency [kHz]	meas. period
ADCP1	13,5	10,5	1,61	1,0	600	15.02.-31.03.
ADCP2	1,3	10,8	0,44	0,1	1200	15.02.-31.03.
ADCP3	33,9	10,3	0,50	1,0	300	15.02.-23.03.
ADCP4	6,8	10,3	0,50	1,0	300	15.02.-23.03.
ADCP5	5,6	11,1	0,80	0,5	1200	16.02.-31.03.

The Portable Current Meter (PCM) is an ultrasonic flowmeter designed for measuring flow (measures depth using a pressure sensor and velocity profile using ultrasonic waves) in various kinds (user input) of cross sections. The sensor is located 40 cm before the leeward end of the culvert (Figure 6 and Figure 8). The central unit and its associated battery are located underneath a concrete slab, but above the maximum sea level to avoid undesired contact with the sea. The CTD probe is located in the culvert next to the PCM sensor (Figure 6 and Figure 8). CTD is often used as an instrument in oceanography whose primary task is to measure the salinity and the temperature at sea. By linking the values of temperature and salinity it is possible to determine the density of the sea which can be a critical generator of flow. Wind speed and direction was measured by anemometer positioned, only for this purpose, on the marina's lighthouse at the head of the breakwater. This is quite important due to uncertainty of wind data from Rijeka meteorological station which is 10 km away and especially due to mountainous configuration of terrain which can change the wind current. An ultrasonic anemometer without moving parts was used to maintain the reliability of the measurement while simultaneously minimizing maintenance and damage potential. The anemometer was plugged directly into the power grid in conjunction with a backup battery that would be used in an occurrence of a black out. Next to the anemometer, a time lapse camera was mounted on the lighthouse. The camera shoots one image every 5 minutes during the measurement period. Number of vessels in marina and their positions, same as picture of a real conditions, are captured by the time lapse camera positioned at the lighthouse. After recovering the equipment from the marina on 31.3.2017., processing of the recorded measurements began.



Figure 8. PCM and CTD probe at the culvert; ADCP2 at the leeward side of the culvert; snapshot of the time lapse camera located at the head of the breakwater

4 Results and discussion

Water level oscillations were recorded on all measuring devices presented in Figure 5. Recorded oscillations are identical so only data from PCM were presented in Figure 9. Calculated residuals are in range between ± 0.1 m what show relatively good agreement between measured and predicted data. Only one situation between March 4 and 6, 2017 shows greater residuals what refers to some stronger atmospheric influence.

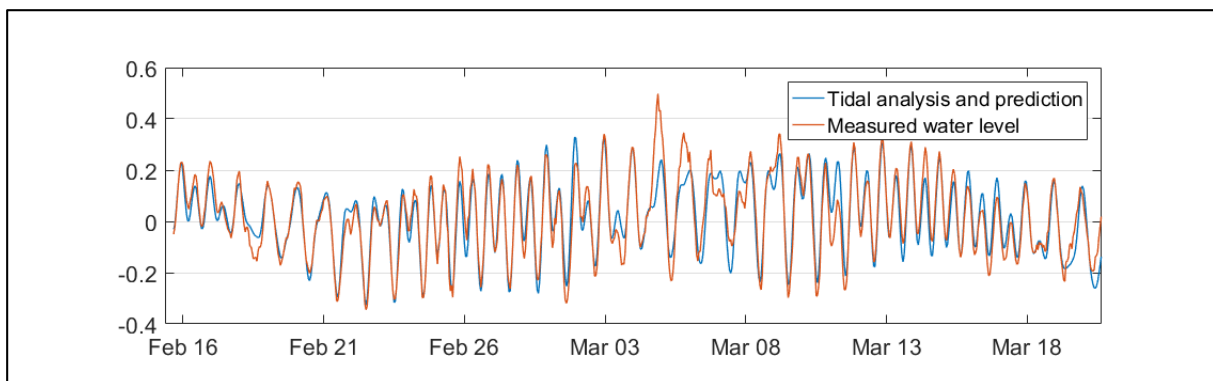


Figure 9 Water level oscillations in marina Opatija recorded on PCM

Wind measurements are presented in Figure 10 as vector diagram of hourly averaged wind velocities. In the measurement period, it was observed several stronger wind situations: Situation 1 (23.2.17. 13:00 - 25.2.17. 20:00); Situation 2 (28.2.17. 5:00 - 1.3.17. 17:00); Situation 3 (4.3.17. 7:00 - 5.3.17. 23:00); Situation 4 (7.3.17. 2:00 - 8.3.17. 1:00) and Situation 5 (10.3.17. 5:00 - 11.3.17. 7:00). First three situations were directed from sector SW-S and other two from sector NE-E. Several other wind situations were recorded but due to smaller velocities these are not underlined hereinafter.

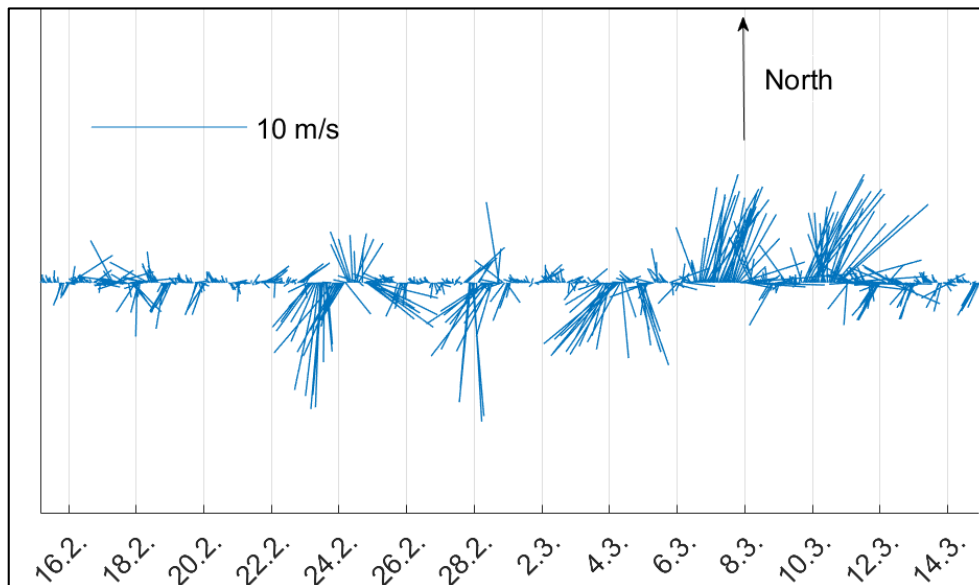


Figure 10 Vector diagram of hourly averaged wind velocities measured with anemometer in a marina

Results from ADCPs are presented in Figure 11 as hourly averaged vector diagrams in measurement period. Each vector represents depth-averaged value in one hour period. The mean value of sea current velocity (in measurement period from 16.02.2017-31.3.2017) calculated on ADCP1 is 4,2 cm/s, what is larger than at the ADCP3 3,1 cm/s which is positioned at outward side of breakwater same as ADCP1. This difference occurs due to averaging throughout the greater depth (33.9m) in the case of ADCP3 than in the case of ADCP1 (13.5m). Lower sea levels at the depths greater than approximately 18m are less influenced by wind what gives smaller velocities and consequently smaller depth-averaged values presented in Figure 11.

The sea currents caused by winds is also observable from Figure 11. That is clearly visible for the wind situation 1 from sector SW-S, which causes sea currents in the same direction. Already mentioned influence of depth averaging is pronounced between ADCP1 and ADCP3 where much larger values of depth averaged velocities are calculated in the case of ADCP1. Greater sea velocities are measured at the surface level, where average value for period of the situation 1 was 26.2cm/s (ADCP1). Similar situations are evident for the situations 2 and 3. Wind situations 4 and 5 from sector NE-E cause occurrence of sea currents with certain delay of approximately 10 hours what is response time of the water body.

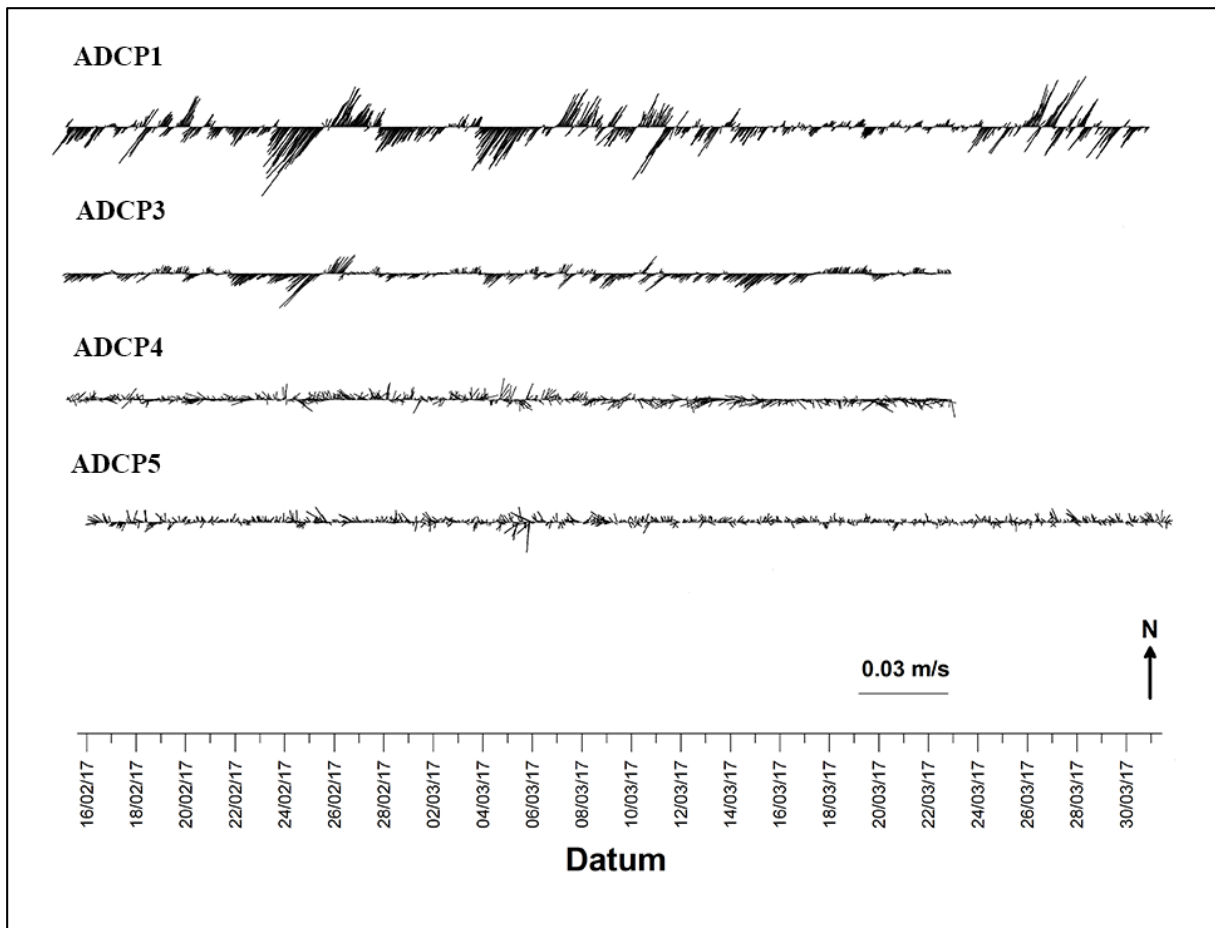


Figure 11 Hourly and depth averaged sea velocities at positions of ADCPs

ADCP 4 and 5 are protected by breakwater so calculated depth-averaged velocities gives lower values. The mean value of sea current velocity (in measurement period from 16.02.2017-31.3.2017) calculated on ADCP4 is 4,1 cm/s and ADCP5 is 0,2 cm/s.

ADCP1 was set up to measure directional wave spectra. The maximum significant wave height measured for situation 1 was $H_s=0.89\text{m}$, for situation 2, $H_s=0.86\text{m}$, for situation 3, $H_s=1.2\text{m}$, for situation 4, $H_s=0.48\text{m}$ and for situation 5, $H_s=0.34\text{m}$. The fetch from sector SW-S is 15km and from NE-E is 5km what describes smaller wave heights in situations 4 and 5.

CTD device was used to measure salinity and temperature in pipe (Figure 12) but also pressure using pressure gauge built-in. Due to variation in sea level (Figure 9) it is possible to record salinity and temperature profiles as it is presented in Figure 12a as hour averaged values. The higher recorded values are 37g/kg in deeper layers below depth 0.6m and the lowest is 14.5g/kg at the depth of 23cm below water surface. It is visible that salinity decreases significantly in the surface layer what reveals that fresh water from underwater springs flows in surface layer with thickness of approximately 0.6m. This fresh water layer moves together with tidal oscillations in vertical direction and cause that flushing culvert is sometimes filled with fresh water in the case of ebb tide and on the other hand in the case of flood tide with sea water. Temperature profile reveals relatively uniform distribution of temperature around 10°C.

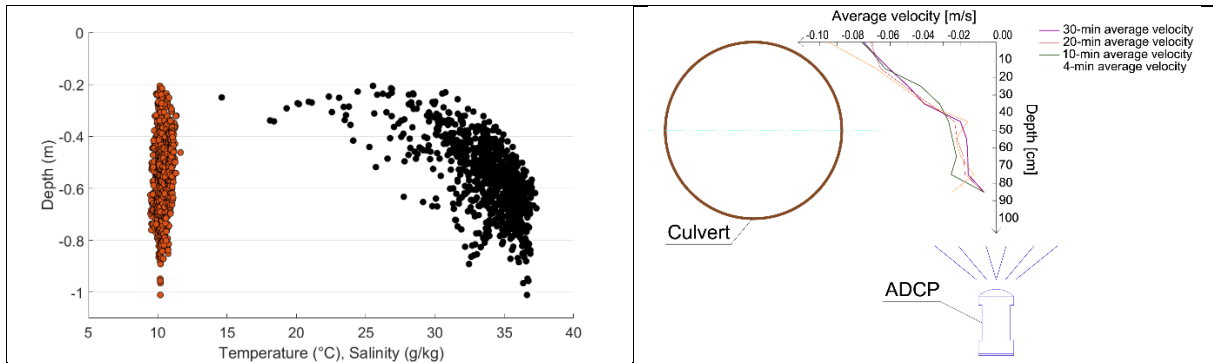


Figure 12 a)Salinity profile measured using CTD gauge positioned in pipe; b)velocity profile measured 15.2.2017. 21:10:00 with ADCP2 for different averaging periods 4, 10, 20 and 30min; velocities directed outward side of marina

In front of the pipe (Figure 6 and **Figure 8**) ADCP2 have been used for measuring of velocity profile. Raw measurements with sampling interval of 1 min. were averaged with periods of 4, 10, 20 and 30 min to analyze influence of averaging on final vertical profile. Example of such analysis is presented in Figure 12b where is visible that surface layer with thickness around 0.6m have greater velocities than deeper layers in that specific period of measurement. This proves outflow of relatively fresh water in the surface layer.

Figure 13 shows flowrate records measured by PCM positioned in the flushing culvert. It is obvious that in relatively calm period (Feb 26 – Feb 28), period without strong wind, recorded flowrate is small value close to zero with negative sign. This means that underwater springs flow is dominant. During the stronger wind situations, it is obvious that flowrate increases altering sign with oscillation periods close to tidal period. During the wind situations, complex mechanism of water exchange through the flushing culverts occurs which includes water movement forced by wind, waves forcing from open sea, sea surface tilt caused by wind and underwater springs flow. Generally, conclusion is that wind produce additional flowrate through the flushing culverts and consequently increase water exchange in closed basin.

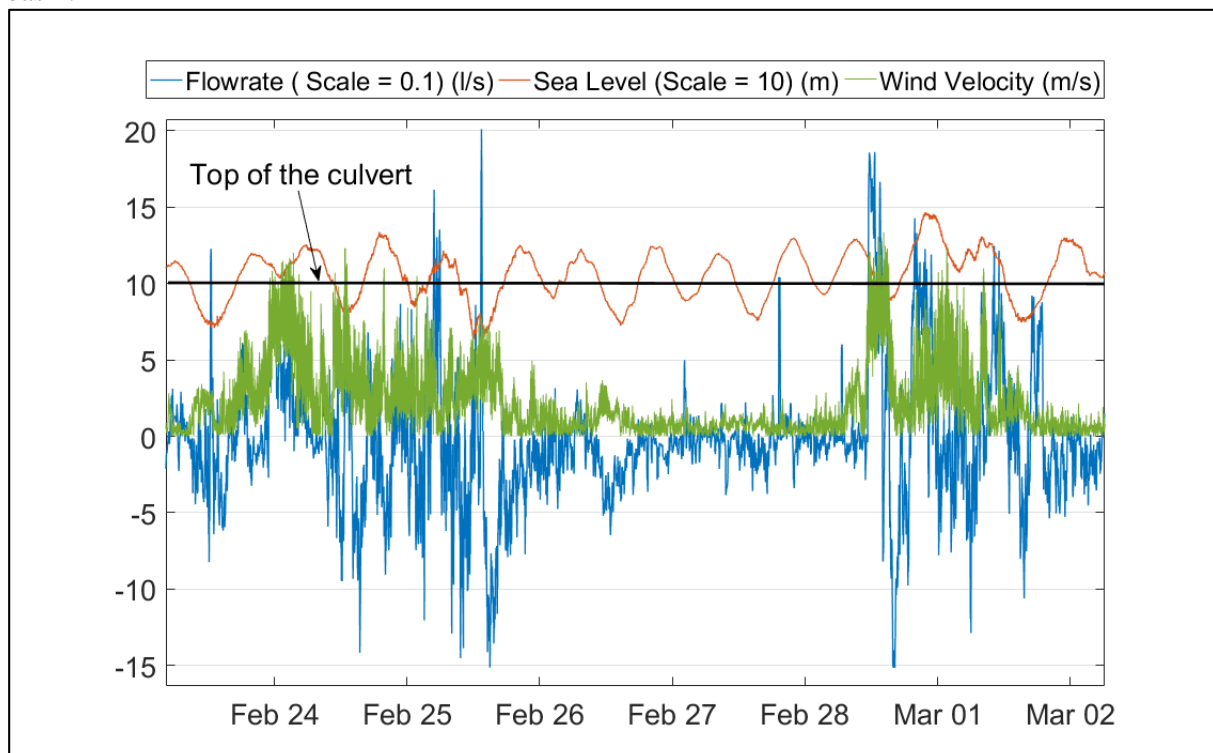


Figure 13 Recorded hourly averaged time series of flowrate through the flushing culvert (+ leeward, - seaward direction), sea level and wind velocity

The total volume of water passed through the one flushing culvert is presented in Figure 14. It is cumulative volume of water which had passed through the flushing culvert in both directions, leeward and seaward side. This curve shows that the flow is dominantly directed toward outward side, the most possibly due to discharge from underwater springs. If one approximates this curve by linear function, the inclination of this function represents average discharge in the measurement period. Such calculation gives 25 m³/h. At the other hand if one calculates average discharge produced by tidal oscillations as $Q=P/T$, where $P=0.4*40000=16000$ m³ is average tidal prism volume and T is 12h25min for semidiurnal tides, it gives $Q=1288.7$ m³/h. Such volumetric comparison leads to conclusion that average discharge caused by tidal variation is ~6 times greater than discharge through eight flushing culverts embedded in breakwater body.



Figure 14 Total volume of water passed through the one flushing culvert

5 Conclusion

Extensive measurements have been conducted in marina Opatija with purpose of gathering of hydraulic data which could reveal natural mechanisms of water exchange in small harbors. Specific for this location is small tidal oscillation range which was in the measuring period around 0.8m. This means that water exchange in harbor is forced not dominantly by tidal oscillations but also winds. Measuring wind speed together with flushing culvert discharge it has been revealed that discharge through the flushing culverts is multiplied several times in periods of stronger wind situations than in the case without it. It has been found that average discharge through the eight flushing culverts embedded in breakwater body is approximately six times smaller value than average tidal discharge. It should be pointed out that discharge through the flushing culverts is caused by strong submarine springs together with tidal oscillations and wind. Sea currents were measured using five ADCP devices aiming to collect extensive database for the purpose of numerical model calibration.

Acknowledgements

This work has been fully supported by the Croatian Science Foundation under the project number UIP-2014-09-6774.

References:

- [1] US Army Corps of Engineers, Coastal Engineering Manual, 2002.
- [2] US Environmental Protection Agency Staff, Environmental Engineering for Small Boat Basins, 1993.
- [3] J. Yin, R.A. Falconer, K. Pipilis, A.I. Stamou, Flow Characteristics and Flushing Processes in Marinas and Coastal Embayments, Proc. 1st Int Conf Marit. Eng. Ports. (1998) 88–98.
- [4] H.B. Fischer, E.J. List, R.C.Y. Koh, J. Imberger, N.H. Brooks, Mixing in inland and coastal waters, Acad. San Diego Calif. 114 (1979) 315–316. doi:10.1017/S002211208223028X.
- [5] R.A. Schwartz, J. Imberger, Flushing Behaviour of a Coastal Marina, Coast. Eng. Proc. 1 (1988) 2626–2640.
- [6] B.R.E. Nece, F. Asce, Planform effects on tidal flushing of marinas, J. Waterw. Port, Coast. Ocean Eng. 110 (1984) 251–269. doi:10.1061/(ASCE)0733-950X(1984)110:2(251).
- [7] R.A. Falconer, Guoping Yu., Effects of depth, bed slope and scaling on tidal currents and exchange in a laboratory model harbour, Proc. Inst. Civ. Eng. Part 2. 91 (1991) 561–576.
- [8] V.K. Tsoukala, C.I. Moutzouris, Wave transmission in harbors through flushing culverts, Ocean Eng. 36 (2009) 434–445. doi:10.1016/j.oceaneng.2009.01.005.
- [9] V.K. Tsoukala, C.K. Gaitanis, A.I. Stamou, C.I. Moutzouris, Wave and dissolved oxygen transmission analysis in harbors using flushing culverts: An experimental approach, Glob. Nest J. 12 (2010) 152–160.
- [10] D. Stagonas, G. Müller, D. Magagna, D. Warbrick, Fundamental investigation of water flow in harbors through a flushing culvert, in: Water Eng. a Sustain. Environ. Ranging, 2009: pp. 7288–7295.
- [11] I. Stamou, I.K. Katsiris, C.I. Moutzouris, V.K. Tsoukala, Improvement of marina design technology using hydrodynamic models, Glob. Nest J. 6 (2004) 63–72.
- [12] G. Fountoulis, C. Memos, Optimization of openings for water renewal in a harbour basin, J. Mar. Environ. Eng. 7 (2005).
- [13] E. Ozhan, E. Tore, Studies for Improving Flushing Ability of Marmaris Marina, Comp Mech Publ. (1992) 267.
- [14] C.K. Gaitanis, E. Douka, V.K. Tsoukala, A.I. Stamou, C.I. Moutzouris, Dissolved Oxygen Transmission in Harbor Basins Through Flushing Culverts, in: Proc. 11th Int. Conf. Environ. Sci. Technol., 2009: pp. 285–292.
- [15] V.K. Tsoukala, V. Katsardi, K.A. Belibassakis, Wave transformation through flushing culverts operating at seawater level in coastal structures, Ocean Eng. 89 (2014) 211–229. doi:10.1016/j.oceaneng.2014.08.009.
- [16] V. Katsardi, G. Boundris, V.K. Tsoukala, K.A. Belibassakis, Study of wave transformation due to flushing culverts in coastal structures, Proc. Int. Offshore Polar Eng. Conf. 4 (2012) 1356–1363.
- [17] K.A. Belibassakis, V.K. Tsoukala, V. Katsardi, Three-dimensional wave diffraction in the vicinity of openings in coastal structures, Appl. Ocean Res. 45 (2014) 40–54. doi:10.1016/j.apor.2013.12.005.
- [18] L. Balas, A. Inan, Modeling of induced circulation, WSEAS Trans. Fluid Mech. 5 (2010).

5. GEOTECHNICAL ENGINEERING

IMPLEMENTATION OF EUROCODE 7 IN THE DESIGN OF FLOOD PROTECTION EMBANKMENTS IN CROATIA

MARIO BAČIĆ¹, MEHO SAŠA KOVAČEVIĆ¹, LOVORKA LIBRIĆ¹

¹ Faculty of Civil Engineering, University of Zagreb, Croatia, mbacic@grad.hr, msk@grad.hr, llibric@grad.hr

1 Abstract

The implementation of Eurocode norms in civil engineering design procedures led to a necessity for certain modification of designer's mindset. The significance of this design approach comes to fore during design of specific structures such as flood protection embankments. To fulfil Eurocode requirements, a designer must consider series of design situations, which are reasonably expected during the lifetime of an embankment. These design situations, present the core of design using Eurocode 7 and it is crucial to identify them. This paper deals with design procedures starting from proper identification and interpretation of investigation works in order to obtain relevant ground model to analysis of both ultimate limit states (ULS) and serviceability limit state (SLS). Further, an importance of designer's role in overall project of flood protection embankment is stressed out.

Keywords: flood protection embankment, Eurocode 7, design situations, ultimate limit states, serviceability limit states, partial factors

2 Introduction

There is a well established hierarchy regarding acts, regulations and norms in civil engineering activities in Croatia, which can be seen on figure 1. Building Act [1], with last version published in 2014, is highest-level document and it consists of articles giving general remarks regarding design and construction of structures, but it is not its purpose to go into specific details for each type of structure. One step below, there are Technical Regulations for Building Structures [2], published in 2017, which give some concise remarks which are obligatory for a designer to take into account. However, this document can still be considered as too general in providing information necessary for design of specific type of structure.

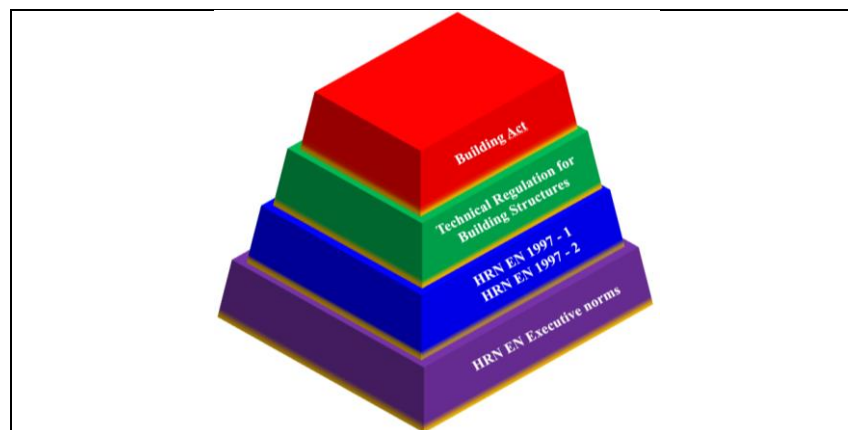


Figure 1. Hierarchy regarding acts, regulations and norms in civil engineering activities in Croatia

More concrete information for design can be found in third level of hierarchy, where Eurocode norms are located. This European standard was adopted in 2004 by European Committee for Normalization (CEN) members [3] and it became a relevant standard for all EU and CEFTA countries. Further, it was defined that by the end of 2006 some specificities will be given through National Annexes. These norms superseded Eurocode pre-norms, relevant from 1994, when they substituted Yugoslavian standards. Current relevant norm, when it comes to design of flood protection embankments as typical geotechnical structure, is HRN EN 1997-1 [4], along with National Annex [5]. By recent publication of newest

version of higher-level Technical Regulations, an additional legitimacy is given to Eurocode norms, since the obligation for their usage is stressed - out, making a step forward of being just a document of 'good practice'. Eurocode norms are also related to Execution Standards, linked with execution of some special geotechnical works, which are located in fourth level of presented hierarchy.

Due to different practice of design of geotechnical structures between CEN member states, mostly due to geological specificities and local experience, Eurocode 7 only gives a sort of design framework which is in line with modern knowledge in field of geotechnical engineering. Norm distinguishes design principles which are mandatory and application rules that meet the principles but are not mandatory. The application rules are general and do not provide detailed instructions for applying particular design procedures, so the designers needs to look for help in other standards or they need to consult the relevant newer expert literature [3]. Unfortunately, this sometimes leads to confusion were flood protection embankments designers have some doubts regarding what needs to be fulfilled, mostly because they expect to have strict design procedures which were, at smaller or larger scale, given in previous standards. This fact came to fore in recent period when there is an increasing trend of reconstruction of existing and construction of new of flood protection embankment in Croatia, where designers are faced with many challenges. This increasing trend is result of fact that condition of most flood protection embankments is generally on a low level, mainly due to lack of investment funding, accompanied with large economic crisis in last few years, what eventually led to the absence of routine maintenance efforts [6]. Additionally, embankments are now subjected to loads for which they were not primarily constructed such as higher water levels due to climate change, etc.

Based on what is mentioned, this paper gives insight in principles of using Eurocode 7 for design of flood protection embankments with the focus on relevant limit states to be checked. Also, a role of a designer in overall project activities will be explained.

3 Design of flood protection embankments according to Eurocode 7

Eurocode generally consists of ten parts where most of them are so called 'material standards' dealing with concrete, steel, composite, wood, masonry and aluminium structures. The other parts, 'basis of structural design' (EC 0), 'action on structures' (EC 1), 'geotechnical design' (EC 7) and 'design for earthquake condition' (EC 8) can be directly applied to all types of structures. Even though designers of flood protection embankments adhere mostly to Eurocode 7, sometimes a design must cover other types of structures such as culverts or locks and therefore other parts of Eurocode should be looked upon. Beside main Eurocode 1997-1 norm [4], designer must consult also National Annexes [5] which should provide information on specific requirements and nationally determined parameters. Since it was shown that this information could still be insufficient to provide comprehensive approach for design of flood protection embankments, but also to prevail difficulties and doubts posed by implementation of Eurocode, some countries have developed Non Contradictory Complementary Information (NCCI) for flood protection embankments. The National Annex may contain references to non-contradictory complementary information to assist the user to apply the Eurocode, but the provision of other material should be in documentation separate from the National Annex, whether endorsed by a national competent authority or published independently [7]. To assist implementation of Eurocode, some institution have published guideline [8] regarding implementation of Eurocode 7 whose aim is '*to improve clarity on key issues relating to flood protection embankments*'. Even though this gives additional interpretations of Eurocode norms which are indeed useful, a guideline covers design through design approach 1, which is not relevant in Croatia. Also, a seismic consideration are not included, due to fact that they were developed as guidance to designers in countries which do not have significant seismic events, which are of importance in Croatia. Generally, a designer of flood protection embankment needs to ensure its hydraulic and overall stability, and some sources [8] stress out that, if required, a resilience to withstand overtopping should be checked, even though the Eurocode 7 does not adhere to this element. To fulfil these requirements, a designer must be familiar with the terminology used in Eurocode 7, which is unique. Even though the range of used terms is large, some of them must be explained such as *resistance – action relationship*, *design situation* and *limit state*.

Resistance - action

A designer's main aim is to ensure that design resistances are greater than the design actions, where resistance is defined as '*capacity of a member or component, or a cross – section of a member of component of a structure to withstand actions without mechanical failure*', while action is defined either as direct actions ('*set of load applied to the structure*') or indirect actions ('*set of imposed deformations or accelerations*'). The actions can be either permanent (for embankments it is usually body mass), variable (for embankments it is usually change of pore pressures), accidental or seismic (earthquake).

Design situation

Design situations are particular sets of circumstances that the design should accommodate in order to fulfil its function, and it is up to designer to take into account all relevant design situation for flood protection embankment. Generally, design situations are classified based on the duration and likelihood of their occurrence as persistent, transient, accidental or seismic. When it comes to flood protection embankments it is common to address the following design situations:

- construction
- normal operating conditions
- flood event
- rapid draw down
- seismic event

Limit states

Eurocode 7 requires verification of not exceeding limit states for each design situation. Limit states represent those states beyond which the behaviour of the structure would be unacceptable. There are two types of limit states:

- ultimate limit state (ULS)
- serviceability limit state (SLS)

3.1 Ultimate Limit State (ULS)

When it comes to the design of flood protection embankments, relevant ultimate limit states include those linked with hydraulic stability – uplift / buoyancy (UPL) and hydraulic heave, internal erosion and piping (HYD). Some other ULS defined by Eurocode 7, such as equilibrium (EQU) and structural (STR), are usually not relevant even though they should be considered if there is structural element in scope of flood protection measures. The embankments are, in Eurocode 7, considered through chapter 12, which is the shortest one in whole norm [9], and which applies to '*embankments for small dams and for infrastructure*'. But it is not elaborated what term '*small*' means. Frank et al. [10] state that it may be appropriate to assume that it deals with embankments of a height up to approximately 10 m. However, a designer will find more design – relevant information in other chapters of norm, where relevant provisions on securing hydraulic stability can be found in section 10 '*Hydraulic failure*' while overall stability is considered in chapter 11 '*Overall stability*'. To understand the concept of dealing with ultimate limit states, some additional remarks must be stressed out.

As it is stated earlier, main aim for designer is to ensure that design resistance are greater than the design action. The question remained on what are design values and how to obtain them. Design values of actions, materials and resistance are obtained by applying appropriate margin of safety through principal of partial factors. Partial factors on actions (γ_f) are applied on representative values of action to obtain design values of action, where partial factors depend on whether the action is permanent or variable, as well as on whether action is favourable or un unfavourable. Design values of material parameters are determined by applying partial factors on materials (γ_m) on characteristic values and design values of resistance are obtained by applying partial factor on resistance (γ_r) on its characteristic values. The complete list of partial factors is given in Eurocode 7 main part, but most of these values are determined as NDP's (Nationally Determined Parameters) through National Annexes.

Since water has crucial role not just in HYD and UPL limit states, but also in GEO through the pore pressure values, it should be noted that Eurocode states that '*design values of ground-water pressures*

may be derived either by applying partial factors to characteristic water pressures or by applying a safety margin to the characteristic water level', but no additional information or partial factor on how to determine design values is given. CIRIA guide [8] goes a step further explaining that characteristic values of the levels of groundwater or free water shall be measured, nominal or estimated upper or lower levels while design water levels for ULS require margin of safety and may be derived by either direct assessment or by adding a margin to characteristic water level. It is also stated that design values of pore water pressures 'shall represent the most unfavourable values that could occur during the lifetime of structure'. Design water levels, and therefore designed pore water pressures, can be determined in several ways:

1. directly assessed using appropriate analysis to determine water level with the required probability of exceedance (very difficult to undertake)
2. add margin to characteristic water level (even though there are no clear guidelines of doing this)
3. factoring of characteristic values of pore water pressure by using partial factors, as given in literature [11]. This is not recommended, mostly due to fact that it is hard to determine whether this action is permanent or variable (or even favourable or unfavourable) and which partial factors on action to use.

Since the explanation on characteristic and design water levels is relatively poorly described in main Eurocode 7 norm, the designers are often confused on what to do. In Croatia, it is common practice that water level which can be expected for some return period (usually 100 years) is given in Terms of references for design of an embankment and these values are usually obtained from previously conducted hydraulic studies. It is additionally defined that a crest of embankment has a certain margin (usually 1 m) above defined water level and designers usually consider water at crest as one of situations in their analysis. In previously used norms in Croatia [12] it was defined that, due to uncertainties linked with calculation of high waters, a so called 'safety height' should be applied as the height between the crest and high water, with values of minimum 1.5 m for dams lower than 15 m and minimum 2 m for those higher than 15 m. Table 1 is derived from CIRIA guide [8], demonstrating most dominant actions on flood protection embankment, which are given concerning favorability or unfavorability of their occurrence.

Table 1. Most dominant actions on flood protection embankment [8]

Type of load	Permanent (P) or Variable (V)	Type of ultimate limit state		
		UPL	HYD	GEO
Soil mass	P	favourable	favourable	both
Imposed load	P or V	either	either	either
Water pressure	P	unfavourable	unfavourable	unfavourable

3.1.1 Hydraulic stability

An UPL ultimate limit state represents loss of equilibrium of a structure or the ground due to uplift by water pressure (buoyancy) or other vertical actions, while HYD ultimate limit state represents hydraulic heave, internal erosion and piping in the ground caused by hydraulic gradients. In regards to later limit state, which is usually more relevant for flood protection embankments, heaving occurs when upwards seepage forces act against weight of soil, reducing vertical effective stress to zero what results in lifting of soil particles through vertical water flow. Internal erosion is result of transport of soil particles within soil stratum or at interface with soil strata, while piping is special form of internal erosion where erosion starts on surface and regresses until a pipe shaped discharge tunnel is formed in soil mass [9]. The examples of internal erosion and hydraulic heave are given on figure 2.

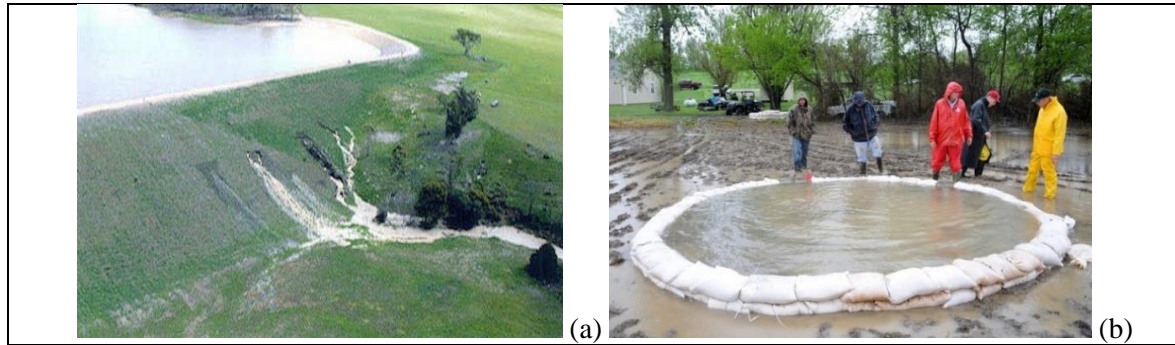


Figure 2. Internal erosion failure [13] (a) and hydraulic heave in Podturen, north Croatia (b)

Hydraulic stability is relevant for design situations of normal operating conditions, flood event (high water) and rapid drawdown. For both UPL and HYD limit states, a designer needs to check that there is not loss of equilibrium with regard to stabilising and destabilising forces.

For UPL an equation must be satisfied:

$$V_{dst,d} \leq G_{stb,d} + R_d \tag{1}$$

where:

$V_{dst,d}$... combined design value of destabilising permanent and variable vertical action

$G_{stb,d}$... sum of the design value of stabilising permanent vertical actions

R_d ... design value of any additional resistance to uplift

For HYD following equations must be satisfied:

$$u_{dst,d} \leq \sigma_{stb,d} \text{ when using total stress} \tag{2}$$

$$S_{dst,d} \leq G'_{stb,d} \text{ when using submerged weight} \tag{3}$$

where:

$u_{dst,d}$... design value of destabilising pore water pressure at the bottom of the column

$\sigma_{stb,d}$... design value of the total vertical stress at the bottom of the column

$S_{dst,d}$... design value of seepage force in the column

$G'_{stb,d}$... design value of submerged weight of the column

However, equations (2) and (3) are mathematically equivalent only if all partial factors are equal to 1. Otherwise, they give different results, where equation (2) is more conservative than equation (3). Using equation (3) may lead to designs where the safety factor calculated according to the classical (not EC7) methods would be very low [14]. List of partial factors, obtained from Croatia's National Annex, for UPL and HYD limit states is given in table 2. It should be noted that in HYD limit state, no partial material factors are provided as no soil strength is involved in failure mechanisms.

Table 2. List of partial factors, obtained from Croatia's National Annex, for UPL and HYD limit states

Action		Symbol	UPL	HYD
Permanent	unfavourable	$\gamma_{G,dst}$	1.1	1.35
	favourable	$\gamma_{G,stb}$	0.9	0.9
Variable	unfavourable	$\gamma_{Q,dst}$	1.5	1.5
Material properties				
Friction angle		$\gamma_{\varphi'}$	1.25	-
Effective cohesion		$\gamma_{c'}$	1.25	-
Undrained strength		γ_{cu}	1.4	-

One of the most important values which needs to be controlled for ensuring hydraulic stability are the values of exit hydraulic gradients. They need to be controlled in order to prevent internal erosion and to

minimize material transport. The allowable values for hydraulic gradients after both Eurocode 7 and JUS norm can be found in table 3.

Table 3. The allowable values for hydraulic gradients after both Eurocode 7 and JUS norm

Allowable hydraulic gradient i [-]				
for filter protected material		for filter unprotected material		
EC7	not defined *			
JUS	10	compacted clay in embankment	0.12	fine grained silty sand
			0.14	fine grained sand $0.063 < d < 0.5$ mm
	12	compacted clay in blanket, at least $d=0.5$ m	0.17	medium grained sand $0.5 < d < 2.0$ mm
			0.20	coarse grained sand $2.0 < d < 5.0$ mm
	3	clayey silt in embankment	0.30	medium grained gravel $10.0 < d < 20.0$ mm
			0.40	coarse grained gravel $20.0 < d < 100.0$ mm
4	clayey silt in blanket, at least $d=0.5$ m	0.50	compacted clay $0.5 < I_c < 1.0$	
		0.65	firm clay $I_c > 1.0$	

* Eurocode 7 does not provide detailed rules for filter design. If the filter criteria are not satisfied, Eurocode 7 requires verification that the design value of the hydraulic gradient i_d is ‘well below’ the critical hydraulic gradient, taking account of the direction of flow, the grain size distribution and shape of grains, and stratification of the soil.

As it can be seen, Eurocode 7 unfortunately does not give a procedure for determining i_d , while the allowable values are clearly defined by previous standard. The lack of straightforward procedure of determination of allowable values of gradients has resulted in ongoing practice of referring usually to previous standards. Some authors, such as Bond et al. [14], suggest that based on previous experience, a safety factor for determination of design gradients from critical ones should be at least equal to 4.0.

3.1.2 Overall stability

A GEO ultimate limit state is considered as failure or excessive deformation of the ground, in which the strength of soil or rock is significant in providing resistance. Some examples of failure by exceeding GEO limit state is given in figure 3.

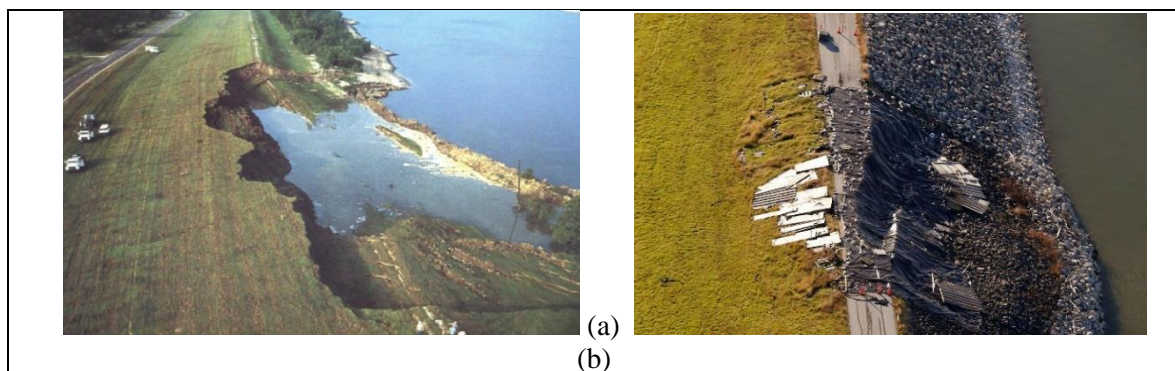


Figure 3. Overall stability failure of flood protection embankments [11, 15]

This ultimate limit state is relevant for all design situations – construction, normal operating conditions, flood event (high water), rapid drawdown and seismic events. When it comes to failure mechanisms, designers should look upon chapter 11 of main norm, which deals with the provisions linked to the overall stability of and movements of slopes and embankments. However, there are no calculation models provided in Eurocode 7 and no specific inequalities to be satisfied in case of stability analysis [9].

The main principle which must be satisfied has form of:

$$E_d \leq R_d \tag{4}$$

where:

E_d ... design values of effect of actions

R_d ... design value of the resistance to the action

Three sets of partial factors need to be considered – for action (A), material parameters (M) and resistance (R). In that sense, Eurocode 7 proposes three design approaches which differ in values of partial factors. Figure 4 gives design approaches (DA) adopted in different European countries for the design of slopes and embankments, given by Bond [16].

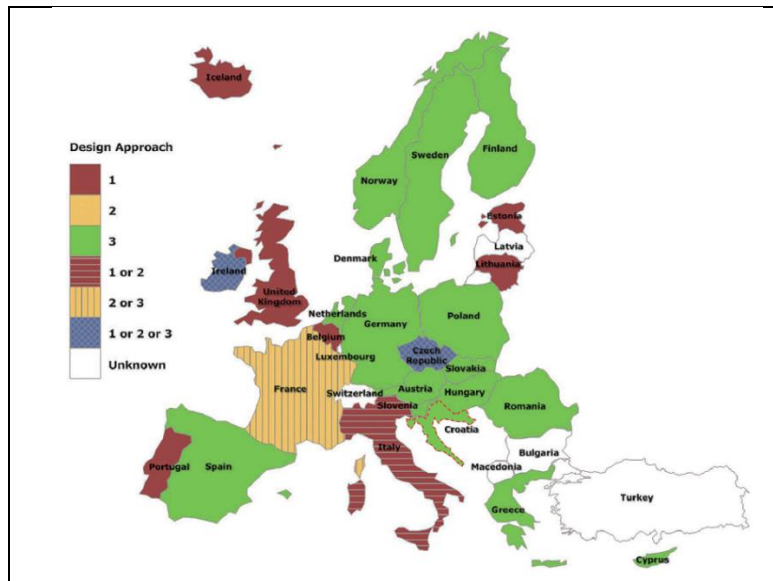


Figure 4. Design approaches adopted in different European countries for the design of embankments [16]

The consensus on which DA should be used was not achieved on EU level, and decision was left to each state. Some analysis show that difference between structures dimensioned by different DA are not too large ($\pm 10\%$) and that they depended from case to case [3]. As it can be seen from figure 4, Croatia has accepted DA3 for the design of slopes and embankments, in which actions on the soil, for example structural loads and traffic, are treated as geotechnical rather than structural actions. The relevant partial factors for this approach are given in table 4, where it can be seen that the reliability of factors of safety is basically derived through reliability of material parameters determined by investigation works.

Table 4. List of partial factors, obtained from Croatia's National Annex, for GEO limit state

Design Approach 3 (GEO)			A1 (A2) + M2 + R3			
Partial Factor Set		Symbols	A1	A2	M2	R3
Permanent actions (G)	unfavourable	γ_G	1.35	1.00		
	favourable	γ_G	1.00	1.00		
Variable actions (Q)	unfavourable	γ_Q	1.50	1.30		
	favourable	γ_Q	0.00	0.00		
Friction angle (φ')		$\gamma_{\varphi'}$			1.25	
Effective Cohesion (c')		$\gamma_{c'}$			1.25	
Undrained strength (c_u)		γ_{c_u}			1.40	
Weight density (γ)		γ_γ			1.00	
Sliding resistance (R)		γ_R				1.00

By applying partial factors to actions (increasing them) and material parameters (decreasing them), a factor of safety to resistance of 1.0 is required. In previously used standards [12], the procedure was somehow different. There was no partial factor concept, so the aim was to satisfy overall factor of safety. The minimum value of factor of safety was defined for dams higher than 15 m as 1.5 (for permanent actions) and 1.3 (for variable actions), while for dams lower than 15 m it was defined as 1.3 (permanent actions) and 1.2 (variable actions). This standard even gave guidelines for seismic actions where it was defined that overall factor of safety in seismic conditions can be lower than 1.0, but in that case a largest possible displacement should be determined. Seismic loading, according to Eurocode, should be also taken into account in accordance with Eurocode 8 [17], where it is necessary to have information of ground acceleration, various amplification factors and foundation soil class. Since most of Croatia is in seismically active area, these calculations need to be addressed properly when designing flood protection embankments. Overall stability in seismic condition should be checked both in drained and undrained condition, weather using pseudo-static analysis or time domain analysis. Stability in undrained behaviour should be checked for materials with permeability less than 5×10^{-4} m/s. Since the probability of coincidence of seismic events along with serious flood events is extremely low, it is not usual practice to take into account, in same analysis, the simultaneous occurrence of these events. However some guidelines [11] mention that seismic events can cause excessive damage to embankments, leaving them vulnerable if not repaired before next major flood event. Therefore, it is suggested to assess resistance of embankments to seismic events in combination with a relatively frequent flood event (for example a five year return period).

Today, numerical methods are most often used for determination of overall stability. They can be divided on those who assume sliding body as rigid where, to overcome static indeterminacy, it is divided on slices. Based on isotropy and homogeneity of materials, sliding surface can be considered as circular or as non-circular. Another approach includes determination of factor of safety based on continuum (FEM) analysis through so called $c-\phi$ reduction method.

3.2 Serviceability Limit State (SLS)

There are several serviceability limit states which need to be considered such as excessive settlement, desiccation or cracking and animal burrowing [8]. While the two later ones needs to be addressed in design through proper selection of materials and other measures (such as protection net), an excessive settlement must be checked in order to prevent occurrence of a serviceability limit state in either the embankment or any adjacent structures road [11]. A following should be satisfied:

$$E_d \leq C_d \quad (5)$$

where:

E_d ... design values of effect of actions

C_d ... limiting design value of the effect of an action

It should be noted that, for serviceability limit states, design values of actions and material parameters are same as representative and characteristic values due to fact that partial factors are equal to 1.0. CIRIA [8] differs settlement assessment for new embankments and for reconstructed ones. For the new embankments, critical situation could be when they are constructed on alluvial soft clays and peats where settlements can be very large, while larger differential settlements may lead to cracking. For reconstructed embankments, differential settlements between new works and existing structures should be considered. Proper assessment of settlements must be conducted by designer through estimation of magnitude, but also of time in which they will occur (consolidation period). Which value of settlement is 'too large' is not straightforward answer, neither it is provided by Eurocode 7. In National Annex for Croatia, there are frame values of allowable settlements, but only for different types of buildings. In the previous standard [12], the limitation on allowable deformation was given for embankments which are not in contact with other objects and whose crest is used for public roads. Allowable deformation is defined as less than 1% for dams lower than 15 m and 1.5% for dams higher than 15 m. In any case, a designer should foresee additional material on crest in order to avoid situation like embankment overtopping during flood events.

4 The role of a designer in overall process

A designer should not be involved only in design process and it is very important for everyone involved in project of flood protection embankment to understand this. Based on guidelines form Eurocode 7, it would be best that designer is involved already in stage of making Terms of References, but because this may pose some difficulties from obvious reasons, a designer should be involved at least from investigation work phase all along to construction phase. To achieve this, a designer must be familiar not just with Eurocode 1997-1 norm [4] on general design rules, but also Eurocode EN 1997-2 [18] on requirements for ground investigation and the performance and evaluation of field and laboratory testing. This is also covered in Technical Specifications [2] where it is stated that the geotechnical design is conducted based on geotechnical data which comprise of selected values of magnitude and spatial distribution of physical – mechanical parameters of soil, rock or groundwater. Parameters relevant for design are determined through interpretation of geotechnical investigation works and other documents and maps (geological, engineering geological, hydrogeological, etc.). Since the designer is responsible for its design, a selection of appropriate design input values must have its basis in selection of a type and volume of investigation works. However, the practice is such that designer usually gets results of investigation work conducted previously without his knowledge. If a designer considers investigation works as insufficient for a design, it should be stressed out and additional investigation should be conducted based on designer's requirements. During selection of investigation works, a designer should take into account design phase (conceptual, main, detailed) as well as history of location (records of maintenance, observations through visual inspection, records of conducted monitoring etc.). Besides being involved in investigation works, a designer should be also involved during construction in form of designer supervision, as well as in process of quality control work for the purpose of verification of its design. An overall design process of flood protection embankment, is presented in figure 5.

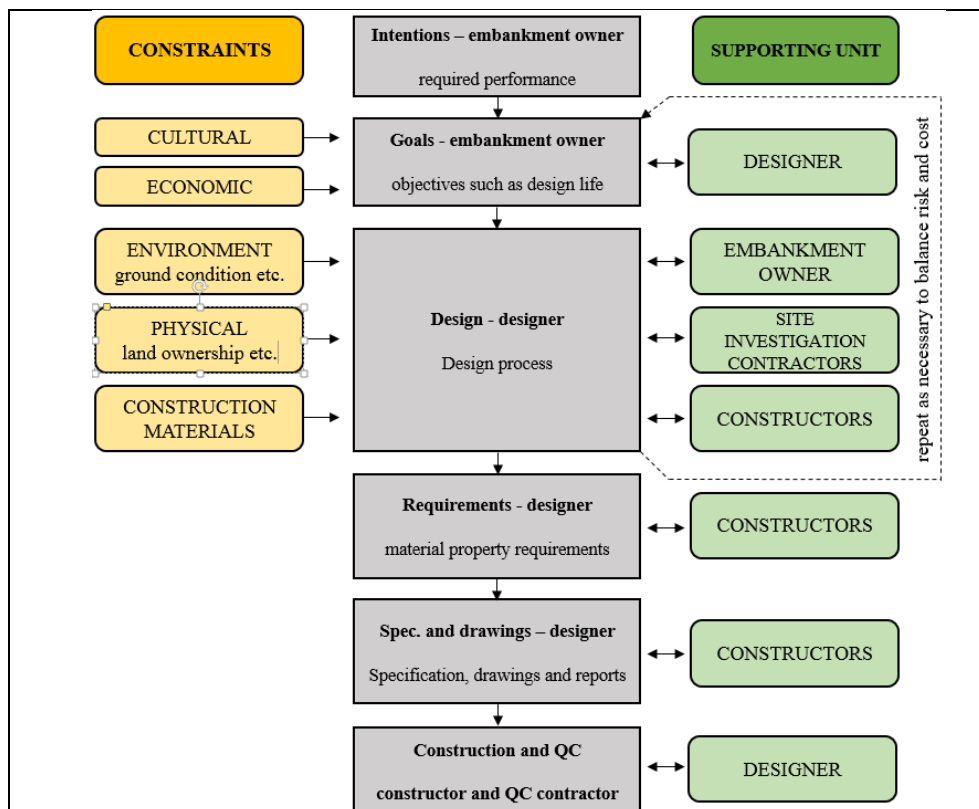


Figure 5. An overall role of designer in project of flood protection embankment [11]

5 Conclusion

This paper gives insight in principles of using Eurocode 7 for design of flood protection embankments. To fulfil requirements posed by Eurocode, a designer must consider series of design situations, which

are reasonably expected during the lifetime of an embankment. These design situations, from construction phase and normal operating conditions to the flood event, rapid drawdown and seismic condition, present the core of design using Eurocode 7 and it is crucial to identify them. However, fact that Eurocode 7 only gives a sort of design framework, sometimes leads to confusion were flood protection embankment designers have some doubts regarding what needs to be fulfilled, mostly because they expect to have strict design procedures which were, at smaller or larger scale, given in previous standards. Paper also explains some basic terms given in Eurocode such as action – resistance relationship, design situations, limit states and partial factor concept. Further, an importance of designer in overall project of flood protection embankment is stressed out where Eurocode suggest for a designer to be involved from planning of investigation works, through design, to construction and quality control.

References:

- [1] Building Act (In Croatian), Official Gazette No.153/13, 2013.
- [2] Technical Regulations for Building Structures (In Croatian), Official Gazette No.17/13, 2017.
- [3] Szavits-Nossan, A., Ivšić, T.: Novi Eurokod 7: geotehničko projektiranje (In Croatian), Croatian Geotechnical Society - Improvement of soil and rocks, eds. Szavits-Nossan, V., Kovačević, M.S., Zagreb, pp. 455-470, 2006.
- [4] HRN EN 1997-1:2012: Eurocode 7: Geotechnical design - 1. part: General Rules, 2012.
- [5] nHRN EN 1997-1:2012/NA: Eurocode 7: Geotechnical design - 1. part: General Rules, National Annex, 2012.
- [6] Bačić, M., Librić, L., Kovačević, M.S.: Application of geosynthetics as hydraulic barriers in flood protection embankments, Proceedings of the 1st International Conference CoMS_2017, eds. Banjad Pečur, I., Baričević, A., Štirmer, N., Bjegović, D. Faculty of Civil Engineering Zagreb, pp. 677-683, 2017.
- [7] www.eurocodes.jrc.ec.europa.eu, 24.06.2017.
- [8] Pickles, A.; Sandham, R.: Application of Eurocode 7 to the design of flood protection embankments, CIRIA C749, London, 2014.
- [9] Bond A.J., Schuppener, B., Scarpelli, G., Orr, T.: Eurocode 7: Geotechnical Design, Worked examples, Workshop “Eurocode 7: Geotechnical Design”, Joint Research Centre Scientific and Policy Reports, Dublin, 2013.
- [10] Frank, R., Bauduin, C., Kavvadas, M., Krebs Ovesen, N., Orr, T., Schuppener, B.: Designers’ guide to EN 1997-1: Eurocode 7: Geotechnical design — General rules, London: Thomas Telford, 2004.
- [11] CIRIA, Ministry of Ecology, USACE: The International Levee Handbook, C731, CIRIA, London, 2013.
- [12] Yugoslavian standard JUS U.C5.020/1980: Projektovanje nasutih brana i hidrotehničkih nasipa, 1980.
- [13] Fisher, W., Camp, T., Krzhizhanovskaya, V.: Detecting Erosion Events in Earth Dam and Levee Passive Seismic Data with Clustering, *Procedia Computer Science*, Volume 80, pp. 577-586, 2016.
- [14] Bond, A., Harris, A.: Decoding Eurocode 7, Taylor and Francis, New York, 2008.
- [15] www.interactives.dallasnews.com, 24.06.2017.
- [16] Bond, A. J.: Implementation and evolution of Eurocode 7, *Modern Geotechnical Design Codes of Practice*, Arnold et al. (eds), Amsterdam: IOS Press, pp. 3-14, 2013.
- [17] HRN EN 1998-1:2011: Eurocode 8: Design of structures for earthquake resistance -- Part 1: General rules, seismic actions and rules for buildings, 2011.
- [18] HRN EN 1997-2:2012: Eurocode 7: Geotechnical design -- Part 2: Ground investigation and testing 2012.

REMOTE SURVEYING OF FLOOD PROTECTION EMBANKMENTS

MARIJAN CAR ¹, DUBRAVKO GAJSKI ², MEHO SAŠA KOVAČEVIĆ ¹

¹ Faculty of Civil Engineering, University of Zagreb, Croatia, mcar@grad.hr, msk@grad.hr

² Faculty of Geodesy, University of Zagreb, Croatia, dgajski@geof.hr

1 Abstract

The need to assess present condition of flood protection embankments becomes more important in recent years. But besides the standard in-situ and laboratory methods for identification of their condition, some novel methods are entering through a “backdoor” and showing high potential, even though designers and investors are in generally not familiar with their possibilities. One of such methods, which can be useful for assessment of current condition, is usage of Unmanned Aerial System (UAS) also known as ‘drone’ which is characterized by an increasing number of engineering applications. First benefit of this method is in interactive approach for visual assessment of condition where a wider aerial picture can be obtained by having a sole operator on site, while the other participants in design of embankment’s remediation (persons who conduct investigation works, designers, investors etc.) can interactively be involved while not being present on site. Also, large areas which are the case for linear structures such as flood protection embankments, can be surveyed in fast manner, reducing the time necessary for standard visual assessment. However, full potential of this method is in possibility for advanced engineering analysis through the formation of orthophoto maps and 3D models using aerial photogrammetry. From this type of models, a complete spatial characteristics of embankments can be obtained with provisional cross sections extrapolated, thus avoiding a current practice where surveying activities are conducted along several profiles. The paper presents the possibilities of using Unmanned Aerial Systems on flood protection embankments, emphasizing their advantages and shortcomings.

Keywords: unmanned aerial system (UAS), remote survey, flood protection embankment, interactive condition assessment, photogrammetry

2 Introduction

Use of UAS for flood protection embankments delivers a highly privileged aerial point of view. Through this kind of assessment and observation, provided data can be viewed in real time or used later on for detailed analysis. Most usual type of data provided by UAS is high resolution photography and video, which makes them ideal for surveying structural objects such are embankments for flood protection. Being characterized as long and narrow objects, embankments usually follow a natural path by the river or canal, which makes them in some cases not easy to approach. Classical technics of surveying embankments in these types of areas, and also all along the route can easily lead to oversight of critical information. With development in technologies, software and materials UAS is becoming a tool which can provide to owners and engineers a much bigger perspective for assessment and surveying respecting accuracy and time, which are being one of the most important parameters in modern time. Being able to make fast and correct decisions from precise and reliable data is putting owners, managers, investors and other interested users in flood protection embankments in a position to see a “bigger picture” from another aerial perspective. In recent times [1] UAS is used in a lot of applications regarding surveying, monitoring and mapping of remote objects (indoors or outdoors), rather if they are hard to reach, hazardous or just more profitable than any other classical method. Various types of final products delivered from UAS data like point clouds, digital terrain models (DTM), digital surface models (DSM) and other types of formats can be used with various software types for planning, designing and remediation of embankments.

3 Methods

3.1 UAS

Unmanned Aerial System (UAS) or Unmanned Aerial Vehicle (UAV), commonly and popularly known as “drone” is a flying device or aircraft without the crew that can be operated by remote controller, or fly independently using a prescheduled flight plan [2]. UAS can take different forms, with different levels of controls and the capacity to carry a very wide range of payloads. There are many types supporting different uses, but they are also subject to different regulations, depending on whether the aircraft is in, or beyond the field of view. They are built with intelligent stabilization systems to keep them flying and carry sensors to perform dedicated functions. One of the most common devices is a camera mounted on gimbals to obtain high-quality video and still photography [3]. They can be divided in two major groups by constructions which are “fixed wing”, Figure 1b and “rotary wing” shown in Figure 1a.

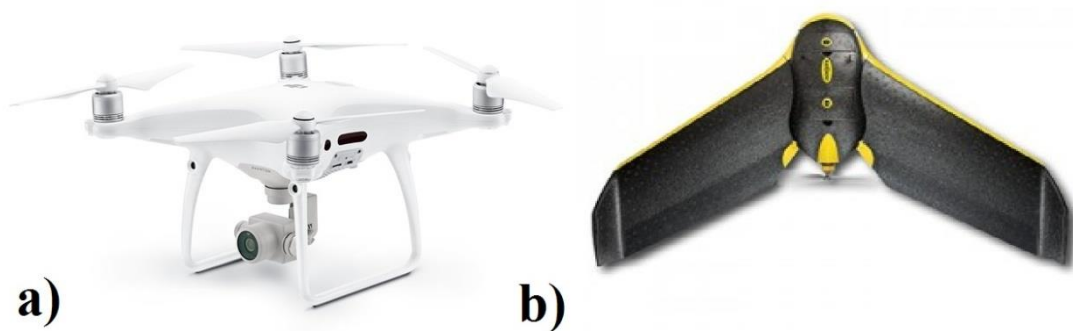


Figure 1a). Rotary wing UAS & **b)** Fixed wing UAS

Each of these types are capable of performing missions for embankment surveying, but still each one has advantages and disadvantages shown in Table 1.

Table 1. Comparison of fixed and rotary wing UAS

	FIX WING	ROTARY WING
PROJECTS	Larger area mapping	Smaller area mapping, inspection
APPLICATIONS	Land surveying, agriculture, GIS, environmental, construction	Urban surveying, real estate, construction surveying and mapping
CRUISING SPEED	High	Low
COVERAGE	Large	Small
OBJECT RESOLUTION	Cm/inch per pixel	Mm per pixel
TAKE-OFF/LANDING AREA	Large	Very small
FLIGHT TIME & WIND RESISTANCE	High	Low

Type of UAS used for embankment surveying field test is rotary wing DJI Phantom 4 Pro [4]. It is a quadcopter drone that can be also called “ready to fly”, meaning all of his components are already built in. In order for using this type of UAS for data collection his most important specifications are camera resolution, flight time, shutter type, built in GPS antenna (Global Positioning System), camera stabilization system and ability to perform autonomous flight operation. It is operated with the remote controller who has attached tablet computer on it, which is used to set up all the drone’s functions and also has live preview from the camera Figure 2.



Figure 2. DJI phantom 4 Pro with corresponding remote controller and tablet computer

Through a mobile data transfer it is possible to send live preview (live stream) to another device or computer with internet connection which can be found very useful. This kind of interactive approach can offer evaluation of embankment condition to the people who are at other locations (offices, cabinets, laboratories). They can focus more on receiving live feed and navigate the on-site operator to take more detailed pictures or videos of specific area of interest [2]. Schematic view on how does it work can be seen on Figure 3.

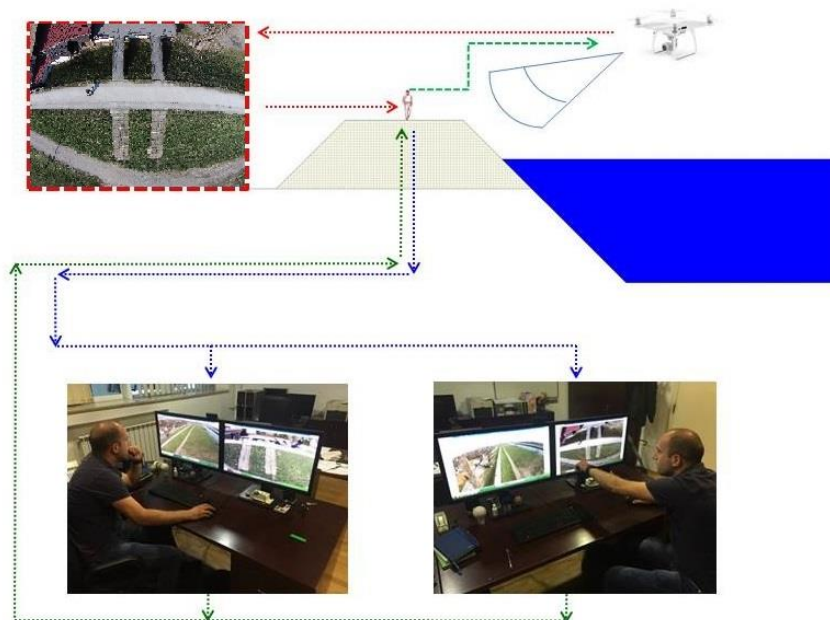


Figure 3. Interactive scheme for embankment surveying

3.2 Field approach

Part of river Sava embankment in Zagreb was chosen for a test field which is shown in Figure 4.

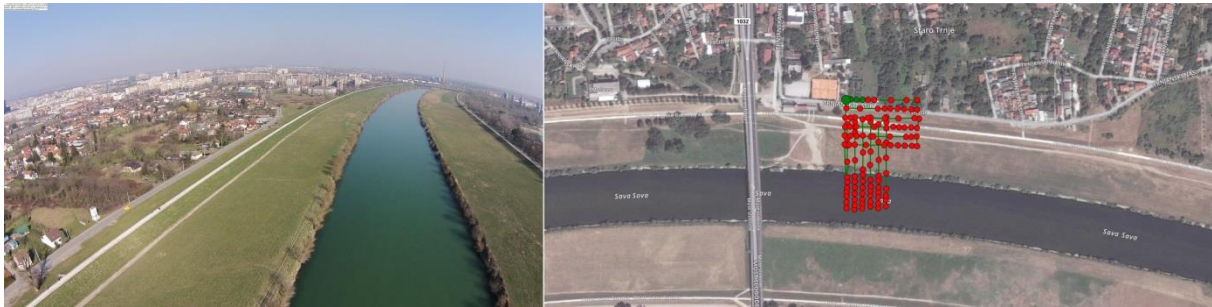


Figure 4. Aerial view of Sava embankment and position of testing area

Upon arrival at the location the first step was to prepare autonomous flight mission for UAS by defining area of surveying [4]. Through that procedure it is needed to set up parameters for flight which are including height of flight, angle of the camera view, longitudinal and side overlapping of the images and drone speed. All these parameters are important for determining GSD (Ground Sample Distance) of the future model [5]. GSD is the distance between two consecutive pixel centers measured on the ground. If the value of GSD is bigger, it will reflect on the spatial resolution of the image and the less visible details will be shown in the 3D model. The GSD is related to the flight height: the higher the altitude of the flight, the bigger is GSD value [6]. The whole procedure is done in interactive application installed on the tablet computer, and the one used in this case is “Pix4Dcapture” [7], Figure 5.

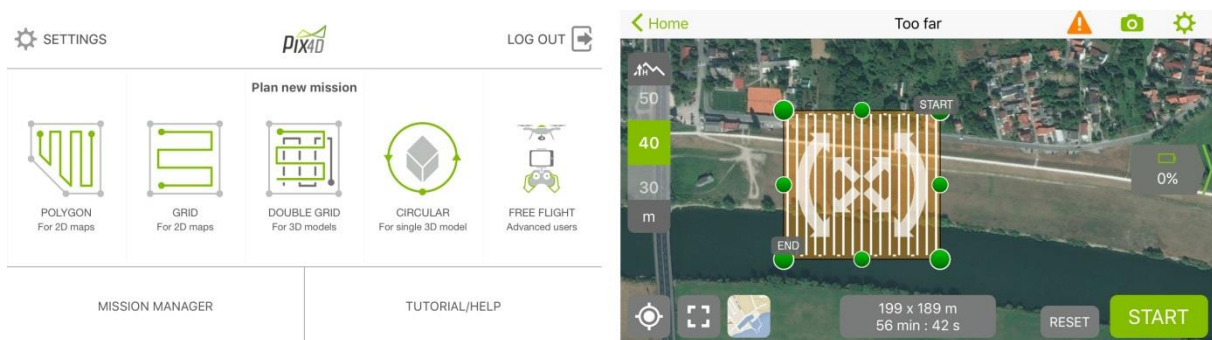


Figure 5. Application screen for setting up flight mission

After setting up the flight mission UAS is ready for take off. Coordinate system used for flight preparation and UAS flight is World Geodetic System (WGS84) [8] which is standard if GPS is used and can be converted to any national datum or coordinate system. Before the flight it is very important to collect local meteorological information and weather conditions. Generally it is good to choose the sunny day without wind for the flight operations [9]. UAS flight preparation and flight time took 30 minutes.

3.3 Pix4Dmapper

Pix4D was founded in 2011 in Switzerland [10]. The purpose of the newly formed company was to make software that will provide a professional tool for processing data obtained by using unmanned aircraft. It started as a spin-off company at the EPFL (Ecole Polytechnique Federale de Lausanne) Computer Vision Laboratory in Switzerland [11] which is one of the two Federal Institutes of Technology. Pix4D is a growing company in collaboration with partners from industry and science involved in many research projects supported by the Swiss government. The company headquarters is now located in Lausanne Switzerland, and also has offices in the United States and China. Pix4Dmapper is software that automatically processes the images that were taken from the air using unmanned aircraft, or from the ground with digital camera. It uses SFM (Structure From Motion) algorithm [12] that works on the principle of recognizing the image content (pixels) in order to make a complete 3D model of the subject in form of creating a point cloud Figure 6. The software is completely adaptable to all types of cameras and image processing results can be converted and used by any GIS or CAD applications. Pix4Dmapper can be used in many different branches of industry and science, such as mining,

agriculture, geodesy, civil engineering, management of natural resources and emergency services, and allows following [10]:

- line and polyline measurement (break lines), making longitudinal and cross sections, contour drawing, measuring areas and volumes directly in the model and their export to other different formats
- generating 3D point cloud, true orthomosaic and orthophoto maps, 3D textured models, DSM (Digital Surface Model), DTM (Digital Terrain Model) from vertical and oblique aerial or terrestrial photos
- it uses a fully automated flow of data processing and calibration of each photo in order to achieve a satisfactory level of accuracy, but also the "Rapid Check mode" for checking the quality of recording directly on the field

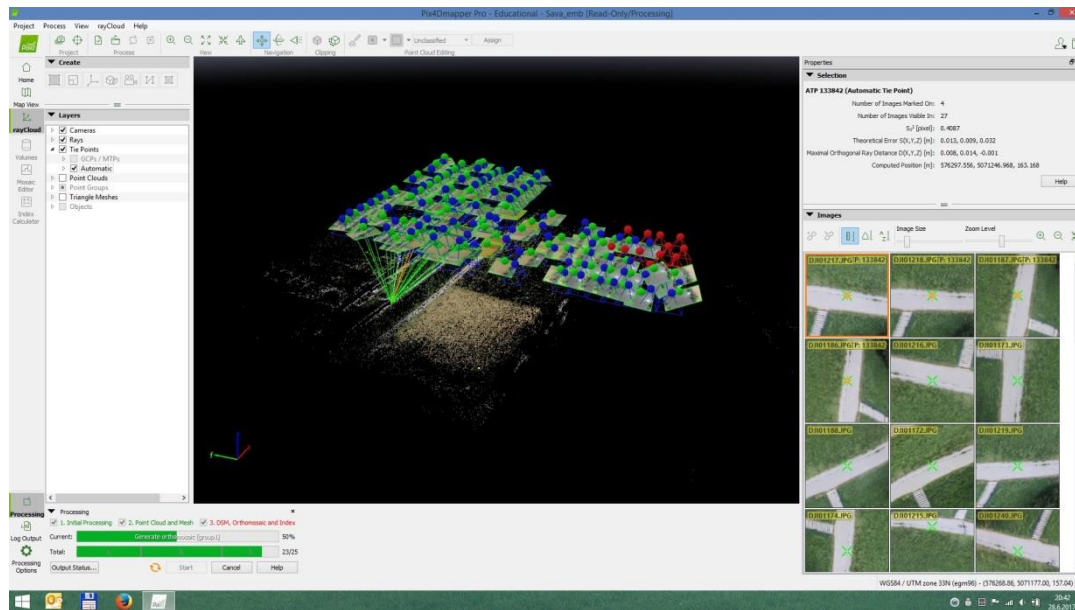


Figure 6. Pix4Dmapper user interface with visible point cloud and aerial positions of images

3.4 Results

At the test field a total of 117 images was taken. All images were geo-located at the time of exposure and overall area covered by images during the flight was 3.69 hectare. Images taken from UAS were imported to "Pix4D mapper" and processed by using default options. One of the first visible things after processing the images was so called "Uncalibrated Cameras". The reason why did it happen is impossibility of the software to find enough matches on neighbouring images to create stereoscopic effect [13] and by that not able to create 3D points. Those 14 images were created above the water, shown in Figure 7., and did not contain any characteristic surface points which would be visible on two or more images. Total image processing time took 90 minutes. Achieved GSD was 2.26 centimeters creating 7.304.850 number of 3D points shown at Figure 8. Inside of the software it is possible to create 3D polylines, surfaces, Figure 9a, volume calculations, Figure 9b. and orthoplanes, which all can be exported to other types of formats such as: *.dxf, *.shp, *.dgn and *.kml. Through inside application of "Pix4D mapper" called "Mosaic editor" generation of DSM [15] and DTM [16] is possible. The difference between those two is in filtering out the surface data and leaving only terrain representing "DTM" Figure 10a, or leaving all the surface data creating "DSM" Figure 10b. Also digital orthophoto map is created using all taken pictures combining it to one high resolution map, Figure 11.

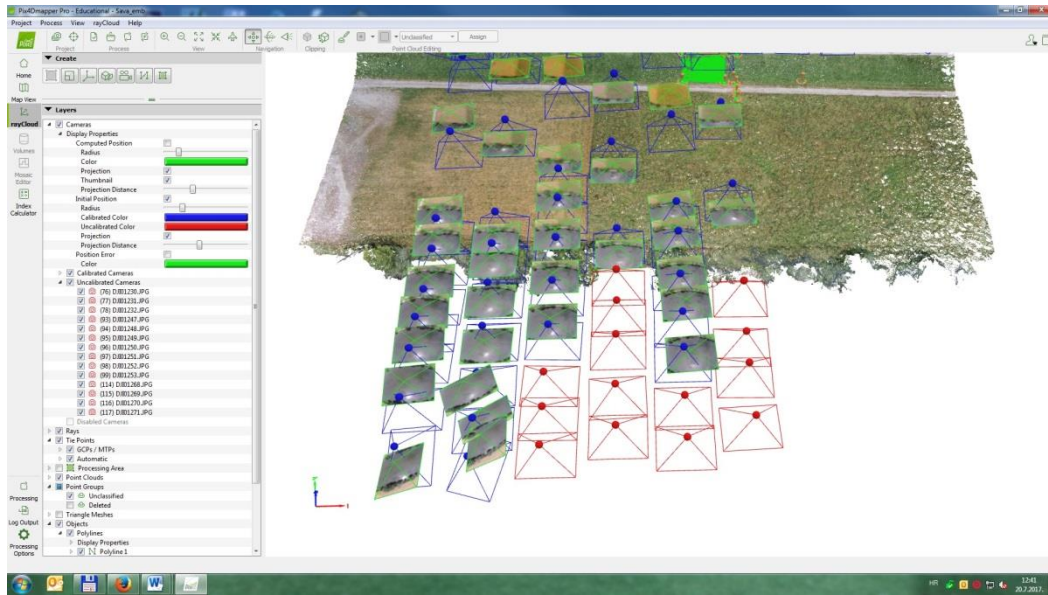


Figure 7. Uncalibrated Cameras visible in red color

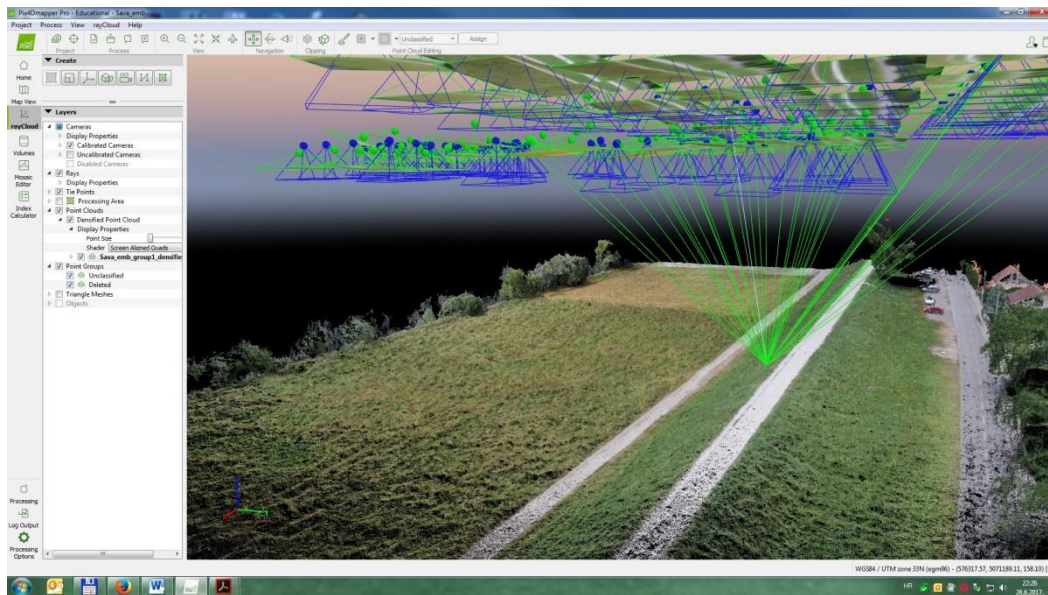


Figure 8. Point cloud containing 7.304.850 3D points

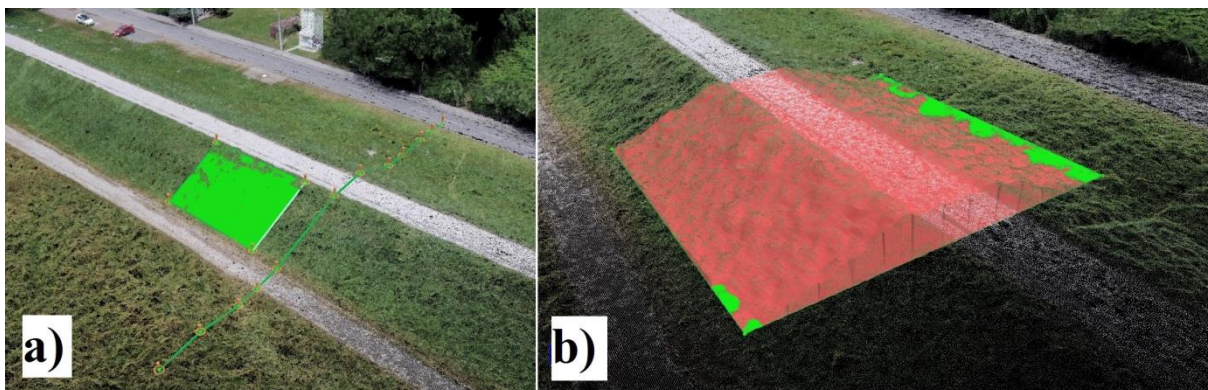


Figure 9.a) 3D polyline and surface & b) Volume calculation

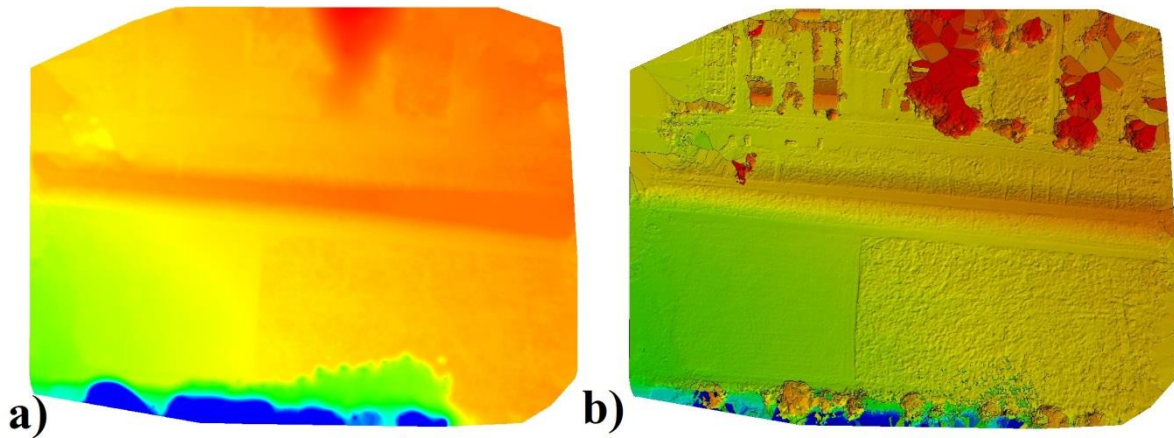


Figure 10. a) Digital Terrain Model DTM & b) Digital Surface Model DSM



Figure 11. High resolution orthophoto map of testing area

One of the useful options, that software provides is being able to generate and extract contours directly from point cloud, making it possible to adjust elevation interval and resolution. It can be exported in three different types of format, *.shp, *.pdf and *.dxf, shown in Figure 12. If large scale objects are surveyed, which in case of embankment is usual, a large amount of data is generated. For clients and investors it is possible to upload data in web cloud, allowing them to review models, make measurements and leave their own remarks and comments Figure 13. Also, all models are compatible with open access maps like “Google Earth” and “Google maps” Figure 14.

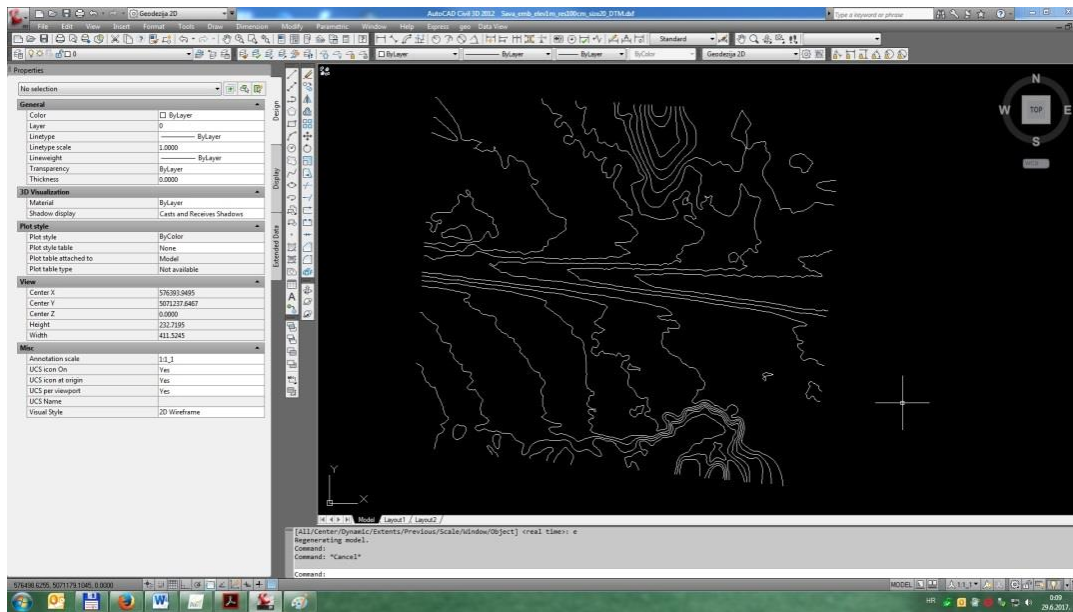


Figure 12. Generated contours in *.dwg format in Auto CAD

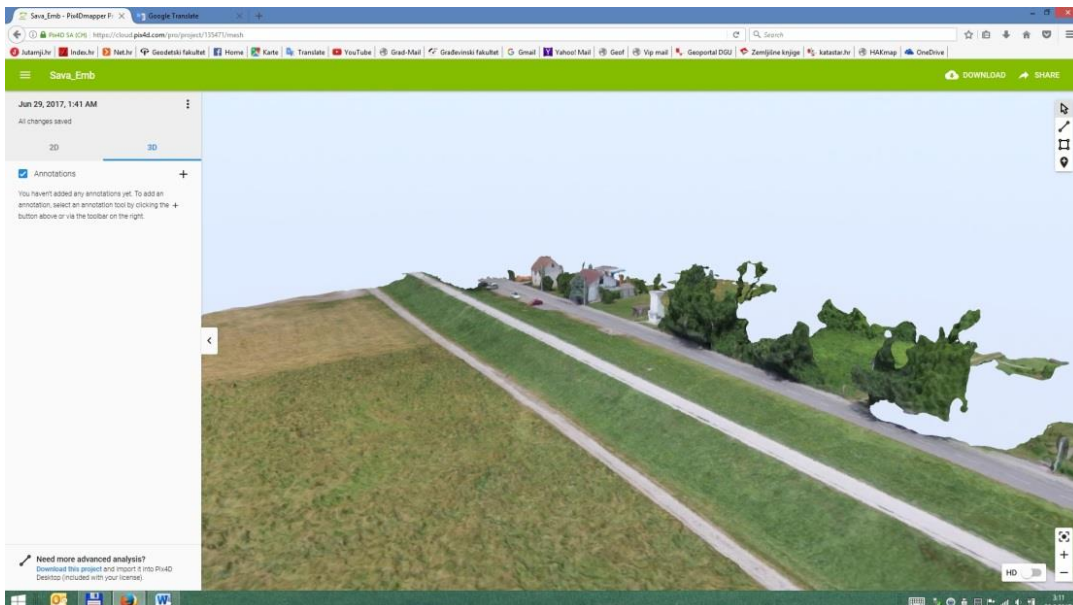


Figure 13. User interface when accessing project through web browser

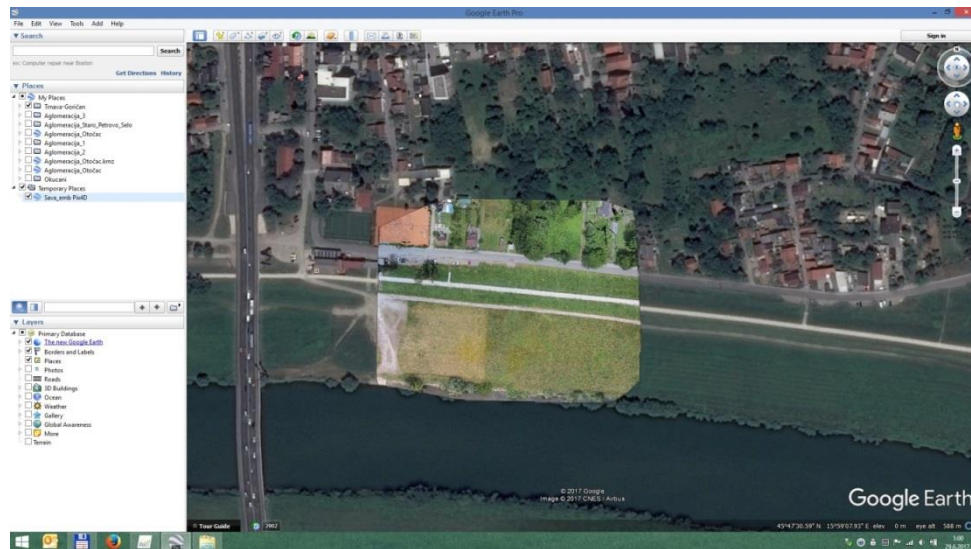


Figure 14. Overlapping orthomosaic in “Google earth”

4 Conclusion

Being able to survey large scale objects like embankments, with new technology like UAS, and have ability to create a “bigger” picture in relatively short time puts this type of survey in the leading place. Advantages shown through this test field can’t be compared with not one classical method of surveying. Regardless to evolving technology, materials, software and precision, a finite number of points are gathered on the field through classical methods of surveying. These methods will always be present and used for various types of assignments. Do to the lack of field operator important spots on embankments can be easily missed, aside from aerial or remote surveying using UAS. Through this example it is shown that all the data provided through this methodology is more than enough accurate and reliable for infrastructure managers and engineers to use in various decision making, remediation measures and management. Future prediction for this type of technology is bringing to us longer flight times, enabling us to cover larger areas, and more robust and durable UAS which could work in bad weather conditions, which is today's biggest flaw. Legal legislation at some countries (like Croatia) can also prevent this type of survey and remote sensing to develop even more.

References:

- [1] Liu, P., Chen, A.Y., Huang, J-N., Han, J-Y., Lai, J-S., Kang, S-C., Wu, T-H., Wen, M-C and Tsai, M-H: A review of rotorcraft Unmanned Aerial Vehicle (UAV) developments and applications in civil engineering, *Smart Structures and Systems* Vol. 13, No. 6. pp. 1065-1094, 2014
- [2] Jurić-Kačunić, D., Librić, L., Car, M.: Application of unmanned aerial vehicles on transport infrastructure network, *GRAĐEVINAR*, 68 (2016) 4, pp. 287-300, doi: <https://doi.org/10.14256/JCE.1382.2015>
- [3] A business approach for the use of drones in the Engineering & Construction industries, https://www.accenture.com/t00010101T000000__w_/fr-fr/_acnmedia/PDF-24/Accenture-Drones-Construction-Service.pdf, 18.06.2017.
- [4] DJI Phantom 4 Pro <https://www.dji.com/phantom-4-pro>, 18.06.2017.
- [5] Pix4D Support Ground Sampling Distance (GSD), <https://support.pix4d.com/hc/en-us/articles/202559809-Ground-Sampling-Distance-GSD-#gsc.tab=0>, 20.06.2017.
- [6] Car, M.; Jurić Kačunić, D.; Kovačević, M.S.: Application of Unmanned Aerial Vehicle for landslide mapping, *Proceedings of the International Symposium on Engineering Geodesy - SIG 2016 / Paar, Rinaldo; Marenić, Ante, Zrinjski, Mladen (ur.)*. Zagreb: Croatian Geodetic Society, 2016. 549-559
- [7] Pix4Dcapture mobile application, <https://pix4d.com/product/pix4dcapture/> 20.06.2017.
- [8] Spatial reference systems, <http://spatialreference.org/ref/epsg/wgs-84/>, 20.07.2017.
- [9] Jing H., Yongshu, L., Keke, Z.: Research of UAV Flight Planning Parameters, *Positioning* 2012, 3,

- 43-45, Southwest Jiaotong University, GIS Engineering Center, Chengdu, China; Engineering Design Co., Ltd., CNPC, Chengdu, China
- [10] Pix4Dmapper desktop software, <https://pix4d.com/product/pix4dmapper-pro/>, 20.06.2017.
- [11] École polytechnique fédérale de Lausanne, www.epfl.ch, 20.06.2017.
- [12] Mancini, F., Dubbini, M., Gattelli, M., Stecchi, F., Fabbri, S., Gabbianelli, G.: Using Unmanned Aerial Vehicles (UAV) for High-Resolution Reconstruction of Topography: The Structure from Motion Approach on Coastal Environments, *Remote Sensing*, ISSN 2072-4292
- [13] Librić, L.; Car, M.; Kovačević, M. S.: Methods of surveying in rockfall protection, Road and Rail Infrastructure III, Proceedings of Conference CETRA 2014 / Lakušić, Stjepan (ur.). - Zagreb: Department of Transportation, Faculty of Civil Engineering, University of Zagreb, 2014. 617-622
- [14] Orych, A.: Review of methods for determining the spatial resolution of UAV sensors, *The International Archives of the Photogrammetry, Remote Sensing and Spatial Information Sciences*, Volume XL-1/W4, 2015 International Conference on Unmanned Aerial Vehicles in Geomatics, Toronto, Canada, pp. 391-395, 30 Aug–02 Sep 2015.
- [15] Devi, S.; Stereoscopic Vision, Stereoscope, Selection of Stereo Pair and Its Orientation, *International Journal of Science and Research (IJSR)*, Volume 3 Issue 9, ISSN (Online): 2319-7064, pp. 99-104, September 2014.
- [16] Anders, N., Masselink, R., Keesstra, S.: High-Res Digital Surface Modeling using Fixed-Wing UAV-based Photogrammetry, *Soil Physics and Land Management*, Wageningen University Wageningen, The Netherlands
- [17] Christian, J.H., Pedersen, Ø., Bayer, T. and Frederiksen, P.: The photogrammetric derivation of digital terrain models in built-up areas, *The Photogrammetric Journal of Finland*, Vol. 22, No. 1, pp. 33-45, 2010.

APPLICATION OF GEOSYNTHETICS FOR REINFORCEMENT OF FLOOD PROTECTION EMBANKMENTS

DANIJELA JURIC KAČUNIĆ¹, MARIO BAČIĆ¹, NICOLA ROSSI¹

¹ Faculty of Civil Engineering, University of Zagreb, Croatia, djk@grad.hr, mbacic@grad.hr, nrossi@grad.hr

1 Abstract

In Croatia, a large number of flood protection embankments were constructed many decades ago and their deterioration is inevitable. These embankments are subjected to series of factors making them prone to different types of failures. Also, a lack of vision for their remediation led to many problems in past few years, such as large-scale flooding events. In the same time, mandatory design standards, which ensure overall stability of embankments, are becoming stricter making the remediation procedure more complex. Designers need to cope with investor's constant aspiration to keep the remediation costs as low as possible. In order to satisfy strict standards and investor's mentioned aspiration, a relative modern solution for reinforcement of embankments is shown in this paper. This solution comprises of application of geosynthetics where, among vast range of types, geogrids are most often used for reinforcement of flood protection embankments. Main advantage of geogrids is in increasing safety aspects, extending embankment work life and potentially reducing overall remediation cost through reduction of earthworks. Characteristics of geogrids, as well as mechanisms, which drive their behaviour through interaction with soil materials, are also presented in paper. Other than reinforcement, geosynthetics can be efficiently used in embankments by means of material separation, filtration, drainage or to ensure its impermeability.

Keywords: geosynthetics, geogrid, reinforcement, flood protection embankment, remediation measures

2 Introduction

Currently in Croatia there is a necessity for remediation of existing flood protection embankments due to their relatively poor condition, which is the result of inadequate maintenance accompanied with lack of investments in last few decades. Rising water tables, influenced by climate changes, are not the only issue when it comes to existing flood protection embankments. The implementation of Eurocode 7 with its stricter design procedures is also to be considered. To satisfy these requirements, the crest of the embankment must be higher than before so that it meets the minimum design height, and in doing so the embankment is not only getting higher but also wider. This usually presents issues due to several constraints, mainly regarding property legalization. Because of legal complexity of this issue, it is common aspiration to keep reconstructed embankment within the cadastral parcels owned by investor. To ensure this, embankments need to be reconstructed with steeper slopes in order to reach design height. A relatively new solution for this problem is the usage of geosynthetics as reinforcement in the embankment to make steeper slopes while still maintaining their stability. Steeper slopes not only mean construction within the restricted space, but usually also less fill material. The range of geosynthetic products is indeed large, but their other role in flood protection embankment is beyond the scope of this paper. Being a relatively new product, questions arise regarding the design of geosynthetic reinforced embankments. The Croatian Ministry of Construction and Physical Planning published in 2017 the "Technical Regulation for Building Structures" [1] which, among other things, regulates that geotechnical designing should be done following the procedures given by Eurocode 7: Geotechnical design – Part 1: General rules [2], Eurocode 7: Geotechnical design – Part 1: General rules – National annex [3], and Eurocode 7: Geotechnical design – Part 2: Ground investigation and testing [4]. However, Eurocode 7 does not give any provision regarding the usage of geosynthetics as materials for reinforcement and are only mentioned in the context of filtration function when used in embankments. All this makes the design of geosynthetic reinforced embankment more challenging and often leads to doubts regarding application of these relatively new products. Regardless of the lack of specific

information about geosynthetic design, Eurocode 7 notes that “embankments shall be designed taking into account experience with embankments on similar ground and made of similar fill material”, thus encouraging and justifying the usage of other relevant literature, which in Croatia include documents such as “General technical requirements” [5] consisting of recommendations from good practice, or any other standard or newer literature which deals with application of these materials.

3 Characteristics of geosynthetics as reinforcement of flood protection embankment

Geosynthetics are products made of natural or synthetic polymers used in contact with soils in geotechnical operations. There are many types used for different purposes:

- 1) separation – for the separation of layers of coarse grained and fine-grained soil
- 2) drainage – to make drainage paths for transporting filtration water to a trench
- 3) filtration – letting filtration water pass through while keeping soil particles in place for avoiding internal erosion which would lead to failure; goes along with separation
- 4) reinforcement – reinforces the soil with which is in contact by using the load – deformation properties of geosynthetics
- 5) impermeability – flow control through an embankment
- 6) erosion control

Table 1 shows the types of geosynthetics used for each of the mentioned applications.

Table 1. Types of geosynthetic and their functions (Bouazza et al.) [6].

Function Geosynthetic	Separation	Drainage	Filtration	Reinforcement	Impermeability	Erosion control
Non-woven geotextile	1	2	1			1
Woven geotextile	1		2	1		
Geogrid				1		
Geosynthetic barrier					1	
Geocells	1			1		
Geosynthetic clay liner					1	2
Geocomposite	2	1	2	2	1	1
Geonet		1				
Geopipe		1				

1 – primary function

2 – secondary function

Even though all mentioned application of geosynthetic can be implemented within a flood protection embankment, the main focus of this paper is on geosynthetics used for reinforcement, specifically geogrids – types of geogrids, failure mechanisms, and geogrid characteristics. Reinforcement geosynthetics give more stability to embankments and produce lower settlements by providing tensile strength to soils, and allow construction of steeper slopes. Figure 1 shows the various usages for geosynthetics in the reconstruction of an old embankment.

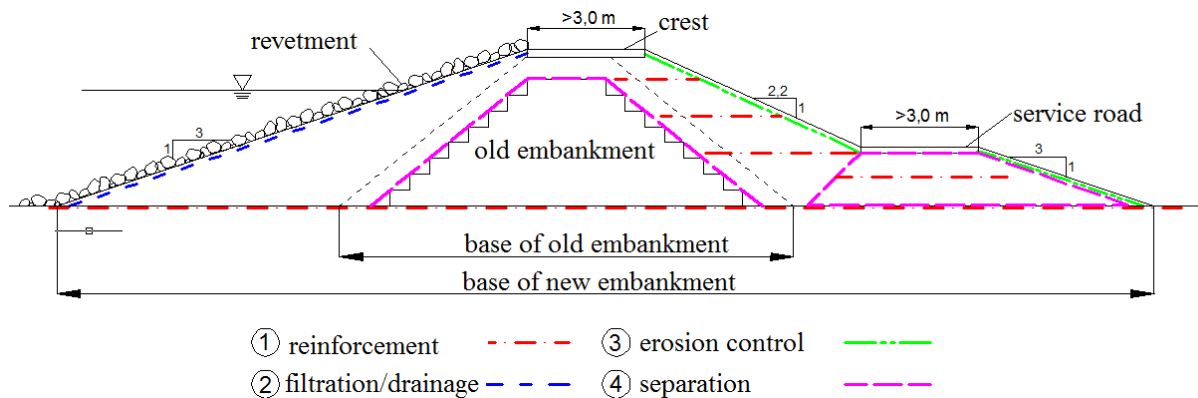


Figure 1. Reconstruction and improvement of old embankment using geosynthetics [7].

3.1 Geogrids

Geogrids are a type of geosynthetic whose sole purpose is reinforcement and increase of overall stability of embankments. They can be produced as monolithic, knitted or by connecting separate pieces together. Monolithic geogrids are made by puncturing a polymer foil and stretching it in one direction to produce a uniaxial grid or two directions to produce a biaxial grid, under controlled temperature and deformations. Polymers which are mostly used are high density polyethylene (HDPE) and polypropylene (PP). HDPE and PP have a Young's modulus that amounts to 0.8 and 1.5-2 GPa [8] respectively, but it should be noted that those are not the moduli of the manufactured and installed geogrid elements which depend on several other factors including the thickness, width and spacing of the geogrid ribs. Knitted geogrids are the most widely spread on the market. They are made from polyester fibers, mostly polyethylene terephthalate (PET) with Young's modulus of 2-2.7 GPa [8]. Their advantage over the other types of geogrids is flexibility. Connected geogrids are made by placing ribs such that they form a grid and connect them together by some patented process. Their characteristics are high stiffness and high tensile strength. As the purpose of geogrids is to transfer different loads, different types of geogrids can be used for a variety of situations. With regard to the main direction of bearing capacity three types of geogrids differ: uniaxial – one main bearing direction; biaxial – two perpendicular direction have high bearing capacity; triaxial – high bearing capacity in three radial directions in a plane. Uniaxial geogrids have ribs only in one direction, mutually connected in the perpendicular direction on specific distances, and are usually made from HDPE. This type is mostly used in embankments where it is placed with the main bearing direction perpendicular to the embankment axis to ensure lateral slope stability. Biaxial geogrids have ribs in two directions. The tensile strength isn't necessary equal in both directions. They are mostly used for point/local loads, and are usually made from PP. Triaxial geogrids, like biaxial, are used for point/local loads but instead of squares the elements form triangles for better load transfer. Biaxial and triaxial grids are usually placed under traffic areas where high traffic loads are expected. Because of this, they are sometimes placed under embankment crests if the crests are designed to be used for traffic purposes. All three types are shown in Figure 2.

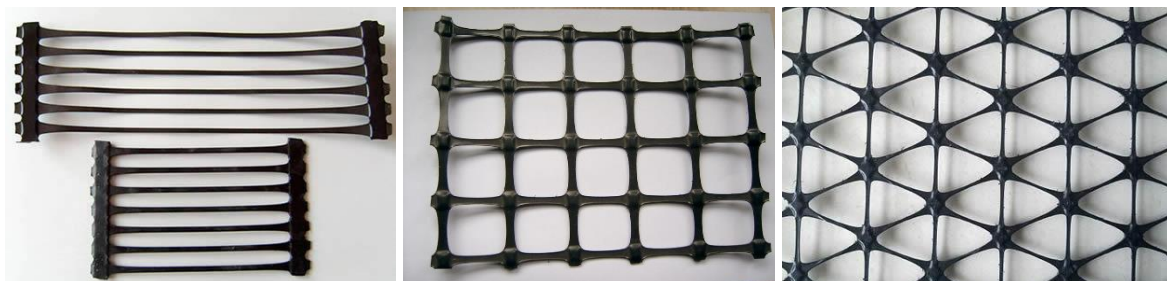


Figure 2. Uniaxial, biaxial, and triaxial geogrids.

Geogrids are delivered in rolls of various widths from 2 – 5m, and as such should be appropriately taken care of during storage, before installation. Geogrids should never be overly exposed to ultraviolet light, precipitations, chemicals, and other environmental conditions that may damage the geogrids' properties. The layer of soil on which geogrids are placed must be adequately prepared. The stronger the geogrids

are, the more flatter the base must be. They should never be placed on frozen ground, on snow, or during rain. Special care should be taken while placing and compacting fill material on top of the geogrid layer. After long periods of time after installation, as a cause of mechanical, chemical, or biological wearing, geosynthetics lose their main function and, as a result, embankment failure can occur. Weakening of geogrid characteristics over time is also associated with creep. When it comes to the service life of these materials there is no straightforward answer mainly due to fact that they are relatively new and geosynthetics installed until now rarely show any sign of significant degradation [9]. Eurocode: Basis of structural design [10] divides structures into 5 categories depending on the required design working life varying between 10 and 100 years. Flood protection embankments, or embankments in general, are not included in this classification. Since they are structures of high importance for public safety, assigning a design working life category of 5, corresponding to 100 years, would be a reasonable assumption. Thus, extrapolation from creep tests performed up until now is needed. Geogrids tend to elongate under constant loads during longer periods of time, as is the case in embankments. Creep design is made by applying a safety factor to the ultimate tensile strength, thus reducing it enough to ensure the long term stability. Generally, manufacturers give creep strength values designed for periods of over 100 years. Geogrids made from polypropylene (PP) and polyethylene (PE) don't have the ability to keep their mechanical properties over long periods of time (10^6 h) [5]. Croatian "General technical requirements for works in water management" [5] specify that yield for PP and PE starts at about 30% of the ultimate tensile strength, thus high safety factors of 3.5 – 4.5 should be applied. Other materials such as PET and polyvinyl alcohol (PVA) have higher resistance. Their yield point comes at around 70% of the ultimate tensile strength and as such they should be used as reinforcement. Safety factors of 1.2 – 2.5 should be applied to geogrids made from these materials [5].

4 Advantages and disadvantages of using geogrids in flood protection embankments

When in contact with soil and under vertical and horizontal stress, they provide tensile strength to the soil by having much higher modulus in their plane than soils. Soil particles at the depth of reinforcement are under vertical stress and, depending on their Poisson coefficient, corresponding horizontal stress. This horizontal stress then leads to horizontal deformations. Particles which are adjacent to the geogrid can interact with it in two ways: by interlocking particles with geogrid apertures and frictionally on the ribs of geogrids, which is usually achieved when the fill material is coarser, such as gravel, or only frictionally with geogrid ribs if the material is finer. Through those contacts the stresses are transferred onto the reinforcement which leads to reduction of deformations due to higher stiffness of soil – geogrid matrix. In the case of slope stability those contacts are used to secure the geosynthetic from being pulled out by the driving forces. Overall stability failure can occur internally or externally, or by the combination of both as shown in Figure 3. Internal failure means that failure will occur by rupture of geosynthetic because of the stress exceeding the ultimate tensile strength, or by being pulled out of the soil because of the interface strength being too low. External failure occurs when the slip surface is beyond the reach of the reinforcement. As geosynthetic reinforcement is installed inside of an embankment, it increases the factor of safety against sliding in two ways according to the mentioned failure mechanisms. In the first instance, the slip surface passes through the geosynthetics but has a higher factor of safety because of bond and tensile strength of the reinforcement material. In the second, the slip surface is moved deeper and beyond the geosynthetic reach thus increasing factor of safety because of larger normal effective stress on the slip surface. Kitch et al. [11] showed that for a target factor of safety and specific reinforcement length there is a minimum value of tensile strength that will generate only external types of failures. Increasing the reinforcement length, while keeping the tensile strength equal or less than the one obtained for an external failure mechanism, will generate internal types with the same factor of safety. An optimum design implies reaching the aimed factor of safety, by controlling the reinforcement vertical spacing, length, value of tensile strength which is defined by manufacturer, and bond strength which depends on the type of fill material as well as on anchoring length.

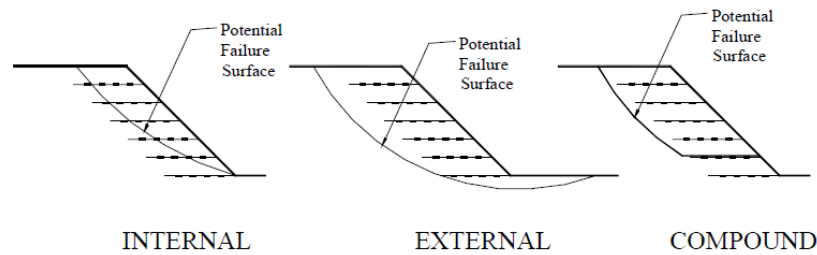


Figure 3. Failure modes of reinforced slopes [12].

Internal properties of geogrids depend on the type of polymer used for their production as well as on manufacture technology. The main characteristics which a designer should look upon are tensile strength at low and large strains, friction and interlocking with soil particles, resistance to damage during construction and exploitation, and durability expressed as strength decrease in percentage during time as a result of mechanical, chemical or biological wearing. Behaviour of geosynthetics doesn't only depend on their characteristics but also characteristics of soils they are in which will be discussed later in this paper.

In the construction of new embankments, geogrids are usually placed through the whole section. Thus, only internal failures can occur. However, in this case some other failure mechanisms can be of importance such as when the bearing capacity of the foundation soil is exceeded, leading to failure of embankment as rigid body. Constructing embankments with steeper slopes by using geogrids can have several advantages which was shown by Varuso et al. [13]. They made a cost comparison between unreinforced and reinforced full-scale test sections on soft foundation soils. When an embankment is built on soft soils then, due to consolidation following a relatively long period after construction, the realized settlements are such that a second lift fill is required in order to maintain the designed height of the crest. With the implementation of geogrids these settlements were reduced. As the geogrids were not used at their full potential in terms of allowable strain, it was possible to consider the same geogrid reinforcement in the revised stability analysis with the second lift. With reduced settlements, and by being able to use the existing reinforcement in the second lift stability analysis, the minimum possible second lift fill was obtained, with estimated savings of 78% compared to the unreinforced embankment, as shown in Figure 4.

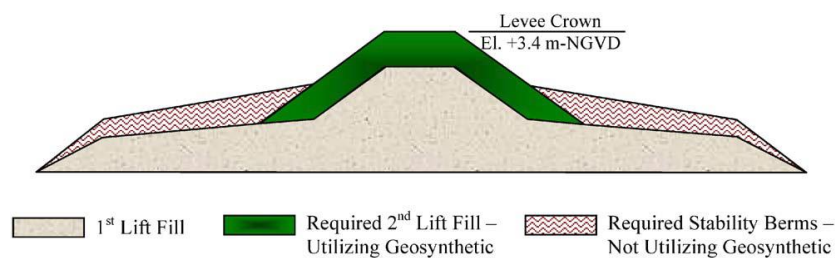


Figure 4. Second lift required fill comparison (Varuso et al.) [13]

For further understanding and optimization of geogrids within flood protection embankments, additional parameters need to be analysed. When reconstructing embankments, geogrids are no longer placed through the whole section but on both sides from the old body to the new slope. This way, external, internal, and combined mechanisms are possible depending on the geogrid characteristics. Ferreira et al. [14] reported that water content and density of fill material have high impact on the shear strength on both geogrids and geotextiles. Moreover, the aspect ratio defined as the ratio of aperture size to medium grain size has significant impact on the interface shear strength according to Mehrjardi et al. [15] (lower aspect ratio corresponds to higher strength). A part of the geogrid's reinforcement mechanism is interlocking between soil particles and geogrid ribs. So, by providing more confinement for soil particles, more confinement stress is induced and the shear strength is increased. This increase in confinement stress lead to improving the interface shear strength of coarse sand much more than for fine sand [15]. This could lead to the conclusion that the interlocking mechanism, as opposed to the frictional part, is the leading component in improving the soils shear strength when using geogrids. Thus, for finer soils smaller apertures should be used, or even wider ribs should be used to produce more frictional

strength since the effect of confinement doesn't affect so much finer soils. While for coarser soils larger openings should be used for more interlocking strength. By having all this in mind, optimized embankment designs could be made.

While designing the reinforced section, construction works must be kept in mind to balance the theoretical optimal design and the construction optimal design in terms of reinforcement spacing, tensile strength, length, type, material, dimensions, availability on the local market, etc.

5 Geogrid modelling methods

There are multiple ways of analysing slope stability reinforced with geogrids, each with their own advantages and limitations. The simplest one is the limit equilibrium (LE) method where a critical slip surface is found by solving force and momentum equilibrium equations for a rigid, non-deformable body. This is done by discretizing the sliding mass into a predetermined number of vertical slices, and by introducing certain conditions to overcome the static indeterminacy of the system. Its advantages are the relative simplicity (due to number of assumptions) to assign strength parameters to soil-geogrid interface, and simple calculation method. The additional force which is the result of geogrid reinforcement is just added in a static equation. Being so simple, this method generates many limitations such as: one global safety factor for the whole slope, neglecting the displacement compatibility, neglecting deformation properties of soils and geogrids. Including them in the analysis would result with more realistic stress redistribution. This can be done by combining the LE method with numerically generated stresses from finite element (FEM) or finite difference methods (FDM) [16]. By doing that, a more realistic stress distribution can be achieved, which is then used for the slope stability analysis to compute the shear stress and strength at the bottom of each slice. Thus, the results depend on the constitution model used to define the soil and interface load-strain characteristics. To get potentially more reliable results, and to more realistically describe the conditions in the soil, influence of other constitutive models should be investigated [17]. A local factor of safety for each slice is also available for assessment after the analysis is completed. The main issue of this method is the complexity of defining geogrid and interface parameters. Because of the insecurities in parameter values linked with the lack of laboratory or field test results, probabilistic analyses can be done instead of deterministic. The deterministic analysis results with a factor of safety (F_s) defined as the ratio of shear strength to shear stress. In the case of probabilistic analyses, the F_s is replaced by the probability of failure or the reliability index [18] which can directly relate to each other when the shape of the probability distribution is known, but there is no direct relationship between them and the deterministic safety factor [16]. The probability of failure is the probability of the F_s being less than 1 (which is considered as boundary value between unstable and stable condition), obtained from counting the number of safety factors less than 1 and showing them as a percentage of the total calculated number of safety factors. The reliability index describes stability with the number of standard deviations between the mean safety factor and 1. When the needed parameters (e.g. interface strength) have "too much" variability, reliability analyses should be carried out instead of the partial factor methodology [18]. Using the reliability analysis for cases where the considered parameter is not directly available would greatly increase the credibility of results.

6 Example of geogrid application for remediation of embankment

In 2015, a design for remediation of old flood protection embankment "Otok Virje – Brezje", situated on river Drava and originally constructed in the 1960s, was made [19]. Due to unfavourable events in 2012 when high waters caused overtopping and breaching of the embankment (Figure 5.), Croatian Waters have decided to completely reconstruct this embankment which directly protects the town Otok Virje as well as surrounding towns and villages. It also protects around 450 ha of agricultural land, forests, and other land. The adopted height for the new embankment is based on the water levels from a hydraulic model corresponding to flows of 3100 m³/s, with additional height of 0.5 m between high water and crest.



Figure 5. Overtopping and breaching of Otok Virje – Brezje flood protection embankment.

To assess the existing state and obtain parameters for stability, hydraulic, and settlement analyses, borings along with standard penetration tests (SPT) and geophysical tests were made. Field investigations were made on 2 occasions, first in 2011 and second in 2013. By interpreting the investigation works, it was found that the foundation materials consisted mostly of sand and gravel sediments with mixtures of silt occasionally. Finally, the new embankment body was constructed out of well graded gravel (GW), as decided by the Investor. All calculations were made according to Eurocode 7 and the respective national annex.

Analyses were performed using the computer program GeoStudio which includes SEEP/W used for hydraulic analyses and SLOPE/W used for slope stability. After making hydraulic analyses to get pore pressures distribution inside the body of the embankment, slope stability analyses were made using the limit equilibrium method, and using the pore pressure distribution as input data. Since there were different characteristic sections regarding materials and geometry as well as various design situations to be calculated, more than 200 analyses were made consisting of both upstream and downstream slope stability analyses. In order to achieve satisfying factor of safety, geogrids were employed. The methodology described earlier in this paper regarding geogrid placement was used: steps were formed on the old embankment body and geogrids were placed from the edges of those steps to the slope faces. The number of steps was chosen according to the embankment height, and geogrids were accordingly placed in 3 layers. Chosen geogrids are HDPE geogrids made by monolithic production with a 120 years design life, and all of equal strength as defined by Eq.(1).

$$P_d = \frac{P_c}{f_m f_d f_e LF} \quad (1)$$

Where: P_d – long term design strength

P_c – long term rupture strength from creep testing

f_m – partial factor for manufacturing

f_d – partial factor for site installation

f_e – partial factor for environmental effects

LF – load factor

From Eq. $P_d = \frac{P_c}{f_m f_d f_e LF}$ (1) can be seen that the tensile

strength value tested in laboratory conditions is reduced by partial factors that take into account strength lowering caused by production, installation damage and environmental effects [20]. Having calculated the required tensile strength adequate geogrids were chosen to be placed in the embankment.

Figure 6 shows a characteristic cross section of the embankment with all its components and highlighted geogrids. Models made for stability analyses are idealisations based on this characteristic cross section in terms of geometry, dimensions, materials, and geosynthetic placement.

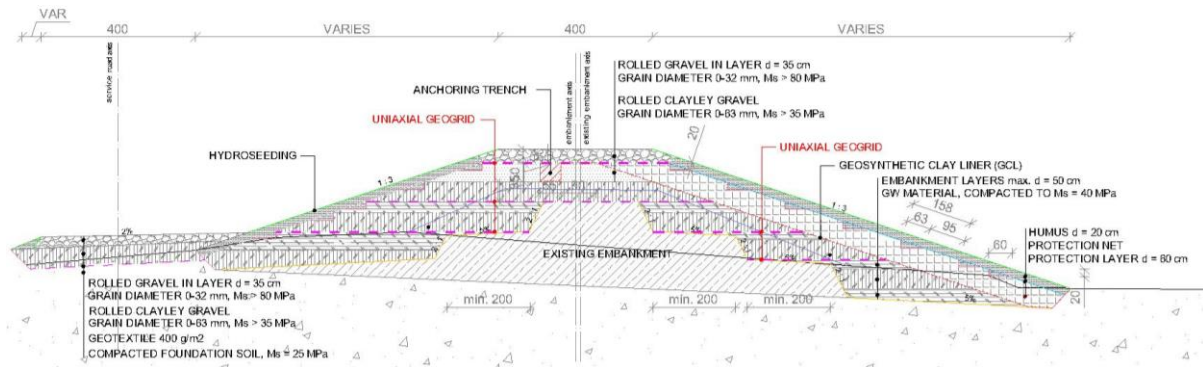


Figure 6. Characteristic cross section of the embankment.

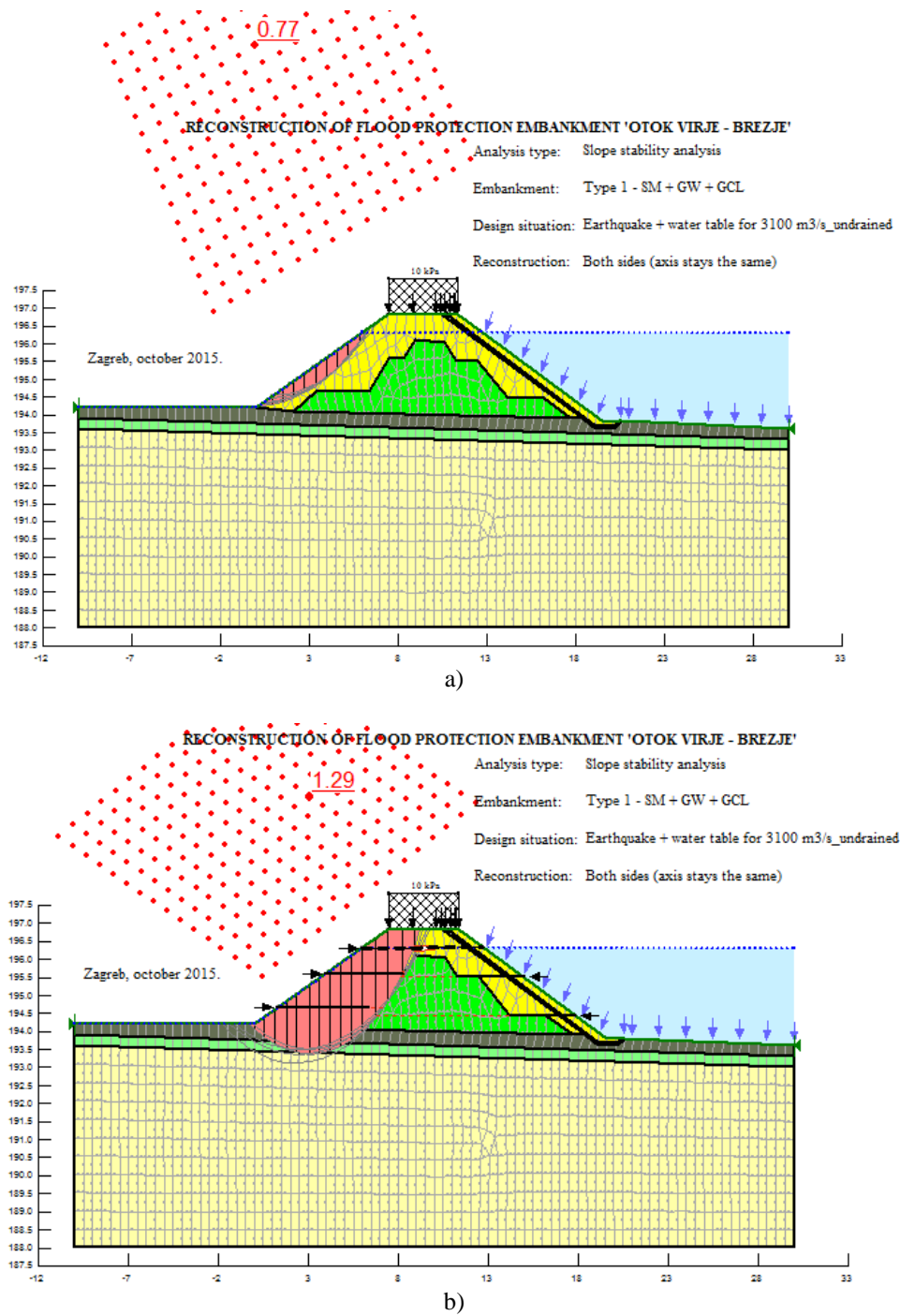


Figure 7. Comparison of a) unreinforced and b) reinforced section.

Comparison between a reinforced and unreinforced section from one of the mentioned design situations is shown in Figure 7. As can be seen from Figure 7, the potential failure mechanism in this instance is combined. The top layer of geogrids is placed across the whole section, thus only producing internal failures, while the other two layers are placed from the existing body to the slope face, susceptible to producing both internal and external failure. Improvement of the safety factor was achieved by the bottom two layers pushing the slip surface deeper, and by the top layer resisting with its interface and tensile strength. The safety factor was improved by 67.5% compared to the unreinforced section.

7 Conclusion

Geosynthetics are attracting new products commonly used in geotechnical engineering. For reinforcement of slopes, geogrids are most often used. There are various types of geogrids considering the method of production, materials, dimensions, and load transfer mechanism. Many researches were made to show the benefits of using geogrids in flood protection embankments in terms of improved stability. Since Eurocode 7 doesn't contain any specific information regarding embankment and geogrid design, the design should be carefully assessed taking into account various parameters of geogrids and adjacent soil. The durability of these materials is of great importance, but since they are relatively new materials, only extrapolations can be made to predict their long term behaviour. To analyse geogrid reinforced slopes various methods can be used. When designing, one has to decide which method to use having in mind the pros and cons of each one and parameters needed for the chosen method. Regardless of the analysis method, geogrids were shown to be effective in improving stability of embankments made from various materials and foundation soils, making them act like semi-rigid bodies.

The reconstruction of the embankment "Otok Virje – Brezje", which suffered big damage during the unfavourable events in 2012, was conducted using the limit equilibrium analysis method. Geogrids were used to improve the stability of the reconstructed embankment, and as a result, stability in terms of safety factor was increased compared to the unreinforced embankment. To prove the stability, more than 200 analyses were performed.

References:

- [1] Technical Regulations for Building Structures (In Croatian), Official Gazette No.17/13, 2017.
- [2] Eurocode 7: Geotechnical design – Part 1: General rules (EN 1997-1:2004/A1:2013), Croatian Standards Institute, Zagreb, 2014.
- [3] Eurocode 7: Geotechnical design – Part 1: General rules – Nacional annex, Croatian Standards Institute, 2016.
- [4] Eurocode 7: Geotechnical design – Part 2: Ground investigation and testing (EN 1997-2:2007+AC:2010), Croatian Standards Institute, Zagreb, 2014.
- [5] Opći tehnički uvjeti za radove u vodnom gospodarstvu (In Croatian), Građevinski fakultet Sveučilišta u Zagrebu, Zagreb, 2011.
- [6] Mulabdić M.: Priručnik – upute za primjenu geosintetika u nasipima za obranu od poplava (In Croatian), Hrvatske Vode, Zagreb, 2016.
- [7] Haselsteiner, R.: Deichertüchtigung in Bayern – Eine Übersicht, Deichertüchtigung und Deichverteidigung in Bayern, Wallgau, pp. 13-28, 2006.
- [8] Modulus of Elasticity or Young's Modulus - and Tensile Modulus for common Materials, http://www.engineeringtoolbox.com/young-modulus-d_417.html, 30.06.2017.
- [9] Bačić, M., Librić, L., Kovačević, M. S.: Application of geosynthetics as hydraulic barriers in flood protection embankments, 1st International Conference on Construction Materials for Sustainable Future, Zadar, pp. 677-683, 2017.
- [10] Eurocode: Basis of structural design (EN 1990:2002+A1:2005+A1:2005/AC:2010), Croatian Standards Institute, Zagreb, 2011.
- [11] Kitch, W. A., Gilbert, R. B., Wright, S. G. (2011) Probabilistic Assessment of Commercial Design Guides for Steep Reinforced Slopes: Implications for Design, Georisk, Atlanta, Georgia, United States, 2011.
- [12] Strata: Global GeoSolutions, Reinforced soil slopes and embankments, 1, Strata Systems, Inc.,

- Cumming, USA, 2010.
- [13] Varuso, J. R., Grieshaber, J. B., Nataraj, M. S.: Geosynthetic reinforced levee test section on soft normally consolidated clays, *Geotextiles and Geomembranes*, 23 (2005), 4, pp. 362-383.
 - [14] Ferreira, F. B., Vieira, C. S., Lopes, M. L.: Direct shear behaviour of residual soil–geosynthetic interfaces – influence of soil moisture content, soil density and geosynthetic type, *Geosynthetics International*, 22 (2015), 3, pp. 257-272.
 - [15] Mehrjardi, Gh. T., Ghanbari, A., Mehdizadeh, H.: Experimental study on the behaviour of geogrid-reinforced slopes with respect to aggregate size, *Geotextiles and Geomembranes*, 44 (2016), 6, 862-871.
 - [16] Geo-Slope Ltd., *Slope/W for Slope Stability Analysis: User's Guide*, Geo-Slope Ltd., Calgary, Canada, 2012.
 - [17] Yu, Y., Bathrust, R. J.: Influence of Selection of Soil and Interface Properties on Numerical Results of Two Soil–Geosynthetic Interaction Problems, *International Journal of Geomechanics*, 17 (2017), 6.
 - [18] Ferreira, F. B., Topa Gomes, A., Vieira, C. S., Lopes, M. L.: Reliability analysis of geosynthetic-reinforced steep slopes, *Geosynthetics International*, 23 (2016), 4.
 - [19] Glavni projekt: Nasip za obranu od velikih voda Otok Virje – Brezje project virje brezje, Građevinski fakultet Sveučilišta u Zagrebu, Zagreb, 2015.
 - [20] Tensar International: *The Properties and Performance of Tensar Uniaxial Geogrids*, Blackburn, 2007

INVESTIGATION WORKS FOR REMEDIATION OF HYDRAULIC STRUCTURES

LUKA PUŠIĆ¹, GORDANA IVOŠ¹, DANIJELA JURIĆ KAČUNIĆ¹

¹ Faculty of Civil Engineering, University of Zagreb, Croatia, lpusic@grad.hr, givos@grad.hr, djka@grad.hr

1 Abstract

Due to climate change, in last decade comes to the frequent occurrence of high water levels, which are higher than those for which are existing hydraulic structures designed. It is therefore necessary to remediate the existing flood embankments. In this paper, the methodology of evaluation of flood embankments is shown. Short overview of investigation methods used is given, as well as examples of implementation of this methodology, which provides data necessary for remediation of hydraulic structures.

Keywords: flood protection embankment, investigation works, borehole drilling, seismic refraction, ground penetration radar, standard penetration test, embankment state evaluation methodology

2 Introduction

Over the last decade, scientists have confirmed the emergence of global warming and warn of the consequences in various forms, some of which may have catastrophic effect on population, agriculture, housing, infrastructure and economic facilities. One of the forms of unwanted phenomena is frequent occurrence of extreme hydrological conditions, like extreme droughts or high water levels with floods. As a result of global warming, in many locations there has been the occurrence of the maximum historical water levels of the river and the emergence of floods that have posed a threat to human life and have devastating consequences in terms of material damage. Because of the above mentioned occurrences, the occurrence of higher water levels than the existing embankments are dimensioned for, it is necessary to carry out an evaluation of the existing flood protection embankments. Since a large number of embankments are in poor condition, these sites need to be reconstructed, and for those that are not high enough to protect them from extreme high waters, it is necessary to perform cambers to meet all the security and functional aspects of flood protection. Figure 1 shows the decision-making process for the reconstruction of the embankment to the performance. The key element for assessing the state of the embankment for flood control is investigation work. According to Eurocode 7 - Part 2, investigative work should be designed to provide relevant data for the relevant project and enable project risk management. Ground investigation work at the design stage should contain: identification and classification of soil and rock, sampling and groundwater measurements, field testing and laboratory tests [1]. In order to evaluate the state of the existing flood embankments, it is necessary to develop a methodology for assessment of flood protection status, i.e. to develop a systematic, interdisciplinary approach using different scientific methods and modern equipment, which would ultimately enable the categorization of the embankments and prioritization in reconstruction of existing flood embankments.

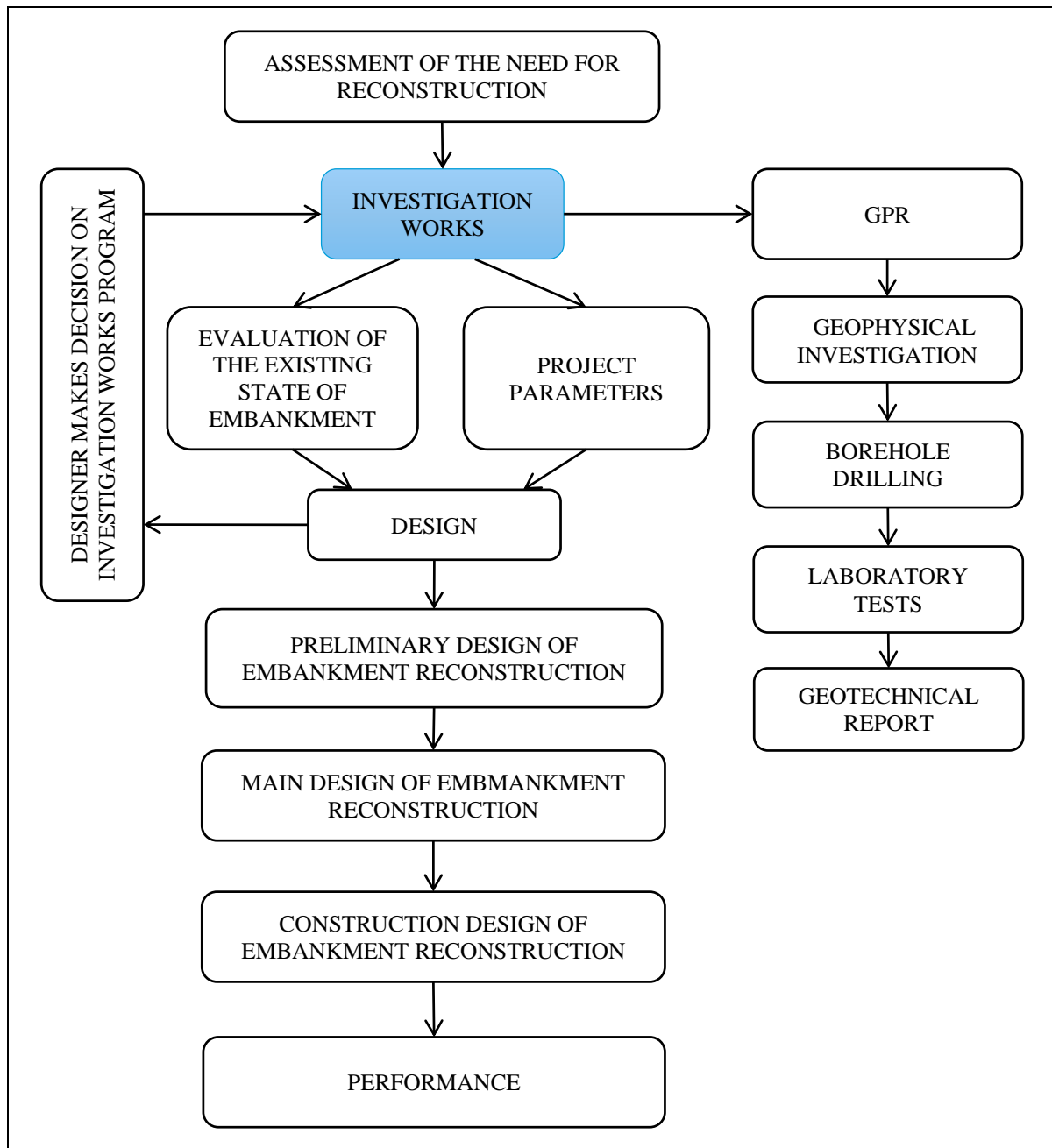


Figure 1. Embankment reconstruction process

The following methodology has been developed for the evaluation of the existing embankments: GPR survey is required to detect anomalies in embankment, such as voids, surface cracks, shallow and deep cavities and inhomogeneity inside embankment fill, or whether there are anomalies in foundation soil [2]. The determined critical sections perform a geophysical test using seismic refraction to obtain a more accurate image of the embankment state and to obtain data for estimating stiffness of embankment material. Seismic refraction and ground penetration radar are non-destructive methods used in geotechnical research and are appropriate for obtaining a wide picture of the existing state. Such tests are relatively quick and financially more favorable than borehole drilling and allow more data. However, these methods do not provide detailed information and do not provide information about the material parameters inside the embankment, but can be used to get an overview of the frame state and to spot locations where certain anomalies appear. Methods are ultimately useful for optimizing the drilling process and selecting the most convenient locations for borehole drilling. To fill the data obtained by GPR testing and seismic refraction, it is necessary to conduct investigative borehole on critical locations along with standard penetration test (determined on the basis of data obtained by non-destructive

methods) to obtain the exact embankment depth profile. Although investigative borehole drilling provides point data (only on the location of drilling) and is more expensive than geophysical and GPR testing, and the process is ultimately slower because it involves obtaining samples for laboratory investigation, borehole drilling is required at critical locations in order to obtain the relevant data for evaluation of embankment state and the parameters for the project. This developed methodology used to evaluate the state of existing flood embankments allows for good engineering-geological images and good foundation for projects.

3 Methods

3.1 GPR – Ground Penetrating Radar

Ground Penetrating Radar (GPR) is a geophysical method, which uses electromagnetic fields to probe lossy dielectric materials to detect structures and changes in material properties within materials. GPR recording is based on the transmission of electromagnetic signals of different frequencies in the soil or rock using the appropriate antennas. Transmitted waves can be attenuated, reflected, or refracted. When the wave hits the anomaly in the soil, the part of the energy is reflected back and processed in the receiver so that a continuous profile of electrical properties of the material is created (Figure 2) [3].

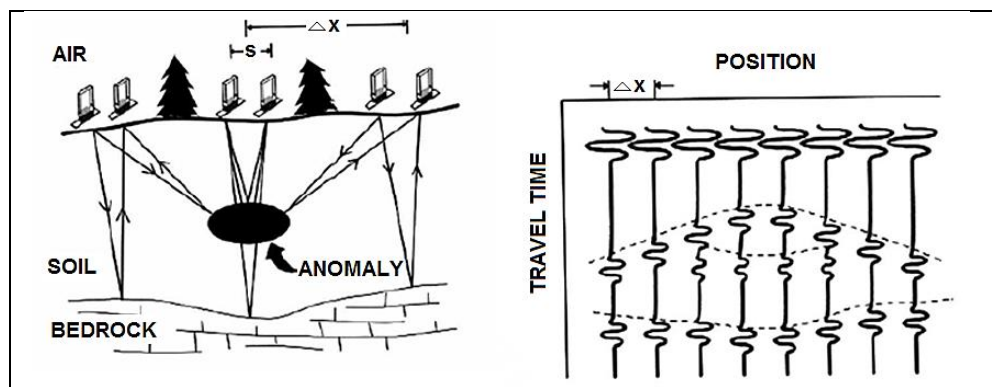


Figure 2. Principle of GPR test [3]

In order to evaluate geophysical method as useful, a change in certain physical characteristic must exist. In case of GPR survey, that physical characteristic is relative permittivity. The relative permittivity of a material for a frequency of zero is known as its dielectric constant. Higher dielectric contrast between two materials will result in stronger reflection in GPR image [4].

Dielectric constant influences velocities of the electromagnetic waves and because of that, velocity analysis conducted in post-processing phase can be used for dielectric constant calibration. Frequency of GPR determines two crucial survey parameters – investigation depth and resolution. When higher frequencies are used, lower investigation depth can be achieved, but with higher resolution. Using lower frequencies, subsurface investigation will result in lower resolution, but larger depths can be investigated. Vertical resolution is smallest distance in vertical direction at which two phenomena can be apart in order to see and distinguish them as separate phenomena. Horizontal resolution is the minimum horizontal distance between two phenomena at the same depth before the radar merges them out into one single event [5].



Figure 3. GPR testing

System for GPR survey is very simple and easy to operate with (Figure 3). It is composed of three parts: an antenna, a control unit, which is 'responsible' for generation of the radar signal and for detection of received signals as a function of time, and the processing system (laptop). GPR survey can be divided into two phases: a pre-processing phase and post-processing phase. Post-processing phase is used for interpretation of collected data from pre-processing phase which include certain noises (can be reduced by averaging) and interferences. Still, in many cases it is possible to use the results from a GPR survey with very modest processing [2].

3.2 Seismic refraction method

The seismic refraction method is based on the analysis of artificially created seismic waves that are generated from the surface. Those waves travel to a particular depth and return to the surface after refraction at the boundaries of layers with different seismic velocities. Surface wave's generator, geophones and computer are used for field data acquisition. The main task of a surface wave generator is to generate a wave with a higher frequency and a wavering energy by impulse or controlled vibration on the surface [6]. Different materials have different stiffness characteristics, so different generators need to be used to cover the larger range of frequencies, to stimulate the deeper layers, i.e. the generation of lower frequencies requires a greater burden than the layers closest to the surface requiring higher frequencies. There are several ways of generating waves on the surface: hammering, using a vibrator and using explosives [7]. The arrival of wave on the surface is detected by measuring sensors - geophones, which are placed at predefined positions [8]. The most common method of generating artificial waves is hammering into a metal plate. The seismic refraction test results (Figure 4) are the velocities of seismic waves and their spatial distribution, from which it is possible to determine the depth of the layers, the position of the fault and the fault zones and the level of the underground power.

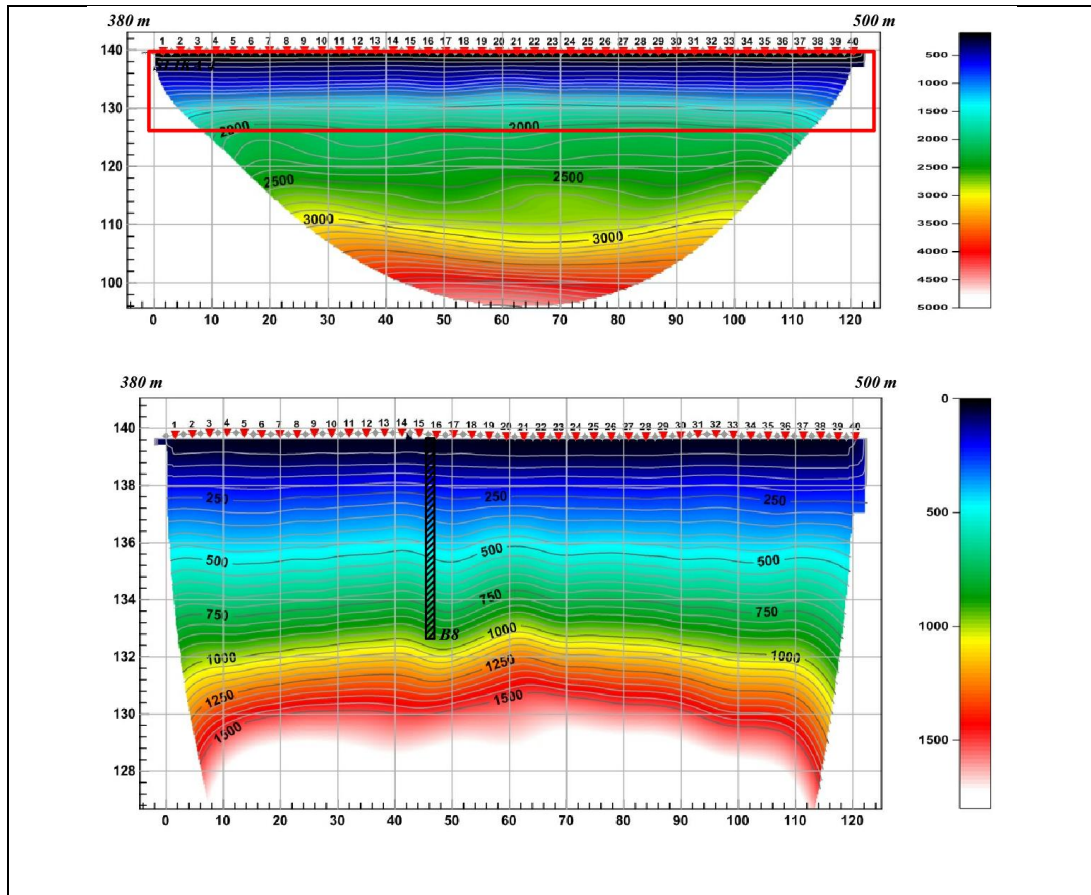


Figure 4. The result of geophysical testing by the seismic refraction method

3.3 Rotary drilling

Rotary drilling (Figure 5) implies swinging momentum on the drill bit, used to form a deep observation borehole or for obtaining representative samples of soil or rock. The drilling method involves a powered rotary cutting head on the end of a shaft, which is driven into the ground as it rotates [9]. The principle of rotary drilling with continuous cores is as follows: a drill tool, which can be a large drill or hollow spindle, which is attached to a series of hollow drill rods, is machine rotated and hydraulically pressed from the surface.

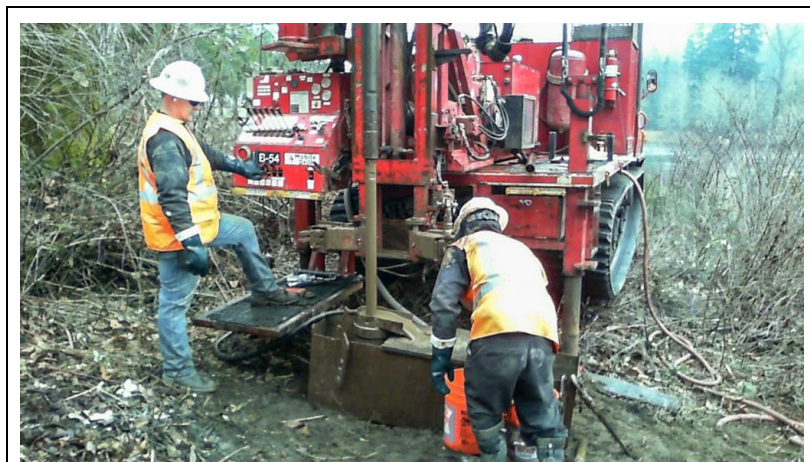


Figure 5. Rotary drilling [10]

In cases where more than one type of research is planned to be performed at a given location, the points of investigation must be separated at an appropriate distance. Since the disadvantage of rotary drilling

is a relatively high price, it is recommended to use geophysical methods to determine locations where rotary drilling is required to make the financial aspect more favorable.

3.4 SPT – Standard Penetration Test

Standard Penetration Test (SPT) is currently the most popular and economical means of obtaining subsurface information. The concept of the test consists of driving a standard 50 mm outside diameter thick walled sampler into the ground at the bottom of a borehole using the repeated blows of 63.5 kg hammer falling freely through 760 mm (Figure 6). The SPT N-value is the number of blows required to achieve a penetration of 300 mm, after an initial seating drive of 150 mm [11].



Figure 6. Standard Penetration Test

One of the advantages of the test is that it is carried out in routine exploration boreholes of varying diameters, so that (in contrast with other in-situ tests) there is no need to bring special equipment to site. Some other advantages of the test are its low cost, simplicity, ability to give a numerical parameter which may be related to crude but straightforward empirical design rules. The disadvantages of the test are that the results affect the way of handling, the differences in equipment and non-standard drilling methods and equipment at the international level. Despite disadvantages, the use of SPT is widely used because of its many advantages [12].

4 Examples of application of developed methodology

4.1 Flood embankment Gornji Hrašćan

For an overview of the 3 km long Gornji Hrašćan embankment (Figure 7) and for obtaining data needed for the reconstruction of the embankment, studies have been conducted in accordance with the developed methodology. In order to gain insight into the state of the embankment, a GPR survey was conducted in total length of 2928 m, to a depth of 4.5 m. For the purpose of checking the critical stocks detected by GPR testing and obtaining information on the best locations for drilling, a seismic refraction test was performed, with three profiles of total length of 720 m (each length 240 m). On critical locations determined by GPR testing and seismic refraction method, a rotary drilling was performed with the standard penetration test. A total of three boreholes of depth of 8 m were performed, and laboratory tests were performed on samples obtained. The use of the proposed methodology resulted in good substrates and quality engineering-geological picture for the needs of the project for the reconstruction of the embankment.

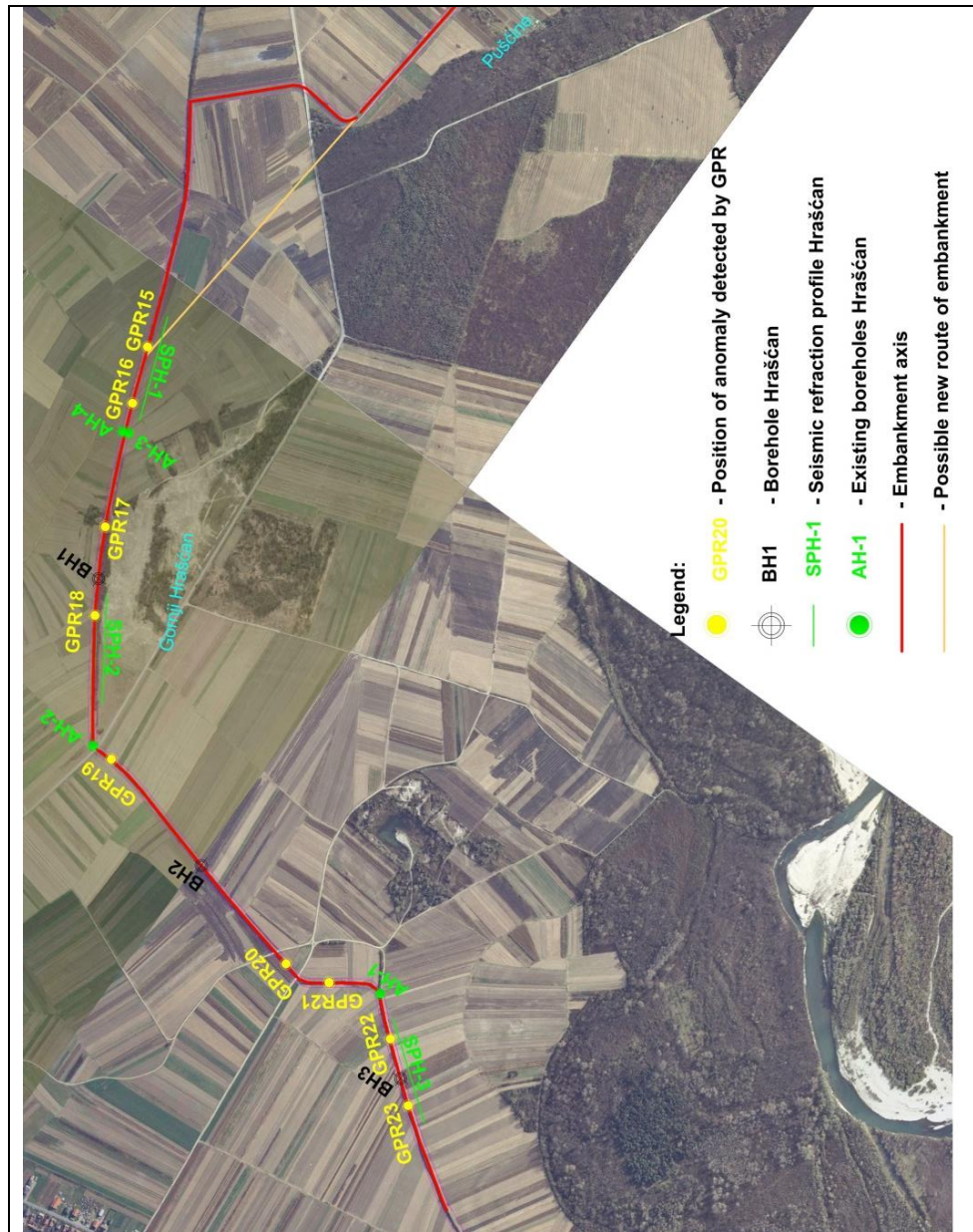


Figure 7. Situation of Geotechnical Investigations for the Gornji Hrašćan Embankment

4.2 Flood embankment Otok Virje – Brezje

Flood embankment Otok Virje – Brezje (Figure 8) is 3.7 km long. Given that the embankment had collapsed and the 100-year high water content increased, the embankment no longer meets the required level of flood protection, so an evaluation of the existing embankment status was needed to determine the extent of reconstruction.

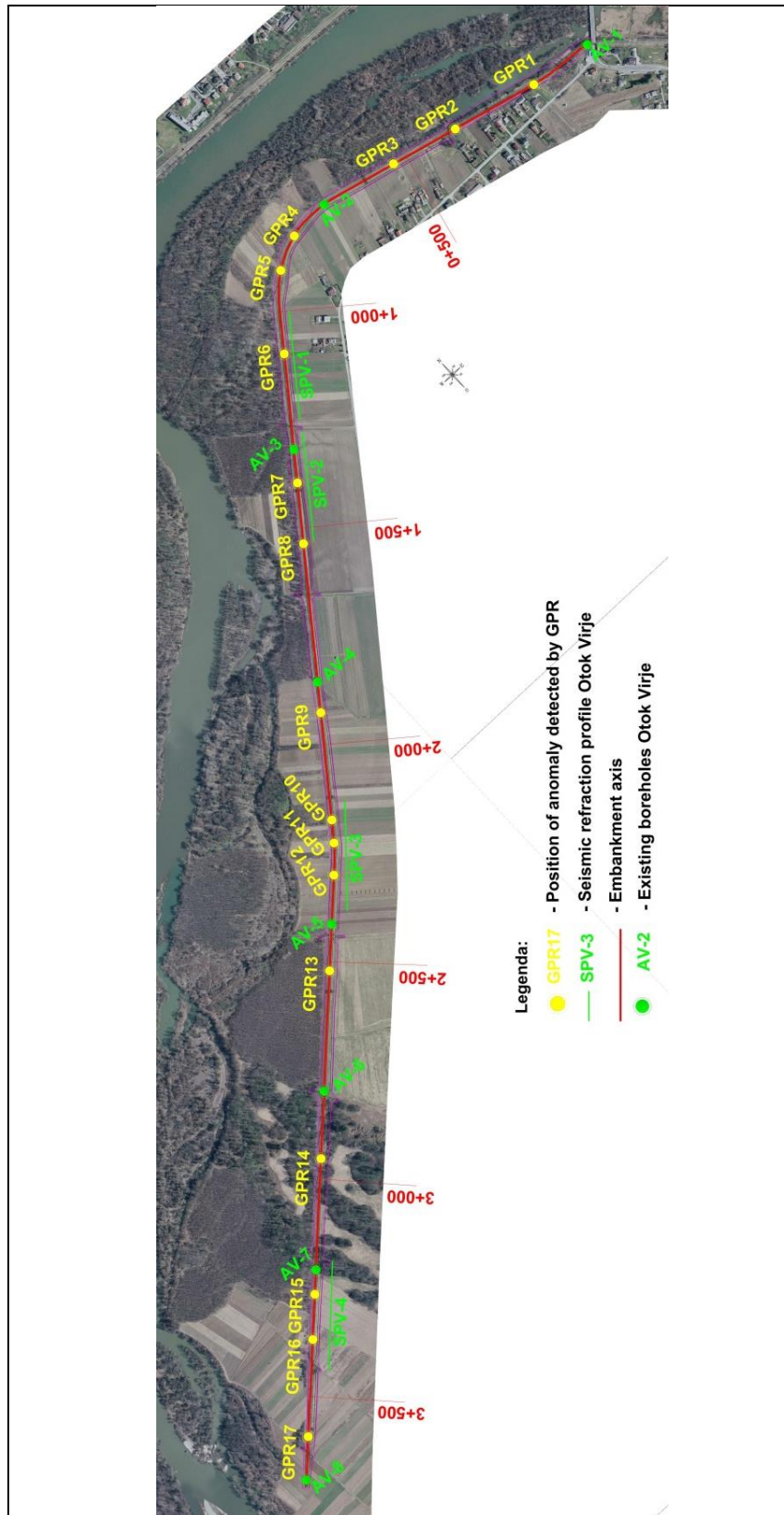


Figure 8. Situation of geotechnical investigation work for the Otok Virje - Brezje flood embankment

A GPR testing of 3669 m, up to a depth of 4.5 m was performed, which proved to be sufficient for testing the embankment body. The tests were carried out along the embankment crown. At sites where anomalies in the embankment were found, geophysical tests were performed using the seismic refraction

method, with four profiles per 240 m (total length 960 m). A total of boreholes of depth of 8 m were performed, and laboratory tests were performed on samples obtained.

4.3 Flood embankment Pušćine

On the left-hand embankment of the 4 km long Pušćine (Figure 9), investigations have been carried out for the needs of the evaluation of the state of the embankment and for obtaining data for the reconstruction of the existing embankment.

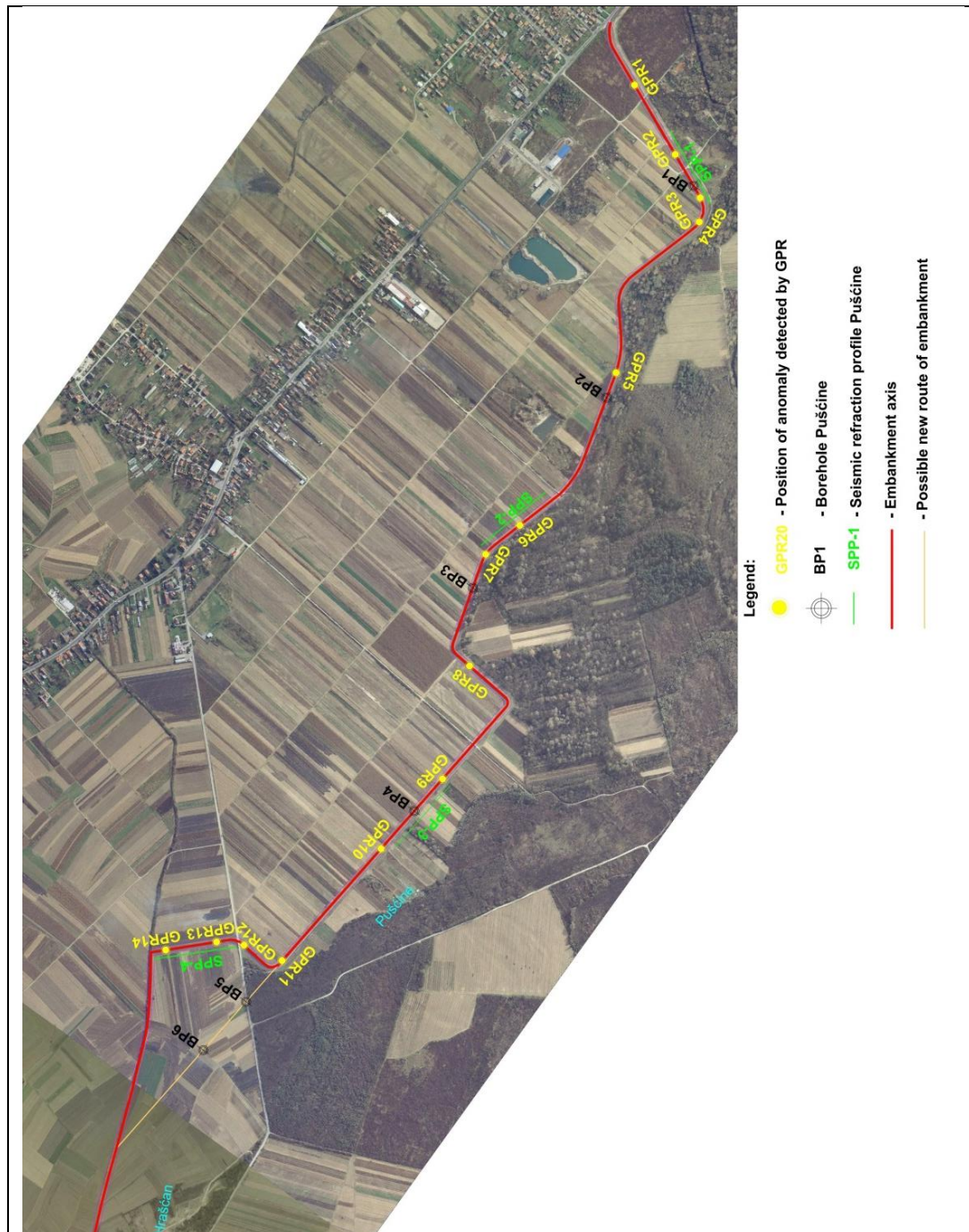


Figure 9. Situation of geotechnical investigations for the embankment of Pušćine

In accordance with the proposed methodology, a GPR test of 3928 m was performed, showing anomalies in certain locations where a seismic refraction test was performed, totally 960 m (4 profiles per 240 m) to determine the borehole positions. GPR test and seismic refraction established 6 locations where

boreholes were performed to depths of 8 m. Also, SPT test and laboratory investigation on samples taken were performed to get a good foundation for further projects.

5 Conclusion

Efficient flood protection becomes lately very important issue in the whole world due to climate change. Concept of flood protection system in Croatia traditionally is based on flood embankments and big foreshores next to great rivers, which has also influenced on preservation of wetlands and water dependent systems. Considering that many flood embankments in Croatia are not in good condition, as well as they are subjected to loads for which they were not primarily constructed due to higher water levels, it is necessary to remediate existing flood protection system. Therefore, a current state of embankments must be identified. This is done by conducting investigation works according to developed methodology. In this process are used different methods. Usage of ground penetration radar and seismic refraction enables getting better insight in overall geological stratigraphy and detecting critical segments and anomalies in embankment body. When general picture of the soil is provided and critical spots are identified on the basis of collected data by using geophysical methods, it is possible to determine an optimal number and position of investigation boreholes. Borehole drilling provides information on type of material of existing embankment and foundation soil and obtains soil samples for laboratory tests. This methodology ensures getting relevant data necessary for identifying state of flood embankments, as well as they provide additional data for remediation of the embankment.

References:

- [1] EN 1997-2: Eurocode 7: Geotechnical design - Part 2: Ground investigation and testing
- [2] Marčić, D., Bačić, M., Librić, L.: Using GPR for detecting anomalies in embankments, 13th International Symposium on Water Management and Hydraulic Engineering, Bratislava, 2013.
- [3] Annan, A.P.: Ground Penetrating Radar – Principles, Procedures & Applications, Sensors & Software Inc., Mississauga, Canada, 2003.
- [4] Kang, Y.V., Hsu, H., Li, K. and Lin, M.: Application of Ground Penetrating Radar method to detect hidden defects in bank revetment, INTERPRAEVENT 2010 - Symposium Proceedings, Taipei, Taiwan, pp. 235-243, 2010.
- [5] Alvarez Cabrera, R.: GPR Antenna Resolution, www.geoscanners.com, 07.06.2017.
- [6] Kovačević, M.S., Marčić, D., Gazdek, M. 2013. Application of geophysical investigations in underground engineering, Technical Gazette 20 (6), pp. 1111-1117., 2013.
- [7] CIRIA, Geophysics in engineering investigations, London, 2002.
- [8] Bačić, M., Jurić Kačunić, D., Kovačević, M.S.: Application of multi-geophysical approach for detection of cavern, Proceedings of International Conference on Testing and Measurement: Techniques and Applications (TMTA2015), Phuket, pp. 53-56, 2015.
- [9] RSA GEOTECHNICS, www.rsa-geotechnics.co.uk, 08.06.2016.
- [10] HOLT SERVICES INC, www.holtservicesinc.com, 08.06.2016.
- [11] Robertson, P.K.: Guide to in-situ testing, Gregg Drilling & Testing, Inc., 2006.
- [12] CIRIA, The Standard Penetration Test (SPT): Methods and Use, January, 1993.

AUTHOR INDEX

A		L	
Amić, Ana	94	Lenart, Stanislav	42
B		Librić, Lovorka	214
Bačić, Mario	214, 234	O	
Barišić, Ivana	27	Obradović, Dino	137
Bogatinoska, Borjana	9	Ocvirk, Eva	165
Bonacci, Ognjen	19	Orfánus, Martin	174
Budinski, Ljubomir	60	P	
Bujak, Damjan	165, 203	Panov, Angelco	69
C		Popovska, Cvetanka	69
Car, Marijan	224	Posavčić, Hana	102
Carević, Dalibor	203	Pušić, Luka	244
D		R	
Dadić, Tamara	27	Rak, Gašper	2
Dušička, Michal	174, 196	Ramušćak, Ratko	203
Dušička, Peter	190, 196	Reyes Perez, Maria Fernanda	113
F		Rossi, Nicola	234
Fischer, Johannes	128	Rumann, Ján	174, 190, 196
Foroughi, Daniel	181	S	
G		Sawicki, Jerzy M.	123
Gajski, Dubravko	224	Schobesberger, Johannes	128
Gašpar, Ante	203	Sekovski, Dimitrija	69
Gilja, Gordon	157, 165	Sharma, Saroj	113
Gronowska-Szneler, Marlena A.	123	Sindelar, Christine	128
H		Slunjski, Tomislav	76
Habersack, Helmut	128	Sočuvka, Valentin	52
Halkijević, Ivan	102	Steinman, Franci	2
Hlavčová, Kamila	52	Stipičić, Matija	60
I		Studvová, Zuzana	52
Ivoš, Gordana	244	Susinov, Bojan	42
J		Szawurska, Dominika	84
Janík, Adam	33	Š	
Jeftenić, Goran	60	Šoltész, Andrej	33
Josifovski, Josif	42	Šperac, Marija	76, 137
Jurić Kačunić, Danijela	234, 244	T	
K		Tadić, Lidija	27, 94
Kennedy, Maria	113	Tečić, Dorja	157
Kinczer, Tomáš	174, 190, 196	Trifunović, Nemanja	113
Kohnová, Silvia	52	Türker, Umut	181
Kolaković, Slobodan	60	Tvrdoň, Miroslav	190
Kolaković, Srdjan	60	V	
Kolerski, Tomasz	84	Velísková, Yveta	52
Kovačević, Meho Saša	214, 224	Vouk, Dražen	102
Kulić, Tin	203	Z	
Kuspilić, Neven	157	Zima, Piotr	147

